

Rashmi Wardhan · Padmshree Mudgal

Textbook of Membrane Biology

 Springer

Textbook of Membrane Biology

Rashmi Wardhan · Padmshree Mudgal

Textbook of Membrane Biology

 Springer

Rashmi Wardhan
Department of Biochemistry
Shivaji College
New Delhi, Delhi
India

Padmshree Mudgal
Department of Biochemistry
Daulat Ram College, University of Delhi
New Delhi, Delhi
India

ISBN 978-981-10-7100-3 ISBN 978-981-10-7101-0 (eBook)
<https://doi.org/10.1007/978-981-10-7101-0>

Library of Congress Control Number: 2017957718

© Springer Nature Singapore Pte Ltd. 2017

This work is subject to copyright. All rights are reserved by the Publisher, whether the whole or part of the material is concerned, specifically the rights of translation, reprinting, reuse of illustrations, recitation, broadcasting, reproduction on microfilms or in any other physical way, and transmission or information storage and retrieval, electronic adaptation, computer software, or by similar or dissimilar methodology now known or hereafter developed.

The use of general descriptive names, registered names, trademarks, service marks, etc. in this publication does not imply, even in the absence of a specific statement, that such names are exempt from the relevant protective laws and regulations and therefore free for general use.

The publisher, the authors and the editors are safe to assume that the advice and information in this book are believed to be true and accurate at the date of publication. Neither the publisher nor the authors or the editors give a warranty, express or implied, with respect to the material contained herein or for any errors or omissions that may have been made. The publisher remains neutral with regard to jurisdictional claims in published maps and institutional affiliations.

Printed on acid-free paper

This Springer imprint is published by Springer Nature
The registered company is Springer Nature Singapore Pte Ltd.
The registered company address is: 152 Beach Road, #21-01/04 Gateway East, Singapore 189721, Singapore

*Dedicated to those who continue to inspire me
My teachers for opening up the world ...
My beautiful daughters who make me proud every day ...
My husband for the endless encouragement and many cups of
tea ...
and to the power above for being the force with and behind me!*

Rashmi Wardhan

*To my parents, who gave me wings, and to family; my husband,
Sukrit, my children, Naman and Khyati who helped me soar
high.*

Padmshree Mudgal

Foreword

It gives me immense pleasure to write the foreword to the book titled Textbook of Membrane Biology. In the last few years, membrane biology has emerged as a very specialized field of study with the development of biotechnology. In effect, the plasma membrane has become the target of various drugs in the process of curing diseases. Plasma membranes are permeable barriers between cell and its environment. They control the flow of information and the movement of substances in and out of the cell.

Rashmi and Padmshree present a complex purview of the studies in plasma membrane in their book. It draws on existing researches on biomembranes, at the same time offering new perspectives on the subject. Such a book, I believe, will be extremely helpful for the undergraduate students in comprehending the basic concepts to recent advances in the field of biomembranes and membrane-associated processes. Students and researchers will find this book abreast of latest developments and findings on biomembranes.

Happy Reading!

April 2017

Debi P. Sarkar
Ph.D., FAScT, FNASc, FASc, FNA
Professor and Head, Former Dean,
JC Bose National Fellow
Department of Biochemistry
University of Delhi South Campus
New Delhi, India

Preface

If there is a book you want to read,
And it is not written yet, then you must write it

Toni Morrison

Charles Darwin had described the process of evolution as “descent with modification.” This phrase best explains the continuous evolution of membrane biology. It is an ever-evolving area of biology and has seen a lot of focus in the last few decades. This book is a very ambitious attempt solely dedicated to membrane biology. The commitment to design each chapter on a skeleton of its key concepts to give students a holistic view of the available knowledge has been maintained throughout the book. The book also juxtaposes the basics of membrane biology with the recent advances in this field. This further aims to enhance the scientific temperament among the readers. This book emphasizes fundamental concepts and scientific inquisitiveness which emerged from decades of classroom experiences and enlightening interactions with the students and subject experts. Each chapter in this book has been designed and crafted to incorporate all the information to cement the concepts of membrane biology even for the beginners. The knowledge of the structural and functional domains of the cell membrane has been harnessed for therapeutic purposes. Membrane and membrane-bound receptors constitute a very large pocket of potential drug targets. The book attempts to embrace the aspects of drug targeting as the modern tool for disease control. The humble attempt to write this book has been gratifying; nevertheless, we echo the thoughts of Thomas Hardy, “The more written, the more it seems to be written.”

New Delhi, India

Rashmi Wardhan
Padmshree Mudgal

Acknowledgements

This book could be possible only because of our publisher Springer's trust in our concept and content of this book. I want to thank my parents for giving me right values of life. I acknowledge Ms. Shachi Saluja for her help in reference arrangement and her contribution to hormone receptors chapter. Far away in the sunshine, my inspiration always guides me to the highest.

Rashmi Wardhan

Padmshree Mudgal acknowledges with thanks Dr. Khyati Sharma for her efforts in proofreading and editing Chaps. 1–5 and 8, and her valuable inputs.

Contents

1	Introduction to Biomembranes	1
1.1	Overview	1
1.1.1	Selectively Permeable Barrier	1
1.1.2	Interaction and Communication with External Environment	1
1.1.3	Energy Transduction	1
1.1.4	Intracellular Transport	1
1.1.5	Transmission of Nerve Impulse	2
1.1.6	Cell–Cell Interaction	2
1.2	Historical Background	2
1.3	Composition of Biological Membranes	7
1.3.1	Membrane Lipids	9
1.3.2	Phospholipids	10
1.3.3	Glycolipids	14
1.3.4	Sterols	14
1.4	Unique Lipid Composition of Cell Organelle Membranes	15
1.5	Transbilayer Lipid Asymmetry	17
1.6	Carbohydrates in Membranes	20
	References	27
2	Membrane Structure	29
2.1	Lipid Water Systems: Thermodynamics, CMC	29
2.1.1	Determination of CMC	30
2.1.2	Surface Tension	30
2.1.3	Conductivity	31
2.1.4	Polymorphic Lipid–Water Systems/Phases	31
2.2	Determinants of Polymorphic Phases: Shapes, Critical Packing Parameter	33
2.3	Lipid Phase Transitions	35
2.4	Technique Used to Study Lipid Phase Transitions	35
2.5	Factors Affecting Lipid Phase Transitions	36
2.6	Polymorphic Lipid Phases and Their Physiological Roles	37
2.6.1	Membrane Curvature	38
2.6.2	Fusion	39
2.6.3	Transbilayer Transport	41
2.6.4	Lipid Rafts	41

2.7	Model Membrane Systems	42
2.7.1	Lipid Monolayers	42
2.7.2	Supported Planar Lipid Bilayer	43
2.7.3	Planar Bilayer at the Tip of Patch Pipette	43
2.7.4	Liposomes	44
2.7.5	Nanodisks	46
2.7.6	Black Lipid Membranes (BLMs)	47
	References	47
3	Membrane Proteins	49
3.1	Types of Membrane Proteins	49
3.1.1	Peripheral Proteins	50
3.1.2	Integral Membrane Proteins (IMP)	53
3.1.3	Lipid-Anchored Proteins	59
3.2	Techniques to Study Membrane Proteins	64
3.2.1	Cell Disruption Methods	64
3.2.2	Membrane Separation and Isolation	67
3.2.3	Solubilization of Membrane Proteins	71
3.2.4	Membrane Protein Purification and Characterization	74
3.3	Membrane Protein Topology	76
3.3.1	The Major Membrane Topology Determinants Are as Follows	78
3.3.2	Experimental Tools to Determine the Membrane Topology of Proteins	78
	References	79
4	Function and Characterization of Cellular Membranes	81
4.1	Plasma Membrane: Specialized Membrane Structures	81
4.1.1	Tight Junctions	81
4.1.2	Desmosomes	84
4.1.3	Hemidesmosomes	85
4.1.4	Gap Junctions	86
4.1.5	Lipid Rafts	90
4.2	The Nuclear Envelope	93
4.2.1	Nuclear Envelope Breakdown During Mitosis	94
4.2.2	The Nuclear Envelope Reformation	96
4.3	Endoplasmic Reticulum	97
4.4	Golgi Apparatus	102
4.4.1	Functions of Golgi Apparatus	103
4.5	Lysosomes	107
4.6	Outer and Inner Mitochondrial Membranes	111
4.6.1	The Mitochondrial Outer Membrane (MOM)	112
4.6.2	The Inner Membrane	116
	References	119

5	Membrane Dynamics	121
5.1	Membrane Fluidity	121
5.2	Motion of Membrane Components	121
5.3	Factors Affecting Membrane Fluidity	124
5.3.1	Lipid Composition	124
5.3.2	Diet.	125
5.3.3	Temperature	125
5.3.4	Osmotic Stress	125
5.3.5	Cell Cycle and Development	125
5.3.6	Disease	125
5.3.7	Anesthetics.	126
5.3.8	Ca ²⁺ and Other Divalent Cations.	126
5.4	Techniques to Determine the Rate of Molecular Motion in Membranes	126
5.4.1	Techniques to Study Lateral Diffusion in Membranes.	126
5.4.2	Confocal Microscopy.	126
5.4.3	Fluorescence Recovery After Photobleaching (FRAP)	127
5.4.4	Fluorescence Correlation Spectroscopy (FCS)	128
5.4.5	Förster Resonance Energy Transfer (FRET)	129
5.4.6	Single-Particle Tracking (SPT)	131
5.4.7	Techniques to Study Rotational Motion in Membranes.	131
5.4.8	Techniques to Study Transbilayer Motion in Membranes.	132
5.5	Barriers Affecting Lateral Diffusion of Molecules in Membranes	134
5.5.1	Physical Barriers	134
5.5.2	The Cytoskeleton	134
5.5.3	Membrane–Membrane Junctions	136
5.5.4	Membrane–Matrix Junctions.	136
5.5.5	Intramembranous Clusters	136
5.6	Polarized Cells	138
5.6.1	Epithelial Cell.	138
5.6.2	Neuron	139
5.7	Organization of the Erythrocyte Membrane	140
5.7.1	Membrane Proteins	141
5.7.2	Integral Membrane Proteins	143
5.7.3	Peripheral Membrane Proteins.	144
5.8	Homeoviscous Adaptation	145
	References.	146
6	Membrane Transport	149
6.1	Introduction	149
6.2	Passive Diffusion	150
6.3	Facilitated Transport of Glucose	151
6.4	Facilitated Chloride–Bicarbonate Transport	154

6.5	Primary Active Transport	156
6.6	P-Type (E_1 - E_2) ATPases	156
6.6.1	Structure of P-Type ATPases	158
6.6.2	Phosphorylation Domain	158
6.6.3	Nucleotide-Binding Domain	158
6.6.4	The Actuator Domain	159
6.6.5	Membrane Domain	159
6.6.6	Transport Cycle of P-Type ATPases	159
6.7	Vacuolar [V-Type] ATPases.	160
6.8	Secondary Transport	163
6.8.1	Secondary Transport of Disaccharide Lactose by Lactose Permease (LacY)	164
6.8.2	Sodium/Glucose Secondary Transport	165
6.9	ABC Transporter	167
6.9.1	Mechanism of ABC Transporter	168
6.9.2	Classification of ABC Transporters in Mammals.	169
6.10	Lipid Transporters in Maintaining Membrane Asymmetry	170
6.11	Aquaporins	171
6.11.1	Structure and Function of Aquaporins	171
6.12	Active Transport Through Group Translocation in Bacteria.	174
6.12.1	Phosphoenolpyruvate (PEP): Carbohydrate Phosphotransferase System	174
6.13	Light-Driven Transport	175
6.14	Pore-Forming Toxins.	179
6.14.1	Activated Signal Pathway and Toxin Effect in Host Cells.	186
6.15	Ionophores.	186
6.16	Porins in Biological Membranes	191
6.17	Transport by Channel Proteins	194
6.18	Transport Through Ion Channel P2X Receptors	194
6.19	The Pentamer Cysteine Loop Gama-Amino Butyric Acid Receptors ($GABA_A$)	194
6.20	Tetrameric Ionotropic Glutamate Receptor Channels <i>N</i> -Methyl- <i>D</i> -Aspartate (NMDA)	196
6.21	Voltage-Gated Ion Channels.	198
6.22	K2P Channels Are Not Leaky Channels	201
	References.	202
7	Nerve Transmission	205
7.1	Introduction	205
7.2	Nernst Equation	205
7.3	Nerve Cell.	207
7.4	Resting Membrane Potential.	209
7.5	Action Potential	210
7.5.1	Refractory Period	212
7.6	Propagation of Action Potential	213
7.7	Saltatory Conduction.	213

7.8	Electrical and Chemical Synapses	214
7.9	Exocytosis of Neurotransmitter	219
	References.	222
8	Bioenergetics and Energy Transduction.	223
8.1	Bioenergetics	223
8.1.1	Difference Between ΔG and ΔG°	227
8.1.2	Energy Currency of the Cell.	228
8.2	Oxidation–Reduction Potential	228
8.3	Types of Electron Carriers	231
8.4	Oxidative Phosphorylation	234
8.4.1	Sequence of Electron Carriers in Electron Transport Chain	234
8.5	Electron Transport Complexes	237
8.5.1	Complex I	237
8.5.2	Complex II.	241
8.5.3	Complex III	242
8.5.4	Complex IV	246
8.6	Chemiosmotic Theory and Proton-Motive Force	250
8.7	ATP Synthesis	251
8.8	The Electron Transport Chain—An Overview.	255
8.9	Regulation of Oxidative Phosphorylation	257
8.9.1	The Availability of Substrates.	257
8.9.2	Proton Permeability of Membranes	259
8.9.3	Reactive Oxygen Species (ROS) Production	261
8.9.4	Apoptosis.	261
8.10	Photosynthesis	263
8.11	Light Energy	264
8.11.1	Site of Photosynthesis	268
8.12	Process of Light Reaction of Photosynthesis.	270
8.12.1	Purple Photosynthetic Bacteria	272
8.12.2	Plants	274
8.12.3	Photoreaction	277
8.12.4	Electron Transport Through PSII.	277
8.12.5	Mechanism of O_2 Evolution	279
8.12.6	The Cytochrome <i>b₆f</i> Connects PSII and PSI	280
8.12.7	Electron Transport Through PSI	282
8.12.8	Physical Arrangement Within the Thylakoid.	282
8.12.9	Cyclic Photophosphorylation	285
8.12.10	The Stoichiometry of Photophosphorylation	285
8.13	Carbon Assimilation	287
8.13.1	Phase 1: Carbon Fixation	287
8.13.2	Phase 2: Reduction	287
8.13.3	Phase 3: Formation of Hexose Sugar and Regeneration of RuBP	287

8.13.4	Alternate Pathways of Carbon Fixation in Hot, Arid Climates	289
8.13.5	Biological Adaptation to Minimize Photorespiration	289
	References.	291
9	Membrane Receptors and Signal Transduction Pathway . . .	293
9.1	Hormone Receptors.	293
9.2	G-Protein-Coupled Signaling Pathway.	293
9.3	G-Protein-Dependent Signaling Through cAMP	295
9.4	G-Protein-Coupled Receptor Kinases.	295
9.5	Tyrosine Kinase-Mediated Receptor Signaling	299
9.6	Transactivation of Epidermal Growth Factor Receptor by G-Protein Couple Receptors.	303
9.7	G-Protein-Independent Signaling.	304
9.7.1	β Arrestin-Dependent Signaling	304
9.7.2	Chemokine Receptors Signaling	309
9.8	The Janus Kinases and Signal Transducers and Activators of Transcription.	310
9.8.1	Cytokine Receptor Signaling via JAKs	311
9.8.2	Signal Transducers and Activators of Transcriptions (STATs)	312
9.9	Receptor Serine/Threonine Kinases	314
9.9.1	Serine/Threonine Kinase Signaling in T-Cell Proliferation	315
9.9.2	Serine–Threonine Kinase Pathways Regulation by Ras.	317
9.9.3	The Serine–Threonine Kinase Akt.	318
9.10	Tumor Growth Factor (TGF- β) Signaling.	319
9.11	Atrial Natriuretic Peptide Signaling.	322
9.12	Cell Adhesion Receptors	326
9.12.1	Selectins	331
9.13	Immunoglobulin Superfamily Receptors.	332
9.13.1	Major Histocompatibility Complex (MHC). . .	338
9.13.2	Surface Immunoglobulins.	342
	References.	343
10	Recycling of Membranes	345
10.1	Introduction	345
10.2	Type of Vesicle Transport	345
10.3	Clathrin-Coated Vesicles Mediated Endocytosis and Recycling of Membrane.	347
10.3.1	The Clathrin-Coated Vesicle (CCV) Cycling	347
10.3.2	Constitutive and Inducible Endocytosis by Clathrin Coating Vesicle	350
10.4	Noncoated Vesicles in Endocytosis	350
10.5	Clathrin-Independent Endocytosis (CIE).	351
10.5.1	Endocytosis by Caveolae	351

10.5.2	The Clathrin-Independent Carrier (CLIC)—GPI-Anchored Protein-Enriched Early Endosomal Compartment (GEEC) Cycling	354
10.6	Coatomer Protein (COP) Vesicles	356
10.6.1	The Coatomer Protein I (COP)I in Transport	356
10.6.2	Coatomer Protein (COP)II Vesicles in Transport	357
10.7	Internalization by the Exomer Complex	358
10.8	Recycling of Synaptic Vesicle	360
10.9	Exocytosis	361
	References	368

About the Authors

Dr. Rashmi Wardhan, Ph.D., was born in Muzaffarnagar, UP, and did her graduation in science from DAV College, Muzaffarnagar, Meerut University, and master's in Biochemistry from Govind Ballabh Pant University of Agriculture and Technology (GBPUAT), Pantnagar, UP. She was awarded doctorate in biochemistry by Meerut University, UP. At present, she is Associate Professor in Department of Biochemistry, Shivaji College, University of Delhi.

She has worked at various prestigious institutes of India like All India Institute of Medical Sciences (AIIMS), Lady Hardinge Medical College (LHMC), Kalawati Saran Children Hospital, Delhi, and LLRMC, UP. She has taught various subjects like metabolism, DNA technology, gene expression, molecular biology, and membrane biology.

She has been involved in developing the course curriculum of the various papers like molecular biology, metabolism, and DNA technology for biochemistry undergraduate students of University of Delhi. She has availed Senior Research Associateship (SRA; Pool Officer), Council of Scientific and Industrial Research (CSIR), after completing her Ph.D. She worked as honorary research associate in Department of Biochemistry, School of Biological Sciences, Flinder University, Adelaide, Australia. She worked on PKC-epsilon signaling in U937 cells during that period and at present is working on L-asparaginase as anticancer enzyme.

She is working on the second Innovation Project of University of Delhi. She has received "Best Poster Presentation Award 2016" from University of Delhi. Her teaching and research experience in diverse field of biological sciences motivated her to write this book on Membrane Biology with the aim to provide readers a new perspective for research.

Padmshree Mudgal, Ph.D., was born in Karnal, Haryana, India, did her B.Sc. (Hons) in Chemistry from Miranda House, University of Delhi, pursued her master's in Biochemistry from Postgraduate Institute of Medical Sciences, Chandigarh, and then earned her Ph.D. in Animal Biochemistry from National Dairy Research Institute, Kurukshetra University.

In 1989, she joined as a faculty member in the Department of Biochemistry, Daulat Ram College, University of Delhi, and is presently an Associate Professor in the same department. For the past 25 years, she has been actively engaged in teaching various undergraduate courses in biochemistry. Her special interest and excitement comes from teaching cell signaling, bioenergetics, and membrane biology. She has also been a member of course curriculum committee, for the designing of undergraduate courses in membrane biology and bioenergetics. She has received many awards, including the "Teaching Excellence Award for Innovation," 2014–15, by University of Delhi.

She established the Zebrafish Research Facility in the department in 2015 and is engaged in research projects using zebra fish as a toxicological and a disease model. This facility is a big draw among students and has stimulated many undergraduate students to take up small research projects using zebra fish model system. She has also conducted many workshops for science faculty of other undergraduate colleges in University of Delhi to popularize zebra fish model system as a teaching tool.

Abbreviations

ANT	Adenine nucleotide translocator
Apaf-1	Apoptotic protease activating factor-1
BChl	Bacteriochlorophyll
BNC	Binuclear center
BNP	Brain natriuretic peptide
CAM	Cell adhesion molecule
Cav	Caveolins
CD4	T helper cells
CD8	T cytotoxic cells
Chl	Chlorophyll
CIV	Complex IV
Cldn	Claudins
CMC	Critical micelle concentration
CNP	C-type natriuretic peptide
COPI, II	Coatomer protein I, II
COX	Cytochrome c oxidase
Cx	Connexins
DC	Desmosomal cadherin
DCCD	Dicyclohexylcarbodiimide
DSC	Differential Scanning Calorimeter
ER	Endoplasmic reticulum
ERES	ER exit sites
ERGIC	ER-Golgi intermediate compartment
ERQC	ER quality control compartment
ESR	Electron spin resonance
ET	Electron transfer
FAD	Flavin adenine dinucleotide
FCS	Fluorescence correlation spectroscopy
Fd	Ferredoxin
FMN	Flavin mononucleotide
FNR	Ferredoxin-NADP ⁺ oxidoreductase
FQR	Ferredoxin-plastoquinone oxidoreductase
FRAP	Fluorescence recovery after photobleaching
FRET	Fluorescence resonance energy transfer
G3P	Glyceraldehyde 3-phosphate

GC	Golgi complex
GLUT	Glucose transporter
HD	Hemidesmosome
HiPIP	High-potential iron–sulfur protein
IBM	Inner boundary membrane
IMS	Intermembrane space
INM	Inner nuclear membrane
ISP	Iron–sulfur proteins
JAM	Junctional adhesion molecules
LAMP	Lysosome-associated membrane protein
LHC	Light-harvesting complexes
LMP	Lysosomal membrane permeabilization
MAC	Mitochondrial apoptosis-induced channel
MAM	Mitochondria-associated membrane
MICOS	Mitochondrial contact site and cristae organizing system
MOM	Mitochondrial outer membrane
MOMP	Mitochondrial outer membrane permeabilization
MTOC	Microtubule organizing centers
NAD	Nicotinamide adenine dinucleotide
NADP	Nicotinamide adenine dinucleotide phosphate
NCAM	Neural cell adhesion molecules
NDH	NAD(P)H dehydrogenase
NE	Nuclear envelope
NEBD	Nuclear envelope breakdown
NP	Natriuretic peptides
NPC	Nuclear pore complex
Nup	Nucleoporin
OEC	Oxygen-evolving complex
ONM	Outer nuclear membrane
PAM	Plasma membrane-associated endoplasmic reticulum
PC	Phosphate carrier protein
PEP	Phosphoenolpyruvate
PFT	Pore-forming toxins
PGA	3-phosphoglycerate
Pheo	Pheophytin
PS	Photosystem
Q	Ubiquinone (coenzyme Q)
RC	Photosystem reaction-center
RER	Rough endoplasmic reticulum
ROS	Reactive oxygen species
RTS	Receptor tyrosine kinases
RuBP	Ribulose 1, 5-bisphosphate
SAM	Sorting and assembly machinery
SER	Smooth endoplasmic reticulum
SOD	Superoxide dismutase
SPT	Single-particle tracking
SQR	Succinate-coenzyme Q reductase
TGN	Trans-Golgi network

TIRF	Total internal reflection fluorescence
TNBS	Trinitrobenzene sulfate
TOM	Translocase of the outer membrane
UCP	Uncoupling protein
VDAC	Voltage-dependent anion-selective channel

1.1 Overview

A **biological membrane** or **biomembrane** is a selectively permeable barrier which defines a living cell or a cellular organelle. It provides a microenvironment in which a cell or individual organelle can function and maintain its identity. Biomembranes are phospholipid bilayers with associated peripheral and integral proteins and bound sugar molecules. The membrane lipid bilayer provides a fluid matrix for the proteins to function. Proteins in a fluid membrane can rotate and laterally diffuse facilitating change in protein conformation and protein–protein interactions which are required for its functioning. From simple unicellular prokaryotes to complex multicellular eukaryotes, membranes perform many important cellular functions, which include.

1.1.1 Selectively Permeable Barrier

Membranes are barriers which separate the inside and the outside of a compartment. The plasma membrane, which encloses the cell, separates the intracellular environment from the extracellular, whereas nuclear and mitochondrial membrane encloses the nucleus and mitochondria, respectively. Yet, membranes are said to be semipermeable; they selectively allow some molecules/solutes to pass through the membrane. This selective permeability is brought about by transport proteins associated with membranes which facilitate the

transport of molecules across the membrane. For a cell to survive, nutrients like sugars, amino acids are taken up by the cell and end products of metabolism are to be transported out.

1.1.2 Interaction and Communication with External Environment

Cells respond to changing external environment by binding to external signal/stimuli through cell surface membrane receptors. Binding of signal/stimuli to cell surface receptors trigger signal transduction pathways in the cell, resulting in varied responses.

1.1.3 Energy Transduction

Membranes are the site of energy transduction in cells. Cytoplasmic membrane in prokaryotes, inner membrane in mitochondria, and thylakoids in chloroplasts are the site of electron transport chain which generate electrochemical gradient across the membrane. The energy conserved in the electrochemical gradient generated during the process of electron transport is then utilized for ATP synthesis.

1.1.4 Intracellular Transport

Many solutes in the cell are transported inside the cell from one compartment to another or exocytosed outside the cell packaged in membrane

vesicles. Proteins to be secreted out of the cell or to the lysosomes are transported in vesicles from ER to Golgi apparatus and then to the targeted site. Uptake of solutes via endocytosis also involves vesicular transport. Vesicular transport of solutes is a highly regulated process which results in specific docking and targeting of solutes.

1.1.5 Transmission of Nerve Impulse

Membrane potential of most cells is ~ 70 mV due to difference in ionic concentration across the cell membrane. Neurons are excitable cells in which membrane potential can change due to change in the membrane permeability of specific ions. An action potential in a neuron is generated when a membrane is depolarized upon influx of positively charged Na^+ ions into the cell. Action potential is then propagated by opening and closing of specific ion channels, finally resulting in exocytosis of neurotransmitter at the synapse. The neurotransmitter released at synapse binds to a receptor at postsynaptic membrane, hence transmitting the nerve impulse across the synapse to the next connecting neuron.

1.1.6 Cell–Cell Interaction

Cells organize to form tissues, and tissues form organs. Cell–cell interactions are fundamental to the development of tissues and organs. Cell–cell interactions adhere to cells in tissues mediated mainly by a group of cell adhesion molecules (CAMs). Cells also communicate with neighboring cells through these interactions. Hence, cell–cell interactions modulate cell growth, differentiation and ultimately the cellular function.

Transient interactions between cells during immune response result in chemotaxis of leukocytes to the site of injury.

Loss of cell–cell interaction can cause cancer. In normal cells, contact inhibition mediated by cadherins results in growth inhibition. Uncontrolled growth results in the absence of this inhibition.

1.2 Historical Background

The term “cell” was first coined in 1665 by Robert Hooke. Hooke observed thin slices of cork under a compound microscope. He saw empty spaces or pores demarcated by walls which could be compared to honey combs. These boxes of cells were in fact the plant cell wall of cork tissue surrounding the inner empty space or the protoplasm. Inspired by Robert Hooke, Anton van Leeuwenhoek (1632–1723), also known as the “Father of Microbiology,” designed more refined simple microscope and observed for the first time, bacteria, protozoa, and animal cells. By the nineteenth century it became clear that a semipermeable barrier separated the inside and outside of the cell. De Vries, 1884, found that plant cell was permeable to water but not to large polar molecules like sucrose. Pfeffer, a botanist considered to be the father of membrane theory, in 1899 for the first time proposed the idea that a thin layer called the plasma membrane separated the protoplasm of the cell from the outside. Charles Ernest Overton, 1895–1899 (distant cousin of Charles Darwin) found a relationship between permeability of molecules across membranes to their partition coefficient between water and oil. He proposed that cell membranes are similar to lipids like olive oil, and molecules pass through the membrane by dissolving in the hydrophobic interior of the membrane. He for the first time showed that cholesterol and phospholipids were the major components of cell membranes even though little was known about their cellular functions and proposed the concept of lipid (oil) plasma membrane.

Irving Langmuir (1917) studied the nature of oil films on water surface using Langmuir trough, a device made of Teflon trough partially filled with water with a movable barrier at one end. He observed that when amphiphilic lipid molecules dissolved in volatile solvent are dropped on water surface a thin monolayer film is formed on the surface with hydrophobic hydrocarbon chains of lipids oriented toward the air, away from water and hydrophilic polar head groups remaining in contact with water. He studied the relationship

between surface pressure and surface areas occupied for different lipids/oils by using a movable barrier block to compress the monolayer surface (Fig. 1.1).

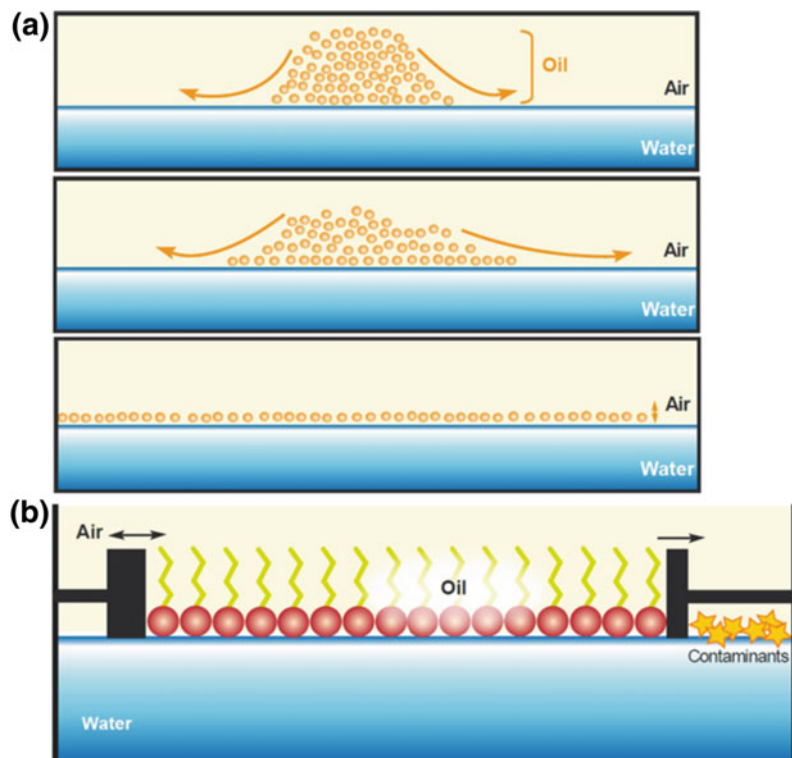
Gorter and Grendel (1925) performed the classic experiment using Langmuir trough. The erythrocyte membrane lipids were extracted with acetone and then dropped on the water surface in the Langmuir trough. Measurement of surface area using movable barrier revealed that the surface area of the monofilm formed was almost two times the surface area of the erythrocyte cell. The only possible explanation could be that cell membranes are made up of bilayers, formed by two lipid monolayers with hydrophobic chains of each monolayer pointed toward the inside of the bilayer and hydrophilic polar head groups pointing outside interacting with the aqueous environment. Hence, Gorter and Grendel experiment gave the first lipid bilayer structural model for membranes (Fig. 1.2).

Though Gorter and Grendel model gave the molecular description of cell membrane

structure, it failed to account for the manifold functions attributed to the cell membrane. Davson and Danielli (1935), a decade later, proposed a membrane model with both lipids and proteins. Their “sandwich” model proposed that the lipid bilayer was sandwiched between two layers of globular proteins on either side. The proteins absorbed to the lipophilic layers contained water-containing outer regions and hydrophobic interiors. These water-containing regions of polar layers were permeable for charged ions (Fig. 1.3).

By the early twentieth century, it was known that the interior of the cell and its extracellular environment varied in their concentration of ions like Na^+ and K^+ . In 1910, Donnan showed that this asymmetric distribution of ions across the membrane resulted from the differences in the permeability of different ions in the membrane. In 1952, Hodgkin and Huxley established that the flow of Na^+ into the cell and flow of K^+ out of the cell resulted in depolarization and hyperpolarization in axon membranes. This discovery

Fig. 1.1 Oil at air/water interfaces. **a** Oil molecules spontaneously spread on the air/water interface until they form a layer one molecule thick. **b** The Langmuir trough allows to precisely measure the surface that these monolayers can spread depending on the applied pressure. *Source* Lombard (2014)



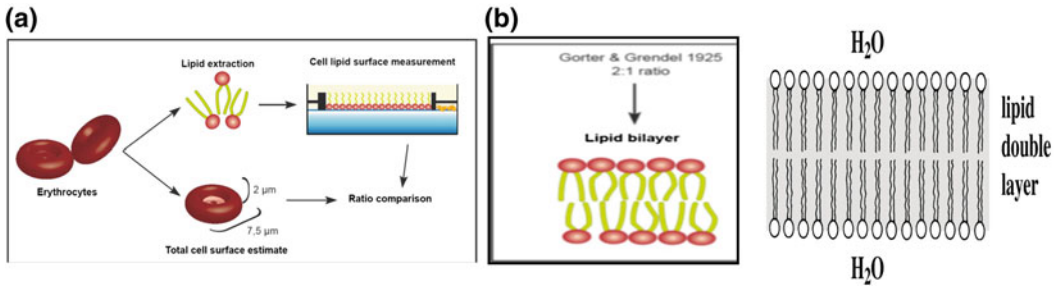


Fig. 1.2 Lipid bilayer model of Gorter and Grendel **a** Lipids extracted from erythrocytes were dropped on the surface of Langmuir trough and minimum

surface area occupied **b** Surface area occupied by extracted lipids to the erythrocyte surface area was found to be 2:1 *Source* Lombard (2014)

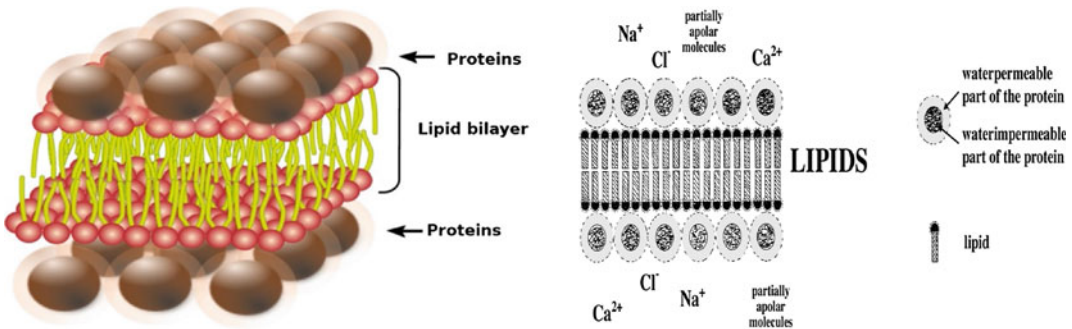


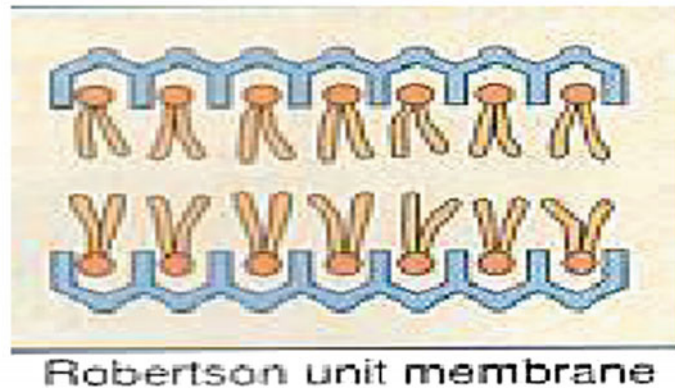
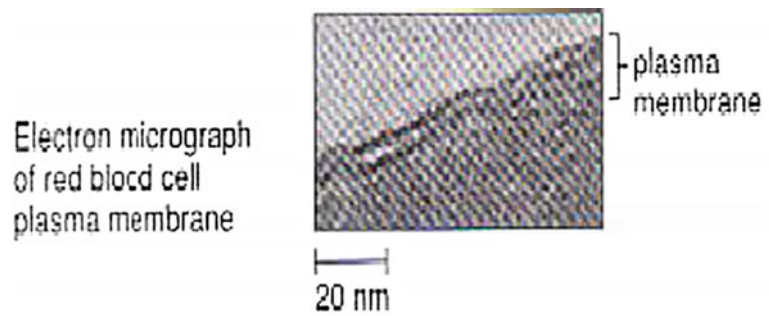
Fig. 1.3 Davson and Danielli membrane model

made excitable tissues a very popular model for the study of active transport of ions. Interest was also generated in the transport of nonelectrolytes across the membranes. It was known that the intestines absorbed some sugar molecules more readily than others. Studies on transporter kinetics revealed saturable kinetics and inhibition by certain molecules. A new transporter hypothesis emerged, suggesting a connection between transporters and enzymes.

Advancement and better resolution in electron microscopy in the 1950s allowed for the first time direct observation of cell membranes. In 1959, J.D. Robertson proposed a modified model based on the electron microscope studies. Transmission electron micrographs showed a “trilaminar” appearance consisting of lighter inner region sandwiched between two darker outer lines, similar to a railroad track (Fig. 1.4). According to Robertson’s “**unit membrane model**,” the two outer dark lines were the protein layers and inner region was the lipid bilayer.

Electron microscopy for the first time revealed the morphological feature at the surface of cells. In potassium permanganate-fixed preparations, this feature is seen as two narrow, dense lines separated by a band of similar width but of low density, the overall width of the unit being of the order of 75 Å. X-ray diffraction studies of the nerve myelin sheath provided further confirmation of membrane bilayer structure. Myelin sheath is an insulating covering of layers of membranes around the nerve axon, which originate from a part of Schwann cell membrane in the peripheral nervous system (PNS) and the oligodendroglial cell membrane in the central nervous system (CNS) (Fig. 1.5). The resulting structure comprises of tightly packed membrane layers of uniform thickness (Fig. 1.6). As X-ray diffraction studies require repetitive structures like in a crystal, multilayered myelin sheaths offered considerable advantage in membrane structure studies. X-ray diffraction electron density plots of the repeating unit of myelin show

Fig. 1.4 Robertson's unit membrane model is based on the electron micrographs of red cell membrane showing trilamellar appearance with two dark lines enclosing lighter inner region. The outer dark lines represent the protein layers and the inner lighter region the lipid bilayer



three peaks which correspond to protein plus lipid polar groups and two troughs which correspond to lipid hydrocarbon chains (Fig. 1.7). In myelin lipid layers, the electron densities associated with the hydrophobic (hydrocarbon) regions would be expected to be relatively low, while the phosphate groups of the phospholipid molecules provide the highest electron densities occurring in this structure. So both electron microscopy and X-ray diffraction studies confirmed the lipid bilayer structure in early 1960s, but still the structural placement of membrane proteins was not clear yet.

Preparation of first lipid bilayers by Mueller and his group in the 1960s, and then preparation of liposomes by Bangham in 1965, provided biologists a tool to study structure and function of membranes. The freeze-etching electron microscopy technique, also known as freeze-fracture technique refined by Moor and Mühlethaller in 1963, for the first time made the interior of the membrane visible (Fig. 1.8). The freeze-fracture technique involves rapid freezing

of cells in liquid nitrogen, fractioning of specimen with a sharp knife, sublimation of surface ice under vacuum (freeze etching), making a platinum/carbon replica of the exposed surface and then imaging by scanning electron microscopy (SEM) or transmission electron microscopy (TEM).

Fracturing can split the membrane along the middle of the bilayer, separating the two halves of the bilayer. Globular proteins protruding out from one-half of the bilayer (seen as bumps) leave a depression in the other half. This technique for the first time showed that proteins are embedded in the membrane lipid bilayers.

Another giant step forward was made by Frye and Edidin in 1970 when they fused human and mouse cell using Sendai virus to monitor the fate of their respective membrane components (Fig. 1.9). Surface antigens of each cell were labeled with a different fluorescent color-labeled antibody, whose movements could be monitored under fluorescent microscope. Human cell surface proteins were labeled with red rhodamine-labeled

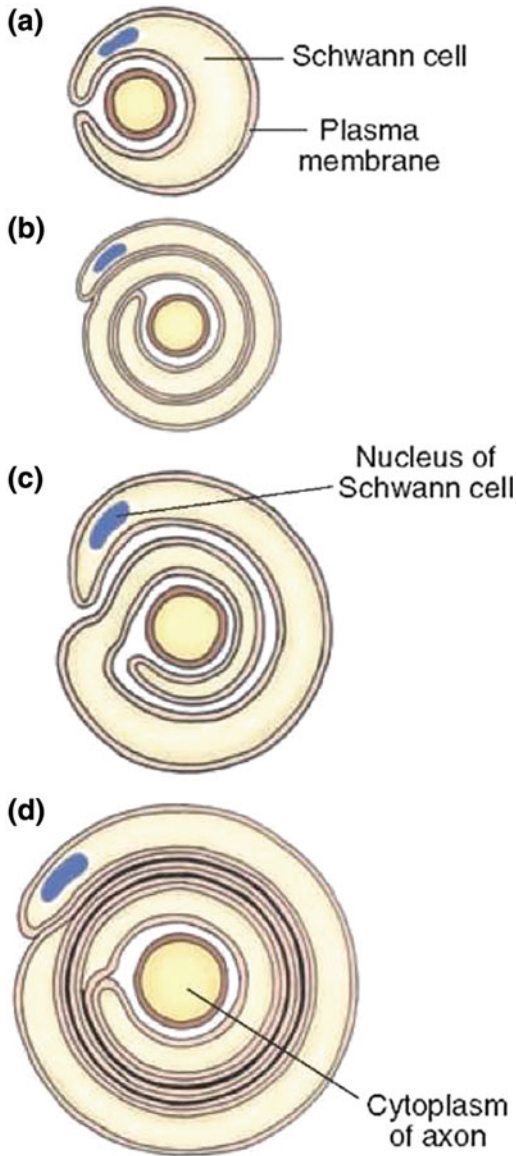


Fig. 1.5 Formation of myelin from concentric layering of Schwann cell membrane on the axon surface: **a** Schwann cell envelops the axon. **b, c** Schwann cell then rotates around the axon. **d** The successive wrappings of Schwann cell membranes around the axon form the myelin sheath

antibodies, whereas mouse cell surface proteins were labeled with green fluorescein-labeled antibodies. As cells fuse to form a heterokaryon, the two separate red and green halves progressively intermix and redistribute resulting in the whole surface appearing brown. This experiment for the



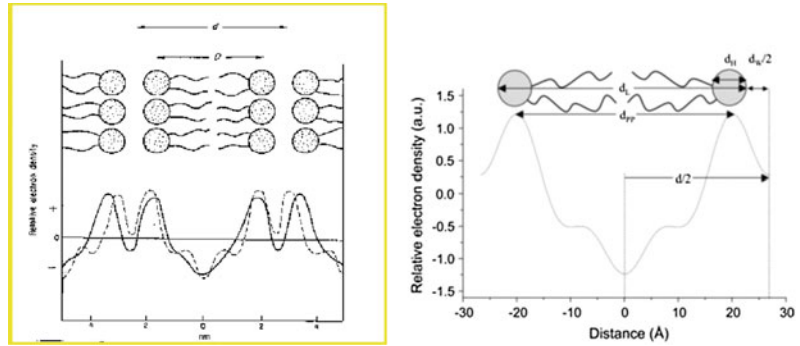
Fig. 1.6 An electron micrograph showing a cross section of myelinated nerve fiber in a potassium permanganate-fixed preparation of human cutaneous nerve

first time proved that membrane components freely diffuse in the membrane plane.

The 1960s also saw a lot of significant development on membrane proteins. Freeze-fracture technique introduced the concept of transmembrane proteins, and Frye and Edidin's fusion experiment provided evidence that proteins are free to move in fluid membranes. The above developments laid the foundation for Singer and Nicolson's (1972) "**fluid mosaic membrane model**" (Fig. 1.10). According to this model, lipid bilayer forms a fluid matrix in which globular proteins float. The proteins either associated with the membrane peripherally or spanning through the membrane appear as a mosaic in lipid matrix. Even after 45 years, this model still remains relevant and is able to explain most biological processes and phenomena.

One of the early landmarks in membrane protein structure was the resolution of the first three-dimensional structure of a transmembrane protein. R. Henderson and P.N.T. Unwin in 1975 (Fig. 1.11) studied the purple membrane of

Fig. 1.7 Electron density curves derived from the low-angle diffraction patterns of myelin in nerve tissue



Halobacterium halobium by electron microscopy and obtained a three-dimensional map of the membrane at 7 Å resolution. They found that the bacteriorhodopsin protein in purple bacterial membrane contains seven closely packed membrane spanning α helices arranged perpendicular to the plane of the membrane. The spaces between the protein molecules were filled by lipids in bilayer. Later, the development of the patch-clamp technique by Neher and Sakmann in 1976 allowed the study and understanding of movement of ions across ion channels.

1.3 Composition of Biological Membranes

Major constituents of biological membranes are lipids, protein, and a little percentage of carbohydrates. While lipids form the structural backbone of the membrane bilayer, proteins are the functional components of the membrane. Carbohydrates are mainly present as covalently linked to either protein or lipid as glycoproteins or glycolipids. Proteins, lipids, and carbohydrates are present in different proportions in different biological membranes (Table 1.1). While plasma membrane of most eukaryotic cells contains equal proportion of lipids and proteins ($\sim 30\text{--}40\%$ by wt.), myelin sheath, a derivative of glial cell

plasma membrane, is much richer in lipids ($\sim 80\%$ by wt.) as compared to proteins ($\sim 20\%$ by wt.). At the other extreme inner membrane of mitochondria/chloroplast and plasma membrane of many bacteria have higher proportion of proteins ($>70\%$ by wt.). This variation in membrane composition is a reflection of diverse biological functions of membranes. The inner membrane of mitochondria or chloroplast contains big protein complexes involved in electron transport and hence, has larger percentage of proteins as compared to other membranes. Bacterial cytoplasmic membranes are also the site of respiration and hence have high protein content in membranes. On the other hand, myelin sheath which provides electric insulation for the nerve axon it encloses comprises of multiple membrane layers rich in lipid and minimal protein (Fig. 1.12).

Membrane carbohydrates are found mainly linked to proteins and lipids as glycoproteins or glycolipids on the extracellular side of the plasma membrane of eukaryotic cells. They are almost negligible in inner mitochondrial membrane, the chloroplast lamellae, and other intracellular membranes. The major sugars found in these glycoconjugates include glucose, galactose, mannose, fucose, *N*-acetyl galactosamine, and *N*-acetyl glucosamine. Glycolipids are present in prokaryotic membranes as lipopolysaccharides, but glycoproteins are totally absent.

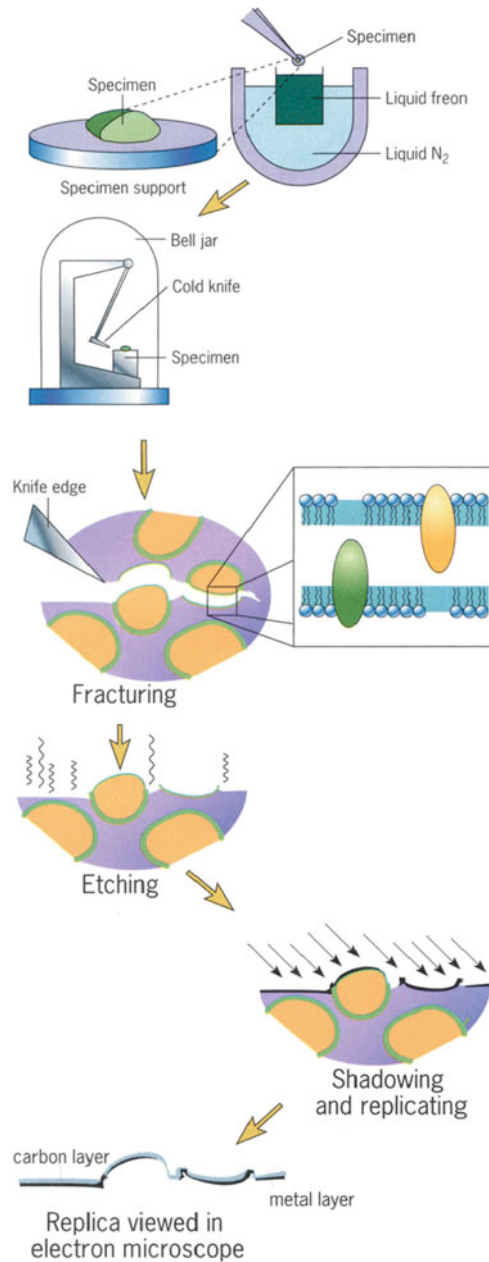


Fig. 1.8 Freeze-etching technique. In **freeze fracture technique**, the cell or tissue is quickly frozen in liquid nitrogen at $-196\text{ }^{\circ}\text{C}$, which instantly immobilizes cell components without forming ice crystals. The block of frozen cells is fractured with a sharp blow, occasionally separating the two leaflet along the fracture surface. Membrane proteins are bound to one or the other leaflet. Next the specimen is placed in vacuum and the surface

ice is removed by sublimation. Thin layer of carbon is then evaporated vertically on to the surface to produce carbon replica. Then a thin layer of platinum is deposited at an angle to the exposed surface to produce a shadow effect. The organic material removed by acid, leaving the carbon metal replica of the tissue ready for examination with electron microscope

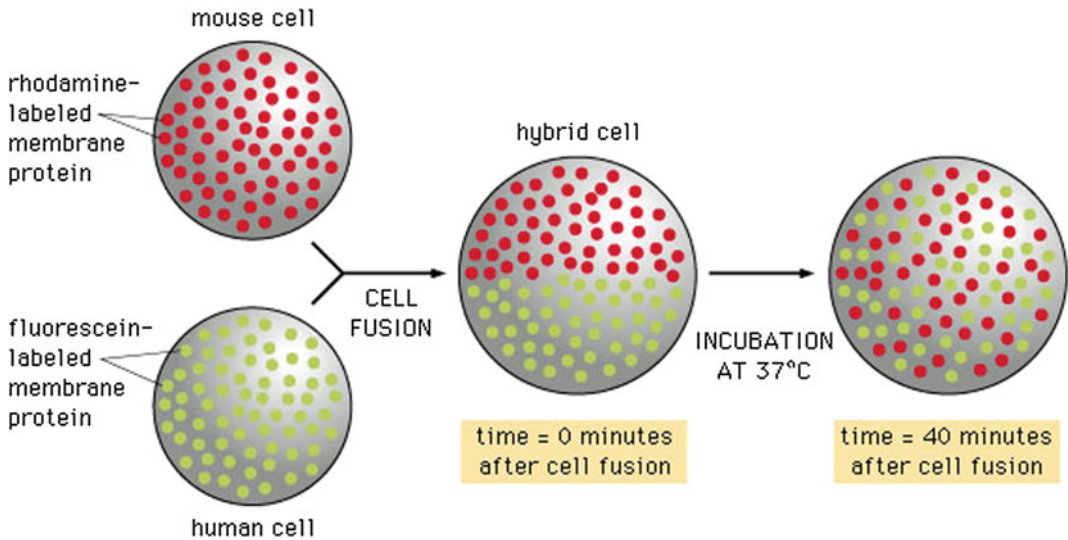


Fig. 1.9 Frye and Edidin cell fusion experiment

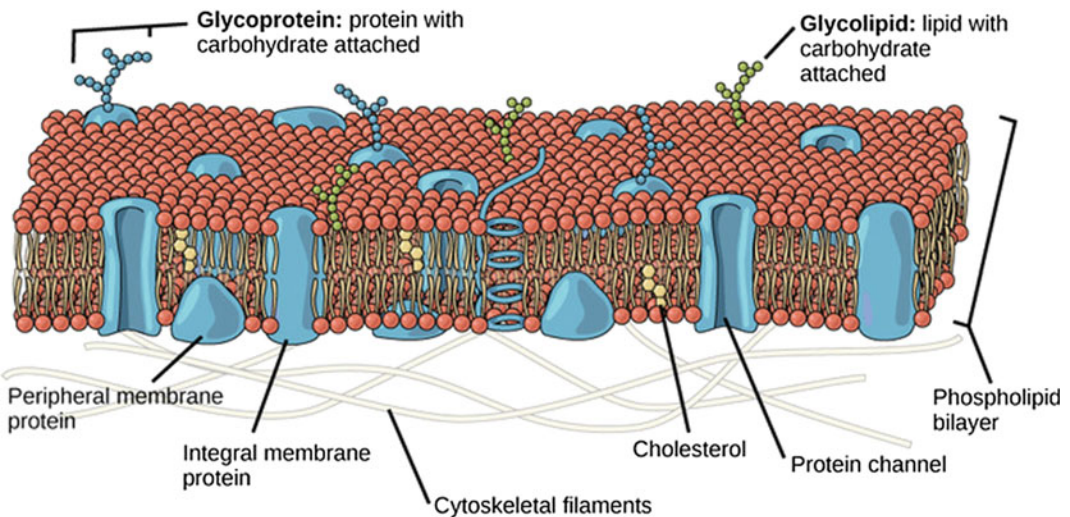


Fig. 1.10 Fluid mosaic model

1.3.1 Membrane Lipids

Lipids form the matrix of cellular membranes, which act as a barrier separating external environment from the internal environment of the cell. The lipids also provide the right physical and chemical environment for the membrane

protein to function. Apart from structural role, lipids in membranes also play important role in signaling, biosynthesis of other molecules, anchoring of proteins, and enzyme regulation. The membrane lipids are amphipathic in nature consisting of a hydrophobic and a hydrophilic polar head groups (Fig. 1.13).

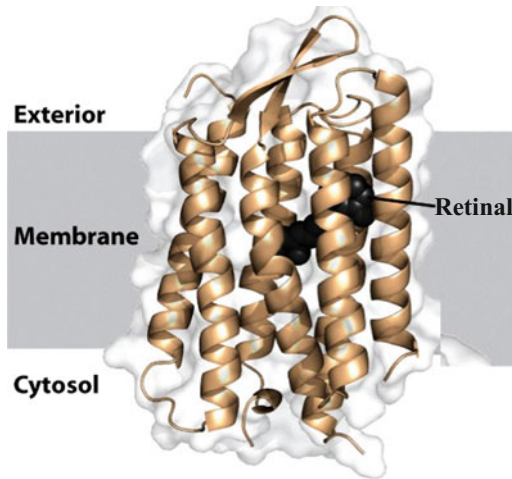


Fig. 1.11 Bacteriorhodopsin: seven transmembrane alpha-helical model

Membranes consist majorly of three classes of lipids: phospholipids, glycolipids, and sterols (Fig. 1.14).

1.3.2 Phospholipids

Phospholipids are the most abundant lipids in membranes. Major phospholipids are glycerol-based phospholipids known as phosphoglycerides. The glycerol backbone of most phosphoglycerides has the phosphate group attached at one end (L-glycerol 3-phosphate, D-

glycerol 1-phosphate, or *sn*-3 position) (Fig. 1.15). The 1- and 2-position of *sn*-glycerol is esterified with long-chain fatty acids to form 1,2-diacyl phosphoglycerides (Fig. 1.16). The two fatty acyl chains may vary in their length and degree of unsaturation. Most glycerophospholipids have saturated C₁₆ or C₁₈ fatty acid at C1 position and *cis*-unsaturated fatty acid, most commonly 18:1, 18:2, 18:3, and 20:4 linked at C2 position. Polyunsaturated chains are generally not conjugated. The phosphate group attached at *sn*-3 position of the glycerol is in turn esterified to -OH of different polar head groups forming the various phosphoglycerol lipids namely, choline (phosphatidylcholine, PC), ethanolamine (phosphatidylethanolamine, PE), serine (phosphatidylserine, PS), inositol (phosphatidylinositol, PI), glycerol (phosphatidylglycerol PG), etc. (Fig. 1.17a).

Phosphatidylcholine (PC), phosphatidylethanolamine (PE), phosphatidylserine (PS), phosphatidylinositol (PI), and phosphatidic acid (PA) are the major structural glycerophospholipids in eukaryotic membranes. Their hydrophobic portion is a diacylglycerol (DAG), which contains saturated or *cis*-unsaturated fatty acyl chains of varying lengths (Fig. 1.17b). PC accounts for >50% of the phospholipids in most eukaryotic membranes. It self-associates spontaneously to form a planar bilayer in which each PC molecule has a nearly cylindrical geometry. PE molecule has a conical geometry because of the relatively small

Table 1.1 Proportions of lipids, proteins, and carbohydrates in different biological membranes (% by wt.)

Membranes	Lipids	Proteins	Carbohydrates
<i>Plasma membrane</i>			
Human RBC	43	49	8
<i>E. coli</i>	25	75	–
Hepatocyte	36	54	10
Myelin	79	18	3
Amoeba	42	54	4
<i>Mitochondria</i>			
Outer membrane	45	55	–
Inner membrane	22	78	–
<i>Chloroplast (spinach)</i>			
Lamellae	30	70	–

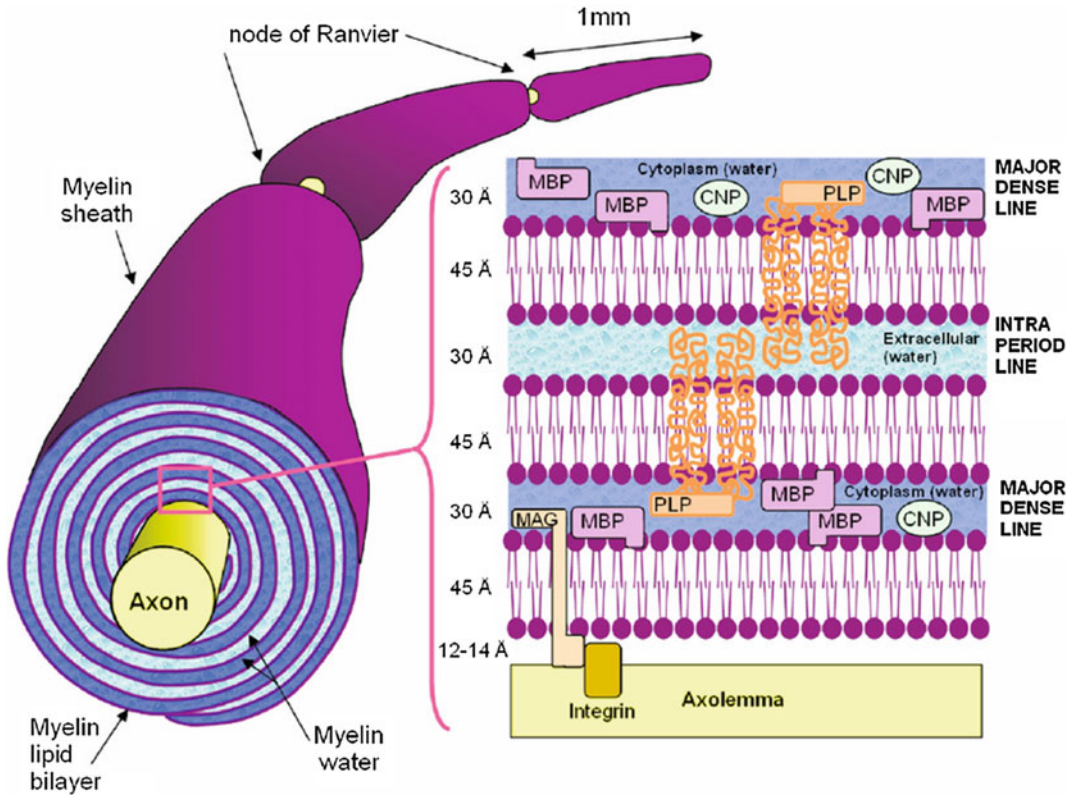


Fig. 1.12 CNS myelin sheath surrounding an axon with inset depicting close up of bilayer, including myelin basic protein (MBP), proteolipid protein (PLP), cyclic nucleotide phosphodiesterase (CNP), and myelin-associated glycoprotein (MAG). *Source* Laule et al. (2007)

Fig. 1.13 Amphipathic membrane lipids associated to form membranes

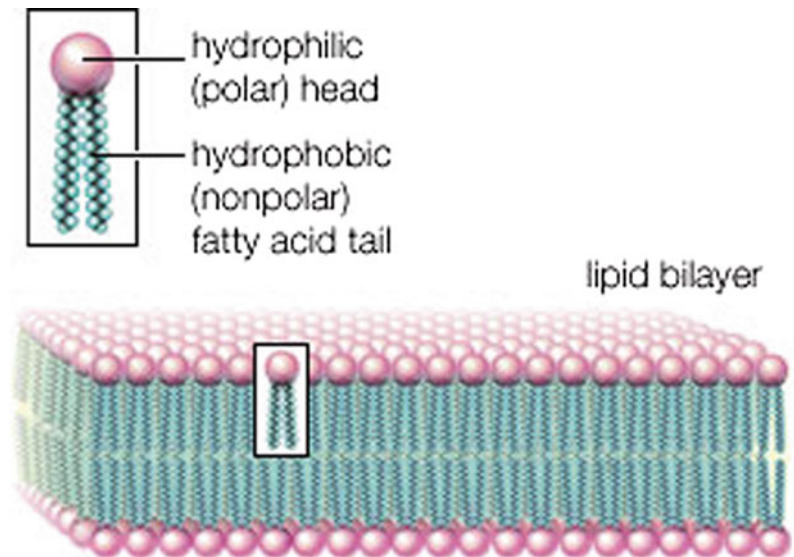


Fig. 1.14 Classification of membrane lipids

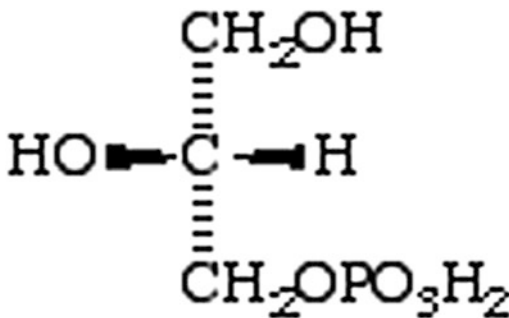
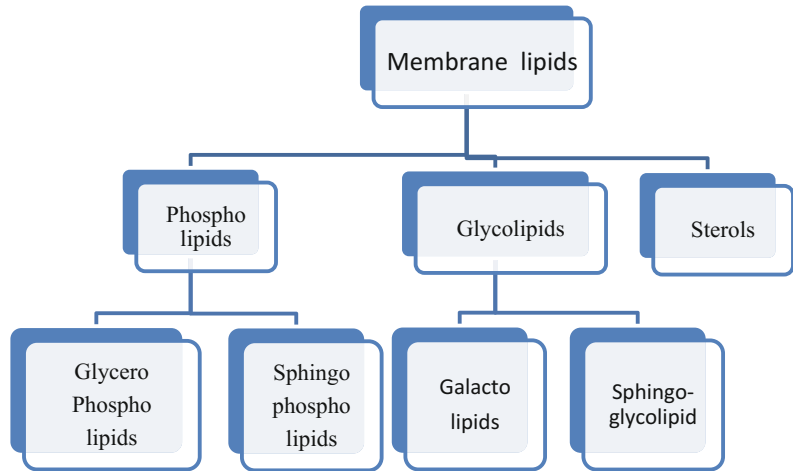


Fig. 1.15 *sn*-glycerol 3-phosphate

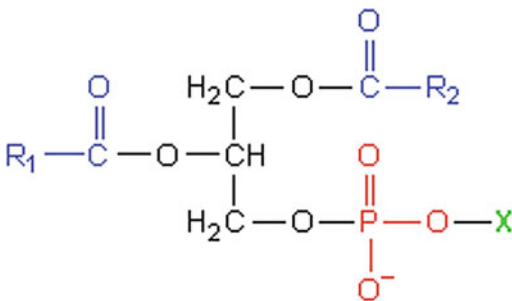


Fig. 1.16 1,2-diacylphosphoglycerides

size of its polar head group. The inclusion of PE in PC-rich bilayers imposes a curvature stress onto the membrane, which is useful for the process of budding, fission, and fusion.

Some rarer phosphoglycerides are found only in some specific membranes in nature. In *archaeobacteria*, for example, the stereo configuration of

glycerophospholipids is reversed, with phosphate attached to *sn*-1 position of glycerol. **Cardiolipids** or diphosphatidylglycerols (Fig. 1.18) are major components of mitochondrial inner membrane, chloroplast membrane, and some bacterial membrane. Cardiolipin (CL) may be used to accommodate membrane proteins and modulate their activities in these membranes. They are rare in other eukaryotic membranes, giving credence to the theory that the mitochondria and chloroplast have evolved from bacteria. **Plasmalogens** (Fig. 1.19), a group of phosphoglycerides, have a long hydrocarbon chain linked to *sn*-1 position via ether linkage. Ethanolamine plasmalogens are an important component of myelin and cardiac sarcoplasmic reticulum. Platelet-activating factor (PAF) has a long ether-linked alkyl chain at C-1 of glycerol, C-2 ester linked to acetic acid, and choline as the polar head group.

Another class of phospholipids, the **Sphingolipids** are derived from long-chain C18 amino alcohol, shingosine. When a fatty acid is attached in amide linkage to the $-NH_2$ on C2, it forms a ceramide, which is structurally similar to a diacyl glycerol. **Sphingomyelins**, the phosphosphingolipids have the polar head groups, phosphocholine, or phosphoethanolamine groups attached to $-OH$ at C1 of ceramide (Fig. 1.20). Sphingolipids have saturated (or *trans*-unsaturated) tails so are able to form taller and narrower cylinders than PtdCh lipids of the same chain length and pack more tightly, adopting the solid “gel”-like phase.

(a)

Name of glycerophospholipid	Name of X	Formula of X	Net charge (at pH 7)
Phosphatidic acid	—	—H	-1
Phosphatidylethanolamine	Ethanolamine	$-\text{CH}_2-\text{CH}_2-\text{NH}_2$	0
Phosphatidylcholine	Choline	$-\text{CH}_2-\text{CH}_2-\text{N}(\text{CH}_3)_3$	0
Phosphatidylserine	Serine	$-\text{CH}_2-\text{CH}(\text{NH}_2)\text{COO}^-$	-1
Phosphatidylglycerol	Glycerol	$-\text{CH}_2-\text{CH}(\text{OH})-\text{CH}_2-\text{OH}$	-1
Phosphatidylinositol 4,5-bisphosphate	myo-Inositol 4,5-bisphosphate		-4
Cardiolipin	Phosphatidylglycerol		-2

(b)

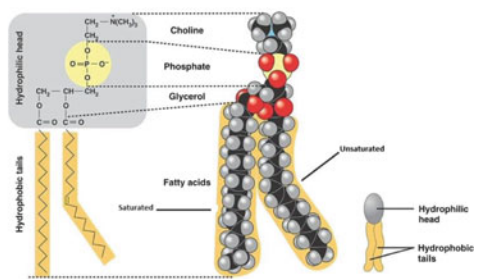


Fig. 1.17 a Phospho glycerolipids in membranes. b The hydrophobic and hydrophilic portion of phosphatidyl choline

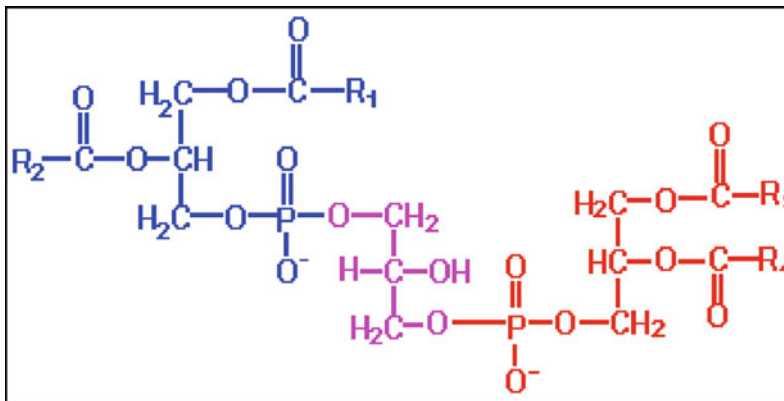


Fig. 1.18 Diphosphatidylglycerol (DPG) or cardiolipin

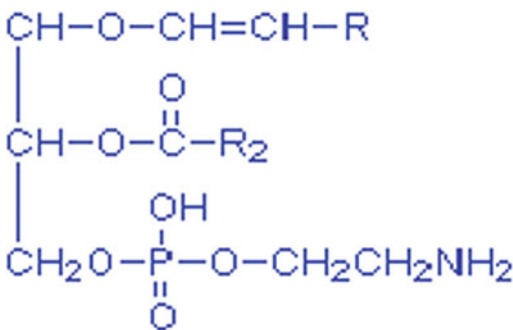


Fig. 1.19 Plasmalogen

Different signaling pathways activate hydrolysis of different glycerolipids and sphingolipids to produce a battery of lipids with second messenger roles; these messenger lipids include lysoPC (LPC), lysoPA (LPA), PA and DAG, IP₃, sphingosylphosphorylcholine (SPC), sphingosine (Sph), sphingosine-1-phosphate (S1P), ceramide-1-phosphate (C1P), and Cer. Messengers like LPC, LPA, SPC, Sph, S1P, and IP₃ are released from the membrane to mediate their action; in contrast, PA, DAG, C1P, and Cer remain in the

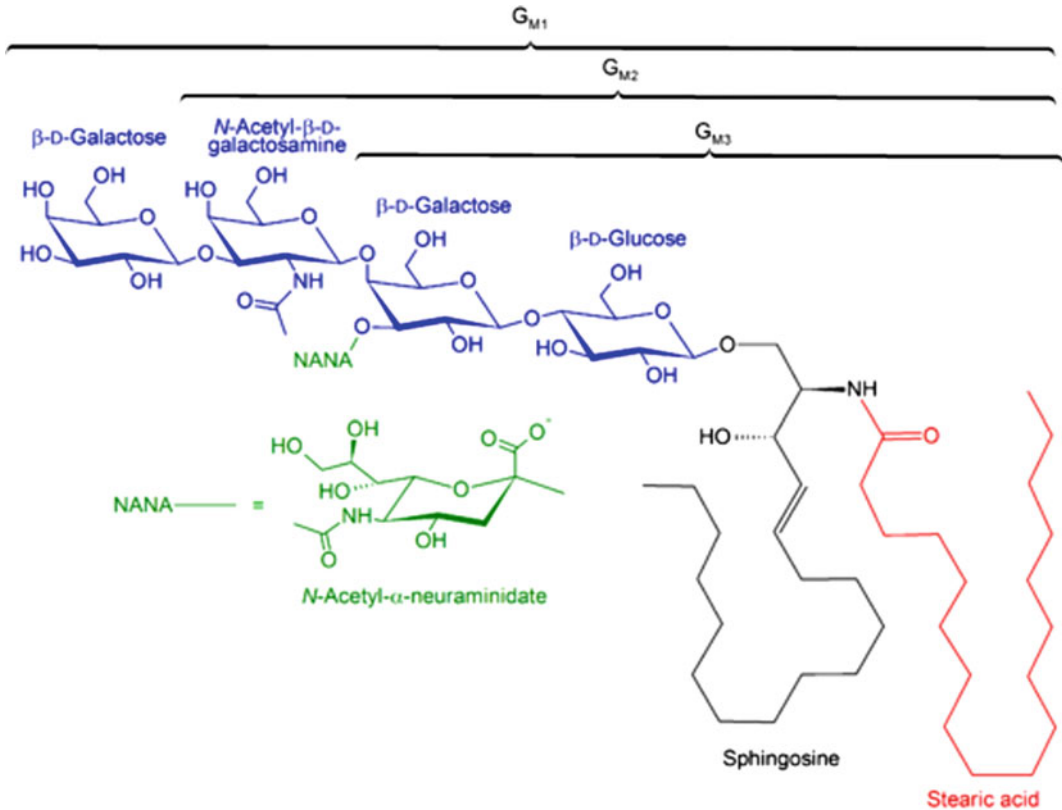


Fig. 1.21 Structure of GM1, GM2, GM3 ganglioside

steroid nucleus of cholesterol is almost planar and relatively rigid, consisting of four fused rings forming the hydrophobic core. The C-3 hydroxyl group forms the polar head group which can be esterified with long-chain fatty acids to form cholesteryl esters. Prokaryotes contain little or no cholesterol in their membranes. Plant membranes have other sterols like sitosterol and stigmasterol, which have an additional side chain at position C-24 and/or a double bond at C-22 position. Ergosterol is found in yeast and other eukaryotic microorganisms (Fig. 1.22).

Lipid composition of different membranes from different types of cells and even different organelles from each cell type distinctly varies from each other determined by the stage of the cell cycle as well as environmental factors (Table 1.2). This unique lipid composition of membranes is a characteristic of its type and also a reflection of its functional specialization.

1.4 Unique Lipid Composition of Cell Organelle Membranes

Cell organelle membranes vary in their lipid composition. The site of structural lipid synthesis and their local lipid metabolism and turnover determine the unique composition of membranes.

The endoplasmic reticulum (ER) is the main site of synthesis of most structural phospholipids and cholesterol (Fig. 1.23). Phosphatidylcholine (PC) constitutes more than 50% of ER membrane lipids and phosphatidyl ethanolamine 20%, and phosphatidyl serine and phosphatidyl inositol together constitute $\sim 14\%$. Lipids like cholesterol after being synthesized in the ER are rapidly transported to other organelles, as ER has extremely low concentrations of sterols. High fluidity of ER membranes and presence of many transporters facilitate the transport of newly

Sterols

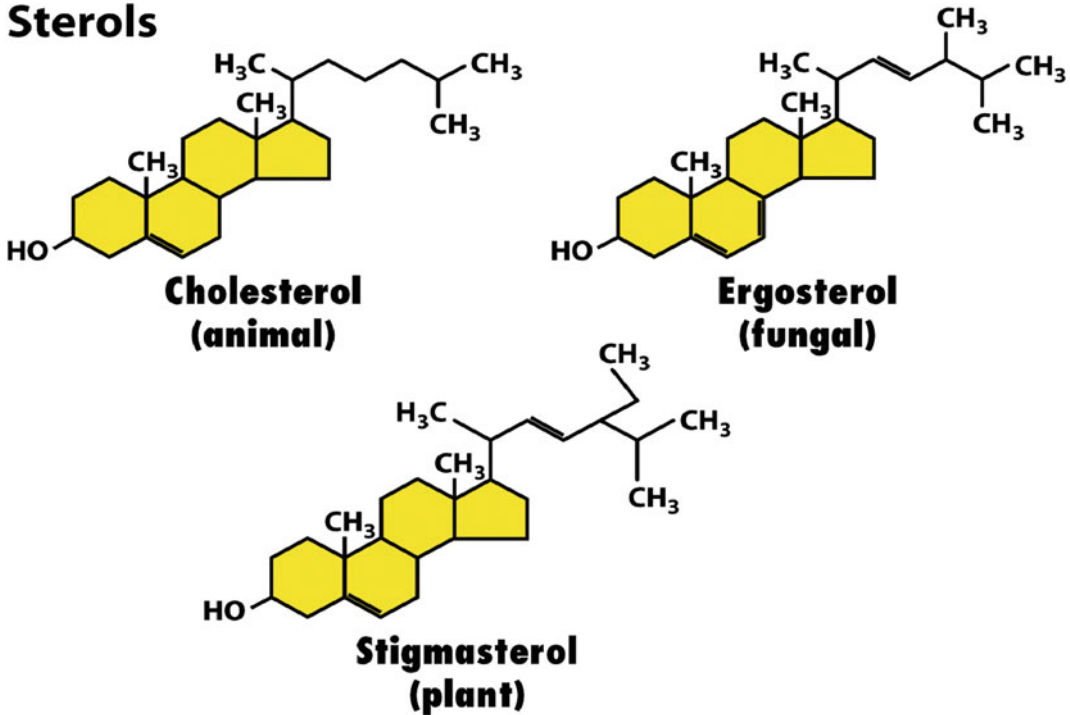


Fig. 1.22 Sterols

synthesized lipids and proteins to other destinations. The ER also has minor lipids that function as intermediates and precursors in many biosynthetic pathways (including ceramide, DAG, CDP-DAG, PA, lysophospholipids) and dolichol.

Golgi complex is another site where significant levels of lipids are synthesized. Sphingolipids are the major lipids synthesized in the mammalian Golgi complex, especially, sphingomyelin (SM), GlcCer, lactosylceramide (LacCer), and higher-order glycosphingolipids (GSLs). These lipids are primarily destined for

export to the plasma membrane, which are richer in sphingolipids than other organelle membranes.

Plasma membrane lipid composition varies with species and cell type, yet on an average, is rich in phosphatidylcholine (PC), phosphatidylethanolamine (PE), cholesterol, and sphingolipids (Fig. 1.23). High percentages of sterols and sphingolipids make the plasma membrane less fluid to resist mechanical stress and increase its stability. Though no lipid synthesis takes place in plasma membrane, turnover of lipid occurs to release signaling molecules and resynthesize membrane lipids from intermediates.

Table 1.2 Lipid composition of cell membranes (lipid %)

Source	Chl	PC	SM	PE	PI	PS	PG	DPG	PA	GL
<i>Rat liver</i>										
Cytoplasmic membrane	30	18	14	11	4	9	–	–	1	–
Rough ER	6	55	3	16	8	3	–	–	–	–
Smooth ER	10	55	12	21	7	–	–	2	–	–
Mitochondria (inner)	3	45	2.5	25	6	1	2	18	0.7	–
Mitochondria (outer)	5	50	5	23	13	2	2.5	3.5	1.3	–
Nuclear membrane	10	55	3	20	7	3	–	–	1	–
Golgi	7.5	40	10	15	6	3.5	–	–	–	–
Lysosomes	14.0	25	24	13	7	–	–	5	–	–
<i>Rat brain</i>										
Myelin	22	11	6	14	–	7	–	–	–	21
Synaptosome	20	24	3.5	20	2	8	–	–	1	–
Rat erythrocyte	24	31	8.5	15	2.2	7	–	–	0.1	3
Rat rod cell (outer segment)	3	41	–	37	2	13	–	–	–	–
<i>E. coli</i> cytoplasmic membrane	0	0	–	80	–	–	15	5	–	–

Chl Cholesterol, *PC* phosphatidylcholine, *SM* sphingomyelin, *PE* phosphatidylethanolamine, *PI* phosphatidylinositol, *PS* phosphatidylserine, *PG* phosphatidylglycerol, *DPG* diphosphatidylglycerol, *PA* phosphatidic acid, *GL* glycolipid

Early endosomes, which pinch off from plasma membrane, are similar to plasma membranes in composition. Early endosomal membranes are also rich in cholesterol, but differ from plasma membrane in their phosphoinositide composition. Plasma membranes are richer in PI (4,5)P₂ and PI(3,4,5)P₃, whereas early endosomes are rich in PI(3)P. A set of kinases and phosphatases play a role in phosphoinositide turnover. Phosphoinositides play an important role in vesicular trafficking. As early endosomes mature to late endosomes, percentage of cholesterol decreases and it becomes rich in a unique phospholipid, lysobisphosphatidic acid (LBPA) also known as bis(monoacylglycero)phosphate (BMP), which is found exclusively in late endosomal membranes. Lysobisphosphatidic acid is found to have a role in multivesicular body generation and fusion processes.

Mitochondria have two membranes, the outer and inner mitochondrial membrane, each distinct in composition from each other. As other organelle membranes, mitochondrial membranes are rich in PC (~40%), PE (~30%) and have low

levels of cholesterol and sphingolipids, but they also have exclusive lipids like phosphatidylglycerol (PG) and cardiolipin (CL). Considerable level of lipid synthesis also occurs in the mitochondria. Cardiolipin, which is synthesized from phosphatidylglycerol (PG), contains three glycerol backbones and four fatty acyl chains and plays an important role in maintaining the structural and functional integrity of the respiratory proteins of inner membrane of mitochondria. Mitochondria are also the source of PE, which is produced by decarboxylation of PS (by a separate pathway from those in the ER), which is then exported to other organelles.

1.5 Transbilayer Lipid Asymmetry

Lipids are asymmetrically distributed over the two leaflets of the membrane bilayer. The choline-containing lipids, phosphatidylcholine (PC) and sphingomyelin (SM), are enriched primarily on the external leaflet of the plasma membrane and correspondingly in the luminal side of the cellular

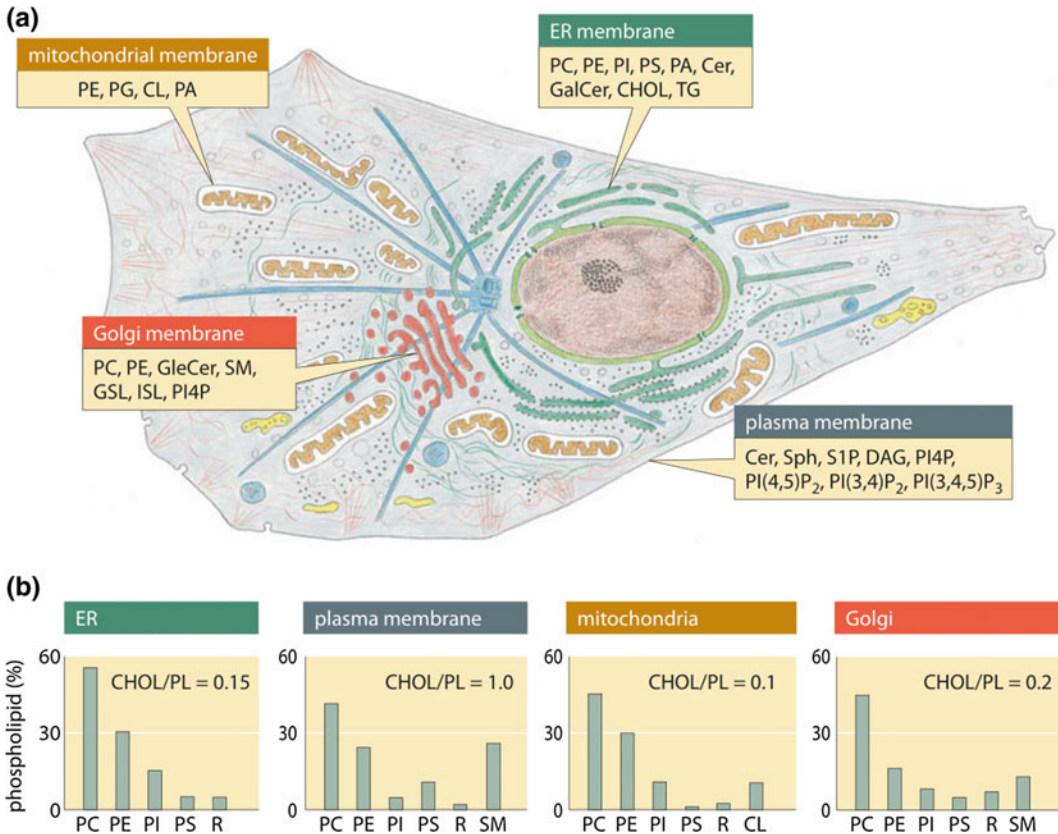


Fig. 1.23 Lipid synthesis and steady-state composition of cell organelle membranes. Lipid production is spread across several organelles. The top panel shows the site of synthesis for the major lipid. The main organelle for lipid biosynthesis is the endoplasmic reticulum (ER), which produces the bulk of the structural phospholipids and cholesterol. The bottom graphs show the composition out

of the total phospholipid for each membrane type in a mammalian cell. As a measure of sterol content, the molar ratio of cholesterol to phospholipid is indicated. SM Sphingomyelin; R remaining lipids. For more detailed notation see previous figure caption. *Source* van Meer et al. (2008)

organelles. In contrast, the amine-containing glycerophospholipids, phosphatidylethanolamine (PE) and phosphatidylserine (PS), are located preferentially on the cytoplasmic side of the bilayer. Other minor phospholipids, such as phosphatidic acid (PA), phosphatidylinositol (PI), phosphatidylinositol-4-monophosphate (PIP), and phosphatidylinositol-4,5-bisphosphate (PIP₂), are also enriched on the cytofacial side of the membrane. Glycosylsphingolipids are present predominantly on the external leaflet of the plasma membrane. The outer leaflet of plasma membrane has higher percentage of saturated acyl chains as

compared to inner leaflet, which has more polyunsaturated acyl chains. The outer leaflet also contains more cholesterol as compared to inner leaflet (Fig. 1.24).

Maintenance of transmembrane lipid asymmetry is essential for the maintenance of the integrity of the membrane and the cell. Loss of it can lead to change in cell surface properties and hence alter cell surface processes. For example, PS externalization is induced early in the process of apoptosis and during platelet activation. This perturbation can also result in increased adhesion and aggregation of cells and also trigger phagocytosis.

Lipid biosynthesis is inherently asymmetric. The *de novo* synthesis of the major glycerophospholipids (PS, PE, PC, and PI) occurs on the cytosolic side of the endoplasmic reticulum (ER). Most of the sphingolipids are synthesized on the luminal side of the ER or Golgi, including SM, galactosylceramide, and complex sugar-linked sphingolipids, except for glucosylceramide (Glc-Cer), which is synthesized on the cytosolic side of the Golgi. The thermodynamic barrier to passive lipid flip-flop prevents rapid spontaneous transbilayer (flip-flop) diffusion of phospholipids. The movement of lipids is further restricted by protein–lipid interactions. Lipids transport from one side of the bilayer to the other side which is mediated by specific transporters. These transporters significantly contribute both to the maintenance and dissipation of transbilayer lipid asymmetry (Fig. 1.25). Three classes of transporters have been described for the transport of lipids across the bilayer, namely, the **flippases**, **floppases**, and the **scramblases** (Fig. 1.26).

Flippases are ATP-dependent aminophospholipid translocases, present in most plasma membranes. Flippases predominantly transport PS from the outer monolayer to the cytoplasmic surface of the plasma membrane. Flippase-catalyzed transport is inhibited by vanadate, suggesting that it belongs to a family of P_4 -ATPases. They are responsible for enriching the cytosolic side of the monolayer in PS and maintaining negligible PS in the outer monolayer.

The second class of ATP-dependent lipid transporters is the floppases. Floppases belong to the ABC transporter superfamily (see Chap. 6).

The most well-characterized lipid floppase activities are those catalyzed by ABCA1, ABCB1, ABCB4, and ABCC1 (Table 1.3). The ABC transporter ABCA1 (ABC1) acts as a floppase for both cholesterol and PS. ABCB1 (MDR1) is a lipid transporter of broad specificity. ABCB4 (MDR3, mMdr2) is a selective transporter for PC. ABCA1 and ABCB1, ABCB4 are mainly involved in lipid efflux to the extracellular side of the monolayer, enriching the outer monolayer in cholesterol and PC.

The third class of transporters, the scramblases, catalyzes the energy-independent bidirectional transbilayer transport of lipids. The ER and Golgi scramblases redistribute newly synthesized lipids or lipid precursors in ER and Golgi membranes. Lipids synthesized on one side of the bilayer are transported to the other side by scramblases. The Ca^{2+} -activated scramblase plays an important role in plasma membrane reorganization in response to cell stimulation, and in conditions such as apoptosis. The dissipation of transbilayer asymmetry of PM results in increased percentage of PS on the outer surface of the cell. This activates blood clotting factors and recognition of the cell by macrophages, triggering phagocytosis. The Ca^{2+} -activated scramblase is relatively nonspecific which randomizes the distribution of all of the major classes of endogenous phospholipids.

Phosphatidylethanolamine is the most abundant lipid class in many bacterial species, whereas phosphatidylcholine is the major lipid class in eukaryotes. Phosphatidylcholine is rarely found in bacteria. Phosphatidylglycerol is also

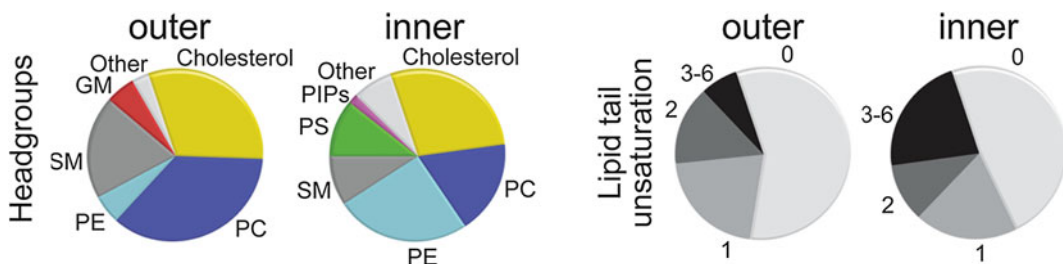


Fig. 1.24 Pie charts showing the distribution of the main lipid head groups and the levels of tail unsaturation in the inner and outer leaflets of mammalian plasma membrane. *Source* Ingólfsson et al. (2014)

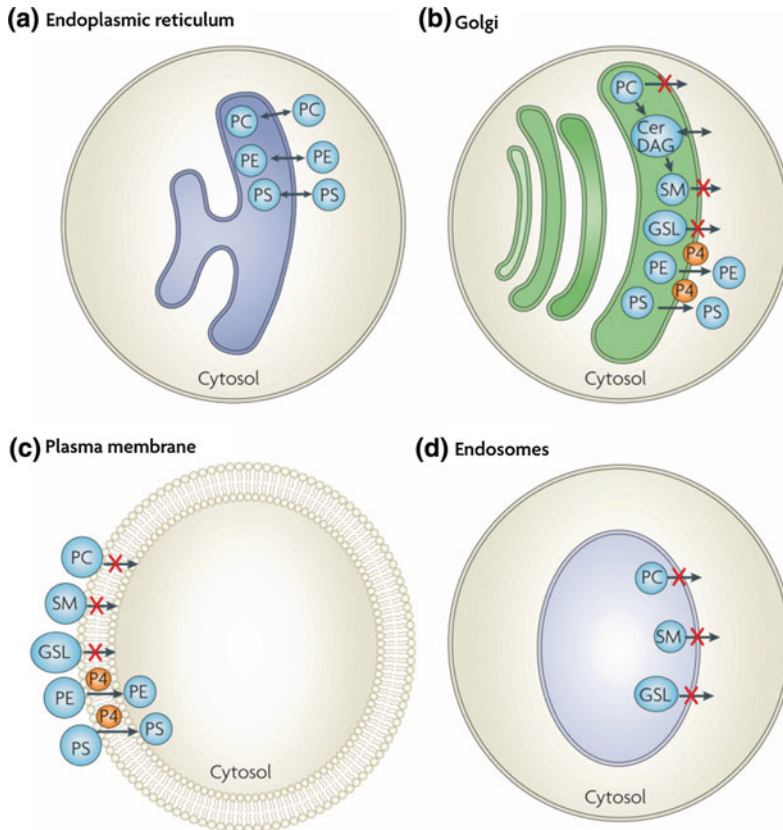


Fig. 1.25 Mechanisms for generating asymmetric lipid distribution in membranes. **a** In the ER, non-specific transbilayer equilibration of phospholipids has been demonstrated, and the membrane exhibits a nearly symmetric lipid distribution between bilayer leaflets. **b** In the Golgi, P4 ATPases translocate PS and PE to the cytosolic face. SM is produced by SM synthase from Cer on the luminal side. Neither PC nor SM molecules that are resident in the luminal leaflet are transported to the cytosolic face. Thus, asymmetry in the Golgi is generated by the specific transport of PS and PE and lack of transport of SM and PC. In SM synthesis, PC is

converted to (DAG), which freely equilibrates across bilayers. DAG can serve as a substrate for the cholinephosphotransferase isozyme, the product of which is SM. **c** At the plasma membrane, P4 ATPases transport PS and PE to the cytosolic face, with little or no transport of PC or SM to the cytosolic face under basal conditions. This homeostatic distribution can be disrupted by activation of scramblase and/or inhibition of the P4 ATPases. **d** Within endosomes, fluorescent PC and SM and GSLs are restricted to the luminal leaflet by a lack of specific transport mechanisms. P4 ATPases are recycled through endosomes. *Source* van Meer et al. (2008)

abundantly present in most bacteria; in fact in cyanobacteria it is the only glycerophospholipid in membranes. Phosphatidylglycerol is only found as a constituent of mitochondrial membranes in eukaryotes. Sphingolipids are also rarely found in bacteria.

1.6 Carbohydrates in Membranes

Carbohydrates in membranes (2–10% of the membranes) are present as oligosaccharides/glycans covalently linked to lipids and/or proteins forming

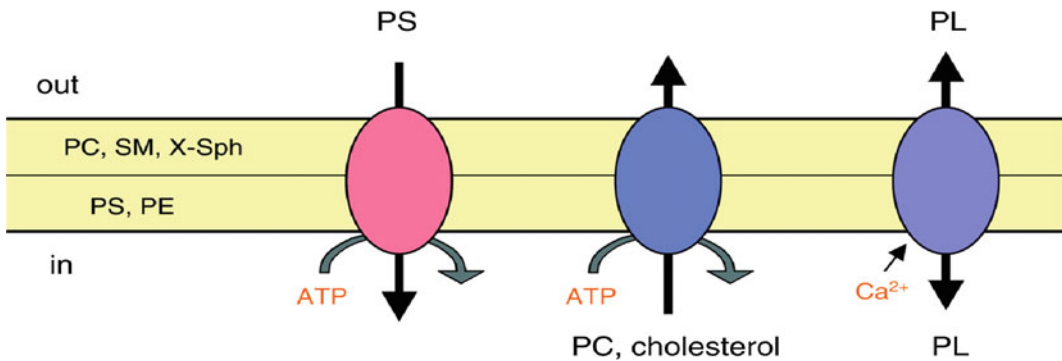


Fig. 1.26 Transbilayer transporters of lipids in the eukaryotic plasma membrane. Phosphatidylcholine (PC), sphingomyelin (SM), and sugar-linked sphingolipids (X-Sph) are enriched in the outer monolayer, while phosphatidylserine (PS) and phosphatidylethanolamine (PE) are sequestered on the cytoplasmic monolayer. This

distribution is maintained by (left) an inwardly directed PS flippase. In some tissues an outwardly directed PC or cholesterol floppase (middle) is responsible for the efflux of these lipids. A nonspecific, Ca^{2+} stimulated scramblase (right) randomizes phospholipid (PL) distribution in activated cells. *Source* Daleke (2003)

Table 1.3 ABC transporters: lipid exporters

Transporter	Presumed substrate	Location	Disease when inactivated
ABCA1	Cholesterol, PtdCho, PtdSer	Plasma membrane	Tangier and familial hypoalphalipoproteinemia
ABCA3	PtdCho, cholesterol	Lung lamellar bodies	Pulmonary surfactant insufficiency
ABCA4	<i>N</i> -retinylidene-PtdEtn	Photoreceptor disks	Stargardt and age-related macular degeneration
ABCA12	GlcCer	Skin lamellar bodies	Harlequin ichthyosis
ABCB4	PtdCho, cholesterol	Bile canicular membrane	Hepatic cholestasis
ABCDL	Very long chain fatty acyl-CoA	Peroxisomes	X-linked adrenoleukodystrophy
ABCGt	PtdCho, SM, cholesterol	Plasma membrane	Pulmonary lipidoses
ABCG5/G8	Sitosterol, cholesterol	Apical membrane	Sitosterolemia and hypercholesterolemia

glycoconjugates. The glycoconjugates are rich in sugars like glucose, galactose, mannose, fucose, *N*-acetyl galactosamine, and *N*-acetyl glucosamine and are predominantly present on the extracellular side of the bilayer. They serve as docking sites in cell recognition, adhesion, and receptor action. They also play an important role in cell–cell interaction during development, chemotaxis of cells during immune response and in processes like blood clotting, wound healing.

The different kinds of glycoconjugates in membranes include glycoproteins, proteoglycans, glycosphingolipids (GSLs), and glycosphosphatidylinositol (GPI) anchors (Fig. 1.27).

Glycoproteins usually have many oligosaccharide chains attached to the protein. The oligosaccharide chains are linked either to the amide nitrogen atom in the side chain of asparagine (termed as N-linkage) or to the oxygen atom in the hydroxyl group of serine or threonine

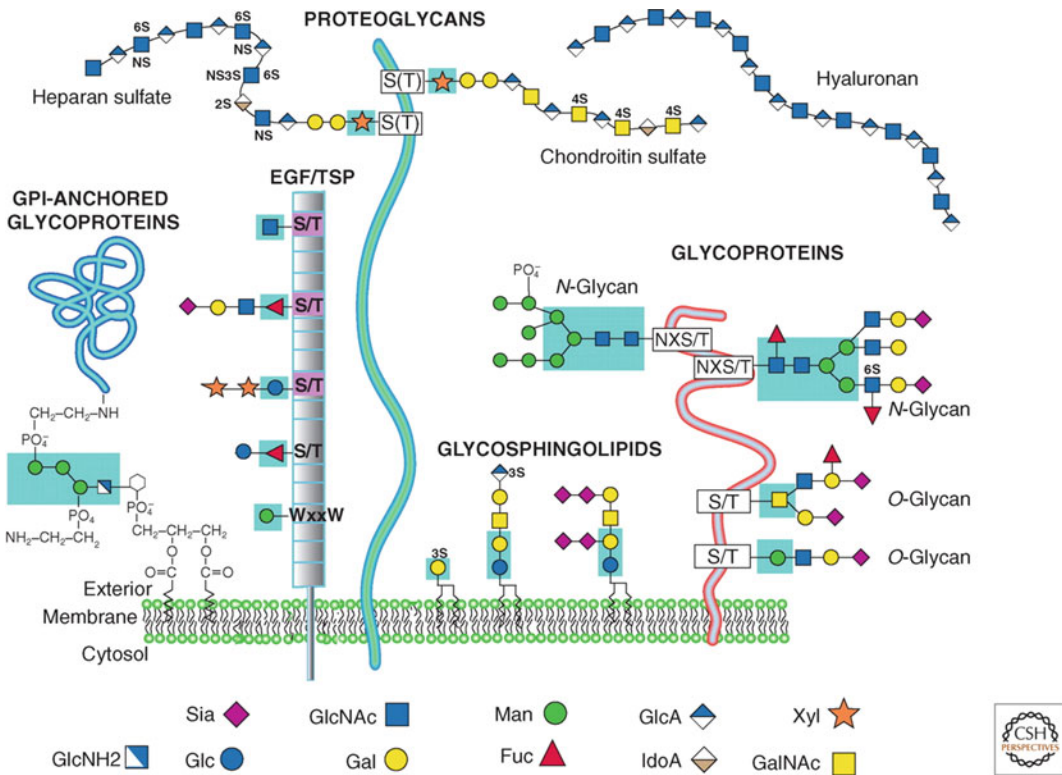


Fig. 1.27 Diagram depicts simple *N*- and *O*-glycans attached to proteins and lipids in the plasma membrane. Rather rare *O*-glycans are found attached to EGF-like repeats (EGF; pink) or thrombospondin repeats (TSR; gray) with a particular consensus sequence. The W_{xx}W motif in a TSR is C-mannosylated. Core regions boxed in teal are sugars added in the ER. The remaining sugars in each class of glycan are added during passage through the *cis*-,

medial-, and *trans*-Golgi network (TGN) compartments of the Golgi. Abbreviations are: Man mannose; Gal galactose; Glc glucose; GlcNAc *N*-acetylglucosamine; GlcNH₂, Glucosamine; GlcA glucuronic acid; IdoA iduronic acid; GalNAc Nacetylgalactosamine; Xyl xylose; Fuc Fucose; Sia sialic acid; 3S, 3-*O*-sulfated; 6S, 6-*O*-sulfated, PO₄ phosphate. *Source* Stanley (2011)

(termed as O-linkage) via glycosidic linkage (Fig. 1.28). The potential glycosylated asparagine residue is part of an Asn-X-Ser or Asn-X-Thr sequence, in which X can be any residue. Yet, the actual glycosylated site is specific to the protein type and is also cell- and tissue-specific. All N-linked oligosaccharide chains in glycoproteins have a common pentasaccharide core consisting of three mannose and two *N*-acetylglucosamine residues. Additional sugar molecules are attached to this core to form the great variety of oligosaccharide patterns (Fig. 1.29).

Protein glycosylation takes place as a post-translational modification in the lumen of the endoplasmic reticulum (ER) and the Golgi

complex. The process of N-linked glycosylation starts in the ER and continues in the Golgi complex, whereas the process of O-linked glycosylation takes place in the Golgi complex exclusively.

The assembly of oligosaccharide chain to be attached to the asparagine residue of a protein starts with dolichol phosphate, a specialized lipid molecule containing as many as 20 isoprene (C₅) units. Dolichol phosphate is part of ER membrane with its phosphate terminus on the cytoplasmic face.

The assembly process proceeds in three stages. In the first stage, 2*N*-acetylglucosamine residues and 5 mannose residues are added to the

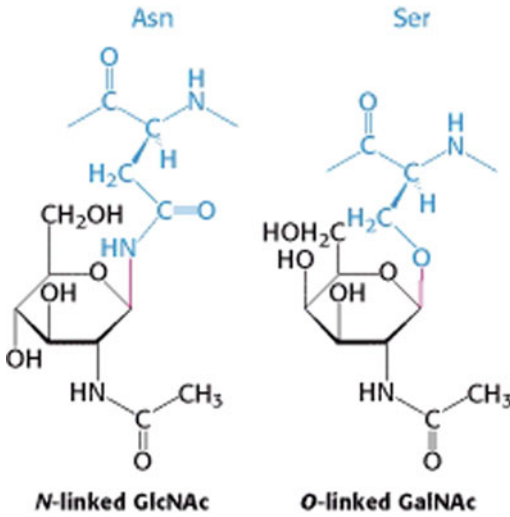


Fig. 1.28 N-linked and O-linked bonds linking carbohydrates and proteins in glycoproteins

dolichol phosphate on the cytosolic side of the ER membrane. A number of cytoplasmic enzymes catalyze the transfer of monosaccharide from sugar nucleotides to the growing chain on dolichol. Then, this large structure formed is translocated through the ER membrane into the lumen of the ER. Further, addition of sugar molecules is catalyzed by ER lumen enzymes. This process results in the formation of a 14-residue oligosaccharide chain attached to dolichol phosphate (Fig. 1.30). The oligosaccharide chain is attached to the phosphate group of dolichol and is then subsequently transferred

to the asparagine residue of the growing polypeptide chain. 3 glucose molecules are removed from the 14-residue oligosaccharide chain before the glycoprotein leaves the lumen of the ER. Further processing of N-linked oligosaccharide occurs in the Golgi apparatus.

O-linked oligosaccharide in membrane-associated glycoproteins is attached via glycosidic linkage to the hydroxyl group of a serine or threonine residue of the protein. Biosynthesis begins in the *cis*-Golgi network with transfer of *N*-acetylgalactosamine (GalNAc) from UDP-*N*-acetylgalactosamine to serine/threonine residue of the protein, catalyzed by the enzyme, GalNAc transferase. After the protein has moved to the *trans*-Golgi vesicles, a galactose residue is added to the *N*-acetylgalactosamine by a specific *trans*-Golgi galactosyltransferase (Fig. 1.31). The terminal sugar of typical O-linked oligosaccharides in vertebrate membrane glycoproteins is negatively charged *N*-acetylneuraminic acid (also called sialic acid) residue. These reactions also occur in the *trans*-Golgi network.

In mammals, glycosylation of lipids begins with the addition of first sugar to ceramide (Cer) in the ER. GlcCer may not be further modified during passage through the Golgi, may have one or two sugars added (Fig. 1.27), or may be extensively modified by a battery of glycosyltransferases localized in different compartments of the Golgi.

The human **A**, **B**, and **O** blood group antigens are a result of one of three structurally related yet

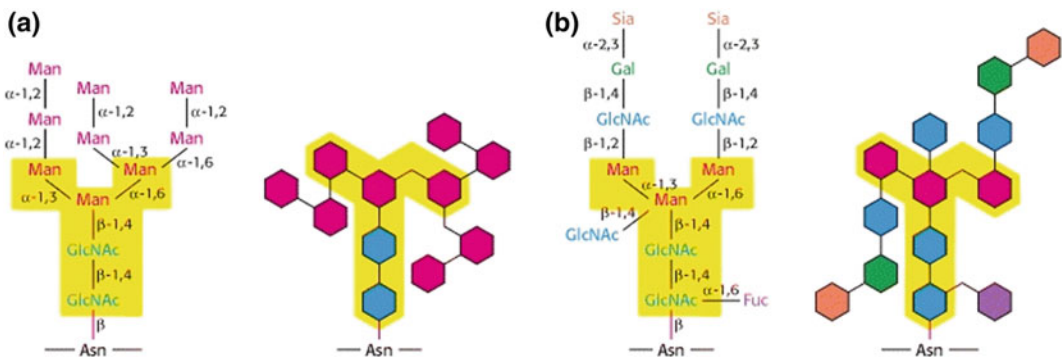


Fig. 1.29 A pentasaccharide core (shaded yellow) common to all N-linked oligosaccharides serves as the foundation for a wide variety of N-linked oligosaccharides, two of which are: **a** high-mannose type; **b** complex type

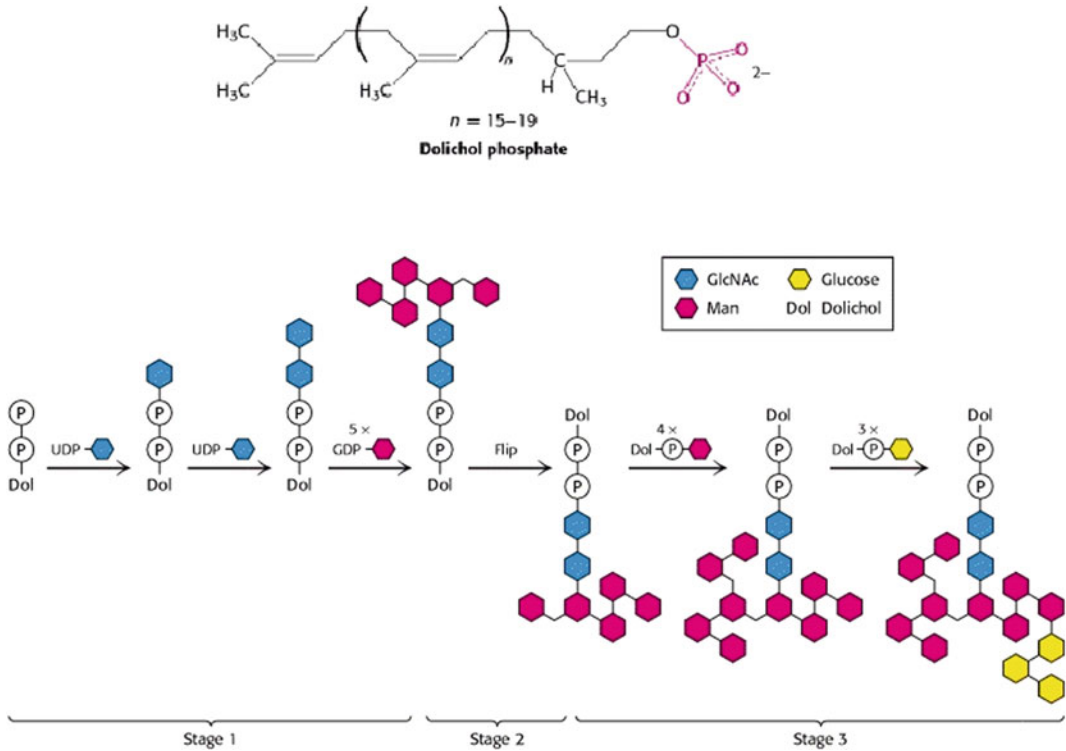


Fig. 1.30 Assembly of an N-linked oligosaccharide precursor starts on the cytoplasm exposed phosphate of a membrane-embedded dolichol molecule. Then dolichol

phosphate and attached oligosaccharide are flipped into the lumen of ER and further synthesis completed

distinct oligosaccharides chains attached to a ceramide lipid or a serine or threonine residue on a protein present on the erythrocytes membrane, and many other cell types (Fig. 1.32). Both A and B antigens arise from O antigen. A antigen contains an *N*-acetylgalactosamine attached to the outer galactose residue, whereas the B antigen contains an extra galactose residue attached to the outer galactose.

The enzymes needed to synthesize the O antigen are present in all individuals. People with type A blood have additional GalNAc transferase that adds the extra *N*-acetylgalactosamine, and those with type B blood have the Gal transferase that adds the extra galactose. People with type AB blood have both the transferases and synthesize both the A and B antigens, but those with type O do not express either of the above two transferases present in A or B type.

The importance of blood groups becomes relevant during blood transfusions (Table 1.4). For example, people with blood types A and O lack the Gal transferase and thus cannot synthesize the B antigen. Such individuals normally have antibodies against the B antigen in their serum. Thus, when type B or AB blood is transfused into such a person, the anti-B antibodies of the recipient bind to the transfused erythrocytes and trigger an immune reaction leading to their agglutination and destruction. To avoid such harmful reactions, blood group testing and appropriate matching of blood donors and recipients are required before all transfusions.

The **glycocalyx**, a proteoglycan/glycoprotein-polysaccharide covering, surrounds the cell membranes of most cell types and some bacteria. A fuzz-like coat on the external surface of plasma membranes has been seen in most animal

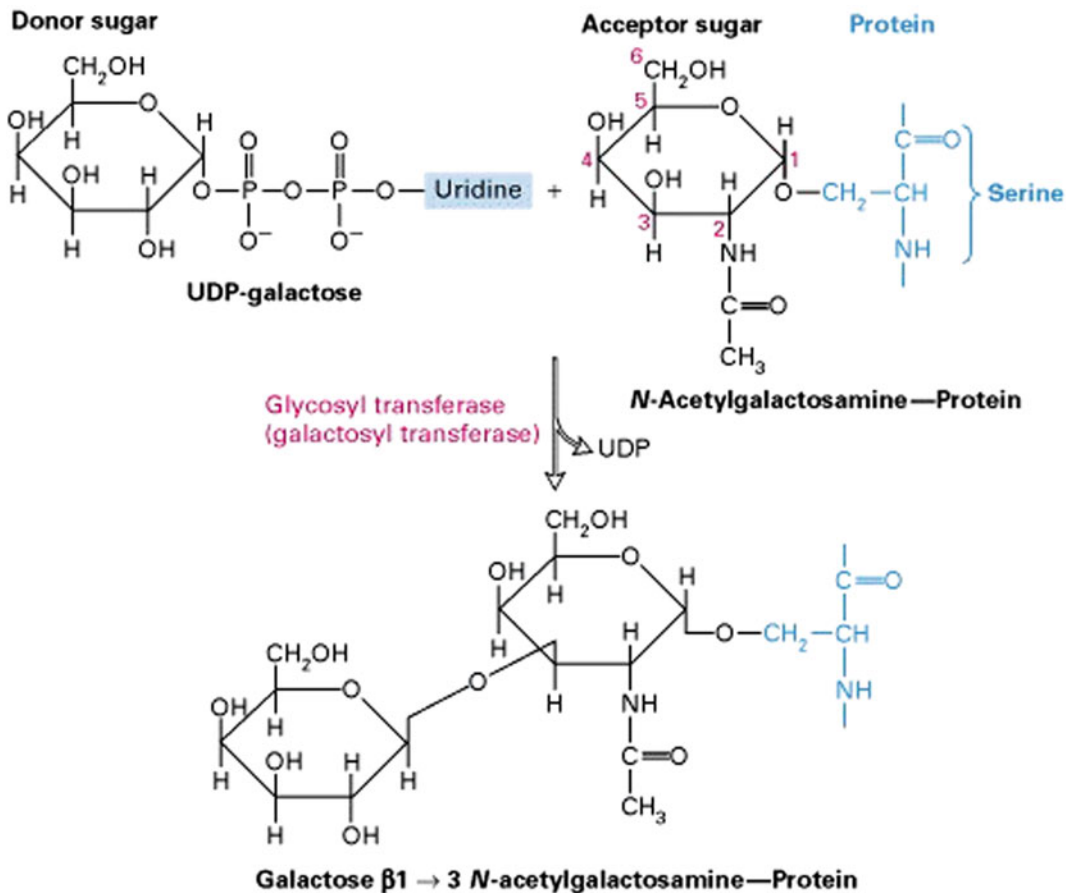


Fig. 1.31 A specific galactosyltransferase catalyzes addition of a galactose residue from UDP-galactose to carbon atom 3 of *N*-acetylgalactosamine attached to a protein forming a β₁ → 3 linkage

epithelial cells. This hydrophilic gel coat on the cell surface protects against physical trauma, regulates ionic and macromolecular access, and also plays an important role in cellular processes like cell adhesion, cell–cell recognition, and communication (Fig. 1.33).

The carbohydrate components of the glycocalyx include both compounds covalently bound to proteins or, to a lesser extent, to lipids on the cell surface, and additionally glycoproteins and polysaccharides are also noncovalently associated with them. The composition of glycocalyx varies with cell type and extracellular matrix environment. In the endothelial cells in small vessels, glycocalyx has the size of 400–500 nm and occupies 10–20% of the vascular lumen

volume. Glycocalyx is considered as a protective layer on the vessel wall, a barrier against leakage of molecules, and provides a porous hydrodynamic environment for intercellular interaction (for example, between the vascular endothelium and the blood cells). Destruction of the glycocalyx often becomes one of the first signs of cell destruction with formation of nano-sized fragments (oligomers glycosaminoglycans products of limited proteolysis of glycoproteins, etc.) characterized by diverse biological activity. It is assumed that the endothelial glycocalyx has a definite ultrastructure that is connected with the cytoskeleton (Fig. 1.33) to serve as a mechanochemical sensor and mediate shear stress response of the cell.

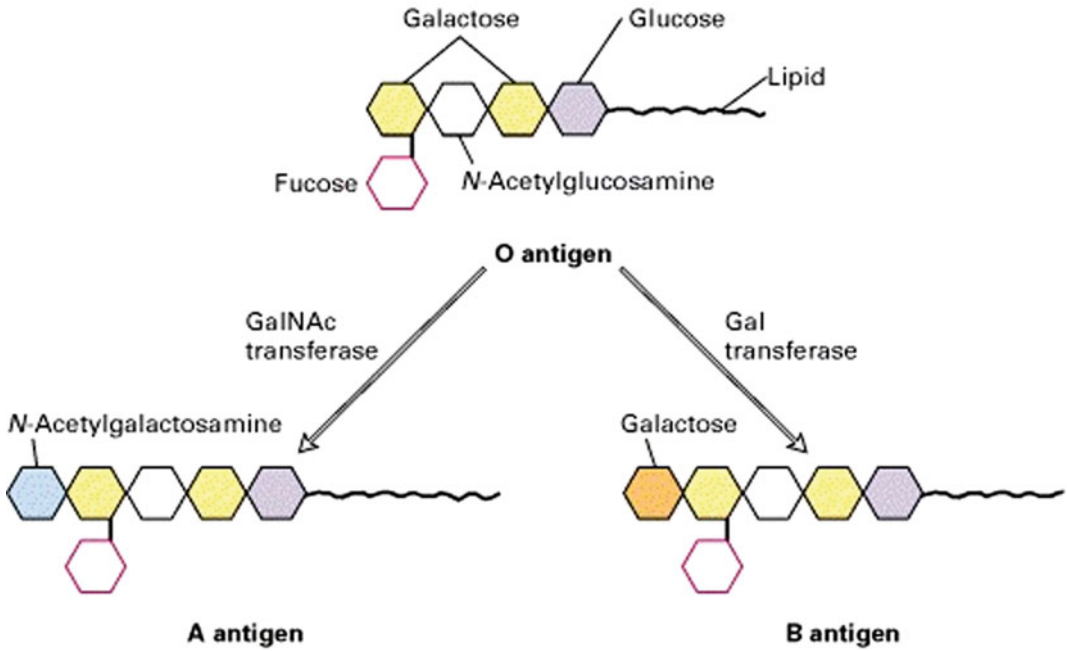


Fig. 1.32 Human ABO blood group antigens. The structure of the terminal sugars in the oligosaccharide component of these glycolipids and glycoproteins

distinguish the three antigens. The presence or absence of particular glycosyltransferases determine an individual's blood type. (See Feizi 1990 for a review)

Table 1.4 Blood group antigens

Blood group type	Antigens on RBCs	Serum antibodies	Can receive blood types
A	A	Anti-B	A and O
B	B	Anti-A	B and O
AB	A and B	None	All
O	None	Anti-A and anti-B	O

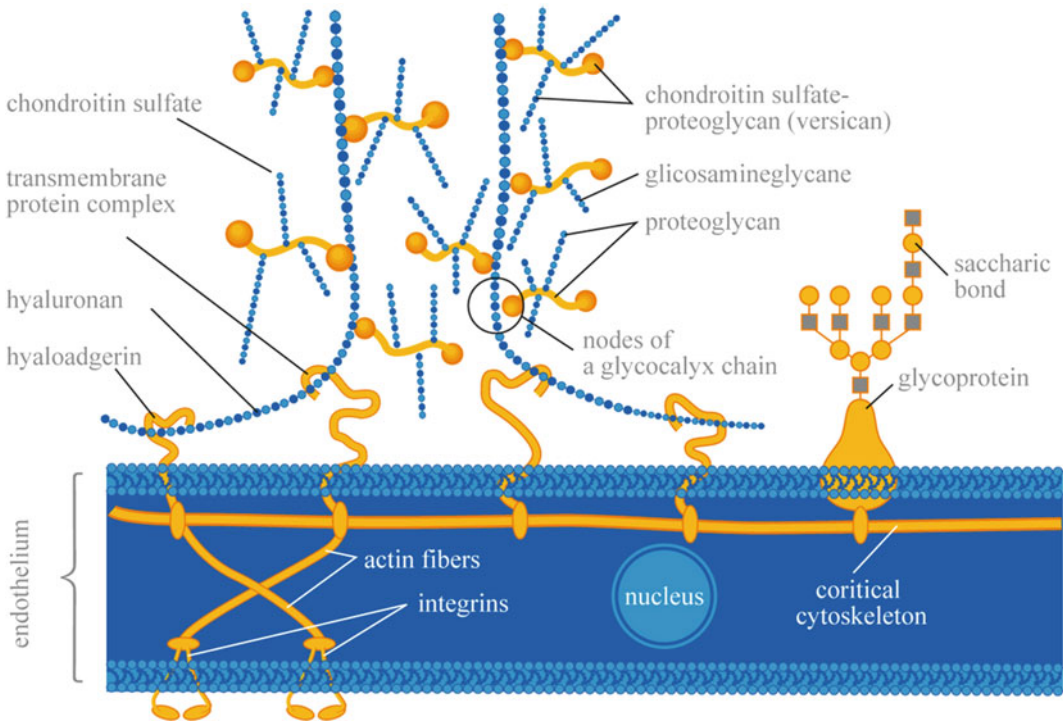


Fig. 1.33 A representation of a glycocalyx chain attached to a cytoskeleton

References

- Bangham AD, Standish MM, Watkins JC (1965) Diffusion of univalent ions across the lamellae of swollen phospholipids. *J Mol Biol* 13:238–252
- Daleke DL (2003) Regulation of transbilayer plasma membrane phospholipid asymmetry. *J Lipid Res* 44:233–242
- Danielli JF, Davson H (1935) A contribution to the theory of permeability of thin films. *J Cell Comp Physiol* 5:495–508
- De Vries H (1884) Eine Methode zur Analyse der Turgorkraft. *Pring Jahrb wiss Bot*, 14:427–601
- Donnan FG (1924) The theory of membrane equilibria. *Chem Rev* 1:73–90
- Feizi T (1990) *Trends Biochem Sci* 15:330
- Frye LD, Edidin M (1970) The rapid intermixing of cell surface antigens after formation of mouse-human heterokaryons. *J Cell Sci* 7:319–335
- Gorter E, Grendel F (1925) On bimolecular layers of lipoids on the chromocytes of the blood. *J Exp Med* 41:439–443
- Henderson R, Unwin PNT (1975) Three-dimensional model of purple membrane obtained by electron microscopy. *Nature* 257:28–32
- Hodgkin AL, Huxley AF (1952) A quantitative description of membrane current and its application to conduction and excitation in nerve. *J Physiol* 117:500–544
- Hooke R (1665) *Micrographia, or some physiological descriptions of minute bodies made by magnifying glasses*. Royal Society, London
- Ingólfsson HI, Manuel N, Melo MN et al (2014) Lipid organization of the plasma membrane. *J Am Chem Soc* 136:4554–4559. <https://doi.org/10.1021/ja507832e>
- Langmuir I (1917) The constitution and fundamental properties of solids and liquids. II liquids. *Am Chem Soc* 39:1848–1906
- Laule C, Vavasour IM, Kolind SH et al (2007) Magnetic resonance imaging of myelin. *Neurotherapeutics* 4(3): 460–484
- Lombard J (2014) Once upon a time the cell membranes: 175 years of cell boundary research. *Biol Dir* 9:32. <http://doi.org/10.1186/s13062-014-0032-7>
- Moor H, Mülhthaler K (1963) Fine structure in frozen-etched yeast cells. *J Cell Biol* 17:609–628
- Neher E, Sakmann B (1976) Single-channel currents recorded from membrane of denervated frog muscle fibres. *Nature* 260:799–802
- Overton E (1895) Ueber die osmotischen Eigenschaften der lebenden Pflanzen und Thierzelle. *Vierteljahrscr Naturf Ges Zurich* 40:159–184

- Pfeffer W (1899) Osmotic investigations. In: Jones HC (ed) *The modern theory of solution*. Harper brothers publishers, New York & London
- Robertson JD (1960) The molecular structure and contact relationships of cell membranes. *Prog Biophys Mol Biol* 10:343–418
- Singer SJ, Nicolson GL (1972) The fluid mosaic model of the structure of cell membranes. *Science* 175:720–731
- Stanley P (2011) Golgi glycosylation. *Cold Spring Harb Perspect Biol* 3:a005199
- van Meer G, Voelker DR, Feigenson GW (2008) Membrane lipids: where they are and how they behave. *Nat Rev Mol Cell Biol* 9:112–124. <http://doi.org/10.1038/nrm2330>

2.1 Lipid Water Systems: Thermodynamics, CMC

Membrane lipids are amphiphilic molecules, containing both hydrophobic and hydrophilic portions. On hydration, lipids self-assemble to form a variety of aggregate structures or phases such that the nonpolar hydrocarbon portions move away from water, toward the interior, and the polar portions interact with the surrounding water.

The formation of different hydrated lipid aggregates is the result of the “**hydrophobic force**,” which drives the nonpolar molecules to move away from polar water molecules and interact with other nonpolar molecules. The other stabilizing factors that stabilize these aggregate structures include the **van der Waals** attraction between adjacent hydrophobic acyl chains, and **hydrogen bonds** and **electrostatic interactions** between polar groups of lipids and water molecules. Contribution of these forces is minor when compared to hydrophobic force in stabilizing aggregate structures.

The structural organization that lipids assume in water is governed by its concentration and the balance of the opposing forces, namely the hydrophobic force that drives aggregation versus the ionic and H-bond interactions and steric repulsive forces of the polar portion which oppose aggregation. At very low concentration, amphiphilic molecules exist as monomers in aqueous solution. As the concentration of the amphiphilic molecule increases, it starts forming

aggregate structures when the hydrophobic force becomes stronger than the opposing favorable polar interactions with water. The concentration of amphiphilic molecules above which any further increase in concentration leads to increase in the concentration of aggregate structures, which are in equilibrium with the free monomer concentration which remains constant, is called **critical micelle concentration (CMC)**. Thermodynamic measurements can quantify the tendency of lipids to form aggregate structures driven by hydrophobic force, excluding water from contact with nonpolar portion of the molecule. When amphiphilic detergent molecule-like sodium dodecyl sulfate (SDS), which like phospholipids has a nonpolar (dodecyl) chain and a highly charged polar (sulfate) group at one end, is dissolved in water, up to a certain concentration remain as monomers, but above that concentration it starts forming aggregate structures called micelles. CMC is also defined as the concentration at which 50% of the detergent is in the form of micelle (Fig. 2.1).

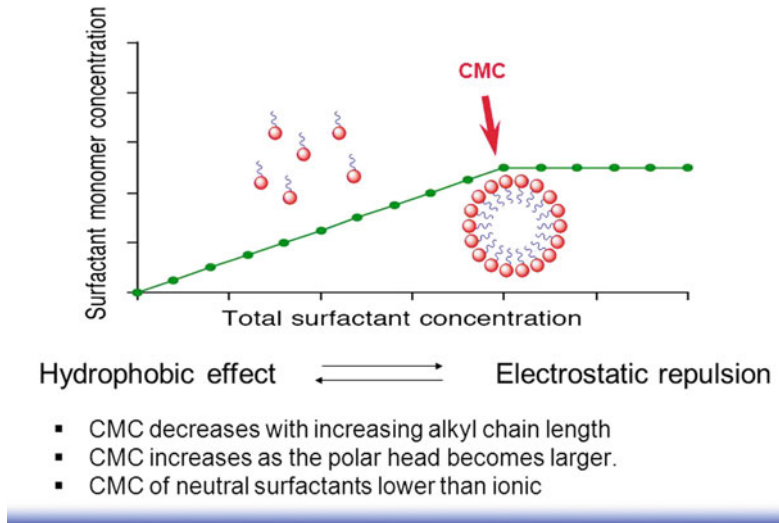
Thermodynamically, CMC is expressed in terms of the Gibbs free energy of micelle formation $\Delta G_{\text{mic}}^{\circ}$ and is given by the equation:

$$\Delta G_{\text{mic}}^{\circ} = kT \ln X_{\text{cmc}}$$

where k is Boltzmann’s constant, T is temperature, and X_{cmc} is concentration at CMC.

The negative Gibbs free energy of micelle formation, $\Delta G_{\text{mic}}^{\circ}$, results from the stabilization of aggregate structures due to the hydrophobic force which drives the hydrophobic regions of the

Fig. 2.1 Critical micelle concentration of a surfactant



amphiphile to move away from water and favorably interact with hydrophobic regions of other amphiphiles inside the micelle. Highly hydrophobic molecules form aggregates at much lower concentrations due to more negative ΔG_{mic}° . CMC decreases with increase in chain length of acyl chain. Membrane phospholipids which are made of two C_{16} – C_{20} long alkyl chains per molecule have a very low CMC of $<10^{-10}$ M. Implying that, the concentration of monomeric phospholipids in aqueous solution is almost negligible. Phospholipids spontaneously form bilayers when they come in contact with aqueous solution. In contrast, CMC of SDS, which has one C_{12} alkyl chain, is 8×10^{-3} M at 25 °C, atmospheric pressure. Below this concentration, SDS is present in monomeric form in aqueous solution.

2.1.1 Determination of CMC

The study of surfactant solutions reveals that the physical properties of these solutions, such as surface tension and electrical conductivity, show an abrupt change near the **critical micelle concentration**. These physicochemical parameters can be

used to determine CMC of a surfactant. The value of the CMC for a given dispersant in a given medium depends on temperature, pressure, and ionic strength. The most simple and commonly used parameters for determination of CMC are surface tension and electrical conductivity (Fig. 2.2).

2.1.2 Surface Tension

The surface active agents decrease the surface tension, σ , of aqueous solutions. With the increase in concentration of the surfactant, the surface tension decreases rapidly till the CMC is reached, and above CMC, no further change in surface tension takes place. As only the monomeric form contributes to the reduction of the surface or interfacial tension, above the CMC concentration, additional surfactant molecules form micelles/aggregate structures. The concentration of the monomeric surfactant molecules remains constant and is equal to the CMC. At the CMC, the interface is considered to be saturated with surfactant molecules, with maximum reduction in interfacial tension, and hence, no further decrease in surface tension occurs above the CMC.

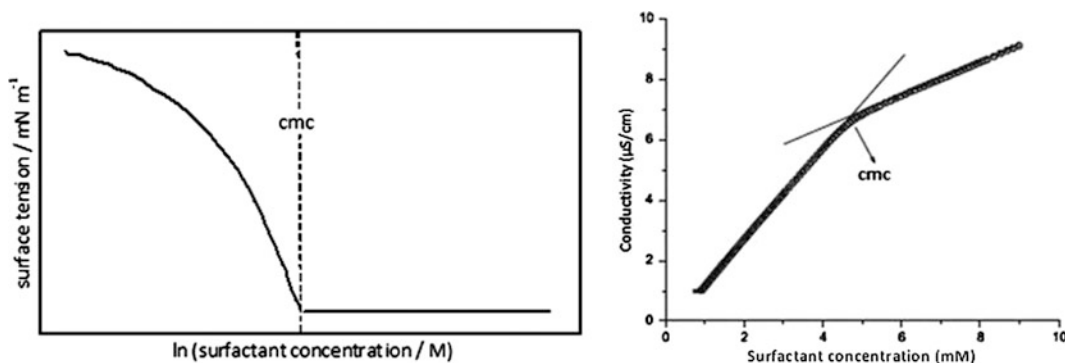


Fig. 2.2 Determination of CMC by surface tension and conductivity method

2.1.3 Conductivity

For ionic surfactants, at low concentrations (below *cmc*), the surfactants behave like a strong electrolyte and dissociate completely. The ions contribute to the electrical conductivity as measured by the specific conductance (κ) or equivalent conductance (Λ). At concentrations below the CMC, conductivity, κ , increases sharply with the increasing surfactant concentration as concentration of the ionic species increases. Above the CMC, further addition of surfactant molecules forms aggregate/micelle structures with the monomer concentration almost remaining constant (at the CMC level). Since aggregate structures/micelles are much larger in size, it shows slower diffusion rates in solution as compared to monomeric molecules. A plot of conductivity against surfactant concentration hence shows a change in the slope above CMC concentration, with a break point at the CMC.

2.1.4 Polymorphic Lipid–Water Systems/Phases

Lipids on hydration self-assemble to form a variety of polymorphic lipid–water systems/phases with different geometry. The type of polymorphic phase formed is determined by a number of factors including the lipid composition and concentration, ionic strength and pH of the aqueous solution, temperature, pressure, and degree of hydration.

The list of different phases formed is given in Table 2.1, and structures are shown in Fig. 2.3.

The nomenclature proposed by Luzzati (1968) is most widely used for naming lipid polymorphic phases. The capital letter denotes the type of lattice, e.g., L stands for lamellar, H is for hexagonal, and Q is for cubic. Subscripts I and II denote normal (oil in water) and reverse (water in oil) phases, respectively. A Greek subscript denotes the type of phase or hydrophobic chain conformation, for example, c denotes crystalline, β denotes ordered gel-like region, α denotes liquid-like region, $\alpha\beta$ denotes coexisting gel- and liquid-like regions, and δ stands for helical chain conformation.

1. Crystalline lamellar phases

Most membrane phospholipids on hydration form lamellar phase, in which lipid bilayers stack on top of one another, separated by a layer of aqueous solution. Crystalline lamellar L_c phase is formed at low temperatures, in which the acyl chains are packed in an ordered manner. The three-dimensional order exhibited in this phase is comparable to a crystalline state.

2. Ordered lamellar phases

At much low temperatures, lipid molecules form a solid-like phase known as lamellar gel phase L_β . The molecules are more tightly packed, and the acyl chains are present in highly ordered, all

Table 2.1 List of different lipid phases

Phase	Description
L_c	3D lamellar crystals
L_c^{2D}	Lamellar stack of 2D crystalline bilayers
L_β	Lamellar gel (untitled)
$L_{\beta'}$	Lamellar gel (tilted)
$L_{\beta I}$	Interdigitated gel
$L_{\alpha\beta}$	Partial gel
L_δ	Lamellar phase of square-packed, helically coiled (δ) chains
$P_{\beta'}$	Rippled gel phase
P_δ	Ribbon phase with δ -packed chains
L_α	Fluid lamellar phase
H	Hexagonal
H^c	Hexagonal, complex
R	Rectangular
M	Oblique
Q	Cubic
T	Tetragonal
Rh	Rhombohedral

Source Seddon and Templer (1995)

transconformation. Strong van der Waals interactions exist between acyl chains.

In the L_β gel phase, the hydrocarbon chains are arranged perpendicular to the membrane bilayer. The $L_{\beta'}$ phase is a gel-like phase, similar to L_β phase, but the molecules are in tilted arrangement. The tilting is due to larger packing requirement of the head group area (twice) than that of the diacyl chains. Tilting accommodates such packing mismatches.

3. Fluid phases

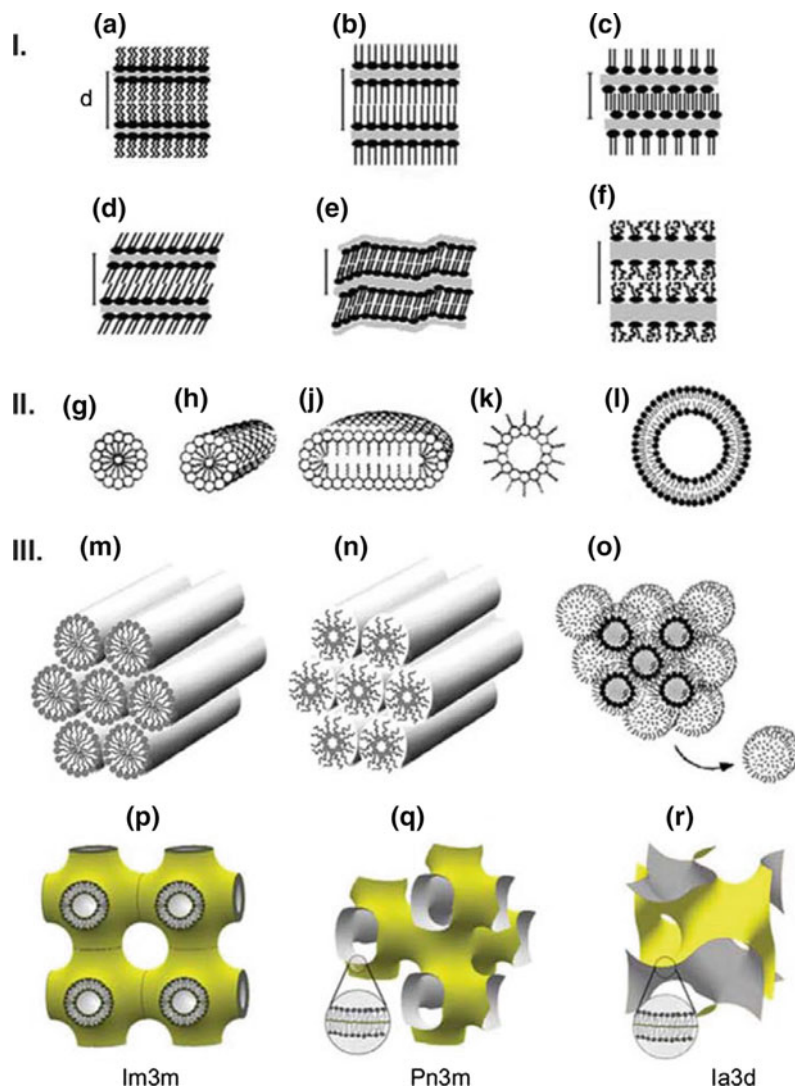
At higher temperatures, the gel phase lipid, the chains transform into a liquid-like, fluid, lamellar liquid-crystalline L_α phase. This form is also called the liquid-disordered phase, which represents the bulk of the lipid phase in biological membranes. This phase is characterized by considerable disorder in the acyl chains due to the presence of kinks in the acyl chains resulting from unsaturated double bonds in *cis*-conformation.

4. 2D fluid phases

Two-dimensional nonlamellar fluid phases are formed when lipid aggregates form indefinitely long cylinders rather than bilayers. The cylinders in water are arranged to form a hexagonal pattern. The most studied 2D fluid phases are the normal hexagonal phases H_I and inverse hexagonal phases H_{II} (Fig. 2.3). In the H_I phase, the lipids aggregate to form circular cylindrical micelles which arrange to form the hexagonal lattice, with a continuous polar aqueous region filling the space between the cylinders. In the H_{II} phase, the lipids are arranged in the reverse, with the polar head groups toward the inside of the cylinder and the hydrocarbon chains toward the outside. The polar head groups enclose water, which forms the central core of the cylinder.

The H_I phase is very common in simple surfactant systems and lysophospholipids, whereas diacyl phospholipids, which form bulk of membrane lipids, are not found in H_I phase.

Fig. 2.3 Structures of lipid phases. I. Lamellar phases: **a** Crystalline lamellar, L_c ; **b** gel, L_β ; **c** interdigitated gel, $L_\beta^{[int]}$; **d** gel, tilted chains, L'_β ; **e** rippled gel, P'_β ; **f** liquid crystalline, L_α . II. Micellar aggregates: **g** spherical micelles, M_1 ; **h** cylindrical micelles (tubules); **j** disks; **k** inverted micelles, M_{II} ; **l** liposome. III. Nonlamellar liquid-crystalline phases of various topology; **m** hexagonal phase, H_I ; **n** inverted hexagonal phase, H_{II} ; **o** inverted micellar cubic phase, $Q_{II}^{[M]}$; **p** bilayer cubic (Q_{II}) phase, $Im3m$; **q** bilayer cubic phase, $Pn3m$; **r** bilayer cubic phase, $Ia3d$. Source Koynova and Tenchov (2013)



Many biologically important lipids, such as DAG or PE, form more stable H_{II} arrangement rather than a flat bilayer. A small weakly hydrated head group and strong head group–headgroup interactions preferentially stabilize the H_{II} phase.

5. 3D fluid phases

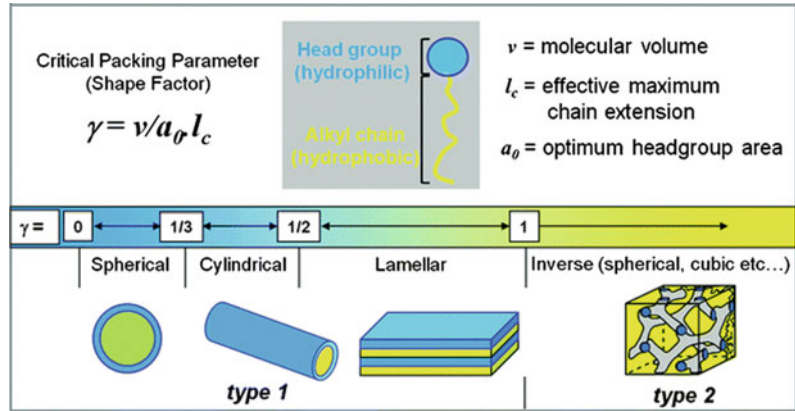
The cubic phase is the most well-characterized three-dimensional fluid phases so far detected. There are two major types of cubic phases. One type consists of curved bicontinuous lipid bilayer in three dimensions which encloses networks of water channels ($Ia3d$, $Pn3m$, and $Im3m$). The

other type is based on complex packings of discrete micellar aggregates ($Pm3n$). The other three-dimensional structures like rhombohedral and tetragonal have also been reported in a few lipid systems at low hydrations (Fig. 2.3).

2.2 Determinants of Polymorphic Phases: Shapes, Critical Packing Parameter

Lipids self-assemble to form aggregates of different geometry, determined by internal factors like the chemical structure and shape of lipids

Fig. 2.4 Critical packing parameter

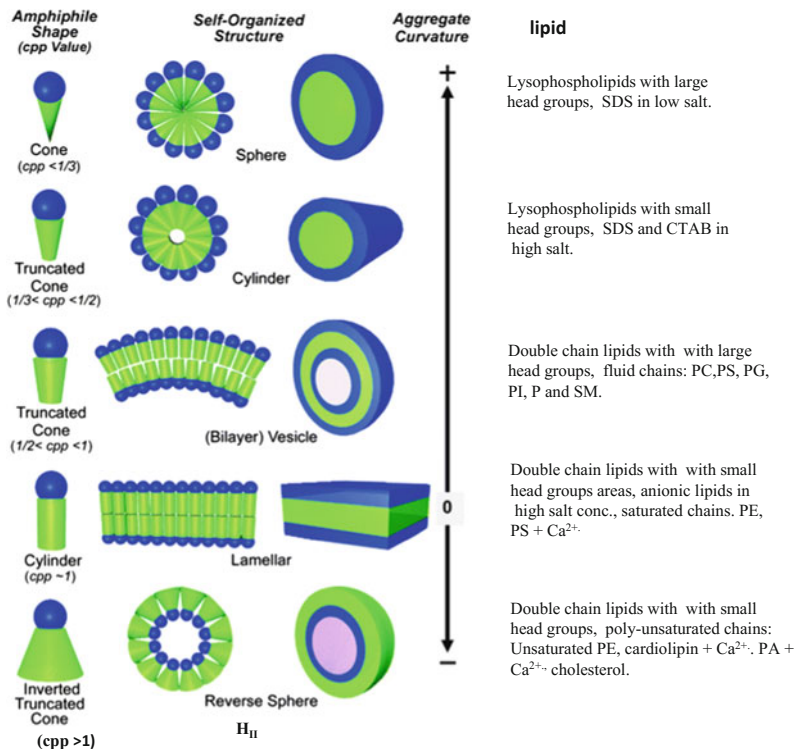


and external variables like temperature, pressure, pH and ionic strength of aqueous phase, and the degree of hydration. Lipid aggregates can take up different shapes like spherical micelles, bilayers, rods, bilayers.

Critical packing parameter of the incorporated lipids determines the most stable aggregate geometry. Critical packing parameter (v/lS_0) is the ratio of the area of the hydrophobic tail region (given by v/l , where v is the volume

occupied by hydrocarbon chains and l is the length of hydrocarbon chains) to the surface area of the polar head group (S_0) (Fig. 2.4). Lipids can be structurally classed as cylinders, cones, or inverted cones based on the relative packing requirements of the two regions, the hydrophobic acyl chains and the polar head groups of the lipid. The critical packing parameter determines the architecture of aggregates formed by different shaped amphiphiles (Fig. 2.5):

Fig. 2.5 Lipid shapes and lipid polymorphic phases. Source Ramanathan et al. (2013)



1. **Spherical micelle:** The sphere micelle is formed by lipids with large ratio of surface area of polar head S_0 to volume of hydrophobic chains (v/l). Lipids with inverted cone shape and critical packing parameter of $<1/3$ form sphere-shaped micelles. For example, amphiphilic molecules with single, small hydrocarbon chain-like SDS in water or solutions of low ionic strength form spherical micelles.
2. **Rod-shaped micelle:** Inverted cone-shaped lipids with critical packing parameter between $1/3$ and $1/2$ form rod- or cylinder-shaped micelles. SDS in high ionic strength solution and lysophospholipids form rod- or cylinder-shaped micelle. High ionic strength lowers the surface area of the polar portion and hence increases the volume to surface ratio.
3. **Bilayer:** Lipids with large hydrophobic volume v , such as lipids with two alkyl chains form cylinder-shaped lipids, with a critical packing parameter between $1/2$ and 1 form stable bilayers. Most membrane phospholipids with cylindrical shape form stable bilayers.
4. **Hexagonal (H_{II}) aggregates:** Lipids which have relatively small polar head groups, cone-shaped, with critical packing parameter >1 , form inverted hexagonal phase (H_{II}) aggregates PS at pH < 4 , and cardiolipin in the presence of Ca^{2+} forms these structures.

Crystalline lamellar (L_c) \leftrightarrow gel phase (L_β) \leftrightarrow
 liquid crystalline (L_α) \leftrightarrow bilayer cubic (Q_{II}^B) \leftrightarrow
 inverted hexagonal (H_{II}) \leftrightarrow inverted micellar
 cubic (Q_{II}^M) \leftrightarrow inverted micelles (M_{II})

With the increase in temperature, a more ordered lamellar crystalline (subgel) L_c phase transforms into lamellar gel L_β phase. Further increase in temperature results in the transition of lamellar gel L_β phase into the disordered lamellar liquid-crystalline L_α phase (Fig. 2.6). This lamellar gel–lamellar liquid-crystalline (L_β – L_α) phase transition is analogous to solid–fluid transition. This results in the increase in disorder in the hydrocarbon chains, headgroup hydration, and intermolecular kinetic energy. Increased hydration of head groups results in large increase in lipid surface area ($\sim 25\%$) and volume ($\sim 4\%$).

On further increase in temperature, a series of phase transitions take place. Some lipids can form two or more intermediate phases, for example, tilted and rippled lamellar gel phases (Fig. 2.3c–e).

Phase transitions can also be brought about by change in degree of hydration at constant temperature. With the increase in degree of hydration at constant temperature, the lipid phase transitions follow the following sequence:

inverted phases ($M_{II}, Q_{II}^M, H_{II}, Q_{II}^B$) $\rightarrow L_\alpha \rightarrow$
 normal phases (Q_I^B, H_I, Q_I^M) \rightarrow
 micellar solution \rightarrow monomers

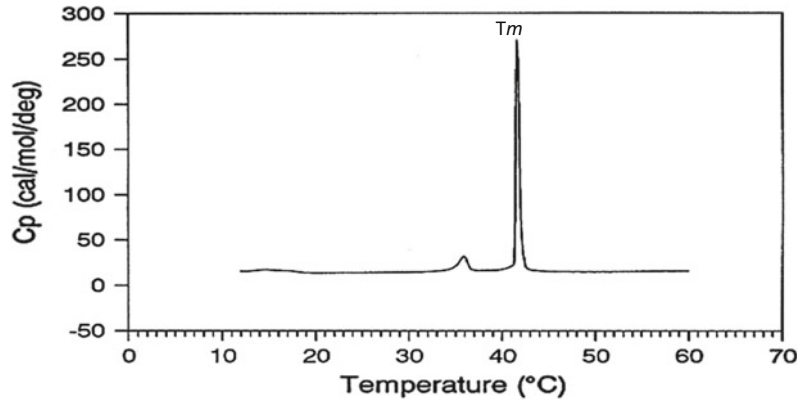
2.3 Lipid Phase Transitions

The different polymorphic lipid phases can transform from one phase to another driven by change in conditions like temperature, pressure, lipid composition, water content. Temperature (thermotropic) and water content (lyotropic) are primary determinants that bring about lipid phase transitions. The thermotropic phase transitions in membrane lipids follow the following sequence:

2.4 Technique Used to Study Lipid Phase Transitions

The **differential scanning calorimetry (DSC)** is a relatively simple and nonperturbing technique for studying the thermotropic phase transitions of hydrated lipid mixtures and of biological membranes. Differential scanning calorimetry (DSC) measures the heat capacity of thermally induced

Fig. 2.6 Differential scanning calorimeter (DSC) scan of phase transition for DPPC (dipalmitoyl phosphatidylcholine)



events/transitions as a function of temperature. It has been used to determine phase transition temperature and associated enthalpy changes of pure single, binary, or ternary mixture of lipids. The amount of heat required to raise the temperature of the sample with respect to a reference standard is measured, when both are maintained at same temperatures. When the sample undergoes a physical transformation, like gel- to liquid-phase transition, being endothermic reaction, much more heat is required by the sample as compared to reference to raise the temperature by one unit.

The gel phase to liquid-crystalline phase transition of pure lipids is characterized by a sharp peak in the heat capacity over a very narrow range of temperature. The process is similar to simple liquid ice/liquid melting. The midpoint of the phase transition, the transition midpoint T_m , is where the transition is 50% complete and is characterized by maximum heat capacity (Fig. 2.6).

2.5 Factors Affecting Lipid Phase Transitions

Phase transition of lipids is affected by various factors which include the following:

1. **Fatty acid chain length:** Longer fatty acid chains have higher surface areas than smaller ones, resulting in stronger van der Waals interactions between long lipid chains. Hence, T_m increases with acyl chain length in lipids (Table 2.2).
2. **Unsaturation in fatty acid chains:** Unsaturation in acyl chains introduces kinks in the acyl chains which prevents tighter packing of adjacent acyl chains. This results in weaker van der Waals interactions between adjacent chains and hence lowers the T_m of the lipid. Introduction of double bond with *cis*-conformation has a larger impact than a double bond with *trans* conformation. As most biological membrane lipids have *cis*-double bond, hence unsaturation in acyl chains reduces the T_m considerably. The position of the double bond in the chain influences the magnitude of the effect, with the maximum decrease in T_m when the *cis*-double bond is near the middle of the chain, as compared to when double bonds are located closer to either end of the chain.
3. **Polar head group:** The size of the polar head groups has an impact on phase transition temperature. Large head groups lower the transition temperature of phospholipids, since they are less “stable” and prevent tighter packing of lipids. Small polar head groups facilitate tighter packing. The vesicles of dipalmitoyl PE and PC have T_m 's of 63 and 41 °C respectively. Saturated phosphatidylethanolamine (PE), which is further stabilized by hydrogen bonding, melts at about 20 °C higher than equivalent phosphatidylcholine (PC).

Table 2.2 Temperatures of melting of some synthetic phospholipids

Fatty acids	The name of the fatty acid residue	Abbreviation	The melting temperature (°C)
14:0	Myristoyl	DMPC	23
16:0	Palmitoyl	DPPC	41
18:0	Stearoyl	DSPC	58
18:1	Oleoyl	DOPC	-21 (<i>cis</i> -form)

3. **Sterols:** Sterols have pronounced effects on the phase transition behavior of lipid membranes. When added to lipids in the gel phase (L_{β}), sterols tend to liquefy the membrane structure by disrupting the highly ordered tilted structure of the hydrocarbon chains. Conversely, cholesterol tends to solidify lipids in the liquid-disordered phase (L_{α}), due to the hydrophobic interaction between the heterocyclic sterol and the lipid acyl chains. In both cases, higher cholesterol concentration results in the formation of an intermediate phase, known as the liquid-ordered (L_o) phase. In the L_o phase, the phospholipid tails have higher order similar to the gel phase, but maintain lateral fluidity similar to the L_{α} phase (Fig. 2.7).

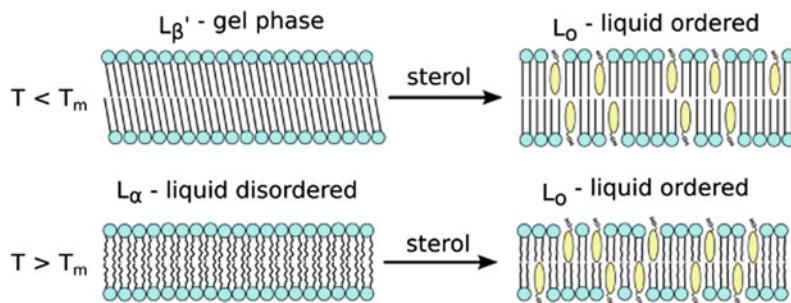
The addition of sterols leads to a dampening and broadening of the enthalpy spikes associated with phase transition (Fig. 2.8), effectively eliminating the phase transitions at higher cholesterol concentrations as the membrane enters the L_o phase. Hence, cholesterol acts as a plasticizer.

Biomembranes are heterogeneous mixtures of lipids with varying composition, differing in acyl chain length, degree of unsaturation, and polar head groups. Lipid phase transitions thus occur at much wider range of temperatures as compared to sharp T_m peaks seen in single lipid studies.

2.6 Polymorphic Lipid Phases and Their Physiological Roles

Biomembranes contain rich diversity of lipids, which can arrange themselves in a variety of morphologies/phases that can play an important role in regulating important membrane-associated processes. Moreover, membranes are organized into domains which have distinct lipid/protein composition, so each domain may be stable in a different polymorphic lipid phase. For example, myelin sheath in neurons is predominantly a gel phase domain.

The polymorphic phases of lipids are important determinants of membrane architecture and function which include:

Fig. 2.7 Sterol-induced liquid-ordered phase

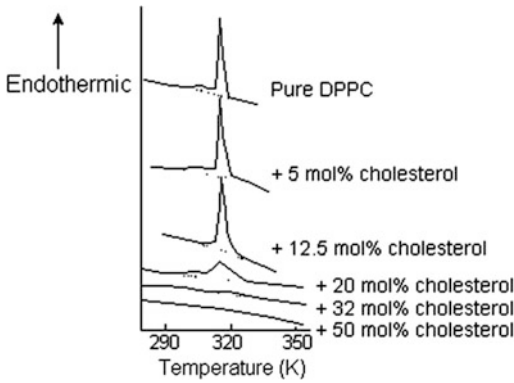


Fig. 2.8 DSC scans for DPPC liposomes as a function of the cholesterol content, and a schematic illustration of the pretransition and the melting transition in DPPC

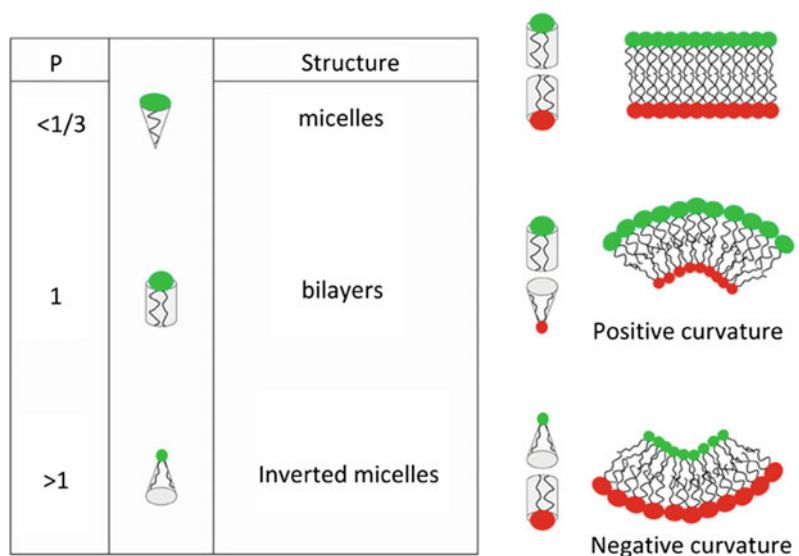
2.6.1 Membrane Curvature

Asymmetric composition of lipids in membranes drives many morphological transformations of the lipid bilayer. Cylindrical lipids like PC and PS form a flat planar monolayer, whereas conical shaped lipids such as PE, PA, DAG, or cardiolipin, with a small polar head group, introduce a negative curvature. A monolayer rich in these conical shaped lipids bends in such a fashion that the head groups come closer together. Conversely, inverted conical shaped lipids like lysophosphatidylcholine (LPC) and phosphatidylinositol phosphates (PIPs)

with a large head group, acyl chain ratio, favor a positive curvature by bending the monolayer away from the head groups (Fig. 2.9). Hence, introduction of conical or inverse conical shaped lipids can introduce negative or positive curvature in the membrane. It has been observed that large positive curvature lipids stabilize the hexagonal I (H_I) phase, whereas large negative curvature lipids stabilize H_{II} or cubic phase. Initiation of membrane curvature is essential for regulating many cellular processes like shaping of organelles like the ER, the Golgi, endosomes, secretory vesicles. For example, H_I phase forms micellar tubules, and hence, lipids present in H_I phase facilitate the formation of ER-like tubular structures. Furthermore, highly curved membranes like the inner mitochondrial membrane, or thylakoid grana margins, are favored by enrichment in H_{II} -forming lipid.

The lipid flippases (type IV P-type ATPases), which translocate phospholipids like PS and PE from the monolayer on the extracellular side to the cytosolic side, regulate membrane curvature by generating a differential partitioning of lipids between the two monolayers. The lipid composition of the monolayers can also be modified by enzymes like lysophospholipid acyltransferases, and phospholipase A, inducing membrane curvature.

Fig. 2.9 Lipid molecular shape and its effect on spontaneous curvature of lipid membranes



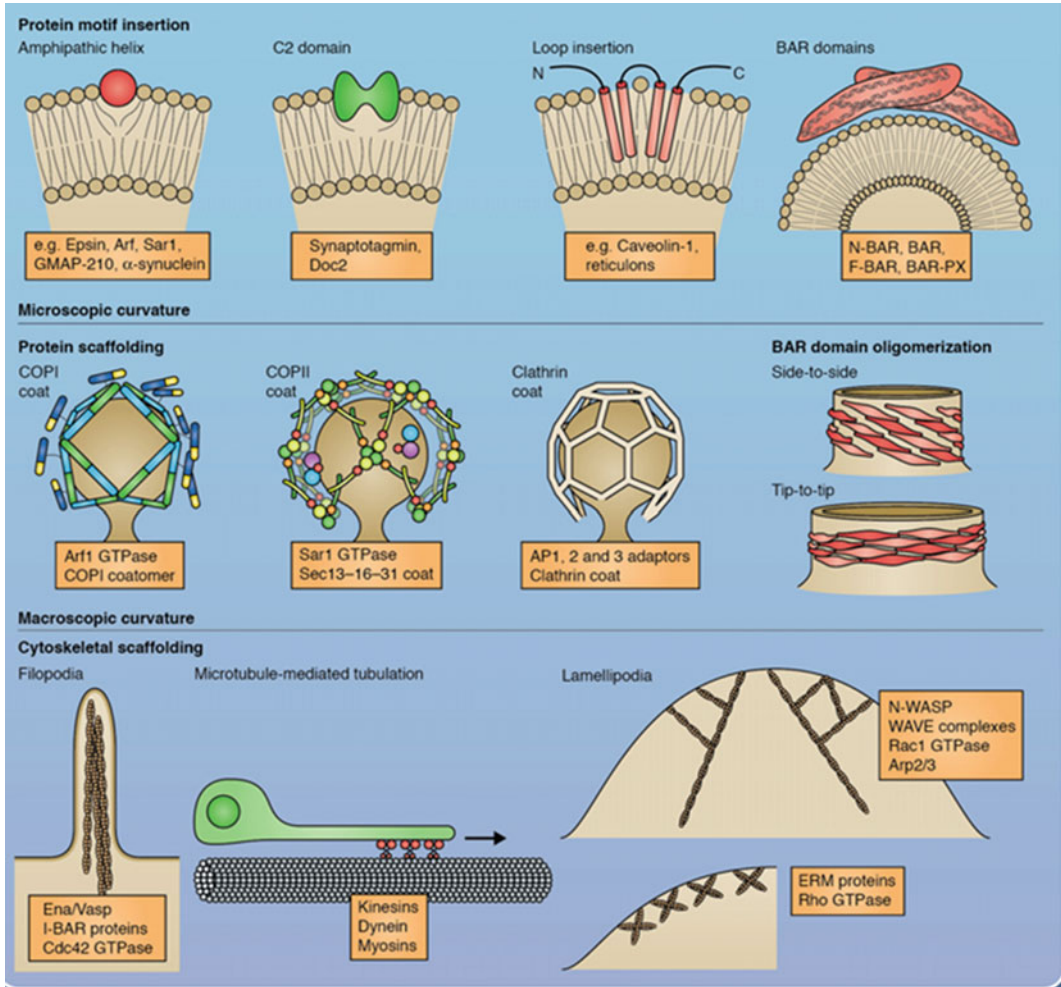


Fig. 2.10 Stabilization of membrane curvature. *Source* McMahon and Boucrot (2015)

Membrane curvature is further stabilized by interactions of various membrane proteins. Curvature can be introduced by insertion of hydrophobic protein domains on one side of the bilayer. These domains can be an amphipathic helix (Arf and Sar1 proteins) or hairpin loops (caveolin-1). Association of oligomerized peripheral proteins like clathrin coat, COPI, and COPII, with the membrane through adapter proteins can also induce membrane curvature. Cytoskeletal elements can create curvature in membranes by polymerization or by stretching the membranes with the help of motor proteins like dynamin. Curved domains of certain proteins like the Bin–amphiphysin–Rvs (BAR) domains

associate with membranes to introduce curvature (Fig. 2.10).

Apart from intracellular tubular network of membranes, membrane curvature is also required in processes like membrane budding, vesicle targeting, and membrane fusion.

2.6.2 Fusion

Lipids which have relatively small polar head groups are cone-shaped, with critical packing parameter >1 , such as dioleoylphosphatidylethanolamine or DOPE, DAG, PS at pH < 4 , cardiolipin in presence of Ca^{2+} , and monogalactosylglyceride. Such

Fig. 2.11 Model of the “blebbing off” process via an inverted cylinder or inverted micellar intermediate. *Source* Cullis and De Kruijff (1979)

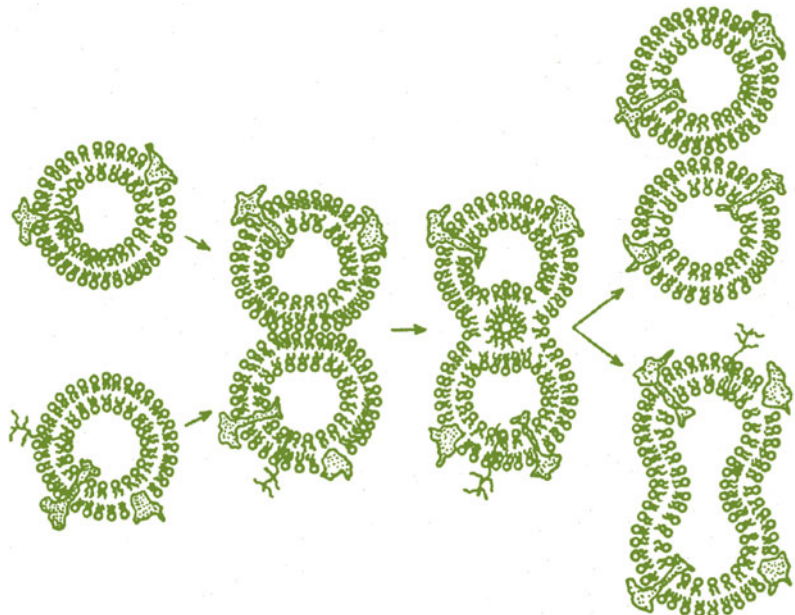


lipids form inverted hexagonal phase (H_{II}). A number of factors like lipid composition, degree of hydration, pH, and cationic concentration can modify lipid phase. For example, a mixture of PE and PC at equimolar concentration at low hydration stabilizes H_{II} phase, whereas forms a bilayer conformation at higher hydration. Acidic (negatively charged) phospholipids such as PS and PA also assume nonbilayer configurations, at higher concentration of divalent cations like Ca^{2+} . In the absence of Ca^{2+} , unsaturated PS adopts the bilayer configuration at high hydration. Hence, increase in Ca^{2+} concentration can stimulate the formation of nonbilayer lipid structures which play a major role in triggering many membrane processes.

Membrane fusion is an important process in vesicular transport in the cell (see Chap. 10). It is well documented that Ca^{2+} is required to initiate membrane fusion. At high intracellular Ca^{2+} concentration, acidic phospholipids like PS and PA show a higher tendency to form hexagonal H_{II} structures. It has now been demonstrated that Ca^{2+} -induced formation of intramembrane inverted micellar or cylindrical (H_{II}) configurations brings about morphological changes in the membrane, resulting in processes like “blebbing off” observed in exocytosis, endocytosis, and membrane fusion (Figs. 2.11 and 2.12).

Nonlamellar lipid assemblies play an important role during the process of acrosome reaction in

Fig. 2.12 Proposed mechanism of membrane fusion proceeding via an inverted cylinder or inverted micellar intermediate. *Source* de Kruijff et al. (1986)



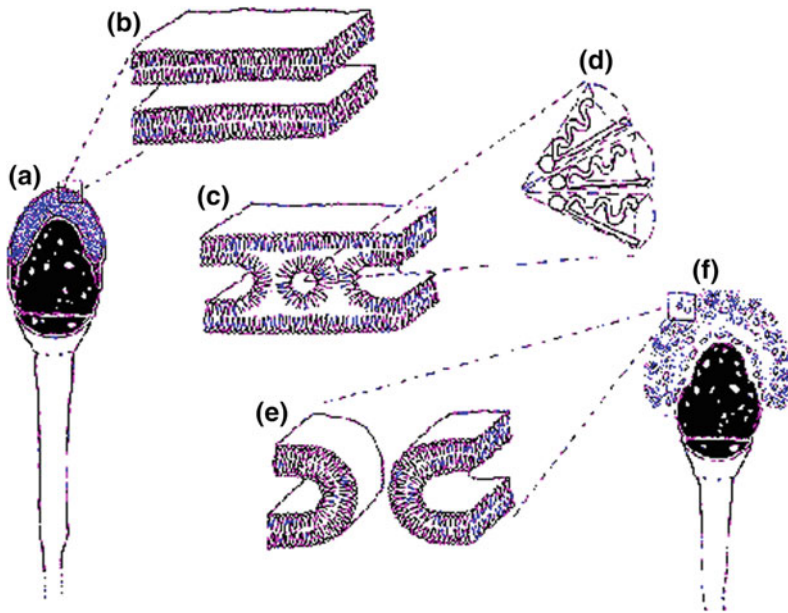


Fig. 2.13 Schematic presentation of the role of lipids in the proposed mechanism of acrosome reaction, via the formation of nonlamellar inverted micellar intermediates. **a** Human non capacitated sperm; **b** apposed plasma membrane (PM) and outer acrosomal membrane (OAM) from human sperm; **c** inverted micellar

intermediate; **d** disposition of the cone-shaped lipids (e.g., polyunsaturated phosphatidylethanolamine plasmalogen) in the formation of a rod-inverted micelle; **e** formation of lamellar vesicles; **f** acrosome-reacted sperm. Adapted from Yeagle (1994)

sperm. The acrosome reaction starts with the fusion of plasma membrane with the outer acrosomal membrane to form vesicles and the release of hydrolytic acrosomal enzymes (Fig. 2.13).

transport of lipids and polar molecules across the membrane (Fig. 2.14).

2.6.3 Transbilayer Transport

Change in lipid composition favors H_{II} structure. The inverted micelle formed can fuse with the opposite monolayer, resulting in transbilayer

2.6.4 Lipid Rafts

Lipid rafts, which are cholesterol- and sphingolipid-rich domains, form liquid-ordered phase, the gel phase which is distinct from the regular liquid-crystalline (disordered) phase in membranes (see Chap. 4).

Fig. 2.14 Inverted micelle H_{II} intermediate formation in transbilayer (flip-flop) transport of molecules

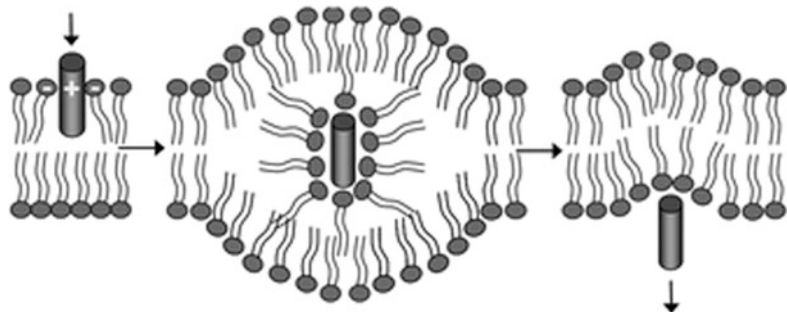
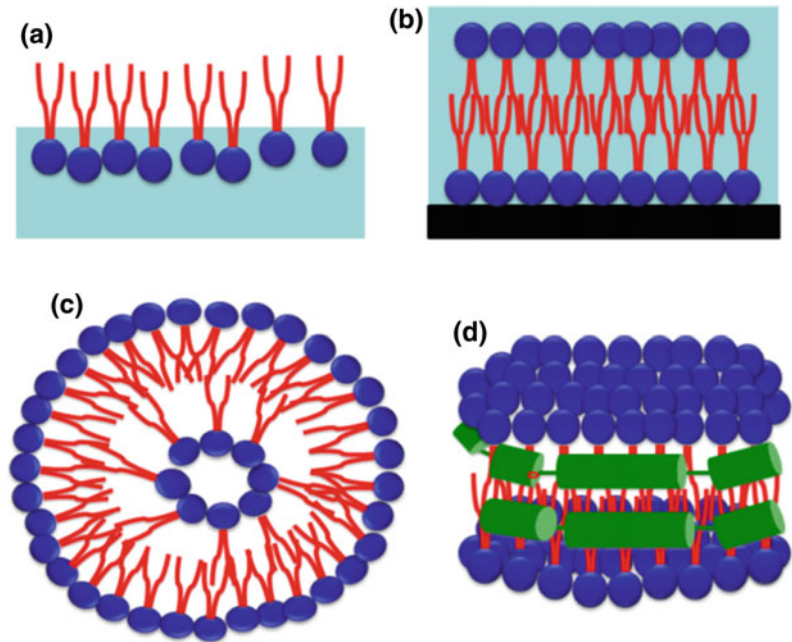


Fig. 2.15 Schematic drawings of model membranes: **a** Monolayer, **b** supported lipid bilayer, **c** liposomes, and **d** nanodisk. Phospholipids contain two fatty acid tails, shown in red, and a hydrophilic head group, shown in blue. Light blue (**a** and **b**) and black in **b** represent water and a substrate, respectively. Nanodisks contain membrane scaffold proteins, shown in green. *Source* Shen et al. (2013) (Color figure online)



2.7 Model Membrane Systems

Various model membrane systems have been developed to study various biophysical and biochemical parameters of membrane structure and function. Bilayer structure and properties have been studied using model membrane systems prepared with single lipids, lipid mixtures, and lipid and protein mixtures. The various model membrane systems developed include (1) monolayers, (2) planar bilayer, (3) liposomes, (4) nanodisk (Fig. 2.15).

Each of these model systems provides certain advantages and also has certain limitations.

2.7.1 Lipid Monolayers

Amphipathic lipid molecules when put in aqueous solution spread as a monolayer at the air–water interface, with hydrophobic chains oriented toward air and polar head groups in contact with aqueous phase (Fig. 1.1). The phospholipid monolayer which is a prototype of one leaflet of a phospholipid bilayer has been extensively used

to study interactions between lipids and lipid protein mixtures. Traditionally, Langmuir trough (see Chap. 1) has been used for studies involving lipid monolayers at air–water interface.

Lipid monolayers are formed when an aliquot of desired amount of lipid or lipid mixtures in volatile organic solvent are spread on the aqueous surface. Langmuir trough film balance allows one to accurately measure the surface area (A) and lateral pressure (π) required to maintain the monolayer. Pressure area curves of monolayers help us to study phase transitions from “liquid-like” phase to more solid-like “gel phase” when monolayers were compressed. “Collapse point” is the point at which molecules in the monolayer are most tightly packed, and any further compression can result in breakdown of the monolayer. This two-dimensional system can be used to study surface area occupied in relation to surface pressure, ionic strength, pH, temperature, and lipid composition. Phase transition studies and lipid–lipid interactions w.r.t changing surface pressure can be studied.

Phospholipid monolayers are less useful for studies involving intrinsic membrane proteins, but are suited to study the interaction of

peripheral proteins at the membrane surface. The kinetics and enzymology of peripheral proteins like phospholipases, which associate and act on phospholipids at lipid water interface, can be studied.

2.7.2 Supported Planar Lipid Bilayer

Tamm and McConnell in 1985 for the first presented a planar lipid bilayer on a hydrophilic solid support as a new model membrane system to study the properties of biological membranes.

The simplest method for the formation of supported planar lipid bilayer is by vesicle fusion. The bilayer can be prepared by the fusion of small unilamellar vesicles. The vesicles are then deposited on the hydrophilic solid support such as SiO₂ and glass and held immobile by van der Waals, electrostatic, and steric forces. However, one monolayer of the bilayer is attached to the solid support affecting membrane fluidity and consequently biological functions. But, the hard support at one end of supported bilayers also offers certain advantages in using mechanical probing techniques like atomic force microscopy, and other techniques.

Although the supported bilayers are not in direct contact with the solid support and have a very thin water gap between them, the interactions between the support and the bilayer restrict the movement of molecules, especially the integral membrane proteins. Polymer-supported planar lipid bilayer has been developed, to investigate the functioning of reconstituted integral membrane proteins into the supported lipid bilayer. Supported planar lipid bilayer has been designed with a polymer (polyethylene glycol) cushion (Fig. 2.16) to minimize the interactions of membrane proteins with the solid support. It also provides a soft support linking the membranes to the supporting quartz or glass supports. At low polyethylene glycol concentration, the bilayers show higher lateral lipid diffusion coefficients ($0.8\text{--}1.2 \times 10^{-8} \text{ cm}^2/\text{s}$) of constituent molecules.

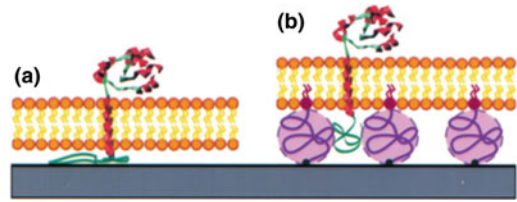


Fig. 2.16 Supported lipid bilayers: **a** The reconstitution of integral membrane proteins into supported lipid bilayer. **b** Polymer-supported lipid bilayers are designed to space the lipid bilayer from the support. Purple represents the polymer cushions which are assembled on a support, shown in blue (Color figure online)

2.7.3 Planar Bilayer at the Tip of Patch Pipette

The patch-clamp technique offers the advantage of studying electrical properties of an ion channel in cell-like environment. Bert Sakmann and Erwin Neher in the late 1970s developed the patch-clamp technique and studied the current flow across a single ion channel in a membrane patch of a frog skeletal muscle. Neher and Sakmann received the Nobel Prize in Physiology and Medicine in 1991 for this study.

A glass pipette called the patch pipette is filled with electrolyte solution and is sealed onto the cell membrane with the application of suction. This can isolate a single ion channel in the membrane patch (Fig. 2.17). The transport of ions across the channel in the membrane patch into the pipette can be recorded by a microelectrode. Recording of this current helps in the understanding of electrophysiology of excitable cells. Several variations of the basic technique have been developed, for example, the whole-cell, outside-out, and inside-out techniques. These techniques are also known as “excised patch” techniques, as the membrane patch is excised (removed) off from the membrane of the cell. In whole-cell technique, the cell membrane is ruptured by applying strong suction and the pipette is exposed to the cytoplasm. In the outside-out mode, the pipette is pulled back, rupturing the membrane, and the resulting two small pieces of membrane reseal to form a small

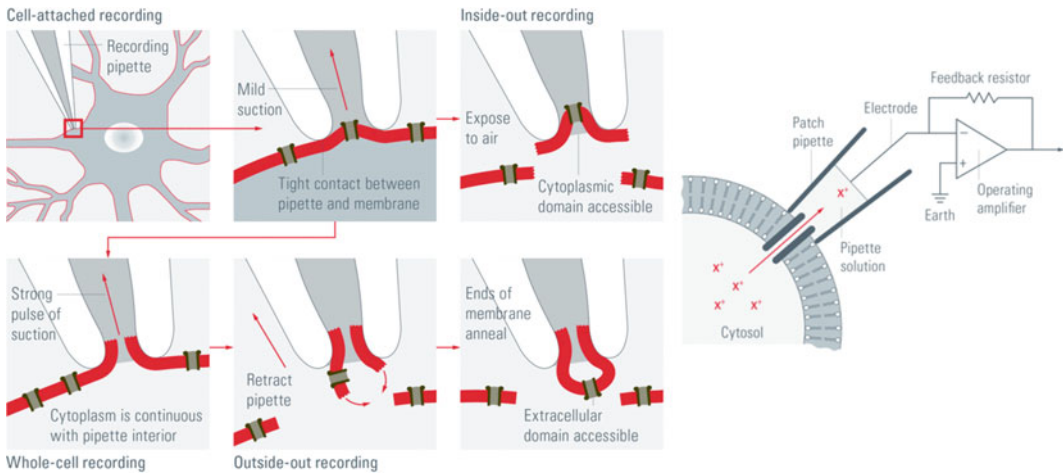


Fig. 2.17 The four patch-clamp methods: (1) Cell-attached: when the pipette is in closest proximity to the cell membrane, mild suction is applied to gain a tight seal between the pipette and the membrane. (2) Whole-cell: by applying another brief but strong suction, the cell membrane is ruptured and the pipette gains access to the cytoplasm. (3) Inside-out: In the cell-attached mode,

the pipette is retracted and the patch is separated from the rest of the membrane and exposed to air. The cytosolic surface of the membrane is exposed. (4) Outside-out: in the whole-cell mode, the pipette is retracted resulting in two small pieces of membrane that reconnect and form a small vesicular structure with the cytosolic side facing the pipette solution. *Source* Molleman (2003)

vesicular structure with the cytosolic side facing the pipette solution. Whereas the in the inside-out mode the pipette is pulled, separating the patch from the rest of the membrane and exposed to air. The inside-out clamp exposes the cytosolic side of ion channel amenable to different studies.

Another variation patch clamp is developing planar membranes over the tip of a small pipette. The formation of bilayers on patch-clamp pipettes from phospholipid monolayers is a powerful technique for the reconstitution of channels of excitable membranes. Bilayers are formed by moving a saline-/buffer-filled patch-clamp pipette out and into a solution that sustains a lipid monolayer at the air–water interface. The lipid monolayer can be spread on the surface of the solution in which the patch clamp is dipped in and out, by adding to the edge of the container the lipid solutions in volatile solvents like pentane, dry lipids, or vesicle suspensions (Fig. 2.18).

This small patch of planar bilayer in the “patch pipette” can be useful tool for sensitive electrical measurements with reconstituted ion channels.

2.7.4 Liposomes

Liposomes were discovered by British hematologist Alec Douglas Bangham in 1961 as lipid bilayer structures which enclose a volume. Bangham had called his lipid structures “multilamellar smectic mesophases” also known as “Banhasomes.” It was Weissmann who later proposed the term “liposome” after the lysosome, which his laboratory had been studying. Liposomes are spherical vesicles that may have one or many bilayer membranes/lamellae. The liposomes can be classified into two categories based of their size and number of bilayers/lamellae: (1) Multilamellar vesicles (MLVs) have multiple bilayers/lamellae separated by layers of aqueous solution, and (2) unilamellar vesicles are made of single phospholipid bilayer with enclosed aqueous core. Unilamellar vesicles can be further classified into two categories: (1) large unilamellar vesicles (LUVs), with diameters in the range of 500–5000 Å, and (2) small unilamellar vesicles (SUVs), with diameters in the range of 200–500 Å. Liposomes can serve as model

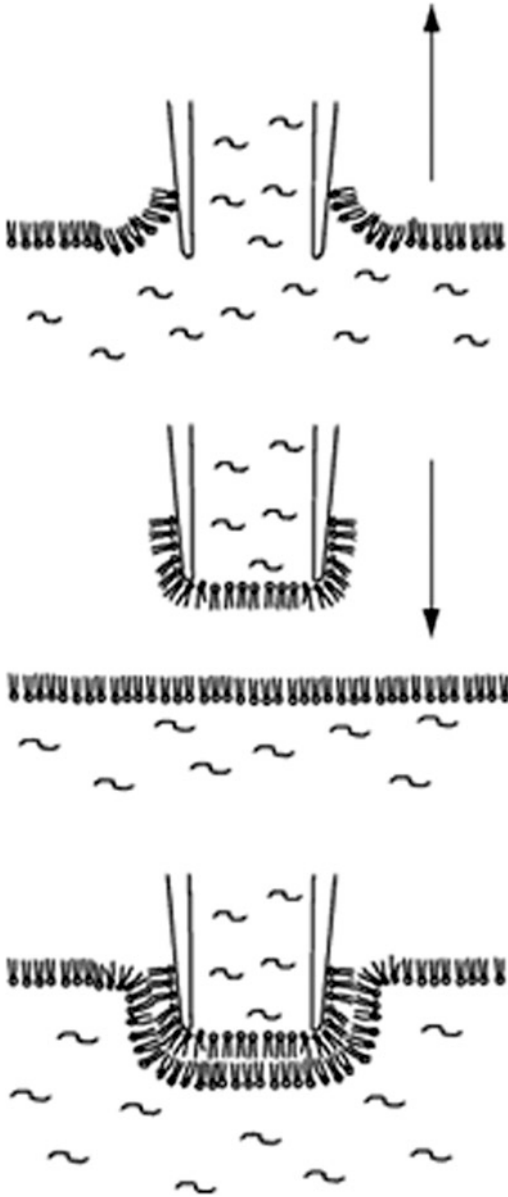


Fig. 2.18 Scheme of lipid bilayer formation at the tip of patch pipette. A monolayer is first derived by dipping the pipette into the solution containing lipid–protein vesicles under positive pressure. The monolayers adhere to the glass pipette by interactions with the lipid head group, leaving the hydrocarbon tails in contact with air. The pipette is then reimmersed into the solution forming a bilayer

membrane system to study the functioning of membrane-associated proteins. Liposomes have also been used as carriers and delivery systems of

encapsulated solutes and drugs to targeted body tissues and organs.

Liposomes can be prepared by many techniques. One of the techniques used is **reverse-phase evaporation**. Mixture of phospholipids is dissolved in an organic solvent, and the solvent is then evaporated from the mixture at low pressure. The resulting lipid film is then hydrated with a solution containing proteins of interest, resulting in the formation of multilamellar vesicles (MLVs). Liquid suspension of MLVs is sonicated to generate unilamellar vesicles (ULVs). To get the desired sized vesicles, sizing can be done using gel filtration chromatography or density gradient centrifugation.

Liposomes can also be prepared using detergents. Excess detergent is codispersed with the lipid or lipid and protein mixture, and the detergent is then removed by dialysis or by dilution. As detergent is removed, phospholipid–detergent or phospholipid–protein–detergent mixture forms LUVs. Detergent with high CMC (e.g., cholate, deoxycholate, octylglucoside) can be removed by dialysis, whereas detergents with a low CMC (e.g., Triton X-100) are removed by simply diluting the mixture to finally reduce the detergent concentration to a point where the lipids spontaneously form liposomes.

2.7.4.1 Applications

Liposomes have been extensively used as model membrane system to study several membrane proteins, transporters, and ion channels by reconstituting these proteins in liposomes. SUVs have been used to study the impact of membrane curvature on membrane protein function. LUVs are the preferred liposomes to study membrane function. Effect of composition of annular and nonannular lipids on membrane function has also been studied. Liposomes have been used to study the kinetics, substrate specificity, obligatory cotransporters, agonists and antagonists of various transporters, and ion channels.

Liposomes have also been used as drug delivery systems. Liposomes provide a biocompatible, biodegradable, and less toxic drug delivery system with the ability to carry both hydrophilic and lipophilic drugs for site-specific

targeting. Yet some modifications have to be made for liposomes to act as drug delivery system in the human body. The liposomes are recognized as foreign object by the mononuclear phagocytic system (MPS) and are then cleared from the blood circulation via endocytosis. Hence, they accumulate in the MPS. They have been used as ideal drug targeting vehicles into the phagocytic cells of the reticuloendothelial system. Several parasitic diseases associated with the cells of MPS like leishmaniasis and several fungal infections can be treated by liposome-encapsulated drugs. The effective dose of drugs, different antimonials in case of leishmaniasis and amphotericin B in antifungal therapy, is highly toxic. Fungal infections are common in immunosuppressed patients with AIDS or undergoing chemotherapy, and antifungal therapy in such patients often proves fatal. Liposome-encapsulated drugs reduce the dosage requirement by site-specific passive targeting to the MPS and hence reduce the associated toxicity and increased efficacy.

To target liposomes to other tissues or organs, liposomes have to evade the MPS; for this, liposomes are coated with PEG, which makes them stealth, and hence are not recognized by the MPS. Thus, liposomes are not taken up by MPS, and consequently, the liposomes are retained in the blood circulation for a longer period of time. Specific targeting or homing of liposomes is done by coating the liposomes with antibodies or ligands that bind to tissue-specific cell surface proteins. Doxorubicin-loaded and PEG-coated stealth liposomes have been used successfully for the treatment of tumors with homing markers.

2.7.5 Nanodisks

Nanodisks, developed by Bayburt and Sligar a decade ago, are soluble phospholipid bilayers in which integral membrane proteins are assembled with the purpose to study their structure and function in aqueous environment. Studying membrane proteins has always been a challenge.

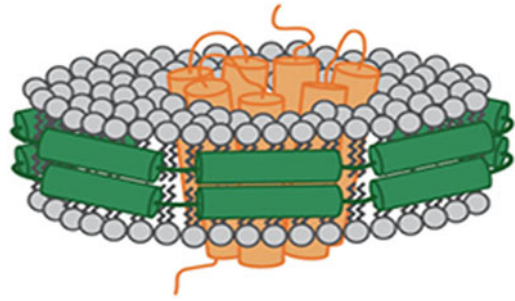


Fig. 2.19 Schematic image of a membrane protein reconstituted into a nanodisk. Green: membrane scaffold protein (MSP), Gray: phospholipids, Orange: reconstituted membrane protein (Color figure online)

Nanodisks form a phospholipid bilayer system, held together by membrane scaffold proteins (MSPs). These MSPs are amphipathic helical segments of apolipoprotein A-1 which wrap around the phospholipid bilayer like a belt, to form a nanodisk. The hydrophobic surface of MSPs interacts with the bilayer lipids and the hydrophilic surface with the surrounding aqueous solution, making nanodisks soluble in aqueous solutions. The diameter of the nanodisk can be modified by changing the number of amphipathic helices of apolipoprotein A-1 by genetically engineering so as to accommodate membrane proteins of various sizes. Membrane proteins assembled into nanodisks can thus be exposed to aqueous solution without the requirement of detergents (Fig. 2.19).

Nanodisks can be prepared by solubilizing phospholipids and membrane scaffold proteins using a detergent, to form a micelle mixture. The detergent is then removed by dialysis or bio-beads adsorbent, resulting in the self-assembly of nanodisks.

Nanodisks provide native phospholipid bilayer-like environment to membrane proteins that is stable, soluble, and free of detergent. Nanodisks have been used to study proteins of varied sizes, including CytP450, GPCRs, transport proteins. It provides the natural conditions to study binding of ligands, interactions of signaling molecules, and functioning of molecular motors in membranes.

2.7.6 Black Lipid Membranes (BLMs)

Mueller et al. (1962) developed the earliest bilayer model system known as the “black lipid membrane” (BLM). To make BLMs, a small hole of diameter of $\sim 10\text{--}100\ \mu\text{m}$ is first made in a thin sheet of a hydrophobic material such as Teflon. The hole is then painted with a solution of lipids dissolved in a hydrophobic solvent. The hydrophobic solvent used should be of very high viscosity to prevent rupture. A mixture of decane and squalene is the most commonly used solvent. After drying of the coat over the hole, both sides of the chamber are filled with aqueous solutions. The hole is painted again with the same lipid solution. A lipid monolayer is formed at the interface of the coated organic solvent and the aqueous chamber solution on either side of the hole. The lipid monolayers fuse at the center of the hole, forming a bilayer. Some residual solvent that remains attached at the edges maintains the stability of the bilayer by acting as a bridge between the bilayer and the thin hydrophobic sheet (Fig. 2.20).

The BLMs are called “black” bilayer because they are dark in reflected light, as the bilayer formed is only few nanometer thick, so light

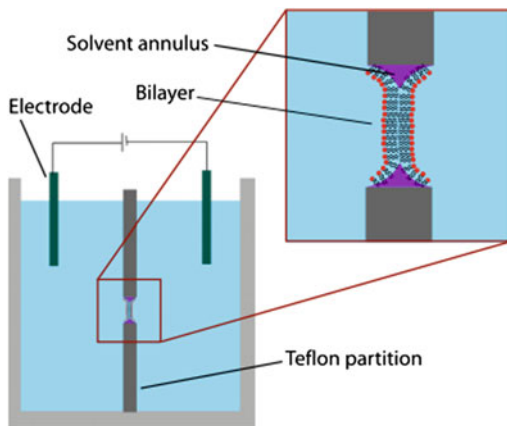


Fig. 2.20 Schematic diagram of a painted bilayer. A sheet of plastic with a small hole in the center separates the two sides of the chamber. The bilayer is formed across this hole, separating the two chambers. The electrical properties of the bilayer can be measured by putting an electrode into each side of the chamber

reflected by the two surfaces interfere with each other. Black lipid membranes are well suited to study electrical transport across the two chambers separated by the bilayer, by use of large electrodes.

The painted bilayers have very low stability, and the residual solvent trapped between the two monolayers of the bilayer can interfere with the normal functioning of the incorporated membrane proteins. A modified technique has been developed that uses volatile solvent such as chloroform, instead of heavy nonvolatile solvent. In this method, lipids dissolved in a volatile solvent such as chloroform are applied to form a monolayer. The solvent is then allowed to evaporate. The chambers are then filled with aqueous solution, and the two monolayers fold down against each other, forming a bilayer across the hole.

References

- Bangham AD, Standish MM, Watkins JC (1965) Diffusion of univalent ions across the lamellae of swollen phospholipids. *J Mol Biol* 13:238–252
- Bayburt TH, Sligar SG (2010) Membrane protein assembly into Nanodiscs. *FEBS Lett* 584:1721–1727
- Cullis PR, De Kruijff B (1979) Lipid polymorphism and the functional roles of lipids in biological membranes. *Biochim Biophys Acta* 559:399–420
- de Kruijff B, Cullis PR, Verkleij AJ, Hope MJ, Van Echteld CJA, Taraschi TF (1986) Lipid polymorphism and membrane function. <http://www.liposomes.ca/publications/86%20Cullis%20et%20al%201986.pdf>
- Koynova R, Tenchov B (2013). Transitions between lamellar and non-lamellar phases in membrane lipids and their physiological roles. *OA Biochem* 1(1):1–9
- Luzzati V (1968) X-ray diffraction studies of lipid-water systems. *Biol Memb* 1:71–123 (D. Chapman (ed), Academic Press, London)
- McMahon HT, Boucrot E (2015) Membrane curvature at a glance. *J Cell Sci* 128:1065–1070. <https://doi.org/10.1242/jcs.114454>
- Molleman A (2003) Patch clamping: an introductory guide to patch clamp electrophysiology. John, West Sussex, England.
- Mueller P, Rudin DO, Tien HT, Wescott WC (1962) Reconstitution of excitable cell membrane structure in vitro. *Circulation* 26:1167–1170
- Neher E, Sakmann B, Steinbach JH (1978) The extracellular patch clamp: a method for resolving currents through individual open channels in biological membranes. *Pflügers Arch* 375:219–228

- Ramanathan M, Shrestha LK, Mori T et al (2013) Nanoarchitectonics: from basic physical chemistry to advanced applications. *Phys Chem Chem Phys* 15:10580–10611
- Seddon JM, Templer RH (1995) Polymorphism of lipid-water systems. In: Lipowsky R, Sackmann E (eds) *Handbook of biological physics*, vol. 1. Elsevier Science
- Shen H, Lithgow T, Martin LL (2013) Reconstitution of membrane proteins into model membranes: seeking better ways to retain protein activities. *Int J Mol Sci* 14:1589–1607
- Yeagle PL (1994) Lipids and lipid-intermediate structures in the fusion of biological membranes. *Curr Top Membr* 4:197–214

3.1 Types of Membrane Proteins

Membrane proteins are the functional components of the membrane and are involved in vital biological functions such as transport of molecules, energy transduction, signal receptor and transmission, cell–cell recognition and interaction, and enzyme catalysis and also maintain the integrity and shape of the cell. Membrane proteins are of great interest as possible targets of drugs for the treatment of whole range of diseases. Elucidation of structure and function of many membrane proteins have increased our understanding of the cause and new approaches for treatment of diseases.

The membrane proteins uniquely function in a highly anisotropic (hydrophobic interior and hydrophilic surface) lipid environment. Additionally, membrane proteins maintain their three-dimensional structure and its functional state in a highly dynamic, yet restrictive fluid state of membranes.

The Singer and Nicolson's (1972) fluid mosaic model (Fig. 1.10) proposed two major types of membrane proteins, the **peripheral or monotopic proteins**, that loosely associated with the membrane surface by noncovalent interactions and can easily be released from the membrane by mild treatment like change in pH or ionic strength, and the **integral or transmembrane proteins** that firmly associated with the membrane span through the bilayer and can only be solubilized using harsher conditions like detergents, organic solvents, or denaturants.

It was in early 1960s when the first protein structure of myoglobin was determined by protein crystallography by Max Perutz and John Kendrew, but it took another twenty years before first structure of membrane protein, of the photosynthetic reaction center of *Rhodospseudomonas viridis* was determined by Deisenhofer et al. in 1985. A lot of advancement in technology and new tools has expanded our knowledge about the structure of membrane proteins. Protein structure predictions can be made using bioinformatics tools. The protein forms secondary structures based on its primary sequence. A series of secondary structures determine the three-dimensional structure of a protein. Sequences of proteins of unknown structure can be matched with the sequences of proteins with known structure. Databases like Structural Classification of Proteins (**SCOP**) are used for structural comparison. SCOP classifies proteins in different hierarchical levels. Proteins with common evolutionary origin are grouped into a *Family*. *Families* which have low sequence homology, but have similar structure, are grouped under *superfamilies*, as they appear to have an evolutionary relationship. Families and superfamilies of proteins have a common *fold*, or a motif, which is formed by the arrangement of the secondary structure units of the protein in a particular pattern. The different folds are grouped into *classes*, for example, all-alpha, all-beta, and alpha and beta classes. The Class, Architecture, Topology, Homologous (CATH) superfamily database classifies protein domains based on their folding patterns. *Domains*

are protein segments that fold and function independent of the rest of the segments of a protein.

Almén et al. in 2009 gave the detailed map of the gene repertoire of human membrane proteins. The total human proteome of 69,731 protein sequences from the International Protein Index (IPI) dataset was used. A dataset of 13,208 human membrane proteins was created based on consensus predictions of α helices with three applications: **Phobius** (a combined transmembrane topology and signal peptide predictor), **TMHMM** (prediction of transmembrane helices in proteins), and **SOSUI** (classification and secondary structure prediction of membrane proteins). By aligning all predicted membrane proteins to the human genome with BLAST-like alignment tool (BLAT) and databases that specialized in receptors like Human Plasma Membrane Receptome (HPMR), transporters like the Transporter Classification Database (TCDB) for membrane transport protein analyses and information, and enzymes (BRENDA: The Comprehensive Enzyme Information System) were used, and 6,718 unique human membrane proteins were identified and classified into groups. The membrane proteins were grouped into 234 families of which 151 belong to the three major functional groups: 63 groups belonged to membrane receptors with 1,352 members, 89 groups of transporters with 817 members, and 7 groups of enzymes with 533 members. Certain membrane topologies are associated with different functional classes, for example, 77% of all transporters have more than six helices while 60% of proteins with an enzymatic function and 88% receptors have only one single membrane spanning α helix except for GPCRs which have seven transmembrane helices.

3.1.1 Peripheral Proteins

Peripheral proteins associate with lipid bilayers reversibly. These proteins interact with integral membrane proteins, or lipids, or peripherally penetrate the lipid bilayer. Numerous membrane-

associated enzymes, transporters, signaling peptides, antibacterial peptides, hormones, toxins, etc., are peripherally associated with membranes. Membrane-associated peripheral proteins can modulate membrane shape, lipid composition, membrane fluidity, and function. They play fundamentally important regulatory role in a variety of cellular processes including cytoskeletal interactions, vesicular trafficking, and signal transduction.

Peripheral membrane proteins interact with membranes through various types of interactions; these include hydrophobic and electrostatic interactions with membrane lipids, and with other membrane proteins.

3.1.1.1 Peripheral Protein–Membrane Hydrophobic Interactions

Many peripheral proteins have specific membrane-targeting domains which associate with specific lipid head groups which form the lipid bilayer. Due to lipid asymmetry in membranes and distinct composition of organelle membranes, different lipid head groups are present in different membranes in different concentrations, for example, PI3P are found predominantly in membranes of early endosomes, PI(3,5)P₂ in late endosomes, and PI4P in the Golgi. Hence, a specific membrane-targeting domain in a protein can target it to a specific membrane. More than ten membrane-targeting domains have been identified, which include C1, C2, PH, PX, FYVE, ENTH, BAR, and PDZ (Fig. 3.1).

C1 domains were first identified in protein kinase C (**PKC**), as binding sites for DAG and phorbol esters. C1 domains which do not bind to DAG/phorbol esters have been found in many proteins such as chimerins. Such C1 domains are called **atypical**, and those that bind to DAG are called **typical** C1 domains. C1 domain has a compact structure of ~ 50 amino acids, rich in cysteine residues. It contains five short β strands, a short α helix, with two zinc ions linked by coordination bonds. PKC δ C1B domain has a polar pocket for DAG/phorbol ester binding located at the tip of the molecule, and this pocket

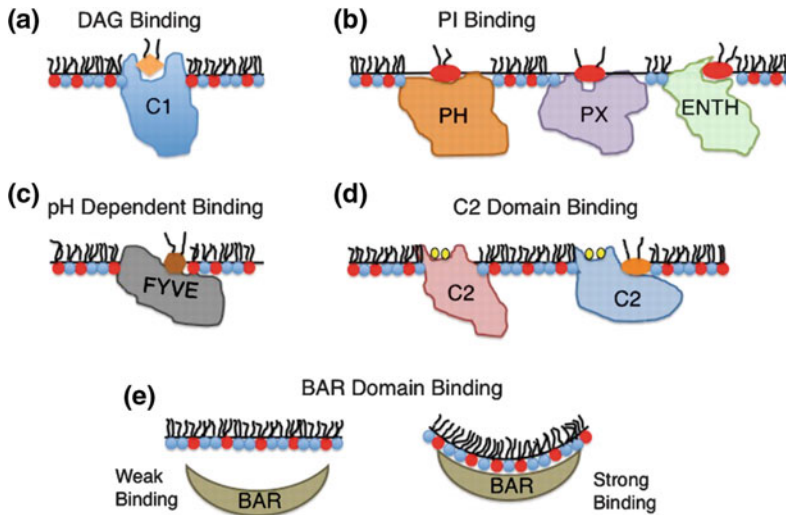


Fig. 3.1 Membrane lipid-binding domains of peripheral proteins. **a** C1 domain hydrophobic interactions associate with DAG or phorbol esters. **b** PH domains can bind a variety of PIs. PIs induce the membrane penetration of PX domains through a reduction in the desolvation penalty surrounding exposed hydrophobic residues adjacent to the PI binding site. The ENTH domain coordinates PIP₂, which induces formation of a N-terminal α helix from an unstructured region. The amphipathic α helix then inserts into the membrane to induce changes in membrane curvature. **c** FYVE domains selectively bind PtdIns(3)P at a site adjacent to the hydrophobic membrane protrusion

loop. **d** Two modes of binding are depicted for C2 domains. Ca²⁺ ions are shown in yellow. Ca²⁺-binding C2 domains can associate with anionic or zwitterionic membranes depending upon the residues present in their Ca²⁺-binding loops. Some C2 domains contain a patch of cationic residues in their β groove that is able to bind lipids such as PIs. **e** Many BAR domains resemble the shape of a crescent moon and are rich in cationic residues on their concave surface. Thus, many BAR domains selectively associate with membranes of high curvature due to the shape of their concave surface. *Source* Stahelin (2009) (Color figure online)

is surrounded by hydrophobic and aromatic residues that penetrate the membrane to stabilize the protein and facilitate DAG binding.

C2 domain is present in proteins such as PKC, phospholipase C, and phospholipase A₂ (cPLA₂ α), which bind to membranes mediated by Ca²⁺. Ca²⁺ ions provide a bridge between the C2 domain and anionic phospholipids like PS. Ca²⁺-binding loops of C1 domain play an important role in phospholipid selectivity and binding with anionic membranes. Different isoforms of PKC contain both C1 and C2 domains.

Pleckstrin homology (**PH**) domains, **PX** domains (phox domains of NADPH oxidase, where phox stands for phagocytic oxidase), and Tubby domains bind to different phosphoinositides. The PH domain a ~ 100 amino acid domain is the most abundant lipid-binding

domain. It binds to different phosphoinositides, which include PIP₃, PI(4,5)P₂, and PI(3,4)P₂. Most PH domains have a conserved sequence [*K-X_n-(K/R)-X-R*] in which the basic lysines and arginines are involved in forming H-bonds with the PI head group.

FYVE, ENTH, and ANTH domains are also phosphoinositides-binding domains, with FYVE domain being more specific for PI3P, ENTH for PI(3,4)P₂ or PI(4,5)P₂, and ANTH for PI(4,5)P₂.

The Bin/Amphiphysin/Rvs (BAR) domain forms a banana-shaped dimer of six helices with positive charges along its concave surface which bind to phospholipids and induce membrane curvature. BAR domain containing proteins include the proteins involved in endocytosis, such as, endophilins, and amphiphysins, and other proteins like RhoGAPs and RhoGEFs.

3.1.1.2 Peripheral Proteins–Membrane Electrostatic Interactions

The peripheral membrane proteins also associate with membranes via electrostatic interactions. Proteins such as Src, K-Ras, and myristoylated alanine-rich C-kinase substrate (MARCKS) have a stretch of basic amino acids, which interact with acidic phospholipids and in the inner leaflet of the plasma membrane via nonspecific electrostatic interactions. In MARCKS protein, a stretch 13 positively charged basic residues interact with negatively charged acidic membrane lipids, such as phosphatidylinositol 4,5 biphosphate (PIP₂) and phosphatidylserine (PS) molecules (Fig. 3.2).

3.1.1.3 Interaction with Other Membrane Proteins

Peripheral proteins reversibly associate with integral membrane proteins. For example, G

proteins interact reversibly with G-protein-coupled receptors (GPCRs), the seven trans-membrane integral membrane proteins to regulate the activity of effector systems of signal transduction pathways (Fig. 3.3). The 2012 Nobel Prize in Chemistry was awarded to Brian Kobilka and Robert Lefkowitz for their work on G-protein-coupled receptors (Kobilka 2007).

Peripheral proteins may have specific domains targeting membrane proteins, such as **PDZ**, **SH2**, **SH3**, and **PTB** domains. PDZ (stands for post-synaptic density protein, in which it was first discovered) domains are small domains consisting of 6 β stranded and small and long α helical strands. PDZ domains recognize and bind to the C-termini of target proteins. The Src **Homology 2 and 3 (SH2 and SH3) domains** are present in proteins participating in signal transduction pathways. SH2 domains dock the proteins to specific phosphotyrosine sequence in membrane-associated proteins

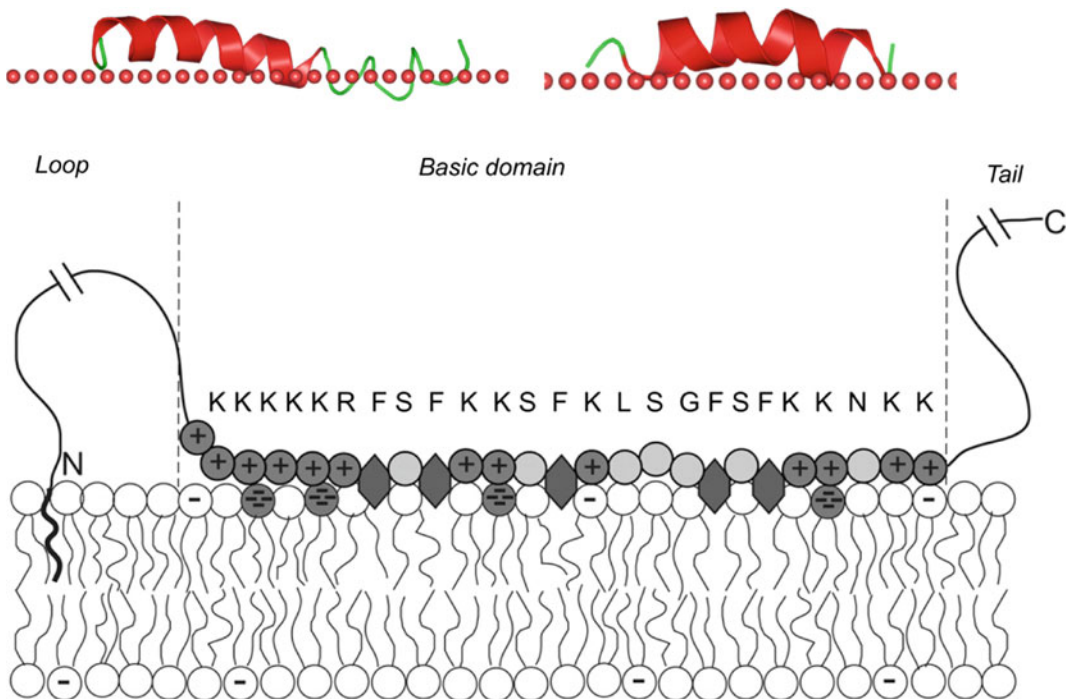


Fig. 3.2 Schematic representation of an adsorbed MARCKS protein. Circles enclosing the + symbol and open circles denote basic and electrically neutral amino acids, respectively. The hydrophobic phenyl groups that tend to insert into the membrane's hydrophobic core are

represented by hexagons. Also illustrated are neutral and several acidic lipid head groups, represented by circles enclosing one (e.g., monovalent PS) or four (tetravalent PIP₂) negative charges. *Source* MARCKS_HUMAN (2007)

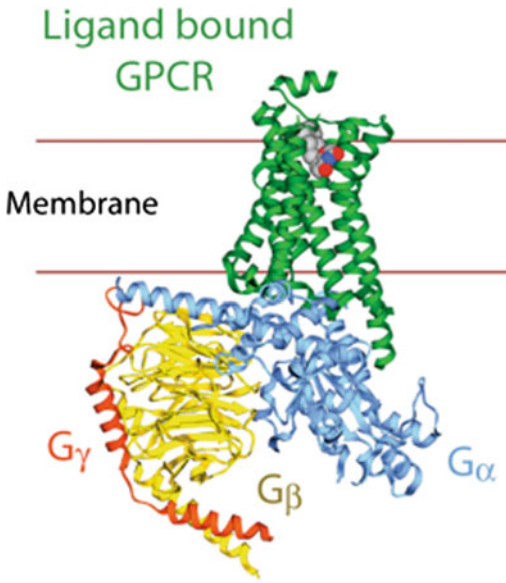


Fig. 3.3 Crystal structure of activated beta-2 adrenergic receptor in complex with heterotrimeric G-protein Gs (PDB entry 3SN6). The receptor is colored red, G α green, G β cyan, and G γ yellow (Color figure online)

like receptor tyrosine kinases. SH3 domains bind to proline-rich sequences in target membrane proteins.

3.1.2 Integral Membrane Proteins (IMP)

Membrane surface is polar and interior nonpolar, hence the integral membrane proteins are amphipathic, and the portion of the integral protein that is embedded in the interior of the membrane is predominantly hydrophobic, composed majorly of amino acids with nonpolar side chains having high hydrophobic index. **Hydrophobic index** of an amino acid is a numeric number based on free energy change (ΔG_t) associated with the transfer of amino acids from aqueous solution to a nonpolar solvent like n-octanol (Table 3.1). An amino acid with positive value is hydrophobic and can associate with the hydrophobic portion of the bilayer. One can create a hydropathy plot of a given protein and identify which region(s) of a given polypeptide that are membrane spanning. A stretch of

hydrophobic amino acids with high hydrophobic index will have a high probability of being a membrane spanning region.

As the membrane interior is essentially void of water, the atoms in the membrane spanning peptide backbone can form hydrogen bond only with the side chains or other atoms in the peptide backbone. The membrane spanning polypeptide region is observed to be stabilized by hydrogen bonds between amide nitrogen and carbonyl oxygen to form either α helix or β sheets secondary structures (Fig. 3.4).

As most acyl chains of lipids in membranes are between 14 and 24 CH_2 in length, the hydrophobic core of the membrane (2x length of tails) is 30–40 Å across the bilayer, so the transmembrane α helix of 18–22 residue length and transmembrane β sheet of 7–11 residue length would be required to cross the hydrophobic membrane core. Hence, the investigators can predict the membrane spanning regions of a protein from the primary sequence of the protein.

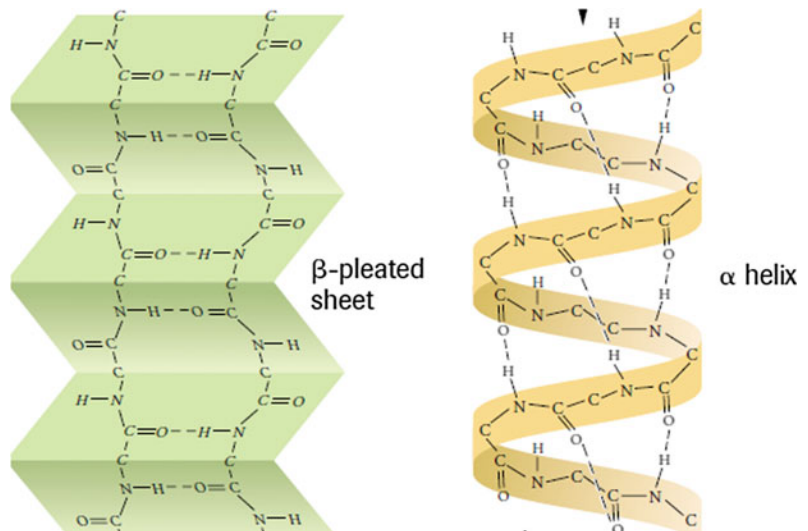
Starting from N terminus, proteins are scanned for a hydrophobic window of a stretch of hydrophobic residues. A region with ~ 20 residues of high hydrophathy index is presumed to be a α helical transmembrane segment, and region with ~ 11 residues to be a β pleated segment. **Hydropathy plots** in which hydrophathy index is plotted against residue number revealed that glycophorin from human erythrocyte has single α helical transmembrane segment with a window of 19 hydrophobic residues (Fig. 3.5), and Bacteriorhodopsin has seven transmembrane helices with seven hydrophobic windows (Fig. 3.6).

It has been observed that the transmembrane domain of all single transmembrane (**bitopic**) proteins is a α helical domain. Most polytopic (**multi pass transmembrane**) integral membrane proteins also span the membrane by multiple helices, and only a few by β sheets. A number of factors contribute to this apparent preference of polytopic integral membrane proteins for α helices. The α helices can accommodate to small changes in the bilayer thickness as compared to β sheet structures. As β sheet is made up of alternating nonpolar and polar amino acids, with nonpolar amino acids

Table 3.1 Hydropathy index for various amino acids

S. No	Amino acids	Hydropathy index
1	Ile	4.5
2	Val	4.2
3	Leu	3.8
4	Phe	2.8
5	Cys	2.5
6	Met	1.9
7	Ala	1.8
8	Gly	-0.4
9	Thr	-0.7
10	Ser	-0.8
11	Trp	-0.9
12	Tyr	-1.3
13	Pro	-1.6
14	His	-3.2
15	Glu	-3.5
16	Gln	-3.5
17	Asp	-3.5
18	Asn	-3.5
19	Lys	-3.9
20	Arg	-4.5

Source Kyte and Doolittle (1982)

Fig. 3.4 β pleated sheet and α helix

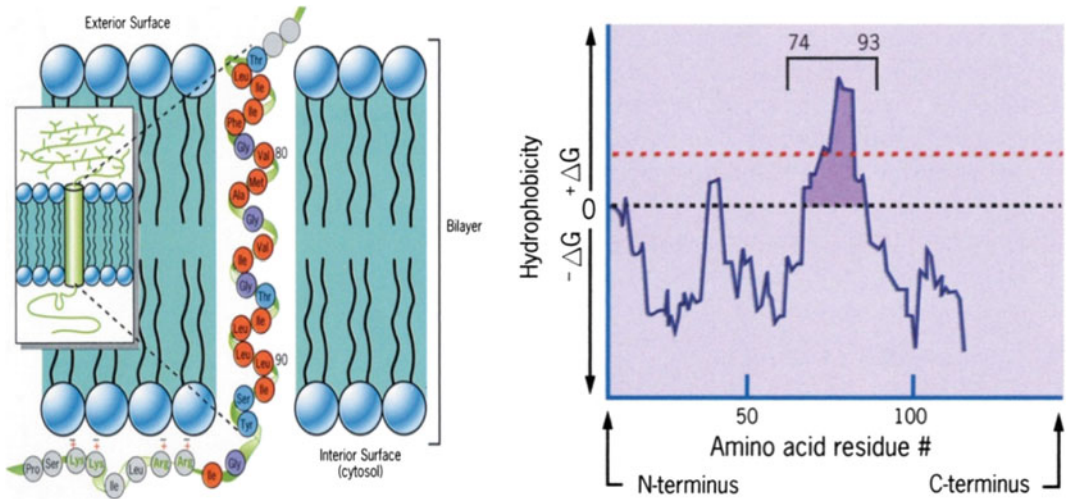


Fig. 3.5 Single transmembrane protein, glycoporin, and its hydropathy plot

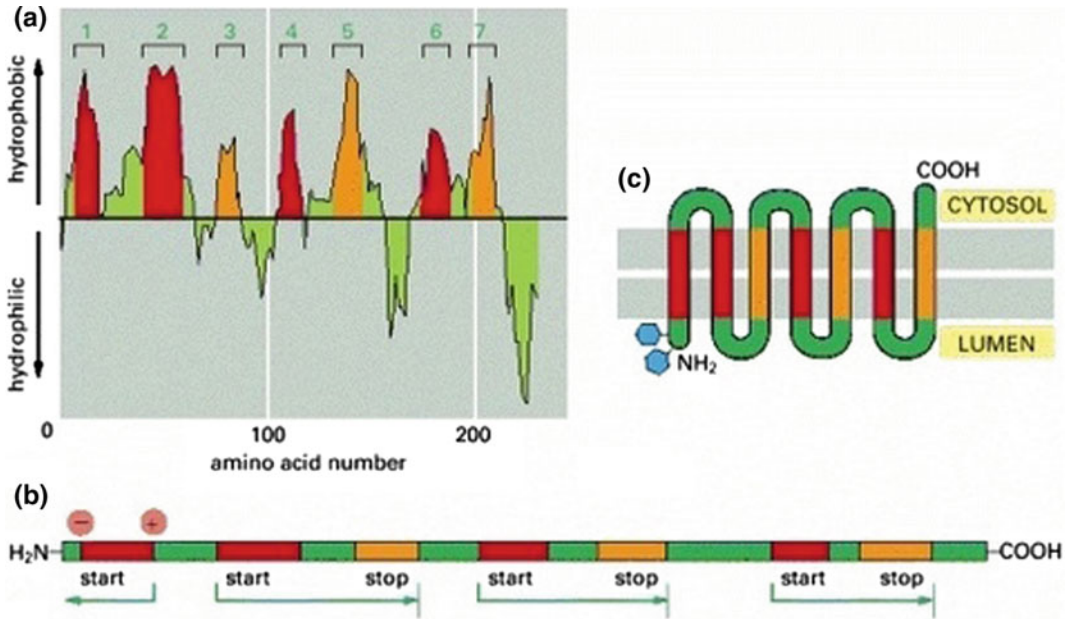


Fig. 3.6 Multipass transmembrane protein with associated hydrophobicity plot to predict TM domains

interacting with hydrophobic lipid bilayer and polar amino acids being involved in inter chain hydrogen bonding interactions, the multiple β strands must align to form sheets before insertion into the membrane, whereas α helices can insert individually and can form stable yet flexible transmembrane structures.

Apart from intrachain and interchain hydrogen bonding, hydrophobic interactions between the and the interior membrane lipids and hydrophobic side chains of amino acids play a major role in stabilizing the overall protein conformation. Additionally, the surface interactions also contribute to the stabilization of a particular

protein conformation. The membrane spanning region of the protein is rich in hydrophobic residues such as Ala, Ile, Val, and Leu and small polar amino acids like Gly which fit in the interior of the α helix. The lipid–water interface is found to be rich in aromatic polar residues like Tyr and Trp. These amino acids serve as membrane interface anchors and are able to simultaneously interact with lipid phase and the aqueous phase on either side of the membrane. Positively charged residues, such as, Lys and Arg, are found at the lipid–water interface region, where they interact with the negatively charged phospholipids. These positively charged residues are preferentially associated with the cytoplasmic side of the membrane.

3.1.2.1 α Helical Membrane Protein

Bitopic (proteins with single transmembrane helix) membrane proteins have been categorized based on their topologies (Fig. 3.7). The type-I integral membrane protein had its N terminus targeted toward the ER lumen during its biosynthesis, whereas in type-II proteins, the C terminus is targeted toward the ER lumen. Integral membrane proteins in which the transmembrane domain has both a signal sequence and a stop transfer sequence are classified as signal-anchored type-II proteins. The TM domain in such proteins is close to the N terminus. The type-IV, C-terminally anchored proteins have a TM domain close to the extreme end of C terminus.

The polytopic (multispanning) α helical membrane proteins have multiple α helical transmembrane domain segment arranged in a helix bundle (Fig. 3.8). Various interhelix interactions including the van der Waals forces, ionic interactions, and hydrogen bonds stabilize the helix bundle. The most studied polytopic proteins are the proteins of G-protein-coupled receptor (GPCR) superfamily, which activate a variety of signal transduction pathways, in response to signals such as hormones, neurotransmitters, light-sensitive molecules, and growth factors.

3.1.2.2 G-Protein-Coupled Receptor: 7 α Helix Bundle Transmembrane Polytopic Protein

G-protein-coupled receptors (GPCRs) (Fig. 3.9) form one of the largest receptor protein superfamily in the mammalian genome. There are over 800 unique GPCR genes in human genome. GPCRs are classified into six major families based on their similarity in sequence and function. These include the rhodopsin-like receptor family, the secretin receptor family, the metabotropic glutamate/pheromone receptor family, the fungal mating pheromone receptors, cyclic AMP receptors, and the frizzled/smoothed receptors.

GPCRs are seven transmembrane (TM-1–TM-7) receptors with an extracellular N terminus and a cytoplasmic C-terminal tail. The transmembrane helices are connected by three

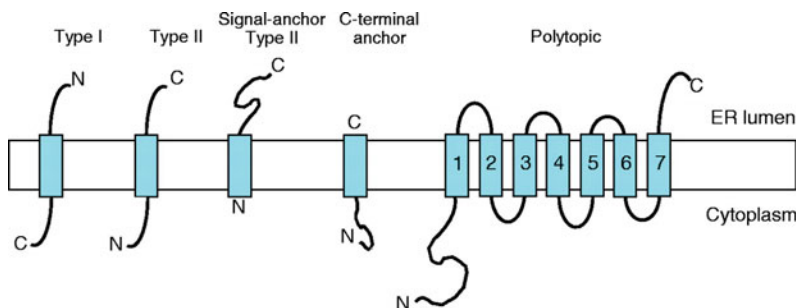


Fig. 3.7 Types of α helical integral membrane protein. Shown here are a type-I integral membrane protein, a type-II integral membrane protein, a C-terminally

anchored integral membrane protein, a type-II signal-anchored protein, and a multispanning membrane protein. *Source* Ott and Lingappa (2002)

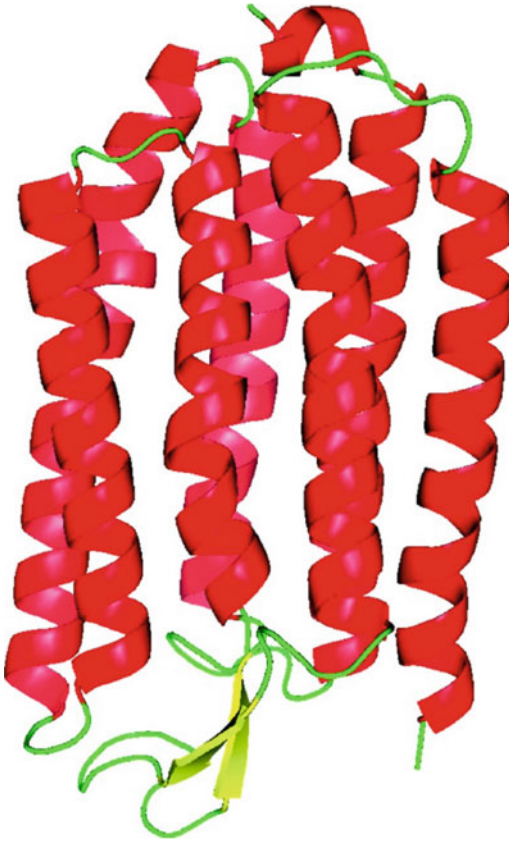


Fig. 3.8 An α helical bundle integral membrane protein (halorhodopsin from *Halobacterium salinarum*). Source Hurwitz et al. (2006)

intracellular loops (IL-1–IL-3) and three extracellular loops (EL-1–EL-3). The seven transmembrane helices are arranged in a barrel-like structure with a cavity inside that serves as a site for ligand binding. The transmembrane helices in GPCRs share the most sequence homology. The N terminus, the intracellular loop connecting TM5 and TM6, and the C terminus form the most variable regions of the GPCR family. For example, the monoamine and peptide receptors have a very short N-terminal sequence of 10–50 amino acids, whereas glycoprotein hormone receptors have much larger sequence of 350–600 amino acids. The extracellular loop region also forms variable secondary structures and disulfide linkages.

The C-terminal tail or the intracellular loops of GPCRs are lipid-anchored by palmitoylation (Fig. 3.12). This positions the C-terminal tail near the membrane so as to interact and activate downstream transducers of signaling pathways. Palmitoylation (see Sect. 3.1.3) can also target the receptors to lipid rafts, where protein–protein interaction with other signaling molecules facilitates rapid and effective signal transduction (see Chap. 9).

3.1.2.3 β Barrel Membrane Protein

β barrel membrane proteins mainly found in the outer membrane of gram-negative bacteria, mitochondria, and chloroplast and are more commonly known as **porins** (see Chap. 6). Proteins of inner membrane of gram-negative bacteria, mitochondria, and chloroplast are mainly single or multiple spanning α helices.

The atomic structure of about 20 β barrel membrane proteins has been determined. They can be monomers or trimers, in some cases dimers. Set of simple rules describes the structural features of all β barrel proteins. All β barrel proteins are cylindrical closed barrels with an even number of TM β strands, ranging from 8 to 22 strands. The β strands are connected in a β meander topology with alternating tight turns on one end and longer loops at the other end (Figs. 3.10 and 3.11). In bacteria, tight turns are found toward the periplasmic side and longer loops toward the extracellular side. The β hairpin forms the basic structural subunit of a β barrel, with a tilt of 20° – 45° out of membrane axis. The β strands that span the membrane constitute of 9–11 amino acids, with polar and nonpolar amino acids alternatively arranged. The smallest known barrels contain 8 TM strands (OmpA), and the largest are the 22-strand TonB-dependent importers.

The hydrophobic amino acids of the β barrels interact with the hydrophobic lipid bilayer, which include Phe, Tyr, Trp, Val, and Leu. The aromatic amino acids are preferentially found at the bilayer interfaces. Small or polar amino acids such as Gly, Thr, Ser, Asp, and Gln are most abundant residues facing the interior of the barrel.

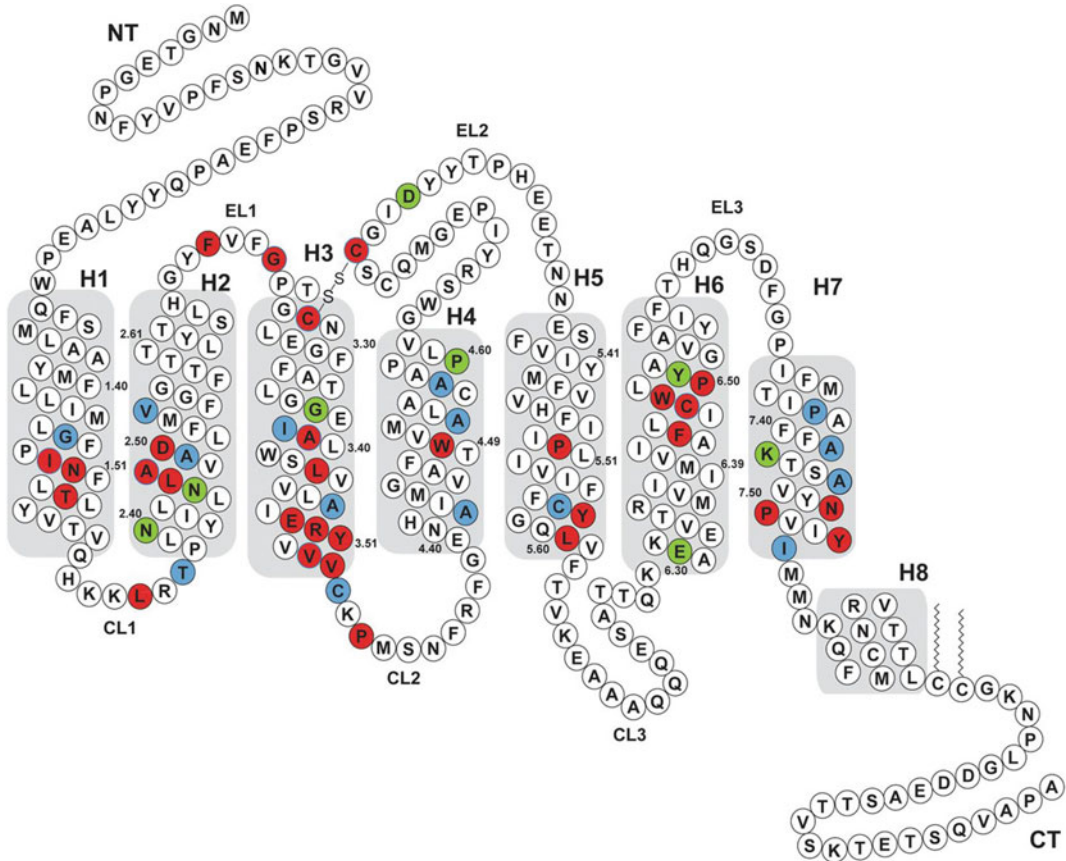
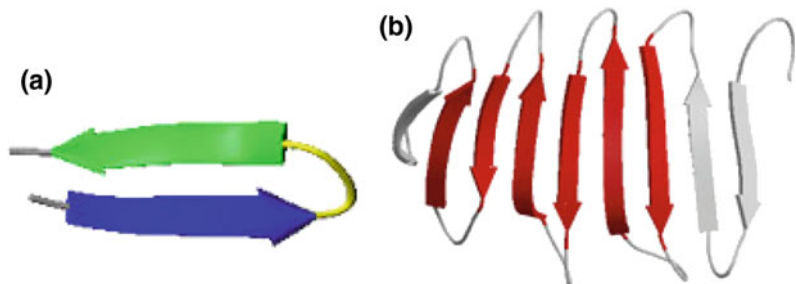


Fig. 3.9 Sequence of the photoreceptor rhodopsin is shown highlighting the amino acid positions conserved in the subfamily of visual receptors (green) and across the large class A GPCR family. The “signature” amino acids (red) are defined as those residues with sequence identities of >70% across the class A GPCR family. The “group-conserved” residues (blue) are those with

conservation of >75% when considered as a group of small and weakly polar residues (alanine, glycine, serine, cysteine, and threonine). These amino acids have been identified in membrane proteins as key determinants in helix–helix interactions (GPCR database <http://www.gpcr.org/7tm/>). Source Smith (2012) (Color figure online)

Fig. 3.10 a β Hairpin. b β meander



Interchain hydrogen bonds between β strands are a dominant stabilizing interaction contributing greatly to the rigidity and stability of β barrel

structure, making them very stable that they rarely undergo conformational changes in membranes.

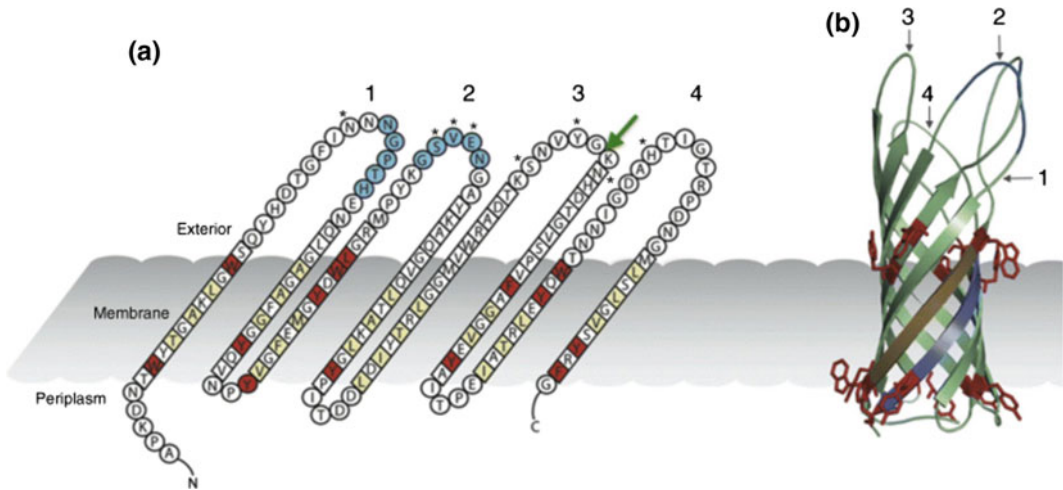


Fig. 3.11 Structure of 8-strand β barrel protein OmpA. **a** A topological model OmpA showing the major features of the protein. Residues in β sheets are in diamonds, those colored in red make up the aromatic girdle while those in yellow are the alternating hydrophobic residues. Loops are numbered. Residues in loops 1 and 2 are important for binding endothelial cells, and C4 bp is highlighted in

blue. Positions that may differ between enterobacteria are asterixed (Gophna et al. 2004; Power et al. 2006). The position of an insertion of three to four amino acids in loop 3 of invasive enterobacteria is indicated (Gophna et al. 2004). **b** Three-dimensional structure of OmpA. The view was generated using PyMOL (PDB-code 1BXW, Pautsch and Schulz 1998) (Color figure online)

Mitochondrial β barrel membrane protein, mitochondrial voltage-dependent anion channel (VDAC), is a new class of β barrel proteins forming an odd numbered 19-stranded β barrel.

3.1.3 Lipid-Anchored Proteins

Lipid-anchored proteins or lipid-linked proteins are covalently attached to lipids in the membrane bilayer. The lipids tether the protein to the cell membrane, facilitating protein interaction with the membrane and other membrane-associated proteins. For example, the GPCR lipid-anchored C-terminal tail interacts with lipid-anchored G-protein and activates downstream signaling pathways. This reversible attachment of membrane lipid to proteins can act as switching device for membrane-associated interactions and processes.

There are three main categories of lipid-anchored proteins which include **prenylated proteins**, **fatty-acylated proteins**, and **glycosylphosphatidylinositol-linked proteins (GPI)**.

3.1.3.1 Prenylated Proteins

The first mammalian prenylated protein identified was nuclear protein lamin B. It is now known that $\sim 0.5\text{--}2\%$ of the mammalian cell proteins are prenylated. Most Ras proteins of the G-protein family are prenylated proteins. Two prenyl groups, farnesyl (15-carbon) and geranylgeranyl (20-carbon) isoprenoid chains, are found to be linked to the cysteine residue at or near the carboxy terminus of the proteins via a thioether linkage (Fig. 3.12).

Protein prenylation is the posttranslational protein modification catalyzed by multisubunit cytosolic prenyltransferases. The majority of prenylated proteins contain a carboxy-terminal CaaX motif (CaaX box) where “C” stands for conserved cysteine residue, “a” for any aliphatic amino acid, and “X” for any C-terminal residue. The CaaX prenyltransferases catalyze the farnesylation and geranylgeranylation on the cysteine residue, using farnesyl pyrophosphate (FPP) or geranylgeranyl pyrophosphate (GGPP) as the substrate (Fig. 3.13). The farnesyl transferase (FTase) recognizes CaaX boxes when X is Ala, Ser, Met, Gln, or Cys, whereas protein

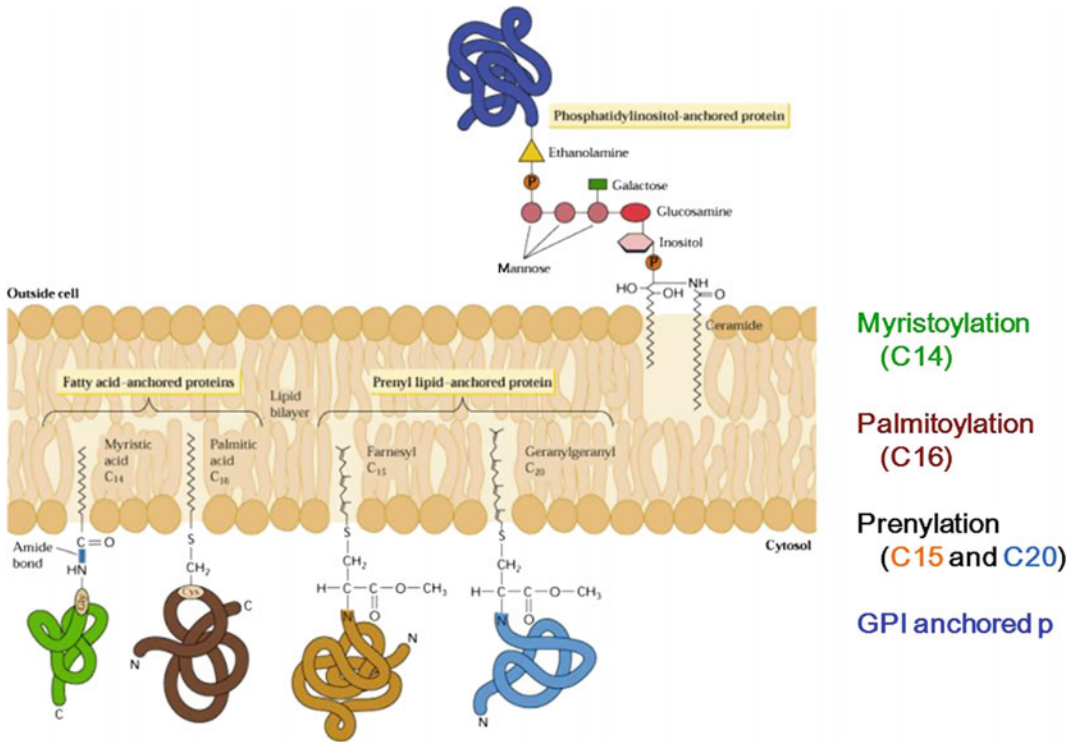


Fig. 3.12 Lipid-anchored proteins: The structures (left to right) represent *N*-myristoyl glycine, palmitate thioester-linked to cysteine, farnesyl thioether-linked to cysteine, geranylgeranyl thioether-linked to cysteine,

cholesterol ester-linked to glycine, and a minimal GPI anchor linked to the ω amino acid in a GPI-anchored protein

geranylgeranyl transferase type I recognizes CaaX boxes when X is either Glu or Leu. Some proteins, such as the Rab proteins, are prenylated at the C-terminal CC or CXC motif, which is recognized and prenylated by geranylgeranyl-transferase type II.

Subsequent to prenylation, Ras and most other CaaX proteins are further processed in the ER. Firstly, a CaaX-specific protease (Rce1) cleaves the -aaX tripeptide leaving prenylated cysteine at the C-terminal. This step is followed by carboxymethylation of the C-terminal prenylcysteine residue by the methyltransferase (Icmt). Methylation converts negatively charged the C-terminal hydrophilic group to an uncharged, hydrophobic group thereby increases membrane affinity of the protein and also serves as a specific recognition motif facilitating protein-protein interactions.

3.1.3.2 Fatty-Acylated Proteins

Fatty acylation of proteins is essential not only for its membrane localization and function, but also for facilitating protein-protein interactions. Many fatty-acylated proteins are involved in regulating intracellular trafficking, signal transduction, and subcellular localization. Myristic acid, a 14-carbon saturated fatty acid, and palmitic acid, a 16-carbon saturated fatty acid, are the two most common fatty acids covalently linked to proteins.

Myristoylated Proteins

N-myristoylation of proteins was first identified in the catalytic subunit of protein kinase A. Many eukaryotic proteins with diverse functions including, ADP-ribosylation factors, recoverin, and calcineurin have been found to be *N*-myristoylated. The *N*-terminal glycine of the target protein is

myristoylated via amide linkage. The enzyme myristoyl-CoA: protein N-myristoyltransferase (NMT) catalyzes the transfer of myristyl group from myristoyl-CoA to N-terminal glycine residues. Before NMT catalyzed myristoylation, the initiation methionine residue is removed by methionyl aminopeptidase, and then the exposed glycine residue at N-terminal is myristoylated. The MGXXXSXX sequence is essentially required to be present in the precursor proteins, with glycine at the second position and serine in the sixth position for N-myristoylation to take place. Myristoylation is an early cotranslational event which occurs in the cytoplasm as the nascent peptide of ~60 amino acids emerges from the ribosomes. However, myristoylation of synthetic peptides can be performed posttranslationally at the N-terminal glycine.

While myristoylation is essentially required for tethering of some proteins to membranes, it is not sufficient to capture large proteins. An additional signal is therefore required for efficient membrane binding. For example, in MARCKS protein, this additional membrane association is provided by electrostatic interaction between positively charged polybasic domain of the protein and the negatively charged phospholipids in the cytoplasmic leaflet of cell membranes.

Palmitoylated Proteins

S-palmitoylated proteins have palmityl group attached to cysteine residue of proteins via thioester linkage. Like prenylation and myristoylation, palmitoylation also tethers proteins to cytosolic membrane surfaces. However, prenyl and myristoyl groups remain attached to the protein throughout its lifetime, whereas palmitoylation is readily reversible due to the labile thioester bond. A variety of soluble and transmembrane proteins can be palmitoylated, hence it acts as a regulatory switch for shuttling proteins between soluble and membrane-associated state, across membrane organelles, and within different regions of the membrane. This large substrate diversity is accommodated by a large array of protein acyl-transferases (PATs). The most studied protein acyl-transferases (PATs)

family is the DHHC domain (a cysteine-rich domain with a conserved asp-his-his-cys sequence) containing enzymes. However, the specific recognition motifs in the substrate proteins are still not fully defined. Only one enzyme, acyl-protein thioesterase-1 (APT1), has been shown to mediate protein depalmitoylation *in vivo*.

Most palmitoylated proteins have more than one lipid anchor, and it can additionally have another fatty acyl or a prenyl group attachment. Based on the type of groups attached, or the site of palmitoylation, the palmitoylated proteins are categorized into four types. Type-I proteins consist of membrane proteins that are palmitoylated on one or several cysteine residues proximal to the transmembrane domain. Type-II proteins include members of the Ras family that are farnesylated at the cysteine residue in the C-terminal CaaX box. A third group of proteins (Type III) is palmitoylated at cysteine residues near the N- or the C-terminal. Type-IV proteins are additionally myristoylated, with the consensus sequence Met-Gly-Cys at their N-termini, where myristoylation occurs at Gly-2-position and palmitoylation at Cys-3-position.

GPI-Anchored Proteins

Glycosylphosphatidylinositol (GPI) anchors a wide variety of proteins either to the outer leaflet of the plasma membrane or to the luminal face of intracellular organelle membranes in eukaryotic cells. Glycosylphosphatidylinositol (GPI anchor) is a glycolipid that can be attached to the C-terminal amino acid of a protein during post-translational modification. It has a conserved core structure consisting of ethanolamine phosphate (EtNP), three mannose (Man), one glucosamine (GlcN), and inositol phospholipid, in the sequence: EtNP-6Man α -2Man α -6Man α -4GlcN α -6myoinositol-P-lipid (Fig. 3.14). GPI-anchored proteins with two fatty acid chains inserted into the outer leaflet of the plasma membrane provide a stable association with the lipid bilayer, and those with saturated acyl chains are preferably associated with lipid rafts. The GPI-anchored proteins are involved in varied functions

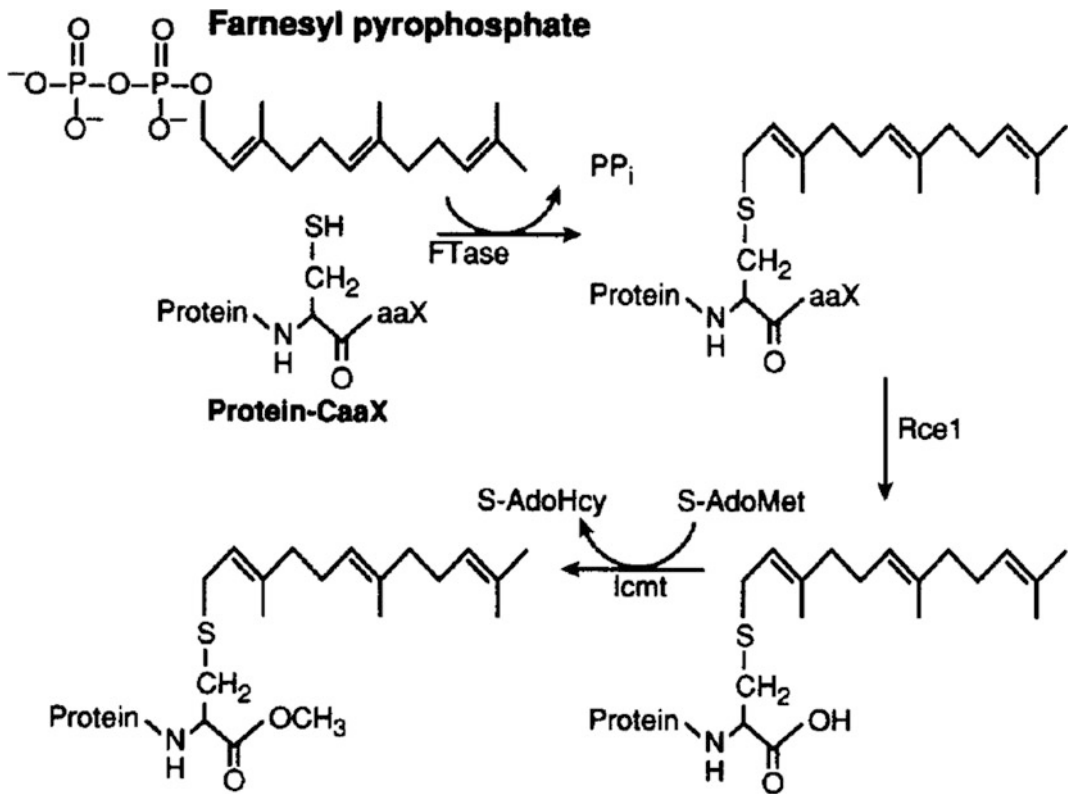


Fig. 3.13 Farnesylation, proteolysis, and carboxymethylation of a CaaX protein. The farnesyl donor is farnesyl pyrophosphate. Ftase Farnesyl transferase; Rce1 CaaX

protease; S-AdoHcy S-Adenosyl homocysteine; S-AdoMet S-Adenosyl methionine; Icmt Methyl transferase

including signaling, cell–cell interaction and communication, cell adhesion, enzymes, and transport. In polarized cells, GPI anchor may serve as a targeting signal for proteins to be trafficked from Golgi to the apical side of the membrane.

GPI anchor is synthesized via a topologically complex pathway similar to N-linked glycosylation of proteins. The synthesis is initiated with the phosphatidylinositol (PI) substrate in the cytoplasmic face of the ER membrane. Sequentially, the monosaccharides are transferred to phosphatidylinositol (PI) from activated sugars (Dol-P-Man and UDP-GlcNAc), yielding the core GPI structure. The GPI core structure is then translocated to the lumen side of ER via the flippases. In the lumen, the transamidase enzyme catalyzes the addition of GPI anchor to proteins

forming an amide linkage between C-terminal carboxyl group of the protein and the amino group of ethanolamine phosphate (Fig. 3.15).

GPI-anchored proteins are associated with a range of diseases. Human disease paroxysmal nocturnal hemoglobinuria (PNH) is attributed to reduced expression of two GPI-anchored proteins, membrane inhibitor of reactive lysis (CD59), and decay accelerating factor (CD55) in hematopoietic stem cells. As these proteins are involved in complement system regulation, the disease is characterized by complement-system-mediated intravascular hemolysis, thrombosis, and bone marrow failure. Another GPI-anchored protein, the prion protein (PrP), is associated with prion diseases including Creutzfeldt–Jakob disease in humans. Variant surface glycoprotein (VSG), a GPI-anchored protein from

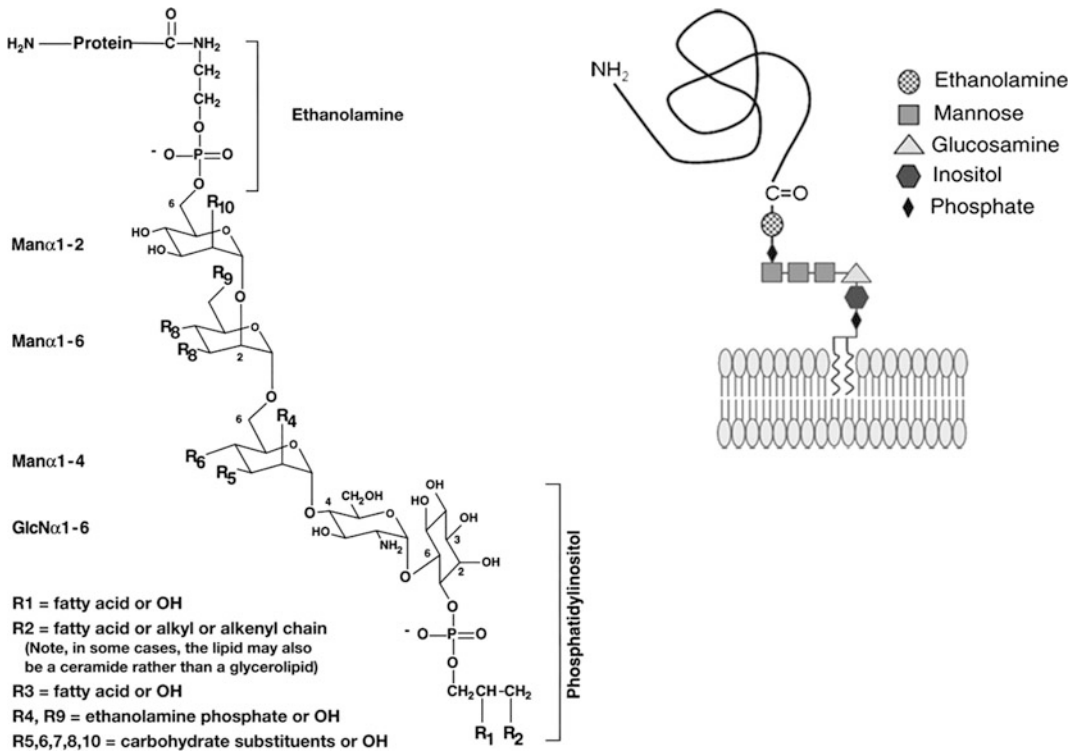


Fig. 3.14 Detailed general structure of GPI anchors. All characterized GPI anchors share a common core consisting of ethanolamine-PO₄-6Man α1-2Manα1-6Manα1-4GlcNα1-6myo-inositol-1-PO₄-lipid

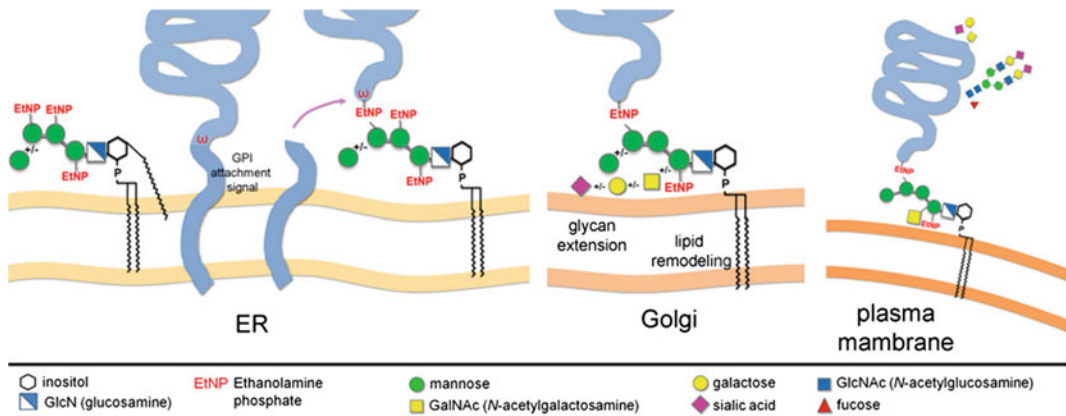


Fig. 3.15 Schematic representation of the main events in the synthesis of GPI-anchored proteins. Proteins (often glycoproteins) acquire a GPI anchor in the ER, a signal sequence is cleaved (at a consensus omega residue) and the GPI anchor is attached via a terminal ethanolamine

phosphate to the C-termini of the acceptor protein. The glycolipid moiety can be later modified in the Golgi. The mature glycoprotein is finally localized to the plasma membrane

Trypanosoma brucei, is involved in the pathobiology of the disease by forming a protective coating around the parasite.

3.2 Techniques to Study Membrane Proteins

Studying membrane proteins still holds a challenge for structural biologists and biochemists. To date, membrane proteins represent only 1% of over 50,000 repository of protein structures in the Protein Data Bank (PDB). There has been some growth in the unique membrane protein structures of both monotopic and multispinning proteins deposited in the PDB, and also, in database of “Membrane proteins of known 3D structure” (http://blanco.biomol.uci.edu/Membrane_Proteins_xtal.html) in the past decade.

Membrane proteins provide a challenge at all levels of purification, crystallization, and expression. Being present in hydrophobic environment, to maintain their native state they can only be extracted from the cell membrane using detergents. Their instability and small starting material still prove to be challenge.

Strategies involved in membrane protein purification include: 1. Isolation of membrane of interest, which would involve cell disruption to release intracellular organelles, followed by membrane separation and isolation, 2. solubilization of

membrane proteins from isolated membranes, and 3. purification and characterization of solubilized membrane proteins (Fig. 3.16).

3.2.1 Cell Disruption Methods

Cell disruption is the breakage of cell wall/membrane to release intracellular contents including cellular organelles, which can be the source of particular membrane of interest. Cell disruption methods can be mechanical or nonmechanical.

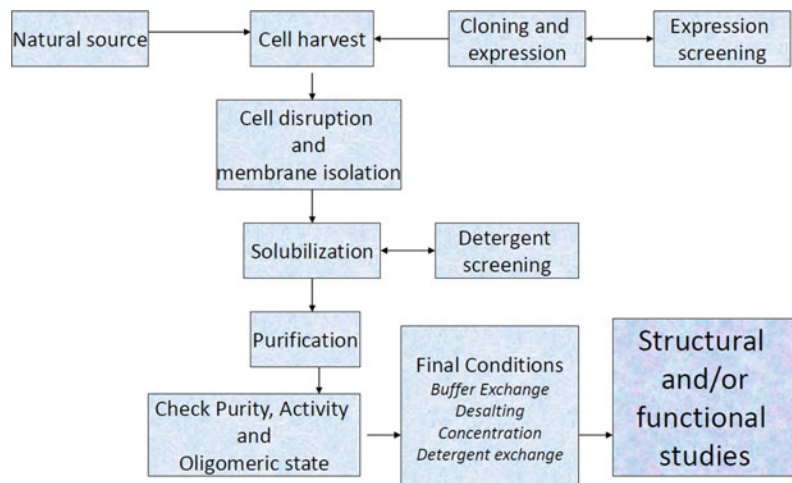
A. Mechanical methods for cell disruption

Mechanical methods use mechanical forces such as shearing, abrasion, pressure, and sonic vibrations for cell disruption.

1. Bead method

The cell disruption by this method is caused stirring or shaking the aqueous solution of the cell sample containing beads of tiny glass, ceramic, or steel. As the beads collide with each other and with the cellular sample, the grinding action disrupts the cell wall/membrane to release intercellular components (Fig. 3.17). This method, also called “bead beating,” has been successfully used for different cell types including bacteria,

Fig. 3.16 Protocol for membrane protein purification



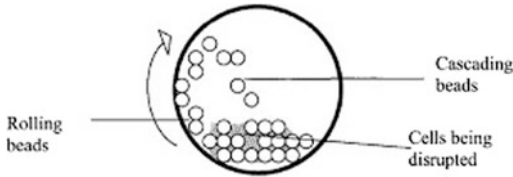


Fig. 3.17 Cell disruption by Bead beating

spores, animal and plant cells. Motorized shaker can be used for bead beating in plastic vials, centrifuge tubes, or microtiter plates. Care is taken to avoid foaming and sample heating.

Depending on the speed of agitation, number of beads used, and bead size, this method can be mild or aggressive, resulting in good membrane or subcellular preparations.

2. Homogenization

Homogenization is one of the most widely technique for cell and soft tissue disruption using shearing forces. The cell or tissue suspension is forced through a narrow space known as clearance space (0.001–0.006 mm), between the vessel and pestle surface, thereby shearing the cell membranes. Different types of homogenizers are used, including a Dounce homogenizer in which a round glass pestle manually homogenizes in a glass tube and Potter–Elvehjem homogenizer which consists of manually or mechanically driven Teflon pestle fitted into a rounded vessel (Fig. 3.18). The type of cell sample determines the number of strokes and the speed required for homogenization.

3. French press

French press method is a high-pressure homogenization resulting in more uniform and complete disruption. The cell suspension is placed in a cylinder fitted with a plunger connected to a hydraulic press. As the pressure is applied, the plunger is pushed down, forcing the suspension to emerge through an orifice in the cylinder at a very high speed in the form of a fine jet. The difference in pressure created and high shearing rates results in cell disruption. The intracellular

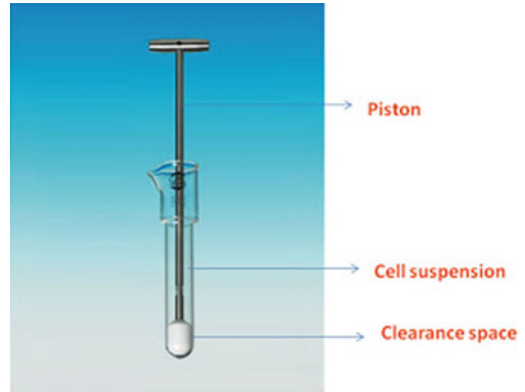


Fig. 3.18 Cell disruption using homogenizer

pressure increases with the increase in pressure in the cylinder, but the external pressure on the cell wall drops rapidly to atmospheric pressure as the sample emerges out through a small orifice (Fig. 3.19). The pressure within the cell also drops but not to the same extent as the outside pressure. This pressure difference across the cell causes the cell membrane to burst. The French press cylinders can be of varying sizes, accommodating whole range of volumes. The pressure generated can range from 10,000 to 50,000 psi.

4. Sonication

Sonication is a process by which electric energy is converted to sound energy. Ultrasonic, high-frequency vibrations >18 kHz are generated

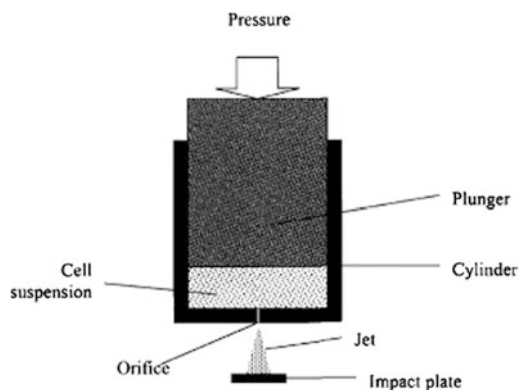


Fig. 3.19 Cell disruption using French press

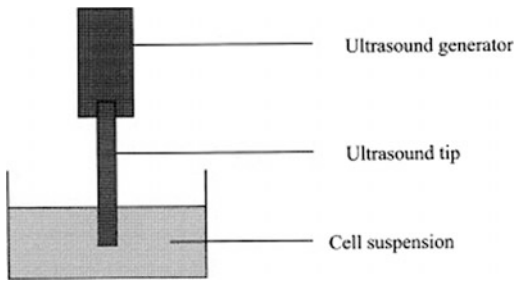


Fig. 3.20 Cell disruption by sonication

by a sonicator that can be used to disrupt cells (Fig. 3.20). Ultrasound emitting tips are immersed in cell suspension. The high-frequency vibrations generated produce cavitation phenomena, which are characterized by production of multiple microbubbles in the fluid. The bubbles initially grow and then collapse after reaching a maximum size. On collapse, a violent shock wave is created in the medium, generating kinetic energy in the cell resulting in its lysis. The whole process of bubble formation, growth, and then its collapse initiated by ultrasonic waves is called **cavitation**.

The exposure time of ultrasound vibrations required depends on the cell type, the sample volume, and the cell concentration. Bacterial cells such as *E. coli* may only require 30–60 s of vibrations, whereas yeast cells could require from 2 to 10 min exposure.

Sonication has many disadvantages that need to be taken care of, for example, high noise levels generated require sound proof enclosures and care has to be taken to prevent too much heat generation. The free radicals generated that can react with other molecules and initiate chain reactions.

Sonication is frequently used in combination with chemical cell disruption methods, thereby significantly reducing the exposure time and frequency required for cell disruption.

5. Cryopulverization

At liquid nitrogen temperatures, cells with a tough outer membrane, or extracellular matrix, such as animal tissue, are ground to a fine

powder. Due to the presence of significant amount of water, biological samples become brittle at very low temperatures, hence are easy to grind with good sample recovery. This technique is known as cryopulverization.

B. Nonmechanical methods of cell disruption

Nonmechanical methods include physical, chemical, and biological treatment of cells, which result in cell disruption.

B.1. Physical methods:

1. Osmotic shock

The difference in solute concentration across a semipermeable membrane results in osmotic shock. Transferring a cell from an isotonic medium to a hypotonic medium would cause a rapid influx of water into the cell. This results in the rapid expansion in cell volume followed by its rupture, for example, red blood cells undergo hemolysis when suspended in water, releasing intracellular contents including hemoglobin. Animal cells can easily be lysed by osmotic shock, but plant, bacterial, and fungal cells have cell walls which need to be lysed before osmotic shock can be applied.

2. Freeze–Thaw method

The freeze–thaw method is commonly used to lyse bacterial and animal cells. The freeze–thaw technique involves alternatively freezing the cell suspension in a dry ice/ethanol bath or in deep freeze and thawing the material at room temperature or at 37 °C. At freezing temperatures, as ice crystals are formed, cell expands and then contracts on thawing. Multiple cycles of freezing and thawing result in cell expansion and contraction, resulting in cell lysis.

B.2. Chemical methods:

1. Detergent

Detergents being amphipathic molecules disrupt the cell membranes by solubilizing the membrane lipids, disrupting lipid–lipid and lipid–

protein interactions. Detergents can also disrupt bacterial cell membrane, following lysozyme treatment which hydrolyzes peptidoglycan layer. The plant and fungal cell walls need to be weakened before detergents can disrupt these cells. Detergents can be cationic, anionic, and nonionic. Nonionic detergents are preferred in cell disruption as they do not denature membrane proteins. Commonly used detergents include CHAPS, Triton X-100, and Tween series of detergents. However, detergents can change the properties of proteins, hence the detergent concentration needs to be subsequently reduced in the final preparation.

2. Organic solvents

Organic solvents like acetone disrupt the cell membrane by solubilizing the membrane lipids. Solvents like toluene have been used to disrupt fungal cell walls. Organic solvents have an advantage that being volatile, and they can be easily removed from the product, but the biggest disadvantage is that they can denature proteins.

3. Acid/Alkali treatment

Acid/alkali treatment is used to isolate DNA from cells. NaOH solubilizes the membrane phospholipid and proteins, but prolonged exposure of cells to extreme pH may denature the proteins. Hence, this treatment is only used for nucleic acid extraction.

B.3. Biological methods:

1. Enzymes

Enzymes have been used to degrade plant and bacterial cell walls for the preparation of protoplasts (cells without cell walls). The commonly used enzymes include lysozyme, cellulase, zymolase, pectinases, mannases, collagenase, and proteases.

Lysozyme disrupts the peptidoglycan layer of bacterial cell walls. After disruption of cell wall, the cell membrane can be disrupted by any of the above-mentioned procedures. Cellulases, pectinases, and

mannases have been used to disrupt plant cell walls. Collagenase and proteases are used for the disruption of extracellular matrix in animal tissues. Enzymes have to be removed before proceeding for further steps of purification.

3.2.2 Membrane Separation and Isolation

3.2.2.1 Centrifugation

Centrifugation separates subcellular components on the basis of their sedimentation rate, which is determined by their density, size, and shape. Different types of centrifugation have been used to separate membrane fractions:

1. Differential centrifugation

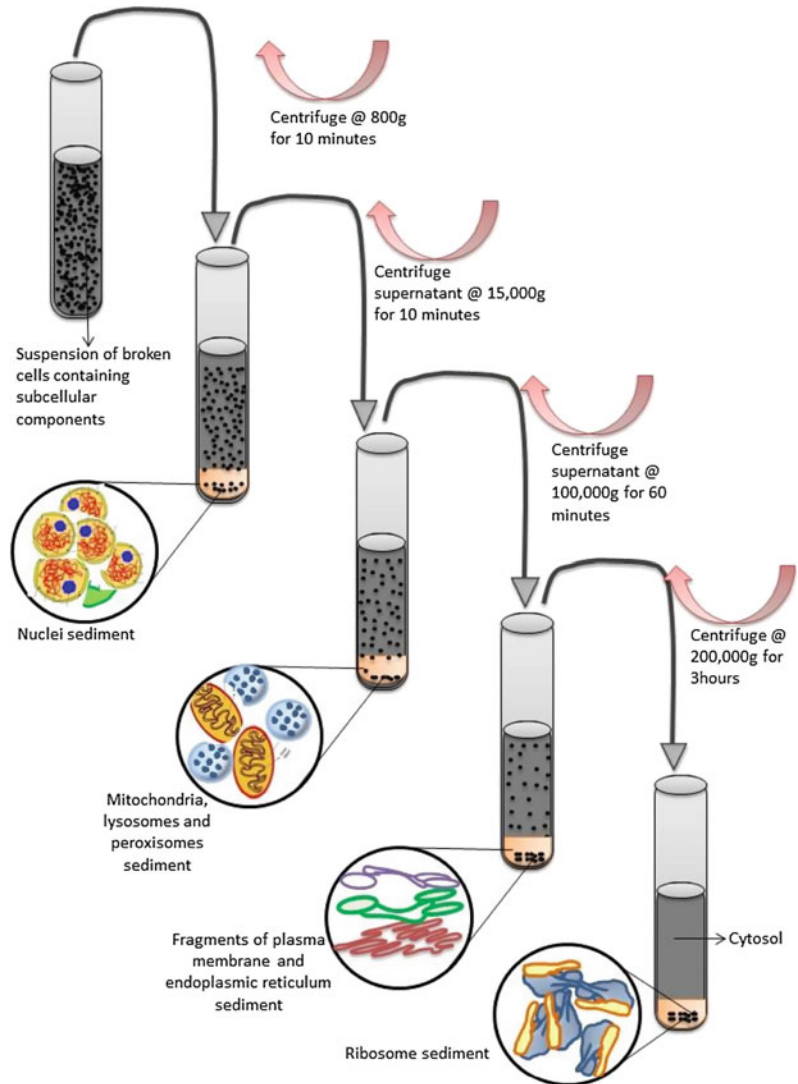
The cell lysate is subjected to series of centrifugations (Fig. 3.21), which will fractionate it into several components. Centrifugation at each step will result in a pellet enriched in a specific component that sediments at that speed and the supernatant contain the remaining components. The separation of components is based on their size and density with highest density component sedimenting first. The cell lysate is first subjected to low speed (~ 800 g for 10 min) centrifugation. At this speed, the nucleus having the highest density/sedimentation rate sediments as a pellet, while the remaining components are suspended in the supernatant.

The supernatant is further subjected to higher speeds (10,000–20,000 g for 10 min) to sediment mitochondria, lysosomes, peroxisomes in the pellet. The supernatant generated in this step is then centrifuged at much higher speed (this time at 100,000 for 1 h) resulting in the sedimentation of plasma membrane and endoplasmic reticulum in the pellet.

Further centrifugations at a very high speed can sediment ribosomes. The final supernatant left is the cytosolic fraction.

The fractions thus obtained are enriched fractions of different organelle components which have to be further purified.

Fig. 3.21 Differential centrifugation



2. Density velocity centrifugation

Density gradient centrifugation can be of two types:

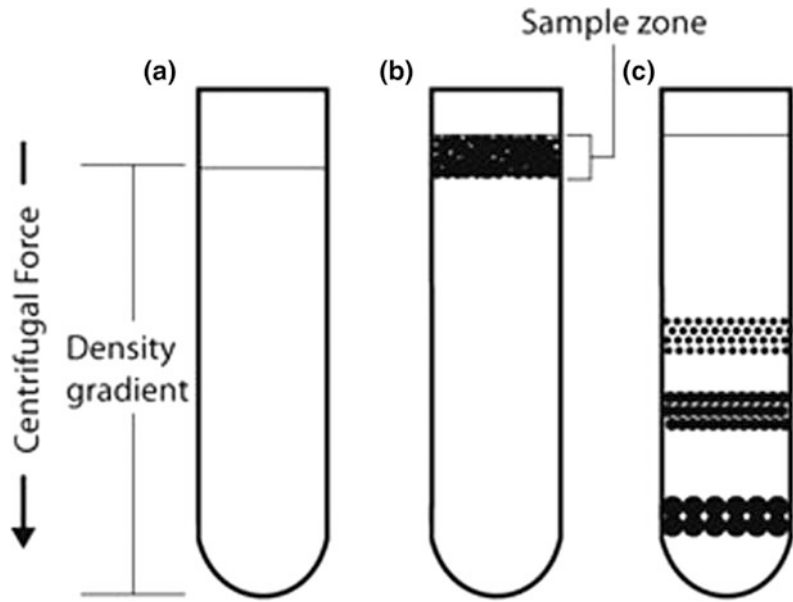
3.2.2.2 Rate-Zonal Centrifugation

Differential centrifugation does not result in pure fractions due to contamination of fast-moving particles with slow-moving particles. Rate-zonal centrifugation involves carefully layering of sample solution as a narrow zone on top of preformed liquid gradient of appropriate

material, with increasing density and viscosity from top to bottom of the tube. The highest density of the gradient is lower than that of densest particle to be separated. Separation of particles by the rate-zonal technique is based on the size, shape, and density of particles (see Fig. 3.22). As the particles in the sample move down the density gradient, they separate as bands containing particles of similar size.

As the density of the particles is greater than the density of the gradient, all the particles will eventually form a pellet if centrifuged long

Fig. 3.22 In Rate-zonal centrifugation (a) preformed gradient with increasing density from top to bottom of the tube is used (b) sample is layered as a narrow zone on the top of a density gradient (c) under centrifugal force, particles move at different rates depending on their mass



enough, so the centrifugation time is very crucial in rate-zonal centrifugation. Small sample size prevents crosscontamination in different bands separated.

3.2.2.3 Isopycnic Centrifugation

Isopycnic separation, also called equilibrium separation, separates particles on the basis of their buoyant density. The density gradient is chosen such that it covers the density range of the species to be separated. The sample is either mixed with the density gradient medium and separates as gradient is generated, or is layering on top of the preformed gradient. In either case, as centrifugal force is applied, and the sedimenting components move along the density gradient to sediment in the zone of same buoyant density and floating over medium of higher density. This is due to the fact that in isopycnic centrifugation, density of the gradient medium is greater than the highest density of the particles to be separated. No further sedimentation occurs after this point, irrespective of how long centrifugation continues, because the particles are floating on the cushion of medium that has density greater than their own (see Fig. 3.23).

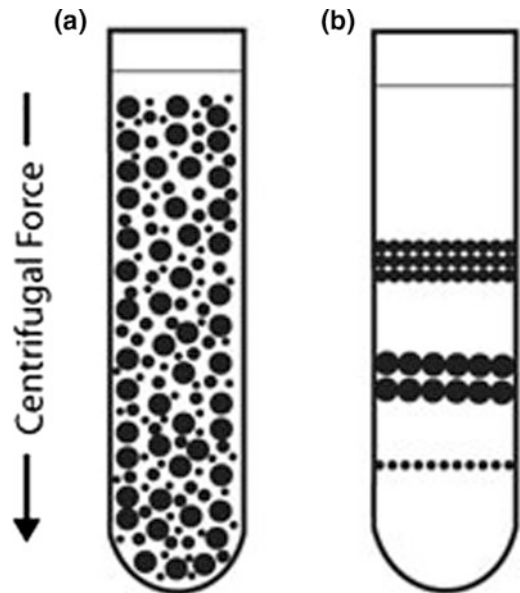


Fig. 3.23 Isopycnic centrifugation starting with a uniform mixture of sample and density gradient (a) under centrifugal force, particles move until their density is the same as the surrounding medium (b)

3.2.2.4 Choice of Density Gradient Medium

The density gradient medium provides a medium for separation of particles, either on the basis of buoyancy density or on the sedimentation rate. A density gradient media should have the following properties: (1) should be sufficiently soluble to generate wide range of densities, (2) should not be hyperosmotic (osmolality of mammalian fluids $\sim 290\text{--}300$ mOsm) or highly viscous in the desired density range, (3) should be compatible with the sample particles to be separated, and (4) can be easily separated from the product.

Over the years, a variety of different density gradient media have been developed for faster separation of different types of particles, maintaining the suitable osmolarity and viscosity (Table 3.2). Different types of density gradient media are used for the separation of different types and sizes of molecules. These include polysaccharides, polyhydric alcohols (sugars), iodinated compounds, inorganic salts, and colloidal silica (Table 3.3).

3.2.2.5 Permeation Chromatography

Population of small membrane vesicles of different diameters can be separated by matrix of porous glass beads. Synaptic vesicles and intestinal brush border vesicles have been successfully separated using columns of carbowax-pretreated glass beads with mean pore

diameter of 300 nm. Phospholipid vesicles have been sized and separated using Sephacryl S-100.

3.2.2.6 Free-Flow Electrophoresis

Free-flow electrophoresis (FFE) is carrier-free electrophoresis, used for the separation of charged or chargeable analytes. High-voltage free-flow electrophoresis has resulted in separation of subcellular membranes with high purity. A mixture of components to be separated is released as a fine stream into a separation buffer flowing through an electric field (Fig. 3.24). Membrane fractions are separated and resolved on the basis of their surface charge with 100% recovery. This technique is applied for separation of Golgi apparatus components (cis, median, trans) and different endocytic compartments (early, late), which are difficult to separate by other methods.

3.2.2.7 Characterization of Membrane Fractions

After separation of subcellular organelle fractions, the fractions have to be identified and characterized. Each organelle fraction has a characteristic structure and function. To carry out these functions, it has specific set of enzymes and proteins. Hence, a set of proteins/enzymes is specifically associated with an organelle or cell compartment. As enzymes are easier to assay, specific **marker enzymes** identify organelle fractions. The marker enzymes can be used to track the fate of a particular organelle during

Table 3.2 Density and dimensions of cellular organelles

Organelle/compartment	Diameter (μm)	Density (g/cm^3)
Nuclei	3–12	1.4
Mitochondria	0.5–2	1.15
Golgi apparatus	–	1.08
Lysosomes	0.5–0.8	1.2
Peroxisomes	0.5–0.8	1.25
Plasma membrane	0.05–3	1.15
Smooth endoplasmic reticulum	0.05–3	1.16
Nucleic acid	0.03	1.7
Ribosomes	0.03	1.6
Soluble proteins	0.001–0.002	1.3

Table 3.3 Density gradient media types and their principle uses

Gradient media type	Principle uses
<i>Polyhydric (sugar) alcohols</i>	
Sucrose	Sucrose organelles, membrane vesicles, viruses, proteins, ribosomes, polysomes
Glycerol	Mammalian cells (infrequent), proteins
Sorbitol	Sorbitol nonmammalian subcellular particles
<i>Polysaccharides</i>	
Ficoll [®] , polysucrose, and dextrans	Mammalian cells (sometimes in combination with iodinated density gradient media), mammalian subcellular particles (infrequent)
<i>Inorganic salts</i>	
CsCl	DNA, viruses, proteins
Cs ₂ SO ₄	DNA, RNA
KBr	Plasma lipoproteins
<i>Iodinated media</i>	
Diatrizoate	Mainly as a component of commercial lymphocyte isolation media
Nycodenz [®] , Histodenz TM	Mammalian cells, organelles, membrane vesicles, viruses vesicles, viruses, plasma lipoproteins, proteins, DNA
Iodixanol	
<i>Colloidal silica media</i>	
Percoll [®]	Mammalian cells, organelles, membrane vesicles (infrequent)

different stages of purification and determine the purity of the membrane preparation. Standard marker enzymes are shown in Table 3.4.

Many membrane fractions are characterized by **chemical markers**, which can be any specific component of that membrane fraction. For example, cardiolipin is a phospholipid confined to inner membrane of mitochondria, clathrin is found exclusively in coated vesicles, nucleoporin found in nuclear membrane, and Rab5a marker for early endosome. But these markers are often require immunofluorescent methods using fluorescent tagged marker-specific antibodies to characterize and identify the membrane fraction.

Organelles may also be identified under microscope using techniques such as immunofluorescent staining and in situ hybridization. Immunofluorescent techniques use fluorescent-labeled antibodies against membrane-specific proteins to identify specific membranes. In situ hybridization is a technique which uses fluorescent or enzyme labels antisense mRNA probes to identify organelle-specific mRNA expression.

3.2.3 Solubilization of Membrane Proteins

Next step in membrane protein purification is the solubilization of proteins from the isolated subcellular membrane fraction into aqueous solution in its native form.

The native environment of membrane proteins is hydrophobic lipid bilayer. Hence, a major challenge of membrane protein purification is to obtain the protein in functionally active, native conformation in aqueous solution.

Detergents are used as invaluable tools to solubilize and isolate membrane proteins for subsequent studies. Detergents like lipids are amphipathic molecules which associate to form micelles above their CMC. At low concentrations, as monomers, detergent molecules partition into the lipid bilayer. Higher detergent concentration disrupts the membrane bilayer forming lipid–protein–detergent mixed micelles. Increase in detergent concentration above its CMC results in a heterogeneous mix of

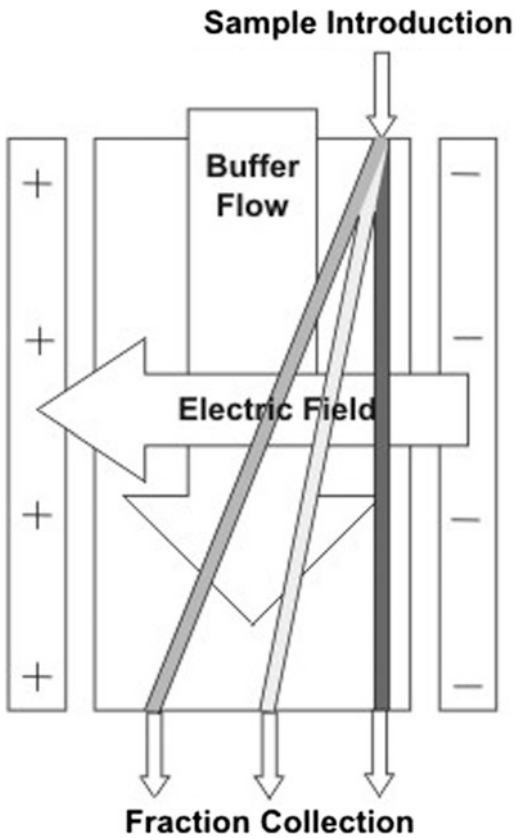


Fig. 3.24 Free-flow electrophoresis

detergent, lipid–detergent, and protein–detergent micelles (Fig. 3.25). The membrane proteins are brought into solution in detergent–protein micelles in which the hydrophobic regions of the proteins interact with hydrophobic portion of the detergent. The protein–detergent micelle can be isolated from the micelle mix and then purified. The choice of the appropriate detergent is crucial for the effective solubilization of a membrane protein. Criteria of choosing a detergent depend on a number of factors, which include (1) the critical micelle concentration (CMC) of the detergent, (2) the solubilizing buffer medium, as the effective CMC of a detergent can be affected by a number of factors, such as pH, ionic strength, and temperature, (3) compatibility with the protein: A detergent should preserve the biological activity of the protein and should not denature the protein and charged ionic detergents can denature proteins, (4) compatibility with subsequent purification methods, for example, ion-exchange chromatography is incompatible with charged detergents, and (5) easy removal of excess detergent. Detergents can be removed by a number of methods including hydrophobic absorption on a resin, gel chromatography (protein–detergent, lipid–detergent, and detergent

Table 3.4 Marker enzymes

Subcellular organelle	Marker
Plasma membrane basolateral	Adenylate cyclase, Na ⁺ K ⁺ ATPase
Apical	5'-nucleotidase
Endoplasmic reticulum	Glucose-6-phosphatase, NADPH (cyt c) reductase
Golgi apparatus	α-Mannosidase II, galactosyl transferase
Mitochondria inner membrane	Cytochrome c oxidase, succinate-dehydrogenase
Outer membrane	Monoamine oxidase
Lysosome	β hexosaminidase, acid phosphatase, β galactosidase
Peroxisome	Catalase
Cytosol	Lactate dehydrogenase

Source Findlay and Evans (1987)

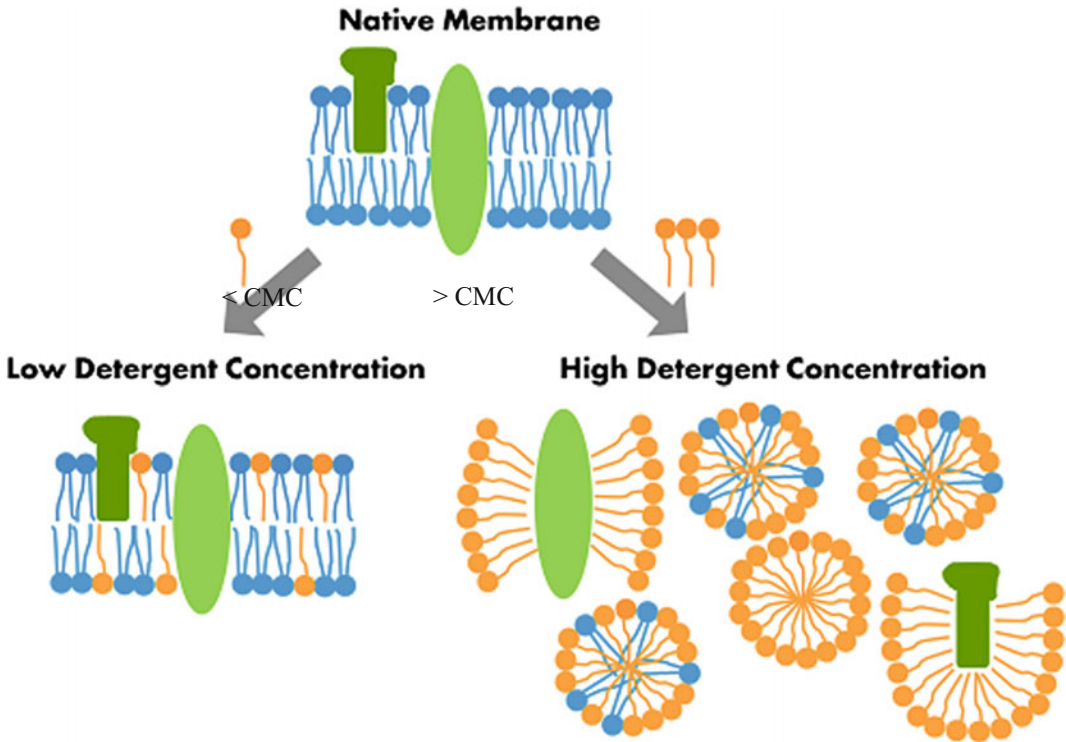


Fig. 3.25 Solubilization of membrane proteins by detergents

micelles are separated on the basis of size), ion-exchange chromatography, dilution, or dialysis.

Classification of detergents

Detergents can be classified on the basis of their hydrophilic groups (Table 3.5).

(i) Ionic detergents have charged hydrophilic groups, which can be positive (cationic) or negative (anionic). Sodium dodecyl sulfate (SDS) and

bile salts such as cholate and deoxycholate are examples of anionic detergents, and cetyltrimethylammonium bromide (CTAB) is an example of cationic detergent. (ii) Nonionic detergents have uncharged hydrophilic groups, such as Triton X-100, which belongs to polyoxyethylene series of detergents, (iii) Zwitterionic detergents combine properties of both ionic and nonionic detergents. 3-[(3-cholamidopropyl)-dimethylammonio]-1-propanesulfonate (CHAPS) is a zwitterionic detergent (Fig. 3.26).

Table 3.5 Commonly used detergents and their critical micelle concentrations (cmc)

Type of detergent	Example	CMC (mM)
Ionic detergent	Anionic: sodium dodecyl sulfate (SDS)	8
	Cationic: cetyl trimethyl ammonium bromide (CTAB)	1
Nonionic detergent	Triton X-100	0.30
	Octylglucoside	25
	Tween 20	0.06
Zwitterionic detergent	CHAPS	6.5

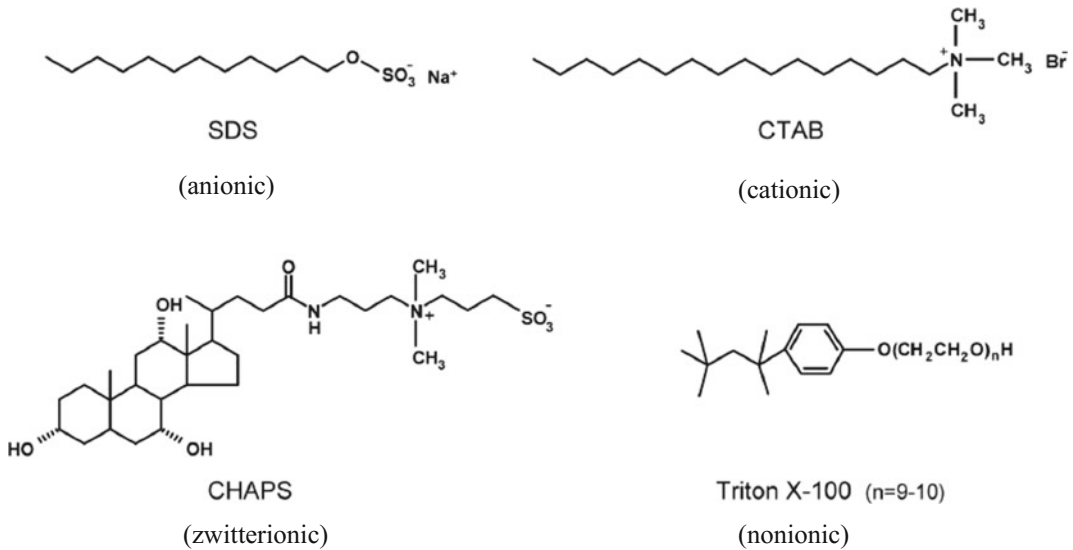


Fig. 3.26 Structures of different types of detergents

Ionic detergents are considered harsh as they disrupt the hydrophilic interactions in the protein leading to its unfolding and denaturation. Non-ionic and zwitterionic detergents are preferred as they retain the structure and function of the proteins. They are considered mild as they affect the lipid–lipid and protein–lipid interactions rather than protein–protein interactions. CHAPS, a zwitterion detergent, and Triton X-100, a mild nonionic detergent, are the most commonly used detergents in membrane studies, yet they both have certain advantages and some limitations. CHAPS, unlike Triton X-100, has very low absorbance at 280 nm, hence does not interfere during optical monitoring of protein purification. Additionally, it can be easily removed by dialysis due to its higher CMC. Triton X-100 on the other hand has a low CMC value and has to be removed by dilution or by bio-beads method. For optimal solubilization, several detergents and conditions need to be screened for each specific membrane protein.

3.2.4 Membrane Protein Purification and Characterization

Membrane proteins solubilized as soluble protein–detergent aggregates, hence need detergents to maintain the three-dimensional structure of the protein. Purification is usually done at detergent concentrations just above the CMC using the same separation techniques as used for soluble proteins.

3.2.4.1 Phase Separation

Phase separation is a simple, efficient, cheap yet powerful, purification protocol that can be used for separating solubilized membrane proteins.

Polymer-based two-phase aqueous systems have been used for the separation of solubilized membrane proteins. Two water-soluble, immiscible polymers such as dextran and PEG are mixed in aqueous solution at high concentrations to form two immiscible aqueous phases. Protein solution is added to the mixture and mixed, as the

two immiscible aqueous separate, the proteins partition into the two phases based on their physical properties. Polymers of opposite charges can also be used for separation (e.g., cationic or anionic PEG derivatives). The pH of the solution can be used to modulate the affinity of the protein to a particular phase for better separation.

Detergent-based phase separation has been developed recently. This phase separation method uses Triton X-114, *tert*-octylphenol poly(ethyleneglycoether)_n ($n = 7-8$). Triton X-114 is a unique detergent in that it solubilizes membrane proteins and also separates them from soluble proteins via temperature-dependent phase partitioning. A solution of Triton X-114 is homogeneous at 0 °C (forms a clear micellar solution) but separates into two phases, an aqueous phase and a turbid detergent phase above 20 °C (the cloud point) as micelles form. So proteins' partition in the two phases of Triton X-114 solution as temperature is raised from 0 to 20 °C.

3.2.4.2 Molecular-Sieve Chromatography

Membrane proteins as protein–lipid–detergent complexes exhibit apparent molecular weights up to twice that expected from their amino acid compositions/sequence. Hence, high-porosity Sepharose, agarose, or polyacrylamides are used for separation. The use of HPLC- and FPLC-based systems for fractionation of integral membrane proteins has also yielded good results. There is a wide range of support material available for gel filtration HPLC and FPLC columns utilizing silica- or polymer-based materials (e.g., hydroxylated polyethers), separating proteins from the range from 500 to 2×10^7 daltons.

3.2.4.3 Ion-Exchange Chromatography

All the classical ion-exchange systems used in protein purification can be used for membrane protein separation provided that the native charge characteristics of the polypeptide have not been altered by addition of detergents especially the ionic detergents. The weakly ionic DEAE and CM-derivatized resins are popularly used for

membrane protein separation in the presence of detergents in conditions such that detergents do not interfere with the interaction between the protein and the resin.

3.2.4.4 Affinity Chromatography

Affinity chromatography is based on the separation of proteins on the basis of some biological specificity of the protein, not present in other proteins. It could be a substrate of an enzyme, ligand of a receptor, or antibodies against the protein. This is one of the most popular methods for membrane protein purification which not only purifies the protein but also concentrates it.

3.2.4.5 Crystallization Membrane Proteins for Structure Determination

Resolution of three-dimensional structures of proteins requires crystallography. Generation of crystals proves to be a major challenge for membrane proteins.

The membrane lipids spontaneously self-assemble into a variety of so-called liquid crystalline phases also referred to as **mesophases**, being more ordered than a liquid but less than a solid phase. This includes the inverted hexagonal and cubic phases (Fig. 3.27). The dominance of a particular mesophase depends on the lipid molecular structure, concentration, and composition and temperature, pressure of the aqueous dispersing medium.

Crystallization of light-driven transmembrane proton pump Bacteriorhodopsin by Landau and Rosenbusch (1996) in a cubic mesophase led to in meso method becoming a popular method of crystallization of membrane proteins.

3.2.4.6 The In Meso or the Cubic-Phase Method

The basic recipe for growing crystals in meso follows the following steps; firstly, two parts of protein solution/dispersion are mixed with three parts of monoacylglycerol lipid (MAG), usually monoolein. The cubic-phase forms spontaneously. Then, precipitant/salt is added and incubated; crystals form in hours to weeks. All operations are performed at 20 °C. Many

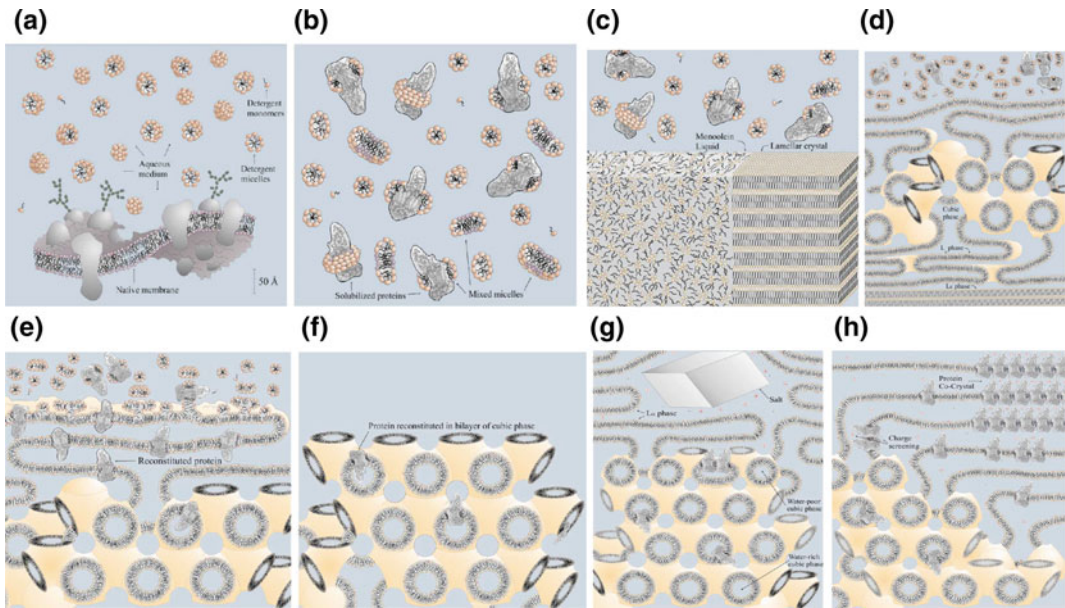


Fig. 3.27 Solubilization, reconstitution, and in meso crystallization of membrane proteins. Cartoon representation of the events taking place during solubilization (**a, b**), reconstitution (**c–f**), and in meso crystallization (**g, h**) of an integral membrane protein as outlined in the text. As much as possible, the dimensions of the monoolein (light brown), detergent (pink), native membrane lipid (purple), protein (gray; RCV, PDB 1PRC (Deisenhofer et al. 1995)), bilayer, and aqueous channels (blue) have been drawn to scale. **a** Isolated biological membrane in the presence of detergent micelle solution. **b** Solubilized membrane proteins exist as mixed micelles in solution. **c** Combining

solubilized protein solution with monoolein in the fluid isotropic and lamellar crystal phases. **d** Hydration of monoolein to form contiguous La and cubic phases. Limited detergent and monoolein exchange occur. **e** Protein reconstitution and dispersion in mesophases. **f** Reconstituted protein in bilayer of cubic phase. **g** Addition of precipitant (salt) to initiate crystallization by water-withdrawing and charge-screening effects. Bilayer curvature in cubic phase increases as water content drops. **h** Reversible crystallization of protein (and bound lipid, in the case of cocrystallization) from cubic phase through lamellar portal. *Source* Caffrey (2003) (Color figure online)

membrane proteins including bacterial rhodopsins, photosynthetic reaction centers, β barrels, and GPCRs have been successfully crystallized by this method.

3.3 Membrane Protein Topology

Integral membrane proteins contain transmembrane (TM) domains that traverse through the membrane and soluble domains that reside on either side of the membrane, i.e., either “in” indicating cytoplasm (cis-side) or “out” indicating extracellular side (trans-side) of plasma membrane in eukaryotes, and luminal side of subcellular organelle membranes such as the ER, Golgi, and lysosomes.

Membrane topology refers to the orientation of different domains of the protein with respect to the plane of the membrane. Topology of a membrane protein is primarily determined during the biosynthesis of the polypeptide as it is inserted into the ER membrane. Membrane proteins like the secretory proteins are synthesized with a N-terminal signal sequence which is recognized by signal recognition particle (SRP). As the protein emerges from the ribosome, the polypeptide’s signal sequence-associated SRP interacts with its receptor (SRP receptor, SR) on the ER surface and transfers the ribosome–nascent protein complex (RNC) to the translocon (Fig. 3.28). The translocon is a protein conducting channel, composed of $\alpha\beta\gamma$ heteromeric Sec61 complex associated with translocating

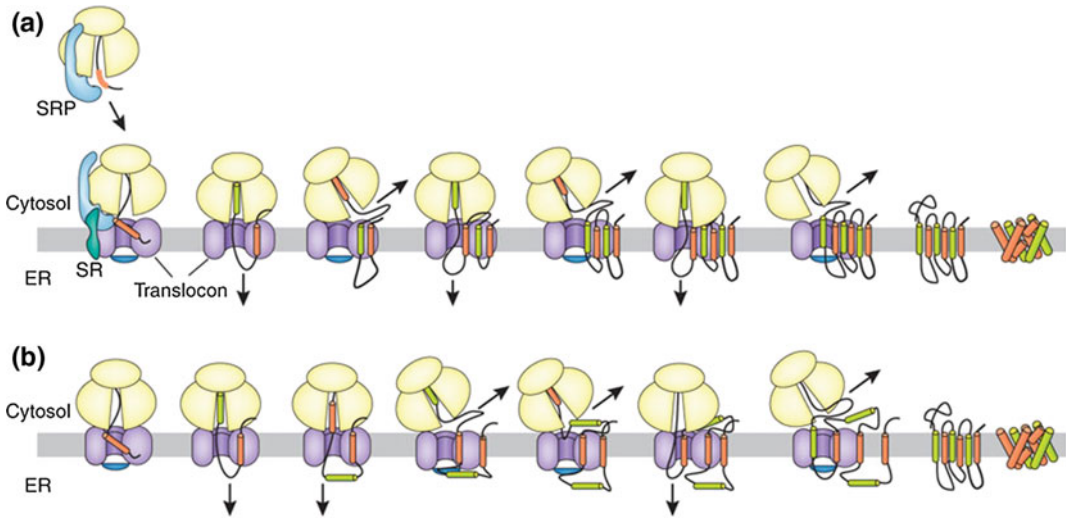


Fig. 3.28 Models of polytopic protein biogenesis. **a** Cotranslational biogenesis is initiated as the signal recognition particle (SRP) interacts with a signal sequence, binds its receptor (SR) at the ER membrane, and transfers the ribosome–nascent chain complex to the Sec61 the translocon. Signal sequences (orange cylinders) stimulate ribosome binding and open the gate of the translocon pore (blue disk) to initiate peptide movement into the ER lumen. Stop transfer sequences (green cylinders) terminate translocation and redirect the elongating nascent chain beneath the ribosome and into the

cytosol. Each sequential TMS therefore alters the direction of nascent chain movement through the RTC (arrow) to establish transmembrane topology from the N- to the C terminus, one helix at a time. **b** During AQP1 biogenesis, TM2 fails to terminate translocation, TM3 is initially inserted into the translocon in a type-I topology, and TM4 transiently resides on the cytosolic face of the membrane. This sequence of events generates a four-spanning intermediate that is converted to a six-spanning topology during or after synthesis of TM5 and TM6. *Source* Skach (2009) (Color figure online)

chain-associated membrane protein (TRAM) and other proteins.

On entering the translocon, the integral membrane proteins, unlike the secretory proteins, are not translocated across the membrane completely due to stop transfer (ST) sequences, instead TM domain sequences move laterally into the bilayer to form a transmembrane segment (TMS) that is termed a “signal anchor” (SA) sequence as it anchors the protein to the membrane. As translation proceeds, different regions of the nascent chain are to be directed either to the lumen, bilayer, or the cytosol without disrupting the membrane. To facilitate this, the ribosome and translocon junctions undergo a series of conformational changes alternatively gating the cytosolic or luminal end of the pore. Gating of pores regulates the passage of the nascent chain into the appropriate compartment. For example, after the transfer of nascent

polypeptide to the translocon, the RNC–translocon junction is sealed to direct the nascent chain into the ER lumen, whereas a TMS signal closes the luminal end of the pore to prevent the passage into the ER lumen. Shortly thereafter, to allow the cytoplasmic domain of the membrane protein to move into the cytosol, the RNC–translocon seal is opened while the luminal end of the pore remains closed. For polytopic membrane proteins with multiple TMSs, besides the alternate gating of the translocon pore at its cytosolic and then its luminal end, a series of alternating signal anchor (SA) and stop transfer (ST) sequences in the native proteins are required to form the polytopic membrane proteins.

Hence, membrane topology is primarily determined by topogenic signals in the amino acid sequence of the nascent polypeptide chain as it emerges from the ribosome and membrane environment.

3.3.1 The Major Membrane Topology Determinants Are as Follows

1. Positive inside rule

It has been observed that positively charged residues in membrane proteins are present in higher percentage in the connecting loops of TM domains in cytoplasmic side of the membrane as compared to the extracellular side. This characteristic property is known as the “positive inside rule.” Sequences rich in positive charged amino acids are retained in the cytoplasm and not translocated through the translocon. Negatively charged amino acids form a stronger translocation signal. Hence, positively charged amino acids in the flanking regions of the TM domain are the prominent “inside” topogenic signals positioning positively charged sequences in the cytosol.

2. Hydrophobicity of the TM segment

The degree of hydrophobicity and the length of the signal sequence and the TM domain influence the N- and C-terminal translocation of single-spanning membrane proteins. Signal sequence and TM segment with higher hydrophobicity and longer length show greater tendency for N-terminal translocation through the translocon into the lumen. Higher hydrophobic sequences translocate faster by interacting with the hydrophobic core of the lipids and have a lower probability to invert their orientation after entering the translocon, whereas moderately hydrophobic TM segments have a much slower rate of translocation and thus have a higher probability to invert their orientation to and acquire $N_{in/cytosol}-C_{out/lumen}$ membrane orientation.

3. Length of N- and C-terminal domains

Studies show that very long N terminus gives rise to higher folding efficiency, resulting in flipping and reversing the membrane orientation of the nascent chain to acquire a $N_{in/cytosol}-C_{out/lumen}$

orientation. Glycosylation of the N terminus in the ER lumen confines the N terminus in the luminal side of the ER, thus acquiring N_{out} membrane orientation. For a single-spanning membrane protein with an N terminus shorter than 20 residues, the C_{out} orientation is favored with increasing length of the C terminus. However, when the N terminus is longer than 20 residues, the impact of the C-terminal length and the hydrophobicity of the TM domain is less prominent. Hence, the N- and C-terminal translocations are influenced by their length and folding efficiency. The membrane insertion of a signal anchor protein can result from the flipping of the N-terminal and then inserted as a hairpin in the membrane.

3.3.2 Experimental Tools to Determine the Membrane Topology of Proteins

1. Proteases

In intact cells and organelles, proteases can cleave only the exposed parts of a membrane protein. The domains embedded in the membrane as well as the inside loops are not exposed, hence are not affected. Migration pattern of cleaved protein can be compared to intact protein on SDS-PAGE, and the peptide segments of the exposed portions can be determined. Oriented membranes, for example, in – side – out, and out – side – out membranes can be made to determine the soluble membrane protein segment exposed on the two sides of the membrane. Both sequence-specific proteases and nonspecific proteases such as proteinase K are used in topology determination.

2. Antibody accessibility

The antibodies bind to specific epitopes of the protein which are exposed on the outside of the membrane. Antibodies tagged with fluorescent probes help in epitope recognition by immunofluorescence studies. The extracellular

domains of membrane proteins can be determined by using this technique.

3. Fluorescence-based assays

Tagging of membrane proteins with a reporter, such as a fluorescent probe, helps in determining membrane topology.

The glycosylation site engineered with a GFP tag does not interfere with the GFP fluorescence intensity, but when glycosylated, it diminishes fluorescence. Thus, gGFP, a GFP-tagged N-linked glycosylation site shows fluorescence in the cytosol as it is not glycosylated, but is nonfluorescent in the ER lumen on glycosylation. Hence, fluorescence measurement and assessment of glycosylated state of a gGFP fusion protein by Western blotting determine the localization of gGFP fusion protein. Two reporter tags, the redox-sensitive GFP (roGFP) and luciferase reporter system, have also been used. roGFP forms a disulfide bond in the oxidative environment of the ER lumen and loses its fluorescence. Luciferase, on the other hand, shows luminescence in an oxidative environment. Therefore, GFP fluorescence and luciferase activity together serve as dual topology reporter tags, with high-GFP fluorescence and low bioluminescence indicative of cytosolic localization, whereas low-GFP fluorescence and high bioluminescence indicate the ER luminal localization.

4. N-linked glycosylation in eukaryotic cells

Eukaryotic secretory proteins are cotranslationally inserted into the ER membrane through the Sec61 translocon. The Sec61 translocon is associated with the oligosaccharyl transferase (OST) in the ER lumen, which recognizes the N-terminal, N-X-T/S (X can be any residue but proline) sequence in the nascent polypeptide, and adds oligosaccharides on the N-terminal asparagine residue. Thus, if the N-linked consensus sequence of a protein segment is glycosylated, that segment resides in the ER lumen. Treatment of the protein with endoglycosidase H (Endo H) followed by SDS-PAGE separation identifies the N-linked glycosylated segment. N-linked

glycosylation adds approximately 2 kDa to the protein mass, thus slows down the migration of glycosylated protein segment on the SDS-gel. As Endo H cleaves off the glycans from glycoproteins, an Endo H-treated sample serves as a unglycosylated protein control. The comparison of the gel mobility of Endo H-treated and Endo H-nontreated protein samples reveals the glycosylated status of a protein. The glycosylated soluble loop is always confined to the luminal side of the ER membrane.

References

- Almén MS, Nordström KJ, Fredriksson R, Schiöth HB (2009) Mapping the human membrane proteome: a majority of the human membrane proteins can be classified according to function and evolutionary origin. *BMC Biol* 7:50. <https://doi.org/10.1186/1741-7007-7-50> (PMC 2739160. PMID 19678920)
- Caffrey M (2003) Membrane protein crystallization. *J Struct Biol* 142:108–132
- Deisenhofer J, Epp O, Miki K, Huber R, Michel H (1985) Structure of the protein subunits in the photosynthetic reaction centre of *Rhodospseudomonas viridis* at 3 Å resolution. *Nature* 318:618–624. <https://doi.org/10.1038/318618a0>
- Findlay JBC, Evans WH (1987) *Biological membranes: a practical approach*. IRL Press
- Gophna U, Ideses D, Rosen R et al (2004) OmpA of a septicemic *Escherichia coli* O78—secretion and convergent evolution. *Int J Med Microbiol* 294:373–381 <http://www.sanger.ac.uk/Software/Pfam>
- Hurwitz N, Pellegrini-Calace M, Jones DT (2006) Towards genome-scale structure prediction for transmembrane proteins. *Phil Trans R Soc B* 361:465–475
- Kenrew JC, Bodo G, Dintzis HM, Parrish RG, Wyckoff H, Phillips DC (1958) A three-dimensional model of the myoglobin molecule obtained by X-ray analysis. *Nature* 181:662–666
- Kobilka BK (2007) G protein coupled receptor structure and activation. *Biochimica et iophysica acta* 1768 (4):794–807. <https://doi.org/10.1016/j.bbame.2006.10.021>
- Kyte J, Doolittle RF (1982) A simple method for displaying the hydropathic character of a protein. *J Mol Biol* 157:110
- Landau EM, Rosenbusch JP (1996) Lipidic cubic phases: A novel concept for the crystallization of membrane proteins. *Proceedings of the National Academy of Sciences* 93(25):14532–14535
- Lefkowitz RJ, Kobilka BK (2012) The nobel prize in chemistry. *Royal Swed Acad Sci*
- MARCKS_HUMAN (2007) Swiss-Prot. <http://www.expasy.org/uniprot/P.29966>

- Ott CM, Lingappa VR (2002) Integral membrane protein biosynthesis: why topology is hard to predict. *J Cell Sci* 115:2003–2009
- Pautsch A, Schulz GE (1998) Structure of the outer membrane protein A transmembrane domain. *Nat Struct Biol* 5:1013–1017
- Perutz MF, Rossmann MG, Ann F, Cullis AF, Muirhead H, Will G, North ACT (1960) Structure of haemoglobin: A three-dimensional Fourier synthesis at 5.5-° A resolution obtained by X-ray analysis, *Nature* 185:416–422
- Power ML, Ferrari BC, Littlefield-Wyer J, Gordon DM, Slade MB, Veal DA (2006) A naturally occurring novel allele of *Escherichia coli* outer membrane protein A reduces sensitivity to bacteriophage. *Appl Environ Microbiol* 72:7930–7932
- Singer SJ, Nicolson GL (1972) The Fluid Mosaic Model of the Structure of Cell Membranes. *Science* 175 (4023):720–731
- Skach WR (2009) Cellular mechanisms of membrane protein folding. *Nat Struct Mol Biol* 16:606–612. <https://doi.org/10.1038/nsmb.1600>
- Smith SO (2012) Insights into the activation mechanism of the visual receptor rhodopsin. *Biochim Soc Trans* 40:389–393
- Stahelin RV (2009) Lipid binding domains: more than simple lipid effectors. *J Lipid Res* 50:S299–S304
- Taylor DR, Hooper NM (2011) GPI-anchored proteins in health and disease. In: Vidal CJ (ed) *Post-translational modifications in health and disease, protein reviews*, vol 13. Springer Science + Business Media, LLC

4.1 Plasma Membrane: Specialized Membrane Structures

The plasma membrane, or the cytoplasmic membrane, demarcates the cell separating the interior of a cell from the outside environment. The plasma membrane primarily functions as a protective barrier and regulates the movement of molecules across the cell.

The plasma membrane has some specialized structures to perform specific functions. It is associated with different types of cell junctions which perform different functions, including attachment to the extracellular matrix, cell–cell adhesion and communication, and maintenance of cell polarity. These junctional complexes include tight junctions, desmosomes, hemidesmosomes, and gap junctions.

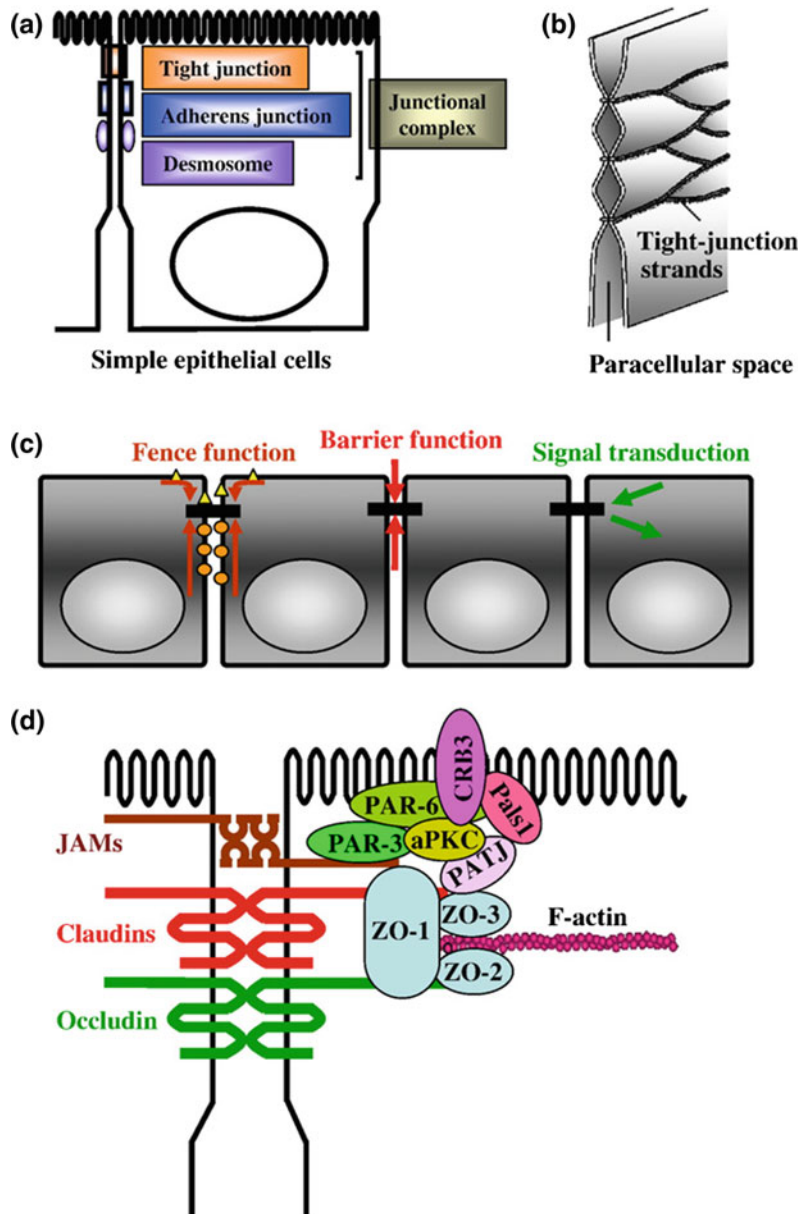
Plasma membranes anchor the cytoskeleton which provides it mechanical strength and give shape to the cell. Sphingolipids, which are present in higher density in plasma membranes (see Chap. 1), associate with cholesterol to form more ordered domains called membrane rafts. Membrane rafts provide an close microenvironment for its associated proteins to interact and function. Plasma membrane contains many such micro- and macrodomains (see Chap. 5), which in most cell types are established transiently, while in others, especially in polarized cells including neurons, oligodendrocytes, and epithelial cells maintain a more permanent distinct domains of membrane proteins and lipids.

4.1.1 Tight Junctions

Tight junctions are observed in epithelial cell plasma membrane at the boundary between the apical and lateral domain. They appear to form a branched network of sealing strands between adjacent cells just beneath their apical surface. Tight junctions act as a intercellular barrier that restricts paracellular leakage (Fig. 4.1). Apart from epithelial cells, they also have a functional role in vascular endothelial cells, mesothelial cells, Schwann cells, oligodendrocytes, and Sertoli cells.

Tight junctions function as a semipermeable barrier preventing the passage of ions, water, and other solutes through the space between the plasma membrane of adjacent cells and hence help in maintaining osmotic gradient. They also function as a fence demarcating the apical and the basolateral domains of plasma membrane and hence play an important role in maintaining polarity of the cell (Fig. 4.1c). In addition, tight junctions also transduce a variety of cell–cell signaling and trafficking signals, regulating variety of cellular events like cell differentiation, proliferation, polarity. Any defect in the structure and function of tight junctions can lead to a variety of diseases, such as infections and cancers. In the brain, the tight junctions present between the endothelial cells lining the capillary wall form the blood–brain barrier (BBB) which restricts the passage of substances from blood into the brain, thereby protecting the brain from any toxic substances present in blood. But it also

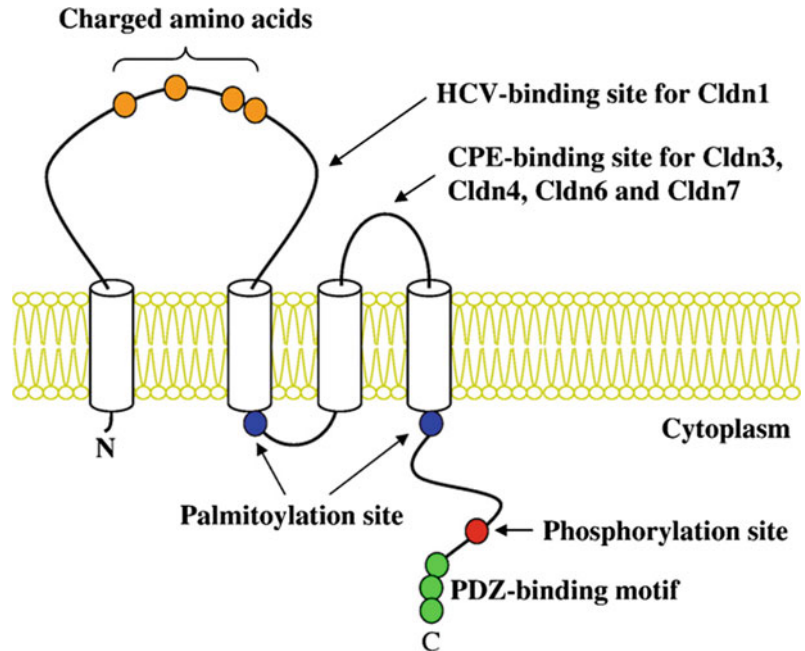
Fig. 4.1 Apical junctional complex and tight junctions. **a** Schematic drawing of the junctional complex. **b** Schematic structure of tight junction strands. **c** Functions of tight junctions. **d** Molecular components of tight junctions. Three families of tight junction transmembrane proteins, occludin, claudins, and JAMs, as well as some scaffold proteins and polarity proteins are shown. *Source* Chiba et al. (2008)



poses a challenge by preventing drug delivery to the central nervous system. Consequently, it becomes critical to develop strategies to overcome this paracellular barrier for successful drug delivery and treatment of many diseases.

Tight junctions are made up of various molecular components, which include the integral proteins, **occludin**, **claudins (Cldn)**, **junctional adhesion molecules (JAMs)**, and **tricellulin**

(Fig. 4.1D). **Occludin** is a ~60 kDa four transmembrane domain protein, whose exact role is still unclear. It has two extracellular loops, one intracellular loop, and N- and C-terminal cytoplasmic domains. The first extracellular loop constitutes majorly of tyrosine and glycine residues (about 60%) with very few charged amino acids. The long C-terminal domain is rich in serine, threonine, and tyrosine residues, which are

Fig. 4.2 A model of claudin protein

the site of phosphorylation by various protein kinases. Occludins, through its C-terminal domain binds to scaffolding proteins like Zonula occludens **ZO-1**, **ZO-2**, and **ZO-3**, which serve as links between the tight junction proteins and the **actin** cytoskeleton. Occludin seems to function as a signal transmitter of tight junctions and is associated with a variety of signaling molecules such as Ser/Thr/Tyr kinases and the phosphatases.

Claudins are 18–27 kDa four transmembrane domain proteins with a short cytoplasmic N-terminal domain, two extracellular loops, one intracellular loops, and a long intracellular C-terminal domain (Fig. 4.2). The claudin family consists of 24 members in mice and humans and exhibits tissue and cell specific expression patterns. Like occludins, the C-terminal domain of Claudins have PDZ-binding motifs to bind PDZ motif containing scaffolding proteins Zonula occludens **ZO-1**, **ZO-2**, and **ZO-3**, linking it to actin cytoskeleton. The C-terminal domain is also the site of posttranslational modification, like phosphorylation and palmitoylation, regulating claudin function and localization.

Claudins are barrier-forming proteins which interact with claudins from neighboring cells to

form a barrier. Claudins also contribute to pore formation, determining the permeability properties of tight junctions. The first extracellular loop (EC1) shows a wide variety in the number and type of charged amino acids (Fig. 4.2) and hence contributes to the ion selectivity of paracellular pores (channels). For example, Cldn15, Cldn2, Cldn12, and Cldn7 which are cationic pores have negatively charged residues within the first extracellular loop, claudin-10a and -17 are anion pores with positively charged amino acids in the first extracellular loops (EC1s). Different tissues/cells have specific combination of different claudin proteins determining the pore selectivity and the barrier properties of tight junctions in that cell/tissue. For example, claudin-16/-19 results in a cation pore and claudin-4/-8 in an anion pore. Cldn16 is observed to be highly expressed at tight junctions of epithelial cells in the thick ascending loop of Henle, where reabsorption of divalent cations takes place. On the other hand, Cldn2 acts as a paracellular channel to Na^+ ions in renal epithelial cells without affecting Cl^- conductance. Cldn2 and Cldn12 mediate paracellular Ca^{2+} absorption in intestinal epithelial cells. Their expression is stimulated by active

vitamin D3, $1\alpha, 25$ -dihydroxyvitamin D3 [$1\alpha, 25$ (OH)2D3] in enterocytes and hence plays an important role in mediating vitamin D-dependent calcium homeostasis.

Claudins are regulated by phosphorylation by different protein kinases, including PKA, PKC, and MAPK.

Mutations in claudin genes have been reported to cause many diseases. The manifestation of the disease depends on the localized expression of claudin genes. Mutations in the *Cldn14* gene, which is highly expressed in outer hair cells of the cochlea, cause autosomal recessive deafness, while mutations in the *Cldn19* gene, which is highly expressed in renal tubules and the retina, have been associated with severe hypomagnesemia due to renal wasting, nephrocalcinosis, progressive renal failure, and severe ocular abnormalities. Claudin-16 gene defect is associated with familial hypomagnesemia, hypercalciuria, and nephrocalcinosis (FHHNC) is expressed at different sites in Henle's loop and is involved in reabsorption of Ca^{2+} and Mg^{2+} .

Tricellulin is a four transmembrane domain protein that is found at tricellular tight junctions, the junctions found where three adjacent cells meet. The bicellular tight junctions between two adjacent cells form a horizontal band of strands, whereas tricellular tight junctions, between three cells form vertical strands. Claudins are major cell–cell adhesion proteins of bicellular tight junctions, whereas tricellulin is the cell–cell adhesion protein of tricellular tight junctions. Its C-terminal sequence (~130 amino acids) has 32% homology with that of occludin. Tricellulin is assembled at tricellular tight junctions in cochlear and vestibular epithelial cells and recessive mutations in the tricellulin gene causes nonsyndromic deafness (DFNB49). Absence of tricellulin from the tricellular junctions in the inner ear epithelia of the mutant animals leads to rapidly progressing hearing loss accompanied by the loss of mechanosensory cochlear hair cells.

Junctional adhesion molecules (JAMs) are proteins that belong to the immunoglobulin (Ig) superfamily (see Chap. 9). They have a single transmembrane domain, two extracellular Ig like domains and one C-terminal intracellular

domain. JAM-A, a subtype of JAMs, is involved in the barrier function of tight junctions in both endothelial and epithelial cells, and in the development of apico-basal polarity in epithelial cells. JAM-B and JAM-C are associated with Sertoli cells and spermatids, respectively. Cox-sackievirus and adenovirus receptor (CAR), another subtype of JAMs, contributes to the barrier function of tight junctions associated with the epithelial cells lining the body cavities.

4.1.2 Desmosomes

Desmosomes are intercellular junctions that strongly adhere cells. Desmosomes are intracellularly linked to the intermediate filament of the cytoskeleton to form a strong adhesive network that provides mechanical strength to tissues. Hence, desmosomes are functionally required in tissues that are exposed to strong mechanical forces such as the epidermis, GI mucosa, and the cardiac muscle.

Desmosomes have a highly organized structure (Fig. 4.3). The desmosome can be spatially divided into three zones: the extracellular region (desmoglea) and the two intracellular regions, the outer dense plaque (ODP) and the inner dense plaque (IDP). Approximately 30-nm-wide extracellular domain (ECD) between the plasma membrane of two adjacent cells is bisected by a dense midline (Fig. 4.3). Desmosomes comprises of five major proteins, which include the Ca^{2+} dependent desmosomal cadherins (DCs), desmoglein (DSG) and desmocollin (DSC), the plakin family cytolinker desmoplakin (DP), and the armadillo (arm), proteins plakoglobin (PG) and plakophilin (PKP). The extracellular domains of the cadherin proteins, desmogleins (DSG), and desmocollins (DSC) mediate extracellular adhesion, whereas their cytoplasmic tails associate with the desmosomal plaque proteins, plakoglobin (PG), the plakophilin (PKP), and desmoplakin (DP). DP links the desmosomal plaque to the intermediate cytoskeleton, and PG and PKP are adaptor proteins that link the cytoplasmic tails of cadherins and DP. Each of the components of the desmosome complex contributes in resisting

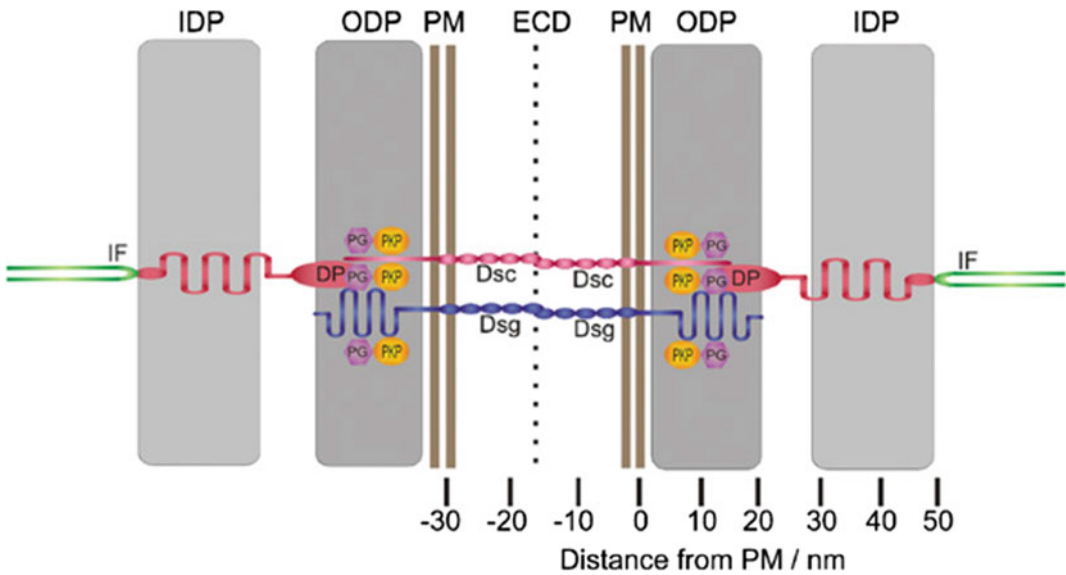


Fig. 4.3 Schematic diagram of a desmosome showing the locations of the five major proteins. The cytoplasmic domain of DSG is folded within the ODP and that DP is

folded within the IDP where it binds to the IF. PKP and PG act as linkers between DP and the DCs. *Source* North et al. (1999)

mechanical stress, and defect in any of them results in human diseases of the epidermis and the myocardium (Fig. 4.4). Mutations in desmoplakin (DP) resulted in detachment of the intermediate (keratin) filaments and severe disruption of the epidermis during birth. Mutations in cadherin protein DSG2 can result in arrhythmogenic right ventricular cardiomyopathy (ARVC). The genetic disease ectodermal skin fragility syndrome results from plakophilin-1 (PKP1) mutations which cause detachment of intermediate filaments and desmoplakin (DP) from the desmosome. This results in epidermal blistering.

Some desmosomes have been found to be resistance to disruption by chelation of extracellular Ca^{2+} . They can adopt a more stronger Ca^{2+} -independent adhesive state known as **hyperadhesion**. Hyperadhesiveness can be modulated by PKC signaling, which mediates the conversion of Ca^{2+} -independent adhesive state to Ca^{2+} -dependent during embryogenesis and wound healing facilitating morphogenetic movement and tissue repair. Desmosomes play an important role in regulating cellular processes such as cell migration and differentiation, alternating between hyperadhesive and normal adhesive state. Downstream

regulation of the two adhesive states would greatly benefit our understanding of processes like wound healing and embryonic development.

4.1.3 Hemidesmosomes

Hemidesmosomes (HDs) are protein complexes that attach cells to the underlying basement membrane in epithelial tissues, such as the skin. They provide a link between the extracellular matrix and the intermediate filament of the cytoskeleton. Hemidesmosomes comprise of at least 5 protein components, which include the $\alpha\beta 4$ integrin, plectin, the bullous pemphigoid antigens BPAG1e (also known as BP230 and BP180), and the tetraspanin CD151. Integrin $\alpha\beta 4$ binds to the extracellular matrix protein laminin-332, whereas P1a, an isoform of the cytoskeletal linker protein plectin forms a bridge to the cytoplasmic keratin intermediate filament network (Fig. 4.5).

The attachment of basal epidermal keratinocytes to the basement membrane (BM) through HDs is important for maintaining the integrity of the skin and epidermal homeostasis. Inherited or acquired

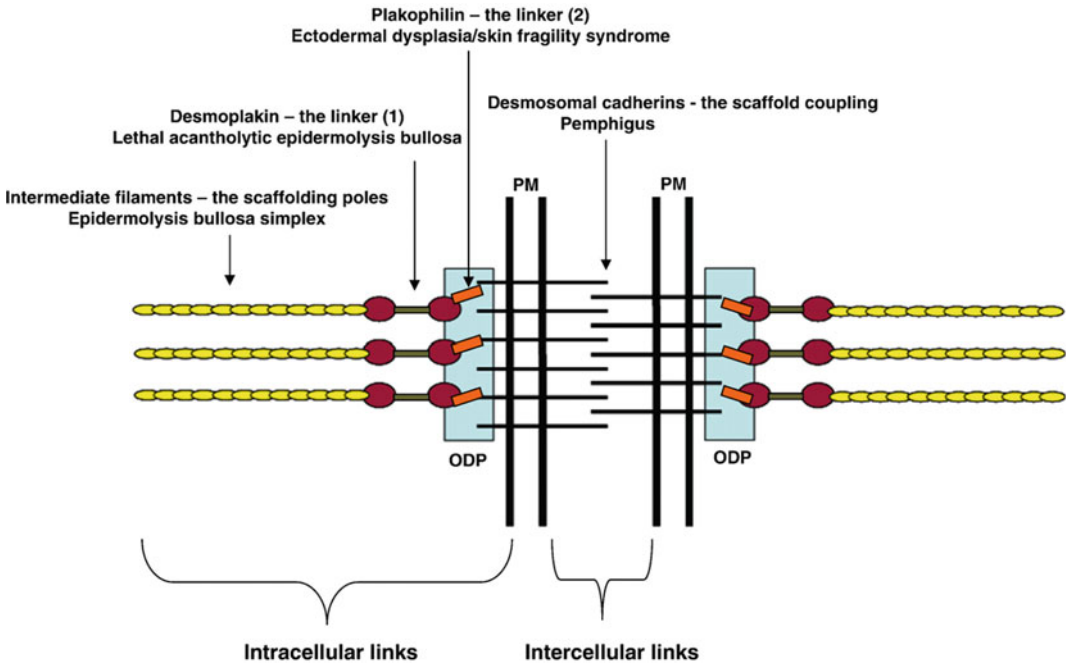


Fig. 4.4 Desmosome-intermediate filament complex showing some of the key links and diseases that weaken them. The interactions between the complex of proteins within the outer dense plaque (ODP) is not fully understood, and plakoglobin (not shown) may contribute to the link in the chain between desmoplakin and the

desmosomal cadherins. Alternatively, desmoplakin may interact with the desmosomal cadherins directly, with plakophilin and plakoglobin mediating lateral interactions (see text). PM plasma membrane. *Source* Garrod and Chidgey (2008)

diseases associated with defects in any of the HD components lead to a variety of disorders involving skin blistering, collectively known as epidermolysis bullosa (EB) which is characterized by tissue separation with blister formation within different layers of the skin.

4.1.4 Gap Junctions

Gap junctions were first discovered in myocardium and nerve providing an electrical connection between adjacent cells. Gap junctions form channels that link the cytoplasm of two cells and allow the passage of ions like K^+ and Ca^{2+} , second messengers like cAMP, cGMP, and inositol 1,4,5-triphosphate (IP_3), and small metabolites like glucose. Intercellular communication through gap junctions is essential for many physiological processes, including electrical

propagation of action potential in nerve fibers, myocardium contraction, organ and tissue development, GI tract motility, myometrium contraction, and coordination of avascular organs like epidermis and lens.

The intercellular gap junction channels are formed by two **connexons** docked in a head to head manner with each cell membrane contributing one connexon. Each connexon is a hexameric assembly of integral membrane proteins, the **connexins** (Cx) which form a half-channel (Fig. 4.6a). Two half-channels of two connexons align to form a continuous channel across the two membranes.

The connexin is a 25–60 kDa protein with four transmembrane domains, C- and N-terminal cytoplasmic domain, one cytoplasmic loop (CL), and two extracellular loops, (EL-1) and (EL-2). The connexin protein is a member of a 21 member large gene family in the human genome.

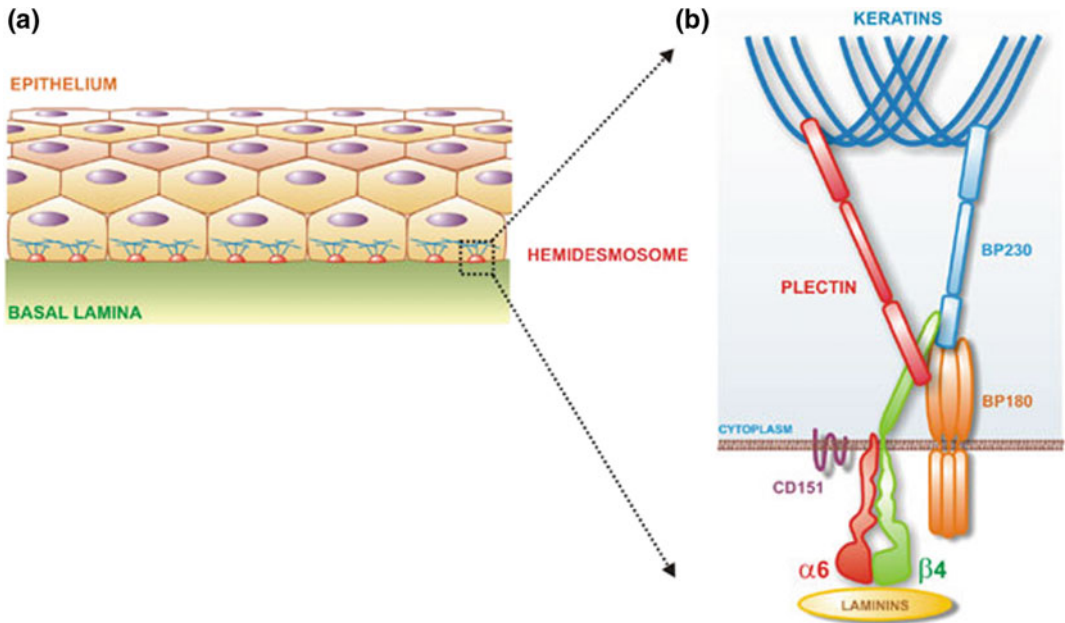


Fig. 4.5 Schematic representation of the components of the hemidesmosomes and the interactions that they establish with each other. *Source* Walko et al. (2015)

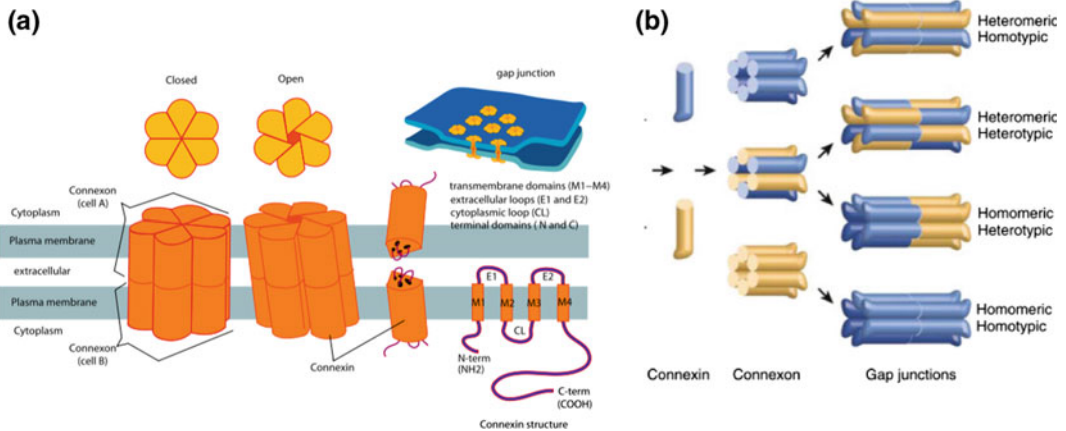


Fig. 4.6 Schematic representation of connexins and gap junctions. **a** Connexins have four transmembrane domains, two extracellular loops, a cytoplasmic loop, and cytoplasmic N- and C-terminal. **b** Six connexins oligomerize to form hemichannels called “connexons,” which then align in the extracellular space to complete the

formation of gap junction channels. **b** Different connexins can selectively interact with each other to form homomeric, heteromeric, and heterotypic channels, which differ in their content and spatial arrangement of connexin subunits. *Source* Meşe et al. (2007)

The various connexins combine to form both homomeric and heteromeric gap junctions (Fig. 4.6b), each of which may vary in pore size, conductivity, and voltage and chemical gating.

There are two conventions used for the nomenclature of connexins, one depends on molecular mass of the connexin (Cx26 represents the connexin protein of 26 kDa; Cx46, connexin

isoform of 46 kDa, etc.), whereas the other uses Greek symbols (*GJβ2* is gap junction beta-2 referring to Cx26, whereas *GJα3* stands for gap junction alpha-3, or Cx46).

Gap junctional intercellular channels are dynamically regulated. The fast mode regulation involves gap junction gating, whereas slow mode regulation regulates the rates of synthesis and assembly, posttranslational modification and/or protein degradation, thereby controlling the number of channels present in the membrane.

The gap junctions are gated by a number of factors, including pH, transmembrane voltage, and calcium concentration. Voltage-dependent gating plays an important role in neuronal communication. Posttranslational modifications of connexin protein including phosphorylation also regulate gap junction gating. The connexin protein can be phosphorylated by a number of kinases, including protein kinase A (PKA) and protein kinase C (PKC).

Biosynthesis and assembly of gap junctions are strictly regulated. The connexin protein is cotranslationally integrated into the endoplasmic reticulum membrane. The oligomerization of six connexins to form a hemichannel called connexon occurs as it progresses from the endoplasmic reticulum to the *trans*-Golgi. Connexons (hemichannels) are then transported to the cell surface via vesicular transport. These hemichannels then diffuse to regions of cell-to-cell contact to align head to head with connexon from an apposing cell to form the intercellular channel. The hemichannels are characterized by a positively charged cytoplasmic entrance, a funnel-shaped pore with a negatively charged pathway, and an extracellular cavity. The pore is narrowed at the funnel, lined by the six amino-terminal helices of each connexin molecule, which acts as a size selectivity filter for the channel.

Gap junctions can form a cluster of few to thousands of units in membranes known as **gap junction plaques**. Gap junction plaques are highly dynamic with the old channels being continuously removed from the center of the plaque and new gap junction added to the

periphery. The gap junctions from the middle of the plaque are internalized via endocytosis into vesicles called the “**annular junctions**,” which are then degraded either in the lysosome or by the proteasomal pathway (Fig. 4.7). This dynamic flux of connexins is regulated by various signaling pathways to provide for the quick adaptation of tissues to different physiological conditions.

4.1.4.1 Some Specialized Functions of Gap Junctions

1. Gap junctions in the vascular system

Arterioles are composed of a layer of endothelial cells lining the lumen, attached to a basal lamina, which is surrounded by circular smooth muscle cells. The smooth muscle cells regulate the lumen diameter. Vascular smooth muscle cells mainly express Cx43 and endothelial cells mainly Cx40, although both cell types also express both connexins and other connexins in minor amounts. Gap junctions in vascular smooth muscle cells conduct vasoconstriction or vasodilation signal along the length of the vessel. Local endothelial stimulation initiates and rapidly spreads a bidirectional wave of relaxation along the vessel. Initially, endothelial stimulation leads to release of an endothelium-derived hyperpolarizing factor (EDHF), which causes hyperpolarization of adjacent smooth muscle. EDHF signaling is mediated through myoendothelial gap junctions, which are permeable to inositol trisphosphate and Ca^{2+} . This is followed by spread of hyperpolarization across the smooth muscle layer through Cx43 gap junctions. Relaxation of smooth muscle can also be stimulated by the release of endothelium-derived relaxation factor (most likely nitric oxide or prostaglandins), which can easily diffuse from endothelium to smooth muscle without the requirement of gap junctions. Hence, vascular gap junctions play a central role in the maintenance of systemic blood pressure. Their expression and functions are modified in disease state of hypertension.

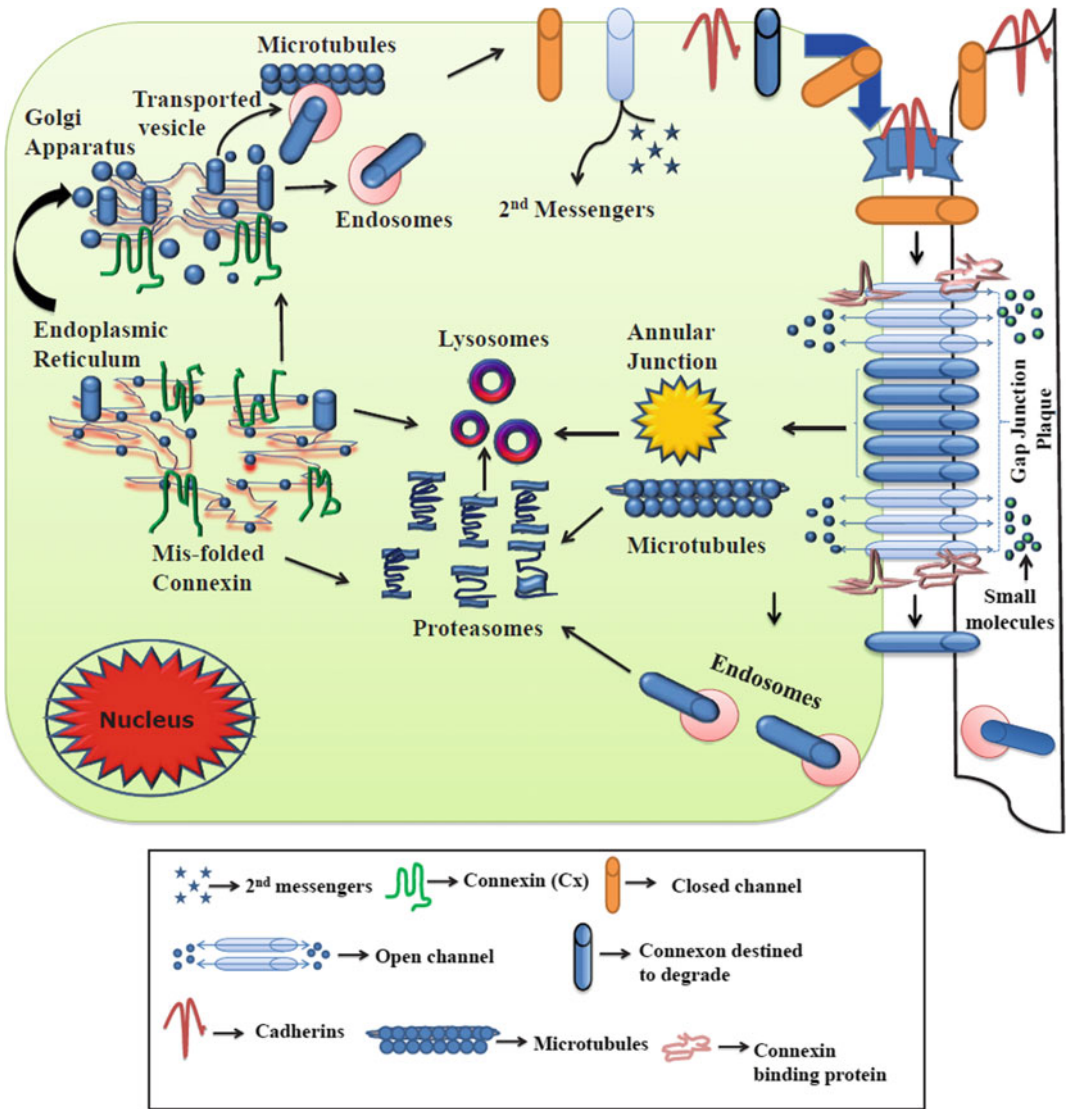


Fig. 4.7 Life cycle of a connexin (Cx). *Source* Laird (2006)

2. Gap junctions in embryogenesis

Gap junctions are also expressed during the early blastula stage and persist throughout embryogenesis. Multiple connexin proteins are found to be expressed during the embryonic phase of neurogenesis. Cx26 and Cx43 are known to be expressed by radial glia and neuronal progenitor cells found within the ventricular zone of the developing brain.

3. Gap junctions in skin

The epidermis, the outermost layer of the skin is composed of four distinct layers: the basal layer, spinous layer, granular layers, and the outer stratum corneum, which is formed of dead corneocytes. Keratinocytes in the basal layer are like stem cells, which differentiate and migrate to upper layers and finally undergo terminal differentiation to form the stratum corneum. Gap junctions are

present in the basal, spinous, and granular layers of human epidermis, but not in the stratum corneum. Different types of connexins expressed in different layers in the epidermis have been implicated to play an important role in wound healing and repair. For example, Cx31.1 and Cx43 are down-regulated after injury, whereas Cx26 and Cx30 expression is unregulated at the wound site, indicating their role in keratinocyte proliferation and/or migration to the wound site, stimulating wound healing

4.1.5 Lipid Rafts

Lipid rafts are more ordered nanoscale subdomain of plasma membrane enriched in sphingolipids and cholesterol with associated proteins. Tight packing of saturated fatty acyl chains of sphingolipids and cholesterol results in more ordered phase separation from the rest of the membrane that is more fluid.

Lipid rafts are resistant to extraction by non-ionic detergents like Triton X-100. That is why they are also known as detergent-resistant membranes (DRMs) or Triton-insoluble membranes (TIMs). Detergent-resistant lipid rafts can be prepared by treating cells with cold buffer containing 1% Triton X-100 and homogenizing the lysate. Rafts are isolated by a 5–30% sucrose density gradient centrifugation, where they distribute in the top few fractions of the gradient.

Lipid rafts are of two types: planar (flat) or nonplanar (invaginated) (Fig. 4.8). Planar lipid raft microdomains are in the same plane as the nonraft membrane, and hence the term planar lipid rafts. Cholesterol is distributed in both the leaflets of the membrane, whereas sphingolipids are mainly concentrated in the outer leaflet. Protein **flotillin** is found in high concentration in planar lipid rafts, associated with cholesterol and sphingolipids.

Rafts are dynamic structures that can laterally diffuse along the plane of the plasma membrane and also continuously flux between the plasma membrane and internal compartments. Lipid rafts preferentially associate with certain proteins

which include glycosylphosphatidylinositol (GPI)-anchored proteins, epidermal growth factor (EGF) and platelet-derived growth factor (PDGF) receptors, fatty acylated α -subunits of G proteins, cholesterol-linked, and palmitoylated proteins such as Hedgehog 9. GPI-anchored proteins and other proteins that undergo hydrophobic modifications have a higher probability to partition into rafts due to their hydrophobic character.

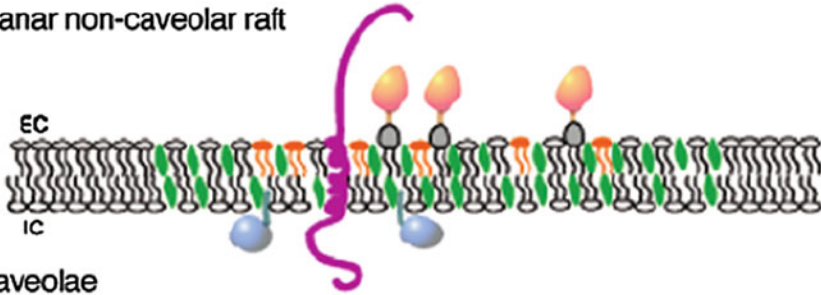
Caveolae (Latin for “little caves”; singular, caveola), were first reported by Palade and Yamada in 1953, are small (50–100 nm) flask-shaped “nonclathrin-coated” invaginations of the plasma membrane. Caveolae are nonplanar lipid rafts, rich in caveolin proteins are found in most cell types, but are especially abundant in endothelial cells and adipocytes.

The caveolae are associated with coat proteins caveolins and cavins which have specific functional roles and are specific to different cell types. Caveolin gene family has three members’ caveolin-1 (Cav-1), caveolin-2 (Cav-2), and caveolin-3 (Cav-3).

Caveolin-1 is highly expressed in adipocytes, fibroblasts, endothelial cells, and smooth muscle cells. Caveolin-2 is associated with caveolin-1, whereas caveolin-3 is predominantly expressed in heart and skeletal muscle cells. Cav-1 and Cav-3 are essential for the caveolae biogenesis. Cav-1 associates with cholesterol with high affinity and forms an oligomer which stabilizes the caveolae structure. The other proteins associated with caveolae are the cavins, which include cavin-1 (polymerase transcript release factor, PTRF), cavin-2 (serum deprivation protein response, SDPR), cavin-3 (srd-related gene product that binds to c-kinase, SRBC), and cavin-4 (muscle-restricted coiled-coil protein, MURC), play important roles in the regulation of caveolae structure.

The study of caveolin proteins reveals that the carboxy and amino-terminal are both cytoplasmic domains with an intervening transmembrane domain (TMD) (amino acids 102–134 in Cav-1), which is in the form of a hydrophobic hairpin loop inserted into the membrane. The two

(a) Planar non-caveolar raft



(b) Caveolae

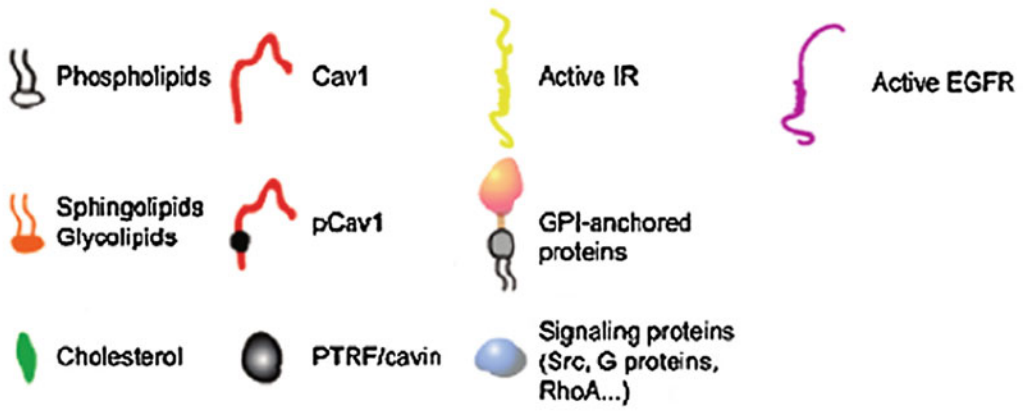
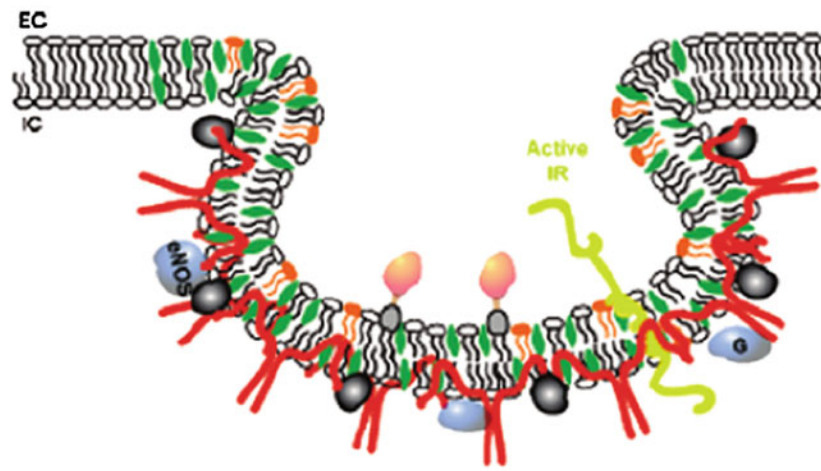


Fig. 4.8 a Planar lipid raft. b Caveolae

adjacent regions that flank the central hydrophobic hairpin loop are the NH₂-terminal membrane attachment domain (N-MAD) (residues 82–101 in Cav-1), and COOH-terminal membrane attachment domain (C-MAD) (residues 135–150 in Cav-1) were found to bind to

membranes with high affinity. Palmitoylation of cysteine amino acids toward carboxy terminus also promote membrane association. Caveolins also contain an oligomerization domain in residues 61–101 in Cav-1, which mediate the homooligomerization (Fig. 4.9).

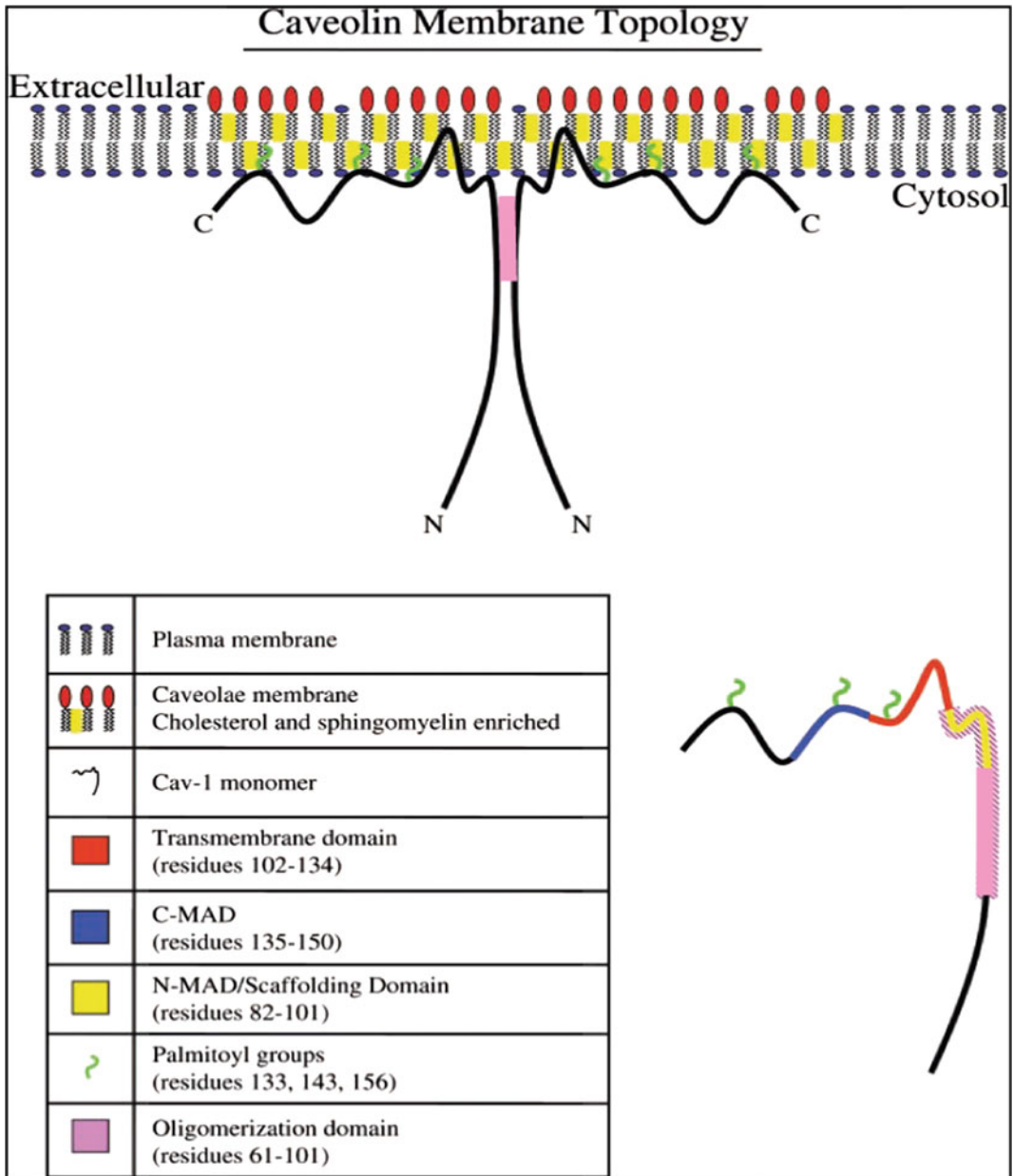


Fig. 4.9 Caveolin-1 membrane topology and protein domains. In this view, caveolin-1 is depicted as a homodimer. C-MAD (blue; residues 135–150) and N-MAD (yellow; residues 82–101) are C-terminal, and N-terminal membrane attachment domain, respectively, while the transmembrane domain (red; residues 102–134) insert into the membrane. Oligomerization is mediated by residues 61–101 (pink). The scaffolding domain (yellow;

residues 82–101) recognizes a hydrophobic caveolin-binding motif present within many signaling molecules. Caveolin-1 is also palmitoylated on three conserved cysteine residues (green; 133, 143, and 156). Note that caveolin-1 is not a conventional transmembrane protein. It is thought to have a unique hairpin topology, with no exposure to the extracellular environment (Color figure online)

The caveolins contain scaffolding domain (CSD) which is thought to be responsible for protein–protein interactions and binding to membrane cholesterol. Many signaling proteins interact with the scaffolding domain of caveolin (CSD) via a signature peptide sequence, the caveolin-binding motif (CBM).

Caveolae have been associated with a wide variety of cellular processes which include endocytosis, transcytosis, cholesterol homeostasis, cell migration, cell polarity, mechanosensation, and signaling.

An alternative clathrin independent, caveolae-mediated pathway for endocytosis was first recognized by the observation of cholera toxin internalization. Many pathogens, including viruses, bacteria and their associated toxins, fungi, and even prions, follow caveolae mode of endocytosis. Clathrin independent of entry allows the pathogen to avoid degradative, endosome–lysosome pathway.

4.2 The Nuclear Envelope

The nuclear envelope (NE) encloses the nucleus in eukaryotic cells. It regulates the flow of materials between the nucleus and the cytoplasm and plays a vital role in the organization of chromatin in the nucleus. During cell division, the NE disassembles at the onset of mitosis, in the prophase stage and then starts to reassemble around segregated chromosomes in anaphase to generate the nucleus compartment in the daughter cells by the end of mitosis.

The nuclear envelope (NE) comprises of two membrane bilayers, the inner nuclear membrane (INM) and outer nuclear membrane (ONM), separated by ~ 50 nm perinuclear space (Fig. 4.10). A large macromolecular nuclear pore complex (NPC) passes through the two bilayers of the NE, hence INM and ONM associated with NPC fuse to form a single membrane known as the pore membrane (POM). The perinuclear space between the outer and inner nuclear membrane is contiguous with the lumen of the endoplasmic reticulum (ER). Despite the continuity between the NE and ER, both the ONM

and INM domains of NE are distinct from ER cisternae.

The INM, ONM, and the pore membrane are associated with distinct proteinaceous structures with specific functions (Fig. 4.11). For example, the INM is in contact with the nuclear lamina and the nuclear chromatin, whereas the ONM is associated with both the cytoskeletal actin network and the centrosome. The pore membrane on the other hand is tethered to the large macromolecular pore complexes.

The nuclear pore complexes (NPCs) are aqueous channels with an outer diameter of ~ 100 nm and a central channel diameter of ~ 40 nm, through which exchange of macromolecules like proteins, RNA, and ribonucleo-protein complexes between the nucleus and cytoplasm takes place. The NPC core structure is an eightfold symmetrical spoke complex that is surrounded by two rings, the cytoplasmic ring and the nuclear ring. The nuclear ring is capped by a fibrous structure called the nuclear basket.

The nucleoporins or Nups, a family of ~ 30 different polypeptides, form the main constituent of the nuclear pore complex (NPC). The nucleoporins are named according to their molecular weight in kDa (kilo Daltons). The different nucleoporins that make up the nuclear pore complex have their own diverse structural and functional roles (Fig. 4.12). Nucleoporins can be categorized into three major groups. The first group comprises of FG nucleoporins, which contain hydrophobic Phe-Gly-rich repeat domains that form the core transport channel involved in receptor-dependent transport across the NE. These FG repeats provide selectivity to the channel. The second group of nucleoporins is devoid of FG-repeat sequences and forms the structural component of the NPC. The third group of Nups is the integral nuclear membrane proteins that anchor the NPC in the nuclear membrane. They are mainly localized in the region where the INM and ONM curve and fuse.

A- and B-type lamin proteins form a mesh-work of intermediate filaments called the nuclear lamina which lines the INM. Lamins provide support to the NE and also interact with the chromatin.

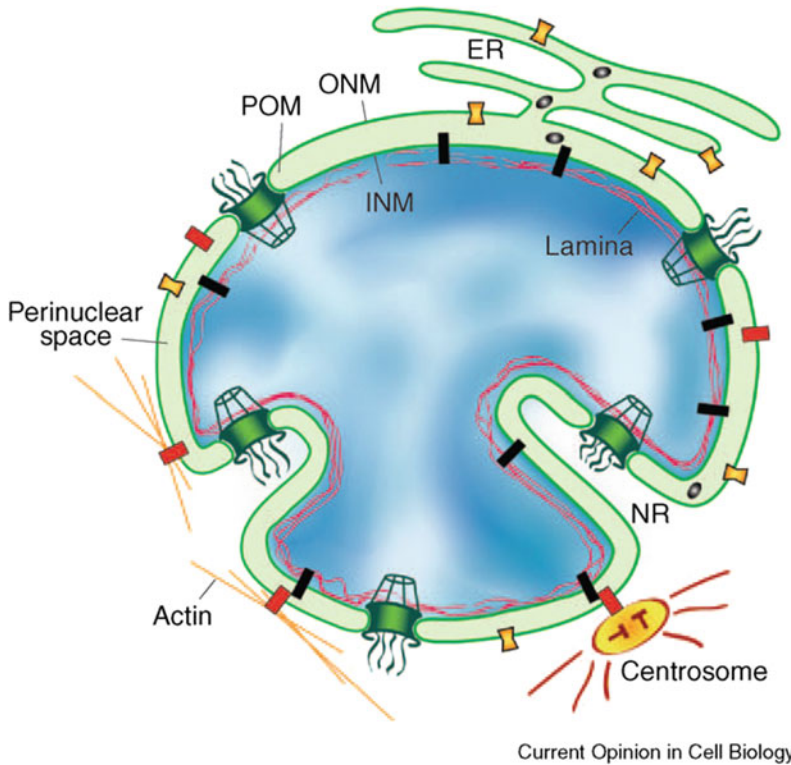


Fig. 4.10 Schematic diagram of the nucleus showing membrane domains of the nuclear envelope (NE) and associated structures. The membrane system of the nuclear envelope consists of the outer nuclear membrane (ONM), the inner nuclear membrane (INM), and the pore membrane (POM). The ONM is contiguous with the endoplasmic reticulum (ER). Portions of the NE extend into the nucleus forming the nucleoplasmic reticulum (NR). The INM contains many distinct proteins (black) that contact the underlying lamina and chromatin. The

pore membrane houses integral membrane proteins of nuclear pore complexes (green). Some ONM proteins (yellow) are also present within the ER and others (red) preferentially localize to the ONM and are proposed to bridge INM proteins to such cytoplasmic structures as the centrosome and actin filaments. Finally, another category of protein (blue ovals) is able to diffuse within the perinuclear space and to interact with luminal domains of NE proteins. *Source* Prunuske and Ullman (2006) (Color figure online)

A group of integral membrane NE proteins associated with INM are the NE transmembrane proteins or NETs. Many of the NETs interact with the lamina, such as lamin B receptor (LBR), lamina-associated polypeptide (LAP) 1, and LAP2. The integral membrane proteins of the ONM in turn interact with the cytoskeleton. The linker of nucleoskeleton and cytoskeleton (LINC) complex is formed within the periplasmic space of the NE with the association of the SUN domain proteins (named for the homology between Sad1 from *Schizosaccharomyces pombe* and UNC-84 from *Caenorhabditis elegans*) of INM and KASH (Klarsicht, ANC-1, Syne

Homology) domain proteins of ONM. Two other related ONM proteins, nuclear envelope spectrin repeat (nesprin)-1 and -2, have been shown to directly interact with the actin cytoskeleton through their amino-terminal actin-binding domain (ABD).

4.2.1 Nuclear Envelope Breakdown During Mitosis

The NE undergoes structural reorganization during the process of cell division. NE is completely disassembled during prophase–metaphase

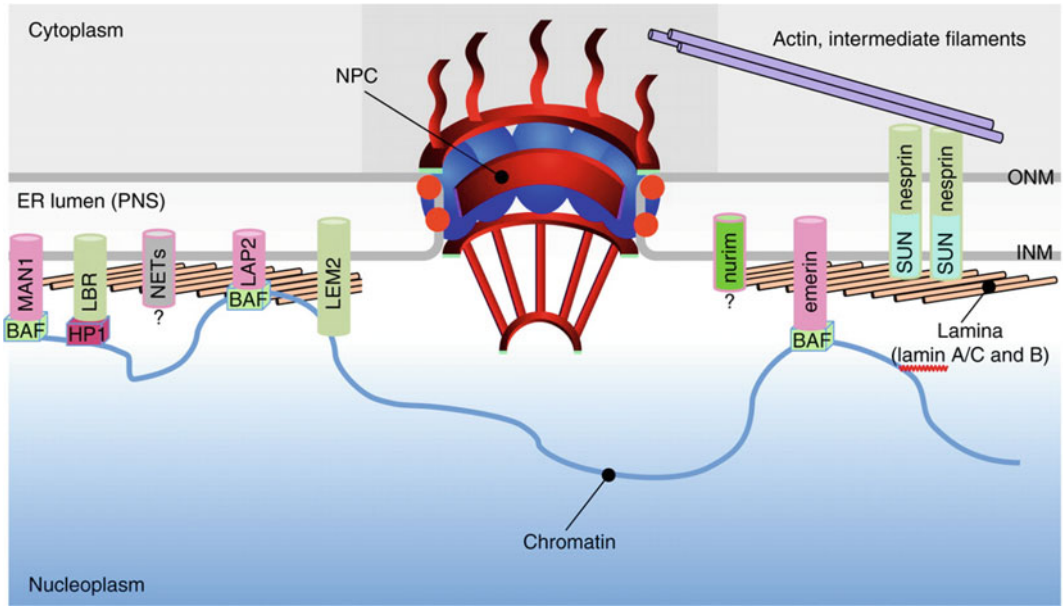


Fig. 4.11 Topology of the nuclear envelope (NE). Inner and outer nuclear membranes (INM and ONM, respectively) are separated by the ER lumen or perinuclear space (PNS). The nuclear lamina interacts with NE proteins and chromatin. INM proteins link the NE to chromatin and the lamina. ONM proteins provide a connection from the nucleus to the cytoskeleton. The lamin B receptor (LBR) interacts both with B-type lamins and chromatin-associated heterochromatin protein 1 (HP1) in conjunction with core histones. Members of the LEM

(lamina-associated protein 2 [LAP2], emerin, MAN1)-domain family (pink) bind to lamins and interact with chromatin through barrier-to-autointegration factor (BAF). SUN proteins (SUN 1 and 2) interact with nesprins in the ONM, thereby forming so-called LINC complexes that establish connections to actin and intermediate filaments in the cytoplasm. Nurim is a multipass membrane protein with unknown function. *Source* Hetzer (2010)

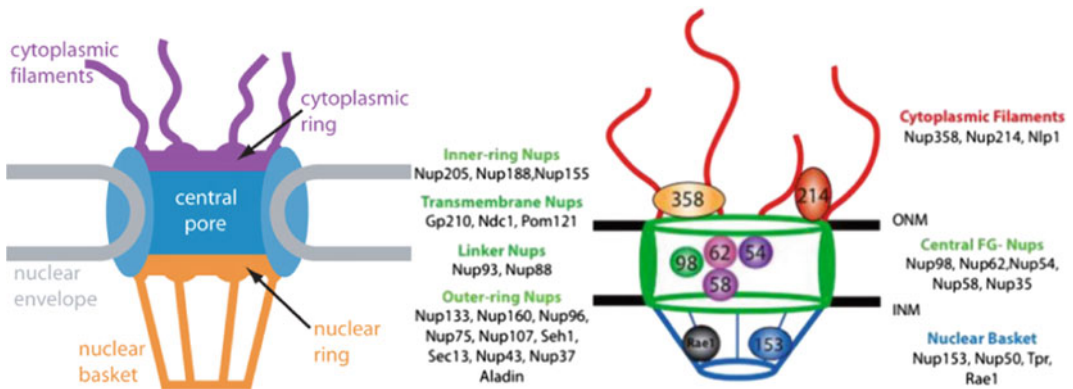


Fig. 4.12 Localization of nucleoporins in the nuclear pore complex. *Source* Le Sage and Mouland (2013)

stage of mitosis and is then reassembled during anaphase–telophase when the NE completely encloses the segregated chromatin mass.

One of the initial events in NE breakdown (NEBD) is the disassembly of the NCPs with the loss of few Nups from the NPCs. Disruption of

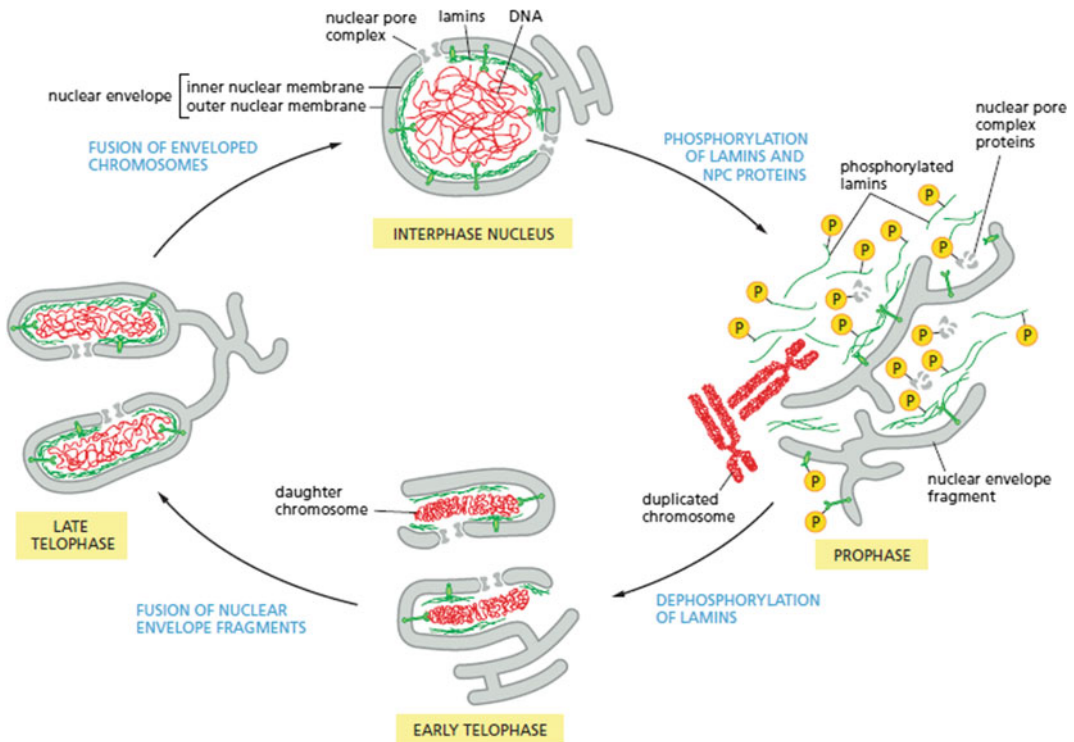


Fig. 4.13 Breakdown and reformation of the nuclear envelope and lamina during mitosis. Phosphorylation of the lamins triggers the disassembly of the nuclear lamina,

which initiates the nuclear envelope to break up. Dephosphorylation of the lamins reverses the process

the permeability barrier allows the influx of molecules into the nucleus, which are critical for further disassembly steps. After the disassembly of NCPs, the lamina disassembles. Permeabilization of NCPs results in exposure of INM proteins and lamins to various proteins kinases including cyclin-dependent kinase 1(Cdk1). Hyperphosphorylation of NE proteins and lamins disrupt protein–protein interactions driving NE breakdown (NEBD). With the disruption of lamina, INM loses its anchor, is no longer associated with the chromatin (Fig. 4.13).

The cytoskeleton components participate in NE disassembly. The dynein–dynactin motor complex is associated with the NE via the ONM, it moves along the microtubules, generating tension which ruptures the NE. As the NE is torn apart, the NE proteins, including the NETs relocate into the ER which serves as “mitotic storage site” for NE components. The

cytoskeleton—NE interactions continue to pull NE fragments away from the chromosomes, toward the centrosome, making the metaphase chromatin free of any membrane associations.

4.2.2 The Nuclear Envelope Reformation

NE reformation starts with the association of ER tubules with the chromatin. As NE proteins are stored in the ER, NETs may play a role in targeting and binding ER tubules to chromatin. After binding of ER tubules to chromatin, the tubular network is flattened into membrane sheets. As the membrane sheets merge and spread across the chromatin to form NE, few small holes between INM and ONM remain. NPCs are then assembled in the NE. The holes could be the site of NPC assembly.

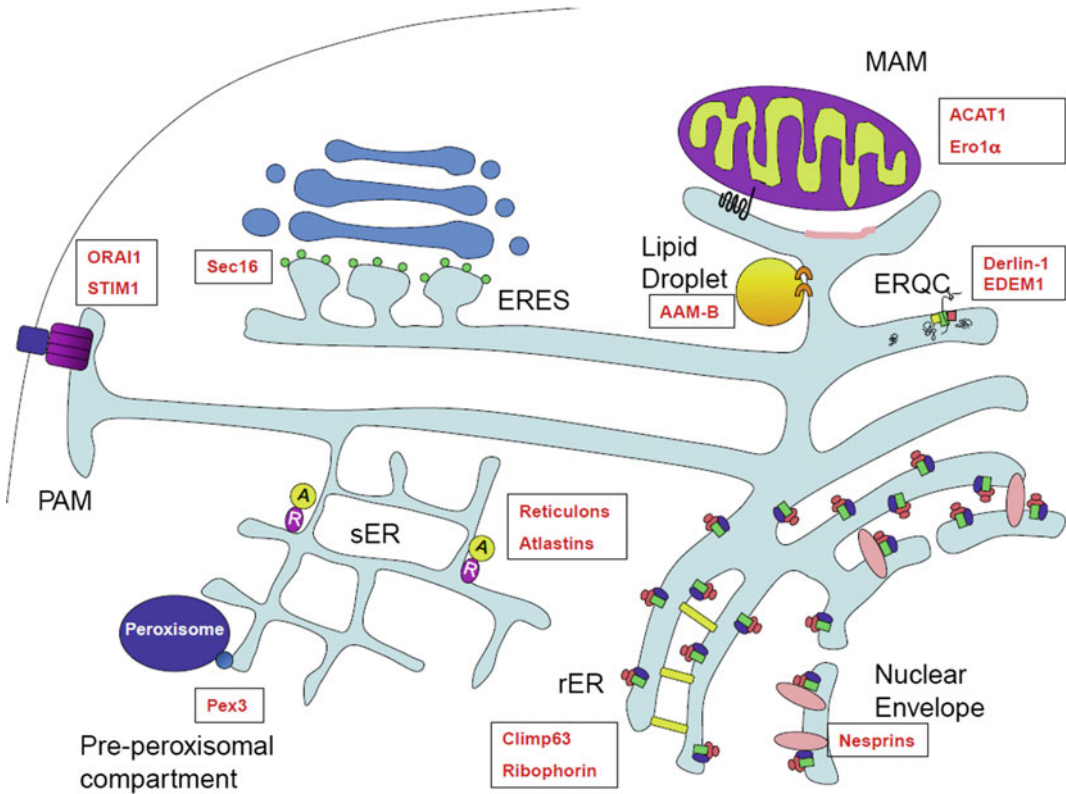


Fig. 4.14 Endoplasmic reticulum (ER) subdomains with specific markers. Rough endoplasmic reticulum (rER) sheets are characterized by ribosomes (pink ovals) which associate with translocon components (green rectangles) and ribophorins (purple ovals). Climp63 (yellow rectangle) is an important structural protein of the rER that also associates with microtubules. The ER quality control compartment (ERQC) is derived from the rER and also features translocon components (green rectangle) and associated proteins such as Derlin-1 (yellow square) and EDEM-1 (pink square) that facilitate the ubiquitination and retrotranslocation of misfolded proteins from the ER. Smooth endoplasmic reticulum (sER) tubule formation is in part mediated by the reticulons (purple circles) and atlastins (yellow circles). At the plasma membrane-associated membrane (PAM), STIM1 (purple rectangle) oligomerizes to form a pore which associates with the plasma membrane calcium channel ORAI1 (dark blue rectangle), mediating store operated calcium entry. The

mitochondria-associated membrane (MAM) is a section of smooth ER that makes close contacts with mitochondria. ACAT1 (black squiggle) localizes to MAMs via a mitochondrial targeting sequence in its cytosolic tail, whereas other MAM proteins target to cholesterol-rich lipid domains within the MAM (pink membrane section). ER exit sites (ERES) at the transitional ER mark the point where COPII-coated vesicles bud off from the ER en route to the ERGIC and Golgi compartments; ERES formation depends on Sec16 (small green circles), which associates with the ER membrane on the cytosolic face. Proteins destined for the peroxisomes sort into the preperoxisomal compartment, where they bud off into preperoxisomal vesicles in a Pex3 (small blue circle)-dependent manner. Lipid droplets are characterized by the presence of selected ER proteins including AAM-B. The nuclear envelope is equipped with ribosomes on the cytoplasmic face, where nesprins (pink ovals) are also found. *Source* Lynes and Simmen (2011) (Color figure online)

4.3 Endoplasmic Reticulum

Endoplasmic reticulum (ER) forms the largest membrane system of the cell. It is associated with varied functions which include protein and lipid

synthesis, incorporation of proteins in membranes, protein modification and folding, carbohydrate metabolism and storage of calcium. ER was first discovered by Keith Porter and his group in 1945 on electron micrographs. ER is broadly classified into ribosome associated rough ER

Table 4.1 ER subcompartments, their main functions and marker proteins

ER subcompartment	Main functions	Marker proteins	Known sorting signals or mechanisms
Rough ER	• Secretory and membrane protein synthesis, folding	Ribophorin/II, Climp63	Interaction with ribosomes (Sec61), CK2 phosphorylation (Sec63, calnexin), cytosolic and transmembrane sequences (Ribophorin II),
Nuclear envelope	• Delineates nucleus	Nesprins	Interaction with inner nuclear membrane proteins using KASH domain
Smooth ER	• Lipid synthesis	Reticulons, atlastins	?
	• Calcium storage		
MAM	• ER/mitochondria calcium homeostasis	ACAT1, FACL4, Ero1a	Cryptic mitochondria interaction signal (UL37, DCAT2), oxidizing conditions (Ero1), lipid raft association (Sigma-1 receptor), resting conditions (calnexin, BAP31)
	• Apoptotic calcium signaling		
	• Lipid transfer		
ERQC	• Export of unfolded proteins to the proteasome	Derlin-1, EDEM-1	ER stress (calnexin, BAP31)
Russell bodies	• Segregation of protein aggregates	Condensed immunoglobulins	Sugar structure and unpaired cysteines
ERES	• Export of proteins from ER to Golgi	Sec16A/B	Interaction with COPII coat (positive charges in Sec16), ER export signal of cargo proteins
PAM	• Calcium import from extracellular space (store operated calcium exchange-SOCE)	STIM1, ORAI1	Mukimerization (STIM1)
	• Sterol trafficking to plasma membrane		
Preperoxisomal compartment	• Peroxisome formation	Pex3	?
Lipid droplets	• Storage of triacylglycerides	AAM-B	N-terminal hydrophobic sequences (AAM-B)

Summary of the main points presented in this review. References and details are found in the text. *Source* Lynes and Simmen (2011)

(RER), and ribosome free, the smooth ER (SER). ER is closely associated with most cellular organelles, including, the plasma membrane, Golgi, mitochondria, and the nucleus. This association results in many subdomains of ER which are structurally and functionally distinct, such as, ER exit sites (ERES), plasma membrane-associated ER (PAM), the mitochondria-associated membrane (MAM), the nuclear envelope and the ER quality control compartment (ERQC) (Fig. 4.14; Table 4.1).

Rough endoplasmic reticulum (RER) is the site for the synthesis of secretory proteins and transmembrane proteins. The RER, is distinctively associated with bound ribosomes and protein translocation channels, the **translocons**. Translocon is a big complex made up of more than 20 polypeptides. The translocation pore consists of the Sec61 trimer complex of Sec61 α , β , and γ proteins. The mRNA of secretory or integral membrane proteins is initially translated on the free ribosomes in the cytosol. The

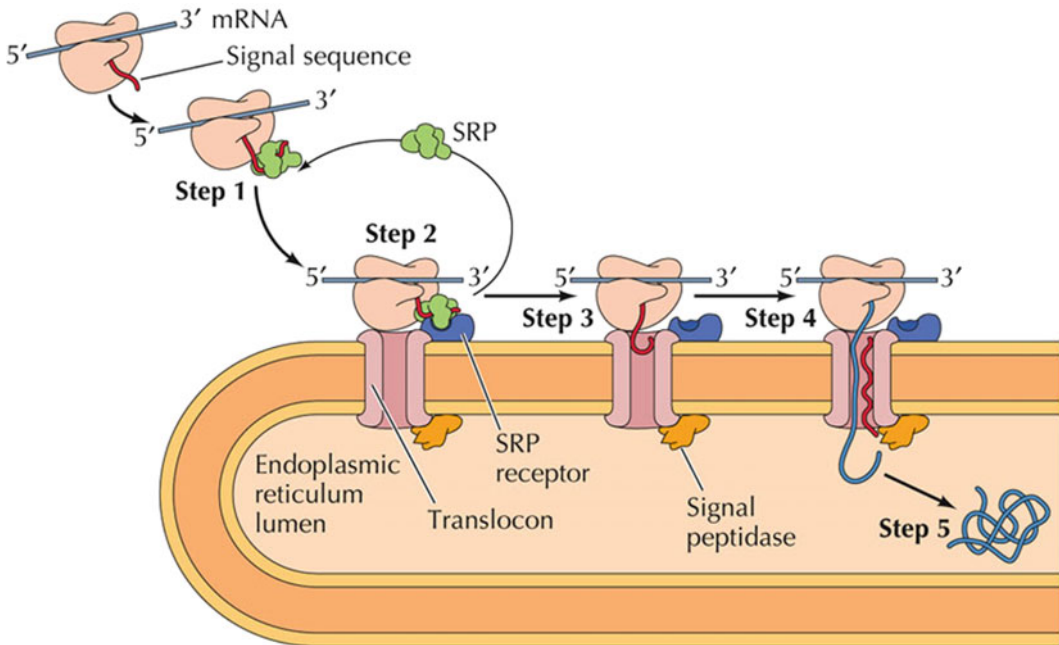


Fig. 4.15 Model of cotranslational translocation of proteins on rough ER

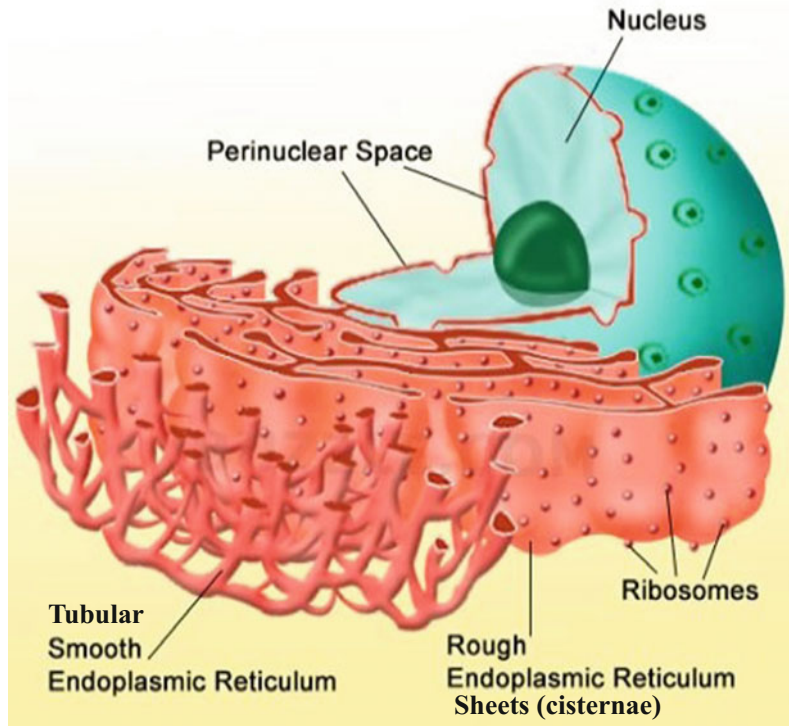
N-terminal signal sequence of hydrophobic acids synthesized recruits the ribosome–mRNA–nascent polypeptide complex to the ER membrane on being recognized and bound by the signal recognition particle (SRP). The mRNA: ribosome: nascent polypeptide: SRP complex docks on the SRP receptor associated with the translocon. As translation proceeds, the emerging polypeptide enters the ER lumen through the translocon (Fig. 4.15). The secretory protein is completely translocated into the ER lumen where, the signal sequence is cleaved off. The integral membrane proteins are characterized by a stretch of hydrophobic residues or stop-transfer membrane anchor sequence, pausing translocation, thereby preventing complete translocation into the ER.

The protein translocated into the ER lumen can undergo chaperones and enzymes aided folding and different modifications like, N-linked glycosylation, disulfide bond formation and oligomerization. Secretory proteins are released packaged in vesicles from the Golgi for transport to a final destination.

The rough ER is characterized by branched stacks of sheet-like flat cisternae (Fig. 4.16). Climp63 (cytoskeleton-linking membrane protein of 63 kDa) protein forms oligomers, and bridge two flat membrane sheets. An ER associated protein, ribosome interacting protein, p180, binds the ribosomes to ER sheets. Both Climp63 and p180 also tether the microtubules to ER. The **nuclear envelope**, which is in continuation with the rough ER, is attached with ribosomes on the ONM, but not in the INM. The ONM is distinct from the rough ER, it has distinct proteins like the nesprin (nuclear envelope spectrin repeat proteins) family of proteins. The (nesprins) proteins establish nuclear-cytoskeletal connections.

The **smooth endoplasmic reticulum (SER)** has no ribosomes associated with it, it is the site of many important functions which include lipid and steroid biosynthesis, detoxification of drugs and metabolites, sequestration and regulated release of Ca^{2+} , and release of glucose by glucose-6-phosphatase enzyme. The SER is organized into tubular network. The architectural organization of SER tubules are quite distinct

Fig. 4.16 Structure of endoplasmic reticulum, showing tubular network of SER and RER sheets or cisternae



from RER sheets, the tubules are more convoluted, and the branch points are frequent giving it a sponge like appearance. A group of proteins called reticulons (RTNs) play an important role in generating curvature in ER membranes and transforming ER sheets into tubular ER. Reticulons are important determinants of ER tubule shape, introduces curvature in membrane by forming a transmembrane hairpin which acts as a wedge, displacing lipids in the outer leaflet of the bilayer introducing bends in membranes (Fig. 4.17). The proteins of atlastin family, related to dynamin and the mitofusins, interacts with reticulons and promote tubular interactions via the homotypic ER—ER fusion and introduce branching in ER tubules. Rab GTPases (Rab10 and Rab18) present in ER membranes also play a role in regulating ER shape and dynamics.

Mitochondria-associated membrane (MAM) is a subdomain of ER, present in close proximity to the mitochondria. MAMs are linked to the mitochondria via protein complexes. The ER-mitochondria encounter structure (ERMES)

complex and the ER membrane protein complex (EMC) bridges ER and mitochondrial membranes. The ERMES complex comprises of the outer mitochondrial membrane proteins (Mdms) and the ER membrane proteins (Mmms). Another set of proteins, mitofusin 1 (MFN1) and mitofusin 2 (MFN2) form homo/hetrodimers to tether ER to mitochondria. Protein links between MAM and mitochondria also facilitate key cellular processes including the transport of calcium from the ER to mitochondria, the import of phosphatidylserine from ER into mitochondria for decarboxylation to phosphatidylethanolamine, regulation of the morphology, dynamics and functions of mitochondria, and cell survival. Impaired contact between MAM and mitochondria could be the basis of the pathology of several human neurodegenerative diseases, including Alzheimer's disease.

ER and mitochondria are major sites for intracellular storage of Ca^{2+} . Together they play a major role in regulating intracellular Ca^{2+} concentration. Calcium binding proteins such as calreticulin and calnexin in ER lumen and ER

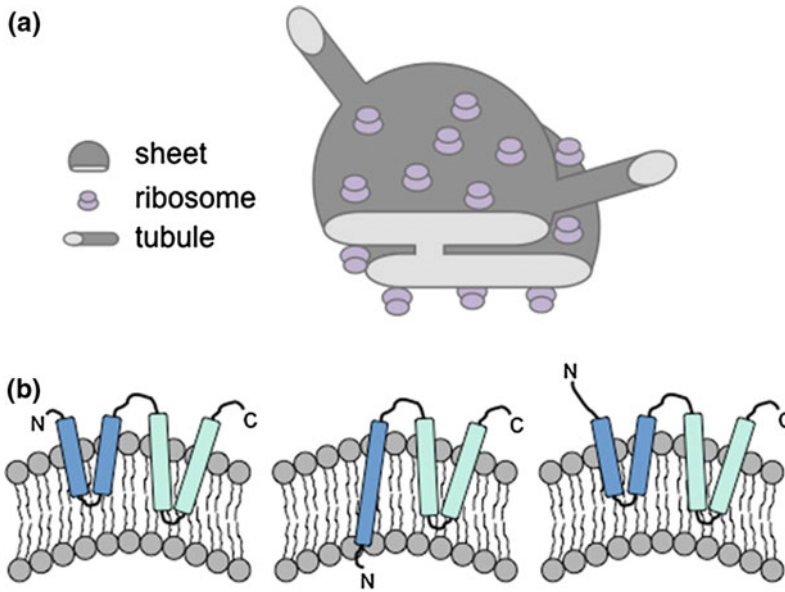


Fig. 4.17 Structure of ER sheets and tubules. **a** ER sheets and tubules have a diameter of 30–50 nm in eukaryotes. Eukaryotic ribosomes are 25–30 nm and localize to the flat regions of ER sheets, giving the sheets a rough appearance (rough ER). Ribosomes are present in

much lower numbers on tubules, giving the tubules a more smooth appearance (smooth ER). **b** Models of potential hairpin topologies of reticulon family of proteins that act as wedges to promote bending of the membrane. *Source* Dianne et al. (2016)

membrane transport proteins like, SERCA calcium pumps, IP₃R and ryanodine receptor calcium channels buffer intracellular Ca²⁺. The MAMs are enriched in inositol 1,4,5-triphosphate (IP₃)-sensitive Ca²⁺ channel which mediates the transport of Ca²⁺ from the ER to the mitochondria. A tripartite complex involving the cytosolic chaperone Grp75 (75 kDa glucose-regulated protein), the mitochondrial voltage-dependent anion channel 1 (VDAC1) and the inositol 1,4,5-triphosphate receptor (IP3R) in the MAM, bridges the MAM and the OMM (Fig. 4.18). This complex promotes efficient transfer of calcium from the ER to mitochondria. Ca²⁺ is then transported into the matrix via Ca²⁺ uniporter (MCU) present in IMM.

A number of chaperones and regulatory proteins regulate the ER–mitochondria junction. Phosphofurin acidic cluster sorting protein 2 (PACS2) controls the translocation of calnexin from the ER to the plasma membrane and thereby modulates ER Ca²⁺ buffering and controls ER–mitochondria appositions during apoptosis. PML

(promyelocytic leukemia) protein regulates Ins (1,4,5)P₃R-mediated Ca²⁺ release from the ER, supports mitochondrial Ca²⁺ uptake and thus has a crucial role during apoptosis.

The domain of smooth ER that is associated with the plasma membrane is known as peripheral ER or plasma membrane-associated membrane (PAM). Phosphatidylserine, which is localized in the cytoplasmic leaflet of plasma membrane, is predominantly synthesized in PAM. Phosphatidylserine, if exposed on the outer leaflet of the plasma membrane triggers apoptosis.

Other smooth ER domains include the **ER exit sites (ERES)** and the **ER quality control compartment (ERQC)**. **ERES** are ribosome free, Ω-shaped membrane system from where the secretory proteins exit the ER to form a transitional compartment called the ER-Golgi intermediate compartment (**ERGIC**) that is enriched in fully folded secretory proteins. This transport is mediated by COPII proteins (Fig. 4.20).

In the ER quality control compartment (ERQC), incompletely folded proteins undergo

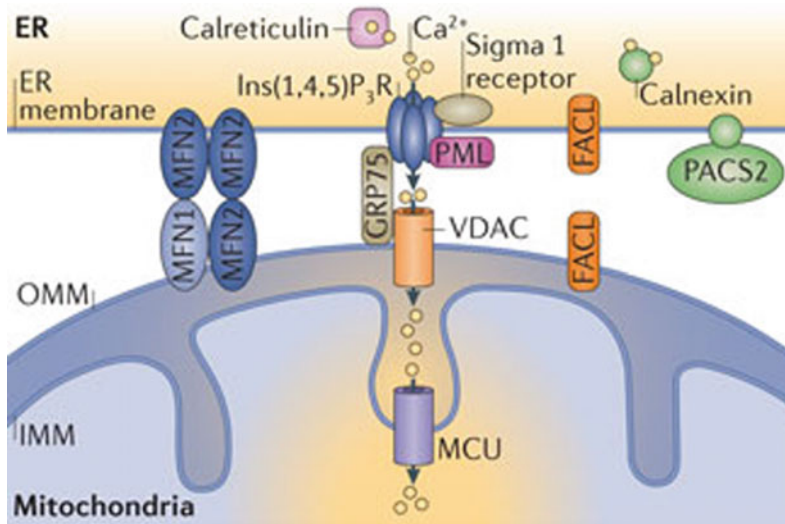


Fig. 4.18 Linking proteins between the endoplasmic reticulum (ER) and mitochondria. Voltage-dependent anion channel (VDAC), mitochondrial uniporter (MCU), phosphofurin acidic cluster sorting protein 2 (PACS-2), glucose-regulated protein 75 (Grp75), long-chain

fatty-acid-CoA ligases (FACL), mitofusin 1 (MFN1) and mitofusin 2 (MFN2) PML (promyelocytic leukemia) protein, which regulates Ins(1,4,5)P₃R-mediated Ca²⁺ release from the ER. *Source* Rizzuto et al. (2012)

ER-associated degradation (ERAD). EREQ can fuse with the lysosomes for complete degradation of such proteins.

The smooth ER is also the site of origin for **Russell body**, **peroxisome**, and **lipid droplet** biogenesis. Russell bodies are exhibited in the plasma cells of multiple myeloma patients. Excessive synthesis of immunoglobulins result in their storage in distended ER cisternae known as Russell bodies where they are neither secreted nor degraded further. The ERES-associated ER proteins ERGIC-53 and ERp44 play a role in the recognition of immunoglobulins and formation of Russel bodies. Russel bodies also contain mucoproteins secreted by the plasma cells and hence are positive to PAS stain.

Peroxisomes also evolve from the smooth ER. Peroxisomes are the site of synthesis of ether lipids like plasmalogens and the breakdown of long chain of fatty acids. A subset of Pex proteins are involved in peroxisome biogenesis, by targeting peroxisome-generating domains of the ER for incorporation into the nascent organelle. Lipid droplet biogenesis essentially requires COPI-coated vesicles mediated trafficking between the ER and the Golgi, with the spatial

confinement of triglyceride and cholesterol ester synthesizing enzymes.

4.4 Golgi Apparatus

In 1898 Camillo Golgi was the first one to visualize the Golgi complex (GC) which he called “apparato reticolare interno,” which was ultimately named after him. Later, electron microscope clearly demonstrated that the GC organelle comprises of stack of flattened membranes surrounded by tubules and vesicles (Fig. 4.19). Palade for the first time established that the proteins synthesized in the endoplasmic reticulum (ER) are transported to the Golgi complex (GC) and then packaged in secretory vesicles to be secreted out of the cell. During the transit through the Golgi, the proteins are modified, sorted, tagged, and then delivered to the final destination. In the last two decades, increasing number of functions has been found to be associated with GC, which includes microtubule nucleation, signaling, and calcium homeostasis. In the last two decades, development of new technologies like live cell imaging, fluorescent microscopy, organelle

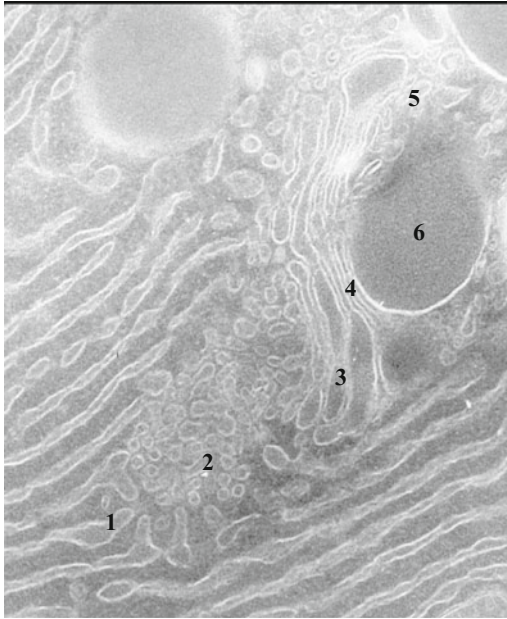


Fig. 4.19 Cryosection of the Golgi complex of rat exocrine pancreatic cells. Typical image of a cross-sectioned Golgi complex. 1 endoplasmic reticulum exit site, 2 tubulovesicular elements associated with ERGIC, 3 tubular membranes associated with the CGN, 4 stack of cisternae, 5 TGN elements, 6 secretory granule. Bar = 200 nm. *Source* Martínez-Menárguez (2013)

proteomics, functional genomics, immunocytochemistry, etc., has expanded our knowledge of Golgi structure and function.

The Golgi apparatus is one of the most elaborate organelles in the cell, consisting of flattened membrane sacs called cisternae. The Golgi complex can be compartmentalized into 3 distinct compartments, cis, medial, and trans. The cis-cisternae receive the cargo of newly synthesized proteins and lipids from the ER, which traversing the medial compartment reaches the transcompartment from where it exits. The transport from cis-trans takes $\sim 10\text{--}20$ min. In each stack, the number of cisternae varies in different species, averaging between 3 and 11. The diameter of the cisternae is quite narrow (10–20 nm) in the center, whereas the ends appear as bulging buds which are usually capped. In a cell, several such stacks are present which are laterally interconnected to each other by tubules.

The ribbon is located near the nucleus, and the microtubule organizing centers (MTOC) in the cell. The microtubule plays an important role in the arrangement and maintenance of the Golgi ribbon. Microtubule depolarizing molecules like nocodazole can cause ribbon fragmentation. The Golgi ribbon stack is also supported by the Golgi matrix present in the area surrounding the cisternae and can be visualized as small fibers connecting the cisternae and the transport vesicles. The matrix structural proteins, like Golgi reassembly stacking proteins (GRASPs) and golgins play a crucial role in organizing Golgi membranes.

Tubule-vesicular networks are present on the cis- and transide of the Golgi stack. The cis-Golgi network (CGN), on the cis-side, is involved in the transport from ER to Golgi. On the other hand, the trans-Golgi network (TGN) on the transide is the site where final steps of protein modification including glycosylation, phosphorylation, proteolysis, and maturation takes place. TGN is also the site of sorting of proteins to the apical or basolateral plasma membranes, early or late endosomes, or the secretory granules takes place. It is the site where the secretory pathway and the endocytic pathway converge.

The Golgi stacks are surrounded by small **vesicles** of different sizes, either budding off or fusing with the Golgi cisternae. Most of the vesicles are coated by either of the three types of coat protein complexes, the COPI, COPII, or the clathrin coat depending on site of origin and the target site (see Chap. 10) (Fig. 4.20). The COPI coat mediates the retrograde transport back to the ER; COPII is involved in ER to Golgi transport, whereas clathrin-coated vesicles are mainly involved in transport from trans-Golgi cisterna and TGN to the endolysosomal system.

4.4.1 Functions of Golgi Apparatus

1. Transport and sorting

The *cis*-Golgi receives neo-synthesized proteins that are to be secreted or targeted to intracellular compartments from the ER. From the *cis*-Golgi,

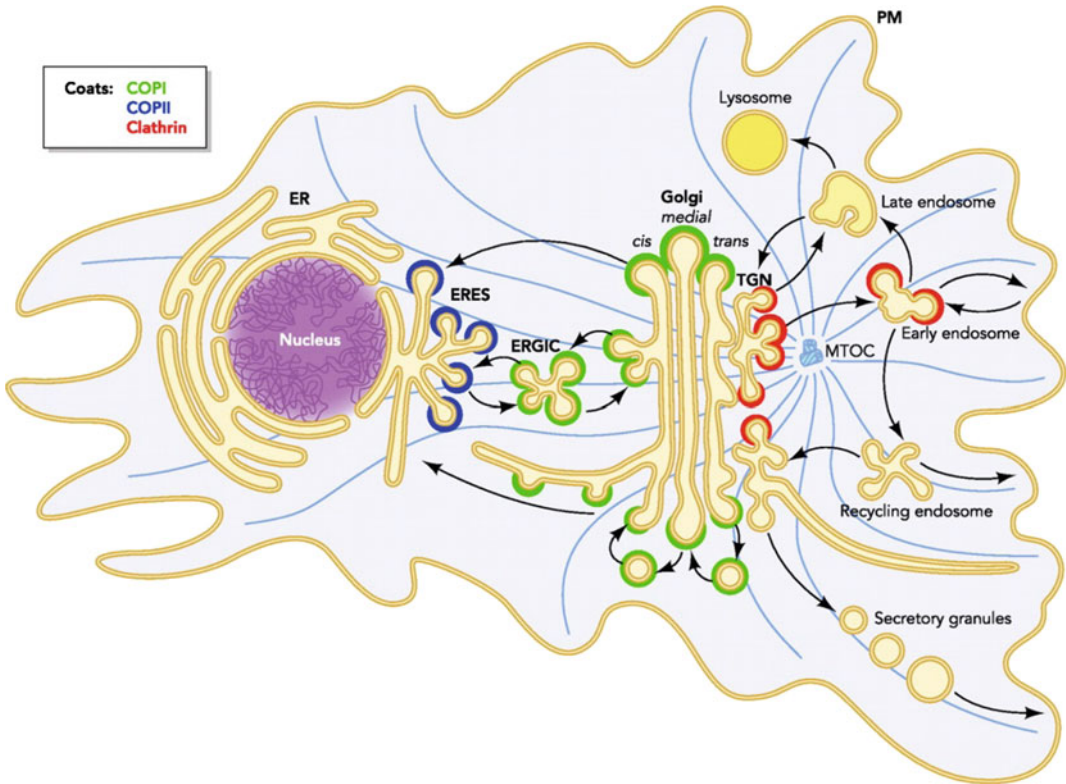


Fig. 4.20 Intracellular transport pathways. The scheme depicts the compartments of the secretory and endosomal pathways. Transport steps are indicated by arrows. Colors indicate the known coats: COPII (blue), COPI (green), and clathrin (red). Secretory cargos are synthesized in the ER, exit the ER at ER exit sites (ERES) in COPII-coated vesicles, and are transported to ER to Golgi intermediate compartment (ERSIC). Cargos are sorted from ERGIC

into anterograde carriers that move them to Golgi. After passage through the Golgi, cargos are sorted at the TGN for delivery to the PM, early and late endosomes, and in some cells to secretory granules. A COPI-mediated recycling pathway retrieves proteins from the Golgi and ERGIC and returns them to the ER. *Source* Szul and Szul (2011) (Color figure online)

cargo molecules then traverse through three to eight cisternae to *trans*-Golgi, some proteins are recycled back to the ER via COPI-mediated retrograde transport. Different mechanisms for the transport of cargo through the Golgi have been proposed. The **vesicular transport model**, launched by Palade in 1975, envisaged that each cisterna is a stable entity, while the vesicles that transport the cargo bud from one cisterna and then move and fuse with the next one. The discovery of COPI- and COPII-coated vesicles supported this model. It was demonstrated that COPII mediate ER to Golgi transport and COPI was responsible for intraGolgi anterograde

transport between cisterna. However, this model is a challenge for the transport of large molecules like procollagen, which are too large to fit in small transport vesicles (having an average diameter of 60–90 nm). The **cisternal maturation model**, postulated by Grasse (1957) based on electron microscopy observations, later updated as cisternal progression-maturation model, proposed that the cis-side of the GC is formed by fusion of ER-derived membranes. These newly formed cisternae move from the cis- to the transside, gradually displacing the older cisternae toward the transside. According to this model, the cargo does not leave the cisterna

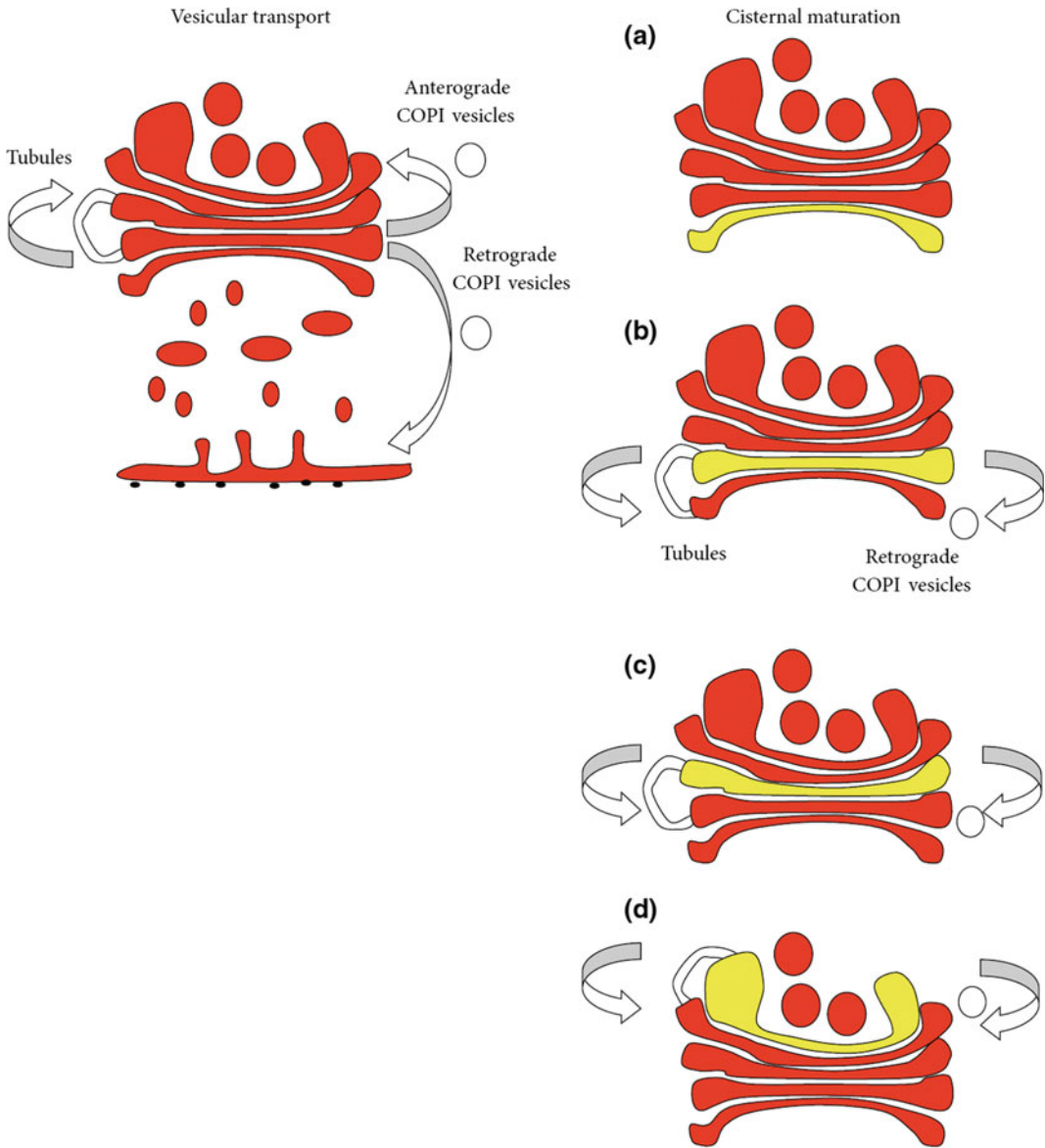


Fig. 4.21 Vesicular transport and cisternal maturation models for intraGolgi transport. According to vesicular transport model, cisternae are static. Anterograde transport may be mediated by COPI-coated vesicles and tubular cisternal connections. Another type of COPI-coated vesicles mediates retrograde transport (i.e., the retrieval of

proteins that have escaped from the endoplasmic reticulum). According to cisternal maturation model, cisternae move from *cis*- (a) to *trans*-Golgi sides (d). COPI-coated vesicles and transient tubules may be involved in the recycling of Golgi resident proteins (retrograde transport). *Source* Martínez-Menárguez (2013)

rather, rather the whole cisterna moves and acts as a carrier (Fig. 4.21). This model can explain the transport of large cargo like procollagen.

A **dual transport model** has also been proposed in which intraGolgi transport of cargo can be mediated by both of the above models

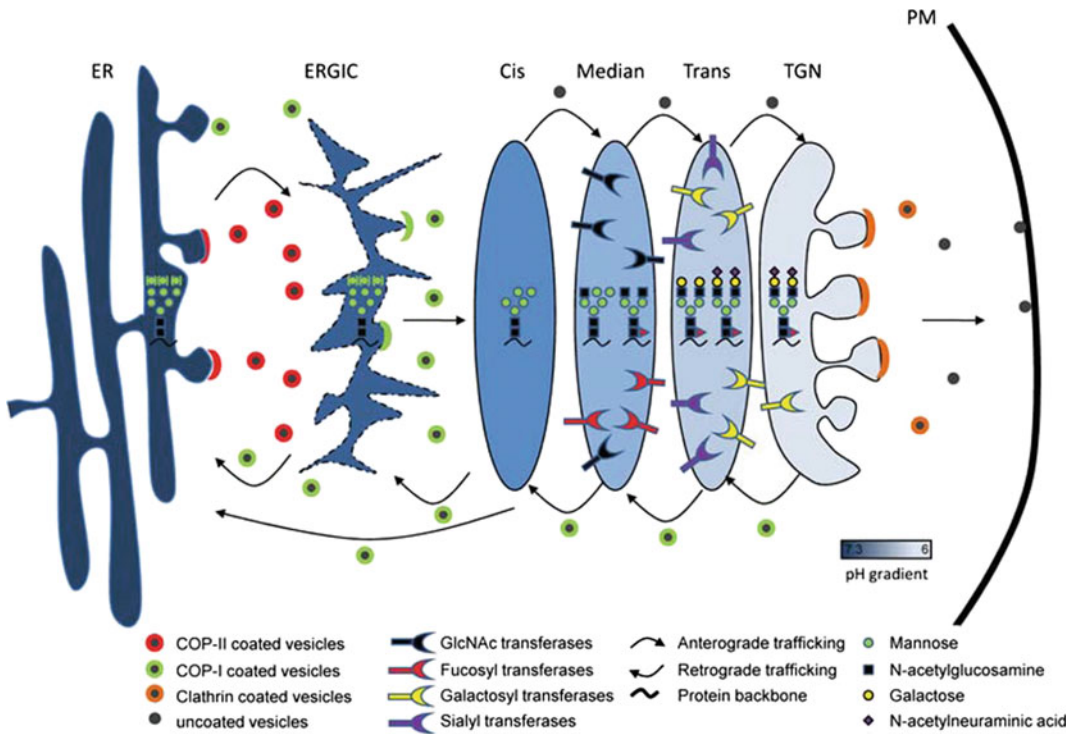


Fig. 4.22 Schematic representation of the Golgi *N*-glycosylation reactions. The glycan structures formed in each cisterna and the trafficking of glycosylation enzymes in the different models are schematically

depicted. The color of the ER, ERGIC, and Golgi cisternae reflects the pH gradient. PM is the plasma membrane. *Source* Reynders et al. (2011)

depending on the type of cargo to be transported. For example, transport of large molecules may be mediated by cisternal maturation mechanism while small molecules can be transported via vesicular transport. The cargo after traversing the Golgi is sorted at the TGN (*trans*-Golgi network) to be transported to different cellular destinations.

2. Protein and lipid biosynthesis

Processing and remodeling of glycosylated proteins and lipids take place in the GC. *N*-linked glycosylation starts in the ER with the stepwise synthesis of a $\text{Glc}_3\text{Man}_9\text{GlcNAc}_2$ oligosaccharide chain which is transferred onto the Asparagine-x-serine-threonine consensus sequence of newly synthesized proteins. This *N*-linked oligosaccharide is then trimmed in the GC with further addition of sugar molecules to generate complex oligosaccharides. The mannose residues of the original

backbone chain are cleaved off mainly in the *cis*-Golgi cisternae, except the trimannosyl core. During the transit to the GC transside, *N*-glycan chain is further modified by addition of two *N*-acetyl glucosamine GlcNAc, two NeuAc, two Gal, and a single fucose residue (Fig. 4.22). The sequence of enzymatic events is highly regulated in the Golgi. The pH of the Golgi stack decreases by ~ 0.5 units from *cis*- to *trans*-Golgi. Presence of gentle pH and ionic gradient could influence the activities of glycosylation enzymes, providing cisterna specific enzyme activities.

GC is also the site of glycosylation of sphingolipids, which include sphingomyelin and GSLs (glycosphingolipids). Ceramide, a precursor of sphingolipid synthesis in the ER, is converted to sphingomyelin on the cytosolic leaflet of the *cis*-Golgi, either via the addition of a phosphocholine headgroup or by glycosylation to GlcCer (glucosylceramide). GlcCer can be further

glycosylated to form different classes of complex GSL (such as gangliosides and globosides) on translocation into the *cis*-Golgi lumen.

Certain lipids are transported from ER to trans-Golgi via nonvesicular transport. CERT (ceramide transport protein) transports ceramide from the ER to the late GC, where ceramide is converted into sphingomyelin. The pool of ceramide is transported through other membrane-bound carriers to the *cis*-Golgi where it is converted into GlcCer. GlcCer transport is in turn mediated by FAPP2 (four-phosphate adaptor protein (2)). CERT and FAPP2 also contribute to the generation of asymmetric distribution of lipids in different Golgi compartments. The late- and post-GC compartments are enriched in sphingolipids, whereas pre- and early Golgi compartments are depleted in sphingolipids. The two cholesterol transfer proteins OSBP1 (oxysterol-binding protein 1) and ORP9 (oxysterol-binding protein-related protein 9) are involved in the transport cholesterol from the ER directly to the *trans*-Golgi, thereby enriching cholesterol in post-GC compartments.

3. Calcium sequestration

In addition to ER, Golgi also stores certain amount of Ca^{2+} which is buffered by Ca^{2+} -binding proteins like CALNUC, Cab45, and P54/NEFA. Two types of Ca^{2+} pumps: the SERCAs (sarcoplasmic/endoplasmic reticulum Ca^{2+} -ATPases) and the SPCAs (secretory pathway Ca^{2+} -ATPases) are involved in Ca^{2+} uptake. The Ca^{2+} and Mn^{2+} pump, SPCA1 insufficiency in humans is associated with Hailey–Hailey disease, a skin disorder disease.

The release of GC Ca^{2+} is mediated by IP_3 (inositol triphosphate)-dependent and -independent channels. Ca^{2+} plays an important role in regulating vesicular transport in different parts of the secretory pathway, from ER-Golgi-plasma membrane. Ca^{2+} also plays an important role in regulating Ca^{2+} -dependent luminal enzymes and transporters.

4. Signaling

The Golgi complex can serve as a signaling platform for various intracellular signaling

cascades. The Golgi can modulate cell signaling generated at the plasma membrane (PM) and can also initiate signaling cascades regulating intracellular transport.

The membrane composition of Golgi is intermediate between the ER and plasma membrane and is enriched in phosphoinositides. Phosphoinositides which are important signaling molecules also regulate membrane trafficking and Golgi function. A variety of other signaling molecules are also associated with Golgi membranes, including heterotrimeric G proteins, protein kinase A, PI(3)kinase, and eNOS.

Golgi-based signaling can thus act as a positive or negative regulator of PM signals. Golgi appears to be an important platform for integrating different aspects of Ras-Raf-MAPK signaling. Ras localization in Golgi can cause inhibition of Ras-Raf-MAPK pathway.

The Golgi also serves as an important platform for GPCR-Adenylate cyclase-cAMP-PKA signaling. GPCR activation in plasma membrane leads to adenylate cyclase catalyzed increase in cAMP concentration which activates Golgi PKA holoenzyme. The regulatory subunits of Golgi PKA remain associated with Golgi, whereas the catalytic subunits move to the nucleus to regulate gene expression. Apart from mediating extracellular signals, PKA also regulates various processes in membrane trafficking.

4.5 Lysosomes

Lysosomes were first discovered and named by Belgium biologist Christian de Duve in the 1950s, for which he received the Nobel Prize in 1974. Lysosome, the major digestive compartment of the cell, known as the “suicide bag,” is rich in acid hydrolases and is found in all eukaryotic cells except erythrocytes. In addition to their role in degradation and disposal of waste, lysosomes also play a crucial role in many cellular processes like plasma membrane repair, bone remodeling, destroying intracellular pathogen, antigen presentation, cholesterol homeostasis, cell death, etc. Lysosomes are rich in various hydrolytic enzymes with optimal activity at

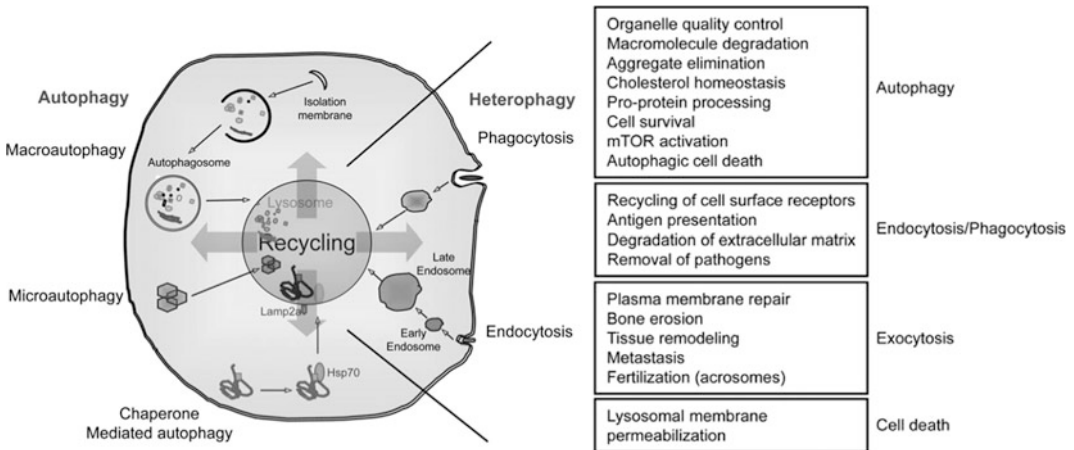


Fig. 4.23 Pathways converging in lysosomes and functions associated with lysosomes. *Source* Boya (2012)

acidic pH. These enzymes include the proteases, phosphatases, glycosidases, lipases, and nucleases. The lysosomes also contain heavily glycosylated proteins like lysosome-associated membrane protein (LAMP)-1 and -2, lysosomal integral membrane protein (LIMP)-2, and CD63 associated with the luminal leaflet of the lysosome membrane. The heavily glycosylated luminal domains of lysosomal membrane proteins form a glycocalyx, protecting the membrane from the acidic hydrolases present in the lysosomal lumen. The lysosomes also contain intralysosomal membrane system, which are the site of membrane degradation.

The mechanism of lysosomal biogenesis is still unclear, but recent evidence reveals that many lysosomal genes are under coordinated regulation of transcription factor EB (TFEB). Many genes encoding lysosomal proteins have a CLEAR (coordinated lysosomal expression and regulation) sequence (GTCACGTGAC) in the promoter region. The transcription factor EB (TFEB) binds to CLEAR sequence in the promoter region and induces gene transcription,

Different degradative pathways including **endocytosis, phagocytosis, and autophagy** converge at lysosomes (Fig. 4.23). The endocytosis, phagocytosis pathways deliver extracellular contents (heterophagy) to lysosomes for degradation, whereas macroautophagy, microautophagy, and chaperone-mediated autophagy

(CMA) involves degradation of intracellular components.

Endocytosis is the process of internalization of the plasma membrane along with cell surface receptors with bound ligand molecules and soluble molecules in the form early endosome (see Chap. 10) (Fig. 4.24). Early endosomes mature into late endosomes which then delivers the cargo to the lysosomes. In addition, late endosomes also deliver new lysosomal hydrolases and membrane proteins to lysosomes from the TGN. Lysosomes have M6P receptors that distinguish them from late endosomes.

Autophagy in mammalian cells can be of three different types, chaperone-mediated autophagy, microautophagy, and macroautophagy. Chaperone-mediated autophagy is a multistep process in which chaperone proteins (usually Hsc70) recognize and bind to cytosolic proteins with a pentapeptide KFERQ-like motif. This chaperone-protein complex is then translocated into the lysosomal lumen for degradation mediated by lysosomal receptor LAMP-2A protein. Microautophagy involves direct uptake of tiny cytoplasmic cargo by the lysosomes for degradation. During macroautophagy, a small portion of the cytoplasmic contents, including damaged proteins and organelles, are sequestered within a newly generated membrane sac called the isolation membrane or the phagophore, which then forms an autophagosome. On fusion of

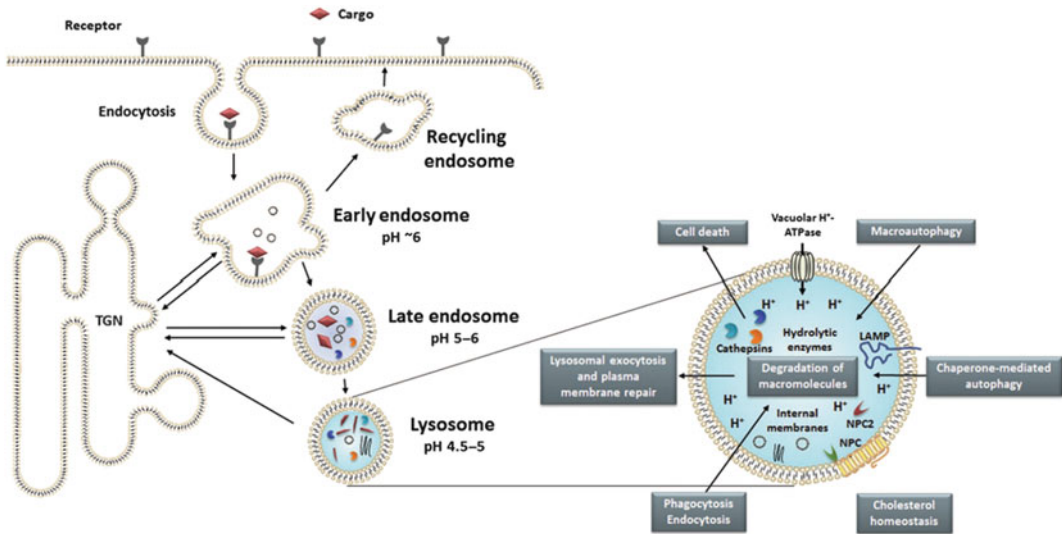


Fig. 4.24 Endolysosomal system. Lysosomes represent the terminal for the degradative endocytic pathway, beginning with early endosomes budding from the plasma membrane. In early endosomes, cargo is either sorted into the recycling pathway back to the cell surface via a recycling endosome or retained for degradation. Through gradual maturation, the early endosome is transformed into a late endosome containing less cargo destined for recycling and higher amount of lysosomal proteins. The formation of intraluminal vesicles (ILVs) starts in early

endosomes and peaks in late endosomes. Internal membranes in lysosomes are mostly seen as lamellar membranes, but some ILVs can be present. To the right is a magnification of a lysosome, showing its critical involvement in many cellular processes, including endocytosis, autophagy, plasma membrane repair, cell death, and cholesterol homeostasis. LAMP lysosome-associated membrane protein; NPC2 Niemann–Pick type C protein; TGN *trans*-Golgi network. *Source* Appelqvist et al. (2013)

autophagosomes with the lysosomes the contents are degraded. The degraded contents are then recycled as building blocks in biosynthesis.

The mammalian target of rapamycin (mTOR), serine–threonine kinases are a key regulator of growth in response to growth factors, stress, amino acids, nutritional status, and energy levels. Under conditions of nutrient sufficiency, TOR is associated with the lysosomal membrane and interacts and phosphorylates TFEB to prevent its nuclear translocation, thereby inhibiting autophagy. In starvation condition, mTOR is inhibited; hence, phosphorylation of TFEB is inhibited, activating gene transcription of TEEB-dependent genes resulting in increased autophagic flux.

Lysosomal **exocytosis** is a secretory pathway by which lysosomal waste is secreted out of the cell. The lysosomes first move from their perinuclear localization to the close vicinity of the

plasma membrane. In response to increased intracellular calcium concentration lysosomes fuse with the plasma membrane. Lysosomal exocytosis plays a major role in plasma membrane repair, immune responses, and bone resorption (Fig. 4.25). The damage of plasma membrane results in the influx of calcium, increasing intracellular calcium concentration. Calcium binds to synaptotagmin VII (SytVII) in the lysosomal membrane which then associates with soluble *N*-ethylmaleimide-sensitive factor attachment protein receptors (SNAREs), resulting in the fusion of lysosome with plasma membrane. Lysosome plasma membrane fusion restores the damaged plasma membrane and its integrity.

Lysosomes are important regulators of **cholesterol homeostasis**. The cholesterol pool in the cell is contributed by the de novo synthesis of

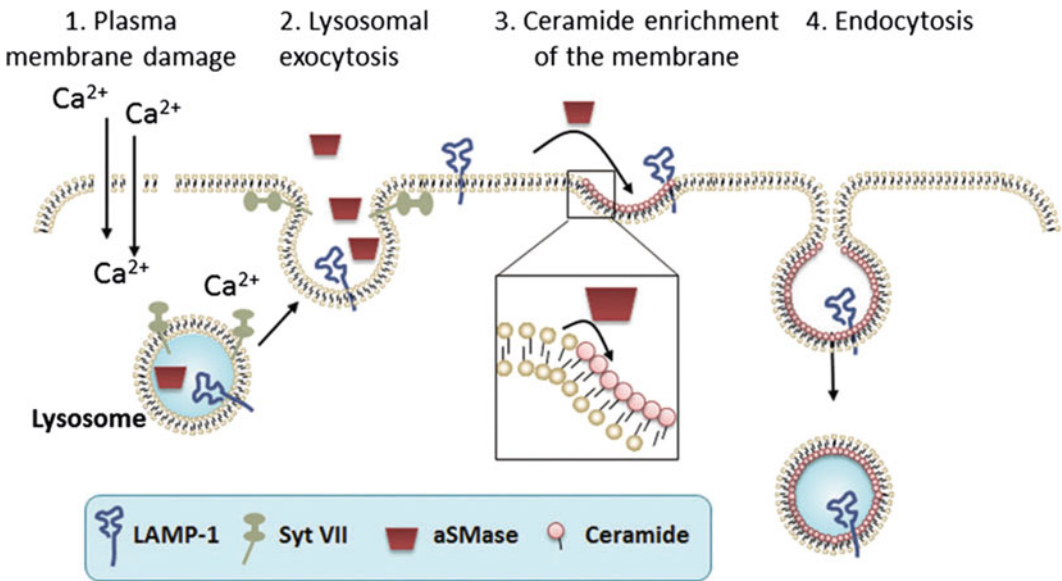


Fig. 4.25 Plasma membrane repair by lysosomal exocytosis. Damage to the plasma membrane results in calcium influx into the cell (1), which triggers a repair process involving lysosomal exocytosis. Lysosomes are translocated to the periphery, where they form a patch that fuses with the plasma membrane in a calcium-dependent manner (2). Lysosomal exocytosis is dependent on the presence of the calcium sensing synaptotagmin VII (Syt VII), which is located at the lysosomal membrane. As a result of exocytosis, the luminal part of LAMP-1 appears

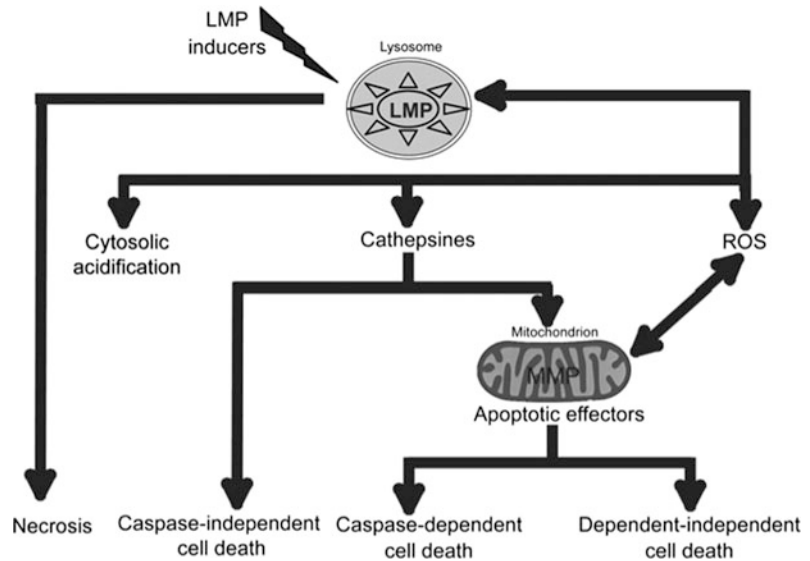
at the plasma membrane. In addition, lysosomal exocytosis results in the extracellular release of lysosomal enzymes, including acid sphingomyelinase (aSMase). At the outer leaflet of the plasma membrane, aSMase converts sphingomyelin into ceramide (3). A high membrane ceramide content results in an inward bending of the membrane, which facilitates endocytosis (4). Thereby, the lesion formed in the plasma membrane is removed and the plasma membrane is restored. *Source* Appelqvist et al. (2013)

cholesterol in the ER and the uptake of extracellular cholesterol via receptor-mediated endocytosis of low-density lipoproteins (LDLs). Endosomes transport LDL-derived cholesterol esters to the lysosomes, where they are acted upon by lipases to liberate free unesterified cholesterol into the cytoplasm. The free cholesterol is then taken up by other cellular organelles such as the ER, Golgi, and the plasma membrane. In conditions of high-cholesterol levels, cholesterol is reconverted to cholesterol esters by an ER enzyme: acyl-coenzyme A:cholesterol acyltransferase (ACAT), which are then stored in cytoplasmic lipid droplets. Two lysosomal proteins, the Niemann–Pick disease type C1 (NPC1) and NPC2 mediate the efflux of cholesterol from the organelle. Defects in the NPC1 or NPC2 protein result in the Niemann–Pick type C

lysosomal storage disease, leading to the accumulation of sphingolipids and cholesterol in the lysosomes.

Lysosomes, the so-called suicide bags, are an important participant in **cell death signaling**. The acidic lumen and the high concentration of hydrolytic enzymes in lysosomes can cause cell necrosis and death in case of lysosomal rupture or leakage. However, controlled lysosomal membrane permeabilization (LMP) can initiate cell death signaling pathway. Hence, apart from other classical apoptosis stimuli, LMP is also an important stimulus of apoptosis signaling. Lysosomal proteases, especially the cathepsins, the main mediators of the lysosomal apoptotic pathway, are released into the cytoplasm upon LMP. The cathepsins that remain active in neutral pH of the cytoplasm, such as cathepsin B, C, L

Fig. 4.26 Cell death pathways after lysosomal membrane permeabilization.
Source Boya (2012)



(cysteine cathepsins), and aspartic cathepsin D, play a prominent role in apoptosis. These caspases trigger both caspase-independent and mitochondria-mediated caspase-dependent apoptotic signaling pathways (Fig. 4.26). Though the molecular mechanism still remains elusive, LMP-induced caspases play an important role in the regression of the mammary gland after lactation.

Lysosome dysfunction contributes to many **diseases**. Lysosomal storage diseases (LSD) are a class of inborn diseases due to the absence or reduced activity of certain lysosomal proteins/enzymes, resulting in the accumulation of substances in the lysosomes. The massive accumulation of substances in the lysosomes impairs its functions autophagy and recycling of substrates, calcium and cholesterol homeostasis, and inflammation. Lysosomal storage disorders are clinically associated with mental retardation, neuronal dysfunction and degeneration, and premature death.

Neurons are selectively vulnerable to lysosomal storage diseases, with their limited regenerative potential the cells are unable to dilute undigested material by cell division. Lysosomes hold future promise for the development of new strategies for the treatment of neurodegenerative diseases such as Alzheimer's and Parkinson's.

Multifunctional lysosomes are also attractive therapeutic targets for many other diseases.

Controlled cell death mediated by LMP opens up a new horizon for cancer treatment.

4.6 Outer and Inner Mitochondrial Membranes

Mitochondria, called the powerhouse of the cell, were first time recognized as an cell organelle by Richard Altmann in 1890, and Leonor Michaelis visualized them under light microscope by Janus green staining. The detailed internal structure was revealed by electron microscope in 1952 (Fig. 4.27).

Mitochondria are believed to have originated by endocytosis of a proteobacteria some 1.6 billion years ago. Its own unique circular genome and protein translational machinery, which resembles the bacterial system, give credence to the evolutionary relationship between mitochondria and bacteria. In the course of evolution though, majority of the mitochondrial proteins (~99%) are now encoded by the nuclear genome. They are then translated in the cytoplasm and then transported into the mitochondria.

The mitochondria is enclosed by a double membrane, the outer and the inner membrane (Fig. 4.27). The mitochondrial outer membrane (MOM) demarcates the mitochondria from the

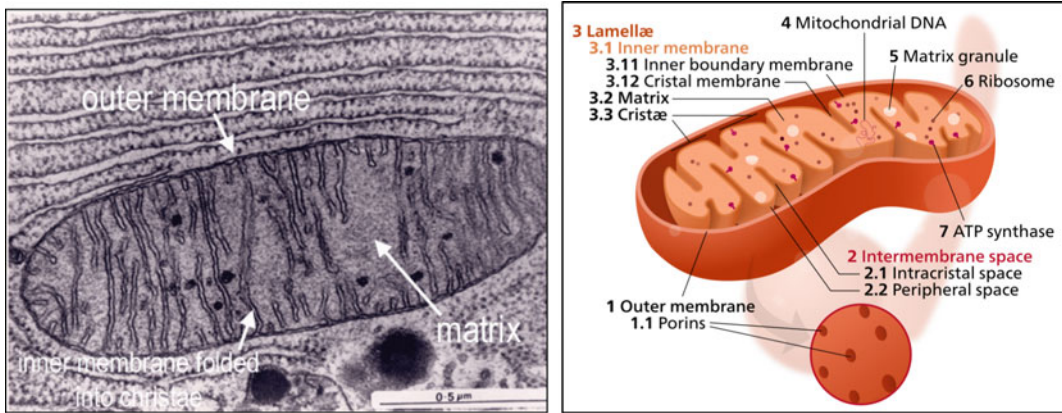


Fig. 4.27 Electron microscope photograph of mitochondria and a schematic diagram of mitochondria

cytoplasm. The mitochondrial inner membrane (MIM) envelops the mitochondrial matrix, which is equivalent to bacterial cytoplasm. The MIM forms extensive folds, called **cristae**, which extend deep into the matrix. This compartmentalizes the MIM into two distinct domains: the **inner boundary membrane (IBM)**, which lies toward the inside of MOM separated by intermembrane space and the **cristae membrane**. Cristae, the tubular membrane structure encloses another mitochondrial compartment, the **cristae lumen**, or the **intracristal space**. Hence, the intermembrane space is demarcated into the peripheral space and the intracristal space. The distinct regions in the mitochondria: the MOM, the intermembrane space, the MIM, cristae, the cristae lumen, and the matrix have their own functional importance and role with distinct protein components.

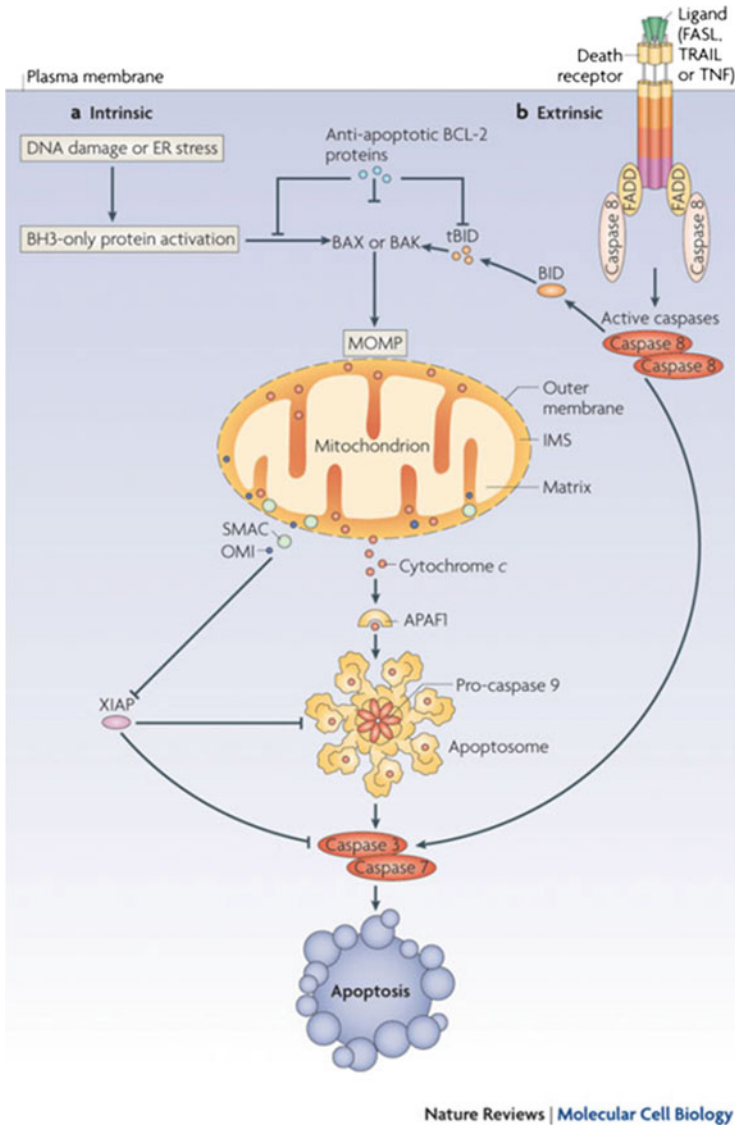
4.6.1 The Mitochondrial Outer Membrane (MOM)

The mitochondrial outer membrane (MOM) connects the mitochondria with the rest of the cell, and also mediates mitochondrial fusion and fission and maintains the mitochondrial morphology. MOM has a protein-to-phospholipid ratio of $\sim 1:1$ by weight, similar to the plasma membrane. It contains large number of transmembrane proteins called porins, which allow

the passage of molecules of 5000 daltons or less through the membrane. Proteins with larger molecular weight can enter the mitochondrion via a large multisubunit protein complex known as the translocase of the outer membrane (**TOM**), which recognizes and binds specifically to a signaling sequence at the N terminus of the protein. The voltage-dependent anion channel (**VDAC**) is the most abundant porin ion channel of the mitochondrial outer membrane (MOM). It can transport small hydrophilic ionic molecules like ATP, ADP, pyruvate, malate, etc. VDAC is also involved in the release of cytochrome c present in the intermembrane space into the cytosol during cell apoptosis.

The MOM is also associated with enzymes which catalyze diverse reactions, including monoamine oxidase, fatty-acid-CoA ligase, rotenone-insensitive NADH-cytochrome c-reductase, and kynurenine hydroxylase. Disruption of the outer membrane leaks intermembrane space proteins into the cytosol, leading to certain cell death. The mitochondrial outer membrane associates with MAM (mitochondria-associated ER membrane) an endoplasmic reticulum (ER) subdomain.

Many pro- and antiapoptotic signal proteins are associated with the MOM in mammalian cells. The two apoptosis signaling cascades, the intrinsic and extrinsic pathways, ultimately converge and activate the caspase cascade to induce apoptosis. The intrinsic pathway triggered by DNA damage, activates pro-apoptotic B cell



Nature Reviews | Molecular Cell Biology

Fig. 4.28 Intrinsic and extrinsic apoptotic stimuli. **a** Intrinsic apoptotic stimuli, such as DNA damage or endoplasmic reticulum (ER) stress, activate B cell lymphoma 2 (BCL-2) homology 3 (BH3)-only proteins leading to BCL-2-associated X protein (BAX) and BCL-2 antagonist or killer (BAK) activation and mitochondrial outer membrane permeabilization (MOMP). Antiapoptotic BCL-2 proteins prevent MOMP by binding BH3-only proteins and activated BAX or BAK. Following MOMP, release of various proteins from the mitochondrial intermembrane space (IMS) promotes caspase activation and apoptosis. Cytochrome c binds apoptotic protease-activating factor 1 (APAF1), inducing its oligomerization and thereby forming a structure termed the apoptosome that recruits and activates an initiator caspase, caspase 9. Caspase 9 cleaves and activates executioner caspases, caspase 3 and caspase 7, leading to apoptosis. Mitochondrial release of second mitochondria-derived activator of caspase (SMAC; also

known as DIABLO) and OMI (also known as HTRA2) neutralizes the caspase inhibitory function of X-linked inhibitor of apoptosis protein (XIAP). **b** The extrinsic apoptotic pathway is initiated by the ligation of death receptors with their cognate ligands, leading to the recruitment of adaptor molecules such as FAS-associated death domain protein (FADD) and then caspase 8. This results in the dimerization and activation of caspase 8, which can then directly cleave and activate caspase 3 and caspase 7, leading to apoptosis. Crosstalk between the extrinsic and intrinsic pathways occurs through caspase 8 cleavage and activation of the BH3-only protein BH3-interacting domain death agonist (BID), the product of which (truncated BID; tBID) is required in some cell types for death receptor-induced apoptosis. FASL FAS ligand; TNF tumor necrosis factor; TRAIL TNF-related apoptosis-inducing ligand. *Source* Stephen and Douglas (2010)

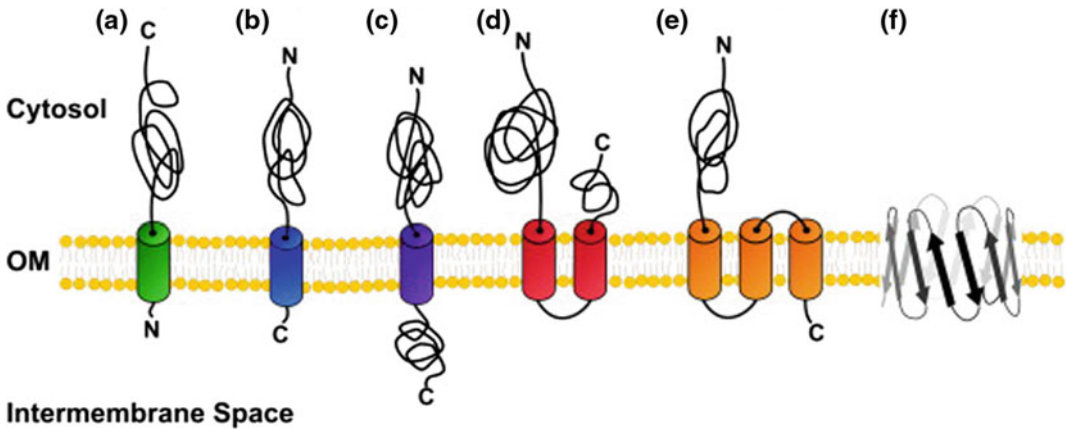


Fig. 4.29 Topologies of proteins in the mitochondrial outer membrane. Proteins span the membrane once, twice, or as multipass polypeptides. One family contains a single transmembrane segment at the N terminus. Examples are Tom20, Tom70, OM45, and Mcr1 (a). These proteins are inserted in an orientation, where the bulk of the polypeptide is exposed to the cytosol and only a small N-terminal segment crosses the outer membrane. Tail-anchored proteins such as Fis1, Tom5, Tom6, Gem1, Bcl-2, and VAMP-1B form another distinct class. These proteins have a single membrane spanning sequence at their C

terminus and display their large N-terminal portion to the cytosol (b). A third type of proteins, like Mim1 and Tom22, traverse the outer membrane once with an N-terminal domain pointing to the cytosol and a soluble C-terminal domain to the intermembrane space (c). Other proteins span the membrane twice (e.g., Fzo1/Mfn1,2, (d)) or several times (e.g., Ugo1 or PBR, (e)). Finally, several proteins (porin, Tom40, Tob55, Mdm10) are predicted to cross the outer membrane as a series of antiparallel β -strands, forming a β -barrel structure (f). *Source* Walther and Rapaport (2009)

lymphoma 2 (BCL-2) homology proteins and causes mitochondrial outer membrane permeabilization (MOMP) (Fig. 4.28). MOMP results in the release of cytochrome c from the mitochondrial intermembrane space. On its release into the cytoplasm, cytochrome c binds to apoptotic protease-activating factor 1 (APAF 1) and induces its conformational change and oligomerization forming an apoptosome complex. The apoptosome, also known as caspase activation complex, recruits and activates caspase 9, which further activates the final executioners, caspase 3 and caspase 7. The extrinsic pathway is initiated on activation of death receptors by ligands like TNF α . The activated receptor recruits many adaptor molecules such as FAS-associated death domain protein (FADD) which then activates caspase 8. Caspase 8 can directly activate caspase 3 and caspase 7, leading to apoptosis.

The integral membrane proteins of mitochondrial outer membrane (MOM) are categorized according to their transmembrane topology

(Fig. 4.29). The majority of MOM proteins are single transmembrane proteins, in which the transmembrane α -helix is near the N or the C terminus of the polypeptide chain. The bulk of the soluble domain of proteins is in the cytosol and only a short tail is located in the intermembrane space. The MOM also contains two span and multispan transmembrane proteins and also the β -barrel proteins (see Chap. 3).

Mitochondrial proteins which are encoded in the nucleus and synthesized in the cytosol enter the mitochondria via the translocase of the outer membrane complex (TOM complex). The TOM complex is a multisubunit complex with comprising of seven subunits with Tom20, Tom70, and Tom22 involved in receptor function, Tom40 forms the central protein conducting channel, and three small proteins Tom5, Tom6, and Tom7 stabilize the complex. The MOM also has the sorting and assembly machinery (SAM complex) and mitochondrial distribution and morphology complex (MDM complex) which are required for protein import and integration

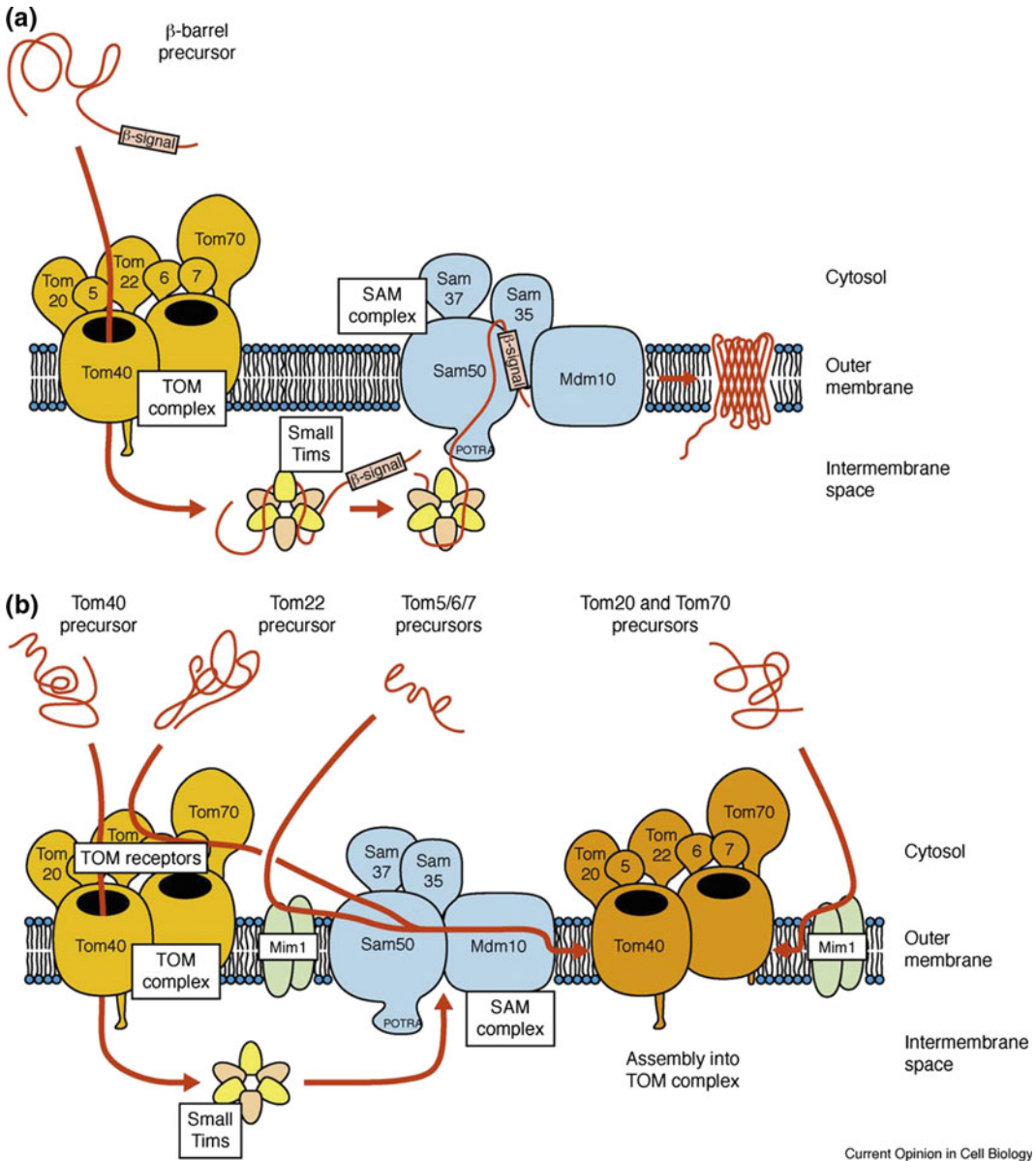


Fig. 4.30 Biogenesis of mitochondrial outer membrane proteins. **a** The precursors of β -barrel proteins are initially transferred across the outer membrane by the TOM complex. The TOM complex consists of the receptor proteins Tom20, Tom70, and Tom22, the small Tom proteins Tom5, Tom6 and Tom7 and the central, channel-forming component Tom40. Small Tim proteins of the intermembrane space take over β -barrel precursor proteins and deliver them to the SAM complex, which mediates integration of these precursors into the outer membrane. Sam50 (Omp85/Tob55) and the two peripheral subunits Sam35 and Sam37 form the SAMcore complex. Sam35 interacts with the β -signal of the incoming precursor. Mdm10 associates with SAMcore to form the SAMholo complex, which is involved in the

final steps of TOM complex assembly. **b** The SAM complex plays a central role in the assembly of the TOM complex. Here, precursor proteins with different types of membrane anchors are assembled, leading to the formation of the functional outer membrane translocase. The SAM machinery not only accepts the precursors of the β -barrel forming Tom40 from the intermembrane space side, but also the precursors of Tom22 and the small Tom proteins, which contain single α -helical transmembrane segments. Mim1 dynamically interacts with SAM components to promote the biogenesis of the small Tom proteins. Mim1 is also crucial for the membrane integration and assembly of Tom20 and Tom70. Mdm10 mediates the association of Tom22 with Tom40 and the small Tom proteins. *Source* Becker et al. (2009)

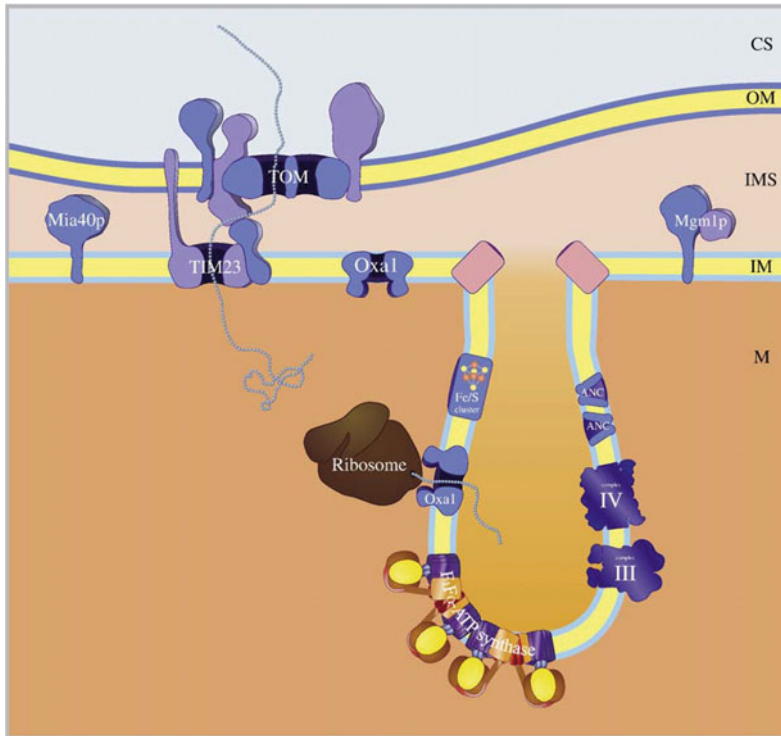


Fig. 4.31 Subcompartmentalization of the mitochondrial inner membrane. The distribution of mitochondrial proteins involved in several major processes of mitochondria has been determined by quantitative immunoelectron microscopy in *S. cerevisiae*. Inner membrane proteins involved in mitochondrial fusion (Mgm1p) or protein translocation (Mia40p, TIM23 complex) are preferentially located in the inner boundary membrane. In contrast,

proteins involved in oxidative phosphorylation (ANC, Complex III, Complex IV, F1FO-ATP synthase) are enriched in the cristae membrane. Proteins dynamically redistribute between the domains depending on the physiological state of the cell. CS Cytosol; OM outer membrane; IMS intermembrane space; IM inner membrane; M matrix space. *Source* Zick et al. (2009)

(Fig. 4.30). Integration of β -barrel proteins in the outer membrane requires SAM complex. The proteins are first translocated across the outer membrane via the TOM complex and then delivered to the SAM complex by small Tim (inner membrane carrier translocase) proteins. The SAM complex then integrates the β -barrel proteins into the MOM. A specific motif in the last β -strand, called the β -signal, is required for binding of precursor proteins to the SAM complex. The SAM core is composed of the integral membrane component Sam50 and two peripheral proteins, Sam35 and Sam37, toward the cytosolic side of the membrane. MDM10 is also associated with SAM complex. Several pathways exist for the import of α -helical proteins of MOM, but they are very well defined.

4.6.2 The Inner Membrane

The mitochondrial inner membrane (MIM) is extensively folded and compartmentalized. The convolutions in the inner membrane was established in the 1950s by Palade and Sjöstrand using electron microscopy. The inner membrane is composed of two distinct subdomains: the inner boundary membrane (IBM) and the cristae membrane (CM). The IBM faces the MOM, whereas the CM is the invaginated inner membrane that protrudes into the matrix space. The cristae are attached to the IBM by a narrow (~ 25 nm diameter) tubular opening which is termed crista junctions (CJs). The CM is found to be enriched in proteins involved in oxidative phosphorylation and protein synthesis, whereas

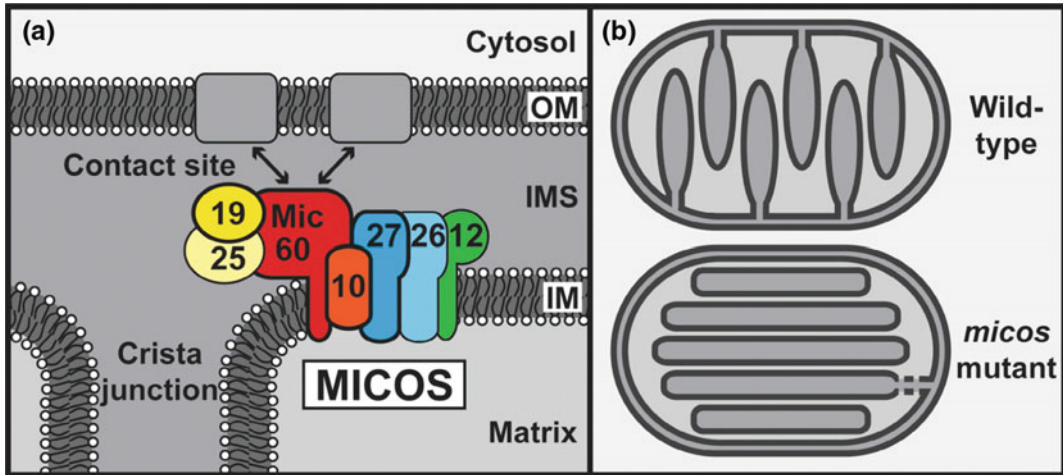


Fig. 4.32 MICOS complex. **a** The MICOS complex (hypothetical model), previously also termed MINOS is required for maintenance of the characteristic architecture of the mitochondrial inner membrane (IM) and forms contact sites with the outer membrane (OM). In budding yeast, six subunits of MICOS have been identified. All subunits are exposed to the intermembrane space (IMS), five are integral inner membrane proteins (Mic10, Mic12, Mic26, Mic27, and Mic60), and one is a peripheral inner membrane protein (Mic19). Mic26 is related to Mic27. The MICOS complex of metazoa additionally contains

Mic25, which is related to Mic19, yet subunits corresponding to Mic12 and Mic26 have not been identified so far. MICOS subunits that have been conserved in most organisms analyzed are indicated by bold boundary lines. **(b)** wild-type architecture of the mitochondrial inner membrane with crista junctions and cristae (bottom). This architecture is considerably altered in *micos* mutant mitochondria: most cristae membranes are detached from the inner boundary membrane and form internal membrane stacks. *Source* Pfanner et al. (2014)

the IBM is enriched in proteins involved in mitochondrial fusion and transport proteins for nuclear-encoded proteins (Fig. 4.31). The proteins can redistribute between the two compartments of the inner membrane with the changing physiological state of the mitochondria. A large multisubunit protein complex of the MIM which is involved in the maintenance of crista junctions, cristae membrane architecture, and formation of contact sites with the MOM has been characterized. The complex was known by different names, including mitochondrial contact site (MICOS) complex and mitochondrial inner membrane organizing system (MINOS); ultimately, the complex is now known as “mitochondrial contact site and cristae organizing system” (MICOS). The MICOS compartmentalizes the MIM into two distinct, CM and IBM domains. The protein subunits of MICOS are named Mic10 to Mic60 (Fig. 4.32). All subunits are exposed to the intermembrane space (IMS), except for Mic19 and Mic25, which are

peripheral proteins, all are integral membrane proteins (Mic10, Mic12, Mic26, Mic27, and Mic60). Some subunits have not been identified yet.

The mitochondrial F_1 - F_0 ATP synthase, the nanomachine that is driven by the proton gradient across the inner mitochondrial membrane to release ATP (see Chap. 8) is present in the cristae as linear arrays of ATP synthase dimers serially arranged in the curved regions along the crista ridges (Fig. 4.33). The respiratory chain complexes Complex I, III, and IV, which generate the proton gradient, assemble into **supercomplexes** or “**respirasomes**” (Fig. 4.34). Each respirasome consists of one copy each of complex I, complex III dimer, and complex IV monomer. The supercomplexes can facilitate effective electron transport and control the ratio of respiratory chain complexes in the membrane. Cytochrome c, a soluble electron carrier between complex III to complex IV is present in the crista lumen.

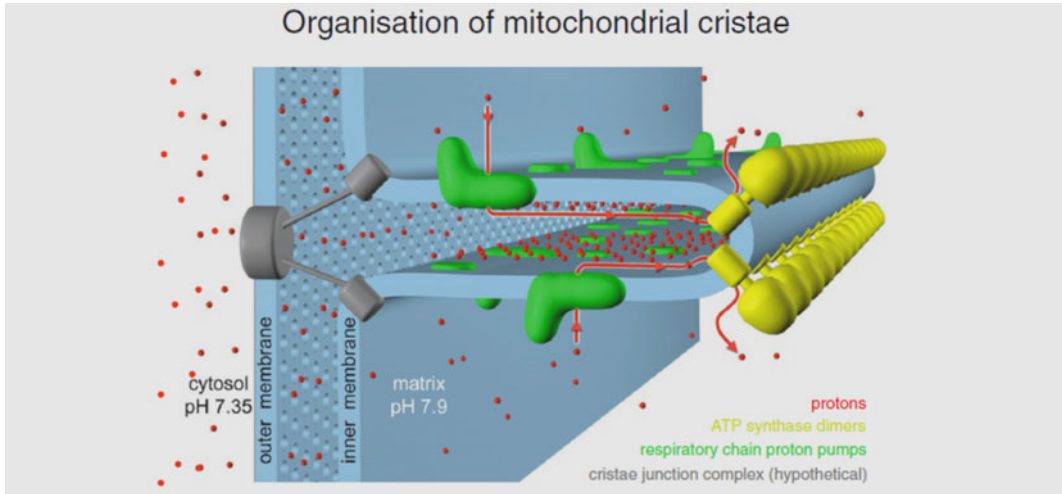


Fig. 4.33 ATP synthase dimer rows shape the mitochondrial cristae. At the cristae ridges, the ATP synthases (yellow) form a sink for protons (red), while the proton pumps of the electron transport chain (green) are located in the membrane regions on either side of the dimer rows. Guiding the protons from their source to the proton sink at

the ATP synthase, the cristae may work as proton conduits that enable efficient ATP production with the shallow pH gradient between cytosol and matrix. Red arrows show the direction of the proton flow. *Source* Kühlbrandt (2015) (Color figure online)

The respiratory chain supercomplex

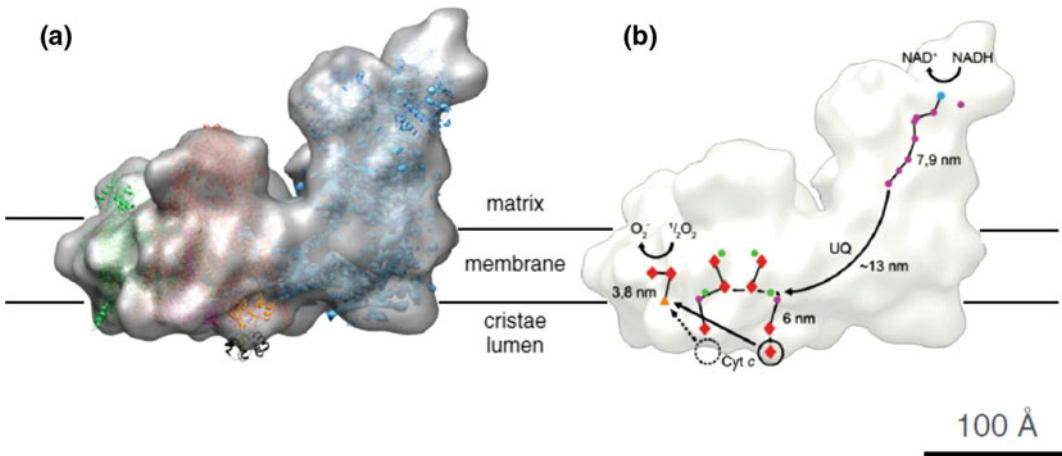


Fig. 4.34 Cryo-EM structure of the 1.7 MDa bovine heart respiratory chain supercomplex. **a** The supercomplex consists of one copy of NADH dehydrogenase (complex I, blue), a cytochrome b-c1 dimer (complex III, pink), and a single copy of cytochrome c oxidase (complex IV, green). **b** The ubiquinol (UQ) binding sites of complexes I and III and the short distance between the

cytochrome c binding sites in complexes III and IV, which would favor efficient electron transfer. Cofactors active in electron transport are marked in yellow (FMN), orange (iron-sulfur clusters), dark blue (quinols), red (hemes), and green (copper atoms). Arrows indicate the electron path through the supercomplex. *Source* Kühlbrandt (2015) (Color figure online)

Even though mitochondria and the respiratory chain protein complexes have been studied intensely for more than five decades, many questions still remain unanswered.

References

- Appelqvist H, Wäster P, Kågedal K, Öllinger K (2013) The lysosome: from waste bag to potential therapeutic target. *J Mol Cell Biol* 5(4):214–226. <https://doi.org/10.1093/jmcb/mjt022> (PMID 23918283)
- Becker T, Gebert M, Pfanner N, Van der Laan M (2009) Biogenesis of mitochondrial membrane proteins. *Curr Opin Cell Biol* 21:484–493
- Boya P (2012) Lysosomal function and dysfunction: mechanism and disease. *Antioxid Redox Signal* 17(5):766–774
- Chiba H, Osana M, Murata M, Kojima T, Sawada N (2008) Transmembrane proteins of tight junctions. *Biochimica et Biophysica Acta* 1778:588–600
- de Duve C (1959) Lysosomes, a new group of cytoplasmic particles. In: Hayashi T (ed) *Suncellular particles*. The Ronald Press Co., New York, pp 128–159
- Dianne S, Schwarz DS, Blower MD (2016) The endoplasmic reticulum: structure, function and response to cellular signaling. *Cell Mol Life Sci* 73:79–94. <https://doi.org/10.1007/s00018-015-2052-6>
- Garrod D, Chidgey M (2008) Desmosome structure, composition and function. *Biochim Biophys Acta* 1778:572–587
- Golgi C (1898) Sur la structure des cellules nerveuses des ganglions spinaux. *Arch Ital Biologie* 30:278–286
- Grasse PP (1957) Ultrastructure, polarity and reproduction of Golgi apparatus. *C R Hebd des Séances del'Académie des Sci* 245(16):1278–1281
- Hetzer MW (2010) The nuclear envelope. *Cold Spring Harb Perspect Biol* 2:a000539
- Kühlbrandt W (2015) Structure and function of mitochondrial membrane protein complexes. *BMC Biol* 13(89):1–11. <https://doi.org/10.1186/s12915-015-0201-x>
- Laird DW (2006) Life cycle of connexins in health and disease. *Biochem J* 394:527–543
- Le Sage V, Moulant AJ (2013) Viral subversion of the nuclear pore complex. *Viruses* 5(8):2019–2042 (PubMed 23959328)
- Lynes EM, Simmen T (2011) Urban planning of the endoplasmic reticulum (ER): how diverse mechanisms segregate the many functions of the ER. *Biochem Biophys Acta* 1813:1893–1905
- Martínez-Menárguez JA (2013) Intra-Golgi transport: roles for vesicles, tubules, and cisternae. *ISRN Cell Biol* 1–15. <https://doi.org/10.1155/2013/126731> (Article ID 126731)
- Meşe G, Richard G, White TW (2007) Gap junctions: basic structure and function. *J Invest Dermatol* 127(11):2516–2524
- North AJ, Bardsley WG, Hyam J (1999) Molecular map of the desmosomal plaque. *J Cell Sci* 112:4325–4336
- Palade G (1975) Intracellular aspects of the process of protein synthesis. *Science* 189(4200):347–358
- Pfanner N, van der Laan M, Amati P, Capaldi RA, Caudy AA, Chacinska A et al (2014) Uniform nomenclature for the mitochondrial contact site and cristae organizing system. *J Cell Biol* 204(7):1083–1086
- Prunuske AJ, Ullman KS (2006) The nuclear envelope: form and reformation. *Curr Opin Cell Biol* 2006(18):1–9
- Reynders E, Foulquier F, Annaert W (2011) How Golgi glycosylation meets and needs trafficking: the case of the COG complex. *Glycobiology* 21(7):853–863
- Rizzuto R, De Stefani D, Raffaello A et al (2012) Mitochondria as sensors and regulators of calcium signalling. *Nat Rev Mol Cell Biol* 13:566–578
- Stephen WGT, Douglas RG (2010) Mitochondria and cell death: outer membrane permeabilization and beyond. *Nat Rev Mol Cell Biol* 11:621–632
- Szul T, Sztul E (2011) COPII and COPI traffic at the ER-Golgi interface. *Physiology* 26(5):348–364. <https://doi.org/10.1152/physiol.00017.2011>
- Walko G, Castañón MJ, Wiche G (2015) Molecular architecture and function of the hemidesmosome. *Cell Tissue Res* 360:363–378
- Walther DM, Rapaport D (2009) Biogenesis of mitochondrial outer membrane proteins. *Biochim Biophys Acta (BBA)-Mol Cell Res* 1793(1):42–51. <https://doi.org/10.1016/j.bbamcr.2008.04.013>
- Zick M, Rabl R, Reichert AS (2009) Cristae formation-linking ultrastructure and function of mitochondria. *Biochim Biophys Acta* 1793:5–19

5.1 Membrane Fluidity

The Fluid Mosaic Model proposed that membrane is a two-dimensional fluid assembly of lipids and proteins.

A fluid state is one which is less viscous, less rigid and the molecules are free to move in the fluid medium. Compared to liquids, in fluid membranes, the molecular motion of membrane components is relatively restricted in terms of direction and rate. Membrane fluidity is essentially required for a functional membrane. Membrane permeability, phagocytosis, endocytosis, signal transduction are just a few of the processes which require a fluid membrane. Adequate membrane fluidity is also required for functional integral membrane proteins, for multitude transformations necessary for cellular functions including transport, division, and differentiation. The molecules in membranes can laterally diffuse in the plane of the membrane, rotate about their own axis, transverse the bilayer, or undergo conformational change. The bulk of most membranes exist in a lamellar liquid-crystalline L_{α} phase. Membranes regulate their lipid composition to maintain the optimal membrane fluidity in order to be functional and preserve its integrity.

Great technological advancements after the 1960s have revolutionized the study of membrane dynamics. Techniques like NMR, ESR, and fluorescent-based techniques like confocal microscopy, fluorescence recovery after photobleaching (FRAP), fluorescence resonance

energy transfer (FRET), fluorescence correlation spectroscopy (FCS), and single-particle tracking (SPT) have helped in visualizing and monitoring membrane dynamics.

5.2 Motion of Membrane Components

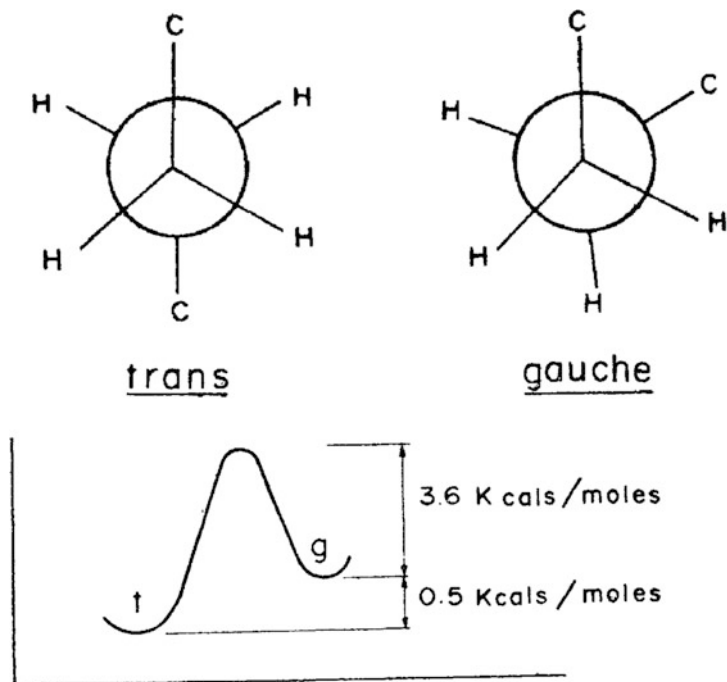
The different types of molecular motions in membranes (Table 5.1):

1. **Gauche-trans transition of methylene residues about C–C bond** (Fig. 5.1): Free rotation about C–C bonds occurs at a high frequency in the straight polymethylene chain of lipid component of membranes. At low temperatures, in crystalline and gel phase of phospholipid bilayers, the all-trans conformation is preferred. In all-trans conformation, polymethylene chain is straight and cylindrical, resulting in close packing of polymethylene chains. Insertion of one or more gauche conformation produces severe distortions in the shape and size of the chain, resulting in larger surface area and shorter length. Hence, at higher temperatures, probability of gauche conformation increases.
2. **Rotational motion:** Both lipid and proteins molecules in membrane show rotational motion along an axis perpendicular to the plane of the membrane (Fig. 5.2). Movement of molecules about their own axis perpendicular to the plane of the membrane is

Table 5.1 Characteristics of different types of molecular motion in biomembranes

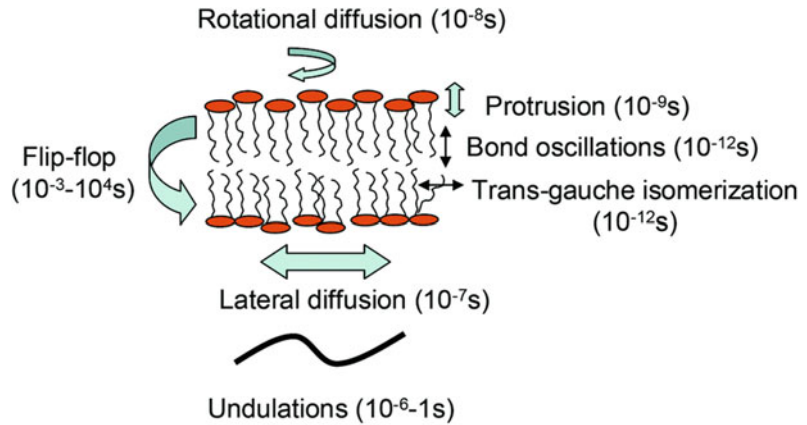
Type of motion	Magnitude (average time)	Structural consequence	Functional consequence
Gauche-trans	10^{-9} – 10^{-11} s	Defect structures Gel-to-liquid phase Regions of mismatch	Passive permeability Regulation of protein functions Permeability, partitioning of solutes
Rotational motion	$>10^{-3}$ – 10^{-7} s	Conformational and relaxation changes	Catalytic and transport functions
Segmental motion	10^{-5} – 10^{-8} s	Fluidity gradient Polarity gradient	Localization of solutes in different regions
Transverse motion	$t_{1/2} > 6$ days	Asymmetry	Several functions are asymmetric
Lateral diffusion	$D = 10^{-8}$ – 10^{-13} $\text{cm}^2 \text{s}^{-1}$	Phase separation Topographical distribution	Turnover, biosynthesis Recognition, catalytic function
Exchange	10^{-5} – 10^{-1} s	Structural integrity	Turnover, biosynthesis

Fig. 5.1 Gauche-trans transition of methylene residues about C–C bond.
Source Jain (1979)



Jump frequency ($t \rightarrow g$) $\sim 10^9 - 10^{10} \text{ sec}^{-1}$ at 25°C
 C–C bond oscillation $\sim 10^{12} \text{ sec}^{-1}$ at 25°C

Fig. 5.2 Rotational, lateral, and transverse motion of membrane lipids



described by **rotational diffusion coefficients** D_g which is characterized by the mean square angular deviation in time interval Δt :

$$\theta^2 = 6D_g\Delta t$$

There is an organizational asymmetry in the environment of a lipid and protein molecules in the bilayer. The long axis of lipid acyl chain has van der Waals interactions with the neighboring chain. In contrast, the polar head groups interact with water and other neighboring polar molecules by electrostatic interactions. Similarly, the transmembrane domain of a membrane protein interacts with nonpolar lipids, whereas domains exposed on the surface of membranes interact by electrostatic interactions with lipid polar head groups and the aqueous environment. Therefore, the rotation of molecules in bilayer is considerably more restricted than in bulk water or in bulk hydrocarbon. The rotational displacement time computed was found to be: ~ 1 ns for phospholipids (MW ~ 700) in liposomes to about <1 μ s for proteins of MW $\sim 100,000$.

3. **Lateral Diffusion:** Diffusion is the random movement of molecules driven by their kinetic energy from area of higher concentration to the area with lower concentration. Lipids and proteins can diffuse laterally in the plane of the membrane. Movement or diffusion of molecules in the plane of the bilayer is described by **lateral diffusion coefficients**

D_T , which is given by the mean square lateral displacement in time interval Δt :

$$r^2 = 4D_T\Delta t$$

Lateral diffusion was for the first time visualized by fluorescence recovery after photobleaching (FRAP) technique. The lateral diffusion coefficients of membrane components have been found to be in the range 10^{-8} – 10^{-13} $\text{cm}^2 \text{s}^{-1}$, in liposomes, which provides unrestricted homogeneous two-dimensional matrix. The lateral mobility of proteins and lipids in biological membranes are much slower than in synthetic membranes, due to a high degree of molecular associations, segregation in membrane domains, or interactions with cytoskeletal components.

Lateral diffusion of membrane components has many functional consequences. To name a few: (1) Lateral diffusion facilitates protein–protein interaction during signal transduction cascades triggered by hormones, neurotransmitters, or antigens, (2) diffusion of ligand-bound receptors in coated pits, resulting in their endocytosis, (3) mediate membrane fusion, (4) electron transport in mitochondria and chloroplast by mobile carriers like cytochrome *c* and plastocyanin, respectively, (5) external cross-linking of the F_c receptor of cell surface Igs is involved in triggering the cellular immune response,

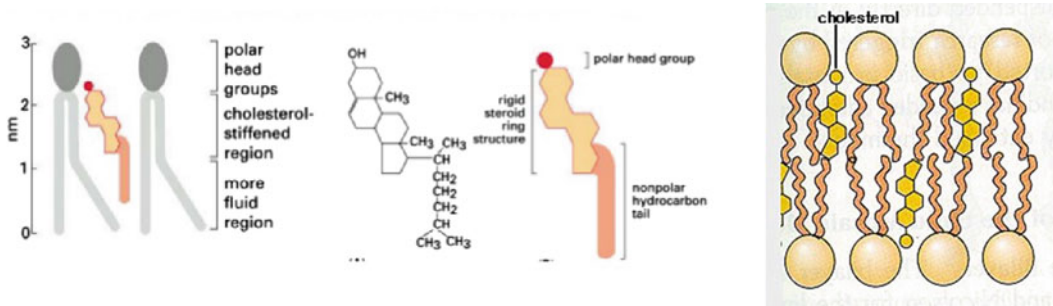


Fig. 5.3 Cholesterol in membranes

(6) provides directionality during cell division and cell development.

4. **Transverse motion or flip-flop movement:** Transverse movement of molecules from one interface of the bilayer to the other is a rather slow process, especially for polar molecules which have to cross an unfavorable hydrophobic interior. Halftimes for flip-flop of cholesterol and phospholipids are greater than 6 days. Proteins being large molecules show negligible transverse motion. Restricted transverse motion results in the asymmetry of membranes across the bilayer.

5.3 Factors Affecting Membrane Fluidity

5.3.1 Lipid Composition

The degree of unsaturation, fatty acyl chain length, and the percentage of cholesterol and sphingolipids impact membrane fluidity. Introduction of unsaturation with *cis*-double bonds in fatty acyl chain introduces a kink in the chain, increasing disorderness and membrane fluidity, whereas increase in saturated or *trans*-unsaturated fatty acyl chains, decrease membrane fluidity. Increase in acyl chain length stabilized by hydrophobic interactions results in more ordered packing leading to decrease in membrane fluidity. Increase in cholesterol/phospholipid or sphingolipid/phosphoglycerolipid ratio also results in decrease in membrane fluidity.

Cholesterol is an important modulator of membrane fluidity. The cholesterol consists of a rigid, planar structure made of series of fused rings with attached hydrocarbon chain at one end, and a hydroxyl group at the other end. Therefore, cholesterol, like other membrane lipids, has both hydrophilic and hydrophobic poles that can position within the lipid bilayer. The hydroxyl group interacts with the phospholipid ester carbonyl, whereas the rigid body of cholesterol is positioned alongside the fatty acid tails of neighboring phospholipids, interacting via hydrophobic interactions increase the order in membranes (Fig. 5.3). As cholesterol fills interstitial spaces between neighboring acyl chains, it increases membrane rigidity and decreases membrane fluidity.

Interaction with the rigid cholesterol ring with hydrocarbon chains of lipids in the liquid crystal phase (L_{α}) and leads to formation of a new phase, the liquid-ordered (L_o) phase (Fig. 2.7). In the liquid-ordered phase, the rotation and lateral diffusion rates are similar to the L_{α} phase, but the acyl chains are predominantly in an all-*trans* conformation; hence, the packing parameters are similar to the L_{β} phase. In cells, cholesterol-rich L_o phase has been strongly associated with lipid rafts.

At low temperatures, cholesterol prevents phase transition of membranes from fluid to the gel phase. Due to its rigid ring structure, cholesterol prevents any higher order of packing hence, acts as an anti-freeze, lowering the phase transition temperature from liquid to gel phase. Some plasma membranes, such as nerve myelin

membranes, contain a high concentration of lipids that form bilayers in gel phase, and the presence of cholesterol keeps these membranes in a fluid phase.

5.3.2 Diet

Biomembranes in animal system remain relatively constant with respect to saturated fatty acid (SFA) and monounsaturated fatty acid (MUFA) levels over a wide range of dietary variation in fatty acids over a short period of time. Yet, changes in membrane composition were observed in diets rich in ω -6 and ω -3 polyunsaturated fatty acid (PUFA) and were most responsive to n-3 PUFA and to the ω -3/ ω -6 ratio. These differential responses are probably due to the fact that both ω -6 and ω -3 PUFA class of lipids cannot be synthesized *de novo* in higher animals and are sourced from the diet.

Long-term intake diet rich in certain lipids can lead to changes in membrane composition. Increased incorporation of cholesterol has been observed in patients with hypercholesterolemia and type 2 diabetes, leading to pathological consequences.

5.3.3 Temperature

The effects of changes in temperature on membrane fluidity have been demonstrated in bacteria and cyanobacteria. Membrane fluidity decreases with a decrease in temperature, whereas high temperatures fluidize the membranes.

5.3.4 Osmotic Stress

Studies on phospholipid vesicles exposed to hyperosmotic stress with the addition of polyethylene glycol, glycerol, sucrose, or NaCl showed that it resulted in decrease in membrane fluidity similar to low-temperature stress. Salt stress is one of the main environmental factors that can inhibit the growth and survival of plants and microorganisms resulting from decreased

membrane fluidity. Hence, organisms that can survive in conditions of high osmolarity, for example, a strain of yeast, *Zygosaccharomyces rouxii* that can grow in high salt media, or plant growing in salt stress conditions develop adaptive mechanisms to reduce membrane fluidity. Sperm membranes with higher fluidity are able to withstand conditions of high osmolarity during cryopreservation.

5.3.5 Cell Cycle and Development

Membrane fluidity fluctuations have been observed during cell cycle and during different stages of development of an organism. Membrane is most fluid during mitosis, whereas cells in G1 and early S phases showed the lowest membrane fluidity. Studies with cultured cells showed that membrane fluidity decreases with aging. Increase in cholesterol/phospholipid ratio could be correlated with decrease in membrane fluidity with aging. Decrease in membrane fluidity could be one of the factors leading to decreased functioning of the aging cells.

5.3.6 Disease

Changes in membrane fluidity affect the functioning of many important physiological signaling pathways, including cell proliferation and cell death.

It has been reported that the activation *de novo* lipogenesis in cancer cells leads to increased membrane lipid saturation, resulting in higher percentage of saturated and monounsaturated phospholipids in membranes. Higher degree of saturation protects the cancer cells from oxidative damage, in contrast to the unsaturated fatty acyl chains which are more prone to lipid peroxidation. The resulting reduced membrane fluidity is a feature of most cancers and tumors. Decrease in membrane fluidity also decreases drug permeability and uptake leading to drug resistance. The increase in cholesterol content in tumors is strongly related with an increase of lipid rafts which are involved in

signaling pathways involved in cell proliferation, differentiation, and migration. Thus, modulation of lipid rafts domains contributes to uncontrolled growth observed in cancer.

Decreased membrane fluidity is also associated with diseases, such as atherosclerosis and diabetes mellitus. Thus, the modulation of membrane fluidity/rigidity emerges as a very useful tool for the treatment of variety of diseases.

5.3.7 Anesthetics

Alkanes, alcohols, benzodiazepines, barbiturates, esters and amides, phenols, ethers, and even inert gases are anesthetics. Anesthetic molecules have been used for local or general anesthesia based on their pharmacological effects.

Most of the local anesthetics now in use are amphiphilic molecules, in which the hydrophilic group is usually consisting of an amino moiety and a hydrophobic group generally contains an aromatic ring. The hydrophobic groups are involved in the diffusion and binding of anesthetics to cell membranes, while the hydrophilic ends confer these molecules water solubility to spread into the tissues.

Anesthetics almost always disorder or “fluidize” membrane, i.e., they increase the mobility of spin labels and reduce order parameters. The lipophilic component of anesthetics penetrates into the membrane, creating disorder, and increasing membrane fluidity. Thereby, anesthetics can impact membrane-embedded ion channels and membrane-associated enzymes. They alter the membrane lipid environments surrounding the transmembrane proteins that can result in change of protein conformation and its activity and function.

Charged anesthetics have differential actions on the two sides of the bilayer because of the asymmetry of the phospholipid distribution. Cytoplasmic side of the bilayer is negatively charged being rich in PS. Hence, positively charged, cationic anesthetics, such as 2-[*N*-methyl-*N*-(2,2,6,6-tetramethylpiperidinoxy)]ethyl p-hexyloxybenzoate, abbreviated as C6SL, preferentially fluidize cytoplasmic leaflet of the membrane

bilayer, modulating the activity of proteins and enzymes such as adenylyl cyclase associated with cytoplasmic side of the bilayer. In contrast, anionic tertiary amine local anesthetics interact with and preferentially fluidize extracellular side of the monolayer and affect the activities and function of proteins and enzymes associated with the outer monolayer. Hence, charged anesthetics have become popular tools in the study of membrane dynamics.

5.3.8 Ca^{2+} and Other Divalent Cations

Fluctuations in intracellular Ca^{2+} concentration in response to signaling pathways or nerve conduction have been observed to modulate membrane fluidity on the cytoplasmic side of the membrane. Increase in intracellular Ca^{2+} has shown to increase membrane order and decrease membrane fluidity. Ca^{2+} decreases membrane fluidity by binding to negatively charged membrane lipids on the cytoplasmic side.

5.4 Techniques to Determine the Rate of Molecular Motion in Membranes

5.4.1 Techniques to Study Lateral Diffusion in Membranes

Microscopy-based techniques have been used to study membrane surface dynamics. The use of membrane tags, such as radioactive label, conjugated dyes, especially the fluorescent dyes (Fig. 5.4) have led to the development of many advance techniques which have enhanced our understanding of membrane dynamics. Some of the advance techniques are discussed below.

5.4.2 Confocal Microscopy

Confocal microscopy is one of the most popular advance imaging techniques in contemporary biology. It was developed by Marvin Minsky in

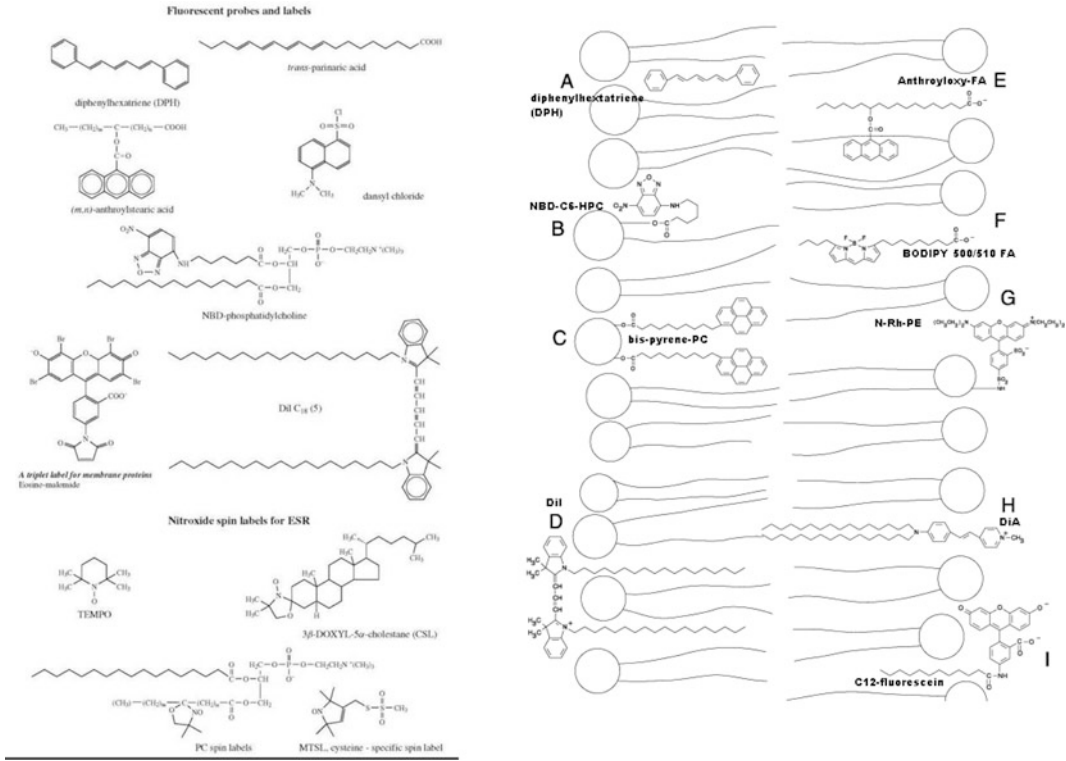


Fig. 5.4 Fluorescent lipid probes and spin labels for ESR. *Source* Gennis (1989)

1950s, as advancement over traditional wide-field fluorescence microscopy. In traditional fluorescent microscope, the whole fluorescent sample is illuminated. The fluorescence from different parts of the sample results in large background noise. In contrast in confocal microscopy, the light is focused on a single point on the sample.

Confocal microscopy, also known as confocal laser scanning microscopy (CLSM), uses laser light for illumination. Coherent laser light passes through a pinhole aperture and falls on the dichromatic mirror, which reflects the laser beams to scan across the specimen in different focal planes (Fig. 5.5). The fluorescence emitted from a point on the specimen in a focal plane is focused as a confocal point at the detector pinhole aperture before reaching the detector. This eliminates out-of-focus light, increases resolution, and decreases background noise. The images obtained at different focal planes provide noninvasive, serial optical sectioning of thick

specimens. Hence, three-dimensional structures can be reconstructed from the set of images obtained at different focal planes.

Confocal microscopy provides noninvasive live cell/tissue imaging of high resolution, with minimum sample preparation. Use of multi-wavelength lasers as light source, sensitive low-noise photodetectors, and fast microcomputers with high-resolution digital imaging enhanced by sophisticated image analysis software packages has added new dimension to the study of b membrane dynamics. Interactions and movement of membrane components tagged with fluorescent dyes can be studied with more precision.

5.4.3 Fluorescence Recovery After Photobleaching (FRAP)

Fluorescence recovery after photobleaching (FRAP) technique (Fig. 5.6) is the most popular

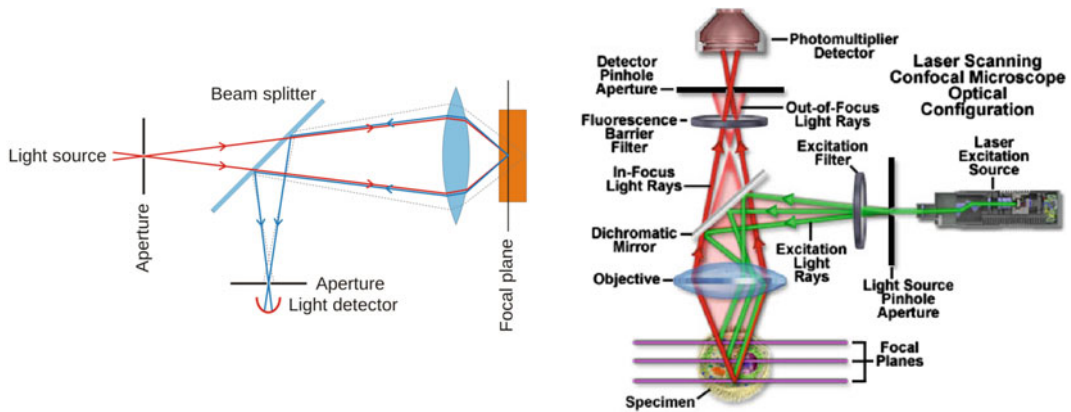


Fig. 5.5 Principle of confocal microscopy: confocals produce an image in quite a different way from wide-field fluorescence scopes. Rather than exciting the entire field at once, the light is focused into a very small spot and this is scanned across the sample and an image is built up. Lasers are used for excitation. The light from the focal

plane passes through the pinhole to the detector. By blocking the light from outside, the focal plane confocals have good z -axis resolution and are great for imaging thick samples because the haze from out-of-focus objects is mostly eliminated

technique to determine the lateral diffusion coefficient D_T of molecules in membranes. The membrane is labeled with appropriate fluorescent probe. A small area (μm) is photobleached using a laser beam and then that specific area is monitored for the recovery of fluorescence caused by diffusion of fluorescent-tagged molecules from the surrounding area. The fluorescence recovery time is a function of the diffusion rate of molecular components in the membrane. Such noninvasive studies are carried out using a fluorescence microscope/confocal microscope in live cells. A typical time curve (Fig. 5.6) shows a remarkable fall in fluorescent intensity on laser-induced bleaching, which is followed by an exponential recovery in fluorescent intensity with a characteristic halftime, when 50% of the intensity is recovered. Hundred-percent recovery is only achieved in synthetic liposomes, but rarely in natural membranes. In natural membranes, the recovery level is usually lower than the initial level due to the presence of barriers and immobile fractions in membranes.

Different extrinsic fluorescent lipid probes have been used (Fig. 5.4) to determine the lateral diffusion rate of membrane lipids and proteins. Lipid fluorophores are attached either to long

acyl chains or to phospholipids. Advent of green fluorescent proteins (GFP) technology using intrinsic GFP-fused protein as a probe to study membrane dynamics has revolutionized the study of membrane protein mobility and interactions with other membrane components.

5.4.4 Fluorescence Correlation Spectroscopy (FCS)

FCS has become an important tool for studying mobility of membrane components in three dimensions with high fluorophore sensitivity. FCS is based on the statistical analysis of fluctuations of fluorescence intensity in a very small volume ($\leq 1 \mu\text{m}^3$). Fluorescence fluctuations occur as the result of molecules diffusing in and out of the focal area under observation (Fig. 5.7). The fluctuations are measured as variation around an average value. The fluorescent signal received from the very small focal volume is recorded at time t and intervals of $t + \tau$ and correlated. This correlation is represented by the autocorrelation function of temporal intensity as a function of temporal average intensity value, given by:

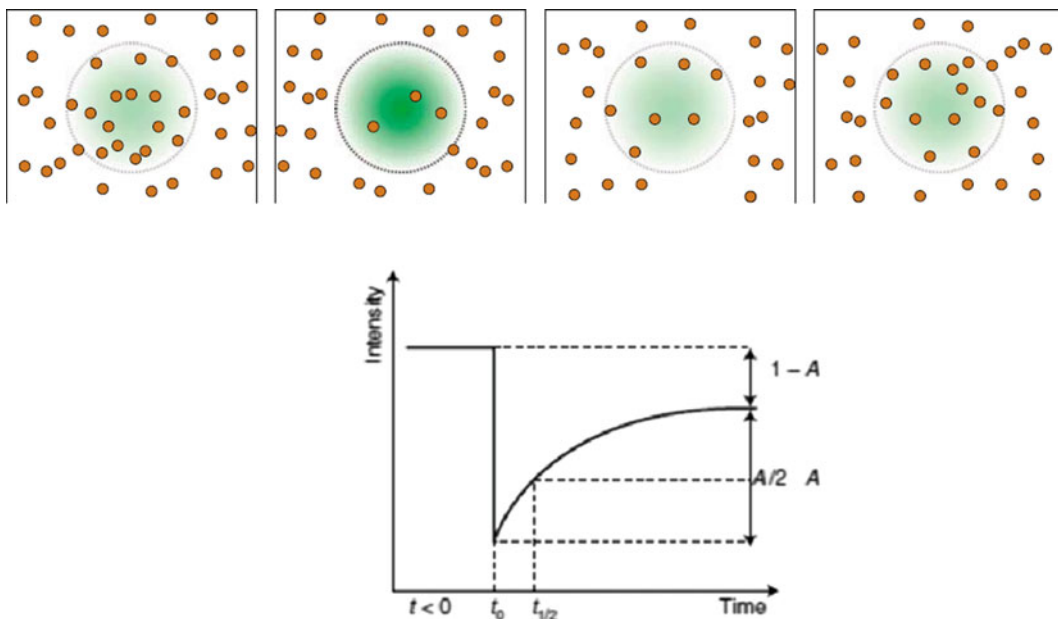


Fig. 5.6 In FRAP, the amount of fluorescence is recorded at low laser intensity in the region of interest (defined here by the laser spot area). A high-intensity pulse is used to bleach most of the molecules within the spot, and the fluorescence is then measured at low laser intensity. Diffusing molecules then replenish the bleached

area, leading to an increase in the detected fluorescence intensity. The characteristic fluorescence recovery time reflects the diffusion time. FRAP parameters $0 < t$ are the time before bleaching, t_0 is the time at bleaching occurs, $t_{1/2}$. A is the mobile fraction and $1 - A$ is the immobile fraction. *Source* Marguet et al. (2006)

$$G(\tau) = \frac{\langle \delta F(t) \cdot \delta F(t + \tau) \rangle}{\langle F(t) \rangle^2},$$

where $\delta F(t) = F(t) - \langle F(t) \rangle$ is the fluctuation around the average intensity and pointed brackets ($\langle \rangle$) denotes the temporal average; τ is the lag time.

The fluctuations can be analyzed by the correlation curves (Fig. 5.7). The diffusion coefficient of molecules is inversely proportional to the width of the correlation curve and the concentration inversely proportional to the amplitude. Hence, FCS provides information about diffusion coefficients, concentrations, and intermolecular interactions of membrane components. However, FCS only records fluorescence fluctuations and ignores immobile molecules. It measures relatively fast-moving molecules ($D_T > 0.1 \mu\text{m}^2 \text{s}^{-1}$), although recent advances have extended its range of application to include slow-diffusion processes ($D_T > 0.001 \mu\text{m}^2 \text{s}^{-1}$).

5.4.5 Förster Resonance Energy Transfer (FRET)

FRET was first proposed by Theodor Förster in late 1940s. FRET is possible when the fluorescence emission spectrum of a donor molecule overlaps the absorption spectrum of the acceptor molecule which is in close proximity of the donor molecule (10–100 Å). The mechanism involves the resonance energy transfer from an excited fluorescent donor molecule to an acceptor molecule in close vicinity in a nonradiative fashion (Fig. 5.8a). The acceptor fluorescent molecule gets excited on absorption of resonance energy and then shows emission fluorescence.

FRET has become a valuable tool to study intermolecular dynamic interactions in living cells. In vivo FRET has greatly advanced by the improvement in the GFP fusion protein technology. Several mutation variants of GFP protein have been developed which have spectrally distinct

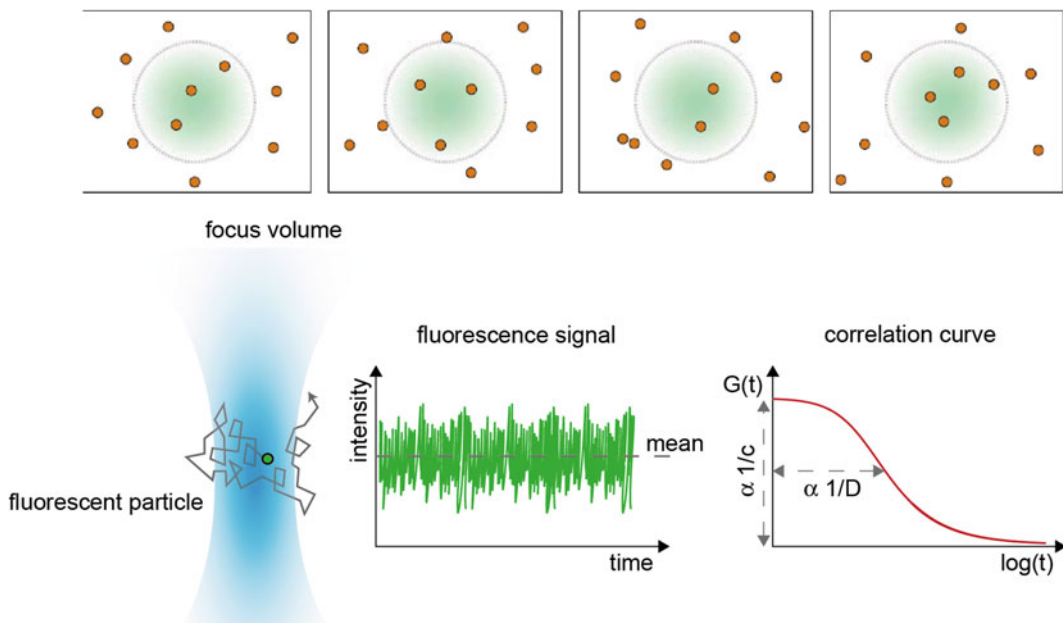


Fig. 5.7 FCS Principle: In FCS, fluorescence fluctuations occur as the result of a small number of molecules diffusing in and out of the observation area defined by the laser spot/focus volume. These fluctuations can be analyzed by calculating so-called correlation curves. The

molecules' diffusion coefficient is inversely proportional to the width of the correlation curve and the concentration inversely proportional to the amplitude. *Source* Marguet et al. (2006)

Fig. 5.8 Principle of FRET. **a** Energy transitions and transfers in donor and acceptor molecules. **b** Study of protein-protein interaction using FRET technique. When Z-CFP and Y-YFP proteins do not interact, illumination with cyan (~430 nm) light results in stronger CFP fluorescence (left). As a result of closer interactions between Z and Y, CFP and YFP are brought into proximity and excitation energy is transferred, resulting in stronger YFP fluorescence (right)

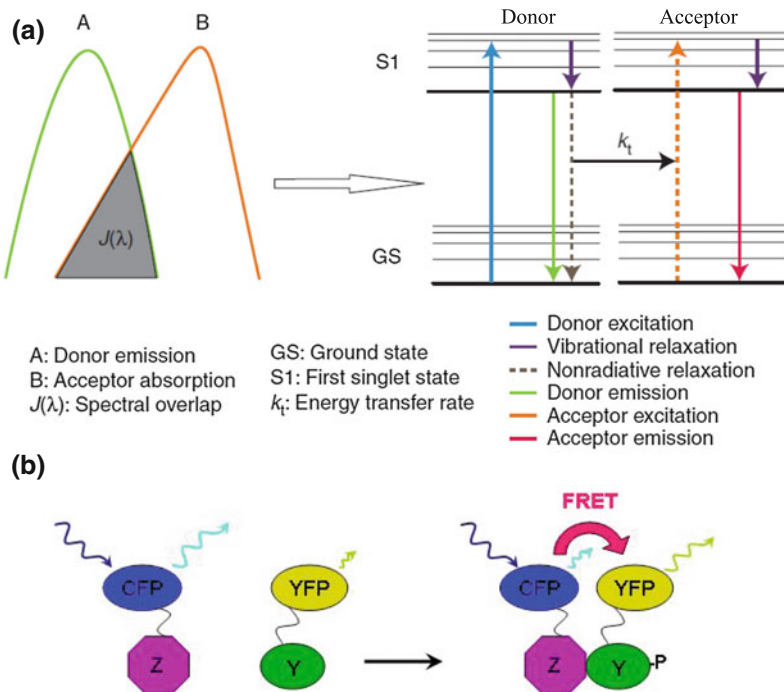


Table 5.2 SPT fitting models

Type of diffusion	Model
3D free diffusion	$6Dt$
3D anomalous subdiffusion	$6Dt^\alpha$
3D diffusion with directed motion	$6Dt + (Vt)^2$
2D free diffusion	$4Dt$
2D anomalous subdiffusion	$4Dt^\alpha$
2D diffusion with directed motion	$4Dt + (Vt)^2$
2D corralled motion	$r(1 - A_1 e^{(4A_2Dt/r)})$

Source Sezgin and Schwille (2011)

absorption and emission spectrum. These variants of GFP include cyan, blue, and yellow fluorescent proteins (CFP, BFP, and YFP). Two variants, whose emission and absorption spectrum overlap but have with distinctively different colored fluorescence emission, such as GFP-RFP, CFP-YFP, or BFP-GFP, are genetically fused with neighboring molecules. FRET technique can be used to study protein–protein interactions in membrane-associated processes in vivo, such as signal transduction and coupled enzymatic reactions (Fig. 5.8b). As the efficiency of resonance energy transfer decreases with the increase in distance between the donor and the acceptor molecule, FRET will be observed only when the two molecules are very close to each other (<10 nm apart).

5.4.6 Single-Particle Tracking (SPT)

SPT technique introduced for the first time by Barak and Webb in 1980s tracks the motion of a single molecule over a period of time in membrane medium. With time-lapse imaging and computer-enhanced videography, the trajectory path of the molecular movement is recorded and analyzed according to the diffusion theory. To analyze the trajectories, the mean square displacement (MSD) which is the average distance that the molecule travels during the lag time, given by the equation below is calculated.

$$\text{MSD}(\tau) = \left\langle (x(t) - x(t + \tau))^2 + (y(t) - y(t + \tau))^2 + (z(t) - z(t + \tau))^2 \right\rangle,$$

where x , y , and z are the coordinates of the molecules, t is the lag time, and $\langle \rangle$ represents the temporal averaging. The MSD can be correlated to the mobility of the molecule in the medium. The trajectory algorithm has been created to investigate molecular diffusion in different conditions (Table 5.2) such as free diffusion, diffusion in confined domains and diffusion with directed motion. In natural membranes, the diffusion of both lipids and proteins is restricted but different types of barriers and associations. The molecular motion is confined to these domains. In contrast, free diffusion is observed in synthetic liposomes and vesicles.

5.4.7 Techniques to Study Rotational Motion in Membranes

5.4.7.1 Fluorescence Anisotropy (Polarization)

Fluorescence anisotropy is an important phenomenon that can be exploited to monitor rotational diffusion of the molecules by using the polarization of light.

The fluorescent-labeled molecule on excitation with plane-polarized light emits polarized light in a fixed plane if the molecules are stationary during the excitation of the fluorophore. However, as molecules rotate, the plane of the polarized light emitted is different from the plane of polarized light used for initial excitation. The emitted light is then said to be “depolarized” (Fig. 5.9).

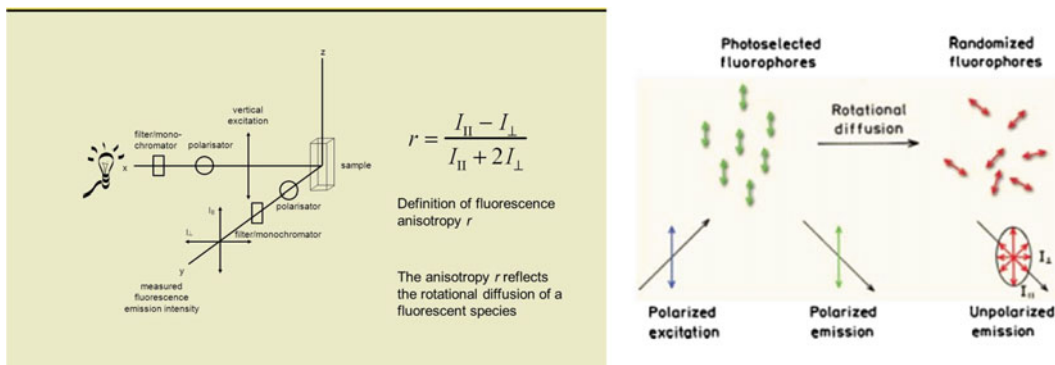


Fig. 5.9 Fluorescence anisotropy: the sample containing the fluorescent probe is excited with linear plane polarized light and the vertical (\parallel) and horizontal (\perp) components of the intensity of the emitted light are measured and the

degree of polarization (P) or anisotropy (r) are determined. Molecules showing rotational motion result in depolarization

Polarization (P) is defined as:

$$P = \frac{I_{\parallel} - I_{\perp}}{I_{\parallel} + I_{\perp}}$$

where I_{\parallel} is the fluorescence emission intensity parallel to the excitation plane and I_{\perp} is the fluorescence intensity perpendicular to the excitation plane. If the emission is completely maintained in the parallel direction, then $P = +1$. If the emitted light is totally polarized in the perpendicular direction, then $P = -1$. In the actual measurement of polarization, there is usually an angle between the excitation dipole and the emission dipole within a molecule. For example, even a fixed, nonrotating fluorophore has some “intrinsic” depolarization. The degree of polarization of emission can also be described in terms of the anisotropy (r), which is given by:

$$r = \frac{I_{\parallel} - I_{\perp}}{I_{\parallel} + 2I_{\perp}}$$

Polarization and anisotropy are interchangeable quantities and only differ in their normalization. Polarization P ranges from -0.33 to $+0.5$, whereas the range for anisotropy r is -0.25 to $+0.4$.

$$P = 3r/2 + r$$

$$r = 2P/3 - P$$

If a molecule in the membrane is restricted due to its association with another big molecule/complex, its rotation is slowed so that the emitted light is in the same plane as the plane-polarized light of excitation. Though both the bound and unbound states of the molecule have an intrinsic polarization value, a high polarized value is observed for the bound state and a low (depolarized) value for the unbound, relatively free state. Thus, fluorescence polarization measurements are also used to study the interactions between molecules to form large complexes.

5.4.8 Techniques to Study Transbilayer Motion in Membranes

Transverse or flip-flop diffusion in membranes can be investigated by electron spin resonance (ESR) or chemical labeling techniques.

5.4.8.1 Electron Spin Resonance (ESR)

ESR spectroscopy is based on the presence of unpaired electrons in molecular species. When molecules with unpaired electrons are exposed to a magnetic field, the electronic energy levels of the molecule are split into different levels. The molecule can be excited from one split level to

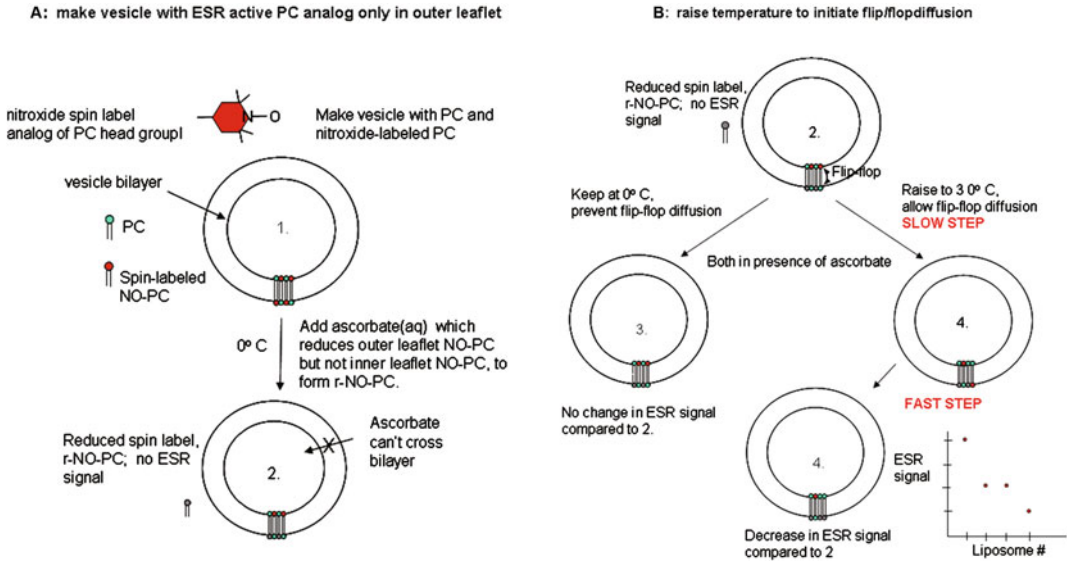


Fig. 5.10 Flip-flop diffusion in liposomes. **a** Make vesicle with ESR active PC analog only in outer leaflet. **b** Raising the temperature to initiate flip-flop diffusion

another on absorption of microwave radiation of frequency corresponding to the difference in energy of the split levels. Such an excitation is called electron magnetic resonance absorption. The ESR absorption signal can be influenced by the local environment and the molecular interactions.

ESR has developed as a very sensitive technique to study membrane dynamics. Spin labels such as **nitroxyl group** can be attached to membrane lipids or proteins to make them ESR sensitive and then monitored. For example, liposomes synthesized with a mixture of lipids, nitroxide spin-labeled and nonlabeled lipids (PC), can be used for the determination of rate of transbilayer diffusion. Both inner and outer leaflets of the membrane have spin-labeled PC. After determination of initial ESR signal, ascorbic acid is used to reduce ESR label in the outer leaflet of the membrane. Rate of regain of ESR signal in the outer leaflet can be monitored with time (Fig. 5.10).

Similar studies can be performed to study protein-protein interactions and mobility.

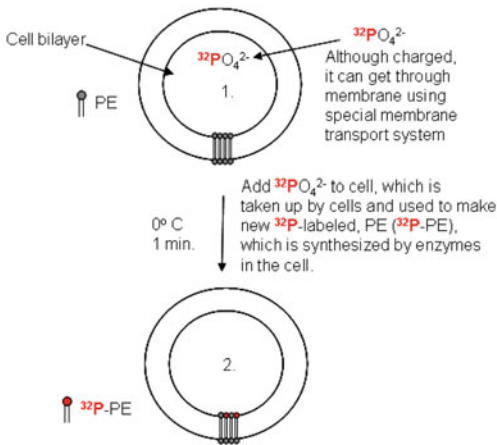
5.4.8.2 Chemical Labeling

Fluorescent or radiolabeled tags can be attached to lipids and proteins and transbilayer movement can be studied.

For example, in bacteria, addition of radiolabeled ^{32}P leads to the labeling of newly synthesized phospholipid (PL) in the inner leaflet of the plasma membrane (Fig. 5.11). At different time interval, the bacteria is exposed to a fluorescent label, for example, trinitrobenzene sulfate (TNBS), which will label only PE in the outer leaflet. Rate of generation of lipids with double labels (TNB and ^{32}P) can be monitored, quantitating transbilayer movement of ^{32}P -labeled phospholipids from inner leaflet to the outer leaflet.

Similar experiments can be done with artificial membranes to compare transbilayer movement of

(a) FLIP-FLOP DIFFUSION IN BACTERIAL CELLS
make cell with ^{32}P -labeled PE only in inner leaflet



(b) FLIP-FLOP DIFFUSION IN BACTERIAL CELLS
Add TNBS as "reporter" label with various times of incubation

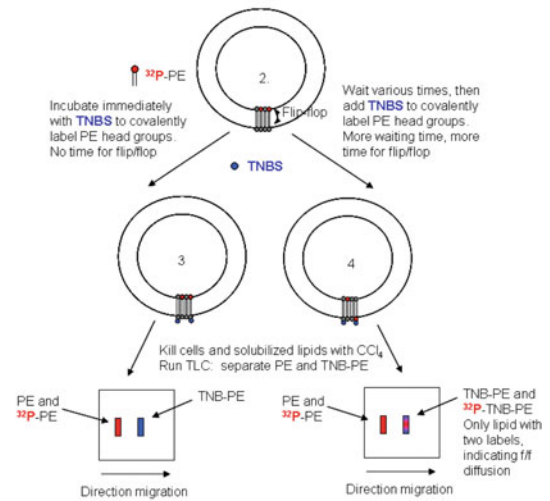


Fig. 5.11 Flip-flop diffusion in bacterial cells. **a** Labeling inner leaflet phospholipids with ^{32}P . **b** Labeling cells in (a) with TNBS to detect flip-flop

different lipids using **phospholipid exchange proteins or flippases** to facilitate transbilayer movement of lipids.

demarcated by different types of physical barriers or may be created due to association of lipid and proteins of specific composition distinct from the remaining bulk membrane.

5.5 Barriers Affecting Lateral Diffusion of Molecules in Membranes

The fluid mosaic model is still relevant after more than forty-five years in describing the basic structure and a variety of functions of biological membranes. Yet, it is unable to explain lateral heterogeneities in the plane of the membrane and confinement of membrane components in compartments or domains. The diffusion rates of lipids and proteins in liposomes are many times higher than the rates observed in biological membranes of similar composition. The free diffusion of membrane proteins and/or lipids in the plane of the bilayer is restricted by the presence of different types of physical barriers or due to molecular interactions.

Biological membranes are compartmentalized into specialized functional domains of distinct composition, which can be transient or persist for the entire life of the cell. These domains may be

5.5.1 Physical Barriers

Physical barriers are created by relatively immobile membrane components that can obstruct the free passage of membrane proteins or lipids. Such barriers can form transiently or form permanent structures in cells. The major physical barriers include the cytoskeleton, membrane–membrane junctions, intramembrane clusters (Fig. 5.12).

5.5.2 The Cytoskeleton

The entire cytoplasmic face of the plasma membrane is lined by a meshwork of the actin-based cytoskeleton, and the cytoskeleton closely interacts with the membrane proteins exposed on the cytoplasmic side of the membrane (Fig. 5.12a). Actin-based mesh of cytoskeleton is present in virtually every eukaryotic cell, constitutes a

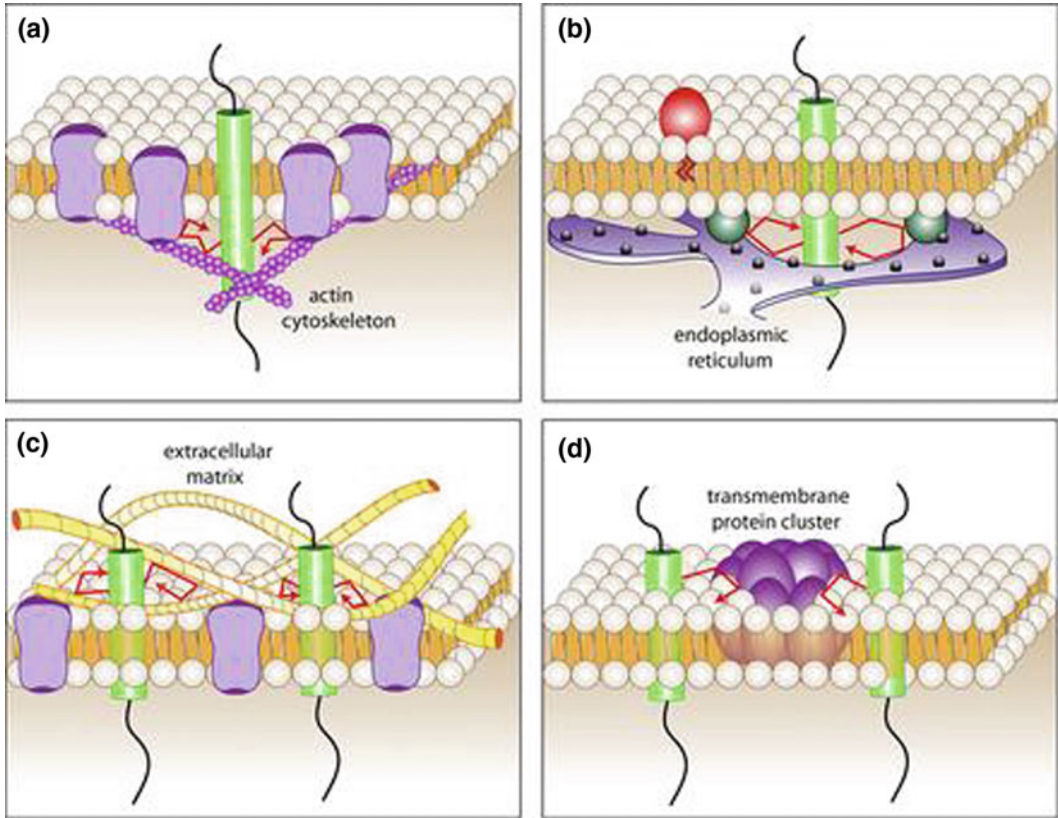


Fig. 5.12 Physical barriers to the diffusion of membrane lipids or proteins. **a** The mesh formed by the cortical actin cytoskeleton serves to underpin a picket fence composed of transmembrane proteins and tightly associated lipids. **b** Regions of intimate contact between two organellar membranes can block the diffusion of molecules along the membrane of either organelle. A site of contact between the ER and the plasma membrane is illustrated as an example. Proteins that bridge the plasma membrane with

the reticulum are shown as blue-green spheres. **c** Linkage of extracellular matrix components (yellow fibers) to membrane receptors can generate a mesh that impedes the diffusion of other membrane molecules. **d** Large, poorly mobile clusters of membrane proteins and lipids can block the passage of diffusing components. Freely mobile transmembrane proteins are illustrated by the green cylinder. Its trajectory is shown by the red arrows. *Source* Trimble and Grinstein (2015) (Color figure online)

variety of proteins which are cell-type specific and also vary between different regions of a cell. A variety of proteins support the actin-rich mesh, the most prominent being, spectrin, ankyrin, Band 4.1, and adducin. The membrane protein domains exposed to the cytoplasmic side interact with actin mesh and the associated proteins to form a fence-like barrier.

High-speed single-particle-tracking techniques have shown that molecules diffuse only within the confines of such fence demarcated area. Based on these observations, Kusumi and

colleagues proposed **the fence-and-picket model**, with the cytoskeletal meshwork forming the fences and transmembrane proteins anchored to the cytoskeleton forming the pickets (Fig. 5.13). SPT shows the zigzag trajectories of membrane molecules within the cytoskeleton fenced compartment termed corrals.

Membrane components have been observed to **hop** between adjacent corrals. This could be attributed to the dynamic nature of actin cytoskeleton which undergoes considerable amount of remodeling. The disruption of actin

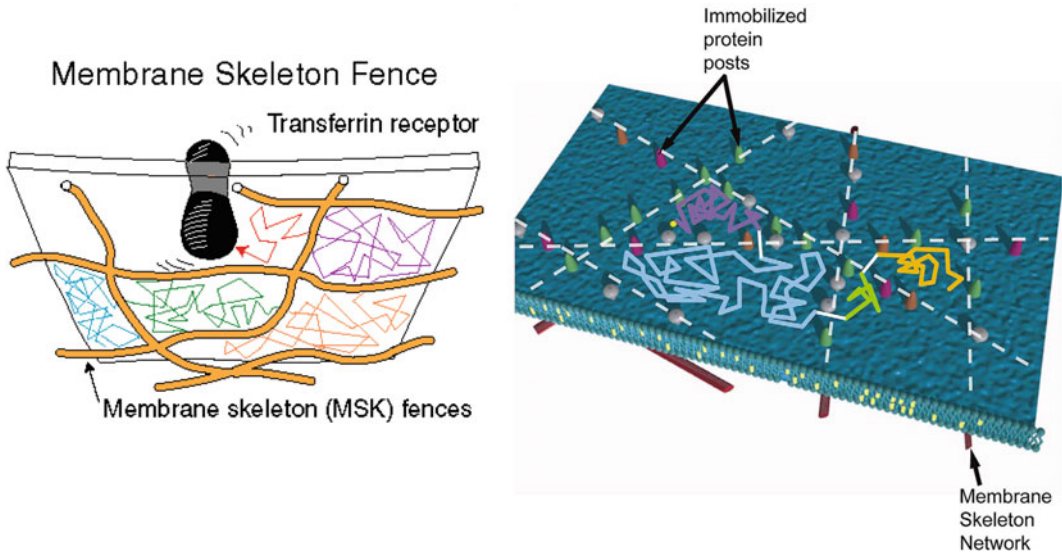


Fig. 5.13 Fence-and-picket model. Lipid/protein diffusion in membranes is compartmentalized, owing to the fraction of transmembrane protein immobilized through binding to the underlying membrane skeleton network.

cytoskeleton dramatically impacts the diffusion of molecules in membranes. Diffusion rates in cytoskeleton deficient membranes are comparable to that in liposomes.

5.5.3 Membrane–Membrane Junctions

Membrane structures like the tight junctions (Fig. 5.14), adherens junctions, and other relatively immobile structures create larger domains of ~ 2 to 300 nm mesoscale, generating impenetrable barriers. The tight junctions also define the polarity of the membrane, demarcating the apical and basolateral domains. The apical and basolateral domains of the membrane have distinct lipid and protein composition, which is maintained throughout the life span of the cell.

5.5.4 Membrane–Matrix Junctions

Membrane components can also be immobilized by latching onto the extracellular matrix

This interaction induces temporal confinement or corraling of transmembrane proteins and membrane lipids into the membrane skeleton mesh. *Source* Fujiwara et al. (2002), Ritchie et al. (2003)

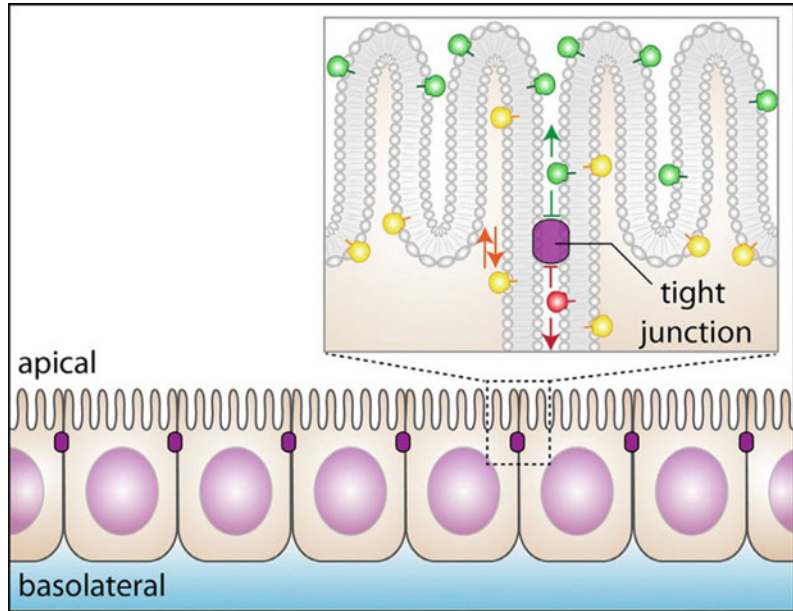
(Fig. 5.12c). Integrins and other receptors bind tightly to matrix components and, if accumulated at sufficiently high densities, could restrict the diffusion of other, more mobile molecules.

5.5.5 Intramembranous Clusters

Relatively short-lived small nanodomains (less than 50 nm in diameters) are formed by passive association of lipids and/or proteins. These include **protein clusters, lipid rafts, caveolae, and clathrin-coated pits**.

Large **clusters of membrane proteins** (Fig. 5.12d) can restrict the mobility of diffusible components. For example, the big protein complexes of electron transport chain of inner membrane of mitochondria render the neighboring membrane lipids and proteins immobile as a result of electrostatic or hydrophobic interactions. Specific lipids or proteins can preferentially associate (partition) with defined regions or components of the membrane, resulting in a decrease in their diffusion rates. The free diffusion of membrane-associated molecules can be

Fig. 5.14 Epithelial tight junctions, are diffusional barriers, occlude the passage of outer leaflet (exofacial) lipids from the apical membrane domain to the basolateral domain. *Source* Trimble and Grinstein (2015)



impeded by collisions with physical obstacles and also by electrostatic interactions. The association of protein PH domains with phosphoinositides or the recognition of phosphotyrosine moieties by SH2 domains typifies this kind of interaction. The multiple PtdIns(4,5)P₂ molecules attracted to electrostatic basin generated by the membrane-associated cationic residues create a negatively charged ring around the protein. These small electrostatic islands thus generated will attract opposite charged molecules and repel similar charged molecules (Fig. 5.16a).

Membrane rafts are defined as dynamic nanoscale cholesterol, sphingolipid-enriched, ordered assemblies of specific proteins, stabilized by specific lipid–lipid, protein–lipid, and protein–protein interactions (see Chap. 4). These saturated lipid- and cholesterol-rich, detergent-resistant microdomains called “rafts” are perhaps the best known example of hydrophobic partitioning (Fig. 5.15b).

Rafts can act as a signaling platform, recruiting signaling proteins to the raft microenvironment facilitating their interaction. Receptors, coupling factors, effector enzymes, and substrates involved in signaling pathway activated

by a hormone would be colocalized in a single raft, for rapid and efficient signal transduction. Enzymes and proteins with opposing effect, for example, kinases and phosphatases could be restricted in separate rafts, fine tuning the regulation of the pathway.

The signaling processes convincingly shown to involve lipid rafts are immunoglobulin E (IgE) signaling and T-cell antigen receptor (TCR) signaling (Fig. 5.16). IgE signaling pathway is activated when F_c segment of IgE binds to receptors (FcεRI) residing in the plasma membrane of mast cells and basophils. The receptor is activated on binding of oligomeric antigens to receptor-bound IgE. Cross-linking of FcεRI by oligomeric antigens stimulate the signaling pathways, ultimately leading to release of mediators of allergic response. FcεRI cross-linking increases the raft affinity of FcεRI, leading to receptor partitioning in rafts. This could lead to increased phosphorylation by raft-associated kinases (Lyn kinase), resulting in further amplification of signal. Receptor cross-linking of TCR receptor also increases its raft residency resulting in phosphorylation of the receptors’ immune receptor tyrosine-based activation motifs (ITAMs) by

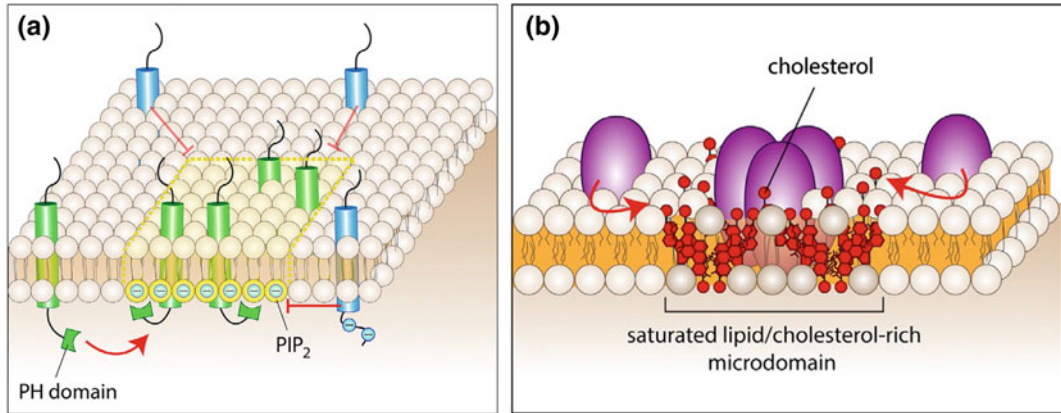


Fig. 5.15 Intramembranous clusters as membrane barriers. **a** Electrostatic impediments: the negative charge of PtdIns(4,5)P₂ (PIP₂) defects proteins with a negatively

charged cytosolic domain. **b** Hydrophobic partitioning occurs in cholesterol-rich rafts. *Source* Trimble and Grinstein (2015)

Src-family protein tyrosine kinases (for example, Lyn, Lck, and Fyn), thereby transducing TCR signaling pathway.

Caveolae, a special type of raft (see Chap. 4), are defined as smooth invaginations (50–100 nm) of the plasma membrane devoid of clathrin coat (Fig. 4.8b).

Caveolins are a family of integral membrane proteins that form the principal membrane components of caveolae (see Chap. 4). The oligomerization of Caveolins leads to formation of caveolin-rich microdomains in the plasma membrane (Fig. 4.8b). Increased levels of cholesterol and association of scaffolding domain of caveolins with the plasma membrane initiates the formation of the caveolar invagination leading to the formation of endocytic vesicle. The ligands of caveolar endocytosis include the bacterial cholera toxin and the nonenveloped virus SV40, both of which bind to the ganglioside GM1 that is enriched in caveolae. Proteins associated with caveolae have been implicated to be involved in cholesterol and lipid metabolism, mechanosensation, and cellular signaling.

5.6 Polarized Cells

Cell polarity exists in some cells in which the cell is organized into distinct domains with specific structure, composition, and function. Epithelial

cells, neurons, and hepatocytes are some of the cells which show cell polarity.

5.6.1 Epithelial Cell

Epithelial cells form sheets that line the exterior surface and interior cavities of our bodies, forming a protective covering separating the body from its external environment. Some of the major organs, such as kidneys, lung, mammary gland, and GI tract, contain ducts or tubules with inner cavities which are lined by epithelial cells. Hence, the epithelial cell surface is exposed to different environments performing different functions. To achieve their specific functions, epithelial cell membrane is demarcated into structurally and functionally distinct domains. For example, the apical domain is exposed to the cavity lumen and is therefore involved in the exchange of nutrients, waste, and gases with the lumen, the lateral domain is in contact with neighboring cells, therefore involved in cell–cell interaction and communication, and the basolateral domain associated with extracellular matrix is involved in the exchange of waste, and nutrients with the interstitial fluid.

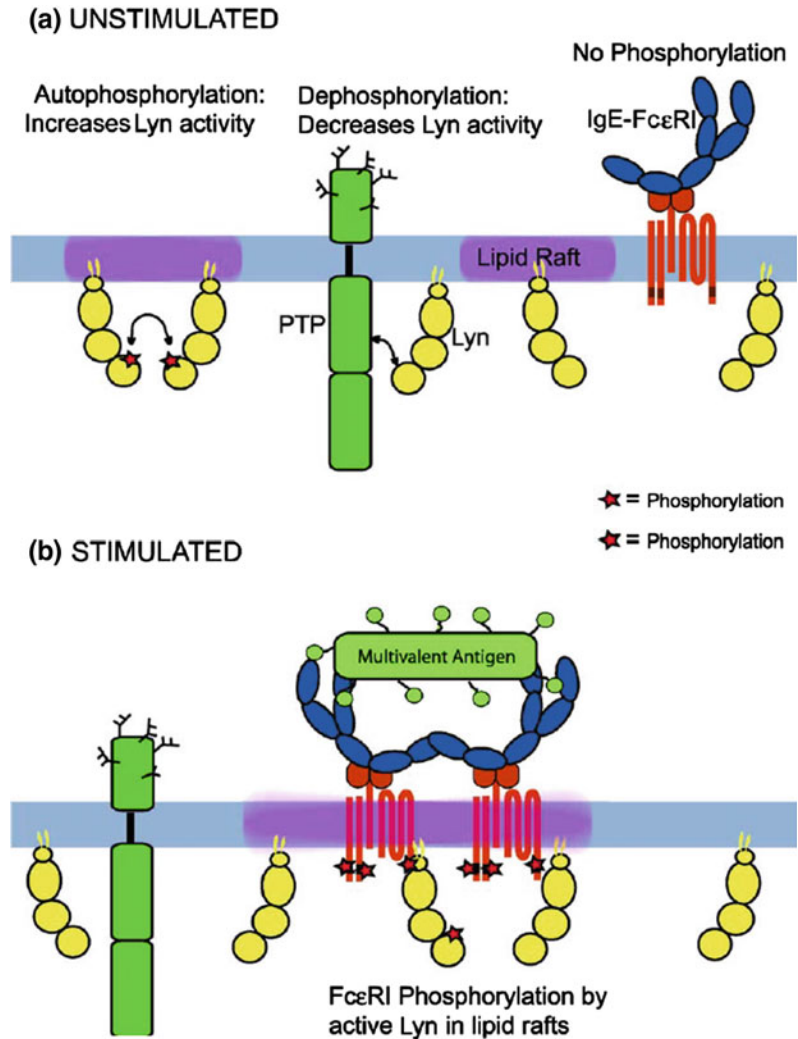
Each domain has distinct lipid and protein composition to perform specific functions. The epithelial polarity is maintained by apical junctional complex (AJC), which demarcates the

Fig. 5.16 Graphic representation of protein segregation by lipid rafts that is relevant to IgE receptor signal initiation.

a Distributions of relevant membrane components in unstimulated cells.

b Distributions of relevant components following signal initiation by antigen-mediated IgE receptor cross-linking.

Source: Alonso and Milan (2001)



domains (Fig. 5.17). The apical junctional complex (AJC) includes the tight junctions (also named zonula occludens) and adherens junctions (or zonula adherens). The tight junctions form a tight seal that prevents the diffusion of lipids and proteins between apical and lateral surfaces, thereby ensuring domain identity. Basal to the tight junctions, adherens junctions form an adhesive belt that encircles each epithelial cell just underneath the apical surface, adhering adjacent epithelial cells.

The unique composition of apical, lateral, and basolateral membrane domains is initially established by the vesicle-trafficking machinery. The

oriented vesicle-trafficking pathways specifically segregate proteins and lipids into the domain in which they are required. The biosynthetic sorting initiated in the *trans*-Golgi network (TGN) and then selective recycling/transcytosis to transport proteins to the correct surface. Specific sorting and targeting motifs target proteins either to the apical or to the basolateral membranes.

5.6.2 Neuron

Neuron is compartmentalized into distinct domains, such as the dendrites, the cell body, the

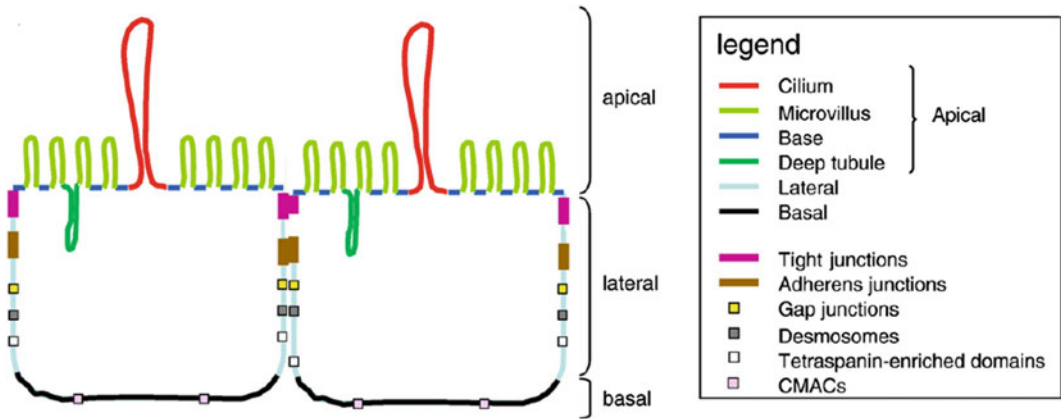


Fig. 5.17 Cartoon depicting the different plasma membrane domains in epithelial cells. *Source* Ben et al. (2009)

axon hillock, the axon, and the axon terminal. Each domain has a specific structure and function, for example, signals are received at the postsynaptic dendrites, from where it is passed on through the cell body to trigger an action potential at the axon hillock and then propagated further along the axon to the axon terminal. At their terminals, the electrical signal is reconverted into a chemical signal by the release of neurotransmitter-containing synaptic vesicles. The cell body compartment localizes most cell organelle, such as the nucleus, mitochondria, ER, and the Golgi bodies. The axon initial segment (AIS) or the axon hillock is a short region of the axon adjacent to the cell body where the action potential is initiated. It is enriched in voltage-gated ion channels, cell adhesion molecules, and cytoskeletal scaffolding proteins. Furthermore, AIS is highly enriched in actin, which associates with AnkyrinG (ankG), and β IV spectrin to form a polymerized complex. The resulting cytoskeletal complex and the AIS membrane-associated proteins form a membrane barrier and cytoplasmic barrier demarcating the somatodendritic and axon domain. Neurons maintain their polarity throughout life (Fig. 5.18).

Neuron initially is a round sphere, during development, lamellipodium (cellular protrusions that contain branched actin filaments) sprout around the cell body. These round spheres later transform into cells containing several neurites,

which have dynamic growth cones at their tips. One of these neurites then grows rapidly to become the axon, and remaining neurites develop into dendrites. Neurons thus develop polarity (Fig. 5.19).

The actin cytoskeleton and microtubules play a crucial role in the establishment and maintenance of polarity in neurons. A variety of extrinsic and intrinsic signaling pathways converge to regulate actin and microtubule dynamics (Fig. 5.20). The highly motile, axonal growth cone is composed of a central region filled with organelles and microtubules and a highly dynamic, actin-rich peripheral region containing lamellipodia and filopodia. The cytoskeleton also regulates the selective trafficking and segregation of cellular components in somatodendritic or axonal compartments.

5.7 Organization of the Erythrocyte Membrane

Red blood cells are unique nonnucleated disc-shaped cells, which can undergo large reversible deformations while passing through the narrow capillaries with cross-sectional area one-third its own diameter, throughout its 120-day life span. Hence, the red cell membrane has to maintain its structural integrity withstanding fluid stresses and cell deformations. The mechanical strength, flexibility, and elasticity of

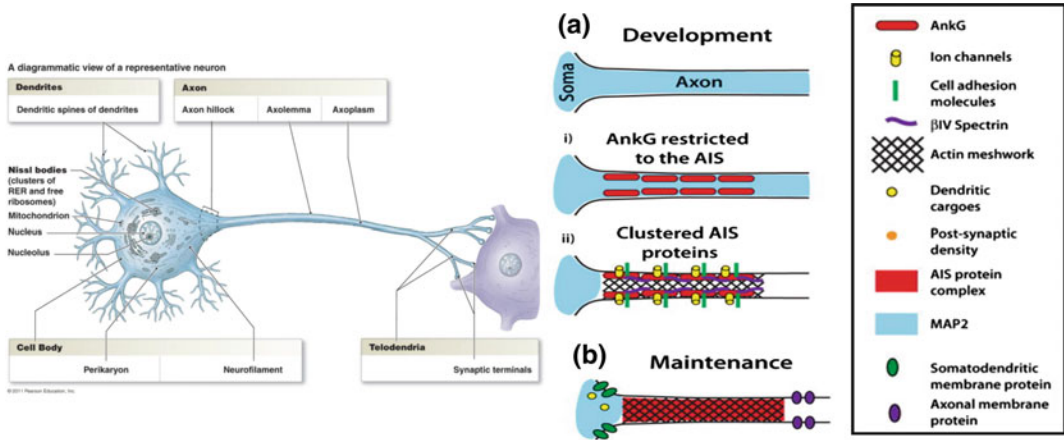


Fig. 5.18 Polarity in neuronal membrane. **a** During early development, neurons become polarized with an axon and somatodendritic domain. This is accompanied by the redistribution of proteins into distinct cellular compartments. After axon specification, ankG becomes restricted to the AIS (i), where it functions as a scaffold to which

many other AIS proteins become attached (ii). Upon assembly of the AIS, MAP2 (blue) becomes excluded from the distal axon. **b** Actin, and ankyrinG play key roles in maintaining neuronal polarity and restricting membrane proteins to either axonal or somatodendritic domains. *Source* Ho and Rasband (2011) (Color figure online)

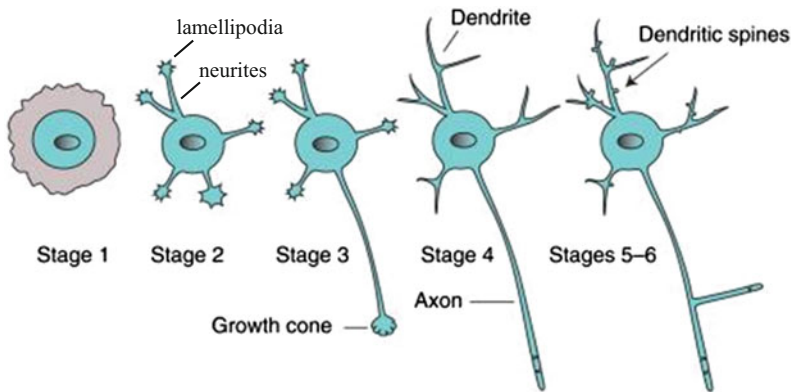


Fig. 5.19 Neuronal polarization in cultured neurons. Hippocampal neurons transform from round cells bearing lamellipodia (Stage 1) into multipolar cells (Stage 2). One neurite enlarges its growth cone and extends rapidly to become the axon (Stage 3). The remaining shorter

neurites will develop into dendrites (Stage 4). This is followed by functional maturation and formation of dendritic spines and synapses (Stages 5–6). *Source* Tahirovic and Bradke (2009)

the red cell membrane are provided by the lipid bilayer capable of resisting bending, and an underlying cytoskeleton network tethered to the cytoplasmic domains of transmembrane proteins embedded in the membrane bilayer. Several skeletal proteins also directly interact with the anionic phospholipids, which present on the cytoplasmic leaflet providing additional binding

sites for the skeletal network to attach to the lipid bilayer (Fig. 5.21a).

5.7.1 Membrane Proteins

The red cell membrane proteins are the most extensively studied membrane proteins as the

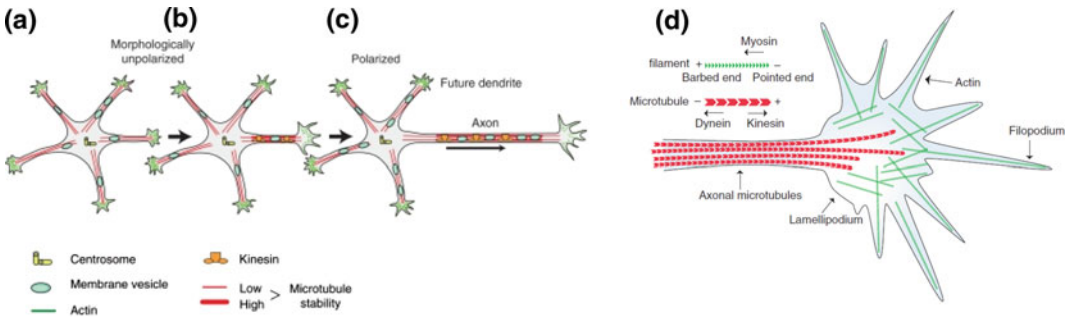


Fig. 5.20 Intracellular mechanisms driving neuronal polarization. Morphologically unpolarized neurons bear several equal neuronal processes. **a** In one of the neurites leads to axon formation. **b** This neurite starts elongating rapidly and a morphologically polarized neuron bearing an axon is formed. **c** Other neurites develop into dendrites.

d Illustration of an axonal growth cone. Microtubules (red) distributed along the axonal shaft protrude into the central region of the growth cone. The growth cone is enriched in F-actin (green) that is organized into long bundles forming filamentous lamellipodia. *Source* Tahirovic and Bradke (2009) (Color figure online)

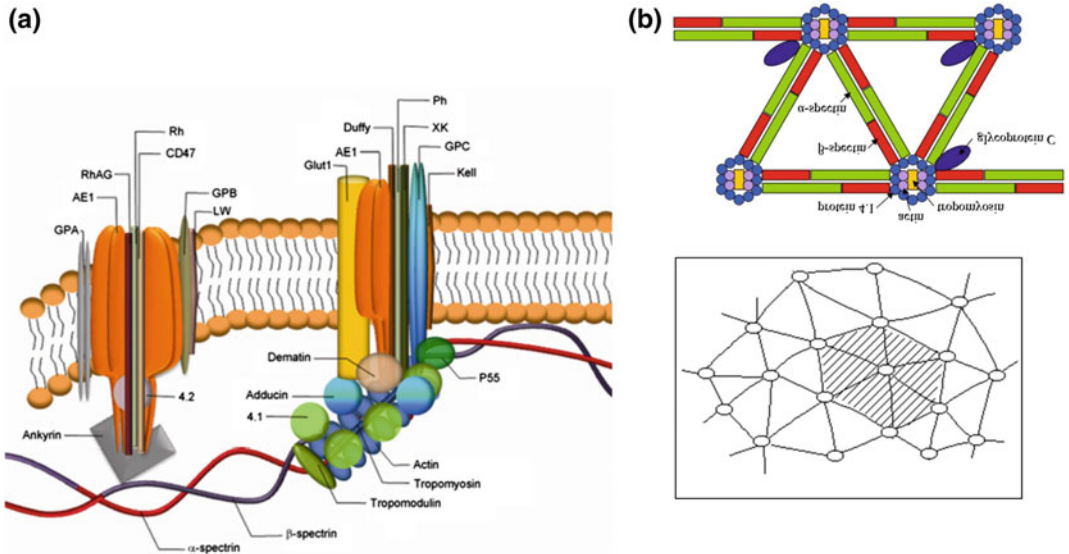


Fig. 5.21 a RBC plasma membrane protein–cytoskeleton interactions. Ankyrin mediates the interactions between spectrin and other transmembrane proteins, such as AE1 and the Rh complex fixed on the spectrin-based skeleton through their interactions with ankyrin. AE1 anion exchanger; GPA glycoprotein A; GPB glycoprotein B; GPC glycoprotein C; Glut 1 glucose transporter 1; Rh

rhesus factor; RhAG Rh-associated glycoprotein. **b** The α - β dimers of spectrin associate head to head to form 200-nm-long tetramers. The ends of spectrin tetramer associate with actin filaments to form junctional complexes leading to the formation of the hexagonal mesh. *Source* Zhang et al. (2013) and Luna and Hitt (1991)

RBC lacks contaminating internal organelle membranes. They can be categorized into integral membrane proteins which include the transporters, receptors, and adhesion proteins, and the membrane-associated peripheral proteins,

which form the two-dimensional membrane skeletal network.

The earliest RBC membrane protein separation and characterization was done by SDS-PAGE electrophoresis of hemoglobin-free

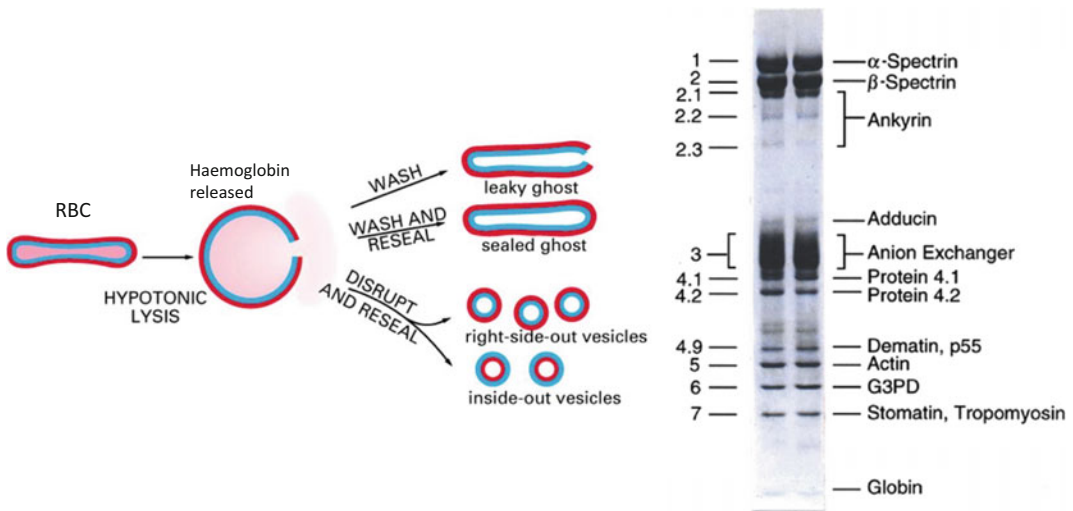


Fig. 5.22 Preparation of ghost cells and SDS-PAGE pattern of RBC membrane proteins

erythrocyte ghost cells. The ghost cells were prepared by hypotonic washing of RBC, which lyses the erythrocytes and releases hemoglobin and other cytosolic proteins. The proteins were named as Band 1, 2, 3... based on the sequence in which they appeared after separation in SDS-PAGE gels (Fig. 5.22). RBC membrane proteins have been found to be deficient in many disease conditions including hereditary spherocytosis, paroxysmal nocturnal hemoglobinuria, and hereditary stomatocytosis.

5.7.2 Integral Membrane Proteins

Band 3 (the anion exchanger), aquaporin-1 (the water channel), and glycophorins are the most abundant integral membrane proteins. More than 50 integral membrane proteins of RBC have been characterized. These transmembrane proteins show diverse structural and functional heterogeneity.

1. **Band 3 protein:** The anion exchanger (AE1), known as the Band 3 protein, a major integral membrane protein, mediates the exchange of the cellular HCO_3^- with Cl^- in plasma. It constitutes around 25% of the total RBC membrane protein. It exists as a homo-dimer or a homo-tetramer in the membrane. Band 3

is the product of a gene in chromosome 17 that encodes a 911-amino acid protein.

Band 3 is composed of three structurally and functionally distinct domains. The hydrophilic N-terminal, cytoplasmic domain (residues 1 to 403) interacts with a variety of peripheral cytoskeleton proteins such as ankyrin, and cytoplasmic proteins and enzymes including, hemoglobin. The hydrophobic multi-spanning transmembrane domain (residues 404 to 882) forms the anion transport channel. The C-terminal domain (residues 883 to 911) interacts with cytosolic proteins such as, carbonic anhydrase and hemoglobin.

Band 3 protein simultaneously performs two important functions. As an anion transporter exchanging $\text{HCO}_3^-/\text{Cl}^-$, it plays a critical role in CO_2 transport and pH regulation in blood, and interacting with cytoskeletal proteins, it anchors the cytoskeleton to the membrane, provides mechanical strength, and maintains the biconcave shape of the cell. The Band 3 proteins also have N-glycosidically linked oligosaccharide chains which possess the blood group antigens of the Diego group.

Targeted mutagenesis to generate RBCs without Band 3 results in spherocytosis and hemolysis with progressive loss of RBC membrane but no change in the skeletal architecture.

2. **Glycophorins:** Glycophorins are sialoglycoproteins, which contain multiple *O*-linked oligosacchride chains with sialic acid linked to serine or threonine residue and a few asparagine N-linked oligosaccharide chains. The presence of high content of sialic acid in glycophorins identifies them in SDS-PAGE gels by staining with periodic acid-Schiff (PAS) reagent. Four glycophorin proteins GPA, GPB, GPC, and GPD identified in RBC membrane comprise ~2% of the total red cell membrane proteins. GPA and GPB have arisen from a common ancestral gene and show considerable sequence homology. GPC and GPD are encoded by the same gene through the use of different translation initiation sites, residing on chromosome 2 and are distinctly different from GPA and GPB, which are the product of genes on chromosome 4.

Glycophorins consist of three domains: a highly hydrophilic, N-terminal extracellular domain, which is heavily glycosylated, a 20–34 residue single α helical membrane-spanning hydrophobic domain, and a C-terminal cytoplasmic domain. The presence of high content of sialic acid in the extracellular domain of glycophorins imparts a strong net negative charge to the cell surface; this is functionally important in reducing the interaction of red cells with one another and with other cells in the circulation. Glycophorins also carry blood group antigens of the MNS group.

3. **Rh blood group antigens:** In contrast to other blood group antigens such as ABO, MNS, and Diego which are carbohydrates, the Rh blood group antigens are proteins. Rh blood group antigens are coded by highly polymorphic genes. Two closely linked genes, RHD and RHCE, undergo numerous genetic rearrangements between them to produce a variety of distinct Rh antigens. The RhD and RhCE proteins are both multipass transmembrane proteins which are also palmitoylated and expressed only in RBC. They are closely associated with a RBC membrane glycoprotein, RhAG. Together, they are present as Rh-RhAG complex which might also be

involved in transporting ammonium or carbon dioxide.

Apart from Band 3 protein RBC membrane is associated with many other transport proteins which include aquaporin 1 (water transporter), Glut1 (glucose transporter), $\text{Na}^+\text{-K}^+\text{-ATPase}$, $\text{Ca}^{2+}\text{ATPase}$, and $\text{Na}^+\text{-K}^+\text{-2Cl}^-$ cotransporter. RBC membrane also has adhesive proteins such as ICAM-4, which interacts with integrins and the laminin-binding protein.

5.7.3 Peripheral Membrane Proteins

Several proteins involved in the formation of filamentous cytoskeleton network underlying the lipid bilayer are anchored to the bilayer via interactions with several integral proteins (Fig. 5.21). This two-dimensional network is largely responsible for membrane elasticity and membrane mechanical stability of the red cell. It also gives the RBC its biconcave shape. The major components of cytoskeleton include spectrin, Band 4.1, Band 4.2, ankyrin, actin, adducin, tropomyosin, and tropomodulin.

1. **Spectrin:** SDS-PAGE separation of RBC membrane proteins from erythrocyte ghost revealed Band 1 and 2 proteins on the gels which represented α spectrin and β spectrin. Spectrin protein is composed of two non-identical subunits, α spectrin and β spectrin that are intertwined side to side in anti-parallel arrangement to form flexible, rod-like molecule. These α - β dimers of spectrin associate head to head to form 200-nm-long tetramers. The ends of spectrin tetramer associate with actin filaments to form junctional complexes leading to the formation of the hexagonal mesh (Fig. 5.21b).

There are two α spectrin proteins, αI and αII encoded by genes, SPTA1 and SPTAN1, and five β spectrin proteins, βI to V , encoded by SPTB, SPTBN1, SPTBN2, SPTBN4, and SPTBN5 genes.

The spectrin subunits have sequence motifs called “spectrin repeats,” which form a

triple-helix super-coil connected by an α helical linker, thus allowing spectrin the flexibility to expand and contract. Furthermore, spectrin has numerous other structural motifs, including actin-binding domain, pleckstrin homology, and Src homology 3 (SH3) domains which mediate interactions with other cytoskeleton proteins. Near the C terminus of β spectrin is an attachment site for ankyrin, which in turn binds to the cytoplasmic tail of Band 3, and near the N terminus tail is an attachment site for protein 4.1, which in turn associates with glycophorin C. These interactions anchor the cytoskeleton network to the membrane bilayer.

2. **Ankyrin:** Ankyrin or Band 2.1 protein links the spectrin skeletal network to the membrane bilayer by simultaneously associating with β spectrin in the skeleton and Band 3 in the bilayer. In humans, there are three major ankyrin isoforms, ankyrin R, B, and G, encoded by three genes, ANK1, ANK2, and ANK3. Ankyrin R is majorly expressed in erythrocytes, ankyrin B is localized primarily in the brain, and ankyrin G is more broadly expressed.

Ankyrin proteins contain four distinct domains, an N-terminal domain that contains 24 tandem ankyrin repeats (ANK repeats) responsible for binding to Band 3 protein and many other membrane proteins, a central domain that is involved in association with spectrin, a death domain that interacts with proteins involved in apoptosis, and a highly variable C-terminal regulatory domain. The ankyrin repeats are similar in structure to spectrin repeats and provide the flexibility to ankyrin. The central spectrin-binding domain that harbors a ZU5-containing subdomain that is essentially required for β spectrin binding.

3. **Actin:** The RBC cytoskeletal junctional complex on the junction of spectrin tetramers bind to a short actin filament. An actin filament consisting of 15–20 monomers is modulated by the proteins tropomyosin and tropomodulin, which maintains its polymeric state.

The tail ends of the spectrin tetramers are associated with actin filaments. Six spectrin ends complex with one actin filament, creating a network with hexagonal lattice. Each spectrin-actin junction is further stabilized by adapter proteins including, adducin, dematin, and protein 4.1.

5.8 Homeoviscous Adaptation

Various types of environmental factors such as temperature and osmolarity impact the membrane structure and function. Poikilothermic organisms including bacteria, fungi, reptiles, and fish cannot regulate their body temperature and must therefore need adaptive mechanism to maintain optimal membrane fluidity for cells to survive. Cells perceive these changes via sensory proteins embedded in their membranes. These sensory proteins then activate signal transduction pathways to regulate gene expression of enzymes and proteins required for adaptation.

Such adaptive responses are termed as homeoviscous adaptations. Homeoviscous adaptation involves changes in membrane lipid composition in order to maintain cell membrane fluidity required for structural and functional integrity of the cell. Homeoviscous response has also been observed in some warm-blooded organisms with a constant body temperature, for example, the lipid composition in the outer extremities in the arctic reindeer which are exposed to extreme cold, show adaptation to maintain membrane fluidity. The bulk of most membranes are in a lamellar liquid-crystalline L_{α} phase (see Chap. 2). Any lipid phase transition can profoundly affect membrane structure and function. The rates of membrane-associated processes like transport, signaling, enzyme reactions and ultimately cell viability requires optimal membrane fluidity.

“Homeoviscous adaptation” was first observed in *E. coli*. *E. coli* grown at higher temperatures incorporates increasing proportions of saturated and long-chain fatty acids into membrane phospholipids. At higher temperatures, due to increase

in kinetic energy, fluidity of membranes increases, which finally lead to the disintegration of the bilayer. Changes in composition of membrane lipids are required to increase the rigidity and viscosity of membranes for cell survival and growth. It was found that biosynthesis of phospholipids with saturated and long-chain fatty acids increased in *E. coli* grown at higher temperatures.

An important strategy adopted by poikilotherms for homeoviscous adaptation to cold temperature is to increase the proportion of unsaturated fatty acids in membrane phospholipids.

Increased activity of stearoyl-CoA desaturase (EC 1.14.99.5), a key enzyme that introduces unsaturation in fatty acids, results in enhancing the membrane fluidity. Studies in cyanobacteria, namely *Synechocystis* sp, showed that three of the four genes for desaturases (desA, desB, and desD) are cold-inducible. The increased synthesis of unsaturated fatty acids in response to cold stress has also been observed in fishes, such as common carp and rainbow trout. Studies of homeoviscous adaptation using physiological models like *Drosophila melanogaster* have shown that flies from all populations show a decrease in PE/PC ratio and the degree of lipid unsaturation in response to warm temperatures (Cooper et al. 2014).

Homeoviscous strategies adapted by organisms to maintain liquid-crystalline phase in membranes include the regulation of fatty acid chain length, degree of unsaturation of fatty acids, the type of lipid polar head groups, the proportion of branched fatty acids, and the cholesterol content.

The archaeon *Thermococcus barophilus*, one of the most extreme members of hyperthermophilic piezophiles known thus far, is able to grow at temperatures up to 103 °C and pressures up to 80 MPa. The archaeal membrane lipids are composed of phytanyl and/or biphytanyl hydrocarbon chains linked to glycerol by ether bonds, which provide increased rigidity, and reduced permeability at high temperature and pressure. In the deepest part of the oceans, high hydrostatic pressures (HHPs) are present, archae bacteria can survive in deep-seas. The diether phospholipid [2, 3-di-*O*-phytanyl-*sn*-

glycerol (DPG)] is the dominant lipid in membranes in some extreme halophilic Archaea. Thermophilic and hyperthermophilic Archaeal membranes also contain bipolar membrane-spanning tetraether lipids such as glycerol-dibiphytanyl glycerol tetraether (GDGT-0; caldarchaeol) which form very tightly packed monolayers instead of bilayers, further contributing to membrane rigidity (Cario et al. 2015).

In response to salt stress, organisms including bacteria, yeast, and plants increase the proportion of unsaturated fatty acids and lower fatty acyl chain length in their membrane lipids. The difference in the concentration of nutrients between the outside and the interior of the cell acts as a sensor to trigger a response to increase membrane fluidity.

References

- Alonso MA, Millán J (2001) The role of lipid rafts in signalling and membrane trafficking in T lymphocytes. *J Cell Sci* 114:3957–3965
- Ben NG, Giepmans BNG, Sven CD et al (2009) Epithelial cell–cell junctions and plasma membrane domains. *Biochim Biophys Acta* 1788:820–831
- Cario A, Grossi V, Schaeffer P, Oger PM (2015) Membrane homeoviscous adaptation in the piezo-hyperthermophilic archaeon *Thermococcus barophilus*. *Front Microbiol* 6:1152. <https://doi.org/10.3389/fmicb.01152>
- Cooper BS, Hammad LA, Montooth KL (2014) Thermal adaptation of cellular membranes in natural populations of *Drosophila melanogaster*. *Func Ecol* 28 (4):886–894
- Fujiwara T, Ritchie K, Murakoshi H, Jacobson K, Kusumi A (2002) Phospholipids undergo hop diffusion in compartmentalized cell membrane. *J Cell Biol* 157:1071–1081
- Gennis RB (1989) Biomembranes: molecular structure and function. Springer, New York
- Ho TSY, Rasband MN (2011) Maintenance of neuronal polarity. *Dev Neurobiol* 71(6):474–482. <https://doi.org/10.1002/dneu.20843>
- Jain MK (1979) Molecular motions in biomembranes. *Prac INSA* 45A(6):558–566
- Kusumi A, Suzuki KG, Kasai RS, Ritchie K, Fujiwara TK (2011) Hierarchical mesoscale domain organization of the plasma membrane. *Trends Biochem Sci* 36:604–615. <https://doi.org/10.1016/j.tibs.2011.08.001>
- Luna EJ, Hitt AL (1991) Cytoskeleton-plasma membrane interactions, *Science* 258:955–964

- Marguet D, Lenne PF, Rigneault H, He HT (2006) Dynamics in the plasma membrane: how to combine fluidity and order. *EMBO J* 25(15):3446–3457. <https://doi.org/10.1038/sj.emboj.7601204>
- Ritchie K, Iino R, Fujiwara T, Murase K, Kusumi A (2003) The fence and picket structure of the plasma membrane of live cells as revealed by single molecule techniques (Review). *Mol Memb Biol* 20:13–18
- Sezgin E, Schwille P (2011) Fluorescence techniques to study lipid dynamics. *Cold Spring Harb Perspect Biol* 2011(3):a009803
- Tahirovic S, Bradke F (2009) Neuronal polarity. *Cold Spring Harb Perspect Biol* 1(3):a001644. <https://doi.org/10.1101/cshperspect.a001644>
- Trimble WS, Grinstein S (2015) Barriers to the free diffusion of proteins and lipids in the plasma membrane. *J Cell Biol* 208(3):259–271. <https://doi.org/10.1083/jcb.201410071>
- Zhang R, Zhang CY, Zhao Q et al (2013) Spectrin: structure, function and disease. *Sci China Life Sci* 56:1076–1085

6.1 Introduction

Every living cell has to exchange molecules across the membrane for cellular functions. The hydrophobic or lipophilic molecules do not require energy for crossing the membrane. They can diffuse freely from higher to lower concentration till equilibrium is established. This process is called **passive transport** or **diffusion**. This is not true for polar or lipophobic molecules because of the nonpolar nature of membrane lipid bilayer. For polar molecules, the cell recruits mediator or transporter proteins in the membrane to facilitate their movement. If the direction of transport is from higher to lower concentration region, the transporter proteins do not use external energy and the process is called **facilitated transport**, because the energy needed for transport is dispensed by molecule's own concentration gradient (unequal distribution across the membrane) in the favorable direction. The free energy is minimal in unequal distribution of polar molecules. If polar molecule is transported from lower to higher concentration region, against the concentration gradient, the energy has to be provided by external source to mediator protein to make the process spontaneous in the cell, and this process is called **active transport**. In the cell, the energy source is mostly adenosine triphosphate (ATP). The facilitated transport unlike diffusion has shown **speed and specificity, saturation kinetics, susceptibility to competitive inhibition, and susceptibility to chemical inactivation**. The active

transport of polar molecules against concentration gradient requires energy for transport. A large group of transporters that hydrolyze ATP to transport molecules across the membrane are known as ATPases. These carrier ATPases are classified into five subclasses according to their structure and physiological functions as P-type ATPases, V-type ATPases, F-type ATPases, ecto-type ATPases, and A-type ATPases. P-type ATPase transporters are multidomain integral membrane proteins involved in the transport of **cation and lipids**. Phylogenetically according to their function, these P-type ATPases are divided into five major types and various subclasses. The vacuolar ATPases are ATP-dependent oligomeric protein **proton pump**, which regulate acidic pH in organelle compartment like phagosome and endosome for the separation of ligand from their receptors transport proton (H^+) across the plasma membrane. The secondary transport, also known as ion-coupled transport involves the use of electrochemical potential generated by an ion transport for the co-transport of another ion against the gradient across the membrane. **ATP-binding cassette (ABC) transporters**, importers, and exporters, the newly identified integral proteins, comprise a large superfamily of integral membrane proteins with diverse functions. There are three major transporters which are known as **flippases, floppases, and scramblases**. The flippases are also known as P4-ATPases, which transport phospholipids to inner leaflet of membrane and have substrate specificity to phosphatidyl serine and phosphatidyl choline. **Aquaporins (AQPs)**, the inte-

gral proteins of membrane, are small, hydrophobic, and homotetramer proteins, which are involved in bidirectional transport. The bacteria take nutrients from their surroundings by various modes of transport but the transport of sugars and its derivatives like sugar alcohols, amino sugars, glucuronic acids, and disaccharides is transported by group translocation with histidine heat resistance protein HPr as high-energy phosphate donor protein. The transporting sugar molecule is also phosphorylated during transport, which makes sugar negatively charged. The various organisms have specialized proteins of rhodopsin family to seize light energy for various physiological functions. The rhodopsin protein part, opsin, is covalently linked to retinal chromophore, which may be in *trans*- or *cis*-configuration. The animal rhodopsin (also known as Type II) are cell G-coupled receptors, while microbial rhodopsin (Type I) may act as ion pump, ion channels, sensors, photosensory receptors and regulator for gene expression and kinases. **Pore-forming toxins (PFTs)**, the bacterial virulence factor, single major family of proteins, are secreted by gram-positive and gram-negative bacteria. **PFTs** may be present either in cytoplasm or in the membrane. The conformational change in cytoplasmic PFTs may translocate them to membrane in need of hour. **Ionophores** are natural and synthetic organic molecules of diverse type, which can transport cations by forming lipid ion-soluble complex. Each ionophore possesses a unique property of **changing transmembrane ion gradient** and **electrical potential**, synthesized by bacteria, and acts as protector against competing microbes. The bacterial and eukaryotic membranes are found to have special proteins in their outer membrane for transport, which are known as porins and form channels for various small size solutes, ions, and other nutrients. The protein ion channels are passive transporters, are made up of transmembrane, are selective for their substrate ions, and have much faster rate of transport than pumps. These channel proteins do not interact with transporting ions and have two conformations, closed and open, to

regulate flow of ions. The trimeric ATP-activated channels are permeable to cations like sodium, potassium, and calcium. There are seven subclasses of the group, which are involved in various physiological functions like muscle contraction, neurotransmitter release and immune responses regulation. The GABA and glycine receptors are anion channels but inhibitory in nature. GABA receptors have two subdivisions as GABA receptors family of ligand-gated channel (ionotropic) GABA_A and G receptor protein family (GABA_B). The *N*-methyl-D-aspartate (NMDA) receptors are known as glutamate-gated cation channel for calcium permeation. The tetrameric ionotropic receptors include NMDA, α -amino-3-hydroxy-5-methyl-4-isoxazolepropionic acid (AMPA), and kainate receptor as per their synthetic ligand binding. The voltage-gated ion channels open or close in response to change in voltage and the unit of membrane potential. In excitable cells like nerve and muscle, the chemical or electrical signaling is initiated through voltage-dependent sodium or calcium influx. The K₂P channels or voltage insensitive channels formerly referred to as leaky or resting channels, are ubiquitously found in all organisms. The functionally active K₂P channel has two subunits, and each subunit is made up of two pore regions (P1 and P2), four transmembrane domains (M1–M4), and two characteristic extracellular helices Cap C1 and C2. This chapter explains all the mechanisms of membrane transport.

6.2 Passive Diffusion

While osmosis is the movement of solution from high concentration to low concentration without transporters across the lipid bilayer, the diffusion is a type of passive transport where small lipophilic or hydrophobic solute moves from higher to lower concentration. The membrane is made up of lipid bilayer to have hydrophobic interior in membrane, which is selectively permeable to small hydrophobic molecules but not to large polar ones. The **passive diffusion** of charged

species across the membrane depends upon the concentration and also on charge of particle Z and the electrical potential difference across the membrane $\Delta\psi$. The diffusion of particle across the membrane is determined by Fick's law of diffusion and affected by magnitude of concentration gradient, molecular weight of solute, distance, permeability, and surface area of membrane. The diffusion coefficient of any solute molecule of Fick's law is proportionality factor, which can be defined as mass of solute diffusing through a unit area in a unit time (unit is square meter per second). The diffusion coefficient depends on the size, temperature, charge on the molecule because of difference between proton and electron and polarity (uneven distribution of charge in the molecule) (Fig. 6.1).

According to Fick's law, for membrane area A , thickness X , and concentration gradient C_2 (higher) and C_1 (lower) across the membrane, the diffusion rate will be proportional to probability coefficient and can be written as follows:

$$\text{The diffusion rate } \frac{dx}{dt} = PA(C_2 - C_1) \quad (6.1)$$

The rate of diffusion is also proportional to partition coefficient K .

So,

$$P = \frac{KD}{X} \quad (6.2)$$

where D is diffusion coefficient.

From Eqs. (6.1) and (6.2),

$$\frac{dx}{dt} = A \frac{KD}{X} (C_2 - C_1) \quad (6.3)$$

Equation (6.3) explains that the rate of diffusion is directly proportional to both partition coefficient and diffusion coefficient and inversely proportional to thickness of the membrane X ; the thickness is constant factor for membrane; that's why diffusion largely depends on partition coefficient. The more hydrophobic molecule will move much faster (Fig. 6.2).

As depicted in Fig. 6.1, the hydrophobic nonpolar molecule diffuses much faster than polar molecule. Among the polar molecules, anionic molecules have higher permeability than cationic molecules. The gases like O_2 and CO_2 are nonpolar and hydrophobic, so they easily diffuse. Glycerol also diffuses across the membrane, but if this is phosphorylated, then this becomes polar. The urea (NH_2CONH_2) is less hydrophobic than diethyl urea ($C_2H_5NHCONHC_2H_5$), so urea diffuses slower than diethyl urea.

The diffusion of molecules and gases from mother to fetus has been observed, and another molecule sodium thiopental is observed to diffuse through blood-brain barrier.

6.3 Facilitated Transport of Glucose

Facilitated transport is mediated by transporter protein, which is found in the membrane without using external source of energy. The transport occurs from higher concentration to lower concentration. In mammal's erythrocytes, the

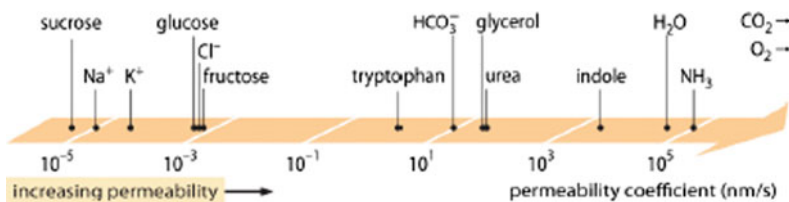
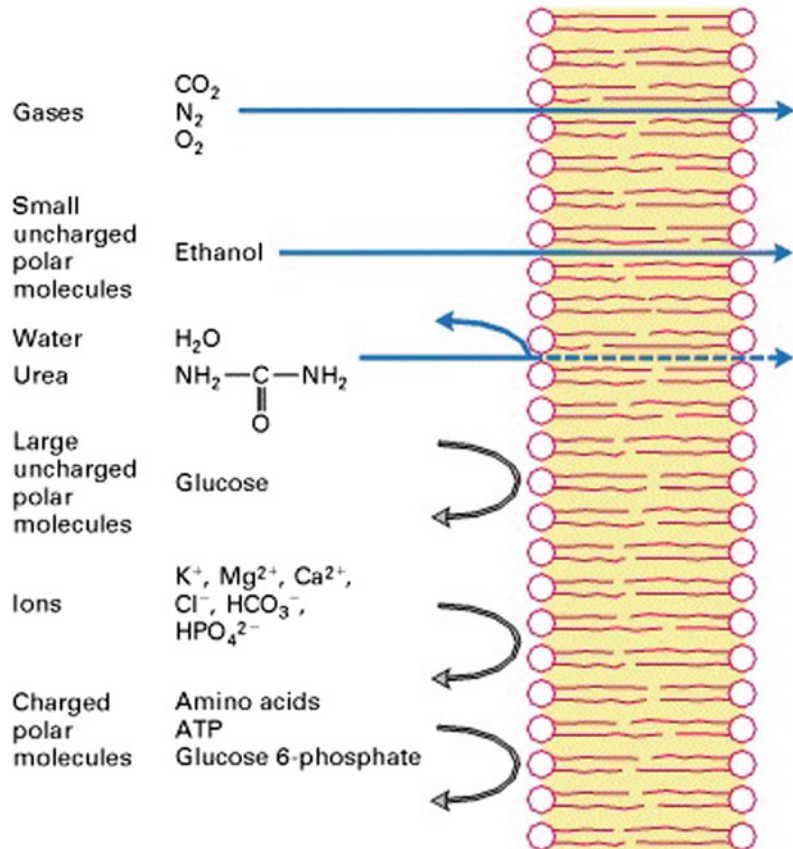


Fig. 6.1 Permeability coefficients of different molecules in the membrane. The nonpolar molecules can diffuse easily across the membrane. <http://book.bionumbers.org/wpcontent/uploads/2014/08/650-fi-PermeabilityAxis-13.png>

Fig. 6.2 Diffusion of polar and nonpolar molecules in the artificial phospholipid bilayer. The small nonpolar molecules move much faster than polar and large molecules



glucose is transported by facilitated diffusion by glucose transporter protein. The facilitated transport unlike diffusion has shown **speed and specificity, saturation kinetics, susceptibility to competitive inhibition, and susceptibility to chemical inactivation** (Fig. 6.3).

The permeability coefficient of the facilitated transport of glucose is much higher than permeability coefficient (2.6×10^{-8} cm/s) of diffusion. The glucose transporter proteins are divided into two major families like Na⁺/glucose cotransporter (SGLTs) and facilitative glucose transporter (GLUTs). The **SGLT** is found in specialized epithelial cells of intestine, proximal tubule of kidney, trachea, heart, brain, testis, and prostate. The Na⁺/glucose cotransporters (SGLTs) are involved in secondary transport of glucose in intestine and nephrons. The 12 members of SGLT class are identified; out of them **SGLT1, SGLT2, SGLT4, and SGLT5**

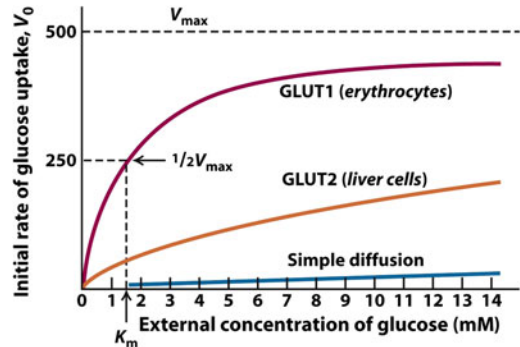


Fig. 6.3 Cellular uptake of glucose mediated by GLUT protein exhibits simple enzyme kinetics and greatly exceeds the calculated rate of glucose entry by simple diffusion

function as sugar transporter and **SGLT3** acts as glucose sensor. **SGLT2** is present in the kidney, brain, liver, thyroid, muscle, and heart. The facilitative glucose transporter (GLUTs) has 14

members, and 11 out of 14 transport sugars. **GLUT1** is present in erythrocytes, fetus placenta, brain, and kidney but low in liver and muscles. **GLUT2** expressed in liver maintains glucose homeostasis. **GLUT3** is neuron-specific glucose transporter with K_m of around 2 mM for glucose. **GLUT4**, a high-affinity, insulin-responsive transporter with approximately 5 mM K_m , is expressed in adipose tissue and muscle tissue. In the process of insulin-stimulated GLUT4 translocation, the various proteins of signal pathway also participate. The high-affinity enzyme **GLUT1** has K_m for glucose around 3–7 mM lower than blood glucose level (5–7 mM), hence transports glucose at significant level even in hypoglycemic conditions. The human erythrocyte glucose transporter (GLUT1) is a type III transporter, having 492-residue glycoprotein with 12 transmembrane (M1–M12) spanning α helices (Mr-45,000). The N-terminal and C-terminal are located in cytoplasm. 33 amino acids in the extra cellular loop between M1 and M2, have n-linked glycosylation sites. The large 65 hydrophobic amino acids are present between M6 and M7. The 3, 5, 7, 8, and 11 amphipathic helices are involved to form hydrophilic channel for glucose transport (Fig. 6.4).

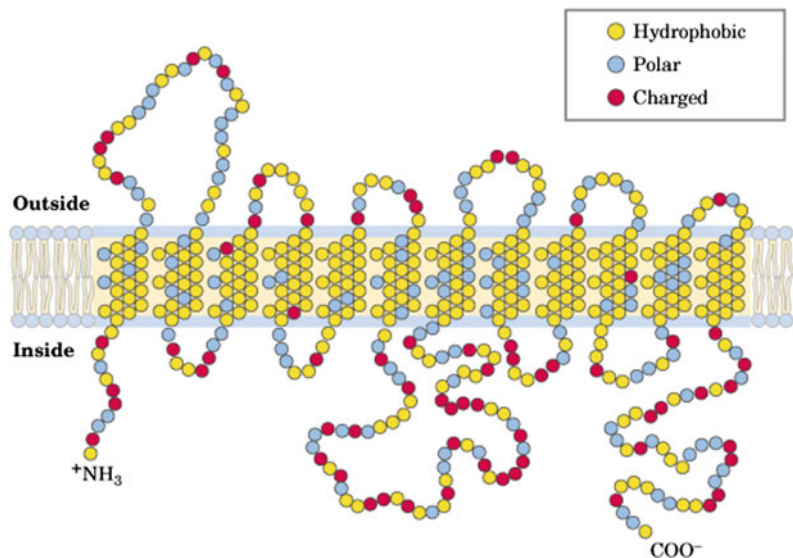
The glucose transporter accounts for 2% of erythrocyte membrane proteins and runs as band 4.5 in SDS-PAGE gels of erythrocyte membranes. It is generally not visible on the gel because the heterogeneity of its oligosaccharides makes the protein band to diffuse (Fig. 6.5).

The glucose concentration is maintained at 4 mM for all metabolic purposes inside the cell. The process of glucose transport can be compared to an enzymatic reaction, where the glucose concentration outside the cell is the substrate (S_{out}), glucose concentration inside the cell is the product (S_{in}), transporter T is the enzyme, initial velocity is (V_0) and (Kt) is the transport constant like Michaelis constant. The graph between velocity of transport and extracellular glucose concentration $[S]_{out}$ shows saturation kinetics. V_{max} and Kt can be calculated from this double reciprocal plot between $1/V_0$ and $1/S_{out}$ when $[S] = Kt$, and the rate of uptake is $1/2$ of V_{max} . The rate equations for this process can be derived like enzyme-catalyzed reactions from Michaelis–Menten equation:

$$V_0 = \frac{V_{max}[S]_{out}}{Kt + [S]_{out}}$$

The glucose molecule does not undergo any chemical change during transport across the

Fig. 6.4 Structure of GLUT1 with 12 transmembranes, and the alpha-helices 3, 5, 7, 8, and 11 are involved to form hydrophilic channel for glucose



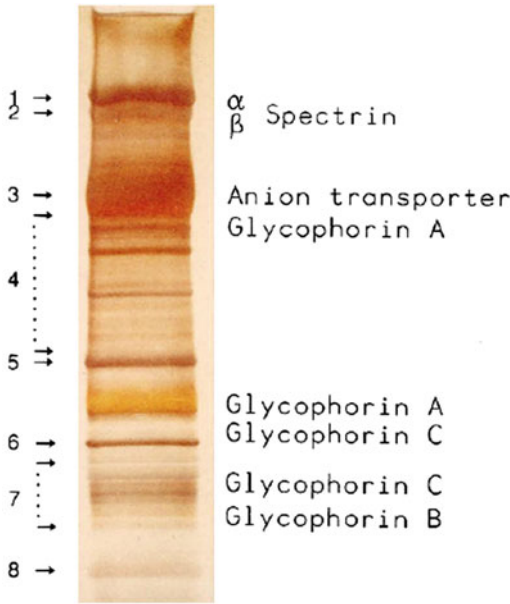


Fig. 6.5 Identification of RBC proteins by SDS

membrane making this a reversible process and helps to achieve equilibrium much faster in the presence of transporter GLUT1 transporter. The transporter protein undergoes a change in conformation on binding to glucose. It has a K_t of 1.5 mM for D-glucose (Fig. 6.6).

6.4 Facilitated Chloride–Bicarbonate Transport

The carbon dioxide formed by cellular respiration of tissues is transported to lung as bicarbonate through erythrocytes and plasma. The

hydration of CO_2 by carbonic anhydrase in erythrocytes forms bicarbonate, which is exchanged with chloride. The anion transporter involved in facilitated transport across the erythrocyte membrane is high-capacity transporter as the diffusion rate of chloride/bicarbonate is never rate limiting for CO_2 transport to lungs. This anion transporter constitutes 30% of erythrocyte membrane. The two identified families of anion exchanger proteins are known as SLC/4A and SLC 26A. The chloride–bicarbonate anion transporter belongs to SLC 26A family. SLC/4A has Na^+ /bicarbonate cotransporter. The anion exchanger can transport bicarbonate in both directions. These transporters regulate pH of the cell, volume, and acid–base secretion.

The carbonic anhydrase enzyme (pKa of 6.2, close to cellular pH) along with CO_2/HCO_3 equilibrium acts as a buffer and maintains pH in the cell (Fig. 6.7).

The human chloride–bicarbonate anion exchanger protein has 911 residues with N-terminal domain, transmembrane, and C-terminal domain. The N-terminal and C-terminal are cytosolic. This comprises 50% of RBC protein. There are 12–14 transmembrane domains involved in transport. The protein is glycosylated at 642 asparagine residue of extracellular domain four. The C-terminal domains of 40 amino acids interact with carbonic anhydrase enzyme (transport metabolon).

In erythrocyte, carbonic anhydrase reaction forms bicarbonate.

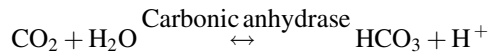
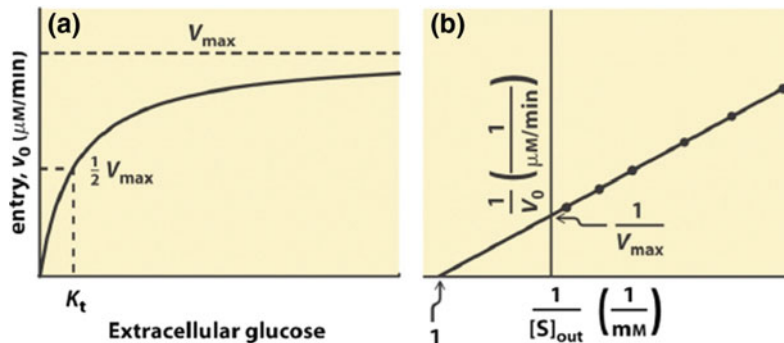


Fig. 6.6 A saturation curve of glucose between velocity and substrate concentration B, the line weaver burk double reciprocal plot of glucose between $1/v$ and $1/S$



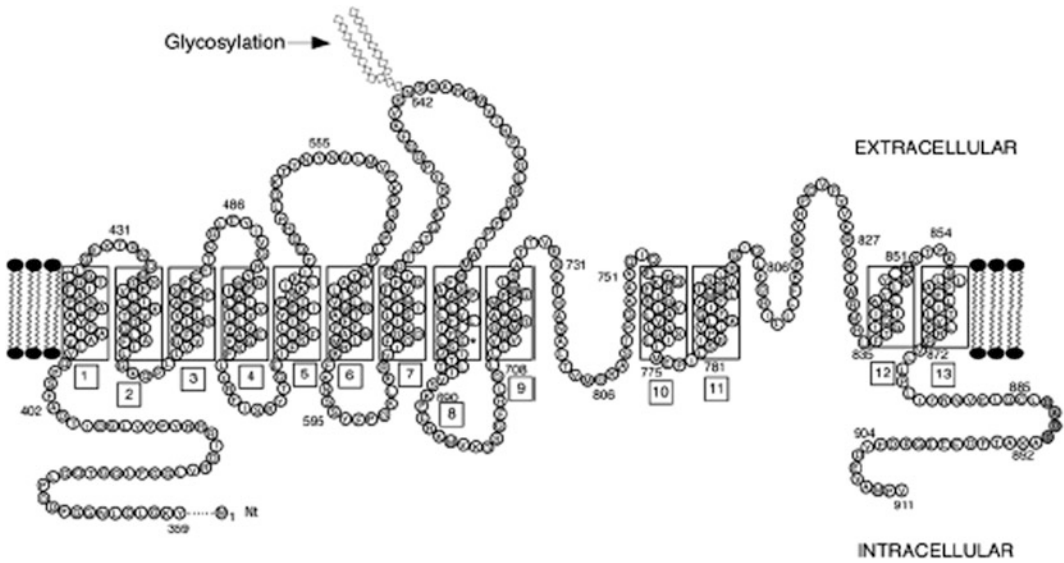


Fig. 6.7 Anion exchanger protein in RBC. Box highlights transmembrane domains. Residue E681 participates in permeability barrier

During mitochondrial respiration, CO₂ is diffused in erythrocytes via capillaries, where it is converted into bicarbonate reaction as shown here. The bicarbonate formed in tissue erythrocytes is released in plasma for lungs. The process is reversed in lungs; the bicarbonate is transported back to lung erythrocytes, which is converted there into CO₂ by carbonic anhydrase II isoform of lung and CO₂ is exhaled from lung by diffusion. In the exchange of one bicarbonate ion,

chloride ion also moves in opposite direction; that’s why this anion transporter is called electroneutral transport (Fig. 6.8).

This anion transporter increases blood exchange capacity for CO₂ and provides flexibility of erythrocytes by interacting with RBC cytoskeleton. This transporter may be dimer or tetramer in erythrocytes. The N-terminal interacts with ankyrin, β-spectrin, 4.1 and 4.2 band proteins of RBC. The mutation in RBC anion

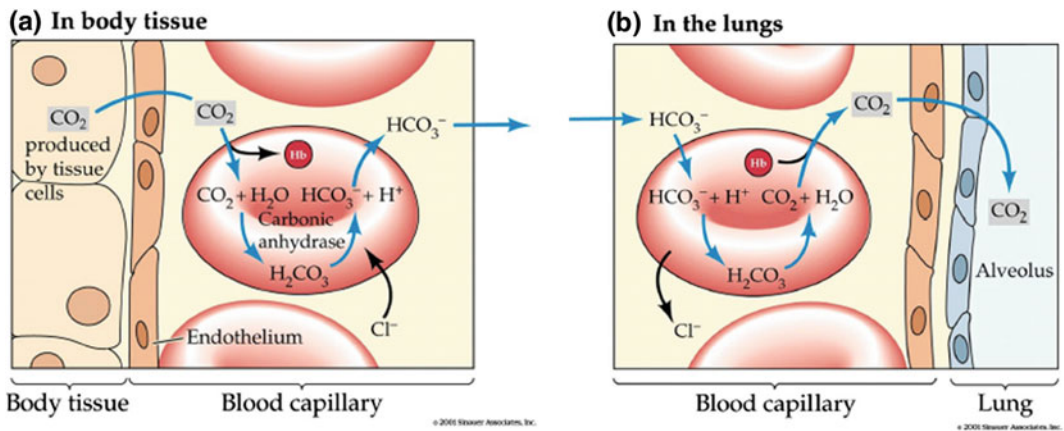


Fig. 6.8 Facilitated chloride bicarbonate anions transport in erythrocytes of tissues and lungs

exchanger results in defective interaction with cytoskeletal proteins to make RBC osmotic fragile and causes disease such as hereditary spherocytosis. In kidney, the anion exchanger protein controls acid–base homeostasis, electrolyte, and fluid concentration.

6.5 Primary Active Transport

The carrier protein as discussed earlier can be involved in **active** or **passive** transport. The active transport of polar molecules against concentration gradient requires energy for transport. A large group of transporters that hydrolyze ATP to transport molecules across the membrane are known as ATPases. These carrier ATPases are classified into five subclasses according to their structure and physiological functions as P-type ATPases, V-type ATPases, F-type ATPases, ecto-type ATPases, and A-type ATPases.

1. **P-type ATPases (E_1 – E_2 ATPases):** These ATPases transport various cations and lipids across the cellular and organelle membrane to regulate cell functions. The various cations may be H^+ , Na^+ , K^+ , Ca^{2+} , Cu^{2+} , Cd^{2+} , Hg^{2+} , Zn^{2+} , Ni , and Pb^{2+} . The phylogenetic study has divided this group into five major types and more than 11 subtypes.
2. **E-type ATPases:** These are cell surface transporters involved in extracellular transport, which can use nucleoside diphosphates and nucleosides triphosphates including extracellular ATP. These transporters depend upon Ca^{2+} and Mg^{2+} and are insensitive to specific inhibitor of P-type. Examples are ecto-ATPase and animal ecto-apyrase. The E-type ATPases participate in termination of **purinergic receptor-mediated responses**. They are also involved in cell adhesion processes and are important for the maintenance of hemostasis in the cardio vasculature.
3. **F-type ATPases (F_1 – F_0 ATPases):** These ATPases are involved in ATP synthesis and localized on bacterial membrane, thylakoid membranes of chloroplasts, and inner membranes of mitochondria.

The detail of these ATPases is discussed in Chap. 8.

4. **V-type ATPases (V_1 – V_0 ATPases):** These ATPases act as proton pump and are found on various organelle membranes to regulate acidic pH in organelles.
5. **A-type ATPases (A_1 – A_0 ATPases):** These ATPases are present in archaeal bacteria and in some other prokaryotes. They functionally resemble to F-type ATPases and structurally to V-type ATPases.

6.6 P-Type (E_1 – E_2) ATPases

P-type ATPase transporters are multidomain integral membrane proteins involved in transport of **cation and lipids**. Phylogenetically according to their function, these P-type ATPases are divided into five major types and various subclasses (Fig. 6.9).

The P-type ATPase or pump is a 70–150 Kd protein having approximately around 900 amino acids. P-type ATPases may have maximum 10 hydrophobic transmembranes from M1–M10 with their N-terminal and C-terminal of proteins in cytoplasm. The cytoplasmic domain is highly conserved and inserted between M2 and M3 and M4–M5. These proteins have characteristic conserved amino acids **DKTGTLT**, where aspartic acid (D) is reversibly phosphorylated during catalytic cycle. The five types of P-type ATPases are divided as Type I, Type II, Type III, Type IV, and Type V.

Type I P-type ATPases are bacterial ion pump like *Escherichia coli*–Kdp ATPases, which are made up of four different subunits with six transmembrane domains namely, Kdp F, A, B, and C. The Kdp B is the catalytic and ion-transporting subunit of the pump. Type IB ATPases of single peptide with eight transmembranes like ZntA and CopA physiologically detoxify bacterial cell by throwing out toxic metals.

Type II P-type ATPases are majorly involved in membrane potential regulation in the

ATPases are regulated by their C-terminal or N-terminal calmodulin-binding domains. The Type IIC ATPases are heterologomers with α - and β -subunits. The sodium–potassium ATPases (Na^+/K^+ ATPase) belong to this class. The α -subunit with maximum ten transmembranes (M1–M10) is catalytic unit with autophosphorylation site and ion binding site, while β -subunit, glycosylated single transmembrane of 55 Kd, is required for insertion and assembly. The renal Na^+/K^+ ATPase has additional γ -subunit with FXYD motif (Fig. 6.10).

The FXYD proteins act as regulator and stabilizer. The FXYD motifs provide stability to pump. The sodium–potassium pump is inhibited by digitalis glycosides and **ouabain**, and H^+/K^+ ATPases are inhibited by **omeprazole**, an antiulcer drug, so these pumps are the site of drug action also. The Na^+/K^+ ATPases transport three Na^+ ions out of the cell and two K^+ ions inside the cell per catalytic cycle. The **Type IID ATPases** are eukaryotic Na^+/K^+ ATPases.

The **Type III ATPases** are prominently found in fungi and plants, where these pumps maintain intracellular pH of 6.6 against extracellular pH of 3.5 and maintain membrane potential in the similar way of animal Na^+/K^+ pump. The H^+ ATPases are regulated by C-terminal autoinhibitory amino acids. **Fusicoccin** is a fungal toxin, which activates H^+ ATPases irreversibly.

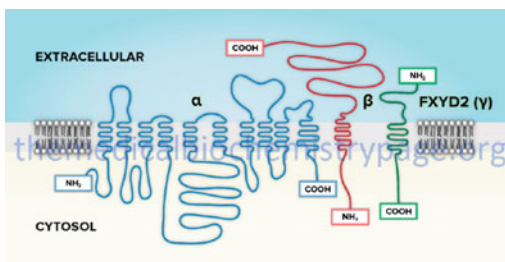


Fig. 6.10 Structure of sodium–potassium ATPases. These ATPases are composed of two subunits (α and β). The α -subunit (113 Kd) binds ATP and ions (Na^+ and K^+) and contains an autophosphorylation site (P) but some isoforms like renal sodium–potassium have extra γ subunit with FXYD2

Type IV and **Type V ATPases**' role is not very clear but structurally they resemble to Type I and are found in eukaryotes. They are also known as **flippases**, which transport phospholipids from outer leaflet to inner leaflet and maintain lipid asymmetry of the membrane. The erythrocyte membrane has Mg^{2+} -dependent flippases. These ion pumps may work in correlation with other lipid transport proteins to maintain asymmetry of membrane.

6.6.1 Structure of P-Type ATPases

X-ray crystallography, NMR spectroscopy and electron cryo-microscopy (EM) studies on various types of P-type ATPases especially, calcium ATPases and sodium–potassium ATPases revealed that **P-type ATPases** have four domains with conserved sequences, namely, **actuator A**, **membrane M**, **nucleotide-binding domain NBD**, and **phosphorylation P-domain**. The variation of amino acids has been observed only in extracytoplasmic loop.

6.6.2 Phosphorylation Domain

The most conserved phosphorylation domain is the catalytic domain with DKTGTLT signature motif, where aspartic acid (D) is phosphorylated and dephosphorylated during catalytic cycle. It has **Rossmann fold** (characteristics of many nucleotides proteins) made up of central seven-stranded β -sheet flanked by α -helices, including the cytoplasmic end of M5.

6.6.3 Nucleotide-Binding Domain

The nucleotide-binding domain inserts into P-domain through conserved hinge region of two antiparallel peptides. Seven strands of β -sheet in central have lysine 515 for nucleotide binding. In Na^+/K^+ ATPases—N-domain phenylalanine clustering is observed whereas acidic residues are rich in calcium ATPases. This might be site for regulator interaction, as observed with EM. In

the nucleotide binding site, adenosine base and phenylalanine 475 interaction forms hydrophobic stacking and three phosphate group bulge out in solution so that γ -phosphate could reach to P-domain aspartic acid for phosphorylation.

6.6.4 The Actuator Domain

The N-terminal actuator domain is highly conserved. Similarly like P-domain, A-domain has two unequal divisions by M1 and M2 helices hairpin structure. The larger part has β -sheet secondary structure with conserved TGE sequence. The TGE sequence interacts with phosphorylation site during transport cycle. Some of ATPases like fungal H⁺-ATPases have extra-long amino-terminal amino acids fused with actuator domain, which might play role in substrate sensing or in regulation.

6.6.5 Membrane Domain

The membrane domain is the largest domain of approximately 405 amino acids with ten trans-membrane segments to enclose ion binding site. This domain is less conserved and is directly connected to catalytic core through M4-M5 and M6-M8 polar ionic side chains. As observed in calcium ATPases, the M6 aspartic acid 800 and M8 glutamate 908 acidic side coordinate Ca²⁺; the other amino acids such as valine 304, alanine 305, and isoleucine 307 of M4 also participate in ion binding. M is the flexible region, which is arranged and rearranged during transport cycle for accommodating different sizes and charge ions and for catalysis (Fig. 6.11).

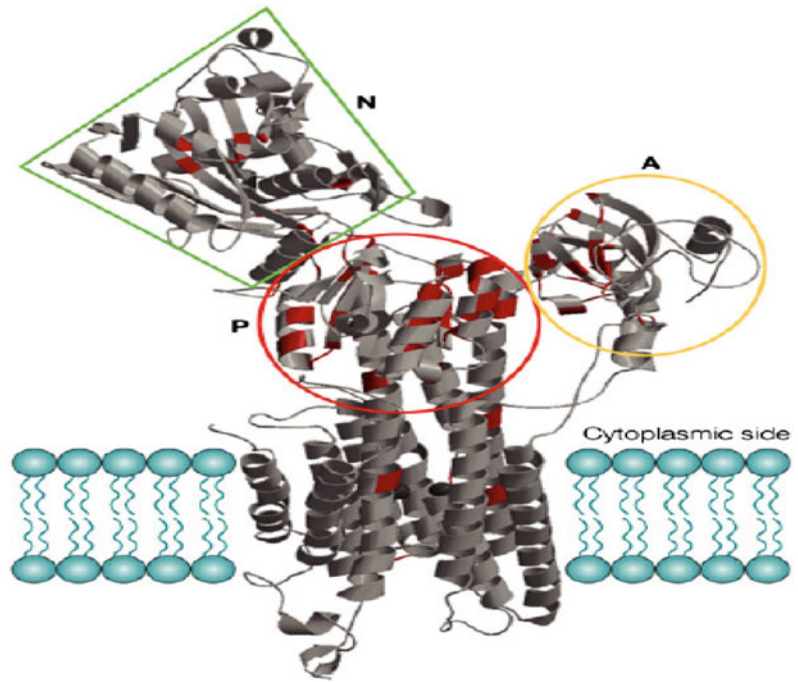
6.6.6 Transport Cycle of P-Type ATPases

The catalytic cycle of ATP binding, phosphorylation, changes in conformation by arrangements

of M-domain helices, hydrolysis of ATP for energy are same in all P-type transporters. That's why P-, N-, and A-domains have conserved residues but M-domain with variable residues regions with ion binding site may change to accommodate various ions. The cycle starts with loading of ion 1 (X⁺) to high-affinity binding site and releasing of extracellular ion 2 (Y⁺) in cytoplasm through cytoplasmic access channel. The interaction of ion 1 (X⁺) with polar group of amino acids near binding site at P-domain twists M4, M1, and M6 helices to move in E1 state. Mg²⁺/ATP binding to NBD domain brings this close to P-domain through slight movement of β -strands. These movements result in correct positioning of γ phosphate group of ATP to P site, and E state of ATPase is changed to E1 ~ P state. In E1 ~ P state, ion1 (X⁺) is trapped in protein, which can be visible from any side of membrane. When ion1 (X⁺) binding is complete, the phosphorylation takes place on aspartic acid residue of P-domain because the energy released by ion binding to E1 ATPase favors the inclination of P-domain to bring more closure γ phosphate group to aspartic acid for reaction (Fig. 6.12).

The reaction may be explained as nucleophilic attack on aspartic acid in P-domain by γ phosphate group. This may be the reason that sodium ATPase needs three Na⁺ ions in comparison with two Ca²⁺ ions in Ca²⁺ ATPases for P-domain movement. A-domain rotates parallel to membrane, and TGE loop becomes closure to phosphorylation site. The E1 ~ P state changes to E2 ~ P state. Simultaneously, M1, M2, and M3 helices of A-domain because of their rearrangement induced by phosphorylation may close polar ion access channel from cytoplasmic site. This might be understood that the inclination of P-domain induces the movement of helices in such a way that E2 ~ P state has low affinity to ion1 (X⁺) and leaves this to extracellular site or into lumen of ER. The E2 ~ P state has high affinity for ion 2 (Y⁺), and binding to this ion may induce the hydrolysis of phosphorylated aspartic acid. The TGE loop interaction with Mg²⁺ ion will leave phosphate group unprotected,

Fig. 6.11 Alignment of various domains in sarcoplasmic reticulum Ca^{2+} -ATPase. The conservative substitutions are shown here in red. The most conservative residues are found in the phosphorylation (P)- and actuator (A)-domains, fewer in the nucleotide-binding (N)-domain, and hardly any in the 10 membrane-spanning helices



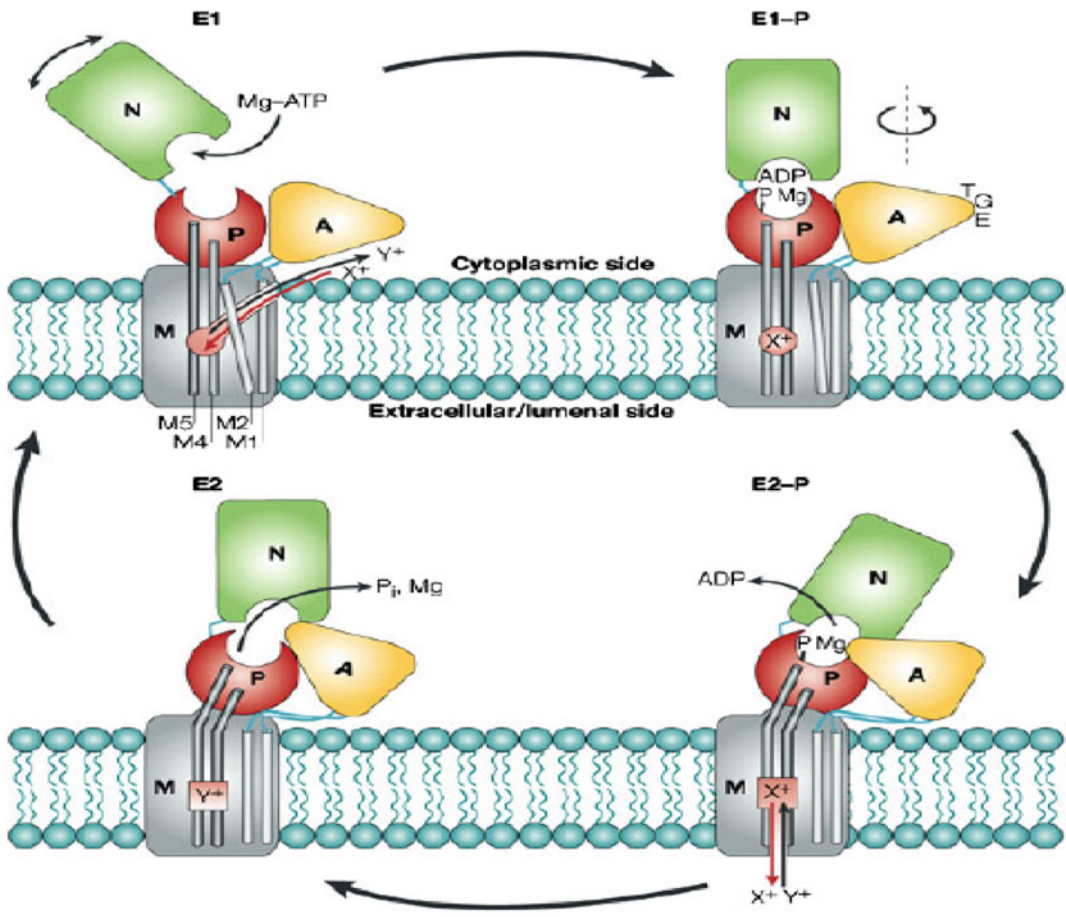
Nature Reviews | Molecular Cell Biology

and this may result in hydrolysis by water. After this hydrolysis, E2 transforms into E2 state with open binding site in cytoplasm for next cycle of transport.

6.7 Vacuolar [V-Type] ATPases

The vacuolar ATPases are ATP-dependent oligomeric protein **proton pump**, which regulate acidic pH in organelle compartment like phagosome and endosome for the separation of ligand from their receptors and transport proton (H^+) across the plasma membrane. The V type ATPases activity can be regulated by reversible disulphide bond formation between conserved cysteine residues at catalytic site. Glutamate uptake in presynaptic vesicle is found to be dependent on V-type ATPases. The V-type ATPases regulate plasma pH by exporting proton through renal intercalated cells of kidney. The mutation in V-type ATPases may cause renal tubular acidosis. The vacuolar ATPases also regulates acidic pH in osteoclasts for bone

degradation, and the genetic defect in V-type ATPases may cause osteoporosis. V-type ATPases are present at the surface of neutrophil and macrophage for maintaining pH. The sperm maturation and storage also need V-type ATPases in epididymis of testis. The cancer cells are also found to manipulate V-type ATPases. The V-type ATPases are potential target for drug in various diseases. The **prerenin receptors'** study has indicated the role of renin/angiotensin signaling in V-type ATPases' regulation. The V-type ATPases are oligomeric protein complex with two different domains, which are known as **peripheral (\mathbf{V}_1)** of eight subunits and **integral (\mathbf{V}_0)** of six subunits. While peripheral proteins (\mathbf{V}_1) carry out ATP hydrolysis, the \mathbf{V}_0 -domain of integral proteins transports proton ions. The peripheral proteins \mathbf{V}_1 are designated in bold alphabet like **$\mathbf{V}_1\mathbf{A}$, \mathbf{B} , \mathbf{C} , \mathbf{D} , \mathbf{E} , \mathbf{F} , \mathbf{G} , and \mathbf{H}** , and integral membrane proteins are known as **\mathbf{a} , \mathbf{b} , \mathbf{c} , \mathbf{c}' , \mathbf{d} , and $\mathbf{V}_0\mathbf{e}$** . The various isoforms of these subunits are found in various tissues and organs. The peripheral proteins are present in stoichiometry concentration of **$\mathbf{A}_3\mathbf{B}_3\mathbf{C}_1\mathbf{D}_1\mathbf{E}_2\mathbf{F}_1\mathbf{G}_2\mathbf{H}_{1-2}$** .



Nature Reviews | Molecular Cell Biology

Fig. 6.12 Transport cycle of P-type ATPases. In the E1 conformation, ion 1 (X^+) binds to its high-affinity site in the membrane (M)-domain through cytoplasmic side. The binding of X^+ ion initiate phosphorylation of aspartic residue in E1 state (P-domain by ATP). Phosphorylated E1P state transporter still is in same state. During transition of E1 to E2 change in conformation (regulated step), the P-domain rearranged itself for bringing TGE loop near to phosphorylation site, which stabilizes phosphoryl group binding and ADP dissociates. The A-domain M1 and M2 segments movement closes access

to cytoplasmic ion access channel (light gray). The P-domain rotation disturbs the high-affinity X^+ binding site through its attachment to helices M4–M6 (dark gray). X^+ is delivered to the outside (extracellular/luminal side) through an exit channel. The ion binding site of E2 P now has a high affinity for second ion 2 (Y^+), which may bind from the outside. The aspartic acid is dephosphorylated leaving enzyme into E2 conformation. Mg^{2+} and inorganic phosphate (P_i) are dissociated, and the enzyme reverts back to the E1 state, in which Y^+ is released into the cell. The ATPases are ready for new cycle

The catalytic domain of vacuolar ATPases contains heterohexamer of alternate A- and B-subunits with the ATP binding site at the interface of A- and B-subunits. Three subunits of A contribute majorly to three catalytic sites, and B-subunits are regulatory in functions. The

remaining peripheral proteins form central and peripheral stalk, which is linked to V_1 - and V_0 -domains. C-, E-, G-, and H-subunits form the peripheral stalk. The V_0 -subunits are present in the ratio of $a_1d_1e_n c_4-c'_1$ and c''_1 (n is variable number of e). The subunits c, c', and c'' have

hydrophobic residues in high concentration and have one **buried carboxyl group** in one of the transmembranes as TM4 (for c and c') and TM3 (for c'') for proton translocation. These buried carboxyl groups may be reversibly protonated during proton translocation. These hydrophobic subunits with single copy of c' and c'' and four copies of c form **proteolipid ring**. The hydrophilic subunit **d** at the cytoplasmic side interacts with V_1 subunits (**D and F**) of the central stalk complex, and this whole complex is referred as **rotatory complex** (Fig. 6.13).

The subunit **a** of V_0 with eight transmembrane domains has buried **arginine amino acid** in seventh transmembrane domain, which participates in proton translocation by forming **two hemichannels** (one toward cytoplasmic side and

other in opposite side). The cytoplasmic proton enters through cytoplasmic hemichannel of subunit **A**, which may protonate buried carboxyl group of V_0 -subunit. The ATP hydrolysis by **A**-subunit induces conformational change in heterohexamer of **AB** resulting in rotation of central motor with **D**-subunit as axle of the motor. **F** is regulatory unit. V_0 **d**-subunit couples this rotation to ion-transporting proteolipid ring of **b**- and **c**- subunits. The **b**-, **c**-, and **a**-subunits form channel for proton transport. The proton moves with rotation of **b**- and **c**-subunits. The V -type ATPases function through rotatory mechanism, where V_1 -induced ATP hydrolysis results in rotation of central rotatory domain with ring of hydrophobic subunits (c , c' , and c'') in relation to other subunits, which causes ion transport.

This proton remains to interact with carboxyl group because of only polar group in the hydrophobic surroundings of V_0 -subunits. When ATP hydrolysis induces conformational change by rotation, the protonated carboxyl group is exposed to luminal hemichannel. These carboxyl groups interact with buried arginine residue of **a**-subunit and stabilize carboxyl group as carbonate ion, so proton gets disassociated and released into the luminal hemichannel. The continued movement of charged carboxyl group because of changes in conformation by rotation of subunit **a** places it once again in contact with the cytoplasmic hemichannel, where it is again available for protonation.

Regulation of V-type ATPases can be observed through the following different ways either induced or natural. The V -type ATPases may be regulated by (1) reversible dissociation of V_1 and V_0 -subunit, (2) by changing or uncoupling of proton transport and ATP hydrolysis, (3) by reversible disulfide bond formation between cysteine 254 and cysteine 532 of catalytic subunit **A**, (4) by modulation proton pump density as in apical membrane of renal intercalated cell of kidney proton pump activity is regulated by reversible fusion of the pump with apical cells induced by bicarbonate-sensitive adenylate cyclase. The net pH of a compartment is the result of active proton transport and

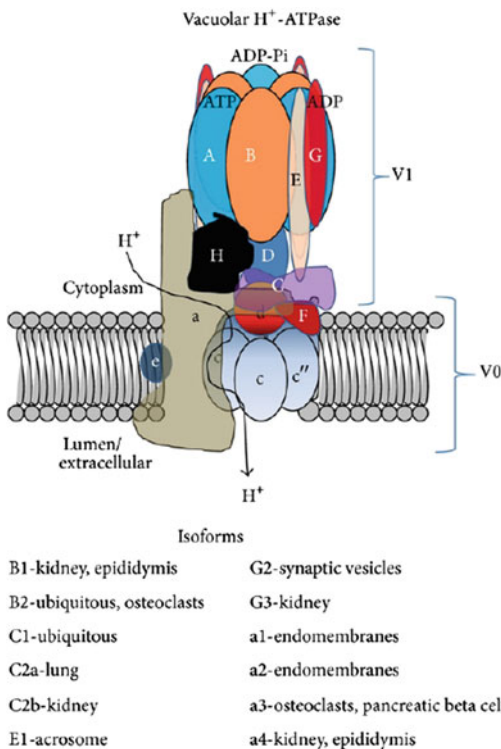
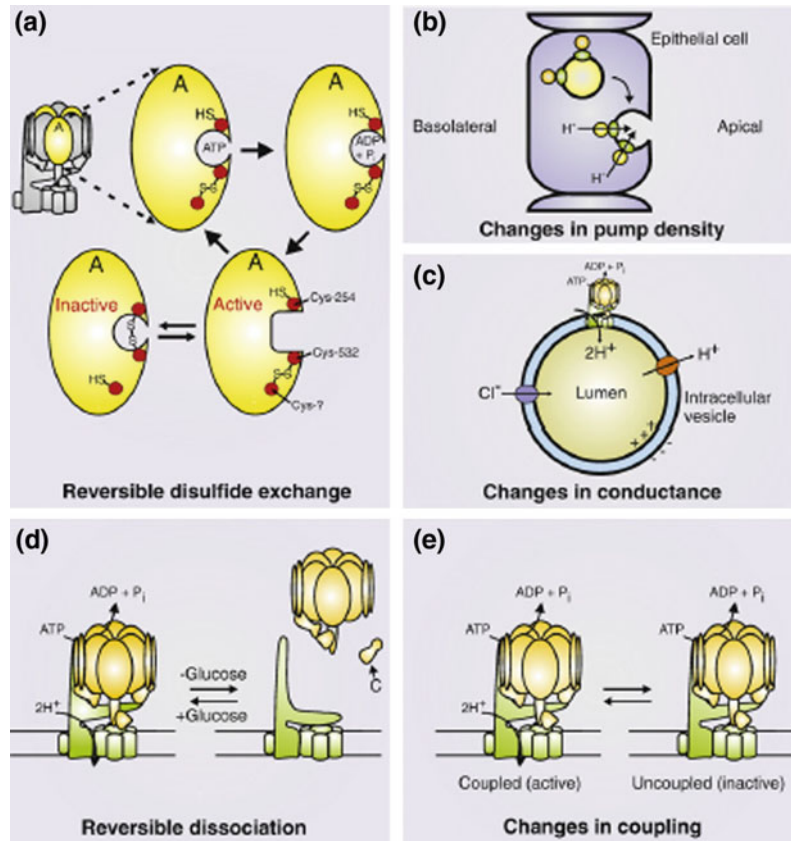


Fig. 6.13 Structure of V -type ATPases with various isoforms in human. **A**-subunit catalyzes ATP hydrolysis. 3 **A** and 3 **B**-subunits of V_1 form heterohexamer. The conformational changes in the **AB** heterohexagon promote turning of the central rotor and the ring of c - and c'' (**b**)-subunits. <https://www.hindawi.com/journals/njots/2014/675430/fig2>

Fig. 6.14 V-type ATPases may be regulated by **a** reversible disulfide bond formation between conserved cysteine residues of catalytic A-subunit, **b** controlling proton ion pump density through fusion with membrane, **c** regulation of other transporters for Cl^- or H^+ , **d** reversible dissociation of V1 and V0 domains and **e** uncoupling ATP hydrolysis and transporting pump subunits. *Source* Cipriano et al. (2008)



passive proton leakage. If passive proton ion diffusion is controlled, proton pump automatically will be regulated (Fig. 6.14).

F-Type ATPases are discussed in detail in Chap. 8.

6.8 Secondary Transport

The secondary transport is also known as ion-coupled transport because the electrochemical potential generated free energy of an ion transport which is used by transporters for other substrate transports across the membrane. These transporters ubiquitously found in all cells constitute a **major facilitator superfamily (MFS)** or solute carrier group of transporters (SLC).

More than 4000 of these transporters are involved in lipid, amino acids, sugar transport, and antibiotics. The important examples may include **Na^+ /glucose (SGLT1)** transporter present in kidney proximal tubule and epithelial cells of intestine. Oligonucleotide/proton transporter (facilitated proton transport and uphill peptide transport), proton/neurotransmitter transports in synaptic vesicle membrane of neuron (neurotransmitter transport against concentration gradient by using electrochemical energy generated by proton transfer), lactose permease LacY in bacteria, sodium taurocholate cotransporting peptide (OATP), apical sodium-dependent bile acids (APSBT). **The major facilitator superfamily transporters** have 12–14 transmembrane segments and

transport substrate by alternating conformations. The bacterial lactose secondary transporters (LacY) and sodium glucose transporters (SGLT1) in human intestines are two well-explored transporters to understand secondary transport mechanism, which is discussed here.

6.8.1 Secondary Transport of Disaccharide Lactose by Lactose Permease (LacY)

Lactose permease (LacY) transporter of *E. coli* bacteria has selective affinity for disaccharides containing a D-galactopyranosyl ring, as well as D-galactose and symport D-galactopyranoside and hydrogen ion together in cell (symport). LacY protein is an integral protein (374 amino acids) of 12 transmembrane helices with a connecting loop between two pseudo-symmetrical six α -helices (7–194 and 214–401 amino acids) bundles. These α -helices form a central hydrophomation. The other conformation with open cavity toward periplasmic side is called **outward-facing** conformation. This alternate conformation of transporter (involved helices II, IV, V in N-terminal and VII, X, XI in C-terminal) exposes bound sugar and proton to cytosol and periplasmic side

alternatively; the basic principle of this type secondary transport is the conformation change in transporter by binding with substrate. The sugar-interacting residues are present in N-terminal region and the proton-interacting amino acids are present in C-terminal side (Fig. 6.15).

The mutagenesis study has identified the role E126 of helix IV, R144 and W155 of helix V in substrate recognition and binding and R302 of helix IX, E325 and H322 of helix X in proton translocation. E269 is required for sugar identification and proton translocation.

LacY has shown affinity toward numbers of D-galactopyranosyl disaccharide and with D-galactose also but not to D-glucose. The 4-hydroxyl group is found to have role in discrimination.

The X-ray crystallography of LacY transporter has explained the mechanism. The transport cycle starts with inward open conformation. In the absence of sugar, lactose permease transporter is closed from periplasmic side. The binding of D-galactosyl pyranoside to LacY transporter induces changes in protein to open periplasmic side by closing cytosolic inward open cavity. The deprotonation of E325 causes closing of inward cavity and opening of periplasmic cavity. The membrane potential has no effect on substrate binding. The five residues R144, W151, E269, N272, and H322 bind

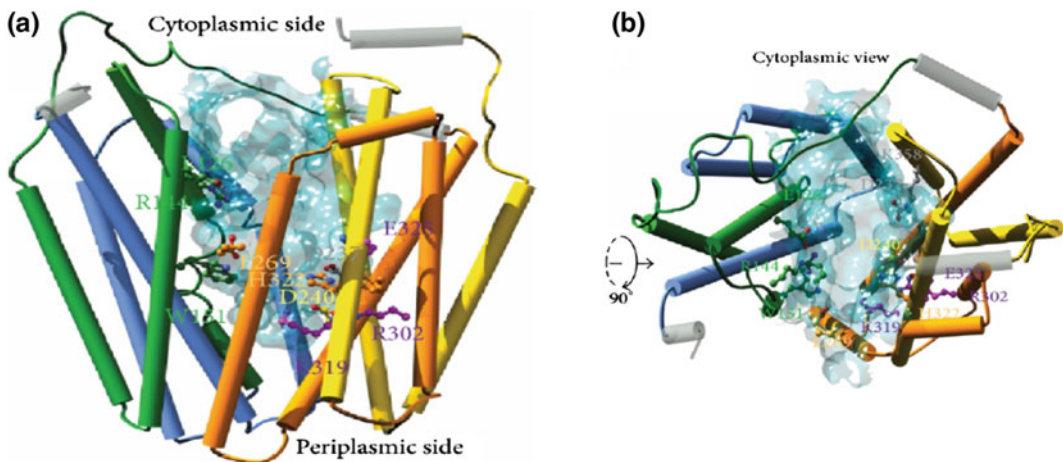


Fig. 6.15 a Structure from top of lactose permease. b Cytosolic view of lactose permease with inward open cavity

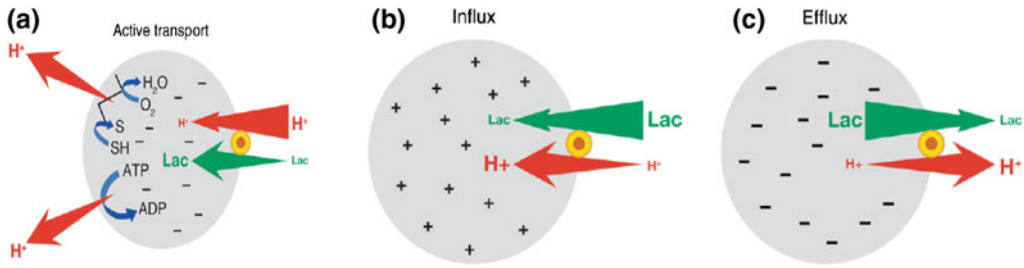


Fig. 6.16 Lactose permease mediated lactose/H symport. In the absence of substrate, LacY does not translocate proton in the presence of electrochemical gradient of membrane. **a** Free energy released from the downhill movement of H is coupled to the uphill accumulation of lactose. Substrate binding generates electrochemical

proton gradients. The polarity depends upon substrate concentration gradient direction. **b, c** Substrate gradients generate electrochemical H gradients, the polarity of which depends upon the direction of the substrate concentration gradient

directly to substrate. The E126 and Y236 stabilize R144 and H322. All these together form substrate binding site in the center of protein. The translocation of substrate may be induced by hydrophobic interaction of W151 indole ring and D-galactosyl pyranoside ring. The binding of this nonpolar substrate to transporter induces major rearrangement of helices in the vicinity of substrate binding site for perfect accommodation. The substrate binding may lower down activation energy for transition between inward open and outward open conformation of LacY. In LacY, the galactose binding induces major conformational change in N-terminal six helices bundle (Fig. 6.16).

The substrate binding and dissociation from transporter promote transition between inward- and outward-facing conformations. The lactose/proton symport has same mechanism in active or facilitative transport for galactose and proton but with the difference in rate limiting steps. The deprotonation step is rate limiting in favorable concentration gradient downhill transports, but in uphill transport, conformation changed induced protonation is rate limiting.

The lactose permease (LacY) transfer potential energy, preserved in proton gradient facilitates galactose transport down the concentration gradient. Hence, the transport is typically a thermodynamically driven and kinetically regulated secondary transport.

6.8.2 Sodium/Glucose Secondary Transport

There are various ways of glucose transporters as discussed earlier. The **sodium/glucose (SGLT1)** transporter is present in epithelial cells of human intestine and also found on incretin (intestinal hormone, which enhances insulin secretion)—secreting vesicles and also in S2 and S3 segments of in kidney proximal renal tubule. SGLT1 has 14 transmembranes (Fig. 6.17).

SGLT1 has specificity for glucose and galactose. In intestine, the sodium/glucose transporters translocate one molecule of glucose per two sodium ions across the epithelial membrane of intestine by using electrochemical gradient of another ion (sodium/potassium). The electrochemical potential is generated by another sodium/potassium pump located in basolateral membrane of these polarized cells of intestine. The another sodium/potassium ATPase pump is present in basolateral membrane to generate electrochemical gradient along with an independent glucose transporter, which also participates in translocation of glucose molecule from intestine to blood vessels. The detail mechanism of secondary transport is discussed above. The sodium–potassium ATPase pump at basolateral membrane transports two potassiums inside the cell and three sodium ions out in blood in

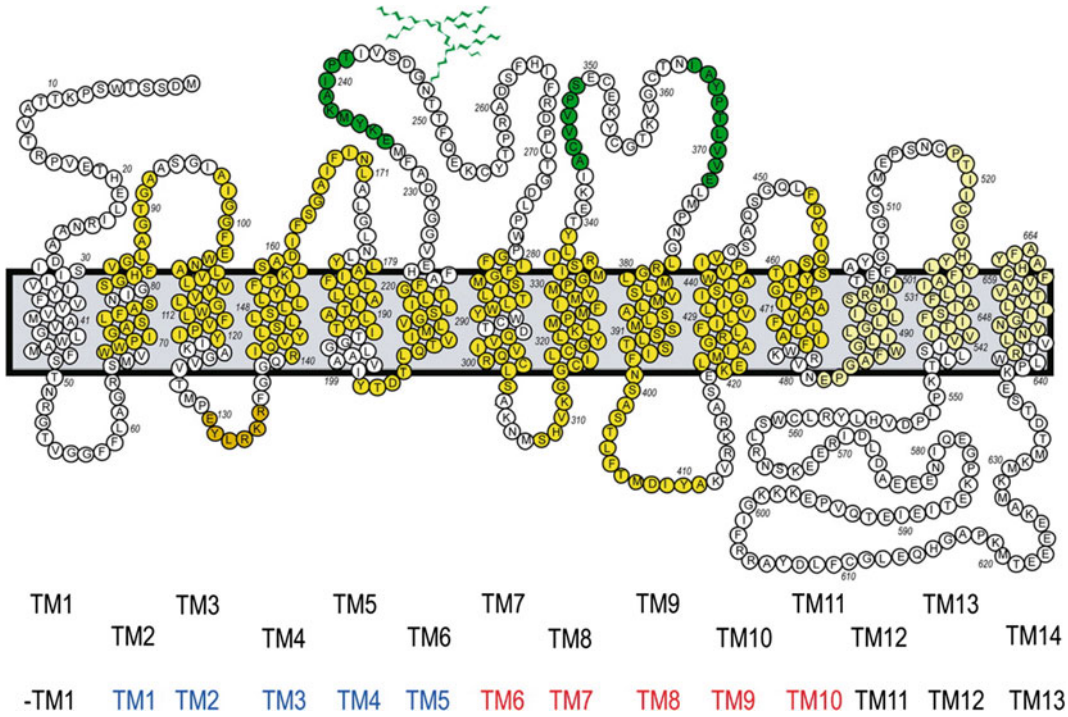
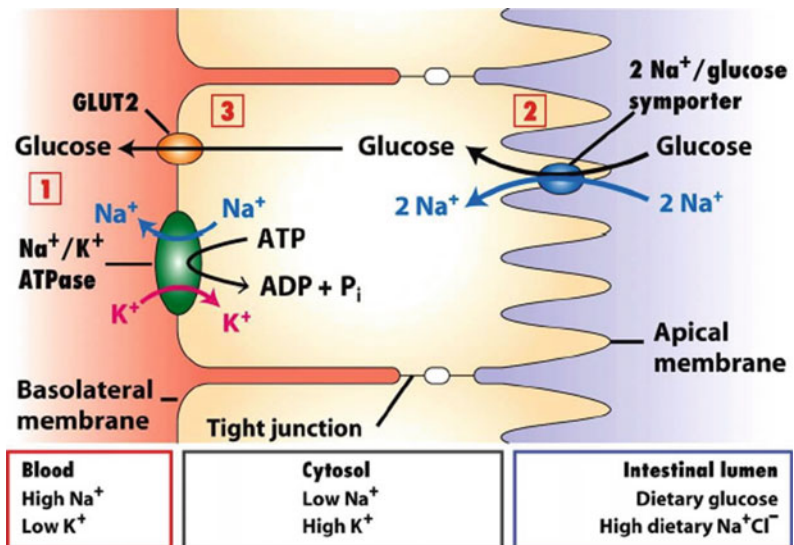


Fig. 6.17 Human glucose/sodium transporter (hSGLT1) structure with 14 transmembrane domains. *Source* Wright et al. (2011)

Fig. 6.18 Summary of glucose transport in human intestine and then to blood vessels by secondary transporter sodium/glucose (SGLT1). The mechanism is discussed in text



ATP-dependent manner. The electrochemical gradient energy generated by this transport is used by SGLT1 transporter in epithelial cell of

intestine to import glucose against concentration gradient. When glucose concentration is accumulated in cell, the other facilitator transporter of

glucose transports accumulated glucose from cell to blood (Fig. 6.18).

6.9 ABC Transporter

ATP-binding cassette (ABC) transporters, importers, and exporters, the newly identified integral proteins, comprise a large superfamily of integral membrane proteins with diverse functions. A total of 48 transporters are identified in human. In bacteria 1% and in archaeobacteria 3% of the genome codes for ABC transporters. They might transport various substrates like amino acids and peptides, monosaccharide, polysaccharides, nucleosides, oligonucleotides, vitamins, coenzymes, and different types of lipid. The ABC transporter proteins are classified on the basis of highly conserved approximately 180 amino acid residues with three motifs like **Walker A/P-loop** (12 amino acids), a **signature motif/C-loop (LSGGQ)**, and the **Walker B motif (five amino acids)**, which participate in ATP hydrolysis.

ABC exporters are physiologically involved in **multidrug resistance** and **detoxification**,

while **importers** play role in **nutrient uptake** and also are used by some prokaryotic pathogens to show **pathogenicity** and virulence in plants, prokaryotes, and archaea. The ABC exporters are also known as **multidrug resistance transporters** because of their role in detoxification. The other distinct classes of energy-coupling factor (ECF) transporters are also as class III ABC importers. The ABC exporters and importers are further classified into subclasses as Type I, II, and III. Functionally, these all transporters may be divided into two major domains known as nucleotide-binding domain (NBD) and transmembrane domain (TMD). The NBD and TMD can be further divided into NBD1 and NBD2 and TMD into TMD1 and TMD2. These domains may be separate, dimer, or fused peptides. In eukaryotes, the ABC transporters are mostly multifunctional with single peptide with four domains but the assemble to form dimers or heteromers. In bacterial ABC transporters NBD and TMD may be separate, dimer or fused. In some bacteria an extra subunit of 30–35 Kd is found for binding to substrate and delivery to TMD. The bacterial ABC transporters may be

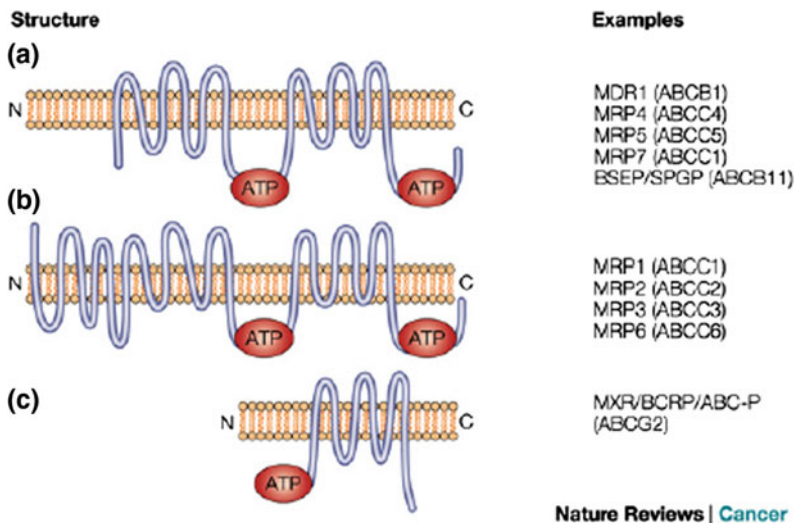


Fig. 6.19 a The three classes of ABC transporters, based on numbers of transmembrane A full transporter such as multidrug resistance MDR1 and multidrug-resistance-associated protein 4 MRP4 have 12 transmembrane domains and two ATP binding sites. **b** The structures of MRP1, 2, 3, and 6 of 17 transmembrane, with two

ATP-binding regions, an additional domain of five transmembrane segments at the amino-terminal end. **c** The “half-transporter” with six transmembrane domains and one ATP-binding region. The ATP-binding camay be on the carboxy-terminal (C) or N-terminal

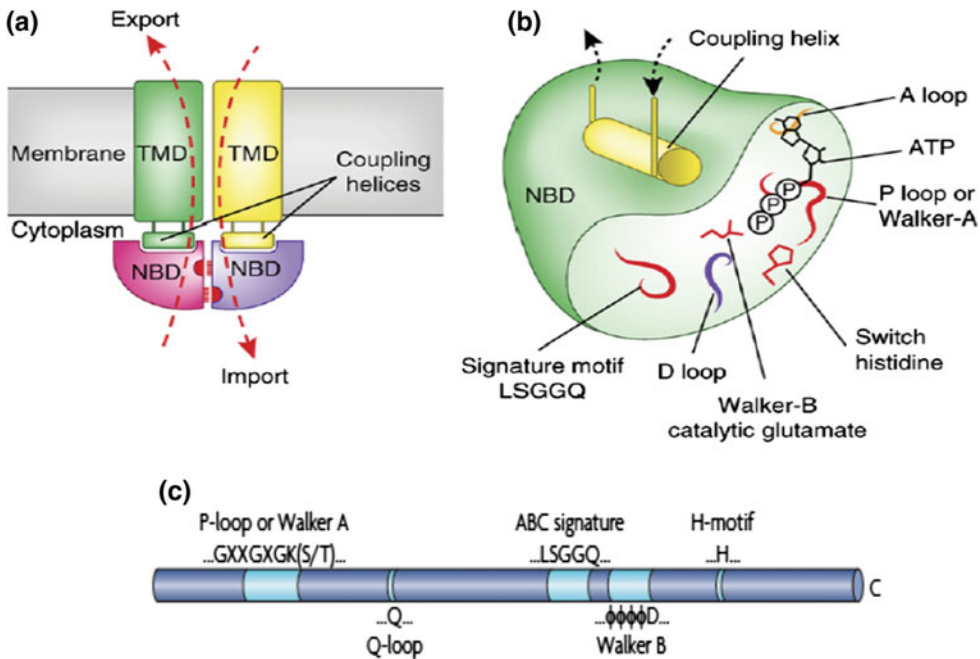


Fig. 6.20 **a** ABC transporters' various domain assemblies. The red half-circles and dashed lines indicate NBD interface, P-loops and conserved signature motifs. In all ABC transporters, coupling helices transmit conformational changes between the NBDs and the TMDs. **b** In

single NBD, various domains like P-loop, A-loop, catalytic glutamate, LSGGQ signature sequence is shown. **c** Linear subunit presentation with conserved sequence

localized in periplasm like gram-negative bacteria or may be membrane bound like gram-positive bacteria (Fig. 6.19).

As mentioned above, the characteristic ABC transporters conserved signature motif like Walker A (GKT/S for phosphate binding domain), LSGGQ, and Walker B motif in NBD are involved in nucleotide-induced conformation change in NBD region. The highly conserved aspartate/glutamate of the Walker B motif forms hydrogen bonds with the threonine/serine of the GKT/S box and with a bound water molecule and facilitates nucleotide hydrolysis (Fig. 6.20).

6.9.1 Mechanism of ABC Transporter

ABC transporters transport substrates against a chemical gradient, a process that requires ATP hydrolysis as a driving force. Under physiological conditions, ABC transporters operate in a

single direction (either import or export) except drug **efflux pump LmrA** having reversible transport under acidic conditions. The transmembrane domain may face outside or inside by changing conformation. The energy for the conformational change in TMD in inward and outward face is provided by the binding of substrate and Mg^{2+} ATP, followed by ATP hydrolysis and substrate release. ABC transporters have similarity to secondary transport in mechanism (Fig. 6.21).

The ABC importers bind to substrate through mediator protein, while exporters directly interact with substrate through their TMD. The NBD forms catalytic domain with Walker A or P-loop, Walker B, Q-loop and H motif (switch region) and conserved sequence LSGGQ in alpha-helical region. The relative orientation of catalytic sequence to alpha-helical region is decided by ATP binding. Usually, in active ABC transporters, its subunits are arranged in head to tail in

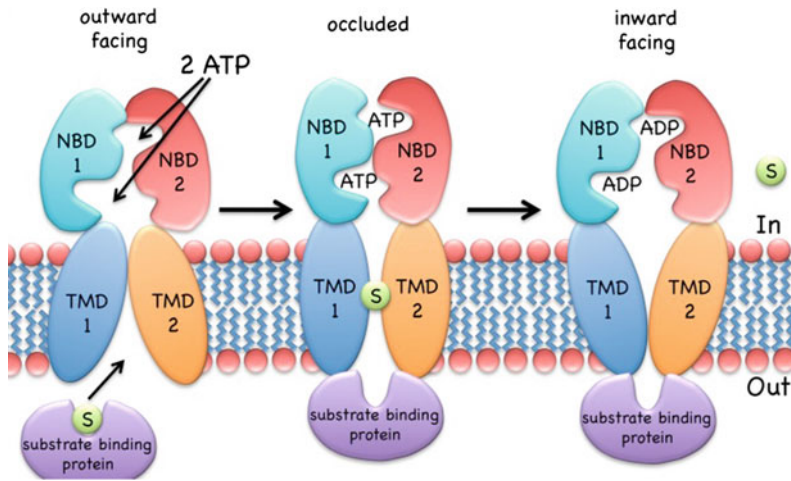


Fig. 6.21 Catalytic mechanism of ABC transporter A. The outward-facing type II importer binds to substrate at binding domain with two molecules of MgATP. The nucleotide domain dimerization because of binding results in the closed conformation with substrate confined to

center of cavity mid-membrane. The ATP hydrolysis and NBD dissociation allow substrate to escape into the cytoplasm. <https://www.ncbi.nlm.nih.gov/pmc/articles/PMC4338842/figure/002/Page3of3>

opposite direction to each other. TMD1 and TMD2 heterogeneous helices are further divided into three separate fold as Type ABC transporter, Type II ABC transporter, and ABC exporters' folds. In outward positions, the TMD helices are in extended wing because of TM1 and TM2 from one subunit and TM3 and TM6 from other subunit. TMD primarily interacts with variable Q-loop with conserved glutamine in α -helical domain. Any change in Q-loop is directly coupled to ATP hydrolysis and conformation change of TMD. Walker B-loop participates in binding. Magnesium interaction with ATP requires D502 of Walker B. ABC transporters utilize two ATPs per one molecule of substrate transport. In addition to substrate binding, two sets of amino acids of D-, Q-, and H-loops are required for catalysis. One set acts as general base to activate water molecule to attack on γ -phosphate group of ATP, and other set of amino acids stabilizes phosphate oxygen. The amino acid E502 near Walker B, Q422 of Q-loop and H534 in H motif essentially contributes to catalysis. ATP molecule is bound at interface between TMD and NBD, and terminal γ -phosphate is positioned between P-loop and LSGGQ signature sequence.

The most important factor in catalysis is the relative position between NBD and TMD domain because of ATP, ADP, and substrate binding. The transport cycles move in order of substrate binding, hydrolysis, substrate release, which induces TMD conformation change from close form with bound ATP to open form without ATP. The change in conformation stimulates substrate translocation also.

6.9.2 Classification of ABC Transporters in Mammals

ABC transporters are ubiquitously found in lung, brain, muscle, spleen, endosome, and rod photoreceptors in mammals. These transporters are classified into various classes as ABCA, B, C, D, E, F. The class ABC A transporters of 12 members are basically involved in transport of phospholipids and cholesterol to HDL. In lung, they protect cell surface (Table 6.1).

These are multidrug transporter and efflux N retinyl-diester-phosphatidyl ethanol amine. The ABC B class of 11 members are found in kidney, brain, ER, liver, and mitochondria. These

Table 6.1 HGNC database of human ABC transporters, genes, classification, and function

Gene	Chromosome location	Exons	AA	Accession number	Function
<i>ABCA1</i>	9q3 1.1	36	2261	NM005502	Cholesterol transport into HDL
<i>ABCA2</i>	9q34	27	2436	NM001606	Resistance to drug
<i>ABCA3</i>	16p13.3	26	1704	NM001089	Multidrug resistance
<i>ABCA4</i>	1p22	38	2273	NM000350	<i>N</i> -retinylidene-phosphatidyl ethanolamine (PE) efflux
<i>ABCA5</i>	17q24.3	31	1642	NM018672	Diagnostic marker in urine for prostatic intraepithelial neoplasia (PIN)
<i>ABCA6</i>	17q24.3	35	1617	NM080284	Multidrug resistance MDR
<i>ABCA7</i>	19p13.3	31	2146	NM019112	Cholesterol efflux
<i>ABCA8</i>	17q24	31	1581	NM007168	Transports particular lipophilic drugs
<i>ABCA9</i>	17q24.2	31	1624	NM080283	Might play a role in monocyte differentiation and macrophage lipid homeostasis
<i>ABCA10</i>	17q24	27	1543	NM080282	Cholesterol-responsive gene
<i>ABCA12</i>	2q34	37	2595	NM173076	Has implications for prenatal diagnosis
<i>ABCA13</i>	7p12.3	36	5058	NM152701	Inherited disorder affecting the pancreas
<i>ABCB1</i>	7q21.1	20	1280	NM000927	Multidrug resistance

are involved in multidrug resistance. They are involved in peptide transport to ER. The C class of 11 members, present in all tissues, is involved in drug resistance, organic anion, nucleoside, chloride ion transport. ABC D of four members are identified in peroxisomes. ABC E class has only one member. The ABC F is also present in all tissues. The ABC G of eight members regulates transport of cholesterol and other sterols.

6.10 Lipid Transporters in Maintaining Membrane Asymmetry

The plasma membrane has to maintain lipid asymmetry for biological functions and requires constant and regulated transport of membrane components for the purpose. The nonpolar molecules can translocate easily from inner to outer in other direction but lipids with polar group are transported by transporters in ATP-dependent manner. There are three major transporters which are known as **flippases**,

floppases, and **scramblases**. The flippases are also known as P4 ATPases, which transport phospholipids to inner leaflet of membrane and have substrate specificity to phosphatidyl serine and phosphatidyl choline. The flippases' transporters may cause change in shape of membrane like bending of the membrane for vesicle formation or vesicle budding. In erythrocyte, amino phospholipid flippases are identified for PS and PC transportation to inner membrane.

ATP8B1 flippase is a phosphatidylserine translocase in human. The other enzyme, **flop-pases**, belongs to ABC transporters' large family, which transport polar lipids to outer membrane in energy-dependent mode for transport. **P-glycoprotein** floppase is a multidrug resistance protein in human.

The scramblases can transfer lipid in both the directions without requiring energy. These are activated by calcium during membrane injury, apoptosis, or coagulation and transport PS and PE to outer leaflet for destroying lipid symmetry. **Phospholipid scramblases (PLSCRs)** are palmitoylated proteins of lipid raft, which is under regulation by phosphorylation and

dephosphorylation. Unphosphorylated form localizes in nucleus, where it interacts with topoisomerases and is required for cell division.

6.11 Aquaporins

Water is the main component of life, and its exchange is characteristic of any living being. First water channel proteins, known as aquaporins were first isolated from RBC and later from renal proximal tubule membrane Peter Agre group in 1992.

Aquaporins (AQPs), the integral proteins of membrane, are small, hydrophobic, and homotetramer proteins, which are involved in bidirectional transport. These proteins are present in all living beings. The aquaporins may facilitate the transport of urea, nitrate, NO, hydrogen peroxide, carbon dioxide (CO₂), and Ammonia (NH₃) along with water. Numerous identified isoforms are differentially expressed and modified by posttranslational processes for tissue-specific osmoregulation in various organisms. In mammal, aquaporins are involved in multiple physiological processes including urine concentration by kidney tubules, nerve transmission, metabolism of lipids, fluid secretion, tissue swelling, cell migration, and salivary gland secretion along with skin hydration. The genetic defects in aquaporins may lead to disorders like kidney dysfunction, loss of vision, and brain edema. According to their substrate specificity and localization, the aquaporins are divided into two subgroups:

1. **Classical Aquaporins** are exclusively water channels.
2. **Aquaglyceroporins** are the proteins with broader specificity for nonpolar molecules like polyols, glycerol, ammonia, CO₂, NO, urea along with water and may participate in nutrient uptake and osmoregulation but bacterial glycerol facilitator GlpF only allows the movement of polyols. The unusual aquaporin 6 acts as anion channel. The aquaporins are mostly found in plasma membrane but may be localized inside the cell organelle

membrane. The movement of water and other solutes through aquaglyceroporins (AQPs) supports bidirectional downhill movement through pore or channel formed by aquaporins. The number of genes identified for coding aquaporins in various organisms is variable with one or two genes in bacteria and yeasts, around 13 in mammals (7 are for Renal tubules to concentrate urine) and more than 38 genes in plants. Aquaporins are highly selective and efficient for the transport of water and glycerol but do not allow hydroxide, hydronium ion, and proton movement. This selective transport protects the membrane electrochemical gradient (Figs. 6.22 and 6.23).

6.11.1 Structure and Function of Aquaporins

The active form of AQPs are homo-tetramers. Each monomer of 26–30 Kd contains 300 amino acids with six transmembrane helices (TM1-6) and five connecting loops (A–E). The primary structure of aquaporin oligomer is made of symmetrical two halves, hemipore-1 (transmembrane 1–3) and hemipore-2 (transmembrane 4–6), as shown in Fig. 6.24. The transmembranes are arranged into two halves of 2, 1, 6 and 5, 4, 3, connected by loops to form channel. The four monomers together form a central pore or channel for ions and gases to move but water is not allowed through this central channel. The water diffuses through individual monomers of aquaporins. The three connecting loops A, C, E are externally located, while B and D face cytosolic side. The two loops, one from each side B and E, have signature motif of aquaporin family (major intrinsic family) asparagine, proline, and alanine (NPA). There are two conserved sequences of NPA in aquaporin channel with two asparagine side chains toward pore at the end of hemipore. All transmembranes have their N-terminal and C-terminal in cytoplasm. The B-loop entering from extracellular side and E from other cytosolic side create seventh

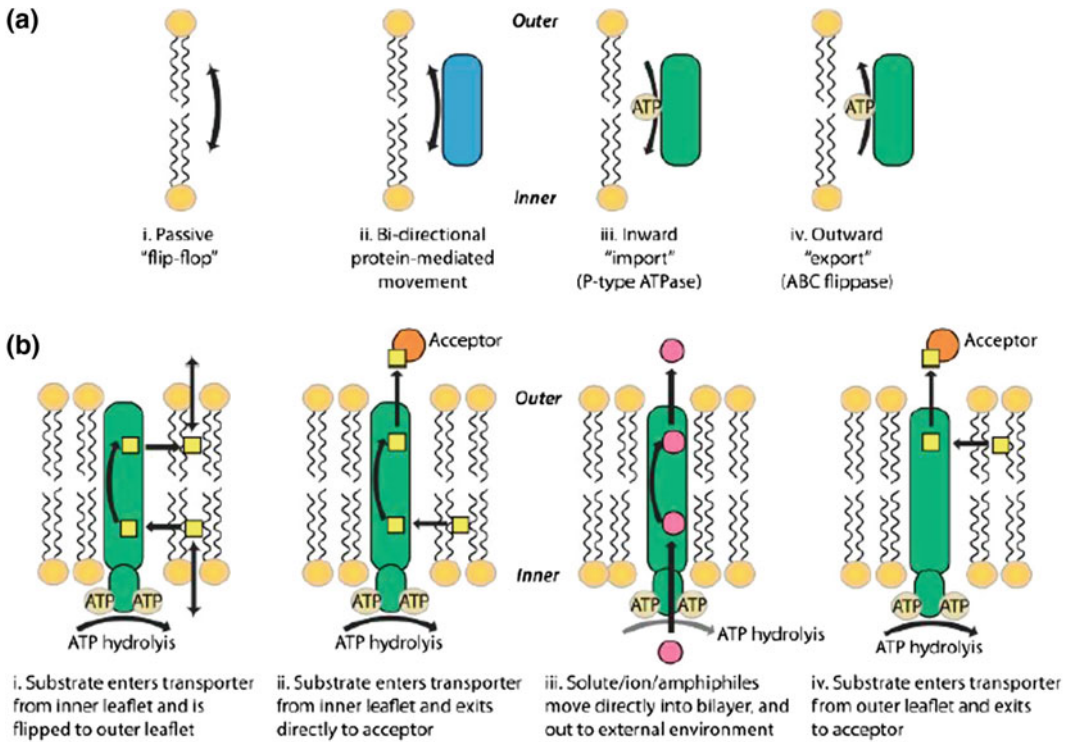


Fig. 6.22 Transporters involved in maintaining lipid asymmetry in membranes. Mechanisms of transbilayer lipid movement

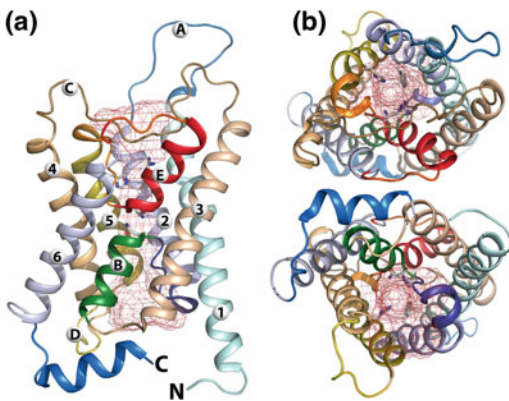


Fig. 6.23 Bovine aquaporin structure. **a** Lateral view showing transmembrane 1–6 and connecting loops A–E with pore of red mesh. **b** Aquaporin from upper side and from lower side

alpha-helical domain to form a part of surface for water channel.

If water is moving from outside to inside, it has to interact with side chain carboxylic group

of amino acid at the surface of aquaporin. The presence of arginine and aromatic amino acids at the narrowest part of the pore is the final selection for any molecule to enter. The overlapping of asparagine, proline, and alanine (NPA) in the center of pore reduces the size of pore for movement, which is important for water molecule interaction for selectivity. The water-specific aquaporin is observed with pore size of 2.8 Å, so bigger molecule or proton will not pass. After interaction with surface protein side carboxylic group, the water molecule will be selected by polar or nonpolar amino acid residues of pore wall proteins, which will provide channel specificity of molecule and will determine the rate of transport.

Figure 6.25 shows the various important amino acids found at pore site. The B and E short helices from opposite side of the pore with positive-charged amino acids with their side group projecting toward center play an important

Fig. 6.24 Aquaporin diagrammatic representations of transmembrane (1–6) and connecting loops (A–E) with signature motif Asn–Pro–Ala (NPA). **a** Shows the linear arrangements of the transmembrane protein showing the two separate regions of helical domains. **b** Two separate regions interact to form the three-dimensional orientation of the protein. The aquaporins pore is composed of two halves (hemipores). The diagram shows the two hemipores interaction to form the functional aquaporin

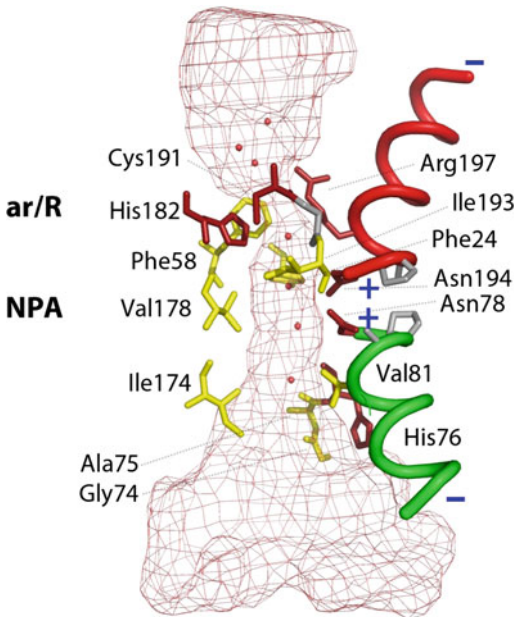
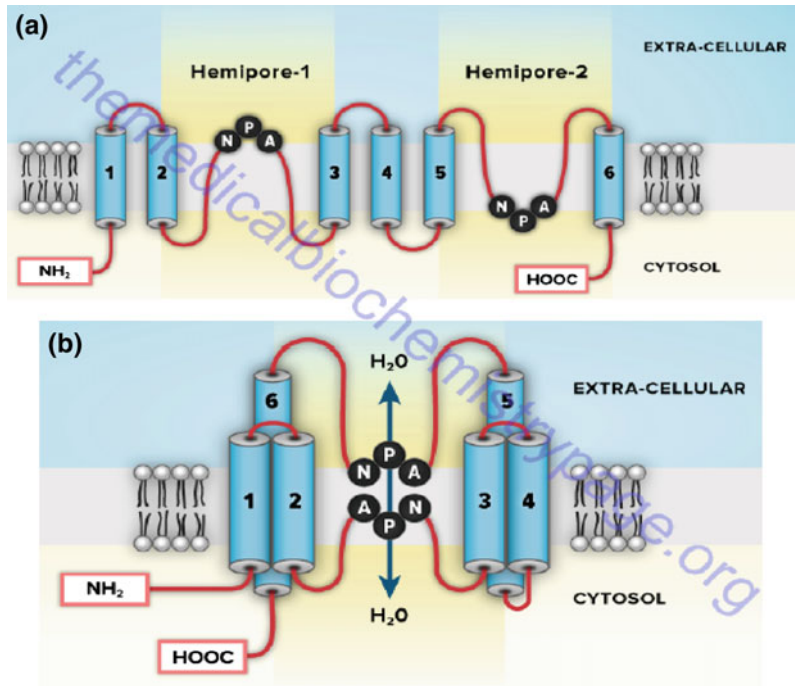


Fig. 6.25 Bovine aquaporin (AQP1) detail structure of pore region with conserved NPA provides interaction mechanism of channel with water. Half helices dipoles and the hydrophilic and hydrophobic residues lining the pore are shown in red and yellow, respectively; the aromatic/R and NPA selective filters are shown as well (Color figure online)

role in selection because of their dipole nature. At the constricted site of NPA with conserved aromatic and arginine amino acids, water ionic bonds become weak. The aromatic amino acids may vary in various aquaporins. In bovine aquaporin (AQP1), phenylalanine and arginine form constriction site. Histidine 182 at surface of pore provides ionic interaction to water molecule, while phenylalanine 58 repels water. After clearing Aro/R constriction site, the water molecule interacts with two conserved NPA sequences and its neighboring amino acids, where protruding valine pulls water molecule to interact with asparagine 194 and asparagine 78 in NPA segment. In the pore, the electrostatic interaction of the NPA repeats and the aromatic/arginine (ar/R) constriction results in the exclusion of protons. These amino acids' segment of NPA is strong lipid anchor for changing water orientation, which is also supported by strong dipole of B and E helices to change water dipole in opposite side to previous one. The NPA amino acids are preceded and followed by hydrophobic residues (isoleucine 193 and phenyl alanine 24 before and glycine 74,

alanine 75 and valine 181 after NPA sequence). These hydrophobic residues stop water interaction with other amino acids of wall proteins for faster movement. Tyrosine 31 of D-loop is found responsible for closing of channel because of its insertion into NPA site. The phosphorylation at serine 107 of aquaporin induces change in conformation, which may open aquaporin channels, because serine 107 is present in B-loop, which is directly connected to tyrosine 31. These channels are very fast to have permeability of water 3×10^9 mol/s.

The aquaporin channels may be regulated by concentration gradient of water, phosphorylation and dephosphorylation, temperature, and pH. This has been observed in plants that decrease in pH may close the channel because of histidine protonation in D-loop. The mercury chloride binding to cysteine at NPA site also closes aquaporins channel. Vasopressin in kidney may activate channels through cAMP-induced phosphorylation. The genetic defect in human aquaporins AQP2 leads to diabetes insipidus. Ca^{2+} is found to regulate translocation of AQP2 to the

plasma membrane. AQP2 overexpression because of **heart failure** leads to water retention. AQP's role in homeostasis of the cerebrospinal fluid (CSF) and neuron excitability is well-established (Table 6.2).

6.12 Active Transport Through Group Translocation in Bacteria

6.12.1 Phosphoenolpyruvate (PEP): Carbohydrate Phosphotransferase System

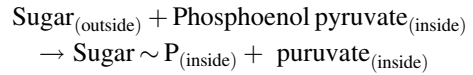
The bacteria take nutrients from their surroundings by various modes of transport but the transport of sugars and its derivatives like sugar alcohols, amino sugars, glucuronic acids, disaccharides is transported by group translocation with histidine heat resistance protein HPr as high-energy phosphate donor protein. The transporting sugar molecule is also

Table 6.2 Classification of aquaporins in mammals

S. No	Name of aquaporins	Classification	Function
1	Aquaporins 1, 2, 4, 5, 6, 10, and 8	Water channels	All are found to be major water channel
	Aquaporins 0, 1, and 6		Transport water, nitrate, chloride ions, and ammonia
	Aquaporins AQP8		Water and ammonia
	Aquaporins 3, 7, and 9	Aqua-glycero-porins	In general, allow diffusion of water, glycerol, urea but some small neutral solutes are also allowed
	AQP9	Nonpolar small solute channel	Transport water, glycerol, urea, purines, pyrimidines, and mono-carboxylates
	AQP11 and AQP12	Intracellular proteins	
	AQP11	Endoplasmic reticulum	Regulate ER integrity
	AQP6		Localized specifically to organelle membrane of endosome

phosphorylated during transport, which makes sugar negatively charged. The phosphorylation of sugar does not change intracellular concentration gradient and also check sugar leakage from cell. The seven families of phosphotransferases have been identified in various groups of bacteria with mostly conserved sequences and dissimilarity in substrate specificity. During this transport, the sugar is chemically modified across the membrane and that's why this transport is also called as group translocation transport. The phosphotransferases complex has cytoplasmic, peripheral, and integral proteins. The cytoplasmic proteins are constitutive and nonspecific, which are involved in group translocation of various other proteins also. The cytoplasmic proteins comprise of heat-resistant histidine protein HPr and Enzyme E1. E1 protein has histidine 189 at N-terminal, which participates in reversible phosphorylation of HPr, and its C-terminal domain is required for protein autophosphorylation by PEP. HPr is small monomeric protein, which is phosphorylated at N-terminal histidine 15 by $E \sim P$. The cytoplasmic PTS proteins or membrane-associated hydrophilic PTS domains undergo **transient phosphorylation** during transport of sugars. The integral membrane proteins are known as Enzyme II (EII), which participate in substrate translocation and its phosphorylation. The EII enzymes are inducible and substrate-specific proteins, which include EIIA, cytoplasmic protein, A peripheral protein associated with inner membrane EIIB, and carrier integral protein EIIC. EIIA and EIIB are sugar-specific proteins. EIIA for glucose is phosphorylated at histidine 90. The EII component may be separate or fused in different organisms. EIIA is conserved; EIIB is hydrophobic which is phosphorylated at conserved cysteine residue by EIIA. EIIC has 6–8 transmembrane regions with one conserved GXXE motif in hydrophobic loop. Protein EIIC has three periplasmic (2, 4, 6 loops) and two cytoplasmic (3 and % loops). In *Bacillus subtilis*, oligo- β -glucoside-specific PTS has three separate enzymes, while in the same organism, mannitol PTS has EIIB fused with EIIC.

The PTS catalyzes the general reaction of sugar transport as



The reaction cycle starts with transfer of phosphate group from PEP to a histidine residue on Enzyme I. The Enzyme EI transfers this phosphate to HPr protein on histidine 15. In the next step, this phosphate group is transferred from HPr to EIIA protein again on histidine residue. The specific Enzyme EIIA for sugar transfers phosphate to the cysteine residue of Enzyme IIB. Finally, Enzyme EIIB transfers phosphate group to EIIC bound sugar, which is phosphorylated and translocated to cytoplasm (Fig. 6.26).

The majority of sugars are transported in phosphorylated form but fucosyl- α -1,3-*N*-acetylglucosamine in *Lactobacillus casei* is translocated in unphosphorylated form exceptionally. Some sugars are immediately dephosphorylated after translocation in cytoplasm like mannose in *Enterobacter faecalis*. The glucose uptake is enhanced by the availability of nitrogen in bacteria through these phosphotransferases.

6.13 Light-Driven Transport

The various organisms have specialized proteins of rhodopsin family to seize light energy for various physiological functions. The rhodopsin protein part, opsin, is covalently linked to retinal chromophore, which may be in *trans*- or *cis*-configuration. The animal rhodopsin (also known as Type II) are cell G-coupled receptors, while microbial rhodopsin (Type I) may act as ion pump, ion channel, sensor, photosensory receptor, regulator for gene expression or a kinase. *Halobacterium salinarum* has normal respiration in the presence of O_2 and high nutrients, but in the absence of nutrients, it survives by using light energy, which is identified with purple patch on the bacterial membrane because of retinal base. The three microbial pumps are well-characterized in their structure and function known as the bacterio rhodopsin H^+ proton pump, channel

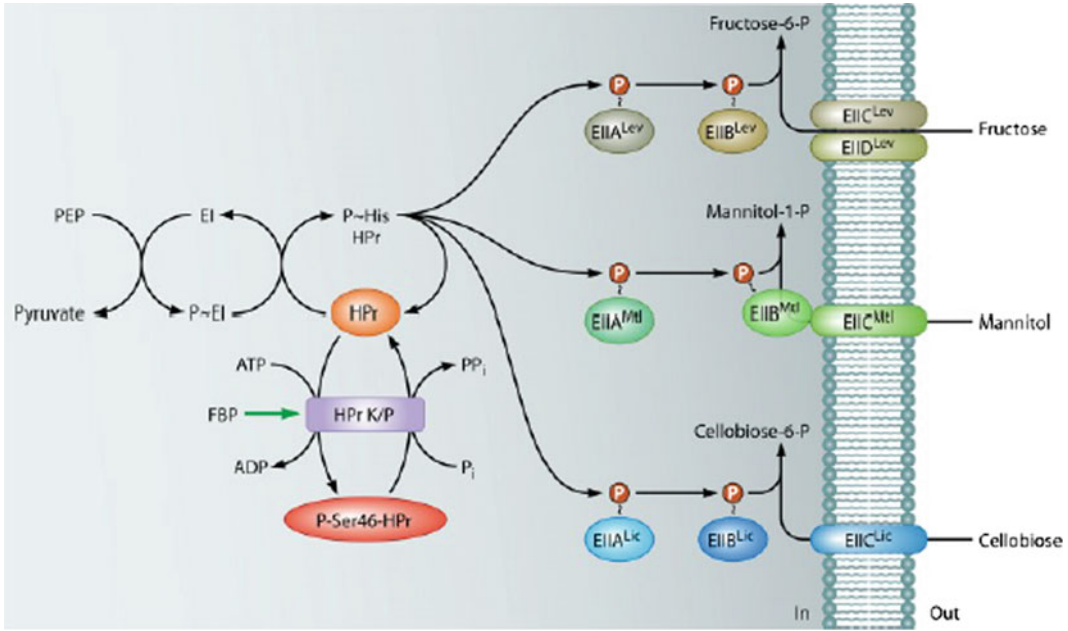


Fig. 6.26 Transport of sugar fructose (PTS), mannitol (PTS), and cellobiose (PTS) by group translocation in *Bacillus subtilis*, which has nine complete PTS, six PTSs without EIIA component, and one PTS without EIIA and EIIB

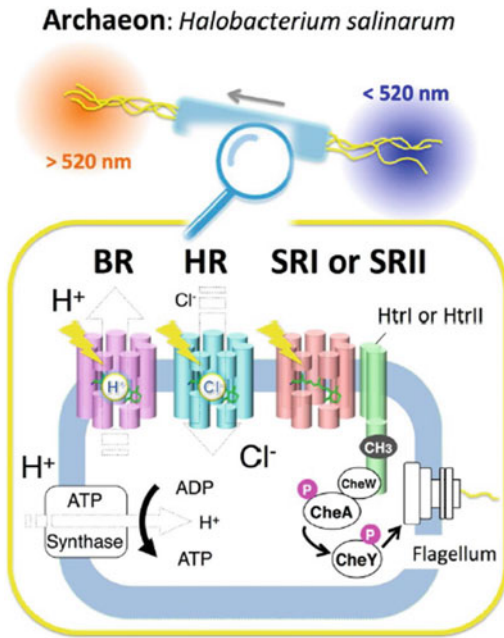


Fig. 6.27 Classical four microbial rhodopsins from the archaeon *Halobacterium salinarum*. The membrane of *H. salinarum* contains four rhodopsins, bacteriorhodopsin (BR), halorhodopsin (HR), sensory rhodopsin I (SRI), and sensory rhodopsin II (SRII, also called phoborhodopsin, pR). BR and HR work as a light-driven

rhodopsin for chloride ion. The *Halobacterium salinarum* has sensory rhodopsin I and sensory rhodopsin II, which activate transducers for senses (Fig. 6.27).

The animal and microbial rhodopsins are transmembrane of 7 α -helices, covalently linked to retinal through lysine residue and form protonated Schiff base with it. The retinal chromophore may be in *cis*- or *trans* configuration. The ground state of microbial and animal rhodopsins has all *trans*- and 11-*cis*-retinal configuration (Fig. 6.28).

Thermodynamically, retinal is preferred in all *trans* configurations in nonpolar environment with absorption maxima at 360 nm wavelength but the protein interaction with retinal shifts this absorption maxima to broader range in visible light range from 400 to 600 nm. The light absorption by retinal stimulates isomerization from *trans-cis* to *cis-trans* in less than a fraction of second. The energy released by this transition isomerization induces change in opsin protein conformation for various activities. The sequences of animal and microbial proteins are quite dissimilar in spite of both having seven

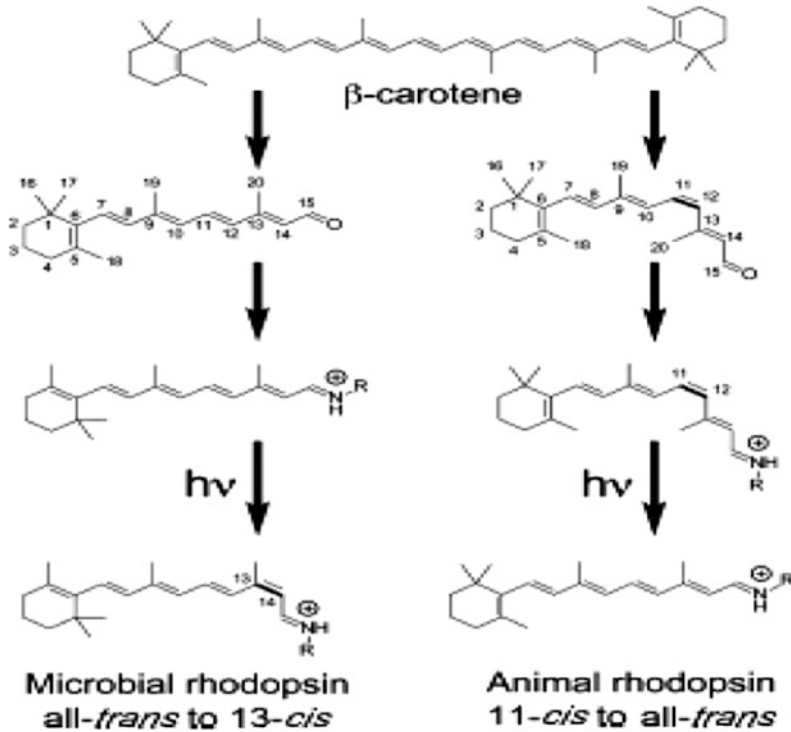


Fig. 6.28 Synthesis of retinal chromophore in microorganism and animal from β carotene. The ground state of microbial and animal rhodopsins possesses all-*trans*- and 11-*cis*-retinal as its chromophore, respectively, bound to a Lys residue via a Schiff base, which is normally protonated and exists in the 15-*anti* configuration. It should be noted that microbial

rhodopsins depend exclusively on all *trans*-retinal, while some animal rhodopsins possess vitamin A2 (C3=C4 double bond for fish visual pigments) and hydroxyl (C3-OH for insect visual pigments) forms of 11-*cis*-retinal. Usually, photoactivation isomerizes microbial rhodopsin selectively at the C13=C14 double bond and animal rhodopsin at the C11=C12 double bond. Post-content

transmembranes. Bacteriorhodopsin translocates one proton inside to outside in cyclic reaction and generates membrane potential across the membrane for ATP synthesis. The channel rhodopsin of *H. salinarum* transports chloride ion from outside to inside of cell for ATP synthesis and for osmotic balance. The sensory rhodopsin I (SRI) acts as stimulator of positive phototaxis, while SRII works oppositely. The bacterial movement toward particular wavelength light is positive phototaxis and moving away is negative. SRI (580 nm λ_{\max}) and SRII (500 nm λ_{\max}) perform through their transducers and cotransducers. The cotransducers are named as HtrI for SRI and HtrII for (SRII). SR proteins with their cotransducers are localized in cell membrane in 1:1 ratio to form tetramer. The signal induced by retinal *trans-cis* isomerization by light is propagated to

cytoplasmic transducers CheA and CheY resulting in phosphorylation and Dephosphorylation for flagellar movement in desired direction (Fig. 6.29).

The crystallographic studies and electron density of catalytic side have explained the photocycle of ion transport. The seven transmembranes of opsin protein may be designated as A B C D E F G, which are arranged to cover centrally linked protonated retinal Schiff base to G-helix by lysine 216. Basically, the light absorption by retinal redistributes its own electrons in protonated base resulting in isomerization, proton transfer between various amino acids at catalytic side, water relocalization, and finally change in protein conformation for physiological function. The water molecule at 402 position in catalytic site accepts proton from retinal and

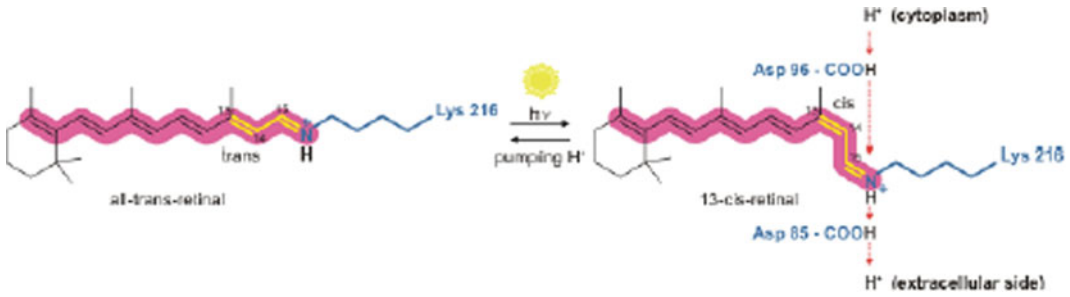


Fig. 6.29 Bacteriorhodopsin molecule is purple and is most efficient at absorbing green light (wavelength 500–650 nm, with the absorption maximum at 568 nm). Bacteriorhodopsin has a broad excitation spectrum

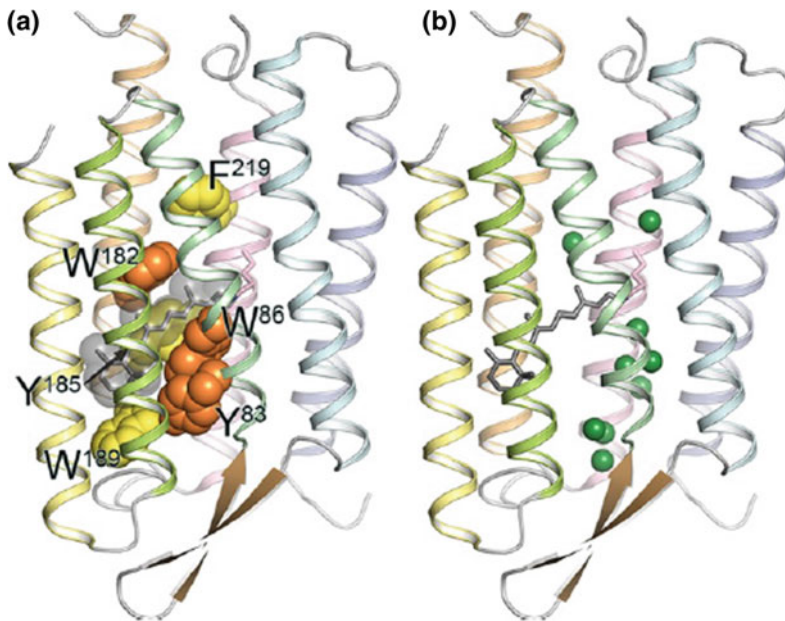


Fig. 6.30 a Structure of bacteriorhodopsin (BR), with conserved aromatic residues highlighted (PDB ID: 1QM8). Tyr83, Trp86, and Trp182 are strongly conserved among microbial rhodopsins (orange). Aromatic amino acids are strongly conserved at the position of Tyr185,

Trp189, and Phe219 (yellow). In BR, Trp86, Trp182, Tyr185, and Trp189 constitute the chromophore binding pocket for all transretinal configuration (gray). **b** Crystallographically observed internal water molecules of BR (shown as green spheres) (Color figure online)

transports it to aspartic acid 85 and asp21. The protonation of Asp85 and retinal deprotonation induce proton movement to outside of membrane, and proton is released. Cytoplasmic proton migration protonates retinal Schiff base to its original position to complete light-induced cycle. The conserved residues involved in proton transfer are shown in Figs. 6.30 and 6.31.

At the ground state of stable active site, the positively charged retinal Schiff base interaction

with three water molecules 401, 402, 406 and aspartic acid (D)85, D212 stabilize separate noninduced light changes fat active site. The H-bond interaction of aspartic acid D85 with threonine T89 asp D212, tyrosine Y57, Y185, and water molecule 406 keeps Asp D85 in anionic form. The aspartic acid D85 and water 406 also interact with positively charged arginine R82. The transition of retinal base from *trans* to *cis* by light will dramatically destabilize this

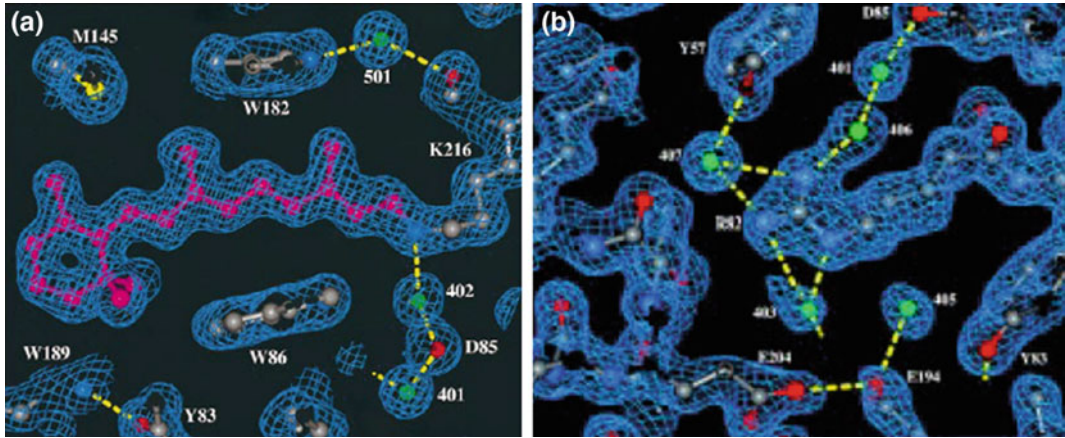


Fig. 6.31 **a** Mechanism of proton transfer by bacteriorhodopsin. The rhodopsin active site detail by electron density map with all transretinal, W86 and W182 covering polyene chain between 9 and 13 methyl group to immobilize retinal site. The H-bond formation from Schiff base to extracellular surface through water 402,

D85 and water 401 is visible. Water 501 links A215 carboxylic group to W185 indole nitrogen, **b** R82 in extracellular half-channel, where its guanidinium group interact with Schiff base through water 406, 401, and D85. Water 407 stabilizes positive charge. Asp85 and Asp212

ground state. The hydrogen bond between these amino acids and water will be disturbed and rearranged, which will cause to disassociation of proton from Schiff base. The asp D85 is first proton acceptor which is centrally located. Water 402 actively participate in hydrogen bond rearrangement because of its position its H^+ and OH^- easily may protonate and deprotonate neighboring residues. The extracellular side of retinal linked to Arginine R82 interacts with three-dimensional hydrogen bond mesh contributed by water molecule 404, 405, 406, and 407 and amino acids. The retinal molecule is linearly connected to arginine 82 through H bonds starting from water 402-D85-water, 412-Arg R82, and other water 402-D212-W57-water407-arg R82 NH_2 /NH $_2$. The whole mesh is interconnected.

The proton release complex with water 403, 404, 405, Glu E 194, Glu E 204 is separated by isoleucine I78 and leuL201 from hydrophilic environment. At the C-terminal of D helices transmembrane, a unpaired buried arginine R134 interacts with salt bridge to glutamate E194 and interacts with carboxylic group of amino acids at 126, 128, and 194 positions. The transmembrane G at cytoplasmic side gets kink because of π

bulging at alanine A215, which results in peptide bending between alanine A 215 and lysine K216. This bending stimulates local rearrangement of H bonding between water and amino acids (Fig. 6.32).

The new hydrogen bonding between molecules and new local arrangements around G transmembrane helices slightly tilt this from center, resulting in C-terminal displacement to outer side, and induce change in conformation. The water molecule at 502 stabilizes this change through interactions with amino acids and carboxylic group of retinal Schiff base. The rearrangement of G helices and water molecule amino acids interactions decrease PKa of aspartic acid D96, which donates proton in photocycle and control reprotonation of aspartic 96 by isomerization of retinal Schiff base from *cis* to all *trans* (Fig. 6.33).

6.14 Pore-Forming Toxins

Pore-forming toxins (PFTs), the bacterial virulence factor, single major family of proteins, are secreted by gram-positive and gram-negative bacteria. **PFTs** may be present either in

Fig. 6.32 Proton transfer interaction of bacteriorhodopsin retinal Schiff base to various amino acids of opsin protein. Representation of retinal Schiff base catalytic domain by electron density map, depicting protonated retinal base and water 402 tightly hydrogen bonded between positive charge Schiff base and two anions D85 and D212. The Schiff base nitrogen atom, water 402, and the two acceptor oxygen atoms of Asp85 and Asp212 are in single plane

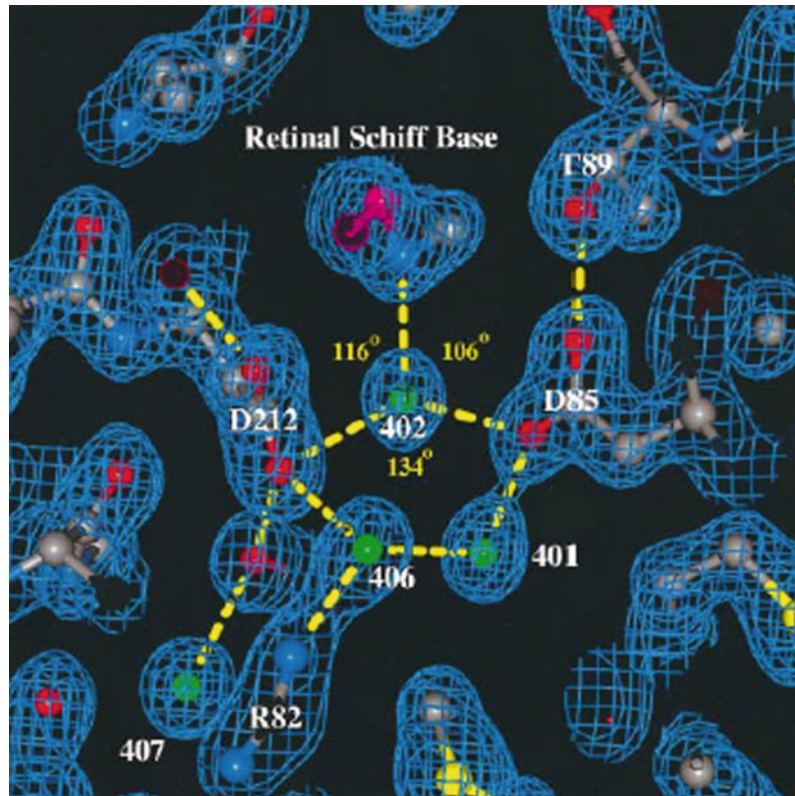
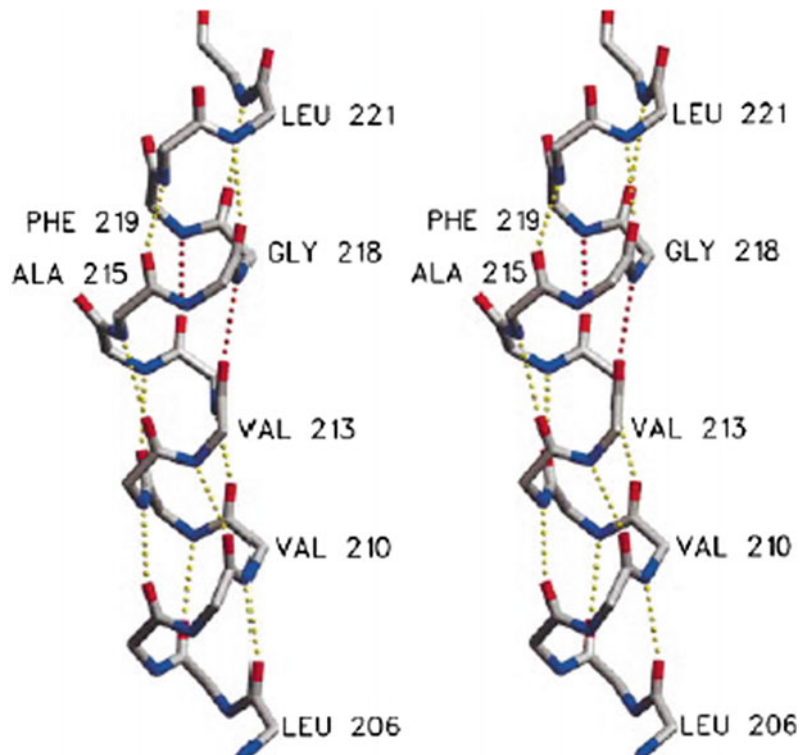


Fig. 6.33 In bacteriorhodopsin helices G at cytoplasmic side, A kink between alanine A215 and lysK216 is produced because of alanine 215 π -bulging. The local hydrogen bonds between water and amino acids are rearranged to release proton



cytoplasm or in the membrane. The conformational change in cytoplasmic PFTs may translocate them to membrane in need of hour. The numbers of bacteria like *Staphylococcus aureus*, *E. faecalis*, *E. coli*, and *Vibrio cholera* had shown the presence of these proteins during pathogenesis. The size of pore may be small (0.5–4 nm) or large (more than 20 nm). Mostly, PFTs are water-soluble. Binding of pore-forming toxin to host cell receptor through sugar, lipids, or protein leads to change in conformation for pore formation. The strength of pore formation is directly proportional to their **virulence power**. As per transmembrane structure of PFTs in host

cell membrane, the PFTs are divided into two groups as **α -PFTs** because of **α -helical pore** and **β -PFTs** because of **β -barrel pore** (Fig. 6.34).

The various molecules in the host membrane may act as receptor molecules like **glycosyl phosphatidyl inositol (GPI)**, **chemokine receptor (CCR5 or CD19)** of white blood cells, **disintegrin** and **metallo-protease (ADAM)**-type proteins, **cholesterol**, and **other lipids**. Pore-forming toxins may change their conformation to adjust in host environment. The pore formed by PFTs may be continuous barrel layer of proteins or may be in toroidal form because of lipid protein interaction.

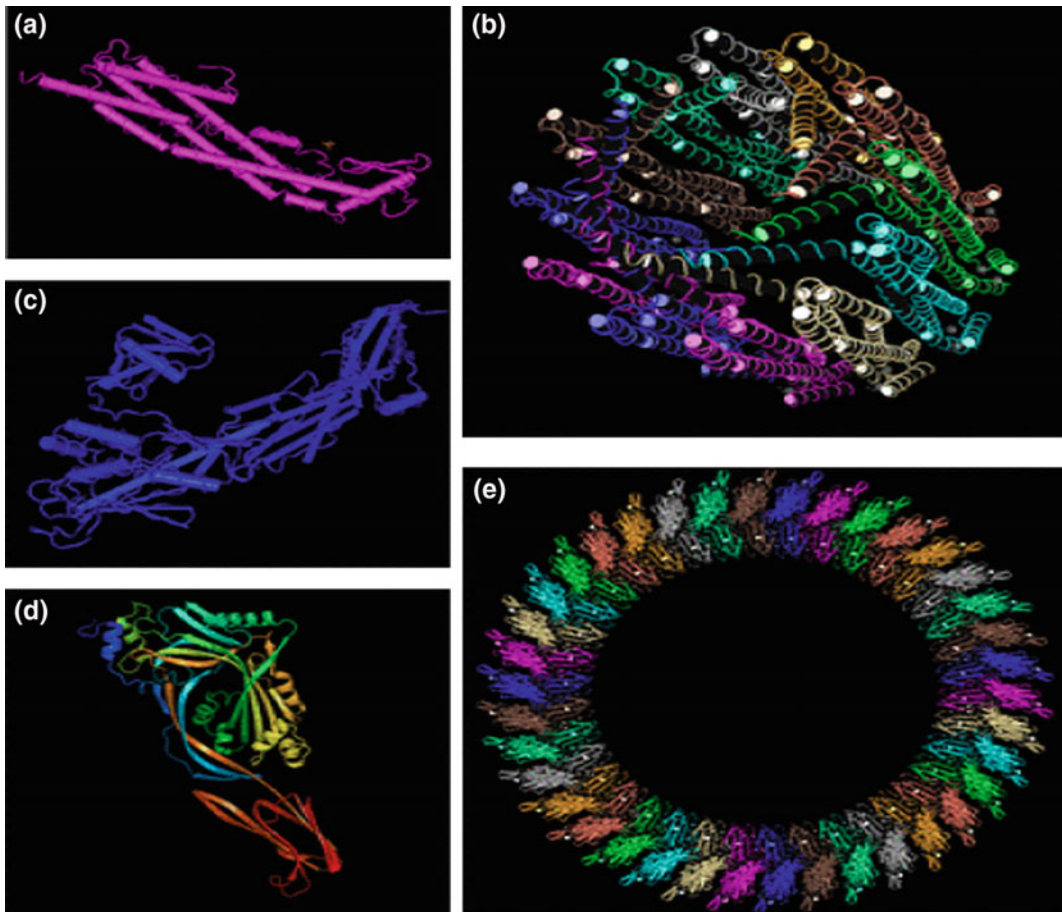


Fig. 6.34 Structure of pore-forming toxin **a** single peptide and **b** multimeric proteins Proteins Data Bank ([PDB] accession number 1QOY). **c** Structure of aerolysin, a β -PFT produced by *A. hydrophila* (PDB accession number 1PRE). **d** PFO monomer (PDB accession number

1PFO). **e** Speculated arrangement of CDC monomers into multimeric pore by mapping PFO monomers onto a PLY cryo-electron microscopy (cryo-EM) image (PDB accession number 2BK1). Structures were visualized using PyMOL (**d**) or MMDB (486) (**a–c** and **e**)

Table 6.3 Pore-forming toxins secreted by common pathogens

Bacteria causing diseases	Major pore-forming toxin proteins
<i>Streptococcus pneumoniae</i> Causes diseases pneumonia	CDC pneumolysins
<i>Streptococcus pyogenes</i> Causes skin disease	CDC streptolysin α (SLO)
<i>Staphylococcus aureus</i> Disease is fatal sepsis and pneumonia	Various small pore-forming β -PSTs Like α hemolysis and γ hemolysis
<i>Mycobacteria tuberculosis</i> Causes tuberculosis	Early secreted antigenic target-6kd (ESAT-6) causes hemolysis by interacting with lipid bilayer
<i>Escherichia coli</i> , though not very virulent, but causes colitis and diarrhea	Two PFTs hemolysin A or α hemolysis and cytolysin or hemolysin E

The major pathogens producing different PFTs proteins are shown in Table 6.3.

The PSTs act first by binding to receptors, which are followed by oligomerization, change in conformation, and insertion into host membrane to form pore. Till date, six families of pore-forming toxins, including three α -PFTs and three β -PFTs, are known. **α -pore-forming toxins** are heterogeneous group with various PFTs like **cytolysin** of *E. coli*, **exotoxin** of *Pseudomonas aeruginosa*, and **diphtheria toxin** from *Corynebacterium diphtheria*.

The various PFTs may form various types of pores with different characteristics. The *E. coli* produced **α -PFTs colicins** family produces pore in other bacterial inner membranes. The isolated colicin A and E1 PFT, according to their function, may be divided into three domains for receptor binding, translocation, and pore formation. The pore-forming domain of colicin has ten α -helices. Two of these hydrophobic helices are surrounded by eight amphipathic α -helices. The hydrophobic α -helices are inserted into inner membrane to make non-specific voltage-gated ion channel. This pore destabilizes membrane potential of host cell. The other α -PFT such as insecticidal **cry** toxin from *Bacillus thuringiensis*, **diphtheria toxin** translocation domain, and eukaryotic protein **Bak**, has shown similar structure like colicin for pore formation. The **colicin** PFT of this group forms the pore by binding to receptor, translocates to periplasm, and causes cell death by forming pore in inner membrane. **Bcl-2**

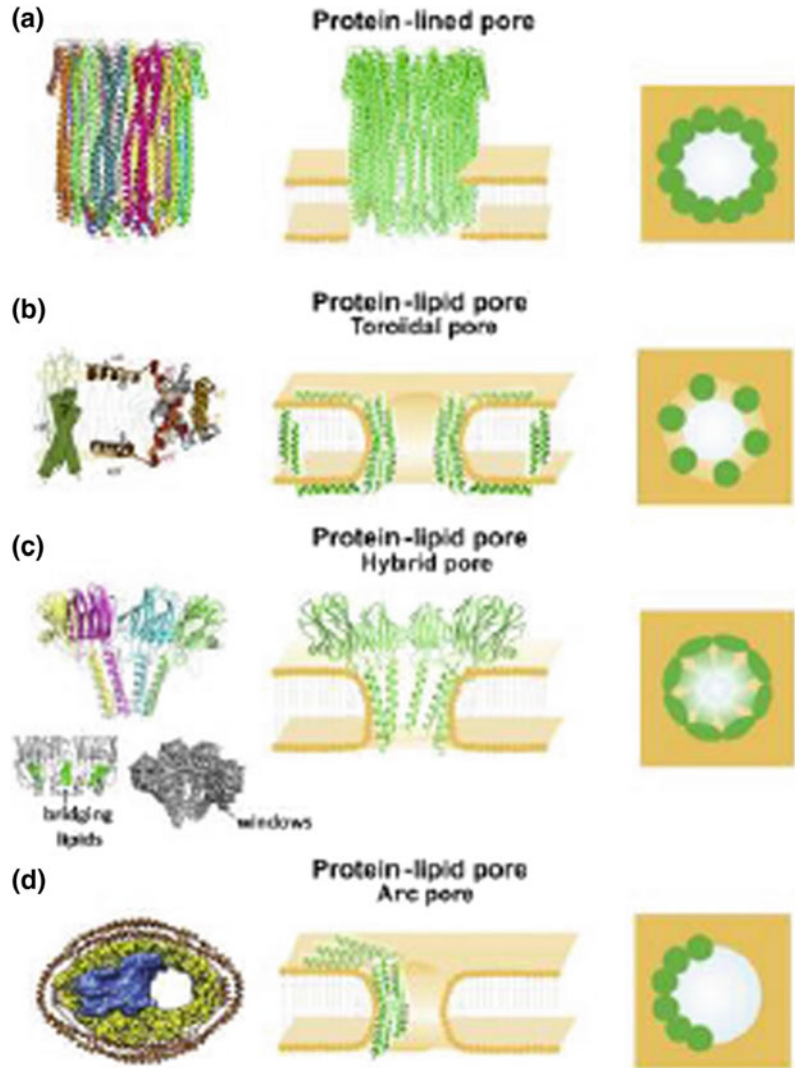
completes pore formation in mitochondria by releasing cytochrome C to activate caspases for apoptosis.

A member of α -PFT **cytolysin** family, cytolysin A(Cly), hemolysin E(Nhe) enterotoxin of *Salmonella enterica* and *Shigella flexneri* and *E. coli* forms pore of 2–7 nm diameter for cation in macrophage leading to apoptosis. Cytolysin A is found to be α -helical protein in elongated shape with short hydrophobic β -strands in tongue shape (β tongue). During formation after assembly, the β -strands become disassociated from the protein for insertion into lipid bilayer; this event causes the rearrangement of N-terminal region of amphipathic helices at the pore site. The N-terminal domain arrangement may vary in length but this variation cause is not clear till now. The conformational change by the N-terminal amphipathic α -helices catalyzes a very organized step-by-step oligomerization of monomers.

There are various ways of protein–protein or lipid–protein interaction for pore formation as shown in Fig. 6.35.

When toxin protein interacts with host lipid for pore formation, lipid may provide a curved nonbilayer shape at pore periphery. In this pore, the protein regulates stress caused by distortion of membrane. As seen in eukaryotic β -barrel **actinoporin** PFT from sea anemones, in which **cation selective pore** is formed by interaction with **sphingomyelin** of host membrane. Usually, the toxins recognize and interact with specific lipid domain of sphingomyelin clustering or cholesterol–sphingomyelin complexes, which

Fig. 6.35 α -PFPs may form pores in various ways (a). Protein-lined pores, **b** protein-lipid pores, **c** protein-lipid pores: hybrid pores, **d** structure of the pore formed by FraC and liposomes (PDB: 4TSY). The bridging lipids connecting two adjacent molecules of FraC are shown in the bottom left side (green) (Color figure online)



support the accumulation of PFTs locally to ease their function of pore formation. This may result in lamellar structure destabilization by lipid transmovement across the membrane (Fig. 6.36).

The β -pore-forming toxins include **aerolysin** and **cholesterol-dependent cytolysin family** (CDC), and these are secreted majorly by gram-positive bacteria and minor by gram-negative bacteria. Gram-negative *Aeromonas* SAPs produces aerolysin as protoxin. The C-terminal cleavage converts protoxin into toxin protein, which is elongated multidomain protein. The aerolysin protein may be divided into four domains; the domains 1, 2, and 4 are together,

and domain 3 is separated. The domain three has multiple short α helices with β -sheet. The domain four (4) interacts with cholesterol for binding by inserting several loops. The domain four (4) has conserved domain of tryptophan residues with three short hydrophobic regions known as L1, L2, and L3. The domain 3 has two transmembrane α -helices in soluble form, which are converted to β -hairpin transmembrane during pore formation.

While α -PFTs start pore formation by the insertion of hydrophobic helices, the β -barrel formation occurs in concerted mode (Fig. 6.37).

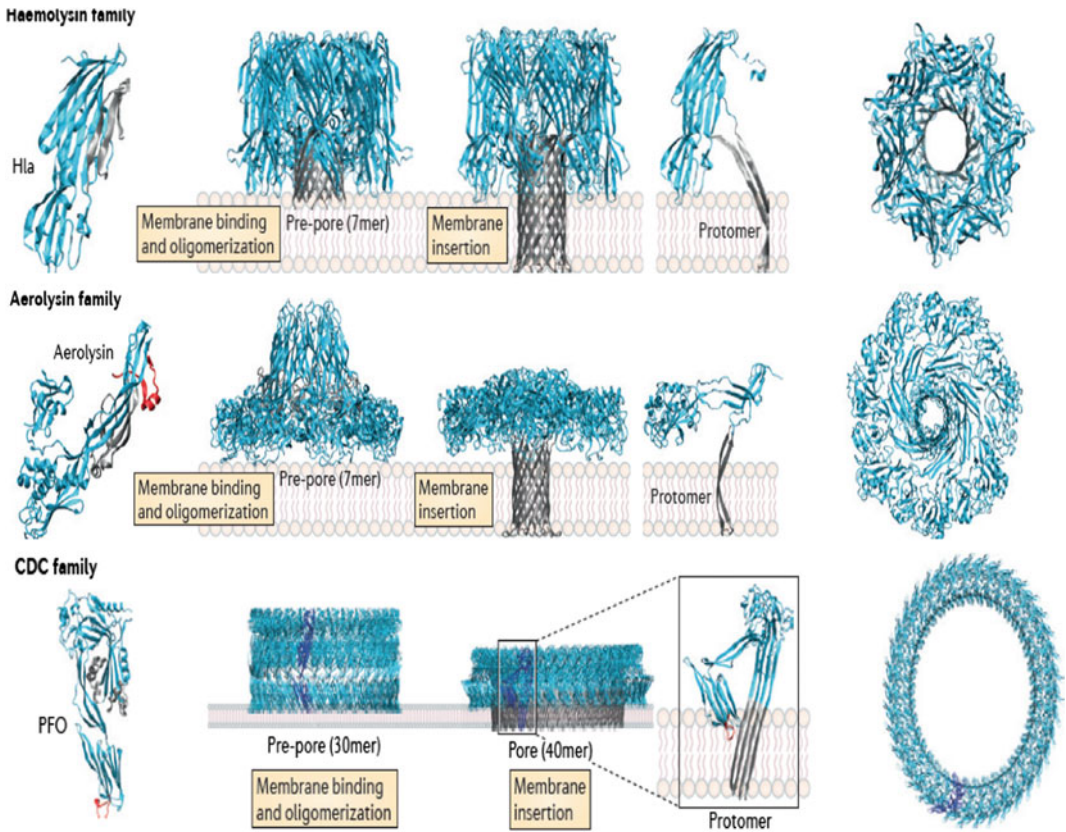


Fig. 6.36 β PFTs, hemolysin, aerolysin, and CDC family pore formation by extraction and insertion and interaction with other monomers of prestem loop of monomers to form beta-barrels

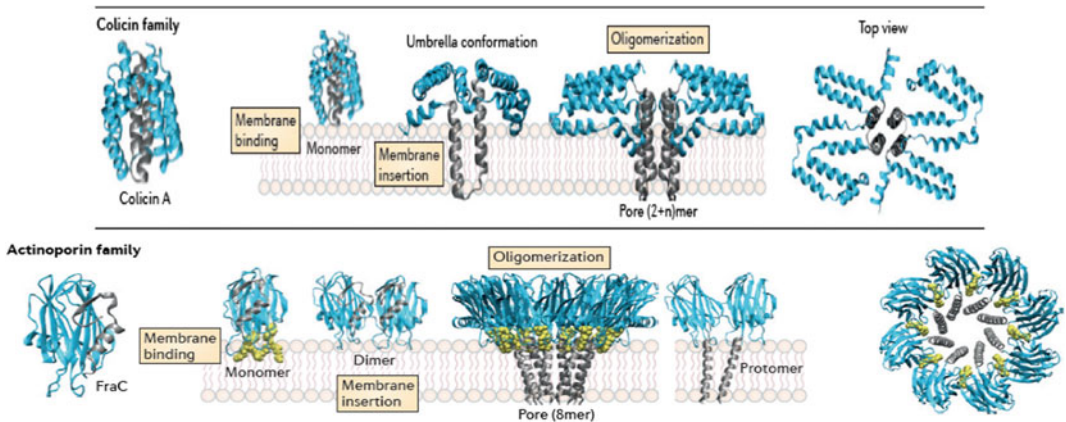


Fig. 6.37 Actinoporin and colicin family PFTs pore formation by monomer alpha-helical hydrophobic segment extraction and insertion into host membrane, umbrella formation, oligomerisation either into two or more peptides

As mentioned above, the other major family of β -pore-forming toxins is **cholesterol-dependent cytolytins (CDC)**, which include perfringolysin O (PFO) of *C. perfringens*, streptolysin O (SLO) of *Streptococcus pyogenes*, pneumolysin of *S. pneumoniae*, and listeriolysin O (LLO) of *Listeria monocytogenes* belong to cholesterol-dependent cytolytin family. These toxins are produced mostly by gram-positive bacteria and by few gram-negative bacteria. The pore formation is dependent on cholesterol for pore formation. In cholesterol-dependent **cytolytin toxin**, pore may contain from 20 to 50 proteins subunits, and each subunit donates 2 β -hairpin for pore unlike other β -PFTs. Cytolysins are produced as monomer or dimer and have some similar features like eukaryotic membrane attack complex (MAC). Cytolysin also has four domains like aerolysin in elongated structure and makes well-defined prepore in the membrane. The CDC,

unlike some other toxins, which rearranges their structure for pore formation, goes under transition from alpha-helices to their β hair pin secondary structure at membrane surface (prepore).

The transmembrane interacts with lipid cholesterol and forms arc-like structure to create Gap (semi pore) in the membrane. At this stage, oligomerization cytolytin monomers occur. The oligomerization transforms the surrounding arrangements of molecules to form functional pore. The conserved tryptophan in toxin and cholesterol play an important role in pore formation (Fig. 6.38).

α -hemolysin (Hla) of cholesterol-dependent cytolytin (CDC) family anchors through N-linked glycan proteins of hosts. Aerolysin binds through glycosylphosphatidylinositol (GPI) anchors. Colicins f α -PFT family interact with lipopolysaccharides (LPS) in the outer

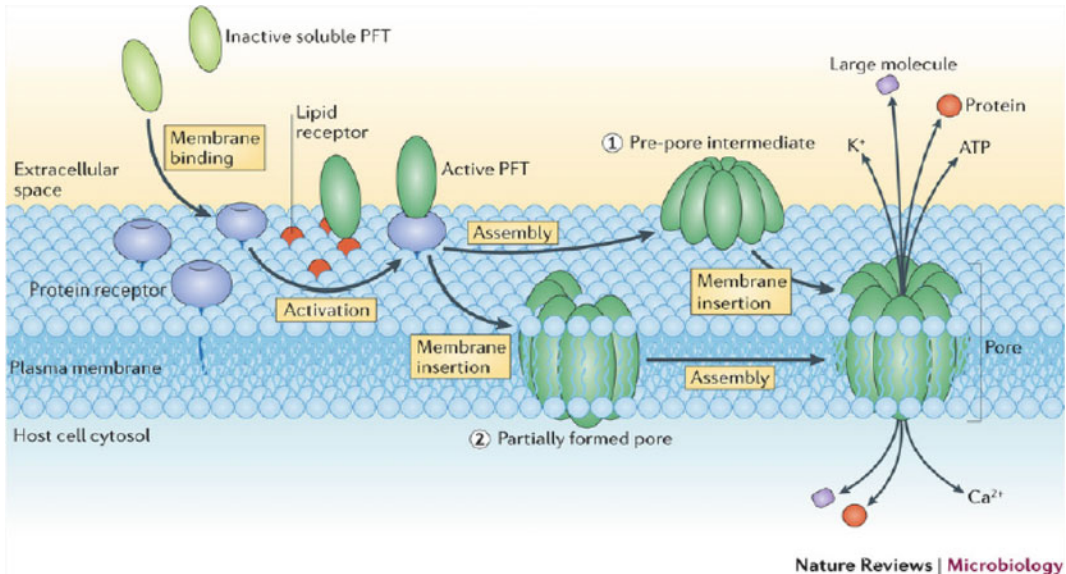


Fig. 6.38 Depiction of pore formation pathway of pore-forming toxins (PFTs). Soluble PFTs are recruited to the host membrane by protein receptors and/or specific interactions with lipids (e.g., sphingomyelin for actinoporins or sterols for cholesterol-dependent cytolytins (CDCs)). Upon membrane binding, the toxins concentrate and start the oligomerization process, which usually follows one of two pathways. In the pathway followed by most β -PFTs, oligomerization occurs at the membrane

surface, producing an intermediate structure known as a prepore (mechanism 1), which eventually undergoes conformational rearrangements that lead to concerted membrane insertion. In the pathway followed by most α -PFTs, PFT insertion into the membrane occurs concomitantly with a sequential oligomerization mechanism, which can lead to the formation of either a partially formed, but active, pore (mechanism 2)

bacterial membrane. α -PFT fragaceatoxin C (FraC) binds to sphingomyelin clustering.

The eukaryotic cell also has pore-forming toxins as the mechanism of their defense, which is known as **membrane attack complex (MAC) or perforin toxins**. The T cell secretes them to destroy pathogen. These toxins like CDC have two transmembrane domains. The **hydrolysin** from cnidaria (phylum of aquatic invertebrate animals), **enterolobin toxin** from *Enterolobium contortisiliquum*, and **human C8** are the examples of eukaryotic toxins.

6.14.1 Activated Signal Pathway and Toxin Effect in Host Cells

The various defense mechanisms against these virulent pore-forming toxins exit in host like human. The binding of toxin to cell membrane may also activate p38 mitogen-activated phosphokinase (MAPK), c-JUN N-terminal kinase like MAPK-KGB1 pathway. *The detail of receptor signaling is discussed in Chap. 9.*

PFTs pore formation may result sometimes in increase in extracellular potassium as a defense mechanism. The potassium efflux activates **nucleotide-binding oligomerization domain (Nod)-like receptors (NLRs)**, which have variable N-terminal domains such as caspase recruitment domain (CARD) and pyrin domain (PYD), which activate apoptosis and inflammation pathways. These receptors are found on immune cells like lymphocytes, macrophages, dendritic cells, and also in nonimmune cells and play a role in innate immunity, phagocytosis, and killing of pathogens. The caspase 1 induces sterol regulatory element binding protein (SREBPs), the regulator of membrane lipid synthesis. The extracellular potassium increases in response to toxin interaction and also activates caspase 2 for inducing apoptosis. The activation of p38 and extracellular response-activated kinase (ERK) brings back potassium level to normal. **α -defensin proteins** are also detected in host to act against PFTs (Fig. 6.39).

Calcium efflux in response to PFTs activates the release of lysosomal enzymes such as sphingomyelinase and hydrolase to degrade pathogenic molecules. Endocytosis is another defense used by host cell. PFTs also interact with cellular signaling, and molecules such as **arthritis** were caused by γ -hemolysin in human. The hemolysin induced the expression of interleukin 6 in osteoclasts. The downregulation of interleukin 12 and nitric oxide synthetase is observed in macrophage by cytolysin toxin.

6.15 Ionophores

Ionophores are natural and synthetic organic molecules of diverse type, which can transport cations by forming lipid ion-soluble complex. Each ionophore possesses a unique property of **changing transmembrane ion gradient and electrical potential**, synthesized by bacteria, and acts as protector against competing microbes. They disrupt membrane's ionic gradient required for proper transport; therefore, they have got **antibiotic properties**. Ionophores increase the permeability of biological membranes to **certain ions and antibiotics**; that's why they are used as growth enhancers as additives in certain animal feed. The various ionophore antibiotics are **macrolides**. The two classes of ionophores are identified as **carriers** and **channels**.

The **carriers** bind to specific ion, shield it from hydrophobic environment, leave the ion on other side of membrane by diffusing across the membrane, and come back without ion to original place. The **carrier polyether ionophores** include approximately more than 130 types having antibiotic properties against bacteria, fungi, and virus. Some of them are found to have antitumor activity also. The antibiotic property of these **polyether ionophores** structure specifies their cation metal binding and is directly correlated to their antibiotic property. The **carrier ionophores** are not found to be effective in gram-negative bacteria because of their cell wall but the opposite is true for gram-positive bacteria. The gram-positive bacterial membrane is permeable for these small molecules. Because of

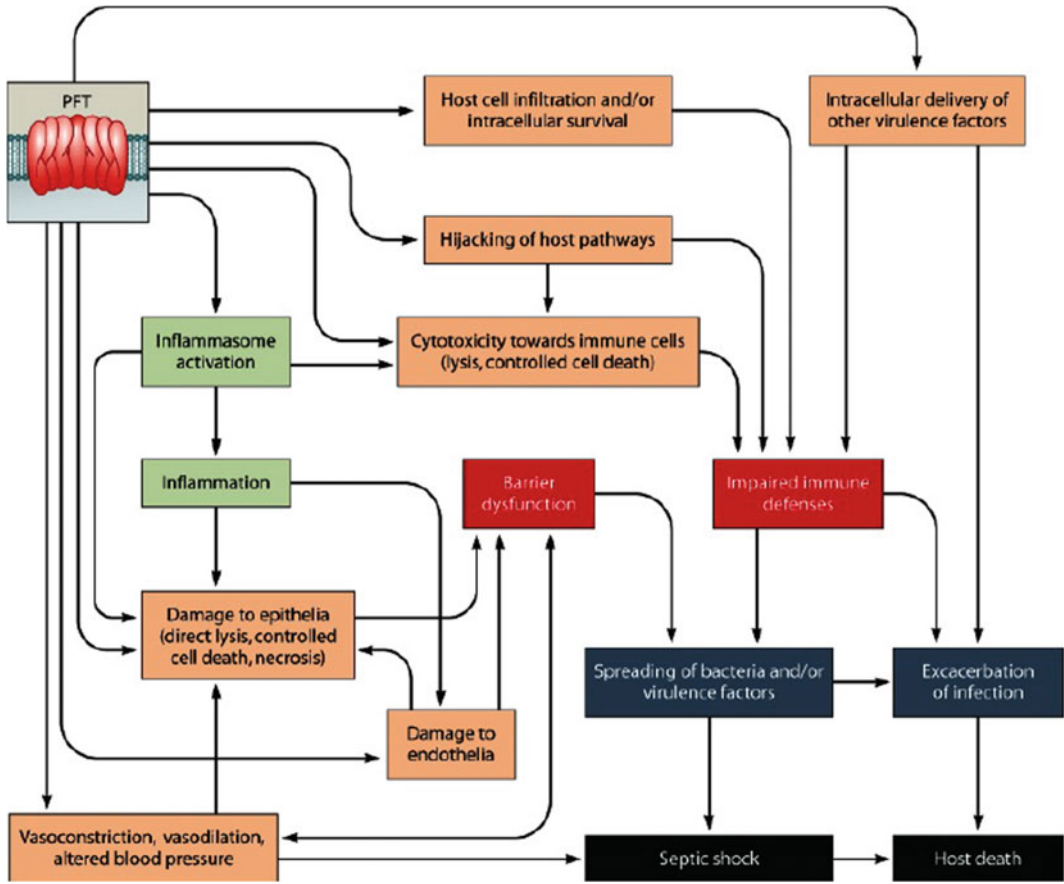


Fig. 6.39 Effect of pore-forming toxin in vivo on host cell by various pathways. *Source* Cosentino et al. (2015)

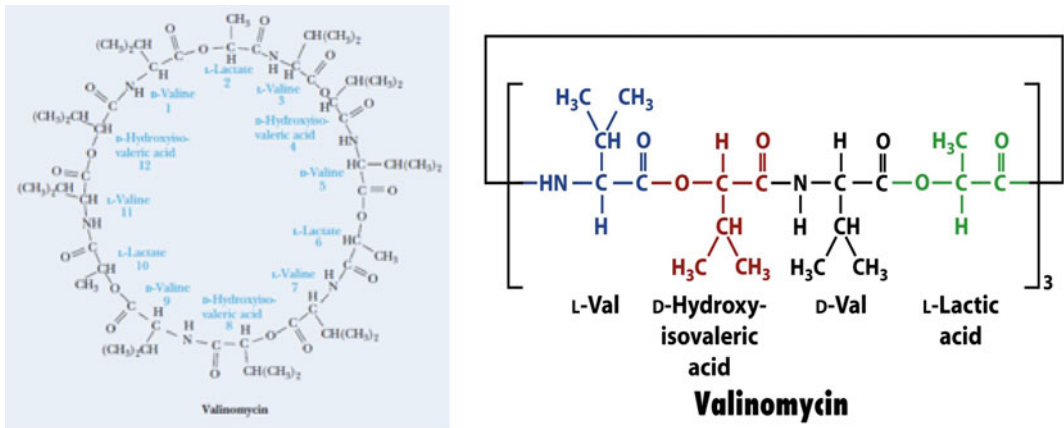


Fig. 6.40 Valinomycin-A carrier ionophore, A, dodecapeptide ring structure, B, L valine-d hydroxy isovaleric acid and D val-L lactic acid, unit arrangement

Table 6.4 Intracellular and extracellular distribution of ions

Ions	Intracellular concentration	Extracellular concentration (mM)
Potassium	148 mM	5
Sodium	10 mM	140
Calcium	Less than 1 μ M	5
Chloride	4 mM	103

this reason, *E. coli* is found to be important for food and human health. The carrier ionophore examples include valinomycin, calcimycin, salinomycin, monensin. Valinomycin is produced by various strains of *Streptomyces* species as *S. tsusimaensis* and *S. fulvissimus*. The valinomycin is highly selective for potassium and Rubidium (Rb^+) ion and does not allow sodium or lithium transport (Fig. 6.40).

The binding and affinity constant for the potassium–valinomycin complex are ten times higher than sodium. Valinomycin was observed to downregulate the lymphocytes multiplication induced by phytohemagglutinins in human. Valinomycin–metal ion interaction essentially requires dehydrating form of ions, and complex is formed in energy-dependent process. The amount of energy required is the deciding factor for forming valinomycin–potassium and rubidium complex but not with sodium (Table 6.4).

As shown in Table 6.3, because of unequal distribution of ions across the membrane, the

electrical potential across the transmembrane is generated, which initiates binding of metal ion to ionophore for diffusion. The movement of ions may decrease or balance electrical potential of membrane. The ionophores may reduce membrane electrical potential through ions movement, which is the basis of their antibiotic property. These metal ion ionophores act as uncouplers like the cell's own uncouplers in mitochondrial respiration. The synthesis of ATP becomes disassociated from electron transport chain. Valinomycin acting as antibiotic may kill the cell by disturbing electrical gradient in transport and energy-generating process. In *S. aureus*, *Listeria innocua*, *L. monocytogenes*, *B. subtilis*, and *Bacillus cereus*, gram-positive bacteria the Valinomycin activity is pH dependent. Recently, the valinomycin is reported to inhibit **severe acute respiratory-syndrome corona virus** survival at 3.3–10 μ M (Table 6.5).

The structural study of carrier ionophore by X-ray has revealed the binding site of ions

Table 6.5 Ionophores specificity to transporting ions

Ionophore	Transporting ions
<i>Carrier ionophores</i>	
Valinomycin	Potassium and rubidium (Rb^+) ion
Monensin	Sodium
Hemisodium	Sodium
<i>Electroneutral carrier ionophore</i>	
Nigericin	Potassium exchange with proton
Calcineurin (A23187)	Calcium-magnesium, calcium-2 hydrogen
<i>Channels</i>	
Gramicidin	Hydrogen > cesium (Cs^+) \approx rubidium (Rb) > potassium (K^+) > sodium (Na^+) > lithium (Li^+)
Nystatin	Monovalent cation and anion

through oxygen atoms in the center of ionophore. Ionophores are neutral complexes with monovalent cations (monensin, salinomycin) and with divalent metal cations (lasalocid, calcimycin). The carboxylic group is deprotonated at physiological pH, so more of neutral complexes are found in the cell. The pseudocyclic structure formed by cation may be stabilized by intramolecular hydrogen bonds of carboxylic group and hydroxyl groups.

The hydrophobic residues of ionophore encircle the ionic interactions for the protection. The polyether ionophore anion ($I-COO^-$) binds the metal (M^+) cation or proton (H^+) and forms either ($I-COO^-M^+$) or ($I-COOH$) depending on pH. This interaction changes Na^+/K^+ ATPases activity to change in gradient of the cell. Resultantly, this may cause the death of the bacteria cell because of increase in osmotic pressure, swelling and bursting of cell by disturbed ATPases. The coordinated geometry between ionophores and ions is important for its function.

The other examples of carrier ionophore, isolated from *Streptomyces chartreuses*, are **calcimycin (A23187)** and **ionomycin** calcium ionophore. Ionomycin hydrolyzes phosphatidyl

inositides in the T-cell membrane to activate phosphokinase C (PKC) through autophosphorylation by phosphorylating T helper cell (CD4) and T suppressor (CD8) cells. The **hemisodium**, synthetic ionophore, transports sodium ions.

The calcium ionophore **calcimycin**, oxidative phosphorylation, and electron transport chain uncoupler are often used for enhancing thyroid and insulin secretion. Calcimycin, because of fluorescent property, may be used as biomarker in membranes for transport study (Fig. 6.41).

Calcium ionophores promote three types of signal in calcium-resistant cell for cytosolic calcium increase: (1) Activate **receptor-mediated calcium** transport into cytosol by native Ca^{2+} channels, (2) **Phospholipase C**-dependent calcium mobilization from intracellular stores like ER, (3) At low concentration of Ca^{2+} , ionomycin in endothelial cell, like histamine, increases cytosolic calcium, while in fibroblast, only intracellular calcium from organelle store releases out. **Beauvericin ionophore** has both antibiotic and insecticidal property. This has phenylalanine and hydroxyl-iso-valine amino acids alternatively to form cyclic hexodepsipeptide. It transports alkaline and alkali metals across the cell membrane. **Beauvericin**, found in *Beauveria bassiana*, wheat, barley, and corn, causes apoptosis in mammals additionally. The other class of **enniatins** ionophores are found in fusarium fungi. Usually, proteins have the characteristic of forming channels in the membrane for transport of various molecules, but some of the ionophore also transport by forming a channel in the membrane. These ionophores have a few unusual amino acids normally not found in proteins. **Gramicidin**, isolated from *Bacillus brevis*, has 15 amino acids, linearly arranged in D and L alternate fashion with amino-terminal formaldehyde and carboxyl terminal ethanol amine. The hydrophobic amino acids in gramicidin support its function in **channel formation**. These channels have outer lining of hydrophobic amino acids to interact with lipid bilayer of membrane with hydrophilic interior for ion interaction. These channels allow very fast diffusion of ions through them in very short period unlike carrier ions. Their size is larger than

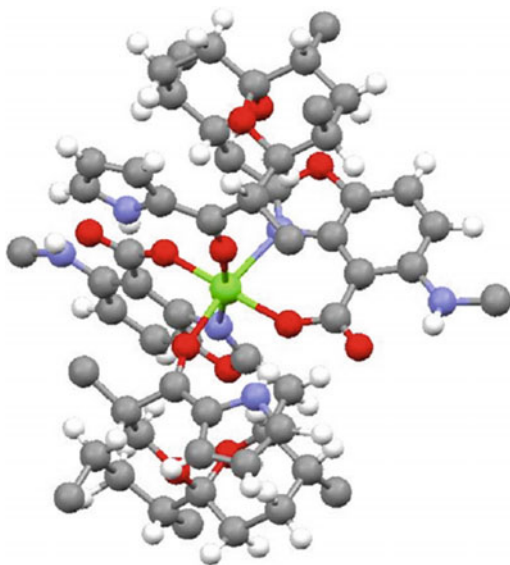


Fig. 6.41 Crystal structure of 2:1 complex of calcimycin with the magnesium cation. <https://www.hindawi.com/journals/bmri/2013/162513/fig6/>

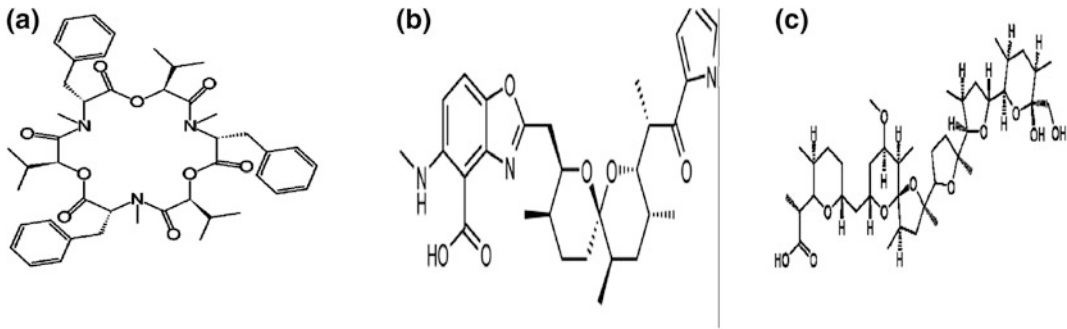


Fig. 6.42 a Structure of beavericin. b Structure of calcimycin and c Nigericin

protein channel. Gramicidin channels allow protons and other cation movements but not of divalent cations like Ca^{2+} , which block them. Gramicidin has antibiotic property against gram-negative bacteria, gram-positive bacteria, and pathogenic fungi but sometimes its hemolytic activity may limit its use. In various solvents, gramicidin has stable amphiphilic antiparallel β -sheet structure with a polar and a nonpolar surface as α -helix is not possible because of alternate D- and L-amino acid residues. Gramicidin has 6.3 residues per turn in β -sheet structure with channel diameter approximately 0.4 nm. The ethanol residue is projected

on the surface and formyl group inserted in membrane. The nonpolar amino acids play a role in microbial specificity, and disrupted beta-sheet structure adds to its antimicrobial activity (Fig. 6.42).

The natural mixture of gramicidin, known as gramicidin A, is observed fluorescent because of tryptophan amino acid. Its antimicrobial activity may be through gene regulation as *E. coli* RNA polymerase was found to be inhibited by gramicidin (Fig. 6.43).

Gramicidin is not synthesized by ribosomes but by cellular enzymes, and at 11 position, it has tryptophan which is replaced by phenylalanine in

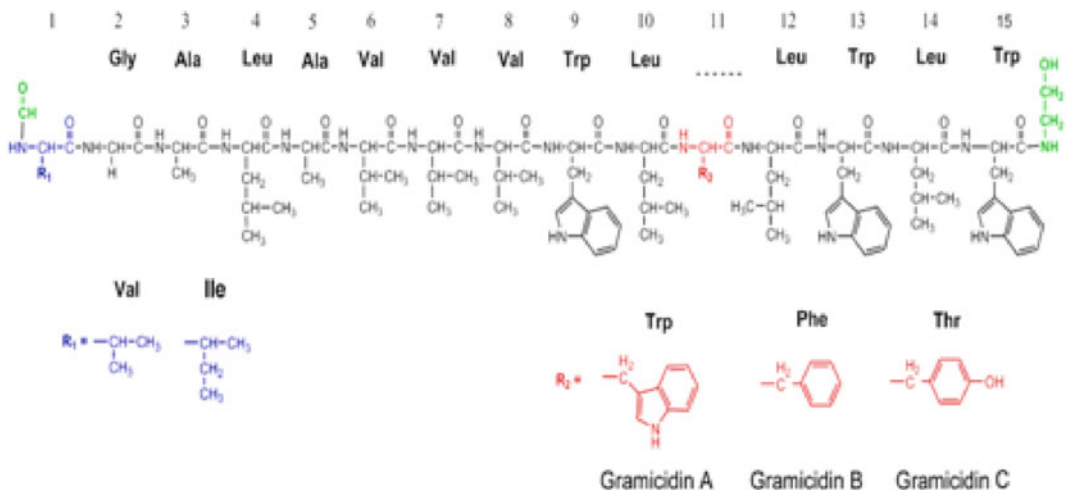


Fig. 6.43 Structure of gramicidin

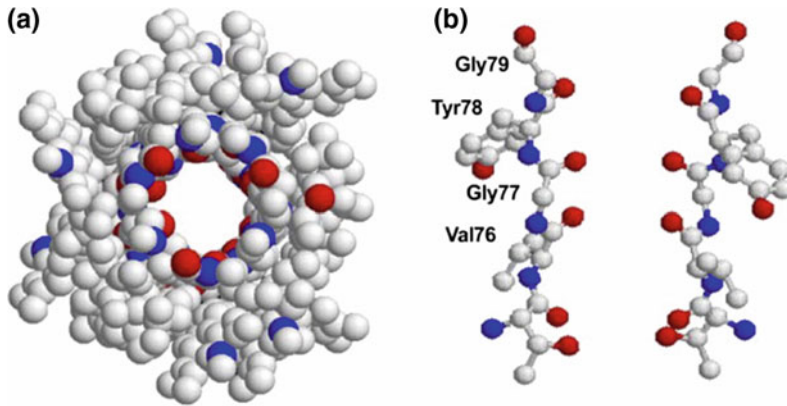


Fig. 6.44 **a** Top view of the gramicidin channel as a space-filling model (color code: white, carbon atoms; blue, nitrogen atoms; red, oxygen atoms) made using RASMOL ver. 2.7.2.1 and using coordinates from PDB 1MAG. Note how the alternating l-d arrangement allows all amino acid side chains to project outward from the channel lumen and the channel lumen is lined by the

peptide backbone. **b** Structure of the selectivity filter (residues 75–79) of the KcsA K⁺ channel. Two subunits are shown in ball-and-stick representation (made as in **(a)**, color code: same as in **(a)**) using coordinates from PDB 1BL8. Note that all amino acid side chains extend outward from the selectivity filter. *Source* Kelkar and Chattopadhyay (2007) (Color figure online)

gramicidin B and tyrosine in gramicidin C, respectively. The interior of the channel is formed by the polar amino acids as discussed above. Gramicidin has affinity for ions in the following order as maximum for cesium and minimum for lithium $\text{Cs}^+ > \text{Rb}^+ > \text{K}^+ > \text{Na}^+ > \text{Li}^+$.

Gramicidin is also used to stimulate the production of cytokines interferon. The property of ionophore to induce apoptosis in cancer cells is being used for drug targeting especially sodium and calcium, because ionophore has capacity to disrupt lysosomal function and can inhibit proteasome function for apoptosis (Fig. 6.44).

6.16 Porins in Biological Membranes

The bacterial and eukaryotic membranes are found to have special proteins in their outer membrane for transport, known as porins which form channels for various small size solutes, ions, and other nutrients. The porins found in mitochondria are also known as voltage-dependent anion channel (VDAC). The mitochondrial conserved porin proteins are tissue specific, but in bacteria, these porins constitute a

diverse group because of bacterial variable environment. The porins are made of 14, 16, 18, or 19 β -barrel strands in slightly tilted form. The porins may be monomer but mostly are trimers. Based on their structure and function, porins are broadly classified as 16-stranded nonspecific β -barrel such as Omp32, OprP, and PhoE, 18-stranded specific β -barrel (LamB from *E. coli*), 14 β -strands and monomeric such as OmpG and multidomain like CymA from bacteria. *T. thermophilus* which is P100 porin protein with N-terminal peptidoglycan binding domain and a coiled coil domain with large pore size. NMR and crystallographic studies have revealed mitochondrial VDAC pore size of 4.5 nm height and 3 nm diameter. The VDAC has 19 β -strands with N-terminal helix buried in pore.

The sugar-specific porins (Fig. 6.45) may allow solute up to 800 Kd. The bacterial porins are oval in shape with pore size 3–3.5 and 5 nm height. The porin first and last β -strands are joined in antiparallel mode to form complete pore.

These β -strands are connected to each other from cytoplasmic side by 8–9 long loops and 7–8 small turns from periplasmic side. The loop 3 from the cytosolic side in all porins is folded in side in barrel as shown in Fig. 6.46 and regulates pore size. Usually, loop 3 is found between 5 and

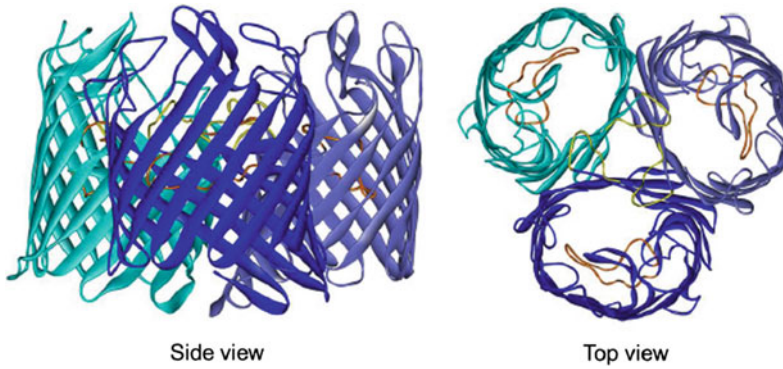


Fig. 6.45 Three-dimensional structure of the porin OmpF from *Escherichia coli*. Surface and internal loops are shown in dark gray. The extracellular space is located at the top of the figure, and the periplasmic space is at the bottom. The trimer is shown (Color figure online)

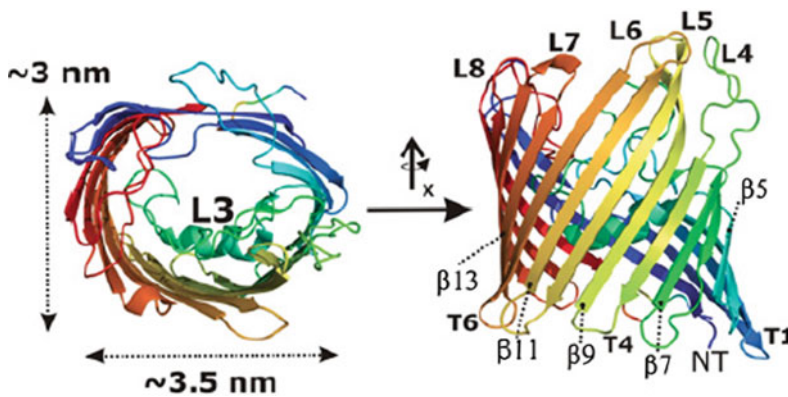


Fig. 6.46 Omp32 porin of *E. coli* from upper side (left-hand side) and lateral view (right-hand side) in colors with the N terminus, blue, and the C terminus, red. The longest loop L3 is labeled, as well as the additional loops (L4–L8), turns (T1–T6), and β -strands (β 5– β 13) structures (Color figure online)

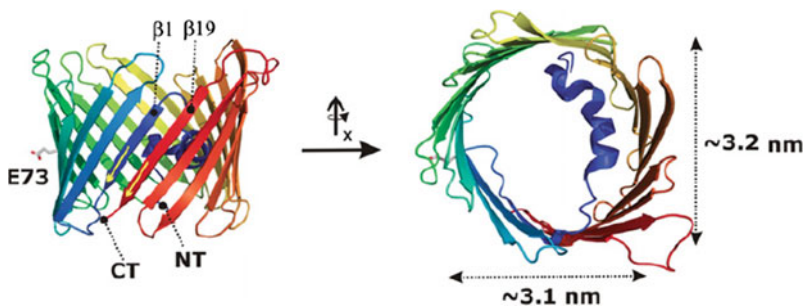


Fig. 6.47 Mitochondrial porins mVDAC, lateral and upper view (PDB code: 3EMN) in ribbon depiction. Color—blue (N terminus), red (C terminus) with approximate molecular dimensions. The first and last β -strands (β 1 and

β 19) are paired in a parallel way (yellow arrows). The upper view highlights N-terminal α -helix localized inside the barrel (Color figure online)

6 strands of barrel. This has mostly polar amino acids aspartic acid and glutamic acids. The L1, L2, and L4 interact with each other monomer to form trimer. L5, L6, and L7 are present on the surface of porin. The loop L8 being folded into interior contributes in channel opening toward extracellular side (Fig. 6.47).

The aromatic amino acids like tyrosine and phenylalanine are predominantly present in inner side and outer side of pore. The tyrosine is more toward outer side and phenylalanine to cytosolic side. All porins are found to have phenylalanine at their C-terminal which is required for proper folding and import. The algE porin from *P. aeruginosa* (18 β -strands) has positive amino acids like arginine inside the pore to translocate negatively charged alginate polymer.

The mitochondrial porins have three isoforms and are of round shape. The first and last β -strands of 19 strands pair parallel teach other unlike bacterial porins. All strands are connected through short loops, little elongated to cytoplasmic side (2–7 number) (Fig. 6.48).

The mitochondrial porins are imported by TOM protein and inserted by sorting and assembly machinery (SAM complex) Bacterial porins are inserted by β -barrel assembly machinery (BAM) complex. In 16-stranded β -barrel porins of nonspecific class, the transport depends on molecular mass and rate of transport is directly proportional to concentration gradient. The specific 18 β -barrel porins like lamb maltoporin of *E. coli* have specific binding site for substrate inside channel and shows Michaelis–Menten kinetics of transport. Many

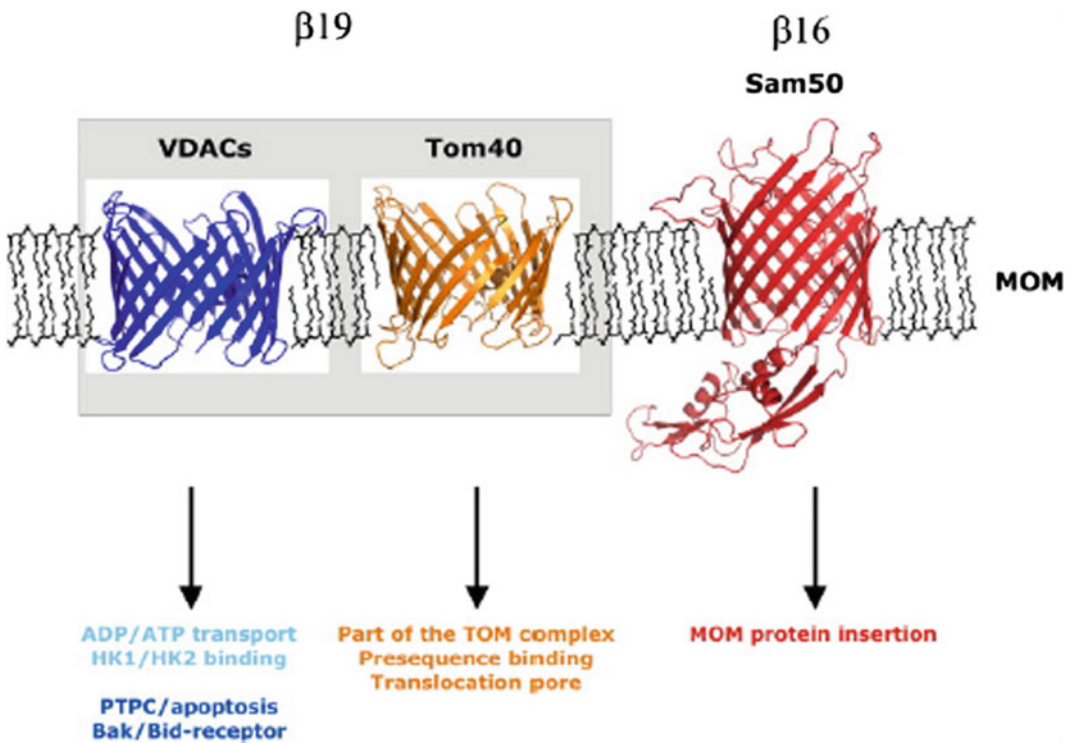


Fig. 6.48 Mitochondrial porins: Summary of MOM structures of β -barrel topology. Summary of the two principle architectures of MOM proteins of β -barrel topology shown embedded in the MOM lipid bilayer. VDAC and Tom40 belong to the protein families comprised by a 19-stranded β -barrel topology. Sam50 is

the only representative of the MOM based on the 16-stranded barrel architecture. Functions assigned to the individual classes of proteins as long as they are clearly confirmed and marked accordingly. All structure figures are prepared using the PYMOL program

prokaryotic porins are closed at high voltage of 100–200 mV. VDAC also has voltage dependence and can be easily gated by change in pH, and their permeability is controlled by membrane potential. They are involved in transport of ATP and ADP; that's why a large number of positively charged amino acids are present in interior wall of pore.

6.17 Transport by Channel Proteins

The protein ion channels are passive transporters, are made up of transmembrane, are selective for their substrate ions, and have much faster rate of transport than pumps. These channel proteins do not interact with transporting ions and have two conformations closed and open, to regulate flow of ions. The channels may be classified into ligand-gated channel and voltage-gated channel. Ligand-gated channel opening and closing depends on the interaction with positive or negative ligand. The binding of ligand induces conformational change in protein for opening or closing. On structural basis, ligand channel (LGIC) is classified into three classes.

1. **Cysteine loop receptors** (Nicotinic Ach) superfamily, which has **pentamer cysteine loop** such as nicotine acetyl receptor 5 hydroxyl tryptamine, Zn-activated channel cation transport, gama-aminobutyrate (GABA_A), strychnine-sensitive glycine receptors for anions, glutamate-gated chloride channel of *C. elegans*.
2. **Tetrameric ionotropic glutamate receptors**, which has four subunits divided into three subclasses like *N*-methyl D -aspartate (NDMA) receptor, α -amino-3-hydroxy-5-methyl-4-isoxazolepropionic acid (AMPA) and kainate receptors.
3. **P2X receptor family**, which has three subunits of cysteine loop. These are cation

permeable-gated channels and opened or closed by ATP interaction (Fig. 6.49).

6.18 Transport Through Ion Channel P2X Receptors

The trimeric ATP-activated channels are permeable to cations like sodium, potassium, and calcium. There are seven subclasses of the group, which are involved in various physiological functions like muscle contraction, neurotransmitter release, immune responses' regulation. P2X receptors are present only in eukaryotes and ubiquitously expressed. P2X are trimers of any three from seven variable subunits (P2x1-7) and exist as homomer or heteromer. Each of the subunit may have two transmembranes. *The detail is discussed in Chap. 9.*

6.19 The Pentamer Cysteine Loop Gama-Amino Butyric Acid Receptors (GABA_A)

In nerve transmission, the neurotransmitter is released in synaptic cleft by presynaptic vesicles. These neurotransmitters have to be internalized by postsynaptic membrane for the propagation of impulses. For internalization, these neurotransmitters bind to receptors on postsynaptic membrane and induce conformational change in receptor to open channel for translocation. The GABA and glycine receptors are anion channels but inhibitory in nature. GABA receptors have two subdivisions as GABA receptors family of ligand-gated channel (ionotropic) GABA_A and G receptor protein family (GABA_B). *The G receptors are discussed in Chaps. 3 and 9.*

The ligand for GABA_A receptor is γ -aminobutyrate. The cysteine loop family in eukaryotes has conserved motif of two cysteine

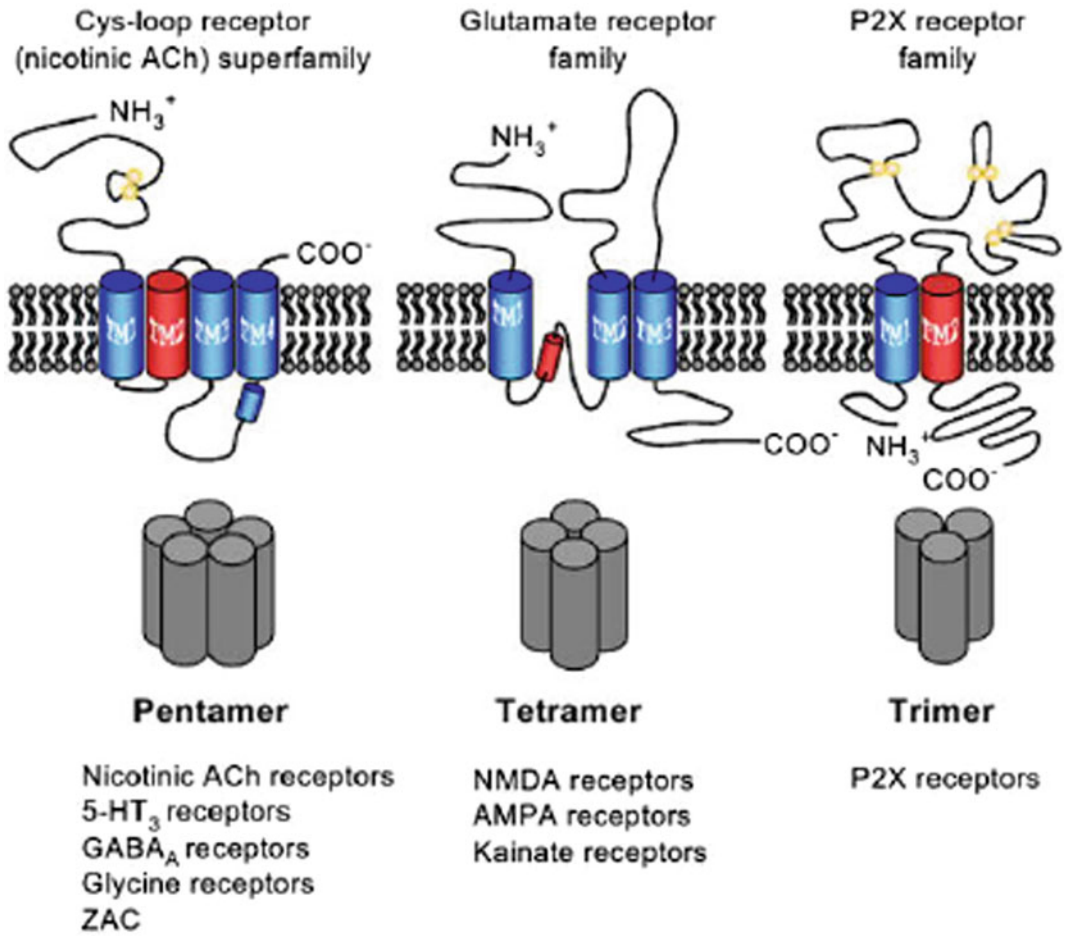


Fig. 6.49 Diagrammatic representation of ligand-gated ion channel subclasses on the structural subunit basis. (1) The pentameric cysteine loop superfamily receptor superfamily. (2) The tetrameric ionotropic glutamate receptors are subdivided into *N*-methyl-D-aspartate (NMDA), α -amino-3-hydroxy-5-methyl-4-isoxazolepropionic acid (AMPA), and kainate receptor subfamilies. The highly

schematic topography of each receptor category indicates the locations of the extracellular and intracellular termini, the number of transmembrane spans (large colored cylinders), and cysteine residues participating in disulfide bond formation (yellow circles). Red cylinders indicate α -helical regions participating in ion conduction/selectivity (Color figure online)

separated by 13 other amino acids. The GABA_A receptors are multisubunits with major isoform of GABA_A.

Receptors are $\alpha 1\beta 2$ and $\gamma 2$. The various isoforms of these proteins are found in human as α -subunits with six isoforms, β -subunits three, γ -subunits three, ρ -subunits three, and ϵ -, δ -, θ -, and π -subunits one copy. The single subunit of GABA_A receptor has around 500 amino acids with both C-terminal and N-terminal that are extracellular. Its half hydrophilic N-terminal has

signature motif of cysteine, and other C-terminal has four transmembrane helices from M1 to M4. The M2 transmembrane forms lining of channel. The large intracellular loop between M3 and M4 constitutes modulation site for phosphorylation. The M3 and M4 domains of receptor may interact with other regulatory proteins. The functional receptors are made up of five subunits as homopentamer or heteropentamer. The ϵ - and δ -subunits enhance polymeric association of monomer (Fig. 6.50).

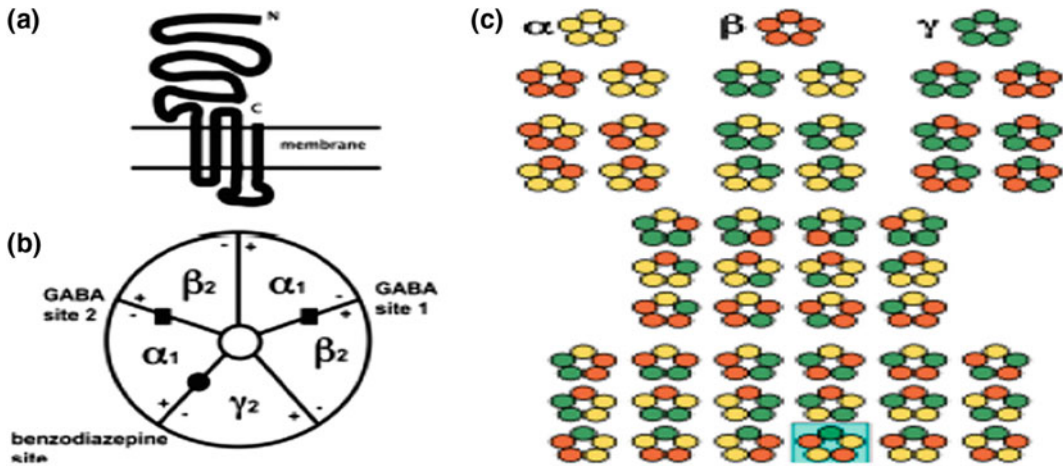


Fig. 6.50 A GABA_A receptor major isoform assembly $\alpha_1\beta_2\gamma_2$. The five subunits are arranged in periphery to form central ion pore. **a** Topology of a single subunit.

b Top view of the pentamer. **c** The various arrangements in a pentamer of subunits three different types, α (yellow), β (red), and γ (green) (Color figure online)

The density of these receptors varies from cell to cell. The GABA_A are found in nerve cells, muscle, and liver and on immune cells. The GABA receptors initially were thought to be only on postsynaptic membrane for opening of GABA chloride channel for hyperpolarization of a depolarized membrane but recent studies have confirmed their presence on dendrites, and other tissues also for the regulation of synapses. The GABA_A receptors are gated chloride anion channels and occasionally may translocate bicarbonate anions. GABA binds to two binding sites at the interface of α -/ β -subunit of receptor. The important region for ion translocation is α -subunit segment (F loop), which bulges out from ligand binding site toward the ion channel, and in γ -subunit, this segment modulates channel activity. The second segment, a lysine residue of the short loop between M2 and M3, is important for the formation of a salt bridge during the process of gating. The third segment resides within the β_4 - β_5 linker of the β -subunit. GABA binding to binding sites at the interface of α -/ β -subunit stimulates conformational change around binding site which passes through open and many closed states (flipped states) for final gate opening.

6.20 Tetrameric Ionotropic Glutamate Receptor Channels *N*-Methyl-D-Aspartate (NMDA)

The *N*-methyl-D-aspartate (NMDA) receptors are known as glutamate-gated cation channel for calcium permeation. The tetrameric ionotropic receptors include NMDA, α -amino-3-hydroxy-5-methyl-4-isoxazolepropionic acid (AMPA), and kainate receptor as per their synthetic ligand binding. These are excitatory neurotransmitters. In excitatory transmission, glutamate released from presynaptic membrane binds to NMDA or AMPA receptor of postsynaptic membrane. The NMDA receptor family have three different subunits known as Glu N1-3. The crystallographic and functional studies have revealed detail structure and mechanism of channel opening. Active NMDA receptors are tetramer with two GluN1 and two GluN2. The monomer subunit may be divided into four distinct domains as extracellular N-terminal domain, ligand binding domain, pore-forming membrane domain, and C-terminal intracellular. The extracellular N-terminal domain is linked to ligand binding domain through small linker, which is also attached to pore-forming transmembrane (Fig. 6.51).

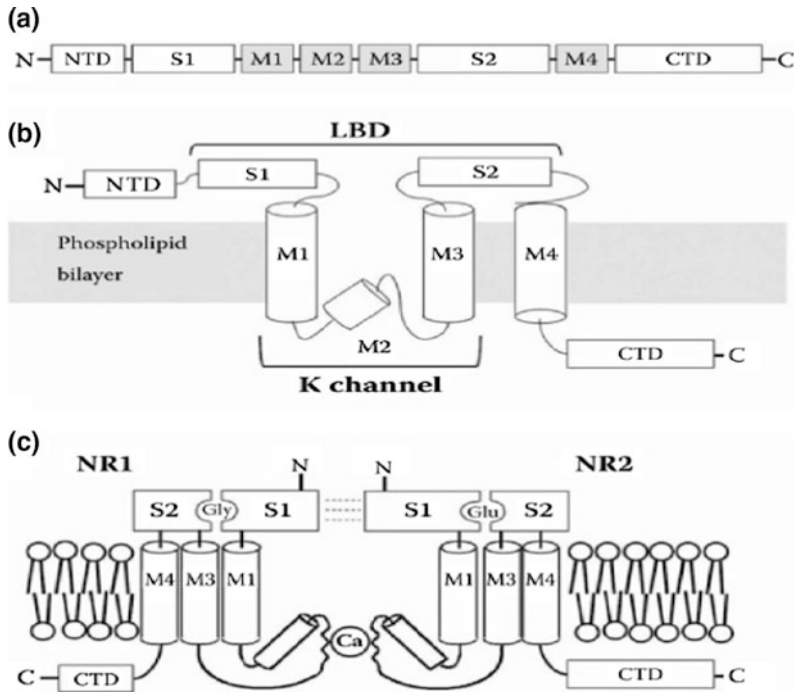


Fig. 6.51 Various domain representations of NMDAR. **a** The arrangement of NMDAR subunits with four hydrophobic domains (M1 through M4), two ligand binding domains (S1 and S2), and amino and carboxyl terminal domains (NTD, CTD). **b** Monomer subunit with N-terminal signal peptide on extracellular side,

transmembrane helices M1, M3, and M4, M2, a cytoplasmic reentrant hairpin loop a link between M1 and M3 and ligand binding domains S1 and S2. **c** Two-dimensional membrane folding model of glycine binding NR1 and glutamate binding NR2 subunits

The transmembrane is linked to C-terminal domain. The channel opening starts in sequential order of ligand binding → change in conformation → channel opening. Two separate ligands are required for NMDA receptors activation. The ligand binding domain of subunit has two subdomains S1 and S2. The S1 domain of two neighboring subunits, at their interface, creates ligand binding site and is rigid in structure but lower one S2 domain is mobile without any interaction. In typical NMDA receptor, GluN1 and GluN2 will interact with two molecules of glutamate and two molecules of glycine. The receptor with GluN1 and GluN3 will require only glycine for the activation. The NMDA receptors have high affinity to glutamate, high calcium (Ca²⁺) permeability, which may be blocked by magnesium ion in voltage-dependent

manner. The NMDA differs from AMPA receptor of the same family in its function. The *N*-methyl-D-aspartate (NMDA) receptors unlike α -amino-3-hydroxy-5-methyl-4-isoxazolepropionic acid (AMPA, activation time 2 ms) are slow in activation (app. 10–50 ms) and deactivation (app. 50–500 ms). AMPA receptor initiates rapid polarization in response to neurotransmitter release during synaptic transmission but NMDA receptors only care for time span of synaptic currents. The glycine is coagonist for NMDA receptor. Two molecules of glycine and two molecules of glutamate bind on separate binding site in receptor for the activation and opening of channel, which results in influx of calcium and sodium with efflux of potassium. The electrical synapses are converted into chemical synapses through NMDA receptor because influx of

calcium in postsynaptic membrane activates calcium-dependent signaling pathway for the modulation of synaptic structure, plasticity, and connectivity.

The signaling is discussed in Chap. 9. The independent binding of two ligands, glycine and glutamate, collectively induces change in conformation to open channel. The closing of channel may result in glutamic acid release and desensitization of receptors. It has been observed that the NMDA receptors may be in desensitized form with bound glutamate for long period. The other function of NMDA receptor in learning and memory can be inhibited by magnesium ion in voltage-dependent mode. In close state of receptor, the magnesium is bound to receptor in inhibition mode, which can be released only by sufficient depolarization of the membrane. This kind of interaction empowers NMDA receptor to act as coincidence detector for pre- and postsynaptic changes. The slow kinetics of NMDAR-mediated excitatory postsynaptic current (EPSC) supports temporal summation and decreases dendritic filtering of synaptic input. The receptors provide strength to synapses through long-term potentiation (LTP) and weakness by long-term depression (LTD) for learning and memory. Through calcium influx, the overstimulation of NMDA receptors may cause Alzheimer, Parkinson, Huntington, and amyotrophic lateral sclerosis (ALS). Physiologically, NMDA receptors may be desensitized by unfavorable interaction between glycine and glutamate to cause close conformation of receptor or calcium influx activate calmodulin to remove actin 2 from receptor to keep receptor in desensitized mode. The receptors activity may be decreased by zinc, polyamines, and proton. The phosphorylation of receptor protein enhances open form of channel by removing magnesium and inducing favorable conformation.

6.21 Voltage-Gated Ion Channels

The voltage-gated ion channels open or close in response to change in voltage and the unit of membrane potential. In excitable cells like nerve

and muscle, the chemical or electrical signaling is initiated through voltage-dependent sodium or calcium influx. The sodium channel protein in human is composed of large α -subunits (260 Kd with 2000 amino acids) and small β -subunits (30–40 Kd); the small β -subunit has two isoforms β -1 and β -2. The sodium channel β -subunits have N-terminal extracellular domain into immunoglobulin-like fold, a single transmembrane segment, and a short intracellular segment. These units may form heterodimer or heterotrimer. The α -subunits are linked noncovalently to β -1 and through disulfide linkage to β -2. The voltage-gated sodium ion channels are also known as Nav channels. In human, α -subunit has various isoforms like Nav1.1, Nav1.2, Nav1.3, Nav1.4, Nav1.5, Nav1.7, Nav1.8, and Nav1.9. The Nav1.7, Nav1.8, and Nav1.9 are found in peripheral nervous system and Nav1.1, Nav1.2, Nav1.3, and Nav1.6 in central nervous system, and the Nav1.5 resides in heart muscle and Nav1.4 in skeletal muscle. The α -subunit is coded by ten different genes in human but one of these codes for nonchannel α -protein is known as sensing helix. β -subunits have four isoforms as β -1, β -2, β -3, and β -4. The β -1 and β -3 associate with α -subunit noncovalently and β -2 and β -4 through disulfide linkage. Nav β -subunits resemble cell adhesion molecules in structure and may have role in localization. The three-dimensional structure of voltage-gated sodium channel has revealed structural detail, mechanism and catalytic amino acids involved, drug target site, and regulatory site. The bacterial sodium channel (NavAb) is seen to have central pore surrounded by four pore-forming helix segments S5 and S6 segments and the intervening pore loop. The four voltage-sensing elements made up of S1–S4 segments are symmetrically associated with the peripheral pore elements.

The structural analysis of bacterial sodium channel (NavAb) has shown the swapping of functional domain of one subunit to other like all individual voltage-sensing elements are found in close associated with the pore-forming element to neighbor as shown in Fig. 6.52 in dark colors. This type of arrangement and association is also observed in potassium channel (Fig. 6.53).

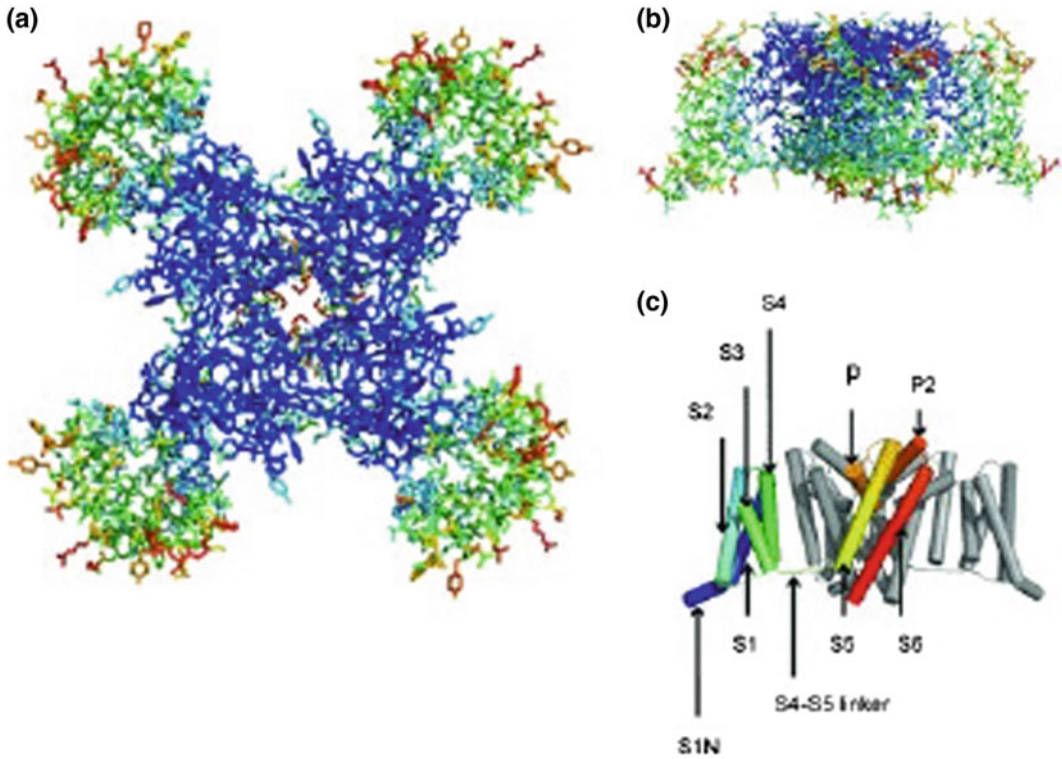


Fig. 6.52 Structure of voltage-dependent bacterial sodium channel (NavAB), **a** view from upper side, **b** lateral view, **c** detail of interacting segments of channel protein

The NavAb sodium channel are found to have large outer entrance with narrow selectivity filter, a large central cavity filled with water and layered by the S6 segments and an intracellular activation gate at the crossing of the S6 segments and intracellular surface of the membrane. Sodium and potassium channel has similar type of structure but differs significantly in permeation mechanism. The potassium ion channels discriminate K^+ by direct interaction with a series of four ion coordination sites created by the carboxyl group of ion selectivity filter amino acid residues in the zone. Water is excluded and does not interact with selection filter, while the NavAb ion selectivity filter has a high-field-strength site for ions at its extracellular end because of the side chains participation of four highly conserved and key determinants glutamate residues. The sodium ion with two planar water molecules for

hydration could fit in this high-field-strength site. On outer side of the field, two carboxylic groups of peptide create coordination site for sodium binding with four planar waters of hydration. These negatively charged group interaction with sodium removes water of hydration partially for permeating sodium as a hydrated ion, which interact on the way with the pore residues through its inner shell of bound waters.

The local anesthetics, antiarrhythmic and antiepileptic drugs may inhibit this channel by binding to inner side of segment 6 (drug receptor site) but binding to this site NavAb channels is solely controlled by the side chain of phe 203, single amino acid residue. The sodium channels open in response to depolarization and within fraction of second are closed also for repetitive firing of action potential in synapse. The short intracellular loop connecting α -subunit III and IV

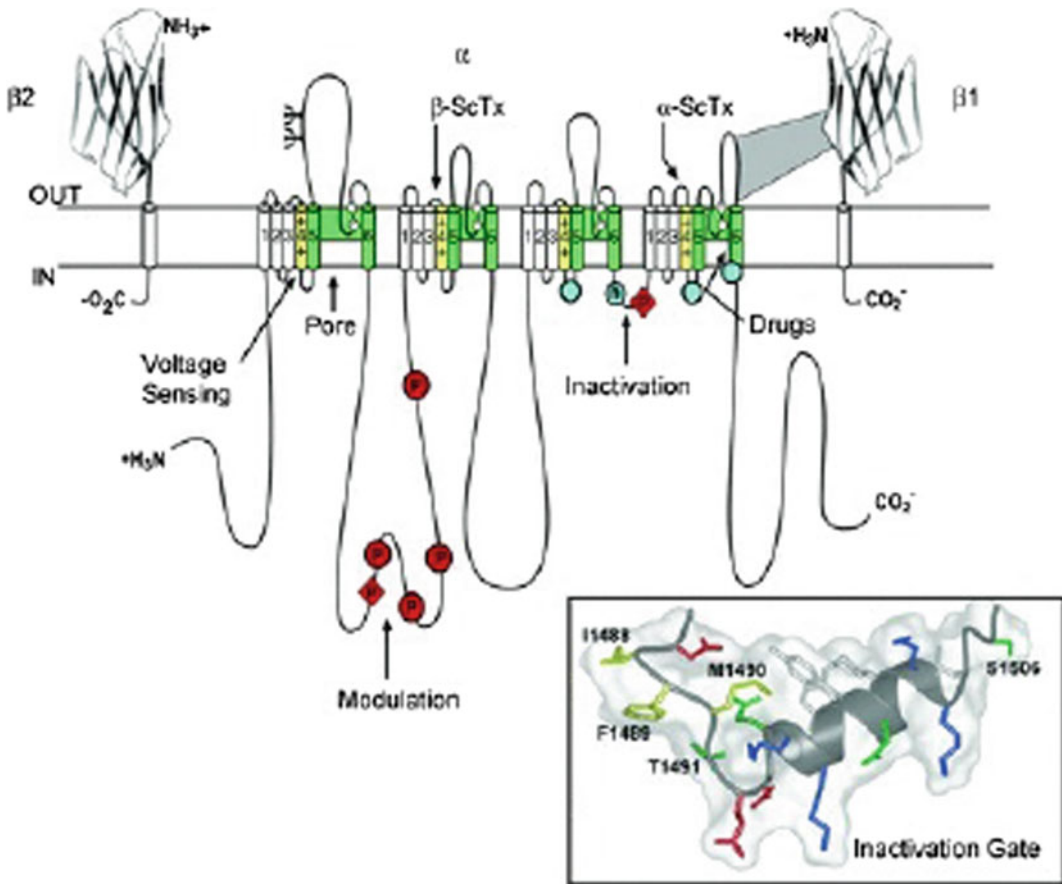


Fig. 6.53 Subunit primary structures of the voltage-gated sodium channels α , sites of probable N-linked glycosylation; P in red circles, sites of demonstrated protein phosphorylation by PKA (circles) and PKC (diamonds); green, pore-lining segments; white circles, the outer (EEEE) and inner (DEKA) rings of amino

residues that form the ion selectivity filter and the drug binding site; h in blue circle, inactivation particle in the inactivation gate loop; blue circles, sites implicated in forming the inactivation gate receptor (Color figure online)

domain acts as inactivation gate in channel inactivation. This acts as an intracellular blocking particle by folding into the channel structure and blocks the pore during inactivation. The NMR study of channel inactivation gate has shown the presence of a rigid α -helix followed by two loops of protein with IFM motif and a neighboring threonine residue on their surface for interaction participate in closing. The inactivation gate bends at conserved pair of glycine residues to fold into the intracellular mouth of the pore. The fast inactivation gate is not found in homotetrameric bacterial sodium channels.

The voltage sensing is executed by the S4 transmembrane segments of sodium channels, which has four to eight repeated motifs of a positively charged amino acid residue (usually arginine), followed by two hydrophobic residues, and shifts the gating charges of sodium channels in the *sliding helix* in voltage sensing. The gating charges are stabilized in their transmembrane position by ionic interacting pairing with neighboring negatively charged residues, which can exchange their ion partners during outward movement.

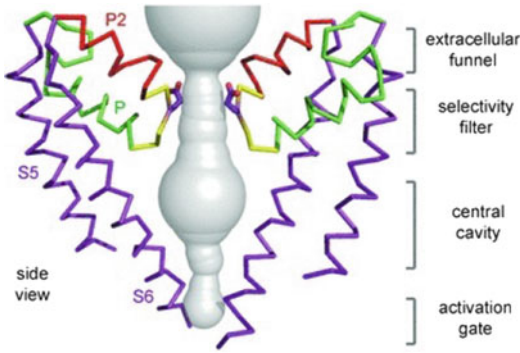


Fig. 6.54 Bacterial voltage-dependent sodium channel selection filter

6.22 K2P Channels Are Not Leaky Channels

The formerly referred leaky channels, resting, back ground, or constitutive channels are now referred as K2P or voltage insensitive channels. The K2P channels are ubiquitously found in all organisms. The functionally active K2P channel has two subunits, and each subunit is made up of two pore regions (P1 and P2), four transmembrane domains (M1–M4), and two characteristic extracellular helices Cap C1 and C2. The Yeast TOK1, KP2 channel with eight transmembrane helices (M1–M8). The TOK1 (2P/8TM) is exceptionally outward rectifier. These channels are highly regulated and functionally important in nervous system, muscles, blood vessels, endocrine system, and kidney. According to sequence homology, eukaryotic K2P channels are classified into six groups; (1) The TWIK clade is weak inward rectifying channels, (2) TREK clade is mechanosensitive and also regulated by lipids, (3) TASK clade channels are regulated by acid pH, (4) TALK clade is alkaline pH-sensitive, (5) THIK clade is inhibited by halothane, and (6) TRESK clade is present in spinal cord.

Unlike voltage-dependent channels (Nav, Kv, Cav), these K2P channel do not have voltage-sensing domain and have two pores. The K2P are not inactivated during depolarization except TWIK-2. The voltage-dependent channels

have one pore made by four transmembranes (Fig. 6.54).

K2P-channels in the cell membrane can be regulated at the transcriptional level. The presence of Cap helices C1 and C2 is unique to these channels, which vertically extends ~ 35 Å on the extracellular side of membrane to cover entrance with two lateral portals for K^+ ions. The pore-lining helices, M2 and M4, traverse obliquely through the membrane and M1 and M3, and the outer helices are more vertically oriented.

The transmembrane segments of the channel have lateral openings between M3 and M4 facing toward lipid environment. The selectivity filter and the pore helices have fourfold symmetry with inner wide open cavity. The extracellular cap, the central cavity, and the inner opening of channel are found in twofold symmetry unlike other potassium channels. The two subunits were found to be assembled in a simple antiparallel manner. The C1–C2 linkers are linked via a disulfide bridge. The two opposite pore helices and the corresponding pore loops contribute to forming the selectivity filter. The M1-helix of one subunit is adjacent to the end to M2-helix of the other subunit. The C-helix is amphipathic with charged residues facing the cytoplasmic side. The human K2P channel cytosolic end of M4 has two to four charged residues and forms an amphipathic helix.

The cytosolic part of the pore participates in gating and permeation. The crystallized K2P-channel has been found to have lateral opening at the interface between the M2-helix of one subunit and the M4-helix of the other subunit to connect the inner cavity with the hydrophobic core of the cell membrane. The lateral cavity, occupied with the hydrophobic tails of membrane phospholipids, may be important in channel gating because of lipid interaction with M2 and M4 domains and alkyl chains of membrane lipids into the cavity through the lateral opening influences the conductance and the pharmacological properties. Like all voltage-dependent channels, the glycine residues are conserved M2 and the M4 helices of all K2P-channels for creating kink in M2 and the M4 domain around the hinge of G268 for moving M4-helix from a

Fig. 6.55 **a** The K2P TRAAK channel from human, **b** diagrammatic representation of two pores and four transmembranes in single unit of K2P channel

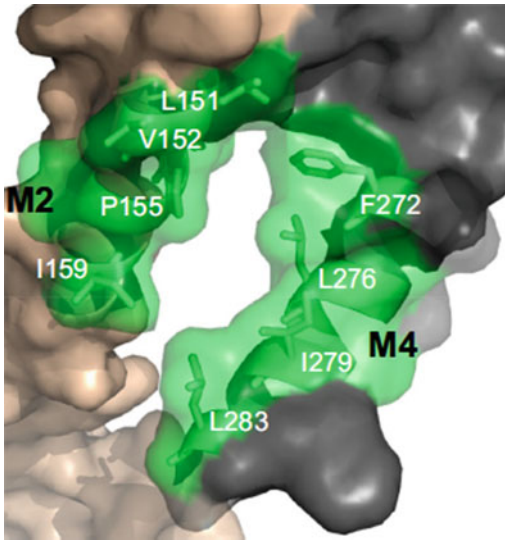
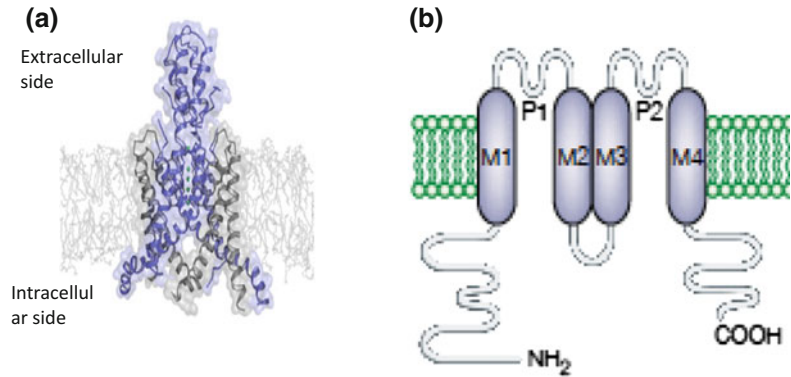


Fig. 6.56 Structure of TRAAK K2P channels space-filling model. The two subunits are color coded. The hydrophobic residues of the lateral cavity (in the down state) are highlighted in green (Color figure online)

“down” to an “up” configuration for transport, where lateral fenestration is closed and ions are passed through the selectivity filter. In down conformation, the central cavity M4-helix crosses the membrane in such a way that lipids of the central cavity blocks the permeation. K2P-channels are lined up with hydrophobic residues in layer. The opening of lower activation gate promotes the opening of upper inactivation gate, and C-type inactivation is promoted unlike voltage-dependent gate. During depolarization, all K2P-channels have shown immediate current

component and following time-dependent component of outward current. This instantaneous component supports all K2P channels to have open probability at negative potentials, and the time-dependent current changes support the regulation of K2P-channels by voltage changes. The steady-state current–voltage relation under physiological conditions (with 4–5 mM K^+ extracellular concentration) of K2P channel, studied at depolarized potentials, is much larger than the current flowing through K2P channel at resting membrane potential to support role of K2P channel in action potential configuration. The anesthetics enhance the leakage of ions in neural tissue and decrease excitability. In various tissues, K2P channels are present to perform various functions and may also play role in apoptosis subjected to further analysis (Figs. 6.55 and 6.56).

References

- Cipriano DJ, Wang Y, Bond S et al (2008) Structure and regulation of the vacuolar ATPases. *Biochem Biophys Acta* 1777:599–604
- Cosentino K, Ros U, Garcia Saez AJ (2015) Assembling the puzzle: oligomerization of alpha pore forming proteins in membrane. *Biochim Biophys Acta* 1858 (3):457–466
- Dawson Roger JP, Locher KP (2006) Structure of a bacterial multidrug ABC transporter. *Nature* 443:180–185
- Deutscher J, Ake FMD, Derkaoui M et al (2014) The bacterial phosphoenolpyruvate: carbohydrate phosphotransferase system: regulation by protein phosphorylation and phosphorylation-dependent

- protein-protein interactions. *Microbiol Mol Biol Rev* 78(2):231–256
- Gomes D, Agasse A, Thiebaud P et al (2009) Aquaporins are multifunctional water and solute transporters highly divergent in living organisms. *Biochimica Biophysica Acta (BBA) Biomembr* 1788(6):1213–1228
- Gutmann Daniel AP, Ward A, Urbatsch IL et al (2010) Understanding poly specificity of multidrug ABC transporters: closing in on the gaps in ABCB1. *Trends Biochem Sci* 35:36–42
- Hollenstein K, Frei DC, Locher KP (2007) Structure of an ABC transporter in complex with its binding protein. *Nature* 446:213–216
- Hosaka T, Yoshizawa S, Nakajima Y et al (2008) Structural mechanism for light-driven transport by a new type of chloride ion pump, Non labens marinus rhodopsin-3. *Br J Pharmacol* 154(8):1680–1690
- Kelkar DA, Chattopadhyay A (2007) The gramicidin ion channel: a model membrane protein. *Biochimica Biophysica Acta (BBA) Biomembr* 1768(9):2011–2025
- Mathie A, Al Moubarak E, Veale EL (2010) Gating of two pore domain potassium channels. *J Physiol* 588 (17):3149–3156
- Morth JP, Pedersen BP, Buch-Pedersen MJ et al (2011) A structural overview of the plasma membrane Na⁺, K⁺-ATPase and H⁺-ATPase ion pumps. *Nat Rev Mol Cell Biol* 12:60–70
- Naftalin RJ, Nicholas Green Y, Cunninghamz P (2007) Lactose permease H1-lactose symporter: mechanical switch or brownian ratchet? *Biophys J* 92:3474–3491
- Palmgren MG, Nissen P (2011) P-type ATPases. *Ann Rev Biochem* 40:243–266
- Postma PW, Lengeler JW, Jacobson GR (2000) Phosphoenolpyruvate: carbohydrate phosphotransferase systems of bacteria. *Microbiol Rev* 57(3):543–594
- Rees DC, Johnson E, Lewinson O (2009) ABC transporters: the power to change. *Nat Rev Mol Cell Biol* 10:218–227. <https://doi.org/10.1038/nrm2646>
- Renigunta V, Schlichthörl G, Daut J, Arch P (2015) Much more than a leak: structure and function of K2P-channels. *Eur J Physiol* 467:867–894
- Tilley SJ, Saibil HR (2006) The mechanism of pore formation by bacterial toxins. *Curr Opin Struct Biol* 16:230–236
- Verkman AS, Anderson MO, Papadopoulos MC (2014) Aquaporins: important but elusive drug targets. *Nat Rev Drug Discov* 13:259–277
- Vyklicky V, Korinek M, Smejkalova T et al (2014) Structure, function, and pharmacology of NMDA receptor channels. *Physiol Res* 63(Suppl 1):S191–S203
- Wright EM, Loo DD, Hirayama BA (2011) Biology of human sodium glucose transporters. *Physiol Rev* 91 (2):733–794
- Weeber EJ, Levy M, Sampson MJ et al (2002) The role of mitochondrial porins and the permeability transition pore in learning and synaptic plasticity. *J Biol Chem* 277:18891–18897
- Wilkens S (2015) Structure and mechanism of ABC transporters. *F1000 Prime Rep* 7:14. <https://doi.org/10.12703/P7-14>
- Zeth K (2010) Structure and evolution of mitochondrial outer membrane proteins of β -barrel topology. *Biochimica Biophysica Acta (BBA) Bioenerg* 1797 (6–7):1292–1299

7.1 Introduction

The human nerve cells may be central or peripheral. The central nerve cells belong to brain and spinal cord, and other nerves are peripheral. The **resting membrane potential** is polarized state of cell membrane having membrane potential -70 mV. Any type of stimulus changes membrane potential from -70 to $+30$ mV by **depolarization**. **Action potentials** are defined as change in the resting membrane potential in response to stimulus, which actively circulate along the cell membrane. When membrane is depolarized by stimulus and membrane potential is lowered than resting potential to a particular value (**threshold potential**), action potential is generated. The polarization and depolarization occur in cycle. Repolarization process brings back membrane potential to -70 mV. The stimulated nerve fiber cannot be restimulated without completing repolarization cycle, and this time duration is called as **refractory period**. The stimulus should be sufficient to start an action potential in the complete nerve fiber for the transfer of signals. Though depolarization and repolarization events are similar in myelinated nerve cells, the action potentials jump from one **node of Ranvier** to the next instead of passing through the myelinated area of the membrane. This jumping of action potential through node of Ranvier is known as **saltatory conduction** (saltation). There are two

types of synapses: **electrical synapse** and **chemical synapse**. The electrical synapses are found in all nervous systems and are the functional correlate of **gap junctions**. The chemical synapse involves the release of neurotransmitters in synaptic cleft. **Neurotransmitters** in the peripheral nerve cells are mostly excitatory, while in the central nerve cells, these neurotransmitters may be either excitatory or inhibitory. Inhibitory transmitters decrease the permeability of the affected membrane for sodium, while in excitatory synapse, it is increased. The summation of excitatory and inhibitory neurotransmitters may determine the fate of action potential.

7.2 Nernst Equation

The direction of any ion transport by channel protein in the membrane depends on **electrochemical gradient** of the ion. Ion concentration gradient (**chemical gradient**) and selective ion channel in the membrane (**voltage gradient**) together form electrochemical gradient. The chemical gradient allows the ions to move from higher concentration to lower concentration across the membrane. The movement of the ion, which is not followed by the other counterion movement, is responsible for the difference in charge across the membrane. This difference is the basis for the establishment of potential

difference across the plasma membrane (**membrane potential V**). Charge difference across the membrane establishes **electrical gradient** that grows in magnitude until it is exactly balanced by chemical gradient. If chemical and electrical gradients are equal, there will be zero electrochemical gradient for the ion and the ion will not move across the membrane. The ion will be in **electrochemical equilibrium state**. In the electrochemical equilibrium state, the membrane potential is also known as **equilibrium potential (V)** for that particular ion.

The **Nernst equation** correlates with equilibrium potential, absolute temperature, and concentration of ions across the membrane. This equation is used to calculate the equilibrium potential of an ion. Nernst equation, given by German Nobel laureate Walther Nernst, is the measure of equivalence between chemical and electrical gradient. The first equation to find membrane potential as result of chemical and membrane potential of the membrane, was given by Goldman Hodgkin Katz.

The equilibrium potential may be written as follows:

$$V = \frac{RT}{zF} \ln \frac{C_o}{C_i}$$

where

V is the equilibrium potential in volts between inside and outside potential
 R is the universal gas constant
 C_o and C_i are the concentrations of ion outside and inside

Absolute temperature is defined as T in degree Kelvin.

F is Faraday's constant
 Z is charge on the ion

(Though Nernst equation is mentioned in Chap. 8, here this equation is used for the calculation of membrane potential.)

The transport of molecule from high concentration to lower concentration has favorable free energy change ($\Delta G < 0$), while the transport from lower to higher concentration carries unfavorable ($\Delta G > 0$) free energy change.

The free energy change per mole of substance to be transported (ΔG_{conc}) is

$$= RT \ln \frac{C_o}{C_i}$$

The free energy change (ΔG_{volt}) of an ionic species from outside to inside in the membrane with voltage V will also depend on the charge of the ion and can be written as

$$\Delta G_{\text{volt}} = zFV, \quad \text{per mole of ion.}$$

At equilibrium potential of the membrane, the electrochemical gradient (chemical gradient ΔG_{conc} + voltage gradient ΔG_{volt}) is equivalent to ion distributed separation across the membrane.

Thus

$$zFV - RT \ln \frac{C_o}{C_i} = 0$$

Therefore

$$V = \frac{RT}{zF} \ln \frac{C_o}{C_i}$$

By converting the natural log into base 10

$$V = \frac{RT}{zF} \log_{10} \frac{C_o}{C_i}$$

For monovalent ion at 37 °C, when $\frac{C_o}{C_i} = 1$.

RT/F may be defined in volts having value equivalent to approximately 61 mV at mammalian cell at 37 °C in log 10 units.

So, $2.303 \frac{RT}{F}$ = approximately 61 mV

Thus for monovalent ion at 37 °C.

$$V = +61 \text{ mV for } \frac{C_o}{C_i} = 1$$

Table 7.1 Intracellular and extracellular concentrations of various ions and Nernst equilibrium potential values for these ions having physiological importance

Ionic species	Intracellular concentration	Extracellular concentration	Equilibrium potential (mV)
Sodium (Na ⁺)	15 mM	145 mM	V _{Na} = +60.60
Potassium (K ⁺)	150 mM	4 mM	V _K = -96.81
Calcium (Ca ²⁺)	70 nM	2 mM	V _{Ca} = +137.04
Hydrogen ion (proton, H ⁺)	63 nM (pH 7.2)	40 nM (pH 7.4)	V _H = -12.13
Magnesium (Mg ²⁺)	0.5 mM	1 mM	V _{Mg} = +9.26
Chloride (Cl ⁻)	10 mM	110 mM	V _{cl} = -64.05
Bicarbonate (HCO ₃ ⁻)	15 mM	24 mM	V _{HCO₃⁻} = -12.55 mV

whereas

$$V = 0 \text{ for } \frac{C_o}{C_i} = 1$$

for example, the K⁺ ion equilibrium potential will be

$$61 \log_{10} \left(\frac{[K^+]_o}{[K^+]_i} \right) \text{ mV}$$

If [K⁺]_o = 5 and [K⁺]_i = 140 mM, the membrane potential will be -89 mV.

At value of *V* zero, no ion will flow across the membrane.

For divalent ions like calcium²⁺, the *ZF* value will be doubled because of two charge of the calcium.

At particular membrane potential (*V_M*) of ions, the resulting driving force for ion movement across the membrane will be equal to the difference of *V_M* and the equilibrium potential (*V*) for the particular ion: For calcium, this will be *V_M* - *V_{Ca}*²⁺; for Na⁺, it is *V_M* - Na⁺; The **Nernst potential** balances the unequal distribution of the particular ion in the membrane. The positive voltage (+55) inside the neuron will inhibit more movement of sodium ions from outside to inside of nerve, and large negative voltage (-90 mV) will accumulate more positive ions like K⁺ inside the cell.

The Nernst equation allows us to predict at any given concentration gradient the membrane potential required to exactly counteract the tendency of an ion to move into or out of the cell. If

concentration gradient changes, the equilibrium potential will change (Table 7.1).

7.3 Nerve Cell

The central nerve cells include brain and spinal cord, and other nerve cells are known as peripheral nerves cells. The cells of nervous system of different organisms may vary in size. The squid nerve cells are 100–1000 times larger than mammalian nerve cell in diameter (1 mm). The nerve cells communicate with each other through signaling molecule in **synapsis**. The speed of action potential conduction depends on the diameter of **axon**; the bigger the diameter is, the faster the conduction will be. According to structure and function, the nerve cell may be differentiated into three major parts: **soma**, the cell body; **dendrites**, the thin projections from cell body soma; and **axon**, the single long nerve tail. The other cells found in nervous system are known as **neuroglia** or **glial cells**, which are present in central and peripheral nervous system, and these cells without axon or dendrites do not participate in signal transmission. These **neuroglia** cells provide voluminous support to nerve cells for proper functioning. The **astrocytes**, **ependymal**, **microglia**, **satellite**, **oligodendrocytes**, and **Schwann cells** are different types of neuroglia cells. The Schwann cells may provide myelin sheath in axon of peripheral nerve cells, while oligodendrocytes synthesize myelin sheath

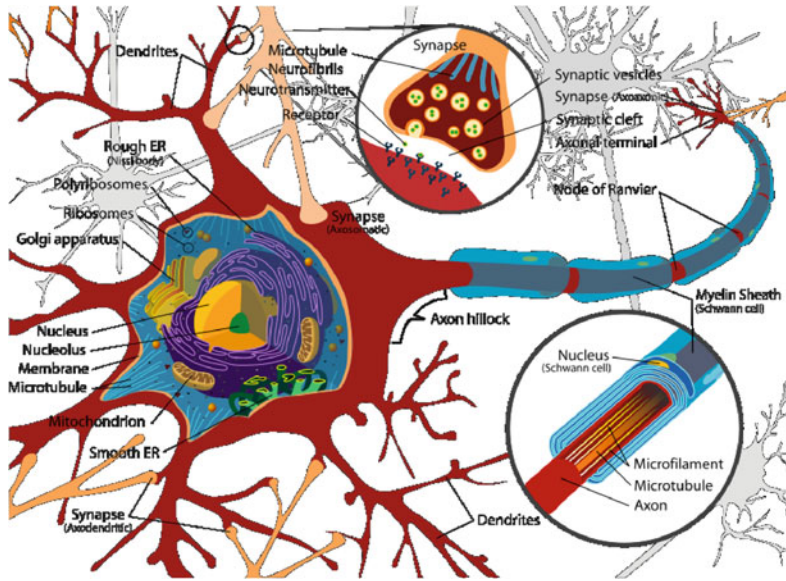


Fig. 7.1 Structure of nerve cell from human. The nervous system is a network of nerves that are spread out to the smallest part of the body so that every part can react to a stimulus. There are about 100 billion neurons in our central nervous system. A stimulus can be mechanical, chemical, electrical or thermal and the body responds to this stimulus as there is a change in the physio-chemical balance at the cell membrane. This disturbance at the cell membrane is called membrane potential. When there is difference in the electric potential, the signal

travels from one neuron to the other through axons. Some axons are myelinated and some are not. The myelinated axons have a couple of breaks in the myelin sheath and these breaks are called as Nodes of Ranvier. When the action potential, passes down the myelinated axon, at the nodes of Ranvier the signal jumps across the nodes and this helps the signal to travel faster than if it were to travel down a non-myelinated axon. This jumping of signals across the nodes of Ranvier is called Saltatory Conduction. Conduction and nerve impulses work in correlation

in axon of central nerve cells. The **axon** of nerve cells carries signal from one cell to another cell of nerve or muscle for signal propagation. The axon may differ in length from few μm as in mammals ($120 \mu\text{m}$) to several meters as in squid giant nerve fiber. Only some of the axons have insulated myelin sheath around them, and this myelin sheath is irregular and interrupted by **nodes of Ranvier**. Nodes of Ranvier, without myelin sheath, is the site for nutrient and waste products exchange for nerve cells. The nerve impulse jumps from one node of Ranvier to another for nerve transmission. The another structure of nerve cell is known as **dendrites**, which originates from soma and branches away from it to accept chemical signals at synapse from other cells for signal transmission to other

cells after converting these chemical signals into electrical signals. Action potential is initiated if electrical signal by dendrites is strong enough, but many neurons are found without dendrites also (Fig. 7.1).

On the basis of projections from cell body soma, the nerve cells are classified into four categories such as **unipolar**, **bipolar**, **multipolar**, and **pseudo-unipolar**. Unipolar nerve cell has only one projection from the soma. Bipolar neurons have one axon projection along with one dendrite extending from soma. Multipolar neurons may have many dendrites and one axon. Pseudo-unipolar neurons have one projection from soma, which is again divided into two distinct structures. The mixed nerves may have inward and outward axons to receive both

incoming sensory signals and can send outgoing signal to muscle cells as in branchial nerve cells and in spinal nerve tissue.

7.4 Resting Membrane Potential

When the cell membrane is not under any stimulus, the membrane potential is known as the **resting membrane potential** (V_{rest}). The resting membrane potential is taken as reference, in which membrane inside has negative charge or potential in comparison with outside and it can be written as **membrane potential** (V_M). The experiment done by Hodgkin and Huxley in squid neuron has explained that **negative potential** inside membrane is because of the more membrane permeability to K^+ ion in comparison with other ions present outside. Because of highly specific permeability effect to potassium, more K^+ ions are accumulated inside the nerve cell membrane than outside. The potassium ion-specific permeability happens because of **K^+ ion concentration** gradient and also because of opened permeable **membrane channels** in the membrane in resting state. The resting membrane potential inside excitable nerve cell is observed around -70 mV. If more potassium accumulates inside with more sodium ions that move outside, the cell is referred as **polarized** at the **resting membrane potential** state of the cell. The cell exists in a steady state with extracellular environment. The open **leaky potassium channel** plays an important role in establishing resting potential by allowing movement of potassium out of the cell down its concentration gradient (refer Chap. 6). In spite of the fact that potassium ion flux has more influence on **resting membrane potential (RMP)** than sodium, the RMP is not equal to potassium equilibrium potential, because few sodium channels are open during this period. In another example of muscle cells, the 10 mM low concentration of intracellular sodium is observed in comparison with extracellular 140 mM sodium, and sodium is transported inside by **nongated Na^+ channels or sodium leak channel** passively. The sodium ions may move out of the cell by **active transport** via the

sodium potassium ATPase with the net result that intracellular Na^+ is maintained constant and at a low level, even though Na^+ continually enters and leaves the cell. The reverse is true for K^+ , which is maintained at a high concentration inside the cell relative to the outside. The passive exit of K^+ through **nongated potassium ion channels** or **leak channel** is matched by active entry via the pump (refer Chap. 6).

The resting membrane potential numerical figure may range from -20 to -100 mV in various types of cells. The resting membrane potential of muscle is around -90 mV in comparison with -70 mV of nerve cell and around -50 mV in epithelial cell.

In **nonexcitable cells** such as **adipose and epithelial** tissues, the membrane potential and the resting membrane potential remain steady with time and more or less has the same value, while in stimulated or **excitable cells**, such as endocrine, muscle, or nerve cells, the membrane potential may change drastically from milliseconds to hundreds of milliseconds in a very small duration of time. These cells have two membrane potentials and two states of cells, polarized and depolarized. The immediate fast change of membrane potential is responsible for signaling in various excitable cells and various physiological functions such as nerve impulses, contraction of muscle fibers, and secretion of various molecules from gland tissues (Fig. 7.2).

According to Hodgkin and Katz experiments on a living squid neuron, if external K^+ concentration becomes equal to the concentration of K^+ inside the neuron, then K^+ equilibrium potential becomes 0 mV. The resting membrane potential change is proportional to the logarithm of ion concentration. The magnitude of resting membrane potential is determined by two factors: difference in specific **ion concentration** and difference in **membrane permeability** of the ions, which depends on the open channel in the membrane. The **Na^+-K^+ ATPase** pump maintains the concentration gradient of these ions and also participates in the establishment of these ion concentrations. This pump moves three sodium ions outside and two potassium ions inside (electrogenic pump). This unequal distribution of ions creates more negative potential inside. In

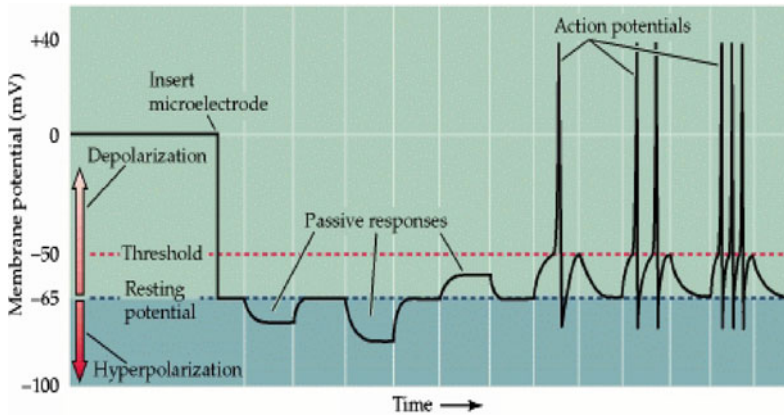


Fig. 7.2 Resting membrane potential and action potential in squid giant axon by the K ion concentration gradient. The resting membrane potential becomes more

positive in response to outside potassium ion. After Hodgkin and Katz (1949)

Table 7.2 Distribution of sodium, potassium, and chloride ions in the neuronal membrane

Ion	Extracellular concentration (mmole/L)	Intracellular concentration (mmole/L)
Sodium	150	15
Potassium	5	140
Chloride	110	10

the cells, which have **chloride channels** but not pumps, the negative membrane potential moves chloride out of the cell and chloride concentration becomes higher outside than inside. Such generated concentration gradient supports diffusion of chloride back into the cell and opposes electrical potential. In the cells with nonelectrogenic active transport, chloride moves out and creates strong concentration gradient by having more electronegative ions inside. The negative interior of the cell is also contributed by negatively charged organic molecule, proteins, and phosphates present inside (Table 7.2).

7.5 Action Potential

The signals are transmitted down the axon because of action potential generation. At **synapse** (the gap between two neighbor nerve

cells), an impulse stimulated releasing of **neurotransmitter** triggers an electrical impulse to conduct in adjacent nerve cell. The nerve cells may have very high number of synapses. The **electrical potential** across the membrane might be calculated by injecting microelectrode into neuron. The microelectrode is made of tube filled with concentrated salt solution with around 1- μ m-diameter opening, and this microelectrode is then connected to a voltmeter (**oscilloscope**) for observing transmembrane voltage of the nerve cell. Incorporation of two separate electrodes in cell is used for membrane potential observation. While one electrode generates current, the other measures the potential current in the neuron. In the membrane interior, a negative potential is observed that is pointing to the resting membrane potential (Fig. 7.3).

The action potential in the membrane can be understood as temporary membrane potential variation from resting membrane potential (RMP) by electrical signal transduction in the membrane. The membrane potential change from RMP is the basis for electrical signal transmission, which may be categorized into short distance signaling like **graded potential** and long distance signaling by **action potential**.

Depolarize, repolarize, and hyperpolarize terms explain the changes in the membrane potential relative to the resting potential in

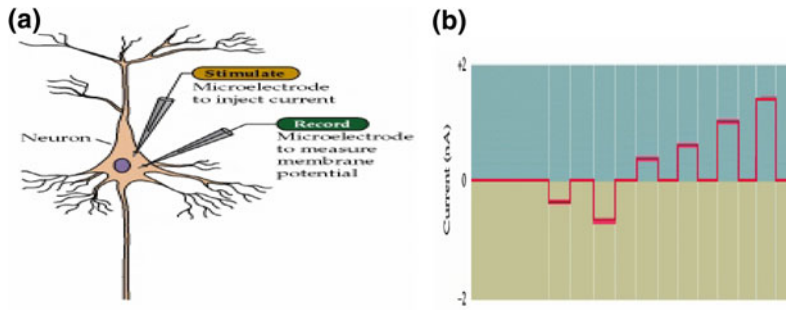


Fig. 7.3 **a** Stimulation of nerve cell for electrical membrane potential. Two microelectrodes are inserted into a neuron; one of these measures membrane potential while

the other injects current into the neuron. **b** Observation of nerve cell's electrical signal

particular direction. The cell at rest is said to be polarized with negative potential inside. When membrane potential becomes zero, the cell is in depolarized state. The term **overshoot** refers to state of the cell, and when the membrane polarity is reversed, the cell interior becomes positive. Returning depolarized cell to resting membrane potential is known as **repolarization**. When the potential is more negative than the resting potential, the cell with more negative membrane potential than RMP is in **hyperpolarized** state.

The electrical current suitable for initiating an action potential can be readily produced by inserting a second **microelectrode** into the same neuron experimentally.

As discussed above, the **graded potential** is confined to a small region of membrane by some specific changes to that particular region. These are also known as **receptor potential** or **synaptic potential**. **Action potential** is very different than the **graded potential** because there are large rapid alterations in membrane potential (from -70 to $+30$ mV). The membrane of nerve, muscle, few endocrine, immune, and some reproductive cells is called **excitable cells** because of their capacity to generate action potential. While all cells are capable of conducting graded potential, only excitable cells are responsible for the generation of action potential. Like resting membrane potential, action potential

can also be explained on the basis of sodium potassium ions. In the resting membrane potential, the **potassium leak channels** are open predominantly and very few sodium ions are open.

The action potential begins with depolarization in response to stimulus. This initial depolarization opens **voltage-gated sodium channel**, which increases membrane permeability to sodium ions several time more and allows more sodium inside. The cell becomes more and more depolarized until a **threshold potential** is generated to start action potential. Once the threshold potential is generated, more voltage-gated sodium channels are opened. The membrane potential overshoots, and cell interior becomes positive and cell exterior becomes negative. The membrane potential at this stage becomes $+60$ mV. At the maximum positive value of membrane potential during action potential, sodium permeability abruptly decreases and simultaneously **voltage-gated potassium channels** are opened. The membrane potential begins rapidly to depolarize its resting potential. Closure of sodium channel alone would restore the potential to resting level because potassium flux outside will be more than the sodium influx. This process would be enhanced by simultaneous increase in potassium permeability. Potassium influx to exterior cell becomes much more than the sodium influx inside, thereby rapidly causing

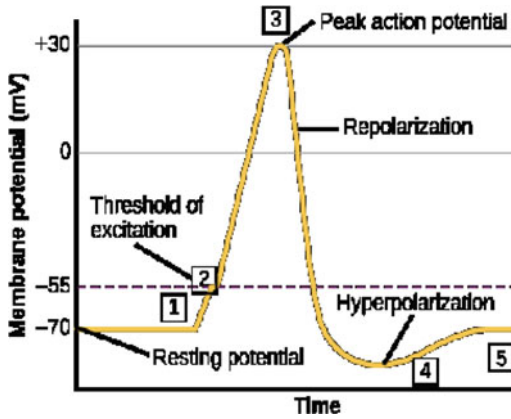


Fig. 7.4 The formation of an action potential can be divided into five steps. (1) A stimulus from a sensory cell or another neuron causes the target cell to depolarize toward the threshold potential. (2) If the threshold of excitation is reached, all Na^+ channels open and the membrane depolarizes. (3) At the peak action potential, K^+ channels open and K^+ begins to leave the cell. At the same time, Na^+ channels close. (4) The membrane becomes hyperpolarized as K^+ ions continue to leave the cell. The hyperpolarized membrane is in a refractory period and cannot fire. (5) The K^+ channels close and the Na^+/K^+ transporter restores the resting potential

potential to rest. In neural cells, many voltage-gated K^+ channels are still open even after the sodium channels became closed and caused **hyperpolarized state** in the membrane. Once the potassium channels are closed, resting membrane potential is restored. **Chloride** permeability is not affected during action potential. The number of ions crossing membrane during action potential is very small compared to the total ions in the cell. The cellular accumulation of sodium inside and loss of potassium are prevented by **sodium potassium ATPases** (Figs. 7.4 and 7.5).

The very first part of depolarization as in **graded potential** is because of local changes by channels, which have been opened by an electrical or chemical or mechanical stimulus. The depolarization increases, and more voltage-gated sodium channel opens as channel protein has voltage sensor, which respond to positive ion by changing conformation of protein. This is called **positive feedback cycle**, and this is responsible for rising phase of action potential. The cells having graded potential but not action potential

are found without voltage-gated sodium channel. The sodium permeability suddenly decreases, and channel spontaneously gets inactivated at the peak of depolarization due to opening of **inactivation gate** in voltage channel.

The sudden change in **voltage-gated sodium channel** starts repolarizing membrane. Potassium channel get activated at this time but slightly delayed. Potassium channel opening makes membrane more negative and contributes to repolarization. Finally, the closure of potassium ion is also delayed. Their slow inactivation after cell acquiring resting potential results in the period of after hyperpolarization and that is brought to an end by potassium channel closing. While sodium is inactive spontaneously, potassium only gets inactivated in response to membrane repolarization. The voltage-gated sodium channels are fast opening and fast closing in comparison with potassium.

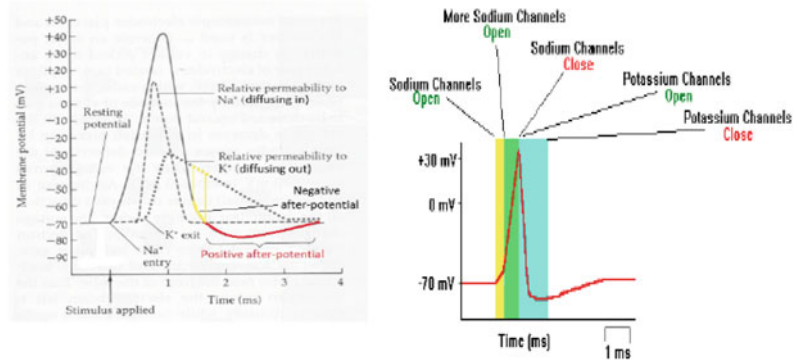
The local anesthetic drugs may inhibit initiation of action potential by stopping voltage-gated sodium channel and preventing their opening in response to depolarization. Ovary of **puffer fish** produces extremely potent toxin **tetrodotoxin**, which binds to voltage-gated sodium channel and stops the generation of action potential.

7.5.1 Refractory Period

The prestimulated cell with action potential may not generate a second action potential when stimulated by a new stimulus during a short period, and the membrane is said to be in **absolute refractory period** during that period. This occurs when voltage-gated sodium channel is open or when inactivation gate of sodium channel blocks the channel at the peak of depolarization of action potential. Following absolute refractory period, there is an interval during which a

The second action potential can only be generated by stronger stimulus after an interval from absolute refractory period. This interval time is called **relative refractory period**. The frequency of action potential is controlled by refractory period, which can be produced by excitable cell

Fig. 7.5 A membrane potential and status of sodium and potassium channels



membrane in a given time. The refractory period distinguishes these action potentials for allowing to pass individual electrical signal down the axon. This period is the key determinant for the direction of action potential propagation.

7.6 Propagation of Action Potential

The flow of action potentials in particular direction is called an **impulse**. The action potential can only be all or none phenomenon if each point along the membrane is depolarized to its threshold potential as the action potential moves down to its axon. The membrane is depolarized at each point along the way with respect to the adjacent portion of the membrane, which is still at resting potential. The difference between the potential causes ion to flow, and the local current depolarizes adjacent membrane. The new action potential produces local currents of its own, which depolarize the region adjacent to it, producing yet another action potential at the next site and so on to cause **propagation of action potential**. There sodium and potassium channels successively open and close along the length of membrane. The membrane areas that have just completed action potential are refractory and cannot start another event of action potential. The only direction of action potential is possible away from the region, which has just gone under action potential.

The excitable membranes cannot conduct action potential in any direction if these membranes are not refractory. The direction of action

potential propagation is decided by stimulus location. Usually, in skeletal muscles, action potential is initiated in middle and from one end in neurons. As already discussed, magnitude and speed of action potential generation is proportional to diameter of axon and also depends on its myelination. Larger fibers show less resistance.

7.7 Saltatory Conduction

Myelin sheath acts as insulator and does not allow movement of ions between extracellular and intracellular compartments. It also has low number of **leakage ions** and low number of **voltage-gated sodium channels**. That's why action potential only takes place at the **nodes of Ranvier** because the nodes of Ranvier have interrupted myelin coating and have more number of voltage-gated sodium channels. Because of all these reasons, the action potential jumps from one node of Ranvier to another and this propagation is called **saltatory conduction** of action potential (Fig. 7.6).

In the unmyelinated nerve cell, impulse is conducted by local current of ions in the active zone of axon membrane by the axon itself and then current passes out in the adjacent area. These local current circuits depolarize neighbor area of membrane in continuous manner, while in myelinated sheath the stimulus at nodes of Ranvier is excited by stimulus and local current is generated. This local current jumps from one node of Ranvier to another one to depolarize without passing through myelinated sheath. The

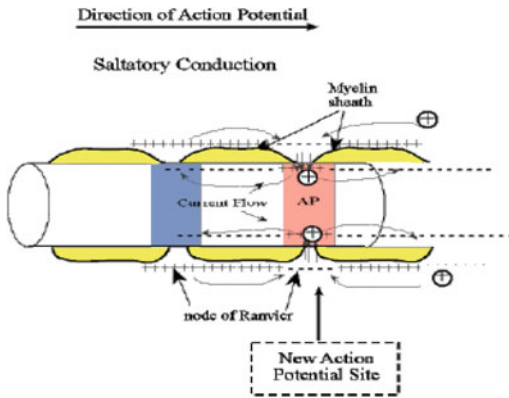


Fig. 7.6 Myelinated nerve cell and mechanism of saltatory conduction of action potential

low capacitance of myelinated sheath ensures less energy requirement to depolarize rest of the membrane between nodes of Ranvier and increase speed of impulse. The conduction velocity in myelinated sheath is proportional to diameter, and impulse conduction velocity in unmyelinated sheath is proportional to square root of diameter. The sodium flux in myelinated sheath is much less than unmyelinated because only node of Ranvier is involved in conduction, contrary to unmyelinated sheath, where the whole membrane is involved in conduction. Saltatory conduction improves energy efficiency in the neuronal cell because of very small amount of ion leakage via membrane.

7.8 Electrical and Chemical Synapses

Nerve cells have to interchange information for impulse conduction, and this occurs at synapse. The first nerve cell is called presynaptic, and the second one is postsynaptic. Majorly, two types of impulse transmissions happen at synapse: One is the electrical synapse, and other is chemical synapse. In electrical synapse, the adjacent nerve cells are internally connected by **gap junctions**, which are intracellular channels and found abundant. In chemical synapses, the two neurons communicate through the release of neurotransmitter at synapse by presynaptic neuronal

membrane. Chemical transmissions occur between axon synaptic terminals of one cell and dendrite or soma of other cell. The nerve cell may also can communicate by **volume transmission**. The volume transmission has process of diffusion through extracellular space of neurotransmitters to approach target cells. Gap junctions directly communicate between two coupled cells so that electrical currents and small molecules such as calcium, cAMP, and IP3 can move in either direction. Gap junctions are formed by each cell of pre- and postsynaptic hexameric hemichannels. These electrical synapses cannot amplify or convert presynaptic signal into other form like chemical synapse, where neurotransmitter release can be converted into electrical synapse.

Electrical synapses polarize the membrane of receptor neuron and initiate the action potential. Communication between cells is very fast, and movement is bidirectional. The hormone-secreting nerve cells of mammalian hypothalamus communicate through electrical synapses and induce hormone secretion. The signal transmitted through an electrical synapse never changes the sign of its polarity: A hyperpolarization in a presynaptic neuron will always cause an attenuated hyperpolarization in the postsynaptic neuron, and a depolarization will always cause an attenuated depolarization. The electrical synapse effectively increases the sensitivity of sensory cells and also causes **lateral excitation**, where neighbor cell may also be excited by already excited nerve cell. These electrical synapses regulate fast turnover number of gap junction channels, which are concentrated in membrane, and this electron dense part of membrane is known as "**semidense cytoplasmic matrix**" as observed by **electron microscopy technique**.

The electrical synapses are efficient in lateral excitation of nerve cells. Because of their bidirection, these synapses do not need action potential and are able to identify simultaneous subthreshold depolarization in adjacent nerve cells (Fig. 7.7).

The chemical neurotransmitter is released from a presynaptic axon in response to action potential at synaptic terminal or in change of

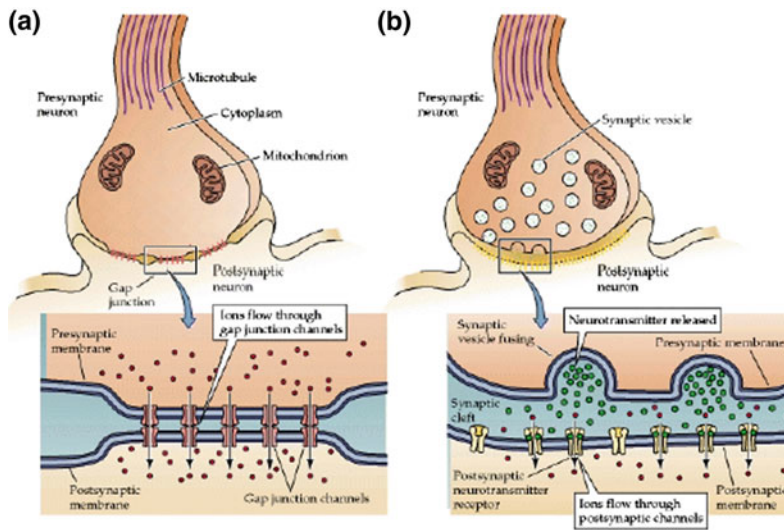


Fig. 7.7 Electrical and chemical synapses are fundamentally different in their transmission mechanisms. **a** At electrical synapses, gap junctions between pre- and postsynaptic membranes permit current to flow passively through intercellular channels. This current flow changes the postsynaptic membrane potential, initiating (or in some instances inhibiting) the generation of postsynaptic

action potentials. **b** At chemical synapses, there is no intercellular continuity, and thus no direct flow of current from pre- to postsynaptic cell. Synaptic current flows across the postsynaptic membrane only in response to the secretion of neurotransmitters which open or close postsynaptic ion channels after binding to receptor molecules

resting membrane potential. When a neuron is fired, this transmitter may **depolarize** or **hyperpolarize** a **postsynaptic** neuron by transmitter binding to its receptors. Neurotransmitters are stored in vesicles, which get fused with presynaptic neuronal cell membrane to release neurotransmitter in **synaptic cleft**, a gap between pre- and postsynaptic cell.

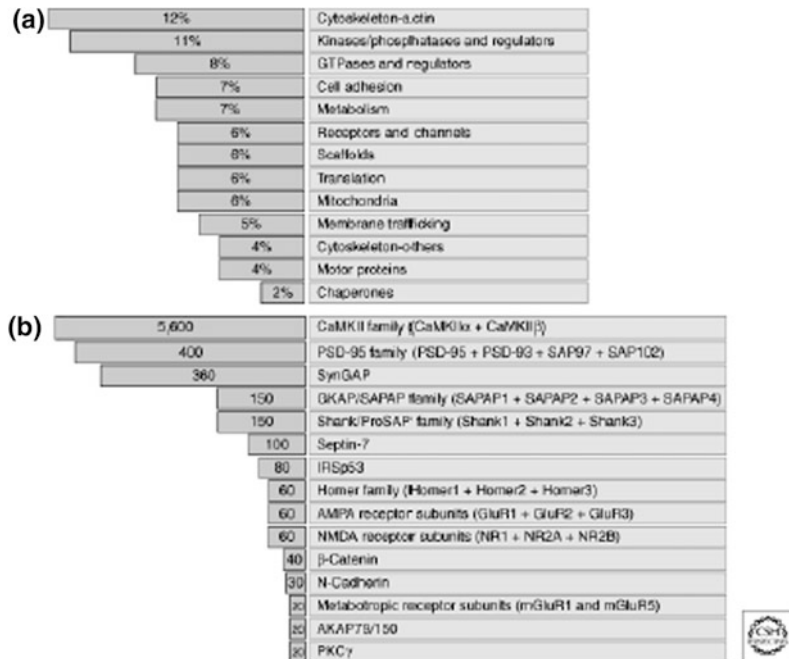
Sometimes, more than one neurotransmitter may be simultaneously released from an axon, which is known as **cotransmitter**. These neurotransmitters have different types of receptors on postsynaptic membranes. The most of chemical synapses unlike electrical synapse operate only in one direction. Neurotransmitters interact with postsynaptic membrane through **ligand-gated channel** or **G protein-coupled receptor** for signal transmission in different ways ranging from change in resting membrane potential to gene expression. Postsynaptic membrane may convert chemical signal into electrical signal. The neurotransmitters may belong to various categories: **monoamines** (epinephrine and norepinephrine); **amino acids** (glutamate, glycine, or

amino acid-derived product such as γ -aminobutyric acid); **peptides** such as enkephalin; and some **ions** and **gas** such as zinc and nitric oxide.

Synaptic transmission may be excitatory or inhibitory at postsynaptic membrane. **Excitatory synapses** are present at dendritic cell tip and known as **postsynaptic density (PSD)** having glutamate receptor, which binds to glutamate neurotransmitter released from presynaptic membrane. PSD is enriched in having accessory scaffold protein, postsynaptic receptors, cytoplasmic signaling enzymes, and adhesion molecule. More than 2000 proteins have been identified in PSD, which might be divided into 13 functional groups including cytoskeletal protein, kinases, and GTPase signaling proteins (Fig. 7.8).

There are multiple forms of various adhesion molecules in postsynaptic density. PSD-95, PSD-93/chapsin 110, SAP97, and SAP102 are found in PSD to bind and support the function of various proteins in PSD. PSD95 binds to C-terminal domain (CTD) of Glu N₂ subunit of **N-methyl-D-aspartate (NMDA)** glutamate receptor. PSD95 also binds to neuroligin,

Fig. 7.8 The proteins categories of the PSD of excitatory synapses. **a** The percentage of PSD proteins (as identified by mass spectrometry of purified PSD fractions) in various functional classes. Proteins with miscellaneous functions comprise ~ 15% (not shown). **b** Copy number of selected proteins in an average size PSD of the forebrain. <https://www.ncbi.nlm.nih.gov/pmc/articles/PMC3225953/figure/A005678F1/>



NGLs (netrin-G ligand), synaptic adhesion-like molecule (SALMs), and leucine-rich repeats transmembrane (LRRTMs). These molecules may also interact with glutamate receptors and other signaling proteins to organize adhesion molecules.

The neural plasticity, neural development, and neurodegeneration are controlled by glutamate receptors. **N-methyl-D-aspartate (NMDA)** receptors and **α amino-3-hydroxy-5-methyl-4-isoxazole propionate (AMPA)/kainate** receptors act as glutamate-gated cation channels. **Metabotropic receptors** (mGluRs) execute their effect through second messenger production via G proteins. The NMDA receptors and **metabotropic receptors** (mGluRs) are active as polymer of various subunits (NMDAR1 and NMDAR2A-2D) and multiple subtypes (mGluR1-mGluR8). The mGluR1 and mGluR5 are found to be involved in inositol triphosphate (IP3)/calcium signal transduction (Fig. 7.9).

Mass spectroscopy has explained the phosphorylation of PSD proteins by neurotransmitters. Cell adhesion molecule in PSD of postsynaptic terminal interacts with specific proteins of presynaptic cell membrane for right synapse formation

and maturation. The N-cadherin in postsynaptic density is required for synapse integrity and transsynaptic signaling. The N-cadherin can also bind to **AMPA receptors (α amino-3 hydroxy-5 methyl-4 isoxazolepropionic acid)**, while β catenin in PSD links N-cadherin to actin filament.

The other scaffolding proteins, G kinase-associated protein (**GKAP**), SAPAP-1-4, **Shank** and **Homer**, form a site of interaction for other proteins in deeper part of PSD. Shank protein promotes dendritic growth and signal conduction. Homer protein also interacts with dynamin 3 protein at PSD to connect it with endocytic region.

The serine/threonine phosphatase 1, tyrosine phosphatase along with various signaling kinase enzymes such as nonreceptor tyrosine kinase, and **calcium calmodulin-dependent protein kinase II (CaMKII α)** are part of PSD. CaMKII α , activated by calcium influx through NMDA (**N-methyl-D-aspartate**) receptor, recruits proteasome to activated dendrites for ubiquitinated protein turnover. The CaMKII α also interacts with F-actin to stabilize dendritic cells.

Small GTPases proteins such as Ras and Rho regulate AMPA receptor cycling and dynamics and morphology of dendritic cells through

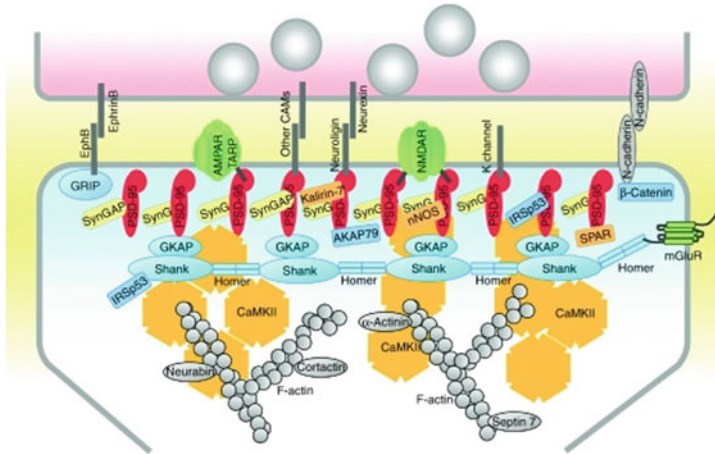


Fig. 7.9 Molecular organization of the PSD of excitatory synapses. Schematic diagram of the major proteins of the PSD, with protein interactions indicated by direct contacts or overlaps between the proteins. The relative numbers of the proteins shown correlate roughly with their relative

abundance in PSDs of forebrain. Copy numbers of most adhesion molecules and ion channels are unknown (indicated by dark gray lines). Each CaMKII shape represents a dodecamer. <https://www.ncbi.nlm.nih.gov/pmc/articles/PMC3225953/figure/A005678F1> (Color figure online)

F-actin polymerization. Activity-dependent protein turnover at the synapses by the **ubiquitin–proteasome system (UPS)** has emerged as a mechanism associated with the **long-term global modification** of synapses.

Guanylate kinase-associated -protein (GKAP or SAPAP), a family of four scaffold proteins, which interact with the guanylate kinase (GK) domain of PSD-95, and DAP for SAP90/PSD-95-associated protein and hDLG-associated protein, respectively, are involved in synaptic scaling. These proteins along with synaptic protein SHANK and CaMKIIa (multifunctional kinase) are found on the cytoplasmic side of PSD.

PSD composition can be rapidly modified by **phosphorylation, ubiquitination, palmitoylation**, and proteasome-mediated protein degradation. GKAP–PSD 95 docks AMPA receptor at the excitatory synapse via AMPA receptor regulatory protein (TARP) for homeostatic synaptic scaling. **Synaptic scaling** is also known as **synaptic plasticity** that adjusts the strength of all neuron’s excitatory synapses up or down to stabilize firing. Inhibitory synapses are majorly found around the nerve cell body and on dendritic shaft.

Inhibitory postsynaptic assembly of proteins is much simpler than the excitatory synapse.

Glycine and **γ aminobutyric acid (GABA)** are central receptors of inhibitory synapse, which directly interact with **gephyrin**, a postsynaptic scaffold protein in postinhibitory synaptic membrane. There are three classes of GABA receptor: **GABA A**, **GABA C** ionotropic receptors (ion channels), and **GABA B** metabotropic G protein-coupled receptors. Gephyrin helps in glycine receptor clustering, while GABA receptor cluster of their own may require gephyrin and associated proteins for postsynaptic differentiation in later stage. Gephyrin protein self-polymerizes to form hexagonal lattice unlike PSD assembly of excitatory synapse. The polymerization is regulated by phosphorylation. The **glycogen synthase kinase 3 β (GSK3 β)** phosphorylation at serine 270 reduces gephyrin polymerization and signal propagation. GSK3 β -inhibitor lithium chloride induces polymerization, and this may be the reason for lithium effect as medicine in psychological disorders. Synaptic adhesion molecules regulate inhibitory synapse development and differentiation via dendritic adhesion function and recruit specific membrane signal protein simultaneously (Fig. 7.10).

Synaptic strength and nerve cell excitability are controlled by regulated turnover cycling of

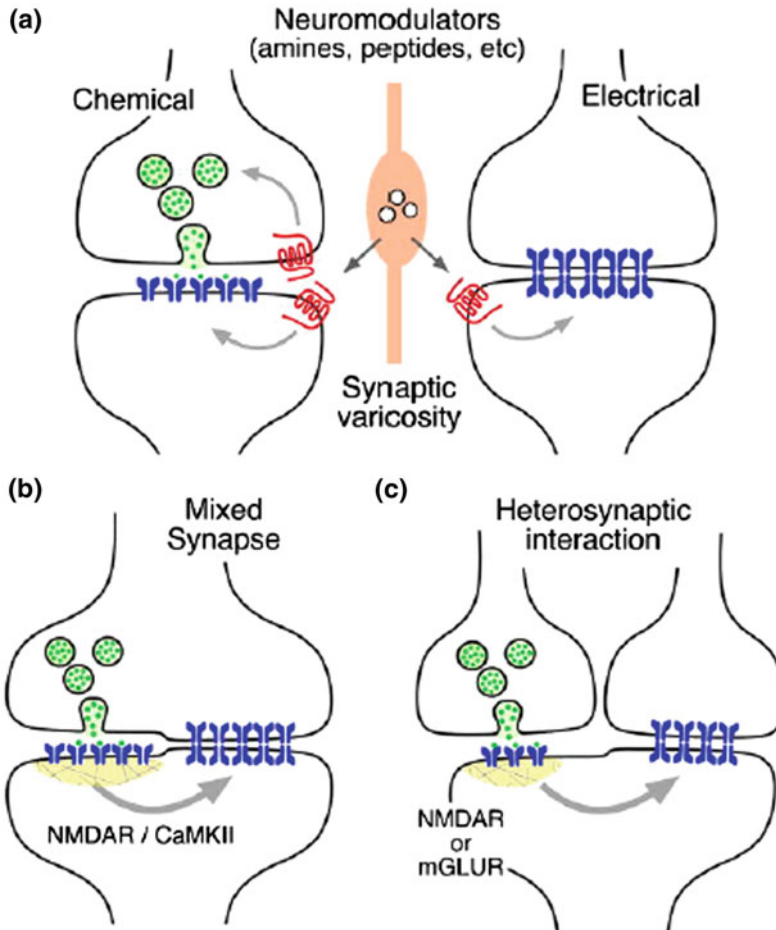


Fig. 7.11 Interaction between chemical and electrical synapse in developed nervous systems. **a** Released neurotransmitter modulators control strength of chemical and electrical synapses via activation of G-protein coupled metabotropic receptors. **b** Co-existence of electrical and chemical synapses at mixed synapses. Glutamatergic synapses regulate the strength of electrical synapses via

a postsynaptic mechanism that includes the activation of NMDA receptors (NMDAR) and CaMKII. **c** Regulation of electrical synapses by glutamatergic transmission could also be heterosynaptic. Nearby glutamatergic synapses can regulate electrical transmission via NMDAR or mGLUR activation. <https://www.ncbi.nlm.nih.gov/pmc/articles/PMC3225953/figure/A005678F1/>

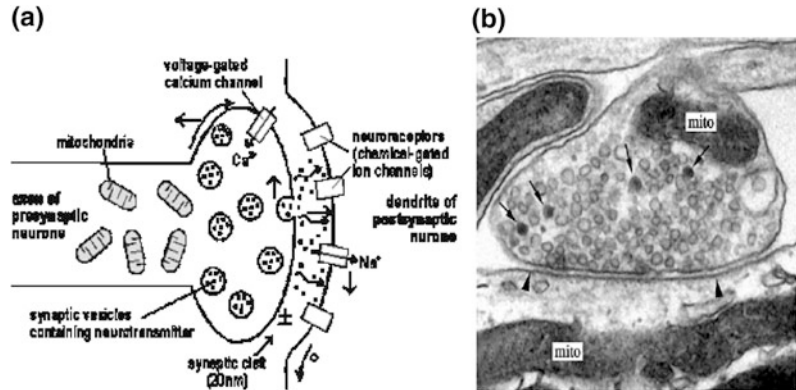
excitatory and excessive inhibitory synapses may cause anxiety or insomnia (Fig. 7.12).

The neurotransmitters are cycled either by degradation or by reutilization after signal propagation. The enzyme acetylcholine esterase hydrolyzes **acetylcholine**. The **catecholamines** and **glutamate** neurotransmitters are reutilized. Some fast-acting neurotransmitters regulate ion channels by inducing a **conformational change** in the **receptor**, which is known as **ligand-gated ion channels** (refer Chap. 9).

7.9 Exocytosis of Neurotransmitter

The vesicles secrete their contents through exocytosis only. Synaptic vesicles are fused with membrane to disrupt membrane for secreting their neurotransmitters. The neurotransmitters are released from vesicles into **synaptic cleft**, the space between pre- and postsynaptic cell. **Synaptic vesicles** (or vesicle precursors) are synthesized in the soma and transported to

Fig. 7.12 a Pre and post synaptic vesicle.
b Micrograph of a synapse



synaptic terminals by axonal transport. These vesicles, loaded with neurotransmitter, are translocated to release sites for docking. The docked vesicles subsequently become aligned for fusion (priming). Initially, Ca^{2+} ions are influxed through **voltage-gated calcium channels** in the presynaptic site. These calcium ions induce movements of the vesicles toward the active sites by dissolving some actin filaments. Calcium ions enhance fusion of the vesicles with the presynaptic membrane. As these vesicles fuse, neurotransmitters are released into the synaptic cleft and bind to the corresponding receptors associated with the postsynaptic density (PSD) on the postsynaptic neuron. To terminate the neurotransmitter signal in the synaptic cleft, the transmitter is either destroyed or transported back into a cell via a **transmitter uptake transporter**. Vesicle membrane that is incorporated into the plasma membrane during fusion is recycled by **endocytosis**. Vesicular components are sequestered into **clathrin-coated pits** at specific area of the membrane, which later on get detached from the plasma membrane as coated vesicles. After the vesicles are uncoated, they fuse with synaptic endosomes. Finally, mature vesicles bud from the synaptic endosomes (*the detail of exocytosis is discussed in Chap. 10*) (Fig. 7.13).

Synthesis of neurotransmitters

The synthesis of **acetylcholine (ACh)** takes place in the nerve terminals with acetyl coenzyme A (also called acetyl CoA) and choline

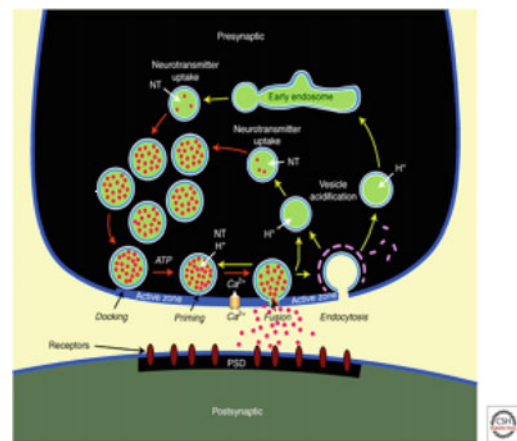


Fig. 7.13 The synaptic vesicle cycle. A presynaptic nerve terminal is depicted schematically as it contacts a postsynaptic neuron. The synaptic vesicle cycle consists of exocytosis (red arrows) followed by endocytosis and recycling (yellow arrows). Synaptic vesicles (green circles) are filled with neurotransmitters (NT; red dots) by active transport (neurotransmitter uptake) fueled by an electrochemical gradient established by a proton pump that acidifies the vesicle interior (vesicle acidification; green background). In preparation to synaptic exocytosis, synaptic vesicles are docked at the active zone, and primed by an ATP-dependent process that renders the vesicles competent to respond to a Ca^{2+} -signal. When an action potential depolarizes the presynaptic membrane, Ca^{2+} -channels open, causing a local increase in intracellular Ca^{2+} at the active zone that triggers completion of the fusion reaction. Released neurotransmitters then bind to receptors associated with the postsynaptic density (PSD). After fusion pore opening, synaptic vesicles probably recycle via three alternative pathways: local refilling with neurotransmitters without undocking, local recycling with undocking, and full recycling of vesicles with passage through an endosomal intermediate. Adapted from Südhof (2004) (Color figure online)

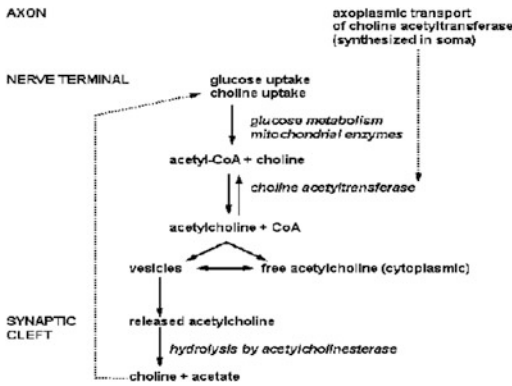


Fig. 7.14 Synthesis and release of acetyl choline

precursor. Acetyl CoA is the product of pyruvate dehydrogenase in mitochondria, and choline is already present in plasma. The enzyme choline acetyltransferase synthesizes acetylcholine, which is released into synaptic cleft through vesicles. Acetylcholine esterase (AChE) hydrolyzes acetylcholine into synaptic cleft after signal propagation into choline and acetyl CoA (Fig. 7.14).

The **botulinum toxin** that produced by a bacteria called **clostridium botulinum** inhibits the release of acetylcholine. Another toxin **α latrotoxin**, a protein found in the venom of the female **black widow spider venom**, increases the release of acetylcholine even in the absence of calcium release. **α latrotoxin** binds to

neurexins, a group of integral membrane proteins found in presynaptic terminals. The neurexins bind to vesicular Ca^{2+} -binding protein **synaptotagmin**, which is required for exocytosis. This interaction may allow α latrotoxin to bypass the usual Ca^{2+} requirement for triggering vesicle fusion. **Glutamate** is a nonessential amino acid synthesized by glutamate–oxaloacetate aminotransferase reaction in cytoplasm, and its decarboxylated derivative γ **aminobutyric acid** (GABA) is synthesized by glutamate decarboxylase, a pyridoxal-phosphate-dependent enzyme which removes alpha carboxyl group from glutamate to produce **GABA**. Glutamate decarboxylase is expressed only in those nerve cells which use GABA as a neurotransmitter. Glutamate decarboxylase enzyme, localized with antibodies or mRNA hybridization probes, is used as **marker for GABAergic neurons** in the central nervous system (Fig. 7.15).

The neurotransmitter **serotonin** is found in the brain, lung, and gastrointestinal (GI) system. It is a major control substance of smooth muscle contractions. Serotonin involved in fear and flight responses is antagonist of epinephrine and dopamine. For serotonin synthesis, tryptophan is hydroxylated by tryptophan 5-monoxygenase to form 5-hydroxytryptophan and 5-hydroxytryptophan is decarboxylated by tryptophan decarboxylase to form serotonin (Fig. 7.16).

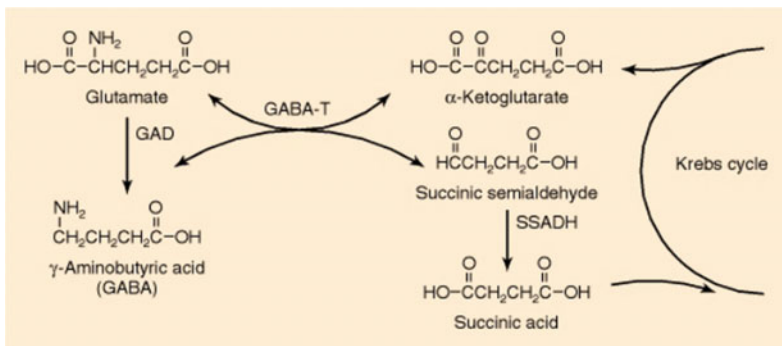


Fig. 7.15 GABA shunt for γ aminobutyric acid. GABA shunt reactions are responsible for the synthesis, conservation and metabolism of GABA. GABA-T, GABA

α - oxoglutarate transaminase; GAD, glutamis acid decarboxylase; SSADH, succinic semialdehyde dehydrogenase

Fig. 7.16 Synthesis of dopamine and serotonin

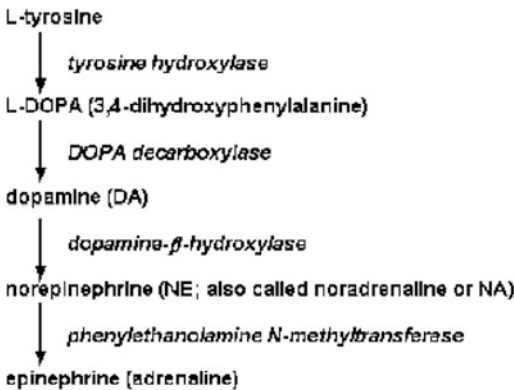
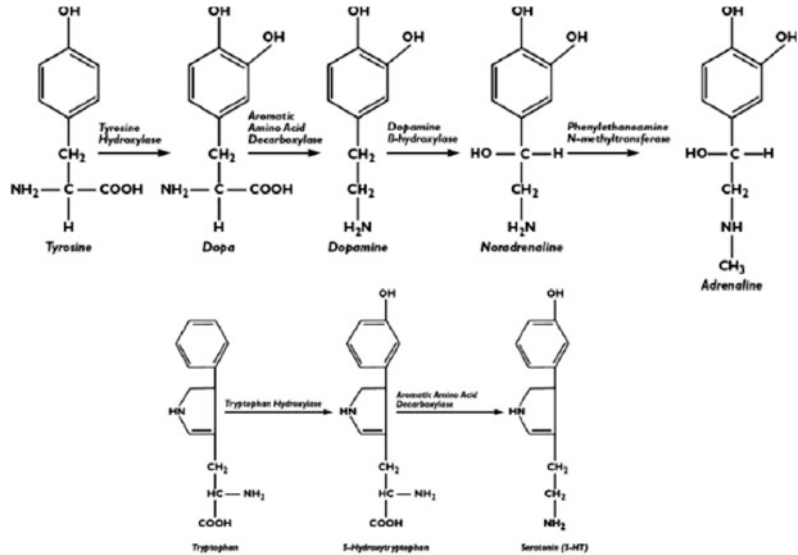


Fig. 7.17 Catecholamine biosynthesis

Catecholamine such as dopamine is a stimulatory precursor for the synthesis of the hormones norepinephrine (nor-adrenaline) and epinephrine (adrenaline). **Histamine** found in the hypothalamus for sending signals to the central nervous system is synthesized from histidine (Fig. 7.17).

Chausson P, Leresche N, Lambert RC (2013) Dynamics of intrinsic dendritic calcium signaling during tonic firing of thalamic reticular neurons. *PLoS ONE* 8:e72275

Chih B, Engelman H, Scheiffele P (2005) Control of excitatory and inhibitory synapse formation by neuroligins. *Science* 307:1324–1328

Chubykin AA, Atasoy D, Etherton MR, Brose N et al (2007) Activity dependent validation of excitatory versus inhibitory synapses by neuroligin versus neuroligin. *Neuron* 54:919–931

Collins MO, Yu L, Coba MP, Husi H, Campuzano I et al (2005) Proteomic analysis of in vivo phosphorylated synaptic proteins. *J Biol Chem* 280:5972–5982

Hodgkin AL, Katz B (1949) The effect of calcium on the axoplasm of giant nerve fibers. *J Exp Biol* 26:292–294

Llinás R (1982) Calcium in synaptic transmission. *Sci Am* 247:56–65

Pereda AE (2014) Electrical synapses and their functional interactions with chemical synapses. *Nat Rev Neurosci* 15(4):250–263

Sheng M, Kim E (2011) The post synaptic organization of synapses. *Cold Spring Harb Perspect Biol* 3(12): a005678

Shin SM, Zhang N, Hansen J, Nashaat Z et al (2012) GKAP/SAPAP orchestrates activity-dependent post-synaptic protein remodeling and homeostatic scaling. *Nat Neurosci* 215(12):1655–1666

Südhof TC (2004) The synaptic vesicle cycle. *Ann Rev Neurosci* 27(1):509–547

References

In heterotrophs, oxidation of carbohydrates, fats, and proteins from food sources generates reducing equivalents in the form of NADH and FADH₂. Oxidation of these reducing equivalents via the respiratory chain, reducing molecular oxygen, is an exergonic process with negative free energy change. The energy so generated is conserved in the form of proton gradient across the inner mitochondrial membrane of mitochondria in eukaryotes. The proton gradient developed then drives the synthesis of ATP by F₀F₁ ATP synthase by the overall process of oxidative phosphorylation.

In autotrophs like plants and photosynthetic bacteria, the light energy from the sun is harnessed to generate ATP and reducing equivalents in the form of NADPH, by the process of photophosphorylation. ATP and NADPH so generated in the light reaction of photosynthesis are utilized for CO₂ assimilation to synthesize sugar molecules in the dark via the Calvin cycle. The sites of photosynthesis in plants are the special organelles called the chloroplast. The chloroplasts have photosynthetic pigments including the chlorophyll molecules which harness the light energy to drive the process of photosynthesis.

8.1 Bioenergetics

Bioenergetics deals with the flow of energy in living organisms. A living organism requires energy to survive, to perform biological functions, to grow and repair. Different organisms

obtain their energy from different sources. **Autotrophs**, like photosynthetic bacteria, green algae, and plants, harness the light energy of the sun via the process of photosynthesis. **Heterotrophs** use organic molecules synthesized by the autotrophs as fuels to generate energy.

The **laws of thermodynamics**, which govern the chemical and physical processes, also govern the biological processes. **Thermodynamics** is the science which deals with the relationship between different forms of energy. In thermodynamic terms, a universe is broadly divided into a **system** and its **surroundings**. The system is that portion of the universe which is under study, whereas the surroundings include those portions the universe, external to the system which is thermodynamically affected by the changes occurring in the system.

A system can be an **open**, **closed**, or an **isolated system** (Fig. 8.1). An open system is one, which exchanges both energy and matter with the surroundings. Living organisms are open systems, and they exchange both energy (heat) and matter with the surroundings. A closed system exchanges only energy with no exchange of matter. Water boiling in a closed container, only exchanges heat with the surroundings, no steam (matter) is let out, as compared to an open container, which lets out both steam and heat. An **isolated system** does not exchange either matter or energy with the surroundings. A truly isolated system is difficult to obtain. A thermoflask can be considered closest to an isolated system.

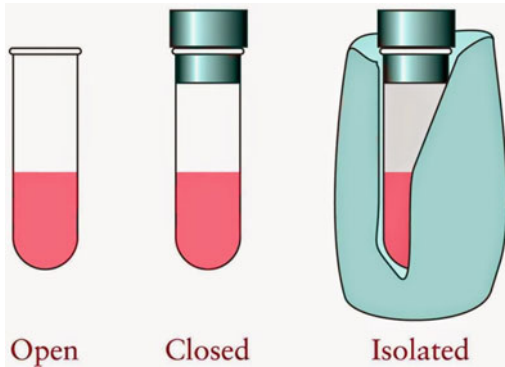


Fig. 8.1 Open and closed and isolated systems

The **first law of thermodynamics** states that the total energy of the universe does not change, and it remains constant. Energy can be changed from one form to another, and it can be transferred from the system to its surroundings or vice versa, but it cannot be created or destroyed.

$$\Delta U_{\text{univ}} = \Delta U_{\text{sys}} + \Delta U_{\text{surr}} = 0$$

In thermodynamics, the **internal energy** of a system (E/U) is energy contained within the system, which is the sum of the kinetic energy and the potential energy of the system. Internal energy is a **state function**; it depends only on the state of the system at any moment in time, not the path used to get the system to that state. The internal energy, E , of any system can change only if energy is exchanged with the surroundings in the form of heat (q/Q) or work (w).

Hence, the change in internal energy (ΔU) of a system is given by the sum of the heat (q) exchanged with the surroundings and the work (w) done on the system by the surroundings:

$$\Delta U = q + w$$

If heat flows into a system, or work is done on it by the surroundings, the internal energy of the system increases and the sign of q or w is positive. Conversely, when heat flows out of the system or work is done by the system, it is at the expense of the internal energy, and therefore, it is negative.

In biological systems, energy is used to perform different forms of work like electrical, mechanical, or chemical, for example, nerve conduction, muscle contraction, biosynthesis of biomolecules. Most biological processes take place under conditions of constant pressure. Work done at constant external pressure is the work of expansion given by: $W = P \times \Delta V$, where ΔV is the change in volume.

Thermochemistry deals with the heat changes associated with chemical reactions. If heat is released in the reaction, the process is said to be **exothermic**, but if heat is absorbed, it is an **endothermic** reaction. Heat change at constant (atmospheric) pressure is Q_p given by:

$$Q_p = \Delta U - p\Delta V = (U_2 + pV_2) - (U_1 + pV_1)$$

Introducing new function H of a system, one may rearrange previous equation to form:

$$H = U + pV$$

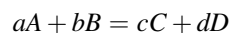
Function H is the state function called **enthalpy**. Although heat is not a state function, the heat change of a process at constant pressure is a state function as it is “path” independent, and therefore it can have only one specific value. The heat change at constant pressure is equal to enthalpy change:

$$Q_p = \Delta H$$

At constant volume, the heat of a process is equal to the change in internal energy:

$$Q_v = \Delta U$$

Heat change of a reaction is the difference in the enthalpies of the reactants and products, at constant pressure, and at a definite temperature, with every substance in a definite physical state: Consider a reaction:



$$\Delta H_{\text{reaction}} = H_{(\text{products})} - H_{(\text{reactants})}$$

$$\Delta H_{\text{reaction}} = (cHC + dHD) - (aHA + bHB)$$

The SI units of measurement of enthalpy are the joule (J) or kilojoule (kJ). If ΔH is negative for a reaction, the heat is released and the process is **exothermic**; if ΔH is positive, the heat is absorbed and the process is **endothermic**. An important law of thermochemistry given by G.H. Hess, known as **Hess's law or the law of constant heat summation**, states that the resultant heat change in a chemical reaction is the same whether it takes place in one step or several stages; i.e., it is independent of the path taken.

A **standard state** has been defined to compare the thermodynamic parameters of different reactions at specific standard conditions. Chemical standard conditions include: 25 °C or 298 K temperature, a pressure of one atmosphere (1 atm or 101.325 kPa), concentration of 1.0 M of reactants and products, when the element or compound is present in their normal physical states, i.e., standard state. The standard thermodynamic parameters like enthalpy and energy are denoted as ΔH° and ΔU° , respectively, in standard state conditions.

In biological systems, all biochemical reactions occur near neutral pH and hence biochemists have adopted a somewhat different **standard state** condition. The activity of pure water is assigned the value of 1, even though its concentration is 55.5 M. This simplifies calculations for reactions in dilute solutions involving water as a reactant, as the $[H_2O]$ term can be ignored. Hence, the **biochemical standard state** is at 298 K (25 °C), 1 atm pressure, pH 7.0, and initial concentrations of 1 M for all reactants and products except protons, which are kept at pH 7.0 ($[H^+] = 10^{-7}$ M). The thermodynamic parameters are symbolized as $\Delta H^{o'}$, $\Delta U^{o'}$, etc.

Thermodynamics can predict whether under a given set of conditions a reaction/process can occur or not. This knowledge is important for the synthesis of new compounds in a research laboratory, manufacturing chemicals on an industrial scale, or trying to understand the biological processes. A reaction that can occur under the given set of conditions without any input of energy is called a **spontaneous reaction**. Examples include a sugar cube dissolving in

water, hot tea getting cold in a cup, or rusting of an iron object in moist air. If a reaction does not occur under specified conditions on its own, it is said to be **nonspontaneous**. Another thermodynamic function, the **entropy** (R. Clausius 1851), is a criterion of determining the spontaneity of a process. Entropy is a measure of the degree of randomness or disorder of a system, and is denoted by symbol S . The relationship between entropy and the spontaneity of a reaction is given by the **second law of thermodynamics**: The entropy of an isolated system always tends to increase ($\Delta S > 0$). In an open system, the total entropy change for any process is the sum of the entropy changes in the system (ΔS_{sys}) and in the surroundings (ΔS_{surr}). Therefore:

For a spontaneous process: $\Delta S = \Delta S_{\text{sys}} + \Delta S_{\text{surr}} > 0$,
For an equilibrium process: $\Delta S = \Delta S_{\text{sys}} + \Delta S_{\text{surr}} = 0$.

Summarizing from these equations, the **second law of thermodynamics** states that the **entropy of the "universe" always increases in a spontaneous process until equilibrium is reached** when no further change can occur.

Living organisms due to their highly ordered structures appear to defy the second law of thermodynamics. Living organisms take in food matter from outside and build macromolecules, cells, tissues, and organs which involve non-spontaneous processes resulting in decrease in entropy. But living organisms also release heat and waste products like water, CO_2 , sweat into the surroundings, and hence, the entropy of the universe as a whole increases.

L. Boltzmann showed that the entropy of a system is related to the natural logarithm of the number of thermodynamic probability of occurrence of the system state (W):

$$S = k \ln W,$$

where Boltzmann constant $k = 1.3807 \times 10^{-23}$ J/K.

Thermodynamic probability of occurrence of the system state equals the number of microstates

that corresponds to a given macrostate of the system characterized by pressure, temperature, and energy. It follows that a system with fewer microstates has lower entropy and a system with more microstates has a higher entropy.

For a reversible (slow) thermodynamic change, where dQ is the heat transferred and T is the temperature at which heat transfer occurs, the entropy change of the system is:

$$dS = dQ_{\text{rev}}/T$$

The third law of thermodynamics states that the entropy of a perfect crystalline substance is equal to zero at the absolute zero of temperature.

Based on the third law of thermodynamics, the increase in entropy of the substance can be theoretically determined when it is heated from 0 K to a given temperature. The change in entropy, ΔS , can be expressed as:

$$\begin{aligned}\Delta S &= S_T - S_0, \\ S_T &= S_0 + \Delta S\end{aligned}$$

As the entropy of a pure crystalline substance is zero at absolute zero, therefore:

$$S_T = \Delta S.$$

The standard entropy values of a compound are measured in J/K mol.

But entropy of a system is difficult to determine. The entropy change of a substance can be calculated from the temperature change and heat capacity of the substance. The change in entropy is given by the equation:

$$\Delta S = C \ln(T_2/T_1)$$

where T_2 and T_1 are the final and initial temperature of the substance, and C is the heat capacity of the substance. The heat capacity of any substance is the amount of heat required to raise the temperature of one mole of the substance by one degree. At constant pressure, the heat capacity is represented by C_p , and the constant volume heat capacity by C_v .

For a constant pressure process:

$$C_p = dH/dT$$

At constant temperature and pressure:

$$\Delta S = Q_p/T = \Delta H/T$$

As at constant pressure, the heat change is equal to the enthalpy change of the system, ΔH .

Given by the second law of thermodynamics for a spontaneous process:

$$\begin{aligned}\Delta S &\geq 0 \\ \Delta S &\geq Q_p/T = \Delta H/T \\ T\Delta S - Q_p &\geq 0 \\ T\Delta S - \Delta H &\geq 0 \\ \text{or,} \\ \Delta H - T\Delta S &\leq 0\end{aligned}$$

A new thermodynamic function, Gibbs free energy (ΔG), named in honor of **Josiah Willard Gibbs** (1839–1903) (Picture 8.1), defined the criteria of spontaneity. The Gibbs free energy (G) expresses the amount of energy available for doing work during a reaction at constant temperature and pressure.

$$\Delta H - T\Delta S = \Delta G \quad (8.1)$$



Picture 8.1 Josiah Willard Gibbs (1839–1903)

A reaction is spontaneous, if: $\Delta H - T\Delta S = \Delta G < 0$.

A reaction is at equilibrium, if: $\Delta H - T\Delta S = \Delta G = 0$.

A reaction is not spontaneous, if: $\Delta H - T\Delta S = \Delta G > 0$.

If an isolated system ($Q = 0$) is at constant pressure ($Q = \Delta H$), then

$$\Delta H = 0.$$

Therefore, the Gibbs free energy of an isolated system is:

$$\Delta G = -T\Delta S.$$

Effect of ΔH and ΔS on spontaneity

ΔH	ΔS	Result
-	+	Spontaneous at all temperatures
+	+	Spontaneous at high temperatures
-	-	Spontaneous at low temperatures
+	-	Not spontaneous at any temperatures

Different representations of free energy change

ΔG Actual free energy change under specified conditions, including actual cellular concentration of reactants and products

ΔG° Standard free energy change, when all reactants and products in their standard states are at 1 molar concentration

$\Delta G^{\circ'}$ Standard free energy change for the **biochemical standard state**, all reactants and products at 1 mol/L except

$\Delta G^{\circ'}$ $[\text{H}^+] = [\text{OH}^-] = 10^{-7}$ mol/L, which allows pH = 7

For a reaction: $A + B \leftrightarrow C + D$

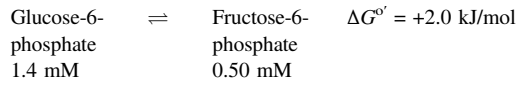
Free energy change:

$$\Delta G = \Delta G^{\circ'} + RT \ln \frac{[C][D]}{[A][B]}$$

R 8.314 J K⁻¹ mol⁻¹, the gas constant

T 298 K

Taking an example of a reaction catalyzed by glucose-6-phosphate isomerase



$\Delta G^{\circ'}$ is positive; however,

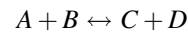
$$\begin{aligned} \Delta G &= 2.0 + \frac{8.314 \times 298}{1000} \ln \frac{0.5 \times 10^{-3}}{1.4 \times 10^{-3}} \\ &= 2.0 + 2.478 \times (-1.030) \\ &= 2.0 - 2.55 \\ &= -0.55 \text{ kJ/mol.} \end{aligned}$$

As ΔG is negative under the given conditions, the reaction proceeds toward right, even though $\Delta G^{\circ'}$ is positive.

8.1.1 Difference Between ΔG and $\Delta G^{\circ'}$

The actual free energy change, ΔG , of a chemical reaction is a function of the actual concentration of reactants and products, and conditions of pH and temperature at which reaction takes place. ΔG changes with changing concentrations of reactants and products. As the reactants are utilized and products are formed, it becomes less and less negative and approaches equilibrium. $\Delta G^{\circ'}$ is standard free energy change under standard conditions and one molar concentration of reactants and products at pH 7. It is a constant value for a particular reaction.

The relationship between standard free energy and equilibrium constant of a reaction.
For a reaction at equilibrium,



The following two relationships are **true**:

$$\Delta G = 0, \text{ and } K_{\text{eq}} = \frac{[C][D]}{[A][B]} \text{ (Equilibrium constant)}$$

Hence,

$$0 = \Delta G'^{\circ} + RT \ln K_{\text{eq}}$$

$$\Delta G'^{\circ} = -RT \ln K_{\text{eq}}$$

For example, the equilibrium constant for the glucose-6-phosphate isomerase reaction can be determined from its standard free energy change $\Delta G'^{\circ} = +2.0$ kJ/mol.

$$2.0 = \frac{8.314 \times 298}{1000} \ln K'_{\text{eq}}$$

$$\ln K'_{\text{eq}} = \frac{-2.0}{2.478}$$

$$\ln K'_{\text{eq}} = -0.807$$

$$\ln K'_{\text{eq}} = 0.45$$

Direction of a chemical reaction and its K'_{eq} and $\Delta G'^{\circ}$ values

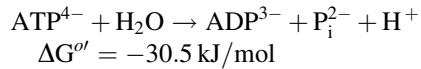
When K'_{eq} is	$\Delta G'^{\circ}$ is	Starting with 1 M components, the reaction
>1.0	Negative	Proceeds forward
1.0	Zero	Remains at equilibrium
<1.0	Positive	Proceeds backward

8.1.2 Energy Currency of the Cell

The cell uses different forms of energy currency, of which adenosine triphosphate (ATP) is considered the primary currency. The energy generated during exergonic reactions is conserved in the form of ATP, which is then used to drive endergonic processes like biosynthesis of molecules, uptake of molecules by cells against the concentration gradient, muscle contraction, etc.

ATP consists of adenosine moiety linked to three negatively charged phosphoryl groups via a phosphoester bond and two phosphoanhydride bonds. Negatively charged phosphoryl groups make the molecule very unstable due to electrostatic repulsion and hence make it a high-energy molecule. On hydrolysis of phosphoanhydride bond of ATP, the electrostatic repulsion is relieved and the phosphate group released is

further stabilized by resonance stabilization. Hence, the reaction is highly exergonic, having negative values for free energy of hydrolysis, also referred to as **phosphoryl group transfer potential**.



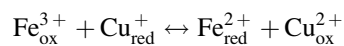
ATP can transfer this inherent high energy by group transfers to drive endergonic processes.

8.2 Oxidation–Reduction Potential

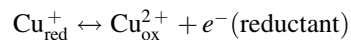
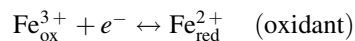
Oxidation–reduction or redox reactions are those chemical reactions in which the oxidation state of the reacting species changes by transfer of electrons. The species donating electrons is the reductant or the reducing agent, and species accepting electrons is the oxidant or the oxidizing agent. The reductant and the oxidant together constitute a redox couple or conjugate redox pair.

Oxidation–reduction or redox potential of a chemical species can be defined as the tendency of a system to gain or donate electrons. Redox reactions can be abstractly divided into two half-reactions, one involving the electron donor and another one the electron acceptor.

For example, for a reaction:



The two half-reactions are given as:



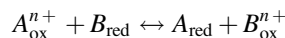
The reducing potential associated to a redox reaction depends on the chemical species involved and their respective concentrations. Relative redox potential is measured by comparing the tendency of a chemical species to gain or accept electrons with respect to a reference electrode. The hydrogen electrode is taken to be the standard reference electrode given by the half-reaction:



Hydrogen electrode half-reaction is by convention given a redox potential of $E^\circ = 0.0\text{ V}$.

Standard reduction or oxidation potentials of chemical species can be determined using a standard hydrogen electrode (SHE) (Fig. 8.2). By using an electrochemical cell, hydrogen electrode is connected through an external circuit to another half-cell in which the oxidized and reduced form of chemical species, whose relative standard redox potential is to be determined, are present at standard concentrations (each at 1 M, each gas at 1 atm). Electrons will tend to flow through the external circuit from the reductant half-cell to an oxidant half-cell. By convention, the half-cell that acquires electrons from standard hydrogen cell is assigned a positive value of E° (in volts), and one that donates electrons a negative value of E° (in volts). Hence, in a redox reaction, chemical species of half-cell with higher redox potential are oxidants, thereby get reduced, and that with lower redox potential are reductants, thereby get oxidized.

Determination of Gibb's free energy change of a redox reaction:



The Gibb's free energy, ΔG , is the negative value of electric work done.

$$\begin{aligned}\Delta G &= -W \\ &= -q \Delta E\end{aligned}$$

A redox reaction equation represents (n) number of electrons transferred. As each mole of electron has a charge of 96,485 C (known as the Faraday's constant, F):

$$q = nF$$

Therefore,

$$\Delta G = -nF \Delta E$$

At standard conditions,

$$\Delta G^\circ = -nF \Delta E^\circ$$

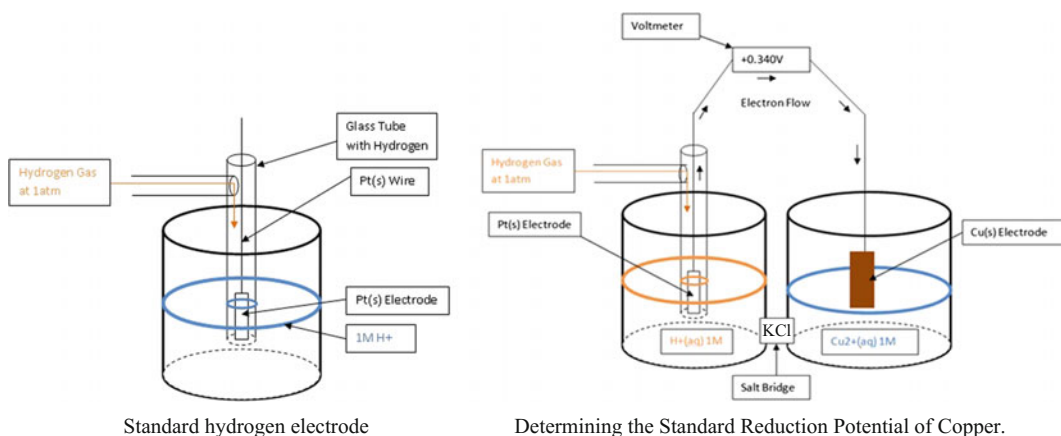


Fig. 8.2 Measurement of the standard reduction potential (E°) of a redox pair. Electrons flow from the test electrode to the reference electrode, or vice versa. The ultimate reference half-cell is the hydrogen electrode, as shown here. The electromotive force (emf) of this electrode is taken as 0.00 V. At pH 7, E° for the hydrogen electrode is -0.414 V . The direction of electron flow depends upon the relative electron “pressure” or

potential of the two cells. A salt bridge containing a saturated KCl solution provides a path for counter-ion movement between the test cell and the reference cell. From the observed emf and the known emf of the reference cell, the emf of the test cell containing the redox pair is obtained. The cell that gains electrons has, by convention, the more positive reduction potential

The general Nernst equation correlates the Gibbs's free energy ΔG and the redox potential of a chemical system.

It has been shown that

$$\Delta G = \Delta G^{\circ} + RT \ln \frac{[C][D]}{[A][B]}$$

and

$$\Delta G = -nF\Delta E.$$

Therefore,

$$-nF\Delta E = -nF\Delta E^{\circ} + RT \ln \frac{[C][D]}{[A][B]}$$

where n , R , T , and F are the number of electrons transferred, gas constant ($8.314 \text{ J mol}^{-1} \text{ K}^{-1}$), temperature (in K), and Faraday constant ($96,485 \text{ C}$), respectively. Thus, we have

$$\Delta E = \Delta E^{\circ} + \frac{RT}{nF} \ln \frac{[C][D]}{[A][B]}$$

This is known as the **Nernst equation**. The equation allows us to calculate the redox potential of any redox reaction for any concentrations. When a system is at **equilibrium**, $\Delta E = 0$ and $Q_{\text{eq}} = K_{\text{eq}}$. Therefore, we have

$$\Delta E^{\circ} = \frac{RT}{nF} \ln \frac{[C][D]}{[A][B]}$$

(for equilibrium concentrations)

$$\Delta E^{\circ} = \frac{RT}{nF} \ln K_{\text{eq}}$$

Thus, the equilibrium constant and ΔE° are related.

The reduction potential of a half-cell depends not only upon the chemical species present but also upon their concentrations. By Nernst equation, the redox potential of a given half-cell relates to the standard reduction potential (E°) and the concentration of oxidized and reduced species in the cell:

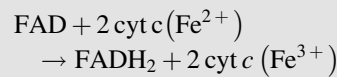
$$\Delta E = \Delta E^{\circ} + \frac{RT}{nF} \ln \frac{[\text{electron acceptor}]}{[\text{electron donor}]}$$

where $R = 8.315 \text{ J/mol K}$, n is the number of electrons transferred, and F is the Faraday constant, 96.48 kJ/V mol . At 298 K (25°C), this expression reduces to:

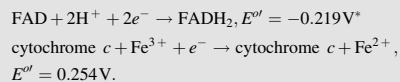
$$\Delta E = \Delta E^{\circ} + \frac{0.026 \text{ V}}{n} \ln \frac{[\text{electron acceptor}]}{[\text{electron donor}]}$$

As standard biochemical free energy change at pH 7 is $\Delta G^{\circ'}$, biochemical standard redox potential at pH 7 is $E^{\circ'}$. The values for standard redox potentials are given in Table 8.1. Each value represents the potential difference when the conjugate redox pair at 1 M concentrations at pH 7 is connected with the standard (pH 0) hydrogen electrode as reference electrode. When the conjugate pair $2\text{H}^+/\text{H}_2$ at pH 7 is connected to the standard hydrogen electrode at pH 0, electrons tend to flow from the pH 7 cell to the standard pH 0 cell; the measured $\Delta E^{\circ'}$ for the $2\text{H}^+/\text{H}_2$ pair at pH 7 is $= -0.414 \text{ V}$.

For the following reaction



determine which of the redox couples are the electron acceptor and which is the electron donor under standard state conditions, calculate the value of ΔE° , and determine the free energy change for the reaction.



$$\Delta E^{\circ'} = E^{\circ'}(\text{electron acceptor}) - E^{\circ'}(\text{electron donor})$$

$$\Delta E^{\circ'} = 0.254 \text{ V} - (-0.219 \text{ V})$$

$$\Delta E^{\circ'} = 0.473 \text{ V}$$

$$\Delta G^{\circ'} = -nF\Delta E^{\circ'}$$

$$= -2(96.5 \text{ kJ/V mol})(0.473 \text{ V})$$

$$= -91.289 \text{ kJ/mol.}$$

Table 8.1 Standard redox potentials for biological redox half-reactions

Reduction half-reaction	E'° (V)
Acetyl CoA + CO ₂ + H ⁺ + 2e ⁻ → Pyruvate + CoA	-0.48
Ferredoxin (spinach), Fe ³⁺ + e ⁻ → Fe ²⁺	-0.43
2H ⁺ + 2e ⁻ → H ₂ (at pH 7.0)	-0.414
α-Ketoglutarate + CO ₂ + 2H ⁺ + 2e ⁻ → Isocitrate	-0.38
Lipoyl dehydrogenase (FAD) + 2H ⁺ + 2e ⁻ → Lipoyl dehydrogenase (FADH ₂)	-0.34
NADP ⁺ + H ⁺ + 2e ⁻ → NADPH	-0.32
NAD ⁺ + H ⁺ + 2e ⁻ → NADH	-0.32
Lipoic acid + 2H ⁺ + 2e ⁻ → Dihydrolipoic acid	-0.29
Thioredoxin (oxidized) + 2H ⁺ + 2e ⁻ → Thioredoxin (reduced)	-0.28
Glutathione (oxidized) + 2H ⁺ + 2e ⁻ → 2 Glutathione (reduced)	-0.23
FAD + 2H ⁺ + 2e ⁻ → FADH ₂	-0.219
FMN + 2H ⁺ + 2e ⁻ → FMNH ₂	-0.22
Acetaldehyde + 2H ⁺ + 2e ⁻ → Ethanol	-0.197
Pyruvate + 2H ⁺ + 2e ⁻ → Lactate	-0.185
Oxaloacetate + 2H ⁺ + 2e ⁻ → Malate	-0.17
Cytochrome <i>b</i> ₅ (microsomal), Fe ³⁺ + e ⁻ → Fe ²⁺	0.02
Fumarate + 2H ⁺ + 2e ⁻ → Succinate	0.03
Ubiquinone (Q) + 2H ⁺ + 2e ⁻ → QH ₂	0.04
Cytochrome <i>b</i> (mitochondrial), Fe ³⁺ + e ⁻ → Fe ²⁺	0.077
Cytochrome <i>c</i> ₁ , Fe ³⁺ + e ⁻ → Fe ²⁺	0.22
Cytochrome <i>c</i> , Fe ³⁺ + e ⁻ → Fe ²⁺	0.254
Cytochrome <i>a</i> , Fe ³⁺ + e ⁻ → Fe ²⁺	0.29
Cytochrome <i>f</i> , Fe ³⁺ + e ⁻ → Fe ²⁺	0.36
Plastocyanin, Cu ²⁺ + e ⁻ → Cu ⁺	0.37
NO ₃ ⁻ + 2H ⁺ + 2e ⁻ → NO ₂ ⁻ + H ₂ O	0.42
Photosystem I (P700)	0.43
Fe ³⁺ + e ⁻ → Fe ²⁺	0.77
½ O ₂ + 2H ⁺ + 2e ⁻ → H ₂ O	0.816
Photosystem II (P680)	1.1

8.3 Types of Electron Carriers

A number of molecules act as electron carriers in biological systems. On oxidation of biomolecules by different metabolic pathways, for example, glycolysis, fatty acid oxidation, and TCA cycle, electrons are transferred to electron carriers, which then ultimately pass on these electrons to molecular oxygen via the electron transport chain.

Most electron carriers are bound to proteins/enzymes except for ubiquinone, which is a mobile electron carrier in the inner membrane of mitochondria as a part of electron transport chain.

1. Nicotinamide nucleotides (NAD⁺/NADP⁺)

Nicotinamide adenine dinucleotide (NAD) and nicotinamide adenine dinucleotide phosphate (NADP) are the coenzyme form of the vitamin niacin.

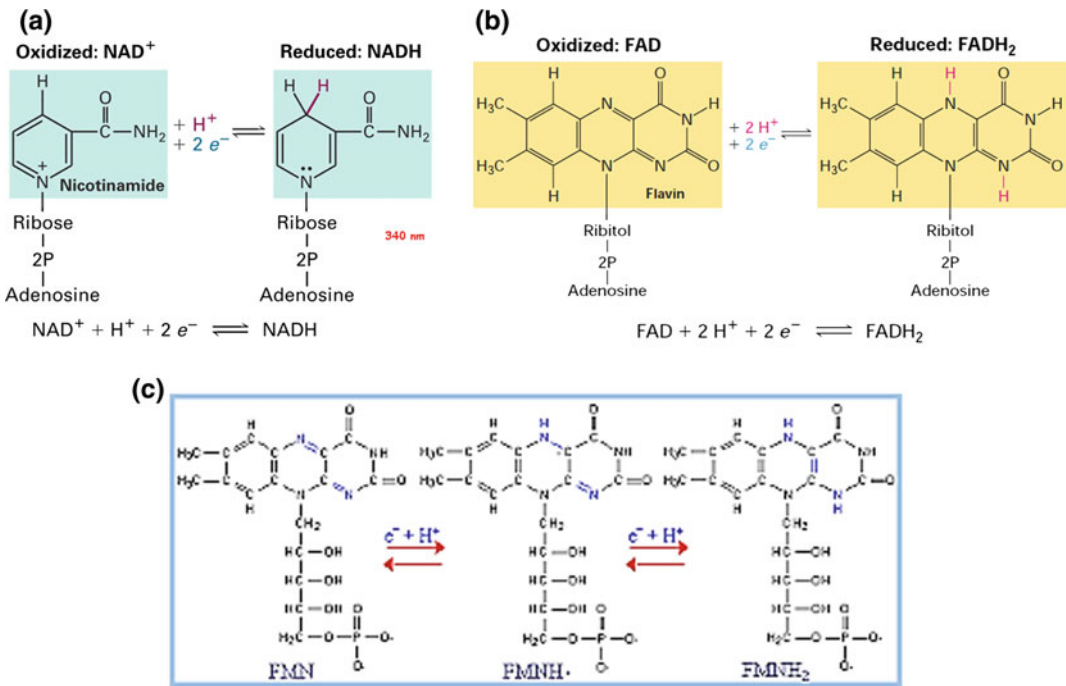
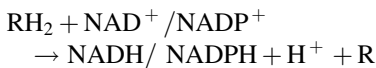


Fig. 8.3 a Nicotinamide nucleotides as two electron carriers. b, c Flavin nucleotides as one and two electron carriers

Nicotinamide nucleotides undergo reversible oxidation-reduction associated with NAD-/NADP-linked dehydrogenases. They are involved in the transfer of two hydrogen atoms from their substrates, nicotinamide adenine dinucleotides act as carriers of one hydrogen atom as hydride ion (H^- which transfers two electrons and one proton), and the other hydrogen is released as H^+ in the medium (Fig. 8.3a).



NADH carries electrons from catabolic reactions into the respiratory chain, whereas NADPH generally supplies electrons to reductive anabolic pathways. Activity of NAD-linked dehydrogenases can be monitored by absorbance at 340 nm, as reduced NADH shows additional absorbance at 340 nm. The standard redox potential of the NAD^+/NADH redox pair is -0.32 V , which makes NADH a strong reducing agent.

2. Flavin nucleotides (FMN or FAD)

Flavin nucleotides (FMN: flavin mononucleotide and FAD: flavin adenine dinucleotide) are covalently linked to proteins and hence are considered as prosthetic group of flavoproteins, the flavin containing proteins. Therefore, the standard redox potential of enzyme-bound flavin nucleotides is different from free flavin nucleotides, and vary between different flavoproteins. The oxidized flavin nucleotide can accept either one electron (yielding the semiquinone form, represented as FADH^\cdot and FMNH^\cdot) or two (yielding FADH_2 or FMNH_2) (Fig. 8.3b, c).

Many flavoproteins have associated metal cofactors like iron and molybdenum to facilitate electron transfers.

3. Ubiquinone (Q or coenzyme Q)

Ubiquinone (also called **coenzyme Q** or simply **Q**) is a lipid-soluble 2,3-dimethoxy-5-methyl-

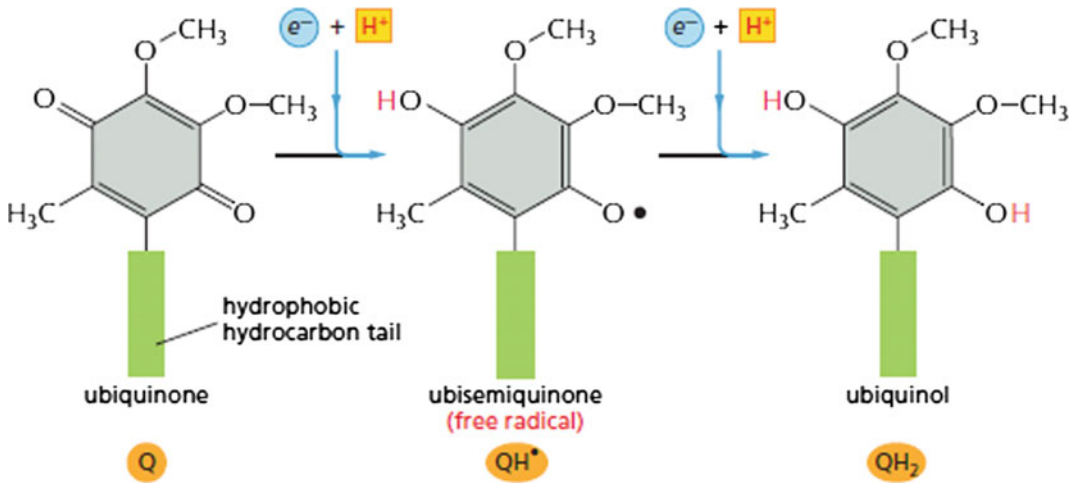


Fig. 8.4 Quinone electron carriers. Ubiquinone in the lipid bilayer picks up one H^+ (red) from the aqueous environment for each electron (blue) it accepts, in two steps, from respiratory chain complexes. The first step involves the acquisition of a proton and an electron and converts the ubiquinone into an unstable ubisemiquinone radical. In the second step, it becomes a fully reduced

ubiquinol (called ubiquinol), which is freely mobile as an electron carrier in the lipid bilayer of the membrane. When the ubiquinol donates its electrons to the next complex in the chain, the two protons are released. The long hydrophobic tail (green) that confines ubiquinone to the membrane consists of 6–10 five-carbon isoprene units, depending on the organism (Color figure online)

6-multiprenyl-1,4-benzoquinone, with a long chain of isoprene units varying between 9 and 10 in number in mammals (Fig. 8.4). Being hydrophobic and small, ubiquinone can diffuse in the membrane bilayer, shuttling electrons from complex I and complex II to complex III of electron transport chain. Ubiquinone can accept one electron and a proton to become the semiquinone radical (QH^\bullet) and additional one electron and a proton to form a fully reduced ubiquinol (QH_2). It plays an important role in quinone cycle in complex III, resulting in translocation of protons across the inner membrane of mitochondria.

Two closely related compounds plastoquinone (of plant chloroplasts) and menaquinone (of bacteria) play roles analogous to that of ubiquinone, carrying electrons in membrane-associated electron transfer chains.

4. Iron–sulfur clusters

Iron–sulfur clusters, discovered by Helmut Beinert (1960), are nonheme iron clusters present as cofactors in proteins. Such iron–sulfur proteins (ISP) are involved in electron transfer and include complex I, II, and III of electron transport chain and other metalloproteins like ferredoxin

and nitrogenase. Iron in iron–sulfur clusters is associated with acid labile, inorganic sulfur atoms, or with the sulfur atoms of Cys residues in the protein, or with both. These iron–sulfur (Fe–S) clusters can be present as simple Fe–S, [2Fe–2S], or [4Fe–4S] cluster (Fig. 8.5).

Rieske iron–sulfur proteins (named after their discoverer John S. Rieske) are a variation to most ISPs, in which one Fe atom is coordinated to two His residues rather than two Cys residues. All iron–sulfur proteins participate in one-electron transfers in which one iron atom of the iron–sulfur cluster undergoes Fe^{2+} , Fe^{3+} transition. The reduction potential of Fe–S proteins varies from -0.65 to -0.45 V, depending on the associated protein.

5. Cytochromes

Cytochromes are heme-containing proteins which have absorption maxima in visible region. The iron attached to heme prosthetic group undergoes one electron Fe^{2+} , Fe^{3+} transition. Mitochondrial electron transport chain complexes contain three classes of cytochromes, designated *a*, *b*, and *c*, of which *b* and *c*₁ are associated with complex III, *c* is a part of cytochrome *c* protein, which is a mobile electron

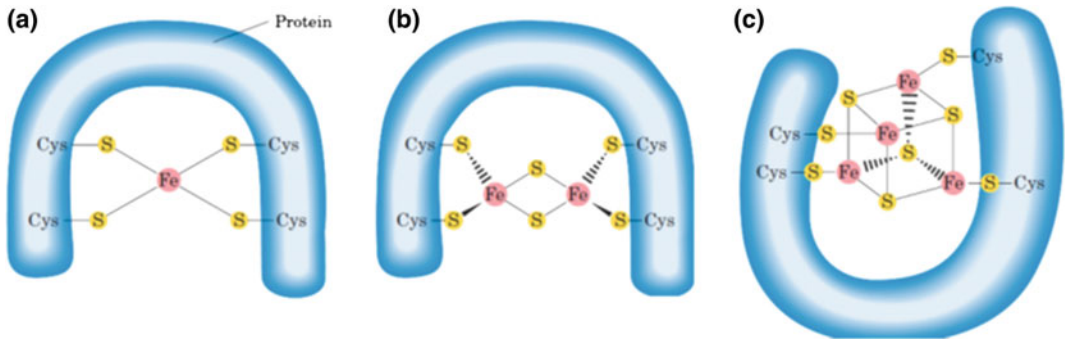


Fig. 8.5 Iron–sulfur clusters. The Fe–S centers of iron–sulfur proteins may be as simple as (a), with a single Fe ion surrounded by the S atoms of four Cys residues. Other

centers include both inorganic and Cys S atoms, as in (b) 2Fe–2S or (c) 4Fe–4S centers

carrier, and a and a_3 are associated with complex IV. Each type of cytochrome is distinguished by their distinct light absorption spectra (Fig. 8.6).

6. Copper (Cu)

Two Cu metal ions are associated with complex IV of the electron transport chain. One Cu forms a binuclear center with SH-groups of the protein, and the other Cu forms a binuclear center with heme a_3 . Cu undergoes Cu^+ , Cu^{2+} transition and is involved in one-electron transfers.

8.4 Oxidative Phosphorylation

Oxidative phosphorylation follows cellular respiration. Oxidation of carbon fuels in the form of carbohydrates, fat, and proteins by oxidative pathways like glycolysis, fatty acid oxidation, and citric acid cycle generates reducing equivalents. These reducing equivalents are collected in the form of reduced coenzymes, NADH and FADH_2 . The electron transport chain channels the electrons from these reduced coenzymes to molecular oxygen, O_2 , the final electron acceptor. When these electrons are transferred to oxygen molecule via electron transport chain, to reduce it to water molecule, a large amount of free energy is liberated, which can be used to generate ATP. **Oxidative phosphorylation** is the process in which ATP is formed as a result of the transfer of electrons from NADH or FADH_2 to molecular

oxygen, O_2 , by a series of electron carriers. In aerobic organisms, oxidative phosphorylation is the major process of ATP generation.

In eukaryotic cells, mitochondria are the site of oxidative phosphorylation, whereas in prokaryotes cytoplasmic membrane is the site of oxidative phosphorylation.

8.4.1 Sequence of Electron Carriers in Electron Transport Chain

Albert Lester Lehninger (1917–1986) (Picture 8.2), a pioneer in the field of bioenergetics, in 1948, with Eugene P. Kennedy, discovered that mitochondria are the site of oxidative phosphorylation in eukaryotes. He authored a number of classic texts, including: *The Mitochondrion*, *Bioenergetics* and, most notably, his series *Principles of Biochemistry*.

The respiratory chain of the inner membrane of mitochondria comprises of membrane-associated four distinct electron carrier complexes, which can be isolated by gentle detergent treatment of the inner membrane of mitochondria. Apart from membrane-associated complexes, two mobile electron carriers, ubiquinone and cytochrome c, also take part in the electron transport.

A number of studies helped in determining the sequence and role of different electron carriers in ETC. The first evidence came from the standard reduction potentials. Electrons tend to flow spontaneously from carriers with lower redox

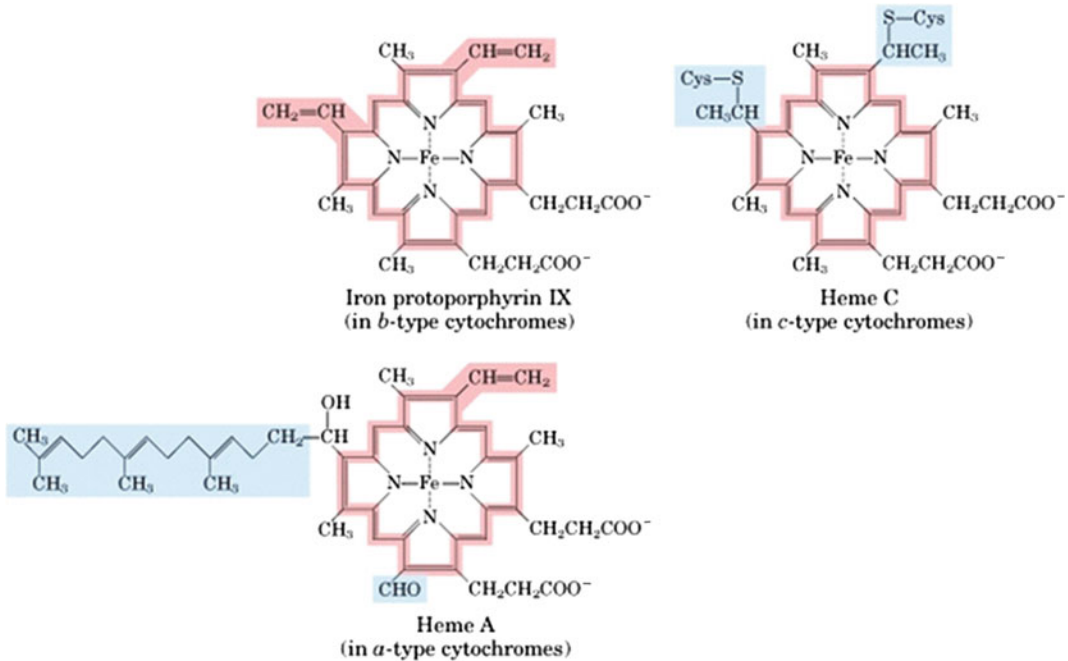


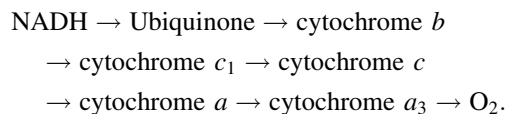
Fig. 8.6 Prosthetic groups of cytochromes. Each group consists of four five-membered, nitrogen-containing rings in a cyclic structure called a porphyrin. The four nitrogen atoms of porphyrin are coordinated with a central Fe ion, which is either in Fe²⁺ or Fe³⁺ oxidation state. Iron protoporphyrin IX is found in *b*-type cytochromes. Heme *c* is covalently bound to the protein of cytochrome

c through thioether bonds to two Cys residues. Heme *a*, found in the *a*-type cytochromes, has a long isoprenoid tail attached to one of the five-membered rings. The conjugated double-bond system (shaded pink) of the porphyrin ring accounts for the absorption of visible light by these hemes (Color figure online)

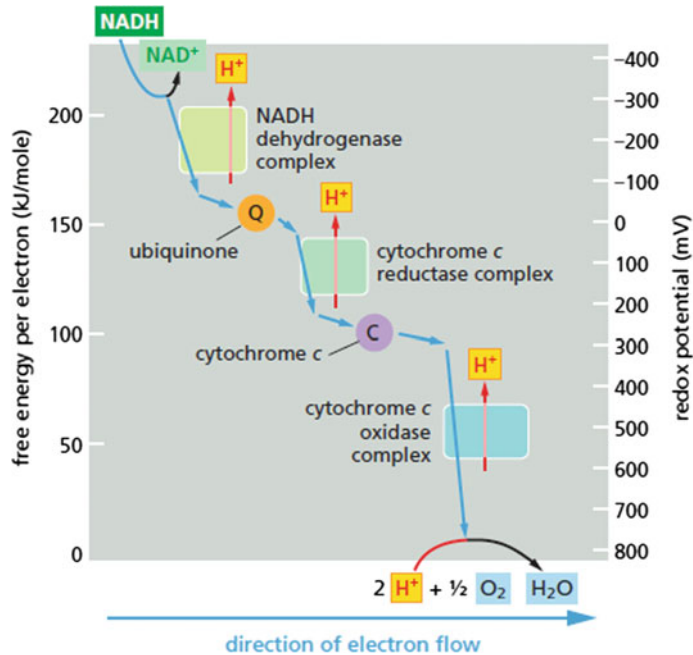


Picture 8.2 Albert L. Lehninger (1917–1986)

potential (E°) to carriers with higher redox potential (E°). Based on the standard reduction potential, moving from most -ve to most +ve, the given sequence resulted (Fig. 8.7):



The actual reduction potential in a cell depends on the concentration of reduced and oxidized forms and not on standard reduction potential. Further proof of the sequence of electron flow in the respiratory chain was provided by use of specific inhibitors. In the presence of O₂ and an electron donor, electron carriers that function before the inhibited step will be in reduced form, whereas those that function after the inhibited



Standard redox potentials of respiratory chain electron carriers.

Redox reaction (half-reaction)	E'° (V)
$2\text{H}^+ + 2\text{e}^- \rightarrow \text{H}_2$	-0.414
$\text{NAD}^+ + \text{H}^+ + 2\text{e}^- \rightarrow \text{NADH}$	-0.320
$\text{NADP}^+ + \text{H}^+ + 2\text{e}^- \rightarrow \text{NADPH}$	-0.324
$\text{NADH dehydrogenase (FMN)} + 2\text{H}^+ + 2\text{e}^- \rightarrow \text{NADH dehydrogenase (FMNH}_2)$	-0.30
$\text{Ubiquinone} + 2\text{H}^+ + 2\text{e}^- \rightarrow \text{ubiquinol}$	0.045
$\text{Cytochrome b (Fe}^{3+}) + \text{e}^- \rightarrow \text{cytochrome b (Fe}^{2+})$	0.077
$\text{Cytochrome c}_1 (\text{Fe}^{3+}) + \text{e}^- \rightarrow \text{cytochrome c}_1 (\text{Fe}^{2+})$	0.22
$\text{Cytochrome c (Fe}^{3+}) + \text{e}^- \rightarrow \text{cytochrome c (Fe}^{2+})$	0.254
$\text{Cytochrome a (Fe}^{3+}) + \text{e}^- \rightarrow \text{cytochrome a (Fe}^{2+})$	0.29
$\text{Cytochrome a}_3 (\text{Fe}^{3+}) + \text{e}^- \rightarrow \text{cytochrome a}_3 (\text{Fe}^{2+})$	0.35
$\frac{1}{2}\text{O}_2 + 2\text{H}^+ + 2\text{e}^- \rightarrow \text{H}_2\text{O}$	0.8166

Fig. 8.7 The sequence of electron carriers in the respiratory chain from NADH to molecular O_2 on the basis of increasing standard redox potential

step are completely oxidized (Fig. 8.8). By using different inhibitors that block different steps in the chain, the entire sequence was determined. The sequence was further confirmed by another method in which the entire chain electron carriers were reduced by providing an electron source but no electron acceptor (no O_2). When O_2 is introduced into the system, the electron carrier nearest to O_2 molecule is oxidized first and furthest is oxidized last. Hence, the rate at which each

electron carrier becomes oxidized (measured spectroscopically) reveals the order in which the carrier is placed in the electron transport chain. Complexes I catalyze electron transfer from NADH to ubiquinone, and complex II transfers electrons from succinate to ubiquinone. Ubiquinone transfers electrons to complex III, which then transfers electrons via cytochrome *c* to complex IV. This completes the sequence of electrons transfer from NADH to O_2 (Fig. 8.9).

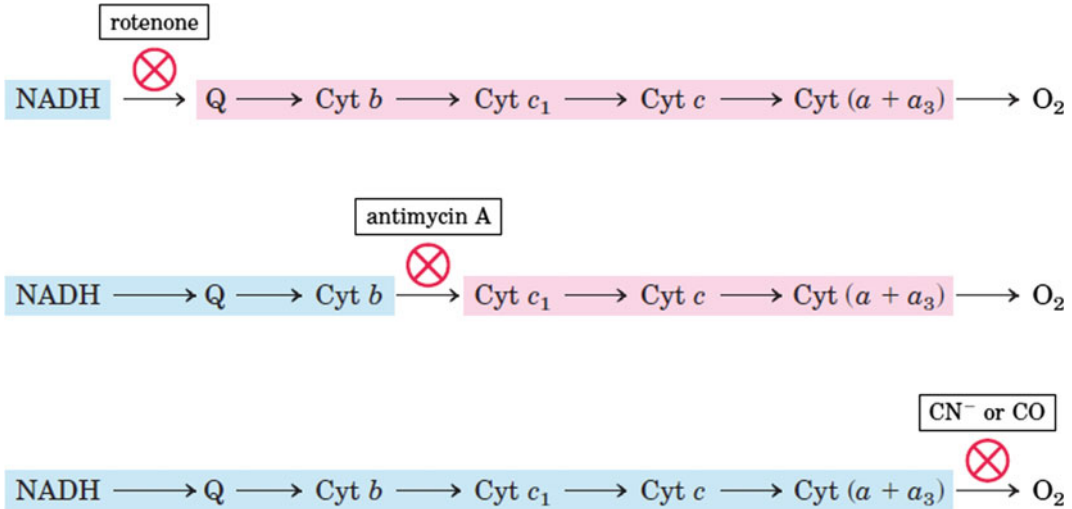


Fig. 8.8 Use of inhibitors for determining the sequence of electron carriers. In the presence of an electron donor and O₂, each inhibitor causes a characteristic pattern of oxidized/reduced carriers: Those before the block become reduced (blue), and those after the block become oxidized (pink) (Color figure online)

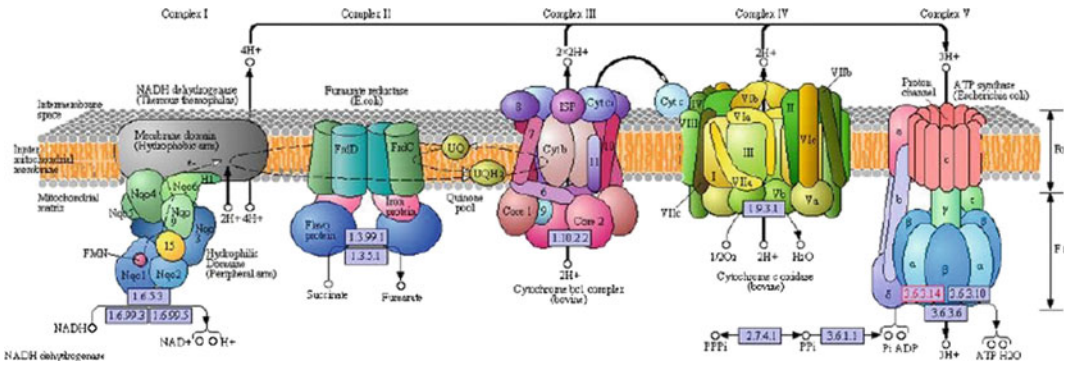


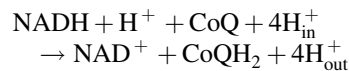
Fig. 8.9 Sequence of complexes I, II, III, and IV in electron transport chain in mitochondria

8.5 Electron Transport Complexes

8.5.1 Complex I

Complex I (NADH:ubiquinone oxidoreductase) is the first enzyme complex of the mitochondrial electron transport chain, which transfers electrons from NADH to ubiquinone. Complex I is the largest enzyme complex of the electron transport chain, having a molecular mass of around 1000 kDa.

The net reaction catalyzed by the complex I is given by:



Transfer of electrons from NADH to ubiquinone results in translocation of protons across the inner membrane, resulting in the generation of the electrochemical potential across the inner membrane of mitochondria.

Mitochondrial complex I dysfunction is implicated in many human neurodegenerative diseases. It is also a major source of reactive oxygen species (ROS), which are associated with Parkinson's disease and aging.

The structure of the eukaryotic complex I still remains to be fully characterized. In mammals, complex I consists of 44 different subunits and electron microscopy studies have revealed that it has a L-shaped structure. One arm of the L is inserted in the membrane (the hydrophobic arm), and the other arm (the hydrophilic arm) projects some 100 Å into the mitochondrial matrix. The bacterial complex I is a “cut down” version of its eukaryotic counterpart, with at least 14 of the subunits are homologous to the mitochondrial enzyme. Sazanov and his group succeeded in solving the structures of the complex I of the bacterium *Thermus thermophilus* (Fig. 8.10a).

The L-shaped complex I consists of a hydrophilic arm toward the mitochondrial matrix, which is involved in electron transfer, and a membrane arm, which mediates proton translocation. The atomic structure of the intact complex I from *T. thermophilus* (536 kDa) consists of 16 subunits, 9 iron–sulfur (Fe–S) clusters, and 64 transmembrane helices. The 95 Å long electron transfer pathway through the enzyme starts from the primary electron acceptor flavin mononucleotide, goes through the seven conserved Fe–S

clusters, then on to the quinone-binding site at the interface with the membrane domain. The four proton translocation channels found in the membrane domain are linked by the central axis containing charged residues. The redox energy of electron transfer is coupled to proton translocation by a mechanism involving long-range control of conformational changes.

The *T. thermophilus* complex I contains 14 strictly conserved core subunits (Nqo1–Nqo14), which are essentially required for its function. The subunits are shared equally between the peripheral, hydrophilic arms, comprising the NADH-oxidizing dehydrogenase module (N-module, which provides electron input into the chain of Fe–S clusters), the connecting Q-module (which conducts electrons to the quinone-binding site), and the membrane-associated hydrophobic arm, which comprises the proton-translocating P-module (Fig. 8.10a).

The **NADH substrate-binding site** is found at the distal end of the hydrophilic arm in subunit Nqo1 (Fig. 8.12), which also has a FMN-binding site. The adenine ring of NADH is held in place by stacking against three phenylalanine residues.

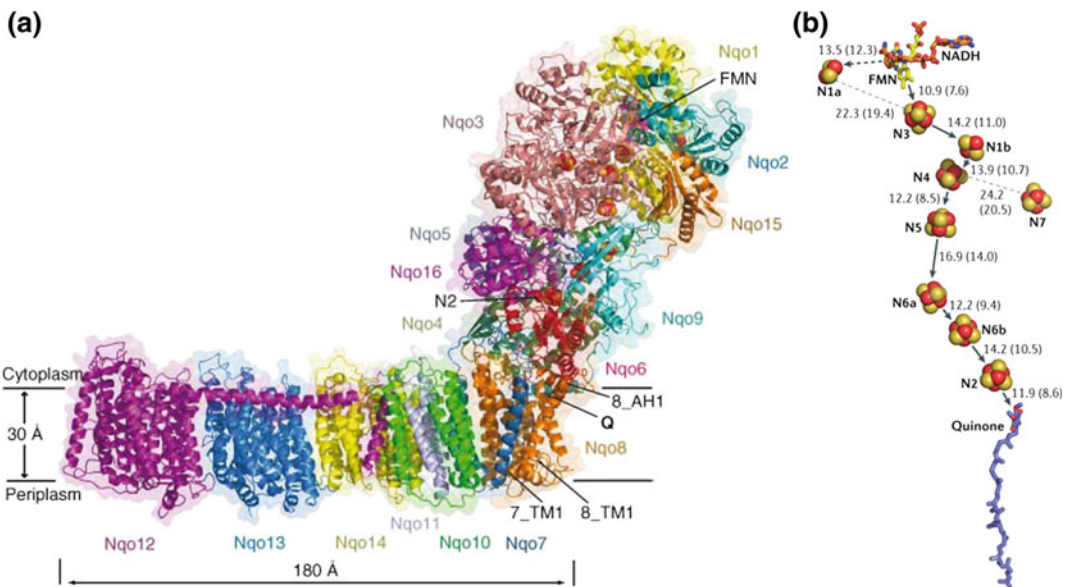


Fig. 8.10 **a** Overview of the complex I from *T. thermophilus* (PDB code 4HEA). Subunits are colored differently and labeled. Key helices around the entry point (Q) into the quinone reaction chamber and the approximate membrane position are indicated. **b** FMN and Fe–S

clusters are shown as magenta and red-orange spheres, respectively, with cluster N2 labeled. All figures were prepared with PyMOL (Schrodinger, LLC). *Source* Berrisfor et al. (2014) (Color figure online)

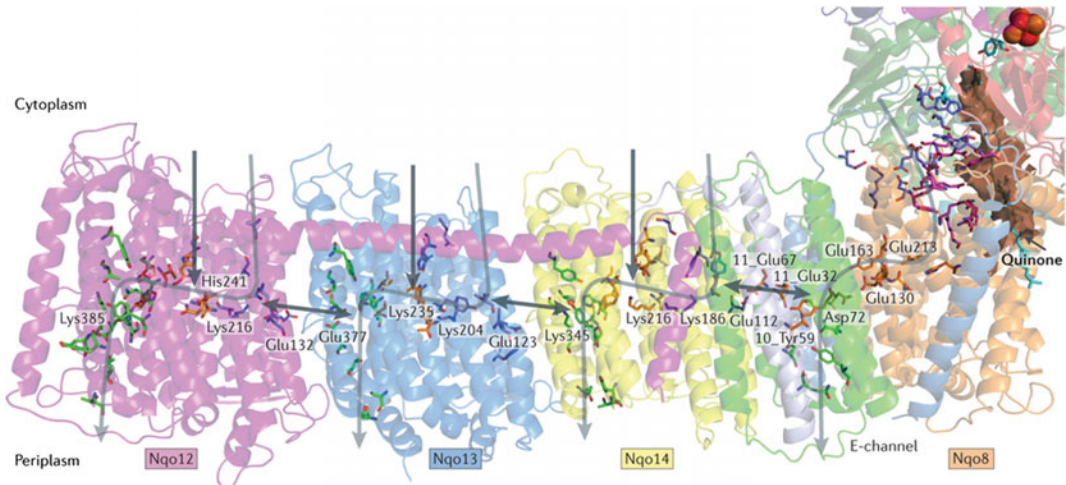


Fig. 8.11 Proton half-channels for proton translocation in complex I: Two sets of five symmetry-related helices in the antiporter-like subunits Nqo12, Nqo13, and Nqo14 each form an apparent half-channel for proton translocation, with TM4–TM8 comprising the cytoplasmic half and TM9–TM13 the periplasmic half (not shown). Polar residues lining the channels are shown as stick models with carbons shown in dark blue for the first (amino-terminal) half-channel, in green for the second (carboxy-terminal) half-channel, and in orange for connecting residues. Key residues for proton translocation in antiporter-like subunits—that is, GluTM5 (132, 123, and 112) and LysTM7 (216, 204, and 186) from the first half-channel, Lys or HisTM8 (241, 235, and 216)

from the connection, and Lys or GluTM12 (385, 377, and 345) from the second half-channel—are indicated. Residues with similar roles in the E-channel are also indicated (Glu–Asp quartet comprises Glu213, Glu163, and Glu130 from Nqo8, and Asp72 from Nqo7; 11_Glu67, 11_Glu32, 10_Tyr59 are also important for proton translocation). The quinone-binding cavity is shown in brown, with the modeled ubiquinone molecule shown in cyan and residues connecting the cavity to the E-channel shown in magenta. Previously suggested proton translocation pathways are indicated by gray arrows and additional proposed paths (new entry sites and intersubunit transfer) by black arrow (Color figure online)

This brings the nicotinamide ring of NADH close to the isoalloxazine ring of the bound FMN. Electron transfer then occurs between the C4 N atom of the nicotinamide ring of NADH and N5 of the flavin ring of FMN. These atoms are only 3.2 Å apart for efficient electron transfer.

Seven iron–sulfur clusters are associated with Nqo1, Nqo3, Nqo6, and Nqo9 subunits in the complex. These form a 90 Å long “wire” which carries electrons from the FMN, to the hydrophilic arm to the quinone-binding site formed by Nqo4, Nqo6, and Nqo8 subunits (Fig. 8.10b). The iron–sulfur clusters are at most 14 Å apart, allowing efficient electron transfer. Nqo2 and Nqo3 also contain additional iron–sulfur clusters, but they do not participate in electron transport.

Menaquinone-8 is the form of quinone which participates in the electron transport in *T.thermophilus*. NADH donates two electrons to the iron–sulfur cluster “wire/chain” which are transferred one at a time along the clusters finally to

the bound quinone and reduce it. Menaquinone-8 binds in a 30 Å long cavity formed by subunits Nqo4, Nqo6, and Nqo8 at the interface between the two, hydrophilic and membrane arms. The cavity has a narrow entrance through which menaquinone-8 has to pass. Hydrophilic residues are present along the length of quinone-binding cavity and may interact with the hydrophilic head group of the quinone as it enters the cavity. Quinone is placed close to the last iron–sulfur cluster in the “wire” by His38, Tyr87, and Asp139 residues in Nqo4, at the distal end of the cavity, for efficient transfer of electrons to quinone. Quinone leaves complex I after it becomes fully reduced, and subsequently transfers its electrons to complex III.

As the complex I reduces the bound quinone, it also **pumps four protons across the membrane**. Complex I contains four potential channels within the membrane which are likely to perform this role (Figs. 8.11 and 8.12).

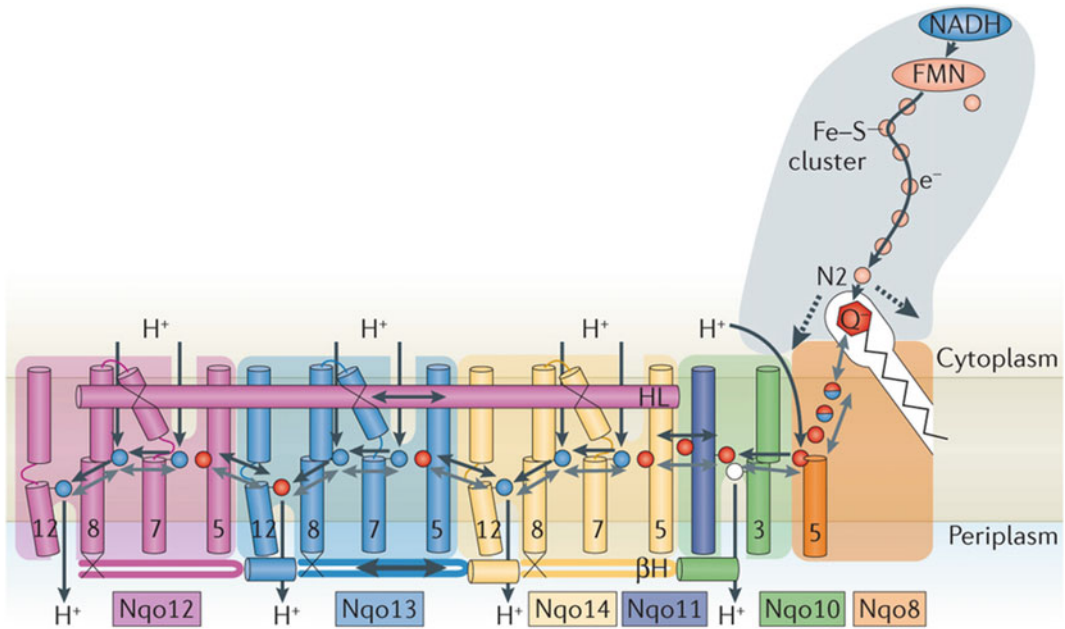


Fig. 8.12 Schematic depiction of electron transport and proton translocation in complex I. Upon electron transfer from the Fe-S cluster N2, negatively charged quinone (or charged residues nearby) initiates a cascade of conformational changes, propagating from the E-channel (at Nqo8, Nqo10, and Nqo11) to the antiporters via the central axis (indicated by gray arrows) comprising charged and polar residues that are located around flexible breaks in key transmembrane helices (TMHs). Cluster N2-driven shifts (dashed arrows) of Nqo4 and Nqo6 helices³³ (not shown) are likely to assist overall conformational changes. Helix HL and the β H element help to coordinate conformational changes by linking discontinuous TMHs between the antiporters. Key-charged residues can be

protonated from the cytoplasm through several possible pathways, including intersubunit transfer (indicated by black arrows). Following the reduction of quinone and completion of conformational changes, Lys or Glu^{TM12} in the antiporters and Glu³² from Nqo11 in the E-channel each eject a proton into the periplasm. TMHs are numbered, and key-charged residues (i.e., Glu^{TM5}, Lys^{TM7}, Lys, or His^{TM8} and Lys or Glu^{TM12} from Nqo12–Nqo14, as well as Glu⁶⁷ and Glu³² from Nqo11, which interacts with Tyr⁵⁹ from Nqo10, Glu²¹³ from Nqo8, and some residues from the connection to the quinone cavity) are indicated by red circles for Glu, blue circles for Lys or His, and white circle for Tyr. *Source* Sazanov (2015) (Color figure online)

Homologous subunits Nqo12, 13, and 14 form the proton-pumping channels 1, 2, and 3, respectively. Subunits Nqo8, Nqo10, and Nqo11 also form the channel 4, which links the other channels to the hydrophilic domain. Each channel contains two transmembrane helices, and a charged residue is present at the break of each helix in the middle. These charged residues appear to form a path for the proton to move through the channel. The proton-pumping channels are connected to each other by other charged residues. The C terminus of Nqo12 (channel 1) consists of a 104 Å long α -helix which runs

horizontally along the surface of the membrane before terminating adjacent to Nqo14. This horizontal helix interacts with one of the two broken transmembrane helices in each of the channels. Additional charged residues play a role in associating proton pumping with quinone reduction by linking quinone-binding site to the channel 4.

NADH, the primary electron donor to complex I, is 85 Å away from the quinone and the quinone 140 Å away from the most distant channel, and hence, remarkably, reduction of quinone results in pumping of protons through a **form of long-distance communication**.

8.5.1.1 Inhibitors

Rotenone, piericidin A, amytal (barbiturates), stigmatellin, and myxothiazol are some of the most commonly used inhibitors of complex I. Rotenone, used as insecticide and fish poison, is extracted from roots of *Derris spec. (Leguminosae)*, and piericidin A from *Streptomyces mobaraensis* cultures.

Rotenone blocks electron transport between iron–sulfur cluster N2 and ubiquinone. Piericidin A is similar to ubiquinone in structure and hence acts as a competitive inhibitor to ubiquinone binding. Amytal is semiquinone antagonist which inhibits the semiquinone intermediate formation. Stigmatellin and myxothiazol inhibit either the formation or release of the fully reduced quinol product.

8.5.2 Complex II

Succinate dehydrogenase or succinate-coenzyme Q reductase (SQR) is the complex II of electron transport chain. It is the only enzyme that participates in the citric acid cycle and is also a part of electron transport chain. The complex II has a large soluble domain projecting into the mitochondrial matrix and a smaller integral membrane

domain (Figs. 8.13 and 8.14). The two domains catalyze two distinct chemical reactions. The soluble domain catalyzes the reversible oxidoreduction of succinate and fumarate, which are part of the TCA cycle, and the membrane-spanning domain catalyzes the reversible oxidoreduction of quinol and quinone of the electron transport chain.

The soluble domain contains two polypeptide chains, which includes a large flavoprotein (Fp; SDHA; ~600 amino acids) with covalently attached flavin adenine nucleotide (FAD) and an iron–sulfur protein (Ip; SDHB; ~250 amino acids) associated with three iron–sulfur clusters: 2Fe:2S, 3Fe:4S, and 4Fe:4S cluster. SDHA and SDHB form the catalytic core of the complex. Succinate binds to SDHA and is oxidized to form fumarate. The electrons released from succinate oxidation are transferred to the FAD cofactor contained in SDHA and then finally to the three [Fe–S] clusters in SDHB.

The membrane-spanning domains of complex II, SDHC and SDHD, anchor the complex to the inner membrane of mitochondria. A heme prosthetic group, heme *b*, is bound at the interface between SDHC and SDHD, but whose role in electron transport is still unclear. At the interface of the two transmembrane domains SDHC/SDHD,

Fig. 8.13 Schematic diagram of complex II.
Source Sun et al. (2005)

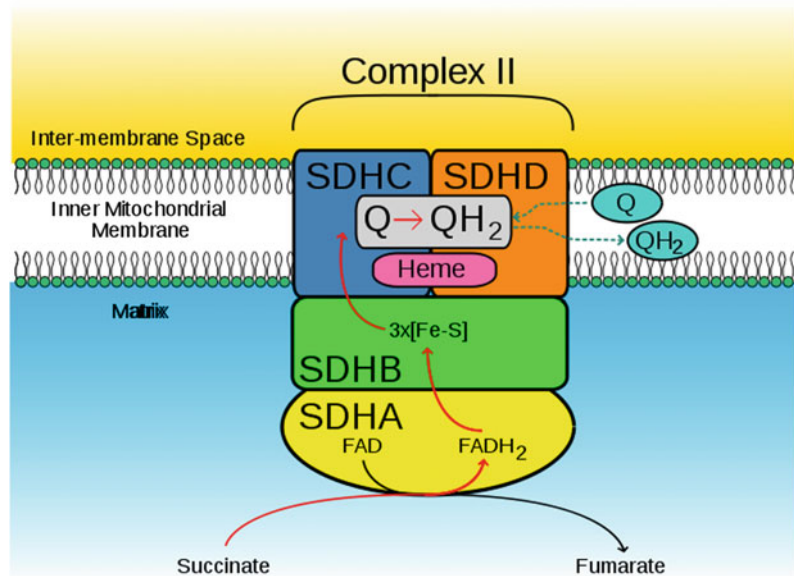




Fig. 8.14 *E. coli* SQR complex (PDB ID: 1NEK). The *E. coli* SQR has been demonstrated to be a trimer, but for clarity, only the monomer is shown. In each case, the flavoprotein (SdhA) is colored purple, the iron–sulfur protein (SdhB) is colored light blue, and the membrane-spanning subunits (SdhC and SdhD) are colored red and green. Cofactors are shown with yellow carbons and bonds. Source Iverson (2013) (Color figure online)

two ubiquinone (CoQ)-binding sites have been found: Q_P (“P” for proximal to the [3Fe–4S] cluster) and Q_D (“D” for distal to the [3Fe–4S] cluster). Ubiquinone binds to the Q_P site, which is the site for ubiquinone reduction. Ubiquinone reduction is a two-step process, first the partially reduced semiquinone is formed by the transfer of one electron, and this semiquinone radical is further reduced by a second electron to produce ubiquinol. The fully reduced ubiquinol then leaves the protein to join the membrane pool (Fig. 8.15).

8.5.2.1 Inhibitors

There are two distinct classes of inhibitors of complex II: those that are analogues of succinate and compete with succinate in binding to succinate binding site in SDHA subunit, and those that

are ubiquinone analogues and compete with ubiquinone to bind in the Q_P pocket. Examples of ubiquinone analogue inhibitors include carboxin and thenoyltrifluoroacetone. The TCA cycle intermediates, malate and oxaloacetate, and the synthetic compound malonate are the most common succinate-analogue inhibitors. TCA cycle intermediate may exert a protective role in minimizing the production of superoxide by complex I. These inhibitors have been used as fungicides in agriculture.

8.5.2.2 Role in Disease

Complex II plays an important role in both TCA cycle and electron transport chain, and hence, any defect can lead to many diseases. An array of tumor syndromes is associated with mutations in complex II proteins. These can also lead to decreased life span and increased production of superoxide ions.

SDHA mutations cause Leigh syndrome (LS), a progressive neurodegenerative disorder of infancy or childhood. Cardiomyopathy and optic atrophy have also been seen.

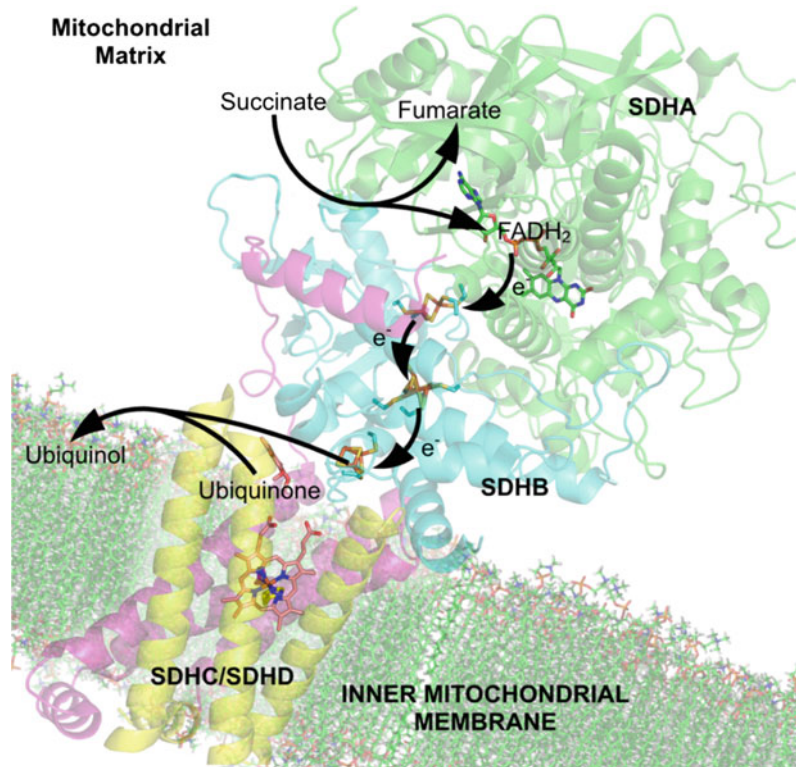
SDHB mutations, the most common of all complex II gene mutations, can lead to tumorigenesis in adrenal chromaffin cells, causing hereditary head and neck paraganglioma and hereditary pheochromocytoma. Tumors tend to be malignant.

SDHC and SDHD mutations are less common and tend to be benign. They have shown to cause hereditary paraganglioma and hereditary pheochromocytoma.

8.5.3 Complex III

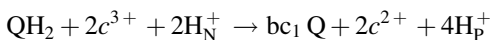
Complex III or the cytochrome bc_1 complex (cyt bc_1), also known as ubiquinol cytochrome c oxidoreductase, is a multifunctional, protein complex localized to the inner mitochondrial membrane of eukaryotes or the cytoplasmic membrane of prokaryotic organisms. This respiratory chain complex contributes to the generation of electrochemical potential. Cyt bc_1 is also an essential part of the photosynthetic apparatus

Fig. 8.15 Electron carriers of the SQR complex. FADH₂, iron–sulfur centers, heme *b*, and ubiquinone



in purple bacteria and reduces cyt *c*₂ which cycles back to the photosynthetic reaction center for oxidation.

The cyt *bc*₁ complex catalyzes the electron transfer from lipophilic ubiquinol (QH₂) to cyt *c*, coupled with translocation of proton across the membrane. For every QH₂ molecule oxidized, four protons are translocated across the inner membrane, and two molecules of cyt *c* are reduced. The net reaction catalyzed by cyt *bc*₁ is given below, where QH₂ and Q represent lipid-soluble fully reduced and oxidized ubiquinone, respectively, *c*³⁺ and *c*²⁺ represent oxidized and reduced cyt *c*, and H_N⁺ and H_P⁺ represent protons at the negative (matrix side) and positive sides (intermembrane side) of the membrane.



Complex III was discovered in mitochondria as early as in 1922, yet it is only recently in 1997 that the first crystal structure of bovine mitochondrial *bc*₁ was published by Xia et al. (1997).

The crystal structures of mitochondrial *bc*₁ found *bc*₁ to be a dimeric structure (Fig. 8.16). The cyt *bc*₁ complex can be divided into three domains: the membrane spanning, the intermembrane space, and the matrix domain. In vertebrates, the cyt *bc*₁ complex contains 11 subunits, out of which 3 subunits are the respiratory subunits involved in electron transport, and they are cytochrome *b*, cytochrome *c*₁, and the Rieske protein (ISP). Additionally, there are two core proteins and six low-molecular weight proteins. Out of the 13 transmembrane (TM) helices present in each monomer of bovine mitochondrial *bc*₁, eight are contributed by the cyt *b* subunit and one each comes from cyt *c*₁, the ISP (Reiski iron–sulfur protein).

In eukaryotes, cyt *b* is the only subunit encoded by the mitochondrial genome. This mitochondrial synthesized transmembrane protein consists of two helical bundles, helices A–E and helices F–H. It has two heme *b* prosthetic groups, and heme *b*_L with lower redox potential and *b*_H with higher redox potential take part in

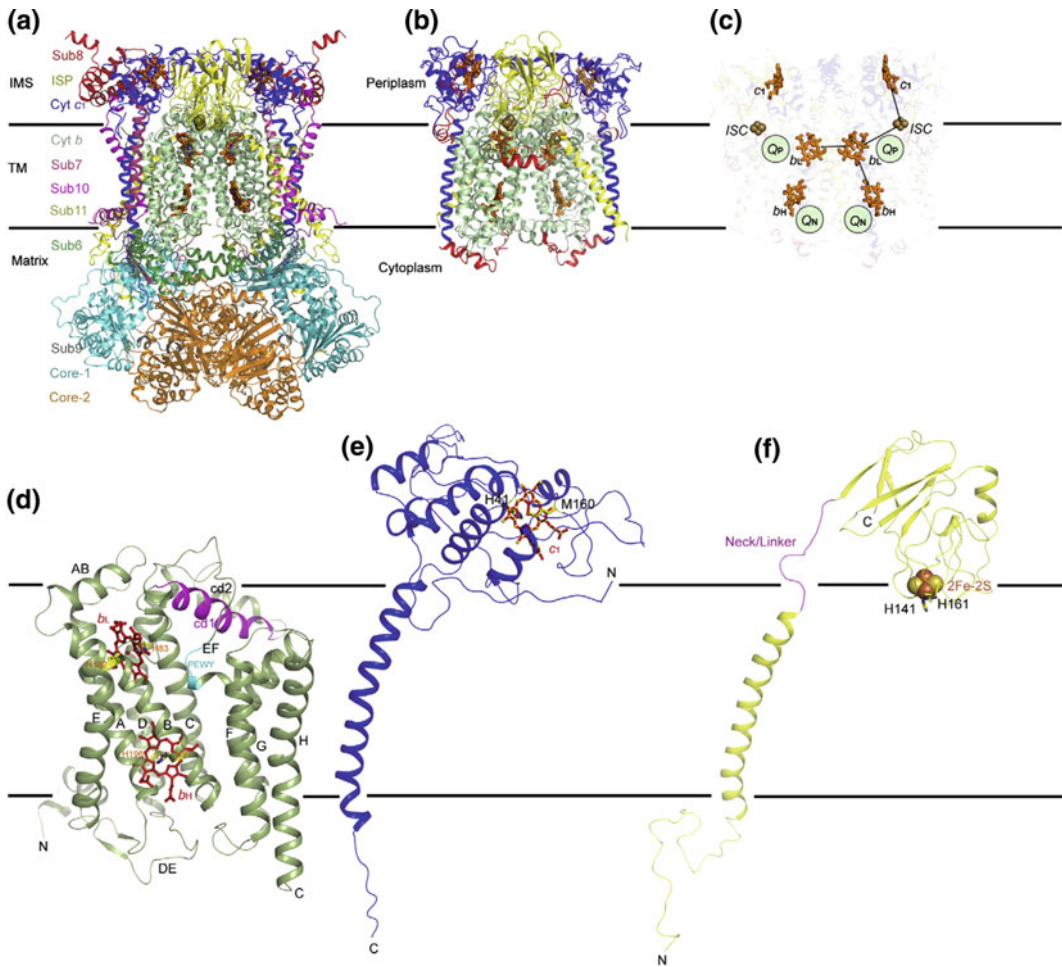


Fig. 8.16 Crystal structures in ribbon representation for mitochondrial and bacterial bc1 complexes. **a** Structural model of the dimeric bc1 complex from bovine mitochondria. The eleven different subunits are represented as ribbons with the color codes and subunit designations given on the left. Prosthetic groups such as the hemes bL, bH, and c1 are shown as stick models. The iron–sulfur clusters are shown as van der Waals sphere models. The two black horizontal lines delineate the boundaries of the membrane bilayer. The three regions of the bc1 complex are indicated as IMS (intermembrane space), TM (transmembrane), and matrix regions, respectively. **b** Structural model of the photosynthetic bacterium *R. sphaeroides* bc1. Color codes for Rsbcl are the same as those for Btbc1 except those in red, which represent insertions in cyt b, cyt c1, and ISP subunits in relation to the corresponding subunits in Btbc1. **c** Positions of and distances between iron atoms of prosthetic groups. Hemes bL, bH, and c1 as well as 2Fe–2S clusters are labeled. Arrowed lines indicate low- and high-potential chains for ET. **d** Ribbon diagram showing the structure of

monomeric bovine cyt b. Eight TM helices are labeled. The two b-type hemes bL and bH are shown as stick models. The axial histidine ligands to the heme groups are also shown as stick models and labeled. The two conserved and functionally important motifs, the cd1 helix and the PEWY sequence, are shown in magenta and cyan, respectively, and as labeled. **e** Ribbon presentation of the structure of bovine cyt c1. Btcty c1 has its N and C terminus on the positive and negative sides of the membrane, respectively. The heme c1 along with its two axial ligands BtM160 and BtH41 is shown as stick models. **f** Ribbon diagram showing the structure of the bovine ISP subunit. The N-terminus of the ISP is on the negative side of the membrane, whereas the C terminus is on the positive side. The 2Fe–2S cluster is shown as spheres; the two histidine ligands H141 and H161 for the ISC are shown as stick models and are labeled. The flexible linker or neck between the TM helix and the ISP-ED is shown as a random coil in magenta. *Source* Xia et al. (2013) (Color figure online)

the electron transport. There are two quinone-binding sites, the Q_P (near b_L heme) site, located near the intermembrane space in mitochondria, which provides access to lipid-soluble QH_2 for oxidation, and the Q_N (near b_H heme) site, situated closer to the mitochondrial matrix, which carries out the reduction of ubiquinone. Q_N site is the site of binding of antimycin, a specific inhibitor of cyt bc_1 complex. Myxothiazol is a Q_P site specific inhibitor of cyt bc_1 complex.

The two helical bundles of cyt b are in contact with each other on the negative side of the membrane, but separate on the positive side, and this gap is bridged by the CD helices (CD1 and CD2) and by the EF loop. Q_P pocket lies in the hydrophobic pocket below the CD helices and next to the EF helix. There are four prominent surface loops; Three are on the positive side (AB, CD, and EF), and one is on the negative side (DE) (Fig. 8.16).

Both the cyt c_1 and ISP subunits are anchored to the membrane by TM helices with their respective peripheral domains which are localized on the positive side of the membrane (Fig. 8.16).

The bc_1 complex uses ubiquinol to shuttle protons across the membrane via the **Q cycle mechanism**. The first step in the Q cycle starts with the separation of the two electrons of QH_2 at the Q_P site. Ubiquinol (QH_2) binds to the Q_P site via hydrogen bonding to His182 of the Rieske iron-sulfur protein and Glu272 of cytochrome b . The first electron of quinol is transferred to cyt c via the “high-potential chain,” consisting of the ISP and cyt c_1 . The second electron is simultaneously transferred through the “low-potential chain” starting with heme b_L , then to b_H , and finally to ubiquinone or ubisemiquinone bound at the Q_N site. On oxidation, ubiquinol (QH_2) is converted to a transient semiquinone, which then leaves the Q_P site of complex III. The semiquinone may then bind to the Q_N site to get reduced (Fig. 8.17).

Having acquired one electron from ubiquinol, the “Fe-S protein” migrates to the cytochrome c_1 subunit, to donate its electron. The cytochrome c_1 then transfers an electron to cytochrome c . The

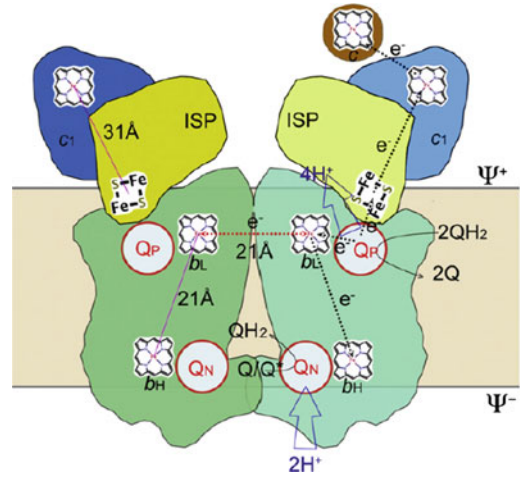


Fig. 8.17 Q cycle mechanism in complex III. The Q cycle mechanism defines two reaction sites: quinol oxidation (center P or Q_P) and quinone reduction (center N or Q_N). It takes two quinol oxidation cycles to complete. At first, a QH_2 moves into the Q_P site and undergoes oxidation with one electron going to cyt c via the ISP and cyt c_1 (high-potential chain), and another ending in the Q_N via hemes b_L and b_H (low-potential chain) to form a ubisemiquinone, and releasing its two protons to the Ψ^+ site of the membrane. The second QH_2 is oxidized in the same way at the Q_P site but its low-potential chain electron ends up reducing the ubisemiquinone radical. Reduced QH_2 is released upon picking up two protons from the negative side of the membrane. As a result of the Q cycle, four protons are transferred to the Ψ^+ side, two protons are picked up from the Ψ^- side, and effectively only one QH_2 molecule is oxidized. Source Xia et al. (2013)

reoxidation of the “Fe-S protein” releases the proton bound to His181 into the intermembrane space, hence translocating protons.

A **second Q cycle** is required to reduce the semiquinone radical at the Q_N site to ubiquinol. Another round of oxidation of reduced quinol (QH_2) at Q_P site transfers the second electron to cytochrome b_H via b_L , reducing the semiquinone radical Q_N site. The two Q cycles ultimately result in translocating four protons across the intermembrane space, two from the matrix and two from the reduction of two molecules of cytochrome c (Fig. 8.18). The reduced cytochrome c then diffuses away from complex III toward complex IV in the mitochondrial inner membrane, to donate electron and itself get oxidized.

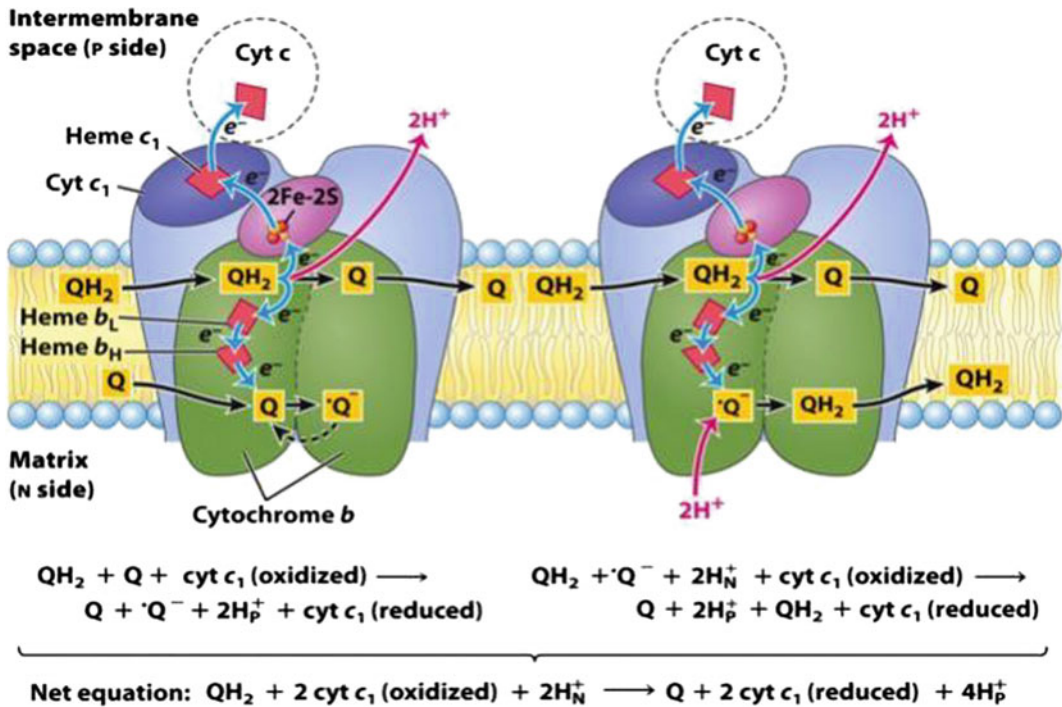
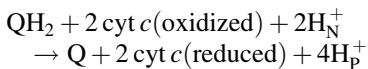


Fig. 8.18 Operation of two cycles of the Q cycle in complex III results in the reduction of cytochrome c, oxidation of ubiquinol to ubiquinone, and the transfer of four protons into the intermembrane space, per two-cycle process

The process is cyclic as the oxidized ubiquinone created at the Q_N site can be reduced by binding to the Q_P , and the reduced ubiquinone generated at Q_P site can be oxidized again at Q_N site. This cycling process results in a proton-pumping efficiency of two protons per electron transferred to from QH_2 to cyt c.

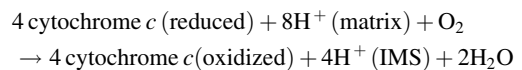
The net reaction catalyzed by complex III is represented as:



8.5.4 Complex IV

The enzyme **cytochrome c oxidase (COX)** or the **complex IV (CIV)** is the last enzyme of the electron transport chain in mitochondria. It receives four electrons from cytochrome c, one at a time, and transfers them to oxygen molecule and reduces it. The complex binds four protons

from the mitochondrial matrix to form water molecules and in addition translocates four protons across the inner mitochondrial membrane. The net reaction catalyzed by complex IV is represented as:



Tsukihara et al. in (1996) for the first time solved the crystal structure of the complete bovine mitochondrial complex IV. It is a dimeric protein with the total molecular weight of 210 kDa. The molecule contains 13 subunits with 28 transmembrane helices. Of the 13 subunits, three subunits, SU1, SU2, and SU3, form the core subunits of complex IV (Fig. 8.19). SU1 has two heme centers (heme a and a_3) and a Cu center (CuB). Heme a_3 and CuB form a **binuclear center (BNC)** which is the site for oxygen reduction. SU2 possesses another Cu center (CuA) with two Cu atoms and accepts the

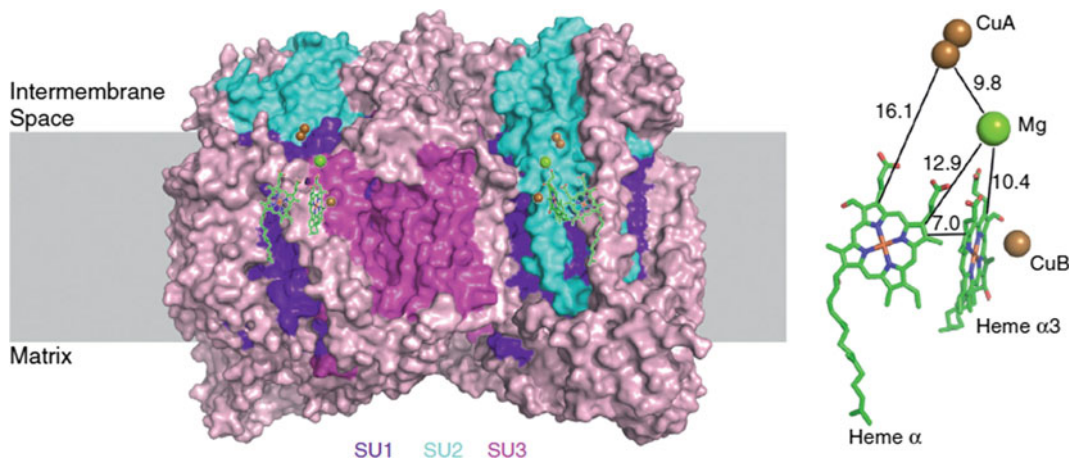


Fig. 8.19 Surface representation of dimerized bovine mitochondrial respiratory complex IV structure (left, PDB code: 1OCC) and the spatial arrangement of its prosthetic groups (right). The membrane region is shown as gray box. The embedded prosthetic groups (left) are shown in sticks for heme groups and spheres for ion clusters, and

superimposed on the surface of complex IV to indicate their relative spatial position. The edge-to-edge distances of prosthetic groups are indicated accordingly (right). The core subunits of complex IV, SU1, SU2, and SU3, are colored and labeled as indicated. *Source* Sun et al. (2013) (Color figure online)

electron donation by cytochrome *c*. SU3 has seven transmembrane helices and interacts with SU1. Besides SU1, SU2, and SU3, other subunits of bovine CIV surround the core and stabilize the whole complex. SU1, SU2, and SU3 are coded by mitochondrial genome and are highly conserved.

The electron transfer pathway through complex IV reducing of O₂ to H₂O requires four electrons that are provided one by one by cytochrome *c*. Cytochrome *c* docks to cytochrome *c* oxidase via electrostatic and hydrophobic interactions at the interface between subunits II and III. The first *e*⁻ acceptor in CIV from cytochrome *c* is CuA. Subsequently, the *e*⁻ is transferred to heme *a* and then the *e*⁻ is transferred from heme *a* to heme *a*₃. The distance between the two hemes, heme *a* to heme *a*₃, is ~5 Å, and the major part of the electron transport (ET) occurs on a timescale of ~3 μs. However, an initial partial nanosecond electron transport from heme *a* to heme *a*₃ is present that is not coupled to the H⁺ translocation. The final step of the ET events is from heme *a*₃ to CuB which occurs on a timescale of hundreds of microseconds due to its coupling to the proton translocation.

The mechanism of the proton translocation is very different from that of electron transport (Fig. 8.20). The O₂ reduction chemistry requires four protons to be delivered to the binuclear center (BNC) for each O₂ molecule reduced [“chemical” protons], and four more protons are translocated across the inner membrane of mitochondria [“pumped” protons]. All eight protons are taken from the mitochondrial matrix. Two diverse proton entry channels, the D- and K-channels, have been identified. The D-channel is named thus after the conserved residue Asp-124 serving as an entrance point to the channel. The D-channel leads from the N-side to a highly conserved residue Glu-278 in the center of the hydrophobic core of the membrane via a sequence of the conserved residues: Asn-199, Asn-131, Asn-113, Tyr-35, Ser-193, Ser-192, and Ser-189. The K-channel is named after Lys-354, a conserved residue located in the channel at about half the distance from the N-side to the BNC. The K-channel is shorter than the D-channel and leads exclusively to the BNC. The K-channel starts from Glu-78 of subunit II or Ser-291 of subunit I and leads to the BNC via Lys-354, Thr-351, and Tyr-280 [which is

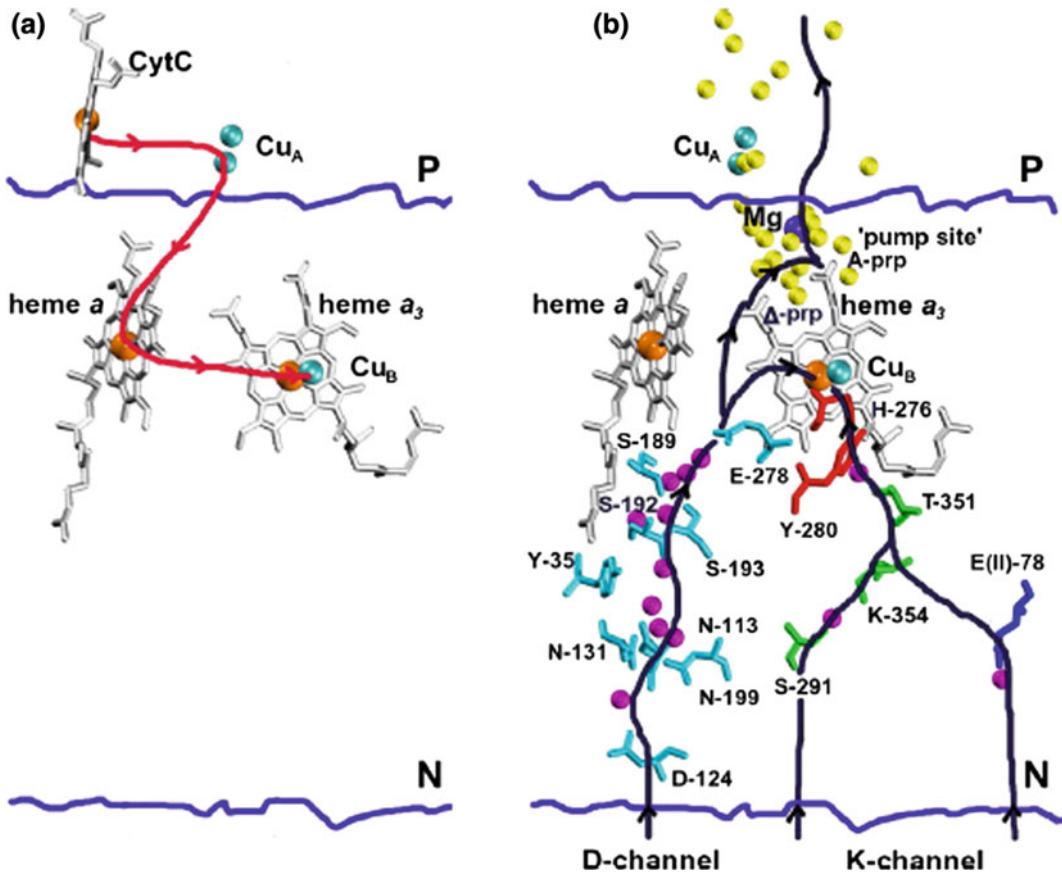


Fig. 8.20 Electron (a) and proton (b) transfer pathways together with the redox centers and water molecules within the H^+ -conducting channels of complex IV structure from *R. sphaeroides* (PDB ID 2GSM). The

amino acid numbering is from *P. denitrificans*. P and N represent the positive and negative sides of the membrane. Source Gorbikova (2009)

cross-linked to His-276]. The D-channel continues to the H^+ exit channel. It should be located above the hemes' propionates and lead to a so-called pump site [where the H^+ to be pumped is preloaded] and further on to the P-side of the membrane (Fig. 8.20). A number of water molecules and polar residues are found above the hemes' propionates which connect the "pump site" with the P-side of the membrane.

The catalytic cycle of CIV consists of oxidative (O) and reductive (R) halves. The catalytic cycle includes several intermediates denoted by a one-letter code, reflecting only the structure of the BNC (Fig. 8.21).

The redox centers of the BNC [heme a_3 and CuB] are reduced in the **R (reduced)**

intermediate. The other two electron transport centers, CuA and heme a , can be either reduced or oxidized. When all four redox centers are reduced, the intermediate is called **fully reduced [FR]** (Fig. 8.21). In the case where only the redox centers of the BNC are reduced, the intermediate is called "**mixed valence**" [MV]. O_2 first transiently binds to CuB, and then to heme a_3 . When O_2 is bound to heme a_3 , compound **A** (ferrous-oxy intermediate) is formed. **P (peroxy)** intermediate is then formed as the dioxygen bond gets broken for which four electrons and a proton are required. One e^- is derived from CuB as CuB is oxidized from cuprous to a cupric state [CuBI \rightarrow CuBII]. The source of the fourth e^- depends on the initial reductive state of CIV: [i]

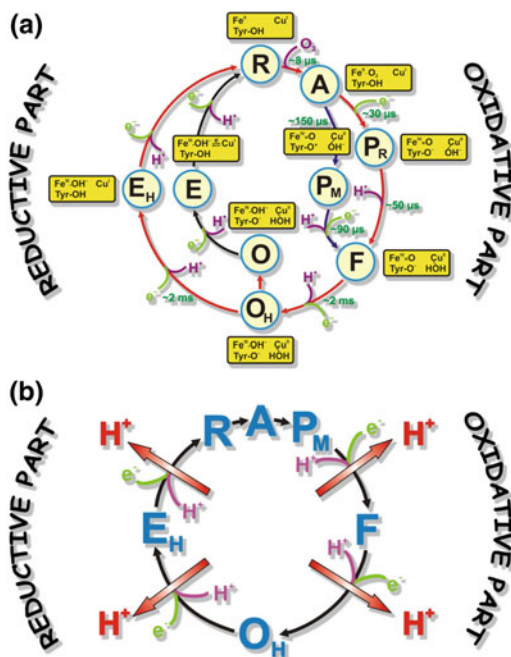


Fig. 8.21 Intermediates of the catalytic cycle in complex IV with the corresponding structures of the binuclear center (a) and the H⁺ translocation events during the catalytic cycle (b). Protons taken by the binuclear center (BNC) for the O₂ reduction chemistry are shown in magenta. Approximate time constants of the catalytic transitions are presented. Altogether four pumping steps occur per O₂ molecule reduced. The H⁺ translocation events are shown as a red arrow and only for the oxygen reaction with **MV** (mixed valence) enzyme. Electrons arriving at the BNC are marked in green. [R] (reduced intermediate), [A] (ferrous-oxo intermediate), [P] (“peroxy” intermediate), [F] (ferryl intermediate), [O] (fully oxidized intermediate), [E] (one-electron reduced intermediate). *Source* Gorbikova (2009) (Color figure online)

heme *a* in the case of **FR** (when all four redox centers are reduced, the intermediate is called **fully reduced**) and [ii] Tyr-280 in the case of mixed valence (**MV**) (where only the redox centers of the BNC are reduced, the intermediate is called “**mixed valence**”) enzyme. Tyr-280 is located in very close proximity to the metal centers of the BNC and is cross-linked to one of the ligands of CuB–His-276. Tyr-280 is in its deprotonated form [Tyr-O⁻] in **P_R** and in a neutral radical form [Tyr-O[•]] in **P_M**. The **PR** intermediate decays rapidly into the **F** (ferryl) intermediate. **F** intermediate is then converted to

O (fully oxidized) intermediate. The enzyme in the **fully oxidized** intermediate “resting” [O] and “pulsed” [O_H] differs in its ability to pump protons in the reductive part of the catalytic cycle: The reduction of the O_H intermediate is accompanied by H⁺ pumping (Fig. 8.21), while the reduction of O is not.

The **E** (one-electron reduced) intermediate is formed from the **O** intermediate when the first e⁻ arrives in the **fully oxidized** BNC. In a kinetically generated **E** intermediate [E_H], the e⁻ ends up on CuB and a proton on Tyr-280. The **EH** → **R** transition should be accompanied with the pumping of H⁺ as well, regenerating the initial **R** intermediate. The **E** → **R** transition is not coupled to H⁺ pumping.

8.5.4.1 Inhibitors

Cyanide, azide, and carbon monoxide bind to complex IV and competitively inhibit the binding of oxygen to the iron of heme *a*₃ in binuclear center (BNC).

Cyanide is the most toxic inhibitor of complex IV. Cyanide binds tightly to heme *a*₃-Cu_B binuclear center in the fully oxidized state (O) and prevents oxygen binding, inhibiting electron transport to oxygen and ultimately ATP synthesis. Due to CIV inhibition, cyanide initiates a catastrophic cascade of reactions leading to neurological and myocardial dysfunction and death.

Azide, like cyanide, also binds to the oxidized state of BNC and prevents oxygen binding to heme iron. **Carbon monoxide** binds to the reduced form of BNC. CO exposure can cause difficulty in breathing, cardiac trauma, brain damage, coma, and ultimately death.

Other ligands, such as nitric oxide and hydrogen sulfide, can also inhibit CIV by binding to regulatory sites on the enzyme, reducing the rate of cellular respiration.

Methanol in methylated spirits is converted into formic acid, which also inhibits the complex IV; however, formic acid is much less toxic than cyanide or azide. Inability to oxidize and detoxify formic acid in humans leads to its accumulation and results in methanol poisoning, which is not seen in other animals.

8.5.4.2 Genetic Defects and Disorders

Genetic mutations affecting complex IV functionality or structure can result in severe, often fatal metabolic disorders, usually manifested in early childhood. Cells and organs with high-energy demands like brain, heart, and muscle are predominantly affected. Therefore, complex IV disorders share many overlapping clinical features with other disorders of the electron transport chain, though some features are distinct. Most diseases are associated with neurological abnormalities and muscle disease.

The complex IV/COX disorders are one of the most frequent causes of respiratory chain disorders in childhood with heterogeneous caused and phenotypes including encephalomyopathy, Leigh syndrome, fatal or benign infantile myopathies, liver failure, and myoglobinuria.

Mutations have been observed in the three mitochondrial complex IV/COX genes (*COXI*, *COXII*, and *COXIII*). The mtDNA is not autonomous, and it requires the nuclear-encoded factors for its replication, transcription, and translation. Defects in the gene or the expression of such nuclear-encoded proteins referred to as assembly factors can lead to dysfunctional assembly of the cytochrome IV complex.

8.6 Chemiosmotic Theory and Proton-Motive Force

Dr. Peter Mitchell proposed the **chemiosmotic theory** in (1961), for which he received the Nobel Prize in Chemistry in 1978.

Peter Mitchell's chemiosmotic theory proposed that the transfer of electrons through the electron transport chain is coupled to the pumping of protons across the inner mitochondrial membrane, from the mitochondrial matrix to the intermembrane space. The energy conserved in the pH gradient and electrical potential so generated across the membrane, represented by the **proton-motive force**, is then used to drive ATP synthesis. Hence, ATP synthesis, representing phosphorylation, is coupled to oxidation of reducing equivalents.

Many experimental evidences provide support to the chemiosmotic theory. This includes observations that (i) when an isolated mitochondria is put in an air tight container in a buffer medium containing electron donor, on injecting oxygen, the pH of the medium is reduced, proving that respiring mitochondria pumps protons across the membrane, (ii) dissipation of the proton gradient (proton-motive force) with specific chemical reagents (uncouplers) prevents ATP synthesis, and (iii) in mitochondria with blocked electron transport reactions the "artificial" generation of a proton-motive force can drive ATP synthesis (Figs. 8.22 and 8.23).

The energy conserved in the **electrochemical gradient** generated due to the pumping of protons across the inner mitochondrial membrane is represented by the **proton-motive force** (PMF). The chemical gradient is due to the difference in proton (H^+) concentration across the membrane and the electrical gradient results from charge separation across the membrane (when the protons H^+ move without a **counterion like** chloride Cl^-) (Fig. 8.24).

The free energy change associated with the electrochemical gradient generated by pumping of protons across the inner mitochondrial membrane coupled with the transfer of electrons to O_2 via the electron transport chain is given by:

$$\Delta G = RT \ln \left(\frac{C_2}{C_1} \right) + ZF\Delta\psi$$

where C_1 is the concentration of the ion (H^+ in this case) in the compartment from where the ion is moving and C_2 is the concentration of the ion in the compartment into which it is moving. Z is the electric charge of the ion (1 for H^+), F is faradays constant, and $\Delta\psi$ is the membrane potential in V across the membrane.

The proton motive force due to the pumping of H^+ across the inner mitochondrial membrane at 25 °C, when $[H^+]_N$ is the proton concentration in mitochondrial matrix, and $[H^+]_P$ is the proton concentration in intermembrane space is given by the following equation:

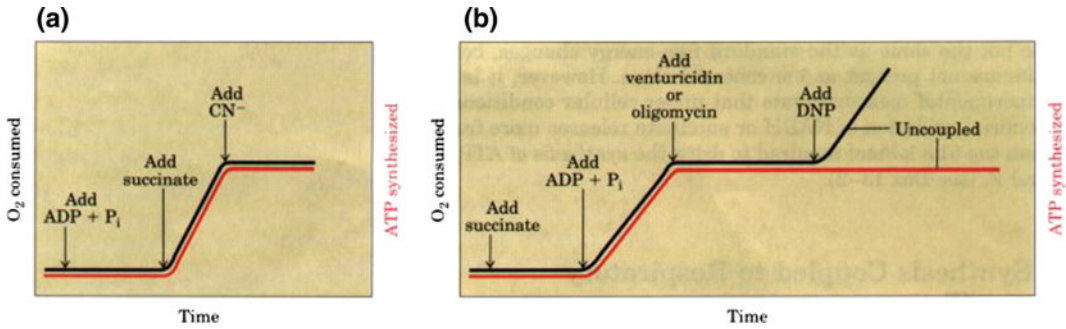


Fig. 8.22 Electron transfer to O_2 is tightly coupled to ATP synthesis in mitochondria, as is demonstrated in these experiments. Mitochondria are suspended in a buffered medium, and an O_2 electrode is used to monitor O_2 consumption. At intervals, samples are removed and assayed for the presence of ATP. **a** The addition of ADP and P_i alone results in little or no increase in either respiration (O_2 consumption; black) or ATP synthesis (red). When succinate is added, respiration begins immediately and ATP is

synthesized. The addition of cyanide (CN^-), which blocks electron transfer between cytochrome oxidase and O_2 , inhibits both respiration and ATP synthesis. **b** Mitochondria provided with succinate respire and synthesize ATP only when ADP and P_i are added. Subsequent addition of venturicidin or oligomycin, inhibitors of ATP synthase, blocks both ATP synthesis and respiration. Dinitrophenol (DNP) allows respiration to continue without ATP synthesis; DNP acts as an uncoupler (Color figure online)

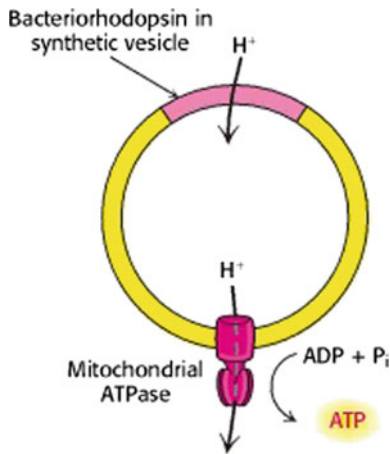


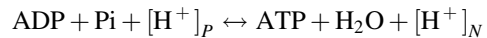
Fig. 8.23 Testing the chemiosmotic hypothesis ATP is synthesized when reconstituted membrane vesicles containing bacteriorhodopsin (a light-driven proton pump), and ATP synthase is illuminated

In actively respiring mitochondria, the membrane potential across the inner membrane $\Delta\psi$ is 0.15–0.20 V and ΔpH is about 0.75.

$$\Delta G = (5.70 \text{ kJ/mol}) 0.75 + (96.5 \text{ kJ/V mol}) 0.15 \text{ V}$$

$$\Delta G = 19 \text{ kJ/mol of protons}$$

The **proton-motive force** subsequently drives the synthesis of ATP, as protons flow passively back into the matrix through $F_0 F_1$ ATP synthase proton pump. The overall reaction of ATP synthesis catalyzed $F_0 F_1$ ATP synthase is given by:



$$\Delta G = RT \ln \left(\frac{[H^+]_P}{[H^+]_N} \right) + ZF\Delta\psi$$

$$= RT 2.303 (\log [H^+]_P - \log [H^+]_N) + ZF\Delta\psi$$

$$= RT 2.303 (pH_N - pH_P) + ZF\Delta\psi$$

$$= 2.303 RT \Delta pH + ZF\Delta\psi$$

$$= (5.70 \text{ kJ/mol}) \Delta pH + (96.5 \text{ kJ/V mol}) \Delta\psi$$

8.7 ATP Synthesis

Mitochondrial **$F_0 F_1$ -ATP synthase** belongs to the family of F-type ATPases, which include the ATP synthases present in chloroplasts and eubacteria (Fig. 8.25). $F_0 F_1$ -ATP synthase, also known as the complex V of electron transport chain, is a large multisubunit complex. It catalyzes the formation of ATP from ADP and P_i , accompanied by the flow of protons from the

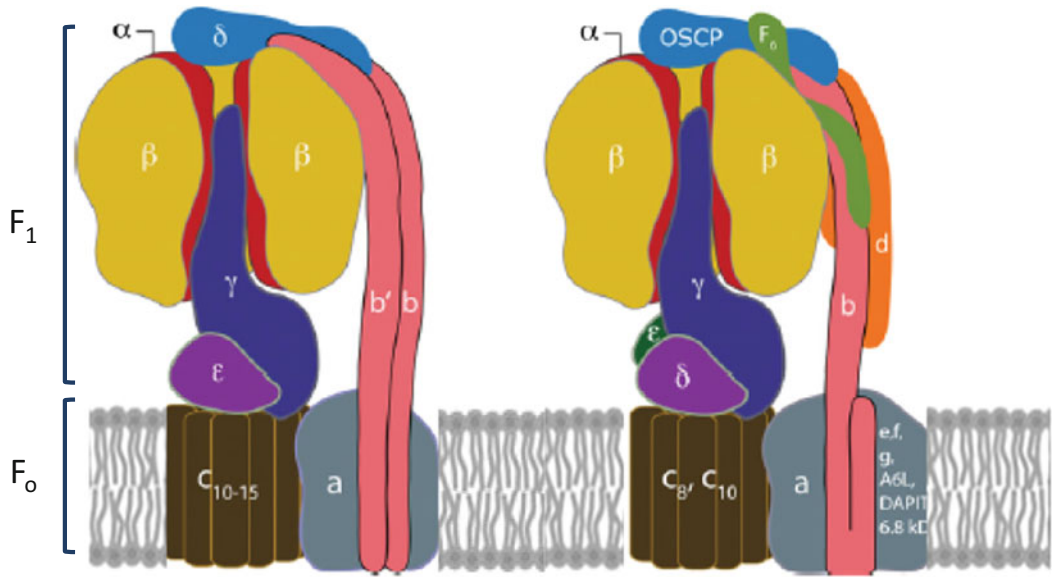


Fig. 8.25 Organization of protein subunits in ATP synthases: The bacterial and chloroplast ATP synthases are depicted on the left, and mitochondrial enzyme is shown on the right. The upper part of each model contains the subunits in the F_1 $\alpha_3\beta_3$ catalytic domain. One of the three α -subunits (red) has been removed to expose the elongated α -helical structure in the γ -subunit (dark blue), which lies approximately along the central axis of the spherical $\alpha_3\beta_3$ domain. The γ -subunit (and associated subunits) is in contact with the F_0 membrane domain, which contains the c-ring (brown) and the associated a-subunit (gray). The rotor of the enzyme consists of the ensemble of the c-ring and the γ -subunit (and associated subunits). The pathway for protons through the F_0 domain is in the vicinity of the interface between the c-ring and a-subunit. The peripheral stalk is on the right of each model. In some bacterial enzymes, it consists of the

δ -subunit (light blue) and two identical b-subunits (pink). In other bacterial enzymes, and in the chloroplast enzyme, the two b-subunits are replaced by single copies of homologous, subunits b and b'. The N-terminal domain of the δ -subunit binds to the N-terminal region of one of the three α -subunits, and the b- and b'-subunits interact with the a-subunit via their N-terminal transmembrane α -helices. In the mitochondrial enzyme, the peripheral stalk consists of single copies of subunits OSCP, b, d, and F6. OSCP is the homolog of the bacterial δ -subunit. The sequences of mitochondrial subunits b, d, and F6 are not evidently related to those of the bacterial b- and b'-subunits. Their structures also differ significantly, although they are both dominated by α -helices, except for the C-terminal domain of OSCP (and presumably the bacterial and chloroplast δ -subunit), which contains β -structures. *Source* Walker (2013) (Color figure online)

required for proton translocation. This carboxyl group can be specifically labeled with dicyclohexylcarbodiimide (DCCD), but bound DCCD inhibits proton translocation-coupled ATP synthesis by the ATP synthase. This proves that the DCCD-sensitive **carboxyl** group of a **c-subunit** plays an important role in proton translocation across the membrane. As protons enter the lower half-channel of a-subunit facing the intermembrane space, it neutralizes the negatively charged carboxyl group of **c-subunit** in the interface between the a-subunit and the c-ring. Once neutralized, this residue moves by Brownian

motion to the more hydrophobic environment of the lipid bilayer, generating a rotation in the c-ring. This rotational step brings another negatively charged carboxyl group into the lower half-channel allowing another proton to be neutralized, generating another rotational substep. Thus, protons appear to be carried around the surface of **c-ring as a result of** these rotations powered by the neutralization of negatively charged carboxyl group. As they come in contact with the second site of a-subunit, the local environment reionizes the carboxyl group, releasing the proton through a second

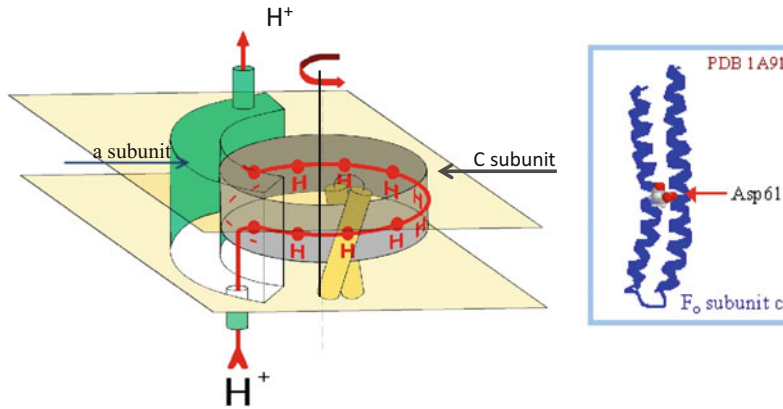


Fig. 8.26 Model to explain the generation of rotation in the F_0 membrane domain of ATP synthases. The a-subunit (green) is shown in contact with the cylindrical ring of c-subunits (brown). The C-terminal α -helix of each c-subunit contains a DCCD-sensitive Asp61 carboxyl group. Protons enter a lower half-channel neutralizing the negatively charged carboxyl group in the interface between the a-subunit and the c-ring. Once neutralized, this residue moves by Brownian motion to the more hydrophobic environment of the lipid bilayer, generating a rotation in the direction indicated. This rotational step brings another negatively charged carboxyl group into the lower half-channel allowing another proton to be

neutralized, generating another rotational substep. Thus, as more negative charge is neutralized by protons, the protons are carried around on the external surface the ring by the neutralized carboxyl group, until they reach a second site in contact with the a-subunit, where the local environment reionizes the carboxyl group, releasing the proton through a second half-channel on the opposite of the membrane from which it entered. The number of protons required to generate each 360° rotation of the c-ring corresponds to the number of c-subunits that form the ring. The γ -subunit (and associated subunits) which is attached firmly to the ring (F_0 -subunit) also rotates 360° rotation along with this rotor (Color figure online)

half-channel on the matrix side of the membrane. The number of protons required to generate each 360° rotation of the c-ring corresponds to the number of c-subunits that form the ring. The γ -subunit (and associated subunits) which is attached firmly to the ring (F_0 -subunit) also rotates 360° rotation along with this rotor (Fig. 8.26).

The association of asymmetric γ -subunit with β -subunits makes each of the three catalytic β -subunits asymmetric with respect to each other and to adopt different conformations with different nucleotide-binding affinities and catalytic properties. **Paul Boyer (1995)** at UCLA proposed a new concept of “binding change mechanism” for ATP synthesis by ATP synthase. According to this mechanism, the energy input for ATP synthesis was not used to form the ATP molecule but to promote the release of an already formed ATP at the reaction site. He termed the three different conformations of β -subunit as open (β_O , which has no affinity for nucleotide

binding), loose (β_L , which binds $ADP + P_i$ loosely), and tight (β_T , which binds ATP tightly).

For this pioneering work, Boyer was awarded the 1997 Nobel Prize in Chemistry with John E. Walker for their elucidation of the enzymatic mechanism underlying the synthesis of adenosine triphosphate (ATP) which they shared with Jens C. Skou for determining the mechanism of ion transport by Na^+ , K^+ -ATPase.

As F_0 c-subunits rotate, associated γ -subunit also rotates. The γ -subunit passes through the center of the $\alpha_3\beta_3$ spheroid, which is held stationary by the b_2 - and δ -subunits (Fig. 8.27). The three β subunits interact with γ -subunit in such a way that one assumes the β_O —empty conformation, the second, the β_L —loose conformation, which binds $ADP + P_i$ loosely, and the third, β_T —tight conformation, which binds ATP tightly with high affinity. With each rotation of 120° , γ comes into contact with a different β -subunit. Suppose given β -subunit starts in the β_L - $ADP + P_i$ conformation, which binds ADP and

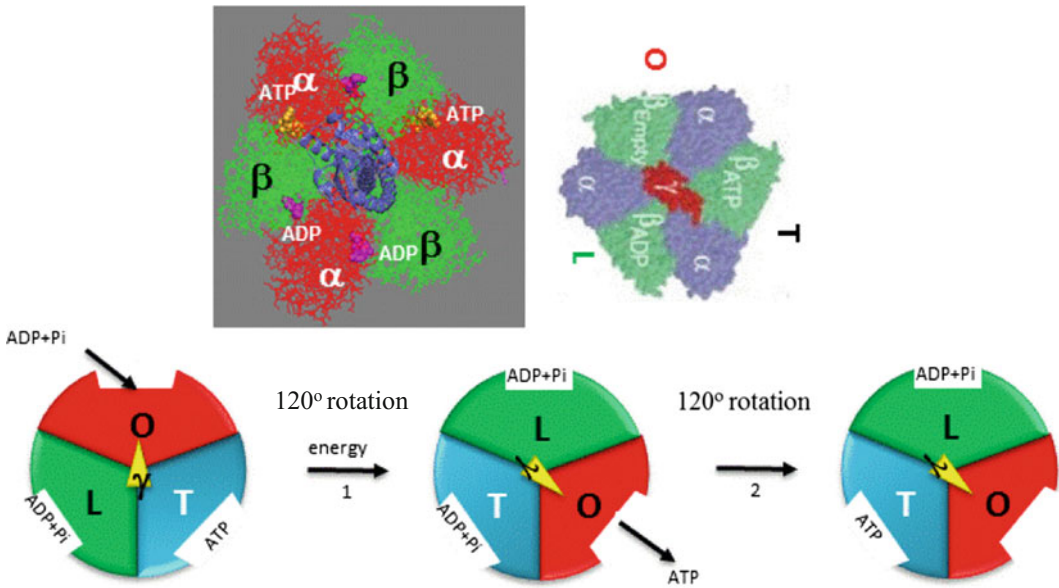


Fig. 8.27 The mechanism of Boyer's binding change mechanism" for ATP synthesis by F_1F_0 -ATP synthase: The three β -subunits of F_1 subunit assume three different conformations, β_O ; which is empty conformation, β_L ; which binds ADP + Pi loosely, and β_T ; which binds ATP tightly due to their differential interaction with γ subunit

of F_0 subunit which rotates as protons flow down the gradient. In one complete 360° rotation each β subunit undergoes all the three conformations. One ATP molecule is released during each β_O conformation. Hence in one complete rotation of F_0 three ATP molecules are released

P_i from the surrounding medium with low affinity. With one rotation, the subunit with β_L -ADP + P_i now changes to the β_T -ATP form that tightly binds and stabilizes ATP, bringing about the conversion of ADP + P_i to ATP on the enzyme surface. With another rotation, the β_T -ATP subunit now changes to the β_O -empty conformation, which has very low affinity for ATP, and the newly synthesized ATP leaves the enzyme surface. Another round of catalysis begins when this subunit again assumes the β_L -ADP + P_i form and binds ADP and P_i . Thus, one complete rotation of 360° of the γ -subunit causes each β -subunit to cycle through all three conformations, and for each rotation, three ATP are released from the enzyme surface.

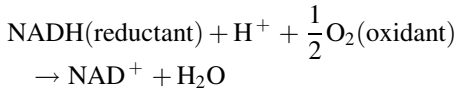
The number of c -subunits in the c -ring appears to range between 9 and 12 in different systems (animal, plants, and bacteria). The number of c -subunits determines the number of protons that must be translocated across the membrane in one complete 360° rotation. Each 360° rotation of the γ -subunit leads to the synthesis and release of

three molecules of ATP. Thus, if there are 10 c -subunits in the ring, complete 360° rotation of c -subunit ring would require 10 protons to be translocated into the mitochondrial matrix. Therefore, to generate one ATP molecule, $10/3 = 3.33$ protons need to be pumped into the matrix. For simplicity, we can approximate that three protons must flow into the matrix for each ATP formed, but the true value may differ.

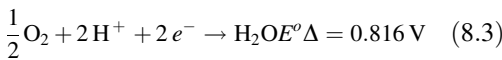
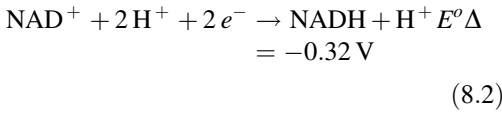
8.8 The Electron Transport Chain—An Overview

The reduced coenzymes NADH and $FADH_2$, generated from the oxidation of fuels like sugars, fats, and amino acids, transfer their electrons to the electron transport chain and are reoxidized. In this reoxidation process, the electrons move from NADH and $FADH_2$ via the electron transport chain to molecular oxygen, O_2 , which is reduced to water molecule.

The net reaction of reoxidation of NADH via the electron transport chain is given by:



This reaction involves the following half-reactions:



Here, half-reaction (8.2) is the electron acceptor and half-reaction (8.3) is the electron donor.

Then, the net redox potential is given by:

$$\Delta E^\circ = 0.816 - (-0.32) = 1.136 \text{ V}$$

and the net free energy change of the reaction is:

$$\Delta G^\circ = -nF\Delta E^\circ$$

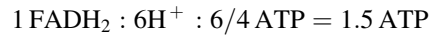
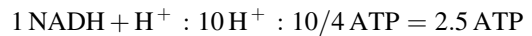
The standard state free energy change, ΔG° , is $= -219 \text{ kJ/mol}$.

We have seen in the previous section that ATP synthase produces 1 ATP/ $\sim 3\text{H}^+$. However, the exchange of matrix ATP for cytosolic ADP and P_i (antiport with OH^- or symport with H^+) mediated by ATP-ADP translocase and phosphate carrier consumes $1\text{H}^+/1 \text{ ATP}$ (Fig. 8.31). As a result of dissipation of the transmembrane

potential during this transfer, the net ratio of ATP generation is recalibrated as 1 ATP/ 4H^+ translocated across the membrane.

The mitochondrial electron transport chain proton pump transfers across the inner membrane 10H^+ ($4e^-$ by complex I + $4e^-$ by complex III + $2e^-$ by complex IV) per electron pair transferred from 1 NADH and similarly 6H^+ ($4e^-$ by complex III + $2e^-$ by complex IV) per pair of electrons from FADH_2 (Fig. 8.28).

So, the final stoichiometry is



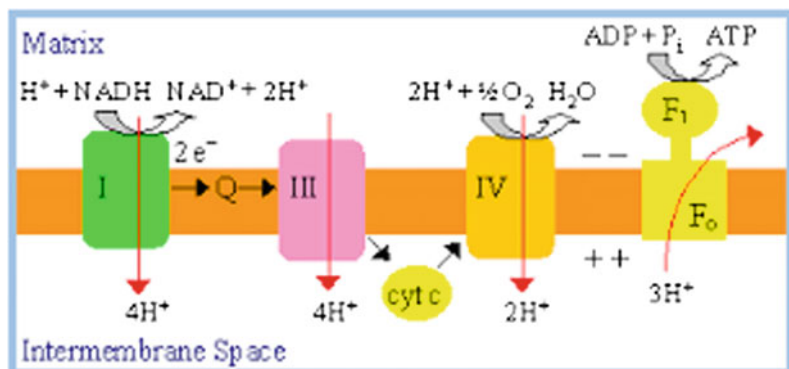
The ratio of ATP produced by oxidative phosphorylation per NADH generated from glycolysis in the cytosol is 2.5 in case of malate-aspartate shuttle transferring cytosolic NADH into mitochondria and 1.5 if transferred via the glycerol phosphate shuttle (Fig. 8.30) located in the inner mitochondrial membrane.

Standard free energy required to synthesize 1 mol of ATP from $\text{ADP} + \text{P}_i$ is $= 30.5 \text{ kJ/mol}$. Assuming oxidation of 1 mol of NADH results in synthesis of $\sim 2.5 \text{ ATP}$, the **thermodynamic efficiency of oxidative phosphorylation** is:

$$\begin{aligned} 2.5 \times 30.5 \text{ kJ/mol} \times 100/219 \text{ kJ/mol} \\ = 35\% \text{ under standard conditions.} \end{aligned}$$

However, under physiological conditions, under cellular concentrations of reactants and products, the thermodynamic efficiency is $\sim 70\%$.

Fig. 8.28 Ten protons are translocated across the inner membrane of mitochondria per pair of electrons transported from NADH to molecular oxygen via ETC



8.9 Regulation of Oxidative Phosphorylation

Rate of oxidative phosphorylation depends on:

8.9.1 The Availability of Substrates

(a) Reducing equivalents like **NADH**, and **FADH₂** are generated by oxidative pathways, predominantly glycolysis, fatty acid oxidation, and tricarboxylic acid cycle (Fig. 8.29). NADH generated by glycolysis in the cytosol is transported into mitochondria via malate-aspartate shuttle or glycerol-3-phosphate shuttle (Fig. 8.30). Intermediates of cytosolic metabolism like pyruvate

enter the mitochondria via the pyruvate transporter (PT). In the mitochondria, it is oxidatively decarboxylated by pyruvate dehydrogenase (PDH) to acetyl-CoA which is then oxidized to CO₂ via the citric acid cycle to generate reduced nicotinamide adenine dinucleotide (NADH) and flavin nucleotides (FADH₂). Fatty acids are imported into the mitochondria bound to carnitine. In the cytosol, fatty acyl-CoA is transferred to carnitine and transported across the mitochondrial membranes, mediated by the carnitine palmitoyl transferases. Fatty acyl carnitine is reconverted to fatty acyl-CoA in the mitochondria and oxidized via β -oxidation. β -oxidation generates both NADH and FADH₂. NADH and FADH₂

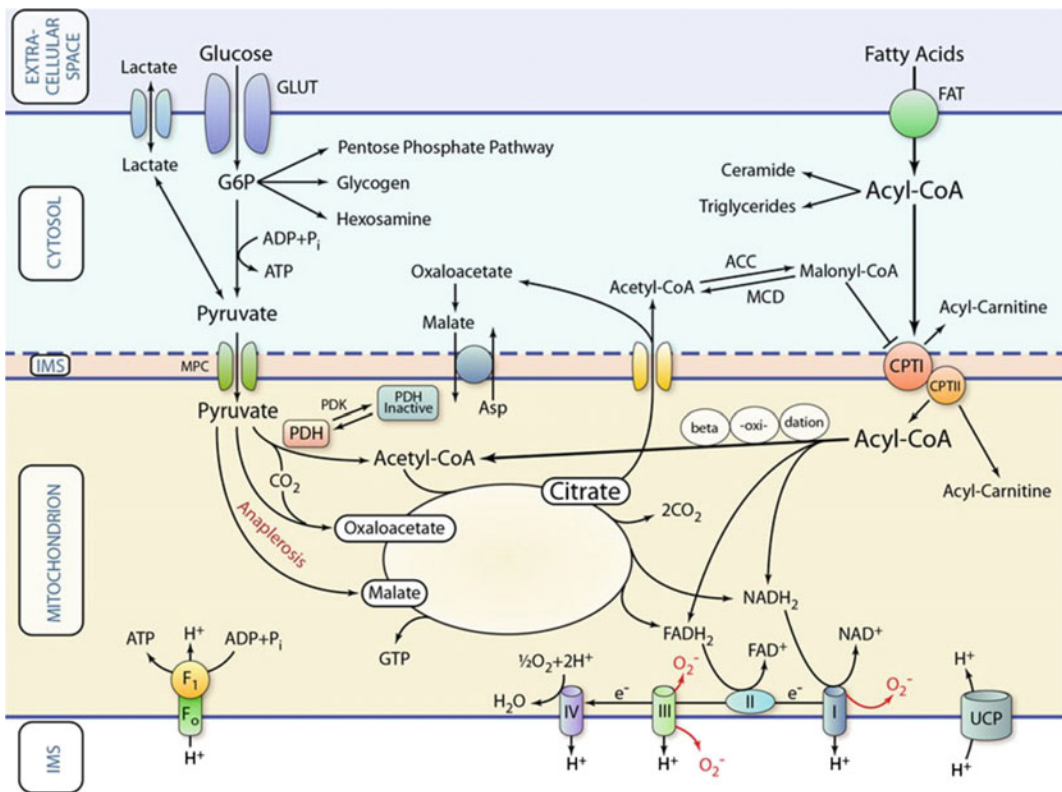


Fig. 8.29 Metabolic pathways generating reducing equivalents, which then enter the electron transport chain at complex I or complex II. ACC indicates acetyl-CoA carboxylase; CPT carnitine palmitoyltransferase; FAT fatty acid transporter; G6P glucose 6-phosphate; GLUT glucose

transporter; IMS mitochondrial intermembrane space; MCD malonyl-CoA decarboxylase; MPC mitochondrial pyruvate carrier; PDH pyruvate dehydrogenase; and PDK pyruvate dehydrogenase kinase. *Source* Doenst et al. (2013)

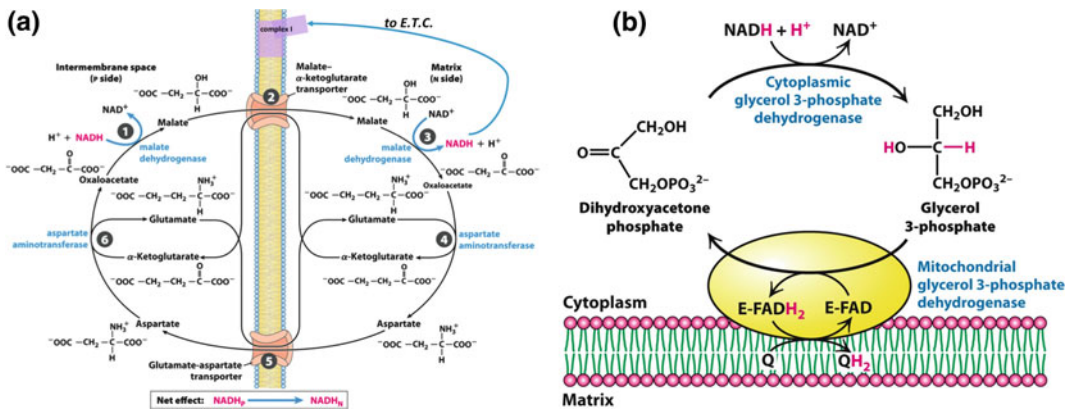


Fig. 8.30 **a** Malate-aspartate shuttle, for transporting cytosolic NADH into the mitochondrial matrix, is used in liver, kidney, and heart. 1 NADH in the cytosol (intermembrane space) passes two reducing equivalents to oxaloacetate, producing malate. 2 Malate crosses the inner membrane via the malate- α -ketoglutarate transporter. 3 In the matrix, malate passes two reducing equivalents to NAD^+ , and the resulting NADH is oxidized by the respiratory chain. 4 The oxaloacetate formed from malate is transaminated to aspartate. 5 Aspartate can leave via the glutamate-aspartate transporter back into the cytosol. 6

Oxaloacetate is regenerated in the cytosol, completing the cycle. **b** Glycerol 3-phosphate shuttle, an alternative means of transporting reducing equivalents from the cytosol to the mitochondrial matrix, operates in skeletal muscle and the brain. In the cytosol, dihydroxyacetone phosphate accepts two reducing equivalents from NADH in a reaction catalyzed by cytosolic glycerol 3-phosphate dehydrogenase. An isozyme of glycerol 3-phosphate dehydrogenase binds to the outer face of the inner membrane and then transfers two reducing equivalents from glycerol 3-phosphate in the intermembrane space to ubiquinone

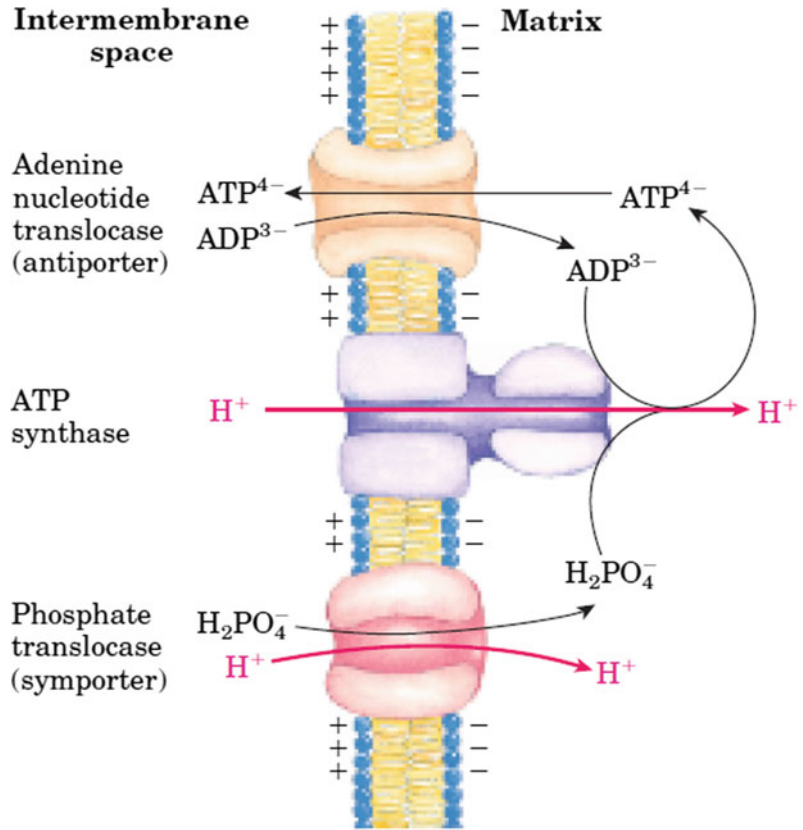
generated in the mitochondria then transfer their electrons into the electron transport chain either to the complex I or via complex II to ubiquinone. High metabolic rate of a cell resulting in high NADH/NAD^+ ratio increases the respiration rate.

- (b) **ADP and P_i** are substrates for ATP synthesis. The regulation of the rate of oxidative phosphorylation by the ADP concentration is called **respiratory control** or **acceptor control**. The ADP level increases with increased ATP consumption, and so the rate of oxidative phosphorylation increases with the utilization of ATP. Electrons flow from fuel molecules to O_2 only on ATP demand. Mass-action ratio, $[\text{ATP}]/[\text{ADP}][\text{P}_i]$, gives a measure of energy status of a cell. Normally, a cell has a very high mass-action ratio, but when energy requiring cellular activities increases, the mass-action ratio falls with the utilization of ATP, and the rate of oxidative phosphorylation increases till the mass-action ratio returns to normal.

Antiporter, adenine nucleotide translocator (ANT) transports ADP and ATP across the inner membrane and mitochondrial phosphate carrier protein (PC) or Phosphate translocase catalyzes the transport of P_i into the mitochondrial matrix. Inhibition of these transporters can inhibit the rate of oxidative phosphorylation (Fig. 8.31).

- (c) O_2 is the final electron acceptor of electron transport chain. Under conditions of ischemia (deprivation of oxygen), as in case of a heart attack or stroke, electron chain transfer to oxygen ceases, inhibiting the pumping of protons, thereby dissipating the proton gradient (Δp). Decreased Δp induces the F_1F_0 -ATP synthase to act in reverse, hydrolyzing ATP to pump protons across the inner membrane, in the attempt to restore the H^+ gradient. Under these conditions, a protein inhibitor, IF_1 , binds to ATP synthase molecules and inhibits its ATPase activity. In O_2 starved conditions due to the accumulation

Fig. 8.31 Adenine nucleotide and phosphate translocases. Transport systems of the inner mitochondrial membrane carry ADP and Pi into the matrix and newly synthesized ATP into the cytosol. Transport of both ATP^{4-} and PO_4^- is coupled to proton gradient



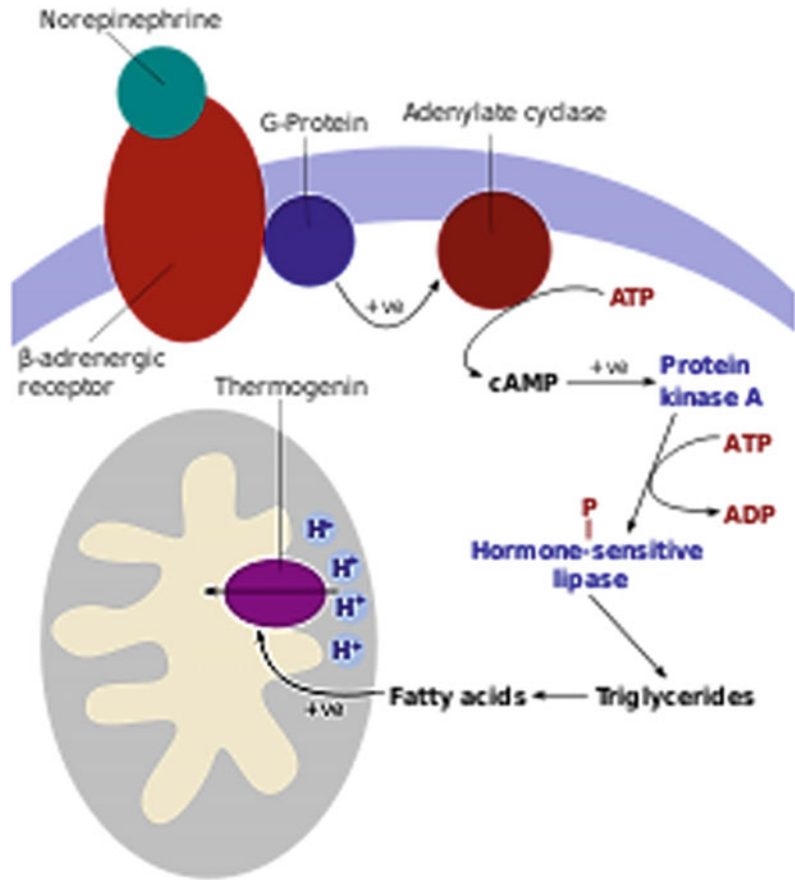
of pyruvate and lactic acid, pH of cytosol and mitochondrial matrix becomes lower than 6.5 which results in the dimerization of IF_1 . In dimeric form IF_1 binds to two ATP synthase molecules thus inhibiting it and preventing wasteful hydrolysis of ATP.

8.9.2 Proton Permeability of Membranes

“Proton leak” across the inner membrane of mitochondria results in the dissipation of proton gradient and uncouples oxidation of fuels from ATP generation, and losing some energy as heat or thermogenesis. The uncoupling of oxidative phosphorylation is a mechanism of generating heat to maintain body temperature in hibernating

animals, in some newborn animals (including human beings), and in mammals adapted to cold. Brown adipose tissue (BAT), which is rich in mitochondria, is specialized for this process of nonshivering thermogenesis. The mitochondrial inner membrane of brown adipose tissue contains a large amount of uncoupling protein-1 (UCP-1), or thermogenin, a dimer of 33-kd subunits that resembles ATP–ADP translocase. UCP-1 forms a channel for the flow of protons down the gradient into the matrix, thereby dissipating the proton gradient which is required for ATP synthesis by ATP synthase. Hence, UCP-1 generates heat by preventing ATP synthase from harnessing the energy inherent in proton gradient. The uncoupling proteins in the brown fat cell are activated by fatty acids and inhibited by nucleotides. On activation of the sympathetic nervous system, norepinephrine is released.

Fig. 8.32 Mechanism of regulation of thermogenin (UCPI) activation



Norepinephrine to a β -3 adrenergic receptor on the plasma membrane of BAT cells activates adenylyl cyclase, which catalyzes the conversion of ATP to cyclic AMP (cAMP). cAMP activates protein kinase A, which in turn phosphorylates and activates triacylglycerol lipase. The active lipase converts triacylglycerols stored in BAT cells into free fatty acids, which activate UCP1, overcoming the inhibition caused by purine nucleotides (GDP and ADP). At the termination of thermogenesis, the mitochondria oxidize away the residual fatty acids, UCP1 inactivates, and the cell resumes its normal energy-conserving mode (Fig. 8.32).

Two other uncoupling proteins, apart from UCP-1, have been identified. UCP-2, which is

56% homologous with UCP-1, is found in a wide variety of tissues. UCP-3 (57% identical with UCP-1 and 73% identical with UCP-2) is localized to skeletal muscle and brown fat. These families of uncoupling proteins, especially UCP-2 and UCP-3, may play a role in energy homeostasis and could have an important role in dealing with oxidative stress by limiting ROS production.

Adenine nucleotide translocator (ANT) and mitochondrial phosphate carrier protein (PC) which catalyze the transport of ATP/ADP and P_i respectively across the mitochondrial membrane, do so at the expense of proton gradient, hence also contribute to the dissipation of proton gradient.

8.9.3 Reactive Oxygen Species (ROS) Production

Reactive oxygen species (ROS), produced in mitochondrial electron transport chain, can cause oxidative damage leading to many pathological conditions. Approximately 1–2% of oxygen consumed during respiration is converted into superoxide ($O_2^{\bullet-}$) by one-electron reduction. There are two pathways in the mitochondrial electron transport chain that can lead to the generation of large amounts of $O_2^{\bullet-}$, predominantly involving the complex I. The first pathway results in conditions of slow respiration or ischemia which can cause a buildup of NADH, and the second pathway occurs when reduced coenzyme Q accumulates resulting from large proton gradient with no ATP synthesis (Fig. 8.33). In first pathway, fully reduced FMN resulting from high NADH/NAD⁺ ratio passes on the electrons to O_2 giving rise to superoxides. Reverse electron transport from reduced coenzyme Q to complex I occurs in the second pathway, when reduced CoQ (CoQH₂) accumulates due to excess supply from succinate, glycerol phosphate, or fatty acid oxidation. Rotenone enhances the superoxide production via first pathway, but inhibits production via second pathway.

Complex III, which transfers electron from reduced CoQ to cyt *c*, is another site of superoxide production. Inhibition of CoQH₂ binding at Q_p site of complex III by antimycin can result in generation of large amounts of superoxides.

Superoxide generated from complex I is released into the matrix, whereas superoxide from complex III can be released on either side of the inner membrane. Superoxides can be transported into the cytosol via outer mitochondria membrane voltage-dependent anion-selective channel (VDAC). Superoxides in the matrix are dismutated to H₂O₂ by the mitochondrial matrix Mn superoxide dismutase (MnSOD, also known as SOD2), while intermembrane space superoxides are dismutated by Cu/Zn superoxide dismutase (Cu/ZnSOD, also known as SOD1). H₂O₂ can be reduced to water by reduced glutathione,

catalyzed by the enzyme, glutathione peroxidase. The oxidized glutathione is reduced by glutathione reductase using NADPH as a reductant. In the presence of reduced transition metals, H₂O₂ can be reduced to hydroxyl radicals ($\cdot OH$), which are the most reactive ROS. In the cytosol, superoxide is converted by SOD1 into H₂O₂, which can be detoxified by the peroxisomal enzyme catalase (Fig. 8.34).

8.9.4 Apoptosis

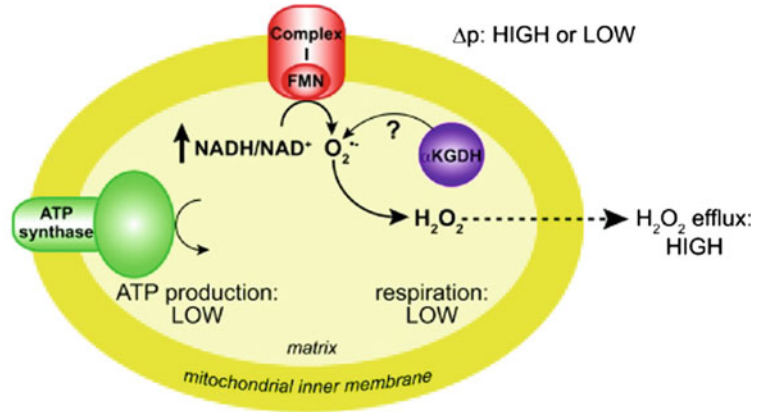
Apoptosis is a process of programmed cell death, which is genetically determined for each cell type. It is a normal process of development and aging, but can be triggered or inhibited in certain conditions which can lead to diseases like autoimmune disorders and cancer. It is characterized by series of morphologically identifiable steps, including shrinkage of cells, chromatin condensation, membrane blebbing, nuclear fragmentation, apoptotic body formation, and finally phagocytosis by neighboring cells.

There are two main apoptotic pathways, the extrinsic and the intrinsic pathway (Fig. 4.26). The intrinsic pathway is also known as the mitochondrial pathway as mitochondria play a major role in it. Apoptotic proteins affect mitochondria by causing mitochondrial swelling through the formation of membrane pores, or they may cause an increase in the permeability of the mitochondrial membrane facilitating the apoptotic effectors to leak out.

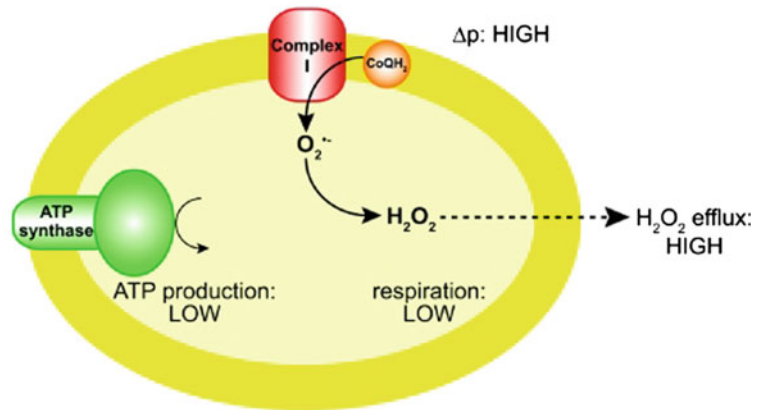
Many apoptosis-regulating proteins govern mitochondrial outer membrane permeabilization (MOMP). These regulatory proteins can be either pro-apoptotic (Bax, BAD, Bak, and Bok among others) or antiapoptotic (including Bcl-2, Bcl-xL, and Bcl-w). On activation of apoptosis signal, there is an increase in the permeability of the outer mitochondrial membrane, allowing the escape of the cytochrome *c* from the intermembrane space. This is due to the formation of mitochondrial apoptosis-induced channel (MAC) in the outer mitochondrial membrane. Once cytochrome *c* is released, it binds with

Fig. 8.33 Modes of ROS production in mitochondria. There are three modes of mitochondrial ROS production. In mode 1, the NADH pool is increased, for example, by damage to the respiratory chain, loss of cytochrome c during apoptosis, or low ATP demand. Other sites such as α KGDH may also contribute. In mode 2, there is no ATP production and there is a high Δp and a reduced CoQ pool which leads to reverse electron transport (RET) through complex I, producing large amounts of $O_2^{\cdot-}$. In mode 3, $O_2^{\cdot-}$ is produced at complex III, and ATP is synthesized and consequently has a lower Δp than in mode 2 and a more oxidized NADH pool than in mode 1 and 2. *Source* Murphy (2009)

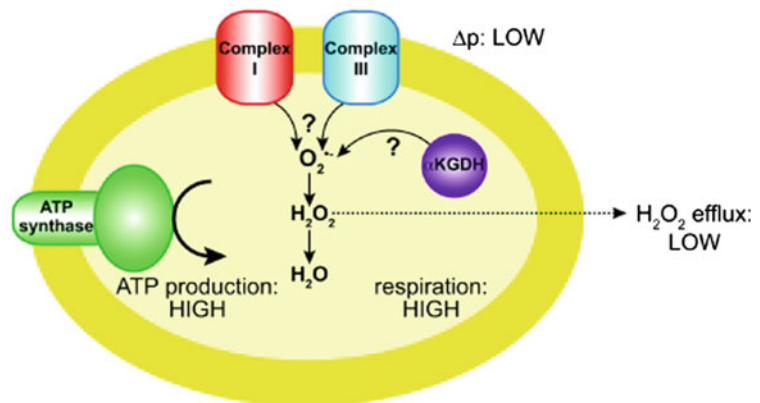
MODE 1: high NADH/NAD⁺



MODE 2: high Δp and high CoQH₂/CoQ



MODE 3: normal mitochondrial function



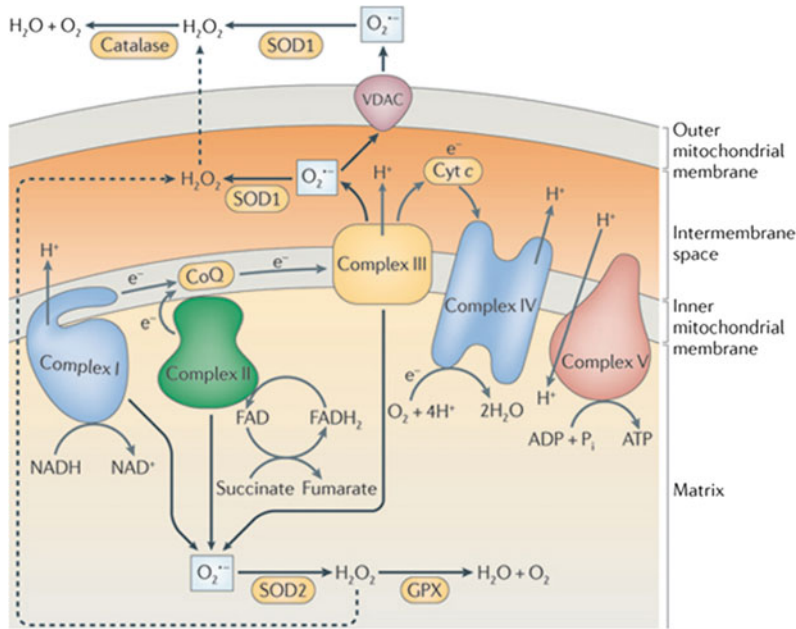


Fig. 8.34 Fate of reactive oxygen species (ROS) generated in mitochondria. Superoxide can then cross the outer mitochondria membrane via a voltage-dependent anion-selective channel (VDAC). Matrix $O_2^{\bullet-}$ is dismutated to H_2O_2 by the mitochondrial matrix (MnSOD; also known as SOD₂), while intermembrane space $O_2^{\bullet-}$ is dismutated by Cu/Zn superoxide dismutase (Cu/ZnSOD; also known as

SOD1). H_2O_2 can be reduced to water by glutathione peroxidase using reduced glutathione as an electron donor. Oxidized glutathione is reduced by glutathione reductase. In the cytosol, superoxide is converted by SOD1 into H_2O_2 , which is further detoxified by the peroxisomal enzyme catalase. *Source* West et al. (2011)

apoptotic protease activating factor-1 (Apaf-1) and ATP, which then bind to pro-caspase-9 to form a protein complex known as an apoptosome.

The apoptosome cleaves the pro-caspase to active caspase-9, which in turn activates the effector caspase-3 and -7. Caspases are a family of cysteine proteases that act in concert in a cascade triggered by apoptosis signaling (Fig. 8.35). This cascade results in the cleavage of a number of proteins in the cell, followed by cell death, and, ultimately, the phagocytosis and removal of the cell debris.

8.10 Photosynthesis

Life on earth is driven by the sun directly or indirectly. **Autotrophs** harness **the light energy of the sun** to produce sugars and other organic molecules from CO_2 and H_2O obtained from the environment. **Heterotrophs** are incapable of

harnessing the energy of the sun directly and derive their energy by consuming sugars and other organic molecules produced by the autotrophs. Autotrophs are hence referred to as *producers* and heterotrophs as the biosphere's *consumers*.

Photosynthesis is a process by which light energy of the sun is converted into the chemical energy of sugars and other organic compounds. Photosynthetic machinery is quite diverse and unique in different autotrophic systems, which include the green plants, phytoplankton, cyanobacteria, and photosynthetic bacteria.

Photosynthesis is a two-stage process. The first stage involves the **light-dependent reactions** or simply the **light reactions**, in which light energy is captured to split H_2O molecule to release O_2 and electrons, which pass on through an electron transport chain, similar to the one in mitochondria, to generate high-energy molecules and reducing equivalents in the form of ATP and

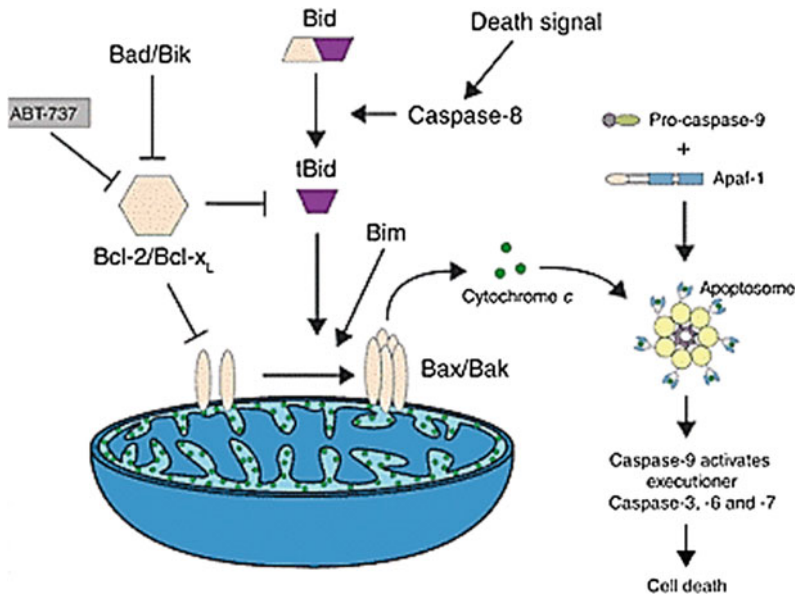


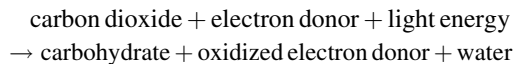
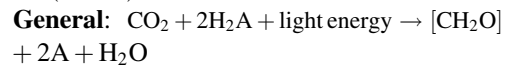
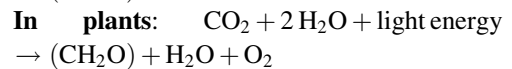
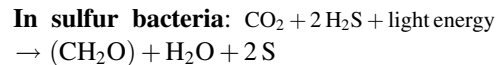
Fig. 8.35 Schematic diagram of the intrinsic or mitochondria apoptosis signaling pathway. Upon the release of cytochrome c from mitochondria, it binds with apoptotic protease activating factor 1 (Apaf-1) to form the apoptosome. The apoptosome activates pro-caspase 9 into

caspase 9, the initiator apoptotic caspase. Caspase 9 then cleaves and activates executioner caspases 3 and 7. Elevated activity of caspase 3 and 7 induces irreversible fate of apoptosis

NADPH, respectively. During the second stage of **dark reactions**, ATP and NADPH generated during the light reaction are utilized to reduce carbon dioxide to synthesize sugar molecules.

In the 1930s, C.B. van Niel, a graduate student at Stanford University, found that photosynthesis in the purple sulfur bacteria does not release oxygen during photosynthesis. It was proposed that in purple sulfur bacteria, H_2S is split during light reaction to release **S** and electrons, which are fed into the electron transport chain. It can be generalized that photosynthetic reactions in different photosystems essentially require an electron donor, which in plants is H_2O and in purple bacteria sulfur bacteria is H_2S . These reducing equivalents generated are then used to reduce CO_2 . Robert Hill in 1937 confirmed that H_2O is the source of electrons in plants required for CO_2 fixation and in turn gets oxidized to O_2 molecule.

The overall reactions in different photosystems are given below:



8.11 Light Energy

Out of the full spectrum of electromagnetic energy radiated by the sun (Fig. 8.36), only a fraction of the radiation reaches the earth. It is only the visible light spectrum of this fraction that is utilized by the process of photosynthesis. Visible light falls in the narrow wavelength range of 400–700 nanometers (nm), between the ultraviolet (higher energy and shorter wavelengths) and the infrared (lower energy and longer wavelengths) light.

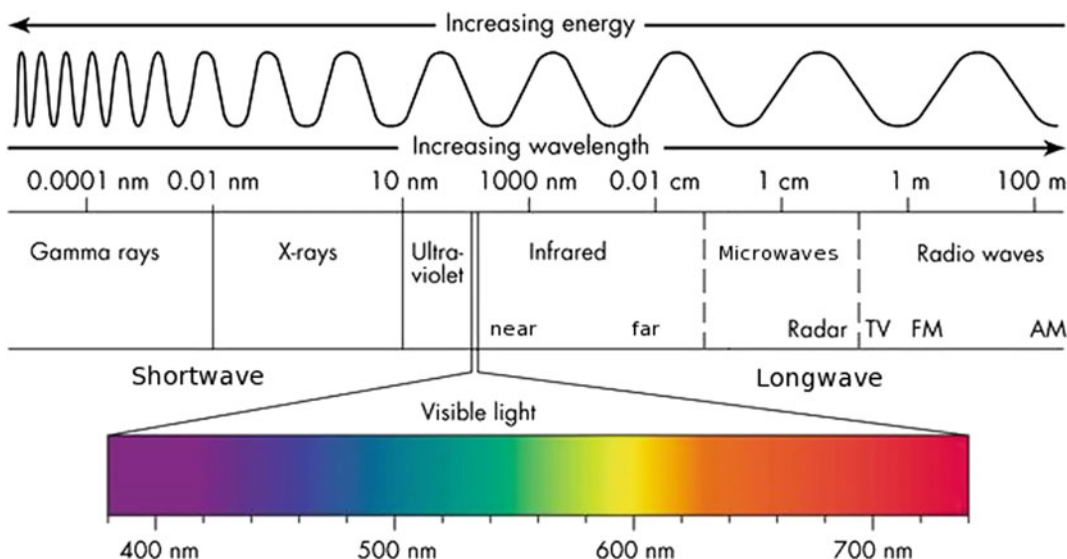


Fig. 8.36 Electromagnetic spectrum

Light has both wave and particle character. A **photon** of light is an elementary particle, the quantum of all forms of electromagnetic radiation.

The energy carried by a single photon, the **photon energy**, is related to the wavelength and frequency of the specific electromagnetic radiation. The photon energy increases with the frequency and decreases with increase in wavelength of the radiation. The photon energy is given by Planck equation:

$$E = \frac{hc}{\lambda}$$

where E is the energy of a photon of light, h is the Planck constant, c is the speed of light in vacuum, and λ is the photon's wavelength. As h and c are both constants, the photon energy is directly related to the wavelength λ of light.

$$\begin{aligned} h & 6.626 \times 10^{-34} \text{ J s} \\ c & 2.998 \times 10^8 \text{ m/s} \\ hc & 1.99 \times 10^{-25} \text{ joules-m} \end{aligned}$$

The energy associated within one mole of photons of blue (400 nm) light is:

$$\begin{aligned} E & = h\nu \\ & = \frac{hc}{\lambda} \left(\frac{(6.626 \times 10^{-34} \text{ J s})(2.9979 \times 10^8 \frac{\text{m}}{\text{s}})(6.022 \times 10^{23} \frac{\text{photons}}{\text{mol}})}{400 \times 10^{-9} \text{ m}} \right) \\ & \quad (\text{Avogadro's number } N = 6.022 \times 10^{23}) \\ & = 300 \text{ kJ/mol,} \end{aligned}$$

whereas the amount of energy in a mole of photons of red (700 nm) light would be = 170 kJ/mol.

Photosynthetic organisms contain light-absorbing molecules called **pigments/chromophores** that absorb specific wavelengths of visible light, while reflecting others. On absorption of a photon of light by a molecule, it is **excited** (electronic and vibrational) to a higher energy level based on Niels Bohr's theory of atomic and molecular structure, from a lower energy level, the **ground state**.

Excited states of molecules are energetically unstable and very short-lived. The excited electrons eventually return back to their ground state. They can do this by either radiative or nonradiative decay (Fig. 8.37). In radiative decay, a photon of lower energy is emitted (after some energy has already been lost by vibrational transitions/relaxation) in a process of either

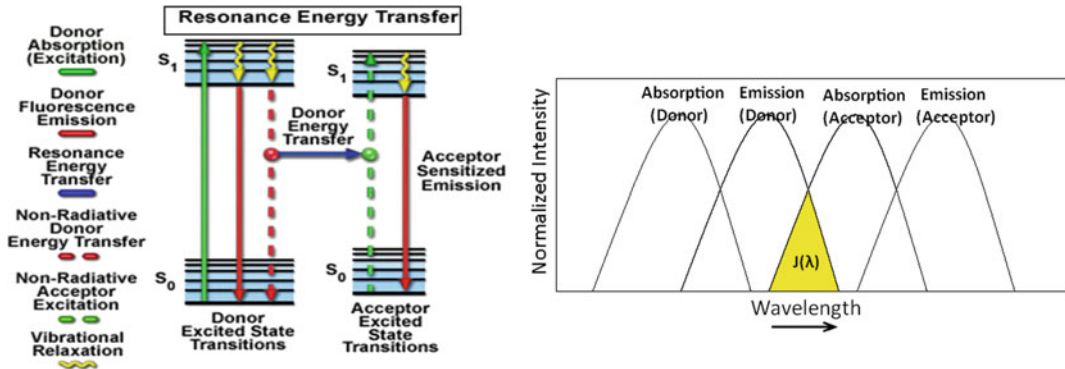


Fig. 8.37 The excited electron in a chromophore can lose its energy by radiative or nonradiative decay. It can also pass on the energy to a neighboring molecule by

resonance energy transfer if donor molecules emission spectra overlap with acceptor molecules absorption spectra

fluorescence or phosphorescence. In nonradiative decay, the energy of an excited electron can be transferred to another molecule, which will then excite the energy of an electron in the second molecule to the same excited state. In this fashion, energy is transferred from one molecule to another. This type of energy transfer from one molecule to another is called **resonance energy transfer** or exciton transfer. The rate of resonance energy transfer depends on the distance between the energy donor and energy acceptor molecules and their spectral overlaps. Hence, in a photosystem pigment molecules are specifically positioned to optimize the transfer rates of exciton transfer. Energy transferred to another molecule can also be lost as heat by vibrational transitions/relaxation resulting in **quenching** by nonradiative decay.

The major **photosynthetic pigments** present in higher plants can be categorized into two major groups, the **chlorophylls** (Chl) and the **carotenoids**. Both types of pigments are bound to proteins in the **thylakoid membranes** in the **chloroplasts**, the site of photosynthesis in plants. The most abundant plant pigments are **chlorophyll a** and **chlorophyll b** which occur in a ratio of approximately 3:1. As is shown in Fig. 8.38, the chlorophylls possess a porphyrin ring with a coordinated magnesium atom at its center, a fused, five-membered ring and a C₂₀ phytol side chain. The only difference between chlorophyll a and b is substituent at the position 3 (ring 3), and

chlorophyll a has a methyl group, whereas b has an aldehyde attached. In plant cell, the chlorophylls serve as the primary photosynthetic pigments present at the reaction center. They absorb light in the blue (450 nm) and red regions (650–700 nm) (Fig. 8.39).

The second groups of plant pigments, the carotenoids, can be further categorized into two different groups, (1) the carotenes which contain only carbon and hydrogen and (2) the xanthophylls which in addition contain oxygen atoms in the form of hydroxyl or epoxide functional groups. The structures for several major carotenoids are shown in Fig. 8.38. They all contain 40 carbon atoms, and because of the extensive conjugation, they are highly colored. Most carotenoids are predominantly yellow, red, and orange. Many of the bright colors found in flower petals are due to the presence of carotenoids (although some are due to anthocyanins). The yellow colors of fall foliage are due primarily to carotenoids as chlorophylls are destroyed. The relative percentage composition of carotenoids in plants varies with growing conditions. On an average weight % ranges are: 13-carotene, 25–40%; lutein, 40–60%; violaxanthin, 10–20%; and neoxanthin, 5–13%.

Carotenoids have two major physiological functions. First, the carotenoids, particularly the xanthophylls, as accessory pigments, funnel the absorbed light energy to the reaction center, by resonance energy transfer. By doing so, the

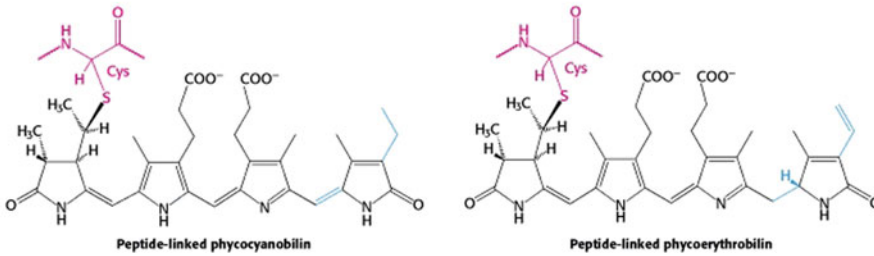
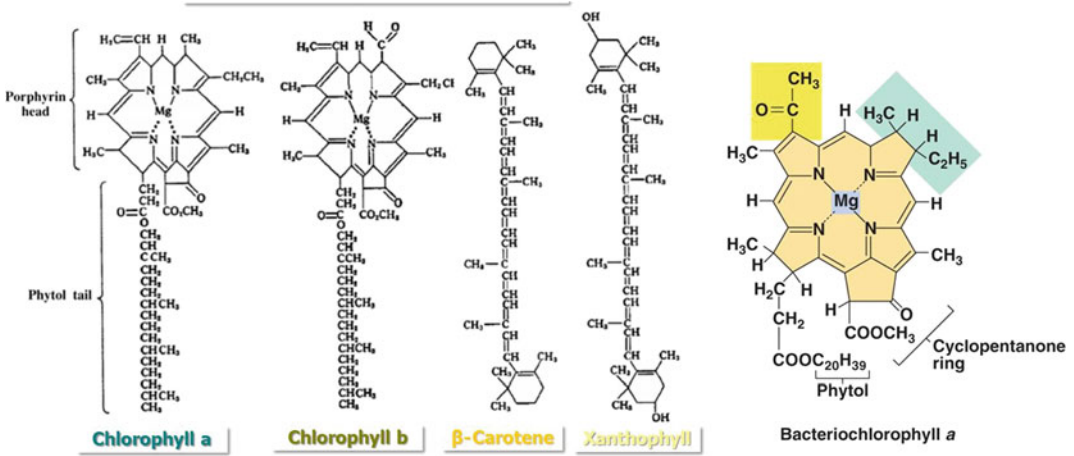
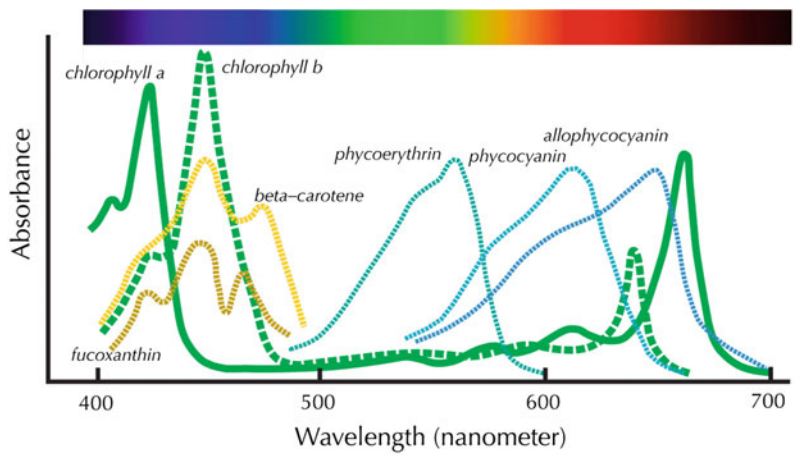


Fig. 8.38 Photosynthetic pigments

Fig. 8.39 Absorption maxima of various photosynthetic pigments



Pigment	Wavelength [nm]	Occurrence
Chlorophyll a	430, 670	All green plants
Chlorophyll b	455, 640	Higher plants; green algae
Chlorophyll c	445, 625	Diatoms; brown algae
Bacteriochlorophyll	365, 605, 770	Purple and green bacteria
α-Carotene	420, 440, 470	Leaves; some algae
β-Carotene	425, 450, 480	Some plants
γ-Carotene	440, 460, 495	Some plants
Luteol	425, 445, 475	Green leaves; red and brown algae
Violaxanthol	425, 450, 475	Some leaves
Fucoxanthol	425, 450, 475	Diatoms; brown algae
Phycoerythrins	490, 546, 576	Red and blue-green algae
Phycocyanins	618	Red and blue-green algae
Allophycocyanin	654	Red and blue-green algae

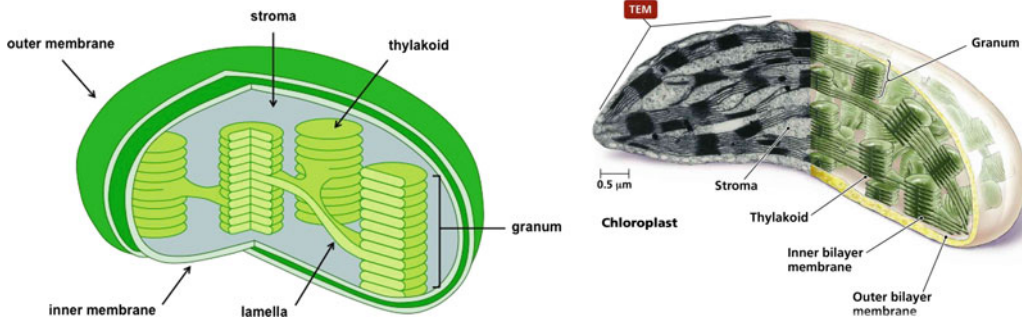


Fig. 8.40 Chloroplast. Diagram and TEM image. *Image courtesy academic.pgcc.edu/03-37_Chloroplasts_L.jpg*

accessory pigments increase the photosynthetic efficiency by extending the range of light wavelengths that a plant photosystem can absorb. The accessory pigments are arranged in numerous **light-harvesting complexes** (LHCs) that completely surround the reaction center. The light-harvesting complex II (LHCII) the most abundant membrane protein in chloroplasts is associated with seven chlorophyll *a* molecules, six chlorophyll *b* molecules, and two carotenoid molecules. Similar light-harvesting assemblies also exist in photosynthetic bacteria.

Carotenoids also play an important role in protecting the photosynthetic apparatus from photodamage by quenching the Chl triplet state and singlet oxygen. Carotenoids have the ability to “vibrate away” their triplet state energy as heat into the surroundings. This enables carotenoids to absorb (“quench”) the energy of excited molecules such as singlet state oxygen and triplet state chlorophyll, thereby preventing the destruction of protein, DNA, and the photosynthetic apparatus. In addition, in higher plants and some algae, a number of xanthophylls can also quench excited Chl under conditions of excess excitation. Hence, the carotenoids inhibit the photooxidative damage of photosystems.

The light-harvesting complexes in cyanobacteria (blue-green algae) and red algae are large protein assemblies called **phycobilisomes** (Fig. 8.41). As little blue or red light reaches algae living in deep seawater, phycobilisomes harvest the green and yellow light that penetrates in deep sea beds. Phycobilisomes are attached to the outer face of the thylakoid membrane, with absorption

maxima in the range of 470–650 nm. Phycobilisomes are very large assemblies (several million daltons) of many **phycobiliprotein** subunits, and each phycobiliprotein subunit contains many covalently attached open-chain tetrapyrrole prosthetic groups known as **phycobilins**, as well as linker polypeptides. Phycobiliproteins can be categorized into four major groups, namely *allophycocyanin* (APC), *phycocyanin* (PC), *phycoerythrin* (PE), and *phycoerythrocyanin* (PEC), containing prosthetic group: *allophycocyanobilin*, *phycocyanobilin*, *phycoerythrobinin*, and *phycoerythrocyanobilin*, respectively.

Highly ordered geometrical arrangement of phycobiliproteins in phycobilisomes, as well as their spectral properties, contributes to the high speed and efficiency of energy transfer, which is greater than 95%. Excitation energy absorbed by phycoerythrin subunits at the periphery is passed on to the reaction center in less than 100 ps.

Bacteriochlorophylls (BChls) and carotenoids are the photosynthetic pigments that occur in various phototrophic bacteria. There are several types, designated *a–g* (Table 8.2). Bacteriochlorophyll *a* and bacteriochlorophyll *b* are similar in structure to the chlorophyll *a* and chlorophyll *b* found in plants.

8.11.1 Site of Photosynthesis

Chloroplasts organelles, the site of photosynthesis, are present in the leaves of most plants and in algal cells. German botanist Hugo von Mohl, in 1837, for the first time gave a

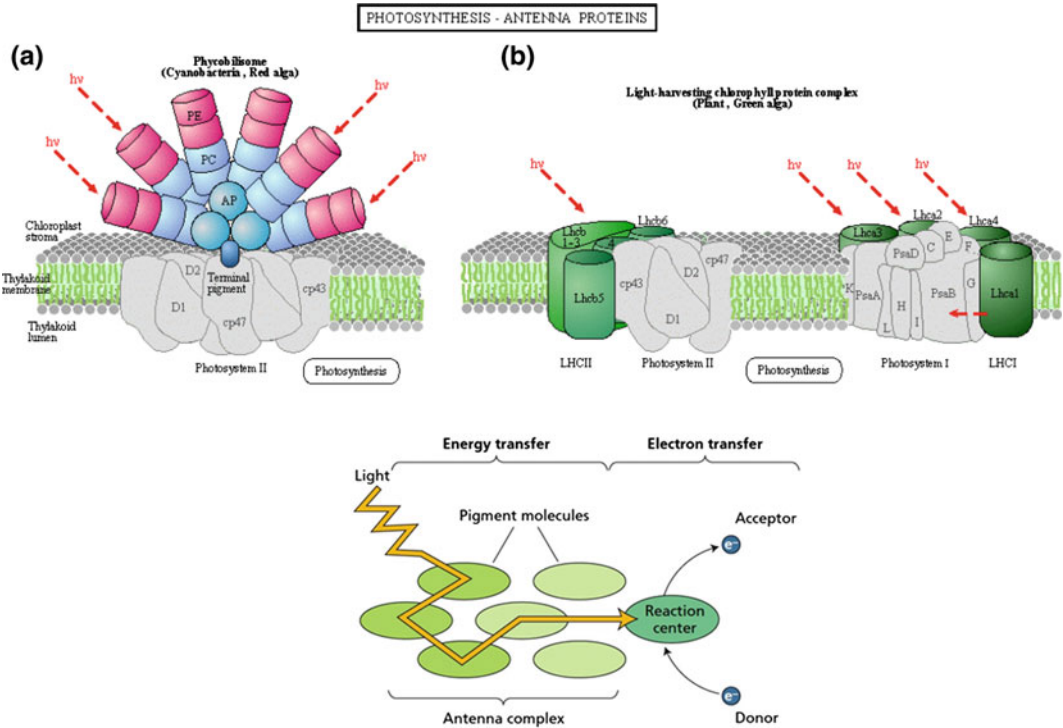


Fig. 8.41 a Antenna proteins in light-absorbing complexes phycobilisomes in cyanobacteria on the left and light-harvesting complexes LHCI and LHCII in plants transfer light energy via exciton transfer to the reaction center (b)

Table 8.2 Bacteriochlorophylls (BChl) a–g found in different types of bacteria

Pigment	Bacterial group	In vivo infrared absorption maximum (nm)
Bacteriochlorophyll <i>a</i>	Purple bacteria, heliobacteria, green sulfur bacteria, chloroflexi, <i>chloracidobacterium thermophilum</i>	805, 830–890
Bacteriochlorophyll <i>b</i>	Purple bacteria	835–850, 1020–1040
Bacteriochlorophyll <i>c</i>	Green sulfur bacteria, chloroflexi, <i>C. thermophilum</i>	745–755
Bacteriochlorophyll <i>c_s</i>	Chloroflexi	740
Bacteriochlorophyll <i>d</i>	Green sulfur bacteria	705–740
Bacteriochlorophyll <i>e</i>	Green sulfur bacteria	719–726
Bacteriochlorophyll <i>f</i>	Green sulfur bacteria (currently found only through mutation; natural may exist)	700–710
Bacteriochlorophyll <i>g</i>	Heliobacteria	670, 788

description of “Chlorophyllkörnern” (chlorophyll granules) in green plant cells, but their discovery is attributed to Julius von Sachs (1832–1697), also called “the Father of Plant Physiology”.

Chloroplasts are found mainly in the **mesophyll cells**, the tissue found in the interior of the leaf. Each mesophyll cell can have 1–50 chloroplasts, depending on the species and age of

the cell. Gases like carbon dioxide and oxygen are exchanged in the leaf via microscopic pores called **stomata** (singular, *stoma*; meaning “mouth” in Greek). Water absorbed by the roots is transported to the leaves in veins. Sugars synthesized in the leaves are also transported to the roots and other nonphotosynthetic parts of the plant by veins.

Chloroplasts belong to a large family of plant cell organelles that are involved in energy storage and the synthesis of metabolic materials, called the **plastids**. Plastids are classified according to the pigments they contain. For example, **leucoplasts** are nonpigmented, colorless plastids, yellow-to-red colored **chromoplasts** contain carotenoids but lack chlorophylls, and the green-colored chloroplasts contain both chlorophylls and carotenoids. All plastids develop from tiny (0.5–1 μm in diameter) organelles present in the rapidly dividing, undifferentiated cells of plant meristems termed **proplastids**. Proplastids then develop into the various types of mature plastids according to the needs of the cells, influenced by the environmental conditions the leaves are exposed to. Plastids are also able to change from one type to another; for example, chloroplasts develop into chromoplasts during the ripening of fruit (e.g., tomatoes) with increased synthesis of carotenoids.

The ellipsoid-shaped chloroplast, like mitochondria, is enclosed in a double membrane, the outer and inner membrane separated by the **intermembrane space**. The outer membrane of the chloroplast is much more permeable than the inner membrane, which is associated with a number of embedded membrane transport proteins. The chloroplast double membranes enclose the **stroma**, a semifluid matrix which comprises most of the chloroplast’s volume (Fig. 8.40). Stroma contains the chloroplast genome (DNA), special ribosomes and RNAs, thylakoid system, enzymes involved in carbon fixation, and starch granules.

Thylakoid system is another membrane system present in the chloroplasts, also considered as the third membrane system of chloroplast, apart from the outer and the inner membranes. **Thylakoids**, a name introduced by Menke

(1962), are differentiated into stacked and non-stacked membrane domains (Fig. 8.40). The stacks of membranes like flattened disks correspond to the **grana** structures, called the **grana lamellae**, and the nonstacked cylindrical membranes are known as **stroma thylakoids/stroma lamellae**, as they are in direct contact with the stroma. The stacks of grana lamellae and unstacked stroma lamellae enclose the **thylakoid lumen**, and this internal space forms a continuous aqueous phase connecting the stroma and grana lamellae.

The thylakoids contain all the protein complexes involved in electron transport chain and energy transduction process of photosynthesis, including the photosystems, light-harvesting complexes, *cyt b₆f* complex, F-ATPase. The grana and stroma lamellae differ in their protein composition and show “lateral heterogeneity.” Photosystem II and light-harvesting complex (LHCII) are concentrated in the stacked grana lamellae, while photosystem I with its LHCI and the chloroplast ATP synthase are localized in the unstacked thylakoid regions, the stroma lamellae. The cytochrome *b₆f* complex (*cyt b₆f*) can be found in both appressed and nonappressed domains of thylakoids.

In bacteria, photosynthetic machinery is located in specialized membrane systems, called the **chromatophores**. In purple bacteria, the chromatophores are in the form of sheets, tubes, or vesicles arising from the plasma membrane, whereas in green bacteria they are cylindrical structures, known as **chlorosomes** underlying the plasma membrane.

8.12 Process of Light Reaction of Photosynthesis

Photosystems are the protein complexes, which are the primary functional and structural units of photosynthesis that together carry out the light reaction of photosynthesis, involving the process of absorption of light and the transfer of energy and electrons. A **photosystem** comprises of a **reaction center complex (RC)** surrounded by several **light-harvesting complexes** (Fig. 8.41).

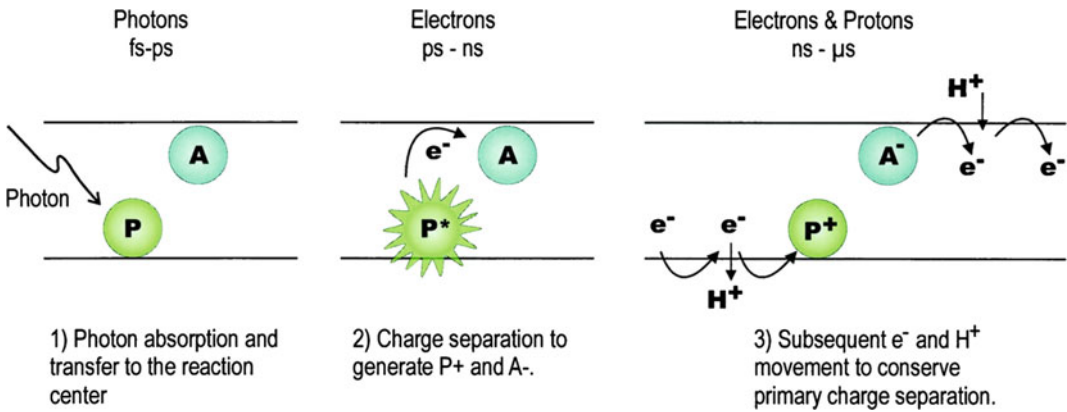


Fig. 8.42 Scheme of the primary processes in the photosynthetic RC. Here, P represents the charge-separating (bacterio) chlorophyll pigments (the primary electron donor) and A represents the first stable acceptor. Energy transfer from the antenna pigments leads to photoexcitation of P on the fs-ps time scale (left). Charge

separation produces oxidized P^+ and A^- on the ps-ns scale (center). The recombination of P^+ A^- to produce PA, heat, and potentially damaging chemical species is efficiently prevented by further forward electron transfer that is now proton coupled

The photosynthetic reaction center is a special pigment-protein complex that functions as a photochemical trap, converting solar energy into biochemical amenable energy. The **light-harvesting complex (LHC)** consists of various pigment molecules (which may include chlorophylls/bacteriochlorophylls and multiple carotenoids) bound to various antenna proteins. The large number of different pigment molecules in the LHC enables the photosystem to harvest over a large spectrum of light, thereby enhancing the photosynthetic efficiency. In light-harvesting complexes, the energy absorbed by one pigment molecule is transferred to another pigment molecule by resonance energy transfer, somewhat like a basketball in a basketball game, until it is passed into the reaction center complex where charge separation occurs (Fig. 8.42).

The reaction center protein complex holds a special pair of RC pigments (bacteriochlorophyll/ chlorophyll *a* molecules), which get excited on absorption of energy, and donates an electron to the **primary electron acceptor**, resulting in charge separation. The reaction center acts as a **primary electron donor** and becomes positively charged, whereas the primary electron acceptor becomes negatively charged. This charge separation initiates a series of electron transfer

reactions that culminate in generation of NADPH. The electron transport is coupled to the translocation of protons across the membrane, generating an electrochemical proton gradient [proton-motive force (pmf)] that can be utilized for the synthesis of ATP.

The bacterial photosynthetic system serves as an important study model to understand the photosystem structure and mechanism of photoreaction in photosynthesis.

Bacterial photosynthesis can be broadly classified into: **anoxygenic photosynthesis** and **oxygenic photosynthesis**. Anoxygenic photosynthetic bacteria consume carbon dioxide but do not release oxygen. Examples of anoxygenic bacteria include purple and green bacteria as well as phototrophic Acidobacteria and phototrophic heliobacteria. Purple bacteria can be of two categories, purple sulfur bacteria (Chromatiales) and purple nonsulfur bacteria (Rhodospirillaceae). Purple sulfur bacteria use hydrogen sulfide as an electron donor, to produce granules of elemental sulfur, which in turn may be oxidized to form sulfuric acid. Purple nonsulfur bacteria use mainly hydrogen as electron donor. The green sulfur bacteria (Chlorobiaceae) are a family of obligate anaerobic photoautotrophic bacteria.

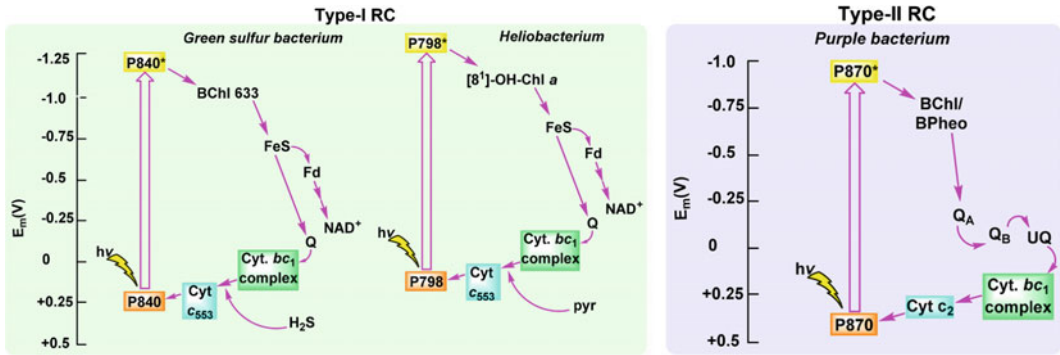


Fig. 8.43 Photosynthetic electron transport system of green sulfur bacterium, heliobacterium, and purple bacterium

They use sulfide ions, hydrogen, or ferrous iron as an electron donor (Fig. 8.43). The process of photosynthesis in **oxygenic photosynthetic bacteria** is similar to that in plants. They have two similar photosystems, light-harvesting complexes, consume carbon dioxide, and release oxygen. **Cyanobacteria (Cyanophyta) or blue-green algae** are the only form of oxygenic photosynthetic prokaryotes known to date. It is thought that cyanobacteria have contributed oxygen to the earth's early oxygen-deficient atmosphere initiating life on earth.

8.12.1 Purple Photosynthetic Bacteria

Purple bacteria have the simplest photosynthetic apparatus, making them an ideal candidate for photosynthetic studies. Purple bacteria reaction center complex was first purified by Roderick Clayton in 1960. However, it was Hartmut Michel, Johann Deisenhofer, and Robert Huber in 1985, who determined the crystal structure of photosynthetic reaction center of *Rhodospseudomonas viridis*, for which they received the Nobel Prize in 1988.

The photosynthetic apparatus of purple bacteria consists mainly of two types of pigment-protein complexes, the photosynthetic RC and LHCs. In most purple bacteria, the photosystem contains two types of LHCs, commonly referred to as B875 (LHCI) and B800-850 (LHCII) complexes based on their *in vivo* absorption

maxima in the near-infrared. LHCI is associated directly with the RCs in a 1:1 ratio, while LHII which is not in direct contact with the RC is sometimes called the “peripheral light-harvesting complex.” It transfers energy to RC via LHI (Fig. 8.44). The two LHCs expand the light-harvesting capacity, both in terms of the area available and in the spectrum of wavelengths that can be used.

Purple bacteria have only one photosystem, P-870. The *Rp. viridis* RC has an overall length of 130 Å (seen perpendicular to the membrane) and the maximum width of about 70 Å (seen parallel to the membrane). The central core of the RC is formed by the L (light)-subunit and the M (heavy)-subunit, with each subunit contributing five α -helical membrane-spanning strands. Both subunits are closely associated with 10 cofactors, which are attached noncovalently. L- and M-subunits are each associated with two bacteriochlorophylls (BChlB), one bacteriopheophytin (BPheo) ϕ and one quinone. The two subunits and their associated cofactors are arranged in a twofold symmetry pattern, perpendicular to the plane of the membrane. The H-subunit is anchored to the membrane by a single membrane-spanning α -helix and is attached to the LM core on the cytoplasmic side. On the periplasmic side, the c-subunit with its four covalently bound heme groups, heme 1-4, is associated (Fig. 8.45).

The L- and M-subunits are similar in structure. The arrangement of cofactors starts with the “special pair” D_L and D_M of two closely

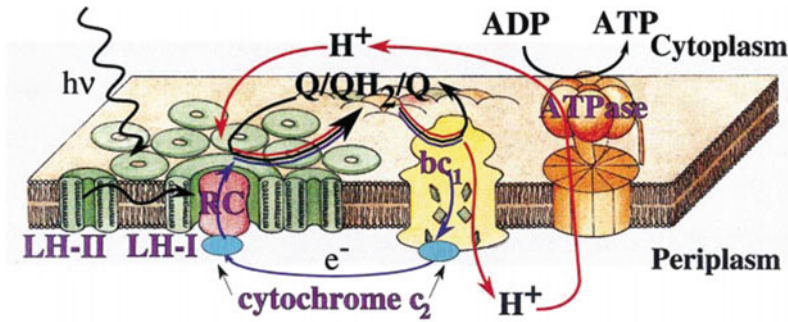


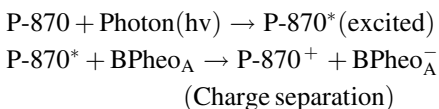
Fig. 8.44 Schematic representation of the electron flow involving photosynthetic apparatus in purple bacteria. The reaction center (RC, red) is surrounded by the light-harvesting complex I (LHI, green) to form the LHI ± RC complex, which is surrounded by multiple light-harvesting complexes (LHII) (green), forming altogether the photosynthetic unit (PSU). Photons are absorbed by LHs, and excitation is transferred to the RC initiating a charge (electron-hole) separation. Electrons are shuttled

back by the cytochrome c_2 complex (blue) from the ubiquinone-cytochrome bc_1 complex (yellow) to the RC. The electron transfer across the membrane produces a large proton gradient that drives the synthesis of ATP from ADP by the ATPase (orange). Electron flow is represented in blue, proton flow in red, quinone flow, likely confined to the intramembrane space, in black. *Source* Xiche Hu et al. (2002) (Color figure online)

associated bacteriochlorophylls near the periplasmic side, each associated with L- and M-subunit, followed by the “accessory” bacteriochlorophyll (BChlB), one bacteriopheophytin (BPheo) ϕ , and a quinone, Q. But only the branch associated with L-subunit is involved in the light-driven electron transfer. Hence, the active cofactors are given subscript A and inactive given B subscript. The electrons excited from D_L reach the electron acceptor, quinone Q_A , via (BPheo) ϕ_A . It is then transferred to quinone Q_B via nonheme iron positioned half way between both the quinones (Fig. 8.45).

On receiving light energy, P-870 (B. Chl.a) gets excited (*). An electron released is immediately (within picoseconds) captured by bacteriopheophytin A (B. Pheo) $_A$.

Thus, charge separation occurs with a positive charge on bacteriochlorophyll and negative charge on bacteriopheophytin:



The reduced pheophytin then passes its electron to a tightly bound molecule of quinone (Q_A), which then passes it to Q_B . Fully reduced quinol

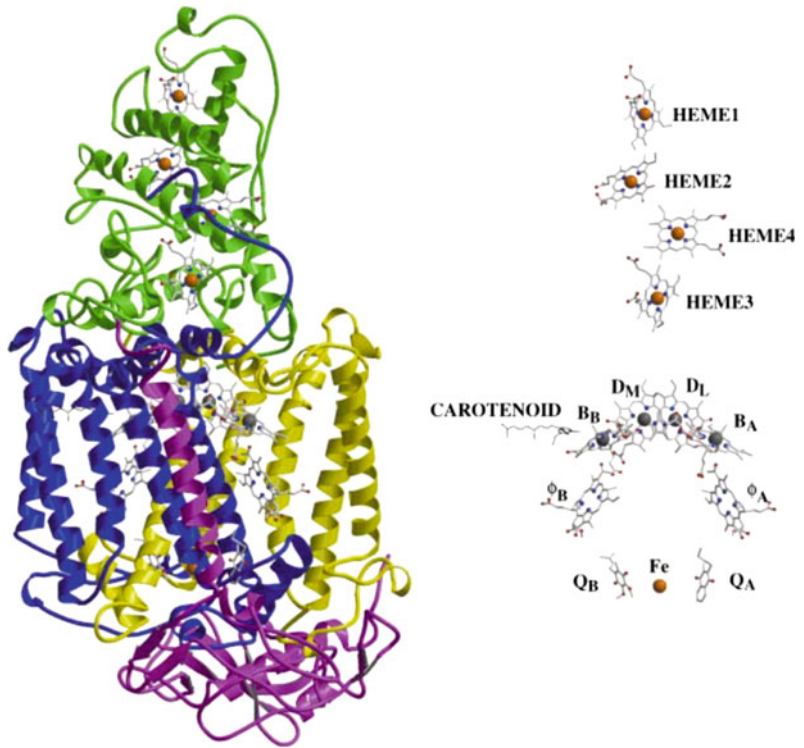
leaves the RC and moves to the cyt bc_1 complex through the membrane. The Cyt bc_1 complex reoxidizes quinol to quinone, through the quinone cycle, and transfers electrons to the soluble electron carrier proteins. The soluble electron carrier proteins can be Cyt c_2 , or the high-potential iron-sulfur protein (HiPIP), depending on the species. Finally, the soluble electron carrier proteins transfer electron back to the photooxidized special pair in RC. In the course of this cyclic electron transfer, the electrochemical gradient of protons is generated via the cyt c_2 **quinone cycle**, similar to the one involving complex III of mitochondria (Fig. 8.44). The resulting energy conserved in proton gradient generated is utilized for ATP synthesis by ATP synthase.

In **green sulfur bacteria**, P-840 constitutes the reaction center. Contrary to the cyclic photosynthetic electron transport of purple bacteria, the photosynthetic electron transport in green sulfur bacteria appears to involve both cyclic and noncyclic routes (Fig. 8.43).

(i) Cyclic photosynthetic electron transport

Excitation of P-840 by a photon of light results in the transfer of an electron from the reaction center to cyt bc_1 complex through a quinone

Fig. 8.45 Schematic representation of the structure of the *Rhodospseudomonas viridis* RC showing the heterotetramer of C-, L-, M-, and H-subunits in green, yellow, blue, and purple, respectively, plus the fourteen cofactors. *Source* Deisenhofer and Michel (1989) (Color figure online)



(Q) and back to the reaction center via soluble electron carrier, cyt C_{553} . The electron transport through the cyt bc_1 quinone cycle results in pumping of proton across the membrane, producing a proton-motive force that powers synthesis of ATP by ATP synthase.

(ii) **Noncyclic photosynthetic electron transport**

During this process, some electrons flow from excited P-840 to a Fe-S protein ferredoxin (Fd), which in turn passes electrons to NAD^+ through Fd: NAD-reductase and ultimately forming NADH (Fig. 8.43). The electrons flow from the reaction center which reduce $NAD^+ \rightarrow NADH$, and are compensated by electrons generated from oxidation of H_2S to elemental S and then to SO_4^{2-} (not shown in figure). This noncyclic process is analogous to oxidation of H_2O in plants.

8.12.2 Plants

The plant chloroplast appears to have originated from an ancestral cyanobacterial endosymbiont. Chloroplast's circular genome is similar to bacterial genome, and the protein-synthesizing machinery is also similar to the one present in bacteria. During evolution though, the cyanobacterium-derived genome has reduced in size, as presently the chloroplast genome contains only 120–130 genes, majority of chloroplast proteins being coded for by the nuclear genome.

The light reactions in plant chloroplast use H_2O to generate NADPH and O_2 . Hill and Bendall in (1960) proposed the revolutionary “Z scheme” of light-driven electron transport with oxygen evolution, and reduction of an electron acceptor, NADP in plant chloroplast using two photosystems (Fig. 8.46).

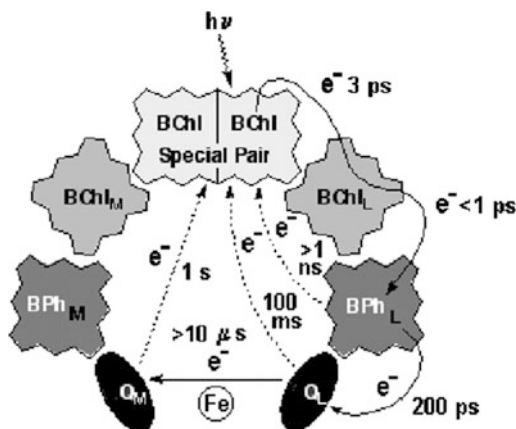
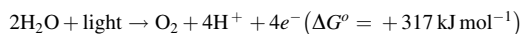


Fig. 8.46 Electron flow in purple bacteria photosystem reaction center

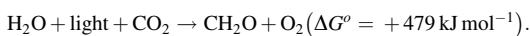
Light reactions:



Dark reactions:



Overall:



It was observed that when chloroplast is experimentally exposed to light above 680 nm, oxygen production decreases whereas oxygen production increases dramatically when exposed to shorter wavelength of light. This “red drop” phenomenon was the first evidence to show that two photosystems of different absorption maxima are required to act in concert to generate oxygen by the process of photosynthesis. The two plant photosynthetic reaction centers are called **photosystem I (PSI)** and **photosystem II (PSII)**. PSI and PSII form supercomplexes with light-harvesting complexes, **LHCI** and **LHCII** (Fig. 8.47).

PSII, also known as **P680** based on its absorption maxima, or **water plastoquinone oxidoreductase**, is based on the process it catalyzes. It is a multisubunit protein complex present in the thylakoid membranes of plants, algae, and cyanobacteria. The **PSII RC** consists of two homologous proteins, D1 and D2, and two closely associated chlorophyll (Chl)-containing antenna proteins (CPs), CP43 and CP47 (Fig. 8.48). The crystal structures of PSII showed that the arrangement of the transmembrane helices of D1 and D2 proteins is similar to L- and M-subunits of the purple bacterial RC.

The PSII RC core complex is also associated with an **oxygen-evolving complex (OEC)** or the **water-splitting complex** attached to its luminal surface. The OEC is composed of polypeptides OEE1 (PsbO), OEE2 (PsbP), and OEE3 (PsbQ), as well as a tetranuclear manganese (Mn) cluster, one calcium ion, and one chloride ion. The **light-harvesting complex II (LHCII)**, associated with the core complex, transfers energy to the RC via exciton transfer. The plant light-harvesting complex of photosystem II (LHCII) is the most abundant chlorophyll and carotenoid-binding membrane protein on earth. The LHCII is a product of the *Lhc* gene superfamily.

Photosystem I (PSI) or **P700**, consists of fifteen core subunits (PsaA to PsaL, PsaN to PsaP), and has associated peripheral antenna proteins, LHCI, consists of up to six Lhca proteins (Lhca1–6) (Fig. 8.49). Out of all the core proteins, only PsaA, -B, and -C are directly associated with cofactors involved in electron transport. The cofactors involved in electron transport include P700 (a chlorophyll dimer), A0 (a chlorophyll a molecule), A1 (a phylloquinone), Fx (a [4Fe–4S] iron–sulfur cluster), F_A and F_B (both [4Fe–4S] iron–sulfur clusters) (Fig. 8.50). The remainder protein subunits perform other functions; for example, PsaF and PsaN are important for interaction with the luminal electron donor

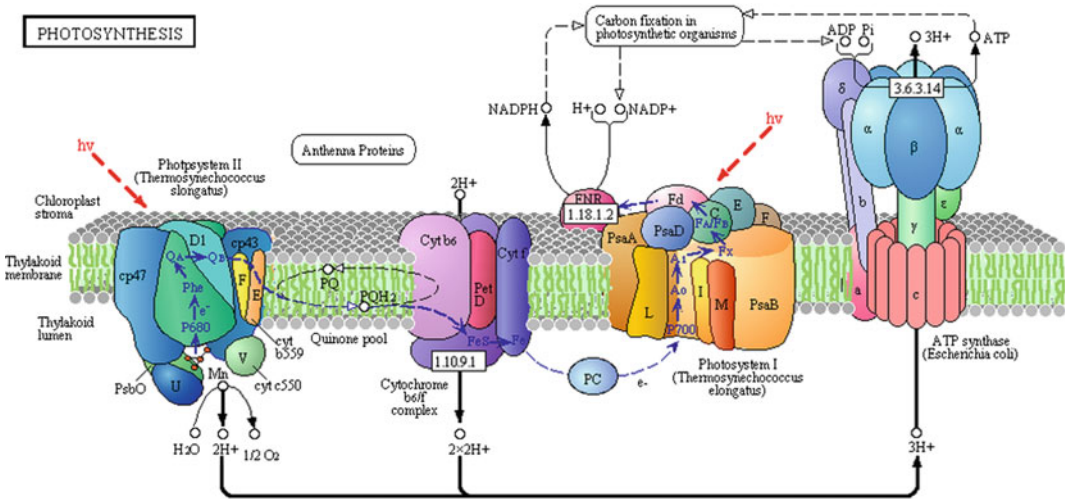


Fig. 8.47 Components of photosynthetic electron transport chain, which includes, PSII, cytochrome *b₆/f* complex, PSI, and FoFiATP synthase in plants, algae, and cyanobacteria. *Source* Horton et al. (1996)

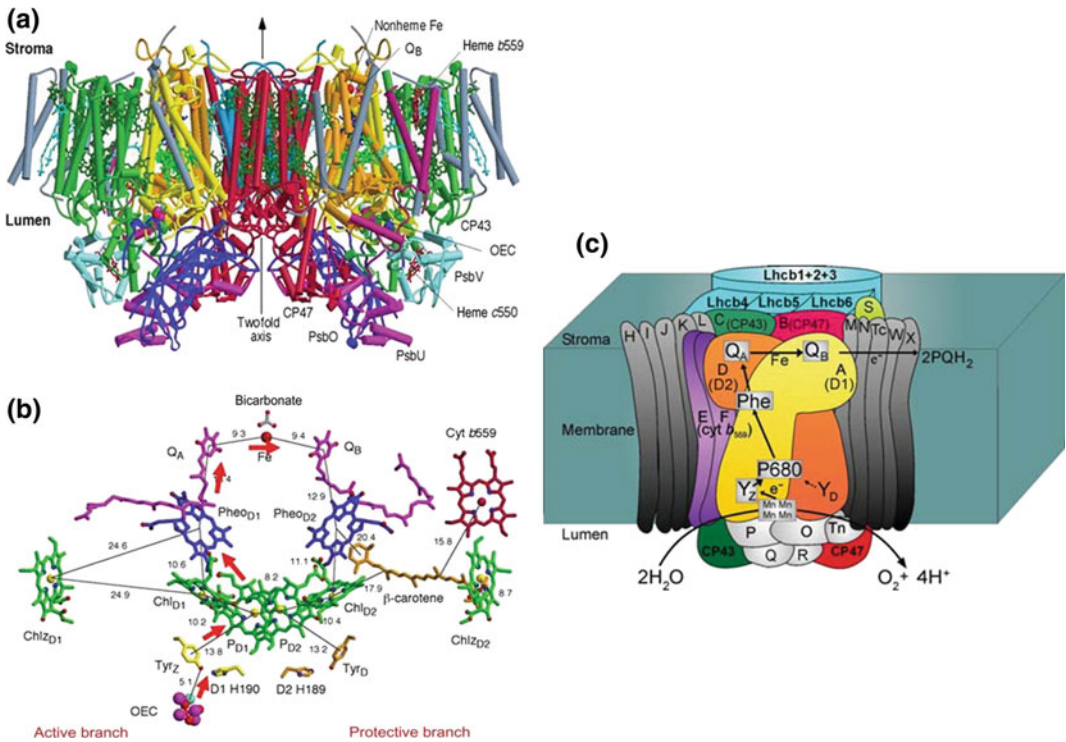


Fig. 8.48 a Side view of the structure of photosystem II, the water-splitting enzyme of photosynthesis. The complex, embedded in the thylakoid membrane spanning their luminal and stromal surfaces, is composed of two monomers related to each other by a twofold axis. Each monomer contains 19 different protein subunits. In total, there are 35 transmembrane helices per monomer. D1 and D2 proteins that comprise the reaction center are shown in

yellow and orange, respectively. The Mn₃Ca catalytic center of the OEC (oxygen-evolving complex) is located on the luminal side of the complex and is stabilized and shielded by three extrinsic proteins: PsbO, PsbU, and PsbV. **b** Organization of the electron transfer cofactors that comprise the reaction center of photosystem II. **c** Schematic model of PSII. *Source* Barbar (2012) (Color figure online)

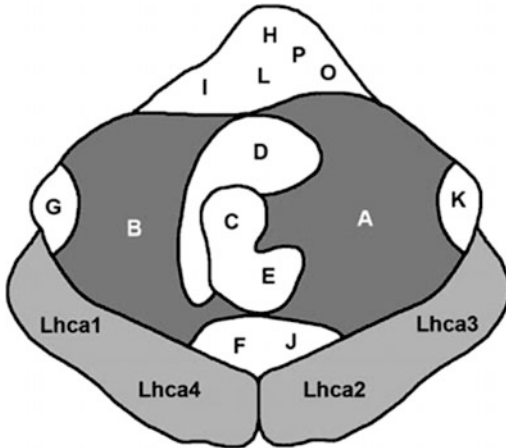


Fig. 8.49 Schematic figure of plant photosystem I viewed from the stromal side, showing the position of the PsaA–PsaL core subunits and the four Lhca subunits. *Source* Jensen et al. (2007)

plastocyanin; PsaD and PsaE provide the binding site for ferredoxin toward the stromal side of the thylakoid membrane.

8.12.3 Photoreaction

The Z scheme or the **noncyclic** electron transport in plant photosynthesis is a redox diagram of electron flow from the water–oxygen couple ($E'^{\circ} = +0.820$ V) via a chain of redox carriers to $\text{NADP}^+/\text{NADPH}$ ($E'^{\circ} = -0.320$ V) resembling the letter **Z** (Fig. 8.51).

The Z scheme of photosynthetic electron transport in plants is driven by two light reactions involving two photosystems, PSII and PSI, which operate in series. The electrons extracted from water by PSII are transferred through the plastoquinone pool involving the cytochrome b_6f complex (cyt_{b_6f}) to PSI via plastocyanin. Ultimately, PSI transfers electrons via ferredoxin to NADP^+ to produce NADPH . Oxidation of water molecule results in the release of O_2 molecule.

The photochemical activity of PSII RC creates a charge separation resulting in a strong oxidant

(P680^+ (P^+)) capable of oxidizing water molecule with the concomitant release of protons and molecular oxygen in the thylakoid lumen. The electrons released from the primary oxidant (P680^+ (P^+)) reduce the primary electron acceptors of PSII, Q_A , and then Q_B , on the stromal side of the membrane. Once it has accepted two electrons, Q_B is released from PSII into the plastoquinone pool and reduced plastoquinone docks to the Q_o site (thylakoid lumen side) of cyt_{b_6f} . This complex acts as a proton pump in a **quinone (Q) cycle**-like process. One electron is transferred through the high-potential chain to the Rieske protein and cytochrome f and subsequently to **plastocyanin** and PSI. The other electron is transferred through the low-potential chain to cyt_L and cyt_H within the cyt_{b_6f} complex and finally to a quinone at the Q_i site (stromal side) to form a semiquinone. Upon oxidation of a second plastoquinol at the Q_o site, this process is repeated and semiquinone is reduced to quinol and released from Q_i site. During the process, four protons are translocated into the thylakoid lumen. The copper protein plastocyanin transfers electrons cyt_{b_6f} to PSI. PSI a light-driven oxidoreductase then oxidizes plastocyanin and transfers electrons through its three internal 4Fe–4S centers F_X , F_A , and F_B to ferredoxin. Ultimately, ferredoxin is oxidized by **ferredoxin-NADP⁺ reductase (FNR)** to produce NADPH .

8.12.4 Electron Transport Through PSII

Water is an extremely poor reductant since the redox potential of the water–oxygen couple is $+0.820$ V. Light energy is utilized to excite a special pair Chl a, P680 (P) at the PSII RC, to P680^* (P^*). P680^* (P^*) then undergoes charge separation by releasing an electron and becomes an extremely oxidizing species, P680^+ (P^+), which has a redox potential of $E'^{\circ} = +1.2$ V, sufficient to oxidize water molecule.

Fig. 8.50 Schematic drawing of photosystem I showing the electron transport. <http://www.bio.ic.ac.uk/research/barber/psIIimages/PSI.jpg>

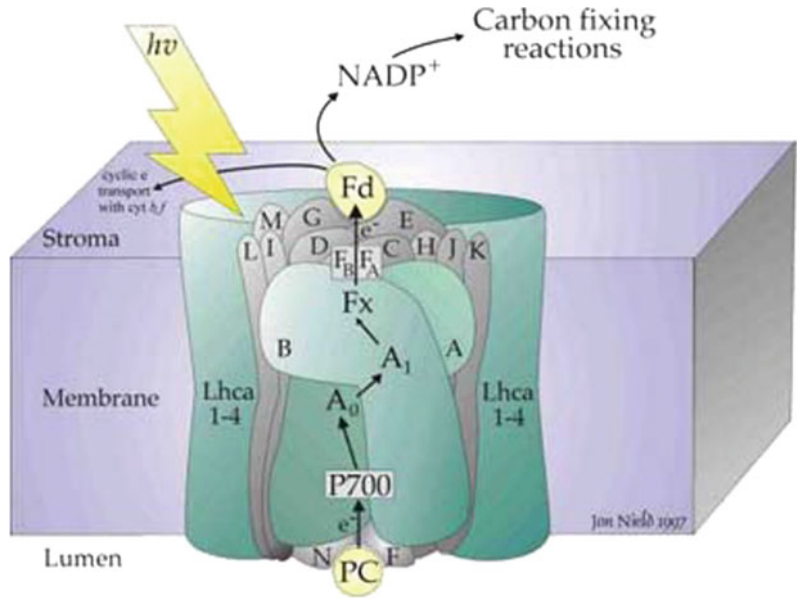
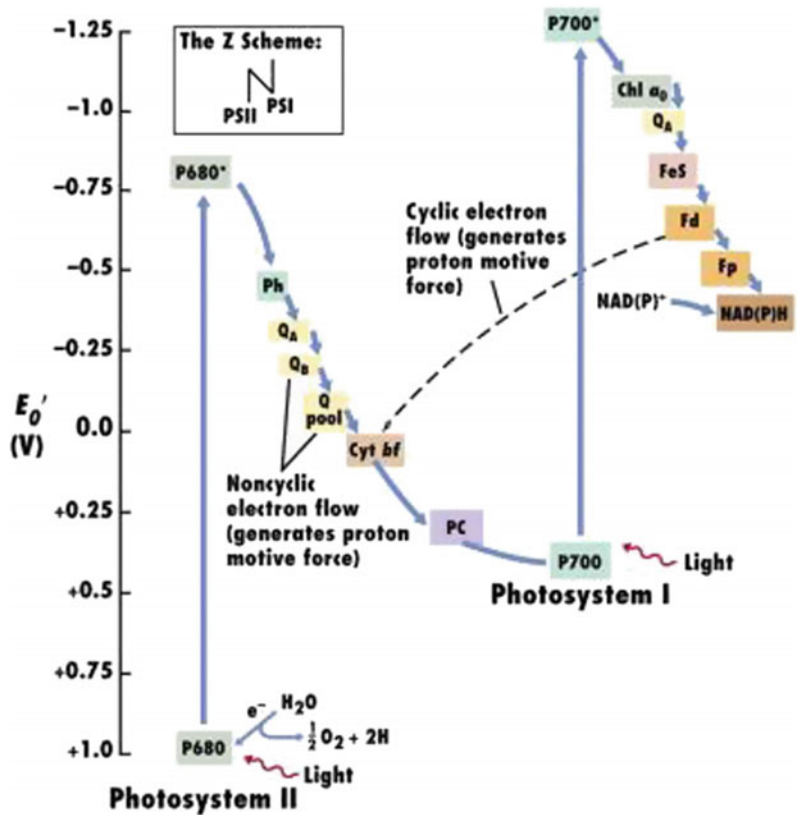
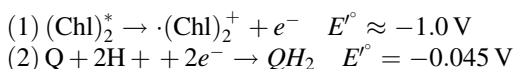


Fig. 8.51 Z scheme of electron transport in plant photosynthesis. The dotted line indicated the electron flow during cyclic photophosphorylation



The electron released by P680* (P^{*}) with redox potential of $E^{\circ} = -1 \text{ V}$ reduces a pheophytin a molecule (Pheo D1) in a few picoseconds to form the radical pair state P680* (P^{*}) Pheo⁻. The net standard free energy change for the process is highly negative:



Thus,

$$\Delta E^{\circ} = -0.045 \text{ V} - (-1.0 \text{ V}) \approx 0.95 \text{ V}$$

and

$$\begin{aligned} \Delta G^{\circ} &= -2(96.5 \text{ kJ/V mol})(0.95 \text{ V}) \\ &= -180 \text{ kJ/mol} \end{aligned}$$

Given that $G^{\circ} = -nF\Delta E^{\circ}$, where n is the number of electrons transferred in the redox reaction and F is the Faraday constant ($96.5 \times 10^3 \text{ kJ mol}^{-1}$), ΔE° is the difference between the standard reduction potentials of the two half-reactions.

No electron flow occurs to PheoD2. Within a few hundred picoseconds, Pheo⁻ reduces a firmly bound plastoquinone molecule PQ_A (Q_A) in D2-subunit to produce Q_A⁻. In the millisecond time domain, Q_A⁻ reduces a second plastoquinone PQ_B (Q_B) in D1-subunit through a nonheme iron (Fe) located midway between Q_A and Q_B. This Fe has four histidine ligands and bidentate ligation with a bicarbonate ion (Fig. 8.48). A second photochemical turnover reduces Q_B to Q_B⁻, which is then protonated to plastoquinol, PQH₂, and released from the Q_B-binding site of PSII into the lipid bilayer, where it is subsequently oxidized via the cytochrome b₆f complex.

P680⁺(P⁺) with its very high redox potential, oxidizes a tyrosine residue Tyr_Z (Y_Z) of D1-subunit. The symmetrically related Tyr_D of D2-subunit is not directly involved in the electron transport. The oxidized Tyr_Z is a neutral radical Tyr_Z[•] which extracts electrons from the oxygen-evolving complexes (OECs).

Photosynthetic inhibitors like triazines (e.g., atrazine), and phenylureas (DCMU

(3-(3,4-dichlorophenyl)-1,1-dimethylurea) act by binding specifically to Q_B binding site in the D1 subunit of PSII, thus inhibiting binding of oxidized Q_B to its site on the stromal surface of the thylakoid membrane. This results in the inhibition of photosynthetic electron transport. They form an important class of herbicides with great agriculture value.

8.12.5 Mechanism of O₂ Evolution

The oxygen-evolving complex (OEC) or the **water-splitting complex** is a metalloenzyme complex containing manganese and calcium as Mn₄CaO₅ cluster (Fig. 8.52). The OEC cycles through five photocatalytic stages (S₀–S₄), from S₀, the most reduced state, to S₄, the most oxidized state. Four electrons are sequentially extracted from the OEC in four light-driven charge separation events by a photooxidized chlorophyll center P680⁺ (P⁺). This water-splitting catalytic cycle is also known as Kok's cycle, named after the person who elucidated it (Fig. 8.53). The reaction of the entire sequence is given as:

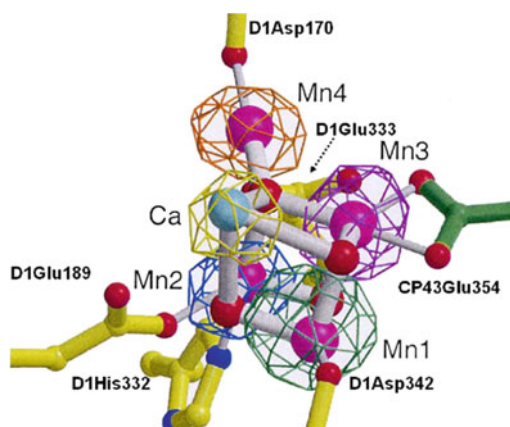


Fig. 8.52 A model of the OEC cluster composed of three manganese ions (magenta) and a calcium ion (cyan) forming a cubane-like arrangement with bridging oxygen atoms (red). A fourth manganese ion (Mn4) is linked to the cubane by an oxygen bridge and is adjacent to the Ca²⁺ (about 4 Å between them). Also shown are five side chains of the D1 protein which form Mn-ligands and one from CP43 (located in the large extrinsic loop of CP43) which is ligated to Mn3 of the cluster. *Source* Nield and Barber (2006) (Color figure online)

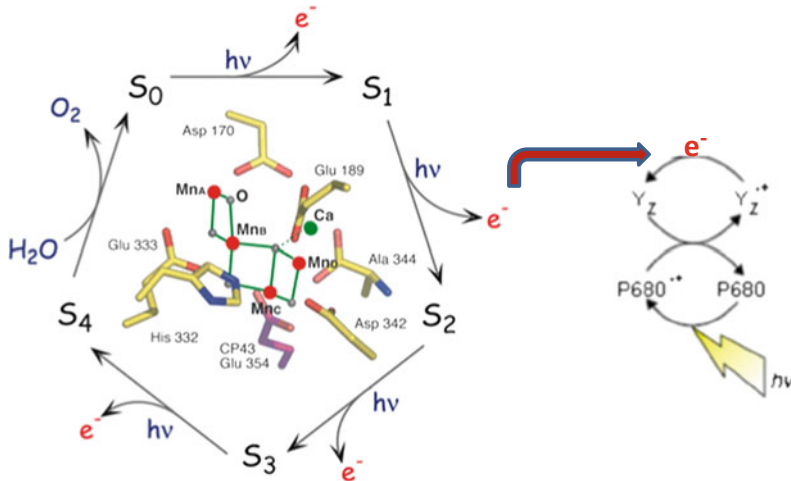
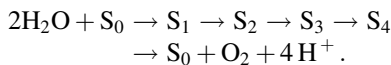


Fig. 8.53 Water-splitting catalytic cycle (Kok's S-state cycle) with the Mn_4CaO_5 cluster structure in the middle. S-state cycle shows how the absorption of four photons of light ($h\nu$) drives the splitting of two water molecules and the formation of O_2 through a consecutive series of five

intermediates (S_0 , S_1 , S_2 , S_3 , and S_4). Protons (H^+) are released into the lumen during this cycle (except for the S_1 to S_2 transition) and electrons are donated to P680^+ via the redox-active TyrZ. *Source* Barbar (2012)



The Tyr radical, TyrZ^{\cdot} generated during photoreaction in PSII RC, regains its missing electron and proton by oxidizing a cluster of four manganese ions in the water-splitting complex. With the transfer of each single electron, the Mn cluster becomes more and more oxidized. Absorption of four photons results in four single-electron transfers, one by one. OEC, with a charge of +4 on the Mn complex ($[\text{Mn complex}]^{+4}$) is transiently produced. In this state, the Mn complex can take four electrons from a pair of water molecules, releasing 4H^+ and O_2 .

The four protons produced in this reaction are released into the thylakoid lumen contributing to the proton gradient. The oxygen-evolving complex hence appears to act as a proton pump driven by photon excitation.

8.12.6 The Cytochrome b_6f Connects PSII and PSI

The crystal structure of the chloroplast cytochrome- $b_6 f$ complex indicates a dimeric

structure, functionally and structurally similar to the mitochondrial cytochrome- bc_1 complex.

Each monomer of cytochrome- b_6f complex contains four large subunits, cytochrome f , cytochrome b_6 , the Rieske iron-sulfur protein, and subunit IV, as well as four small hydrophobic subunits, PetG, PetL, PetM, and PetN (Fig. 8.54). Cytochrome b_6 and subunit IV are homologous to cytochrome b and the Rieske iron-sulfur proteins of cytochrome- bc_1 complex of mitochondria. However, cytochrome f is not homologous to cytochrome c_1 . Cytochrome b_6f contains seven prosthetic groups (Fig. 8.54 b). Four prosthetic groups are common in both cytochrome b_6f and bc_1 which include the c-type heme of cytochrome f , the two b-type hemes, b_L and b_H in b_6f , and the $[2\text{Fe}-2\text{S}]$ cluster of the Rieske protein. Three unique prosthetic groups of unknown function are also found in cytochrome b_6f , including chlorophyll a, β -carotene, and a heme (also known as heme x).

In the chloroplast cytochrome- $b_6 f$ complex (Fig. 8.54), the oxidation of a reduced plastoquinone (PQH2) that is bound at the luminal Q_o site results in the release of net two protons to the aqueous lumen. One electron is transferred from the reduced quinone to **plastocyanin (Pc)** via a

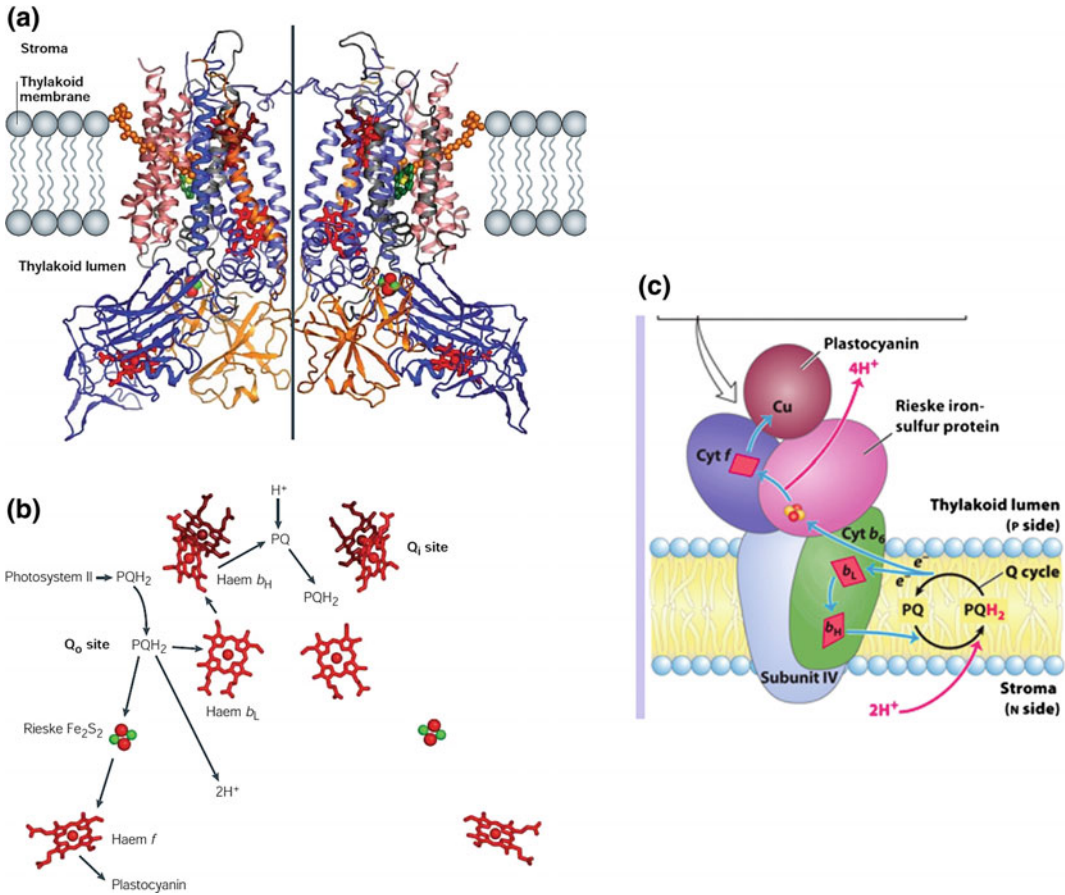


Fig. 8.54 Structure of the cytochrome-*b6f* complex from *Chlamydomonas reinhardtii*. **a** A view of the cytochrome-*b6f* complex dimer perpendicular to the membrane normal. The axis of symmetry of the dimer is highlighted by a line. The cytochrome-*b6* subunits are shown as purple ribbon structures, the subunit IV as gray ribbon structures, and Rieske iron-sulfur proteins are in orange ribbon structures and cytochrome *f* subunits in dark-blue ribbon structures. The small subunits (PetG, PetL, PetM, and PetN) are shown as light-pink ribbon structures. Hemes *b_H*, *b_L*, and *f* are shown in a red stick representation (the central red spheres represent iron ions), and the extra hemes are shown in dark red. Orange spacefill

structures represent β -carotene, chlorophylls are shown in a dark-green stick representation (with the central magnesium ions shown as yellow spheres), and iron-sulfur clusters are represented by red and green spheres. **b** The cofactors that are involved in electron transport are shown in the same positions as in Fig. 8.3a. The arrows indicate the electron transport that occurs during the Q cycle of plastoquinone (PQ)-plastocyanin oxidoreduction and the proton transport activity of the complex. The extra hemes (dark red) are not directly involved in the Q cycle. **c** Schematic representation of **cytochrome-*b6f***. Source Nelson and Ben-Shem (2004) (Color figure online)

high-potential chain that consists of the Rieske iron-sulfur protein and cytochrome *f*, whereas the second electron is translocated across the membrane, through two heme groups (*b_L* and *b_H*) of cytochrome *b6*, to reduce a quinone that is bound at the stromal *Q_i* site. A second reduction cycle starts at the *Q_i* site, two protons are taken

up from the stroma at this site, and the reduced quinone is released into the lipid bilayer to join the reduced quinone pool. Therefore, a proton-motive force is generated across the membrane. The two cycles of **Q cycle** in cytochrome-*b6f* complexes operate in a similar manner to cytochrome-*bc1* of mitochondria. The

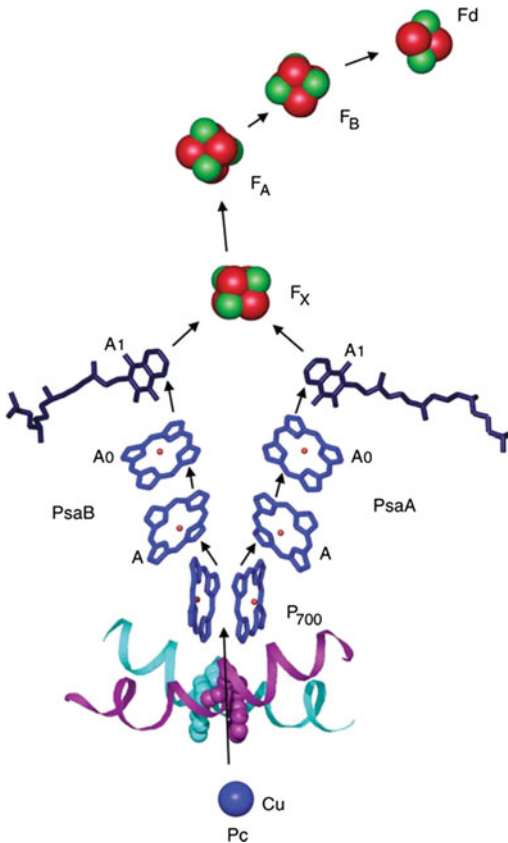
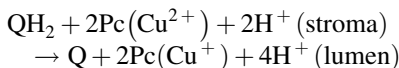


Fig. 8.55 Structural model of light-induced electron transport from plastocyanin to ferredoxin in photosystem I. Chls (blue), quinones (black), the copper atom of PC (blue), and Fe (red balls) and S (green balls) of the three Fe4-S4 clusters, and the Fd Fe2-S2 are depicted. Two tryptophan residues (light-blue and light-pink space-filling structures) that might be involved in electron transport from PC to P700 are also shown. *Source* Nelson and Yocum (2006) (Color figure online)

net reaction catalyzed by cytochrome *b6f* is given by:



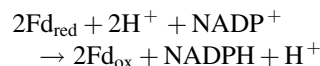
The reduced plastocyanin, a Cu-containing electron carrier protein analogous to mitochondrial cytochrome *c*, transfers electrons to PSI.

Cytochrome *b6f* also participates in another electron transfer reaction of **cyclic photophosphorylation** (Fig. 8.51). The electron from ferredoxin (Fd) is transferred to plastoquinone,

and then involving the cytochrome *b6f* complex reduces plastocyanin. Plastocyanin transfers electrons to P700 in photooxidation of PSI. The exact mechanism for how plastoquinone is reduced by ferredoxin is still not very clear. One proposal is that there exists a specific ferredoxin: plastoquinone reductase or an NADP dehydrogenase.

8.12.7 Electron Transport Through PSI

At the **PSIRC**, special pair of Chl *a* and Chl *a'* of P700 on excitation is converted into a charge separated state, P700^+ (P^+), which then reduces the primary electron acceptor A0, a modified chlorophyll. P700^+ is a strong oxidizing agent, which quickly acquires an electron from plastocyanin, the soluble Cu-containing electron transfer protein. A0^- then transfers electron to **phylloquinone** (A_1), also known as vitamin K_1 , which then passes it to an iron-sulfur protein through three Fe-S centers, F_X , F_A , and F_B in PSI. The electron is then transferred to **ferredoxin** (Fd), another iron-sulfur protein loosely associated with the thylakoid membrane. The final electron carrier in the chain is the flavo-protein **ferredoxin: NADP⁺ oxidoreductase**, which transfers electrons from reduced ferredoxin (Fd_{red}) to NADP^+ (Fig. 8.55). The reaction catalyzed by ferredoxin: NADP + oxidoreductase is given by:



8.12.8 Physical Arrangement Within the Thylakoid

Photosystem II absorbs photons of higher energy than photosystem I, and as a result, photosystem II, rather than initiating electron transfer reactions, would tend to act as a light-harvesting protein for PSI and transfer energy to it. This would leave PSII chronically underexcited and

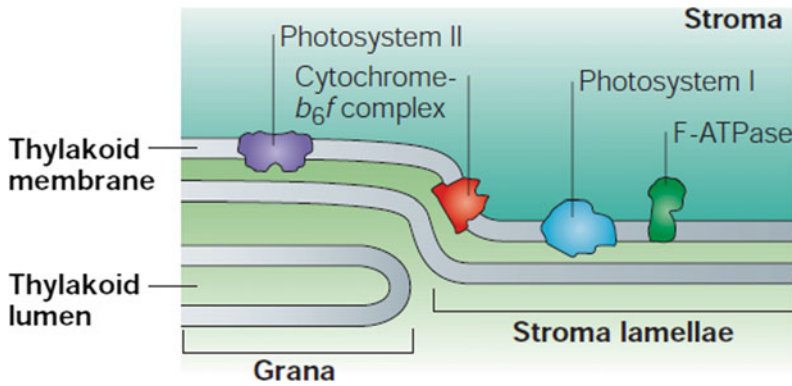
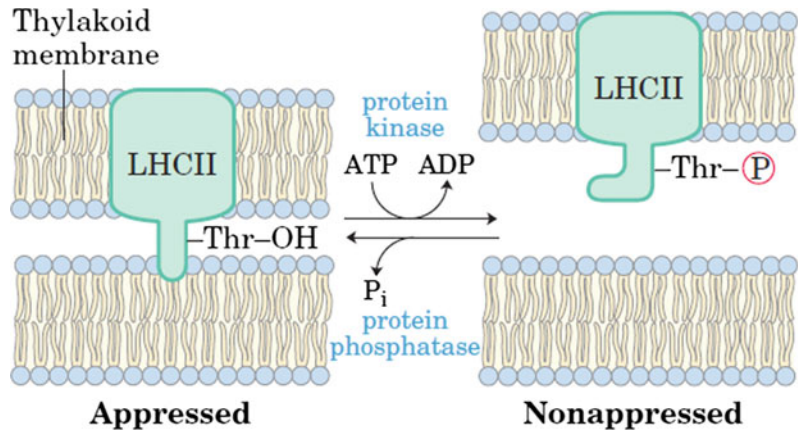


Fig. 8.56 Diagram showing the distribution of the four protein complexes in the thylakoid membranes of chloroplasts. PSII is located almost exclusively in the grana (granal lamellae); PSI and the ATP synthase complex are

located almost exclusively in the stromal lamellae, and cytochrome *b6f* complex is present throughout the thylakoid membrane

Fig. 8.57 The stacking of the thylakoid disks is maintained by LHCII, which is regulated by phosphorylation and dephosphorylation

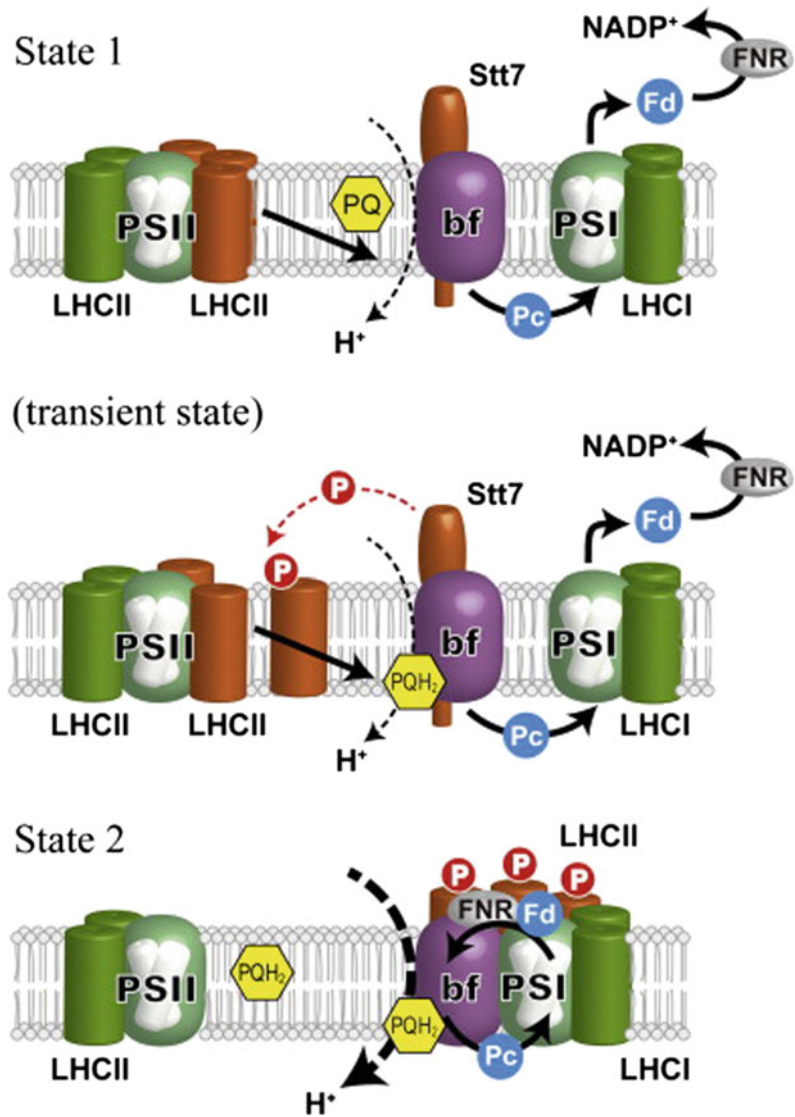


interfere with the operation of the two photosystem electron flow. This “**exciton larceny**” is prevented by separation of PSII and PSI as physically distinct entities. This physical separation of the two photosystems is maintained by the structure of the thylakoid. The photosystem II is segregated in the stacked portions of the membrane, the grana lamellae, while photosystem I is segregated in the unstacked sections, the stroma lamellae (Fig. 8.56). The stacking of the disks is maintained by LHCII, which forms links between disks (Fig. 8.57). This stacking function of LHCII is regulated by phosphorylation/dephosphorylation mechanism. Imbalances in the excitation of the two photosystems are sensed by the redox regulators in the thylakoid

membranes, which can regulate LHCII phosphorylation. PQ appears to act as one such redox regulator.

Exposure to high intensity and high-energy light results in greater excitation of photosystem II than of photosystem I. As a result, reduced plastoquinone gets accumulated. Reduced plastoquinone (PQH_2) docks to the Q_o site of cyt *b6f* leading to the activation of a serine/ threonine kinase, which can phosphorylate LHCII. On phosphorylation, a part of the LHCII pool, the mobile LHCII (*orange*) undocks from PSII (see Fig. 8.58). The phosphorylated LHCII also causes **partial unstacking** of the disks. The mobile LHCII then reassociates on the PsaH side of PSI (state 2) that is on the opposite side of the LHCI

Fig. 8.58 Schematic representation of the regulation of state transitions. State 1, when PSI is preferentially excited, the PQ pool is oxidized. In this state, LHCII_s are bound to PSII. In the transient state at the onset of the preferential excitation of PSII, the PQ pool gets reduced. Docking of PQH₂ to the Q_o site of *cyt bf* leads to the activation of the *Stt7* kinase, which is required for the phosphorylation of LHCII_s, causing the undocking of the mobile LHCII_s (orange) from PSII. State 2, the reassociation of mobile LHCII occurs on the PsaH side of PSI that is on the opposite side of the LHCI belt. *Cyt bf* and FNR are also bound to PSI to form a super-supercomplex (CEF supercomplex). *Source* Minagawa (2011) (Color figure online)



belt. *Cyt bf* and ferredoxin: NADP + oxidoreductase are also bound to PSI to form a super-supercomplex (CEF supercomplex), resulting in higher rate of electron transfer in PSI.

On associating with PSI, LHCII can transfer energy directly to photosystem I and to a lesser extent to photosystem II. This process is reversible as overexcitation of PSI leads to the oxidation of the plastoquinone pool, which results in inactivation of the LHCII kinase and activation of a phosphatase, causing dephosphorylation of

LHCII. Dephosphorylated mobile LHCII diffuses back to PSII (state 1).

The stacking and unstacking processes can alter the physical separation of the two photosystems and, as a result, the ability to transfer energy from one system to the other. This phenomenon of “**state transition**” balances the absorbed light energy between the two photosystems in a short time by relocating light-harvesting complex II (LHCII) proteins resulting in change in association with LHCII

between the two photosystems. In plants, thylakoid membrane remodeling has been observed during state transitions with breakage and fusion of grana layers.

A LHCII-specific protein kinase and a LHCII-specific phosphatase have been identified as Stt7/STN7 kinase and PPH1/TAP38, respectively, giving further credence to the above model.

8.12.9 Cyclic Photophosphorylation

Under certain conditions, photoexcited electrons in plant photosystems can take an alternative path called **cyclic electron flow**, which uses only one photosystem, instead of two. (Fig. 8.51). The electrons flow back from ferredoxin (Fd) to the cytochrome b₆f complex and from there continue on to a P700 chlorophyll in the PS I reaction center complex, back to ferredoxin (Fd). As electrons from ferredoxin are not transferred to NADP⁺, and PSII is also not involved, the cyclic photophosphorylation, unlike noncyclic photophosphorylation, does not produce either O₂ or NADPH.

The plants follow cyclic and noncyclic photosynthetic route of electron transport similar to that in green sulfur bacteria in varying conditions. In C₄ plants, in which PSII is largely absent from bundle sheath cells, cyclic electron transport plays a predominant role.

In high light energy conditions, the migration of light-harvesting complexes (LHCII) from PSII (state 1) to PSI (state 2) occurs in response to an over-reduction and accumulation of electron carriers (PQ pool). This redistribution of energy between the two photosystems results in decrease in PSII activity and PQH₂ oxidation, and increase in PSI activity and NADPH accumulation. In order to reduce NADPH accumulation and enhance ATP synthesis, electrons flow via the **cyclic electron flow** to provide for extra ATP. This extra ATP is also utilized for NADPH reoxidation via the Calvin cycle. Cyclic electron flow has not been observed under state I conditions.

Two possible routes for cyclic electron transport have been proposed (Fig. 8.59). In the first Fd-dependent pathway proposed, electrons are transferred from Fd to cyt b₆f complex via a route involving proton gradient regulatory proteins in the thylakoid membrane like PGR5 and PGRL1 and possibly ferredoxin-NADP⁺ oxidoreductase (FNR) as well as hypothetical ferredoxin-plastoquinone oxidoreductase (FQR). Alternatively, electrons may be transferred from Fd to PQ pool via the NAD (P)H dehydrogenase (NDH)-dependent pathway, which functions in two steps. Electrons are first transferred from NADPH to NDH-1 complex, and then the PQ pool is reduced by the NDH-1 complex.

8.12.10 The Stoichiometry of Photophosphorylation

The overall stoichiometry for the photosynthetic light reactions can be determined. On absorption of four photons by photosystem II, one molecule of O₂ is generated and four protons are translocated into the thylakoid lumen. The two molecules of plastoquinol oxidized by the Q cycle of the cytochrome b₆f complex translocate eight protons into the lumen. Finally, the plastocyanin carries four electrons from cytochrome b₆f complex, one at a time to PSI. On absorption of four additional photons by PSI, four electrons are transferred to NADP⁺ via ferredoxin. Two molecules of NADPH are generated. The overall reaction is given as:



The 12 protons translocated into the lumen can then flow through ATP synthase, back into the stroma. As the c-subunit in the F₀ portion of chloroplast cF₀F₁ ATPase has an apparent stoichiometry of 12 subunits, 12 protons would be required to pass through cF₀ to complete one full rotation of cF₁. As one full rotation of cF₁ generates 3 molecules of ATP, 12 protons flowing

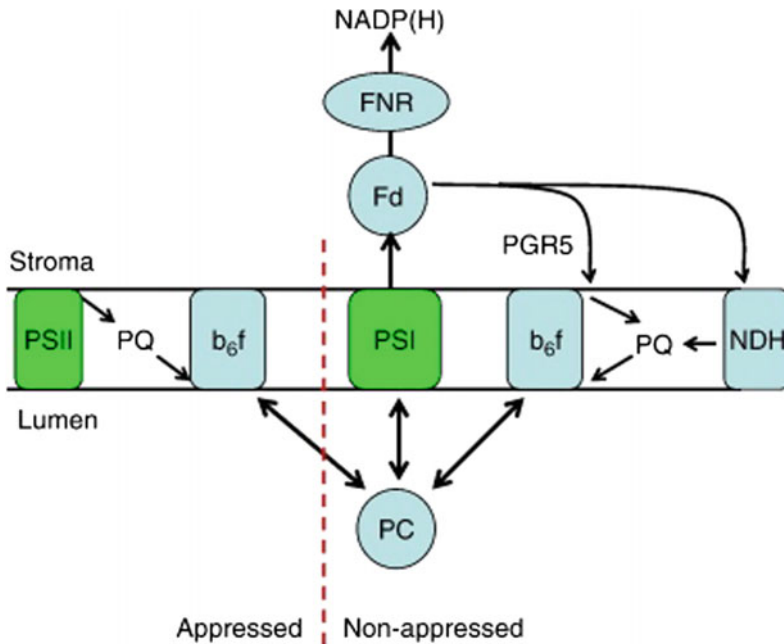
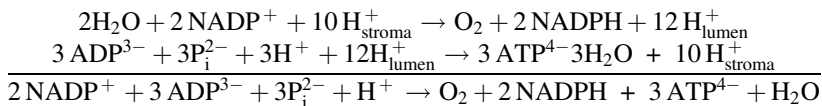


Fig. 8.59 Model of possible interactions between linear and cyclic electron transport pathways. Electrons flowing into a plastoquinone pool from photosystem II reduce cytochrome *b₆f* complexes in the appressed regions of the thylakoid membrane. These flow via plastocyanin to PSI and from there to ferredoxin. Reduced ferredoxin can reduce NADP, via FNR, or can feed electrons to a plastoquinone pool in the stromal lamellae via either a PGR5-dependent pathway or an NDH-dependent

pathway. Reduced PQ then reduces cytochrome *b₆f* complexes in nonappressed membrane regions. This in turn reduces plastocyanin and PSI. Plastoquinone in the stacked and unstacked regions represents isolated pools due to restricted diffusion in the membrane. Plastocyanin is able to move more or less freely in the thylakoid lumen and exists in equilibrium with P700 and cytochrome *b_f*. *Source* Johnson (2011)

through *cF₀F₁* ATPase into the stroma generate 3 ATP molecules with the absorption of 8 photons. Thus, one molecule of ATP is produced at the

expense of four photons absorbed. The overall reaction is given by:



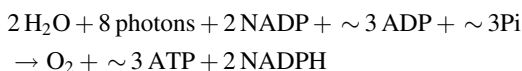
Cyclic photophosphorylation is little more productive with regard to ATP synthesis. The absorption of four photons by photosystem I results in the release of eight protons into the lumen by the cytochrome *b₆f* system. As these protons flow through *cF₀F₁* ATPase, two molecules of ATP are generated (four protons/ATP). Thus, one molecule of ATP is produced at the expense of two photons absorbed, and no NADPH is produced though.

acidic, with the pH approaching 4. The light-induced transmembrane proton gradient generated across the thylakoid membrane is about 3.5 pH units. The energy inherent in the proton gradient, the proton-motive force (Δp), is described as the sum of two components: the charge/electrical gradient and the chemical gradient. In chloroplasts, pH gradient is the major contributor to Δp , whereas, in mitochondria, the contribution of membrane potential is larger. As the thylakoid membrane is quite permeable to Cl^- and Mg^{2+} , the electrical gradient generated

With the translocation of protons into the thylakoid lumen, the lumen becomes markedly

due to the light-induced proton translocation across the thylakoid membrane is dissipated by the transfer of either Cl^- in the same direction or Mg^{2+} (1 Mg^{2+} per 2 H^+) in the opposite direction. A pH gradient of 3.5 units across the thylakoid membrane corresponds to a proton-motive force of 0.20 V or a ΔG of $-4.8 \text{ kcal mol}^{-1}$ ($-20.0 \text{ kJ mol}^{-1}$).

The overall light-driven photosynthesis reaction stoichiometry is:

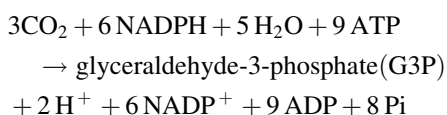


8.13 Carbon Assimilation

The Calvin cycle uses ATP and NADPH generated during light reaction to reduce CO_2 to sugar molecule in **light-independent reactions**. Hence were referred to as dark reactions.

The Calvin cycle, Calvin–Benson–Bassham (CBB) cycle, reductive pentose phosphate cycle or C3 cycle of CO_2 assimilation or CO_2 fixation involves series of biochemical redox reactions that reduce CO_2 to form sugar molecules. Calvin cycle takes place in the stroma of chloroplast in photosynthetic organisms.

The net reaction of Calvin cycle is given as:



Calvin cycle generates a three-carbon molecule, **glyceraldehyde 3-phosphate (G3P)**. A series of enzymatic reactions are then required to synthesize a sugar molecule like glucose. For the net synthesis of one molecule of G3P, three cycles are required, fixing three molecules of CO_2 , one per cycle (the term carbon fixation refers to the initial incorporation of CO_2 into organic material). Calvin cycle can be divided into three major steps: carbon fixation, reduction, and regeneration.

8.13.1 Phase 1: Carbon Fixation

In the first step of carbon fixation, CO_2 is accepted by ribulose 1, 5-bisphosphate (RuBP) already present in the cells to form a six-carbon addition compound which is unstable. It is soon broken down to generate two molecules of 3-phosphoglyceric acid (3PGA). Both these reactions are catalyzed by **ribulose 1,5-bisphosphate carboxylase/oxygenase (RuBisCo)**. 3-phosphoglyceric acid, a 3-C compound, is the first stable product of dark reaction of photosynthesis, and hence, Calvin cycle is also known as **C₃-pathway** (Fig. 8.60).

8.13.2 Phase 2: Reduction

Each molecule of 3-phosphoglycerate receives an additional phosphate group from ATP, to become a high-energy molecule, 1, 3-bisphosphoglycerate. Next, 1, 3-bisphosphoglycerate is reduced by **glyceraldehyde 3-phosphate dehydrogenase**, with a pair of electrons donated by NADPH to glyceraldehyde 3-phosphate (G3P) (Fig. 8.61).

8.13.3 Phase 3: Formation of Hexose Sugar and Regeneration of RuBP

Some of the molecules of 3-phosphoglyceraldehyde isomerize into dihydroxyacetone phosphate, catalyzed by **triose phosphate isomerase**. 3-phosphoglyceraldehyde and dihydroxyacetone phosphate combine in the presence of the enzyme **aldolase** to form fructose 1, 6-bisphosphate. Fructose 1, 6-bisphosphate is converted into fructose 6-phosphate by the enzyme fructose 1, 6-bisphosphatase (Fig. 8.61). Some of the molecules of 3-phosphoglyceraldehyde produced in earlier step instead of forming hexose sugars are diverted to regenerate ribulose 1, 5-bisphosphate through a series of reactions catalyzed by transketolase and transaldolase similar to pentose phosphate pathway. Fructose 6-phosphate formed is converted into glucose, sucrose, and starch.

8.13.4 Alternate Pathways of Carbon Fixation in Hot, Arid Climates

CO₂, the substrate for dark reaction of photosynthesis, enters a leaf (and the resulting O₂ exits) through stomata present on the leaf surface. However, stomata are also the main site of transpiration. On a hot, dry day, in order to prevent loss of water by transpiration, most plants close their stomata. This also results in decrease in photosynthetic rate as less CO₂ diffuses in. With stomata even partially closed, CO₂ concentrations begin to decrease in the air spaces within the leaf, and as the O₂ released during photosynthesis cannot leave, its concentration begins to increase.

O₂ competes with CO₂ to bind at active site of Rubisco. At high concentration of O₂, Rubisco catalyzes the addition of molecular oxygen to ribulose-1,5-bisphosphate to produce 3-phosphoglycerate (PGA) and 2-phosphoglycolate (2PG or PG) in a process called **photorespiration**. PGA is an intermediate of Calvin cycle and hence enters the cycle; however, 2-phosphoglycolate has to be salvaged by a series of reactions in the **glycolytic pathway** (Fig. 8.62). It also inhibits certain enzymes involved in photosynthetic carbon fixation.

Glycolytic pathway in higher plants additionally involves two more organelles, peroxisome and mitochondria. In the peroxisome, it is converted into glycerate. Glycerate then reenters the chloroplast by the same transporter that exports glycolate. In the chloroplast, glycerate is converted to 3-phosphoglycerate (PGA) by phosphorylation, at the expense of 1 ATP molecule. PGA generated can now enter the Calvin cycle.

The whole process of photorespiration is a wasteful process, with no carbon fixation, and consumes significant amount of cellular energy to salvage 2-phosphoglycolate. Hence, to prevent wastage of energy, plants develop strategies to minimize the availability of O₂ to RuBisCo and prevent photorespiration.

8.13.5 Biological Adaptation to Minimize Photorespiration

1. The C-4 pathway or the Hatch-Slack pathway of CO₂ fixation

Plants that grow in hot tropical climates develop mechanisms to minimize the wasteful oxygenase activity of **RuBisCo**. The **C-4** plants that have adapted to hot climates overcome this problem by creating a high local concentration of CO₂ in the stroma of the chloroplasts. In these plants, photosynthesis involves two types of cells, **mesophyll and bundle sheath cells** in the leaves. CO₂ is converted to four carbon compounds (C₄) such as aspartate and malate in the mesophyll cells, which are in contact with air. These C₄ carbon compounds then diffuse into the neighboring bundle sheath cells through **plasmodesmata**, which are the major sites of photosynthesis. The decarboxylation of the C₄ compound in the bundle sheath releases CO₂ and creates a high local concentration of CO₂ at the site of the Calvin cycle. The decarboxylation also generates a three-carbon compound such as pyruvate which can return to the mesophyll cell and become recarboxylated.

The first step of CO₂ fixation in mesophyll cells is carried out by a specific enzyme called **PEP carboxylase**. This enzyme carboxylates phosphoenolpyruvate (PEP) to give four-carbon product, oxaloacetate. PEP carboxylase has a much higher affinity for CO₂ than rubisco and does not bind O₂. Oxaloacetate generated is then reduced to malate by a NADPH-specific malate dehydrogenase. Malate from the mesophyll cell then diffuses into the bundle sheath cells, where it is decarboxylated by the malic enzyme to yield CO₂ and pyruvate. The CO₂ released is fixed via the Calvin cycle, and pyruvate returns to the mesophyll cell where it is reconverted into PEP and carboxylated to form oxaloacetate (Fig. 8.63).

Conversion of pyruvate to PEP in mesophyll cell is an energy (ATP)-consuming step catalyzed

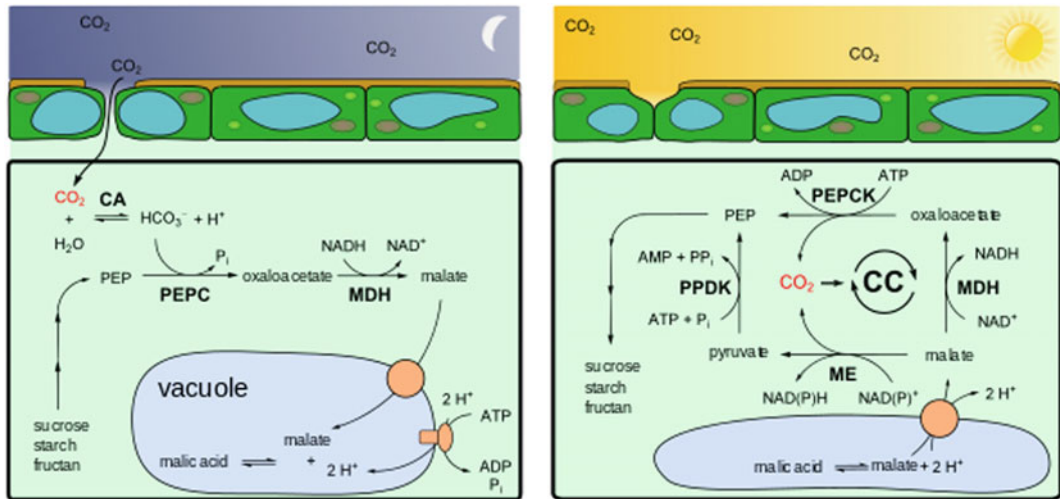


Fig. 8.64 Crassulacean acid metabolism or CAM pathway of carbon dioxide fixation

by pyruvate kinase. In this way, C4 photosynthesis minimizes photorespiration and enhances sugar production at the expense of energy. This adaptation is especially advantageous in regions of high temperatures with intense sunlight.

2. Crassulacean acid metabolism or CAM pathway of carbon dioxide fixation

Another photosynthetic adaptation to hot, arid conditions has evolved in many succulent (water-storing) plants, numerous cacti, pineapples, and several other plant families. These plants have adapted temporal (time) method of separation of CO_2 and O_2 . To conserve water, these plants close their stomata during the day and open them during the night. In the night, when the stomata are open, CO_2 diffuses in and is fixed by phosphoenolpyruvate carboxylase (PEPC) to give C4 organic acid, oxaloacetate. Oxaloacetate is then reduced into malate by NAD^+ malate dehydrogenase. Malate is transported via malate shuttles into the plant vacuole, where it is converted into the storage form malic acid. The next morning, as stomates close, malic acid is transported out of vacuole and releases CO_2 and pyruvate on decarboxylation. The CO_2 released diffuses into chloroplasts to be assimilated by RuBisCo in Calvin cycle. As this pathway was first observed in *Crassulaceae* plant

family, it is called **crassulacean acid metabolism** or **CAM pathway** (Fig. 8.64).

References

- Barbar J (2012) Photosystem II: the water-splitting enzyme of photosynthesis. *Cold Spring Harb Symp Quant Biol* 77:295–307
- Berrisfor JM, Baradaran R, Sazanov LA (2014) Entire respiratory complex I from *Thermus Thermophilus*. *Encyclopedia of inorganic and bioinorganic chemistry*, pp 1–16
- Boyer PD (1995) “From human serum albumin to rotational catalysis by ATP synthase”, *FASEB J.*, 9 (7):559–561
- Deisenhofer J, Michel H (1989) Nobel lecture. The photosynthetic reaction centre from the purple bacterium *Rhodospseudomonas viridis*. *The EMBO J* 8 (8):2149–2170
- Deisenhofer J, Eppo O, Miki K, Huber R, Michel H (1985) Structure of the protein subunits in the photosynthetic reaction centre of *Rhodospseudomonas viridis* at 3Å. *Nature* 318(6047):618–624
- Doenst et al (2013) Cardiac metabolism in heart failure implications beyond ATP production. *Circ Res* 113:709–724
- Gorbikova E (2009) Oxygen reduction and proton translocation by cytochrome c oxidase. Academic dissertation. <http://ethesis.helsinki.fi>
- Hill R, Bendall F (1960) Function of the two cytochrome components in chloroplasts—a working hypothesis. *Nature* 186:136–137
- Horton P, Ruban AV, Walters RG (1996) Regulation of light harvesting in green plants. *Annu Rev Plant*

- Physiol Plant Mol Biol 47:655–684. <https://doi.org/10.1146/annurev.arplant.47.1.655>
- Iverson TM (2013) Catalytic mechanisms of complex II enzymes: a structural perspective. *Biochim Biophys Acta-Bioenergetics* 1827(5):648–657
- Jensen PE, Leister D (2014) Chloroplast evolution, structure and functions. *F1000Prime Reports*, 6, 40. <https://doi.org/10.12703/P6-40>
- Jensen PE, Bassi R, Boekema EJ, Dekker JP, Jansson S, Leister D, Robinson C, Scheller HV (2007) Structure, function and regulation of plant photosystem I. *Biochimica et Biophysica Acta* 1767:335–352
- Johnson GN (2011) Physiology of PSI cyclic electron transport in higher plants. *Biochimica et Biophysica Acta (BBA)—Bioenergetics* 1807(3):384–389. <https://doi.org/10.1016/j.bbabi.2010.11.009>
- Menke W (1962) Structure and chemistry of plastids. *Annu Rev Plant Physiol* 13:27–44
- Minagawa J (2011) State transitions—the molecular remodeling of photosynthetic supercomplexes that controls energy flow in the chloroplast. *Biochim Biophys Acta* 1807 (8):897–905
- Mitchell P (1961) Coupling of phosphorylation to electron and hydrogen transfer by a chemi-osmotic type of mechanism. *Nature* 191:144–148
- Murphy MP (2009) How mitochondria produce reactive oxygen species. *Biochem J* 417(Pt 1):1–13. <https://doi.org/10.1042/BJ20081386>
- Nelson N, Ben-Shem A (2004) The complex architecture of oxygenic photosynthesis. *Nat Rev* 5:1–12
- Nelson N, Yocum CF (2006) Structure and Function of Photosystems I and II. *Ann Rev Plant Biol* 57:521–565
- Nield J, Barber J (2006) Refinement of the structural model for the Photosystem II supercomplex of higher plants. *Biochim Biophys Acta* 1757:353–361
- Sazanov LA (2015) A giant molecular proton pump: structure and mechanism of respiratory complex I. *Nat Rev Mol Cell Biol* 16:375–388. <https://doi.org/10.1038/nrm3997>
- Sun F et al (2005) Crystal structure of mitochondrial respiratory membrane protein complex II. *Cell* 121:1043–1057
- Sun F, Zhou Q, Pang X, Xu Y, Rao Z (2013) Revealing various coupling of electron transfer and proton pumping in mitochondrial respiratory chain. *Cur Opin Struct Bio* 2013(23):526–538
- Tsukihara T, Aoyama H, Yamashita E, Tomizaki T, Yamaguchi H, Shinzawa-Itoh K, Nakashima R, Yaono R, Yoshikawa S (1996) The whole structure of the 13-subunit oxidized cytochrome c oxidase at 2.8 Å. *Science* 272:1136–1144
- Walker JE (2013) ATP synthase: the understood, the uncertain and the unknown. *Biochem Soc Trans* 41 (1):1–16. <https://doi.org/10.1042/BST20110773>
- West AP, Shadel GS, Ghosh S (2011) Mitochondria in innate immune responses. *Nat Rev Immunol* 11:389–402. <https://dx.doi.org/10.1038/nri2975>
- Xia D, Yu CA, Kim H, Xia JZ, Kachurin AM, Zhang L, Yu L, Deisenhofer J (1997) Crystal structure of the cytochrome bc1 complex from bovine heart mitochondria. *Science* 277:60–66
- Xia D, Esser L, Tang WK, Zhou F, Zhou Y, Yu L, Yu CA (2013) Structural analysis of cytochrome bc1 complexes: implications to the mechanism of function. *Biochimica et Biophysica Acta* 1827:1278–1294
- Xiche Hu X, Thorsten Ritz T, Ana Damjanovic A, Felix Autenrieth F, Schulten K (2002) Photosynthetic apparatus of purple bacteria. *Quart Rev Biophys* 35 (1):1–62

9.1 Hormone Receptors

For a unicellular and multicellular organism to function properly, it is paramount that its cell-to-cell communication happens unhindered. This communication may take by direct physical contact between cell or indirectly by secreting specific molecules as messenger from one cell that transmit signal by binding and activating receptors at the surface or inside the other cells. These molecules should have receptors in the membrane of the receiving cell to initiate sequence of interacting proteins after binding and transmitting signal from the bound receptor to the nucleus. The secreted signaling molecule is called ligand and the receiving proteins in the membrane as receptors. The sequential interaction of ligand-bound receptors to intracellular various molecules between the cell membrane receptors and nucleus is called **signal transduction pathways**. These molecules activate the producer cell itself, autocrine stimulation, cells in vicinity, paracrine stimulation, cells in distant organs, endocrine stimulation. GPCRS is found in endoplasmic reticulum, Golgi complex, nuclear membrane and inside the nucleus also (Fig. 9.1).

The Extracellular ligand-binding region is a characteristic feature of the cell surface receptors. They have a transmembrane segment and an intracellular effector region. Each receptor type responds to a family of ligands. Usually, one ligand can bind more than one receptor; similarly, one receptor can bind more than one

ligand. The most commonly observed activation of receptor is through ligand-induced dimerization. In some cases, accessory molecules help to stabilize the dimerization. Most receptor tyrosine kinases are activated by phosphorylation. Different ligand has a varied pathway for activation of its respective receptor. The signal received by membrane receptor may be hormone, light, neurotransmitters, or foreign molecules as have been discussed in other chapters.

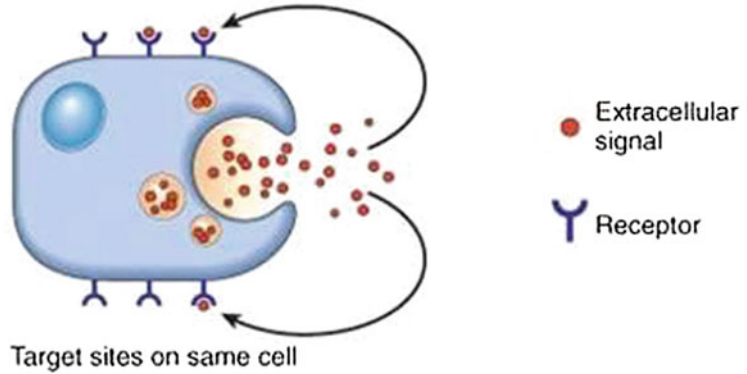
9.2 G-Protein-Coupled Signaling Pathway

The signal received by membrane receptor may be hormone, photons, protons (H^+), ions (Ca^{2+}), neurotransmitters, foreign antigen, peptides, and lipids as has been discussed in other chapters. The ligand-induced change in conformation of receptor may interact with effector molecules and releases various second messenger to pass signal from membrane to nucleus like Inositol 1,4,5-triphosphate, cAMP, cGMP, diacylglycerol and arachidonic acids. The GTP-binding protein (G-proteins), a very large family, found in plant, eukaryotes, and few prokaryotes constitute a prominent signal cascade with **G-protein-coupled receptors (GPCRs)**. These GPCRs have no intrinsic enzymatic activity and work through the coupled heterotrimeric G-proteins.

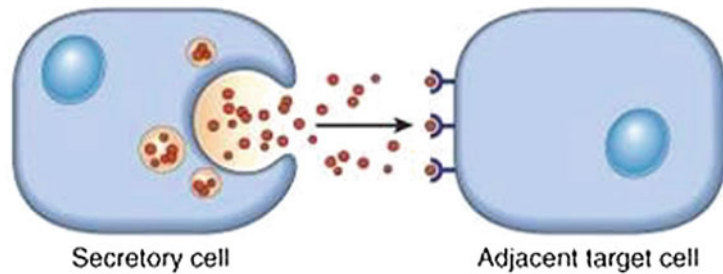
These receptors are seven transmembrane heterotrimeric of one α , two β , and two γ subunits, which have three extracellular and three intracellular and three N- and C-terminal

Fig. 9.1 Modes of cell–cell communication in living organism. <https://www.studyblue.com/notes/note/n/inflammation/deck/9226686>

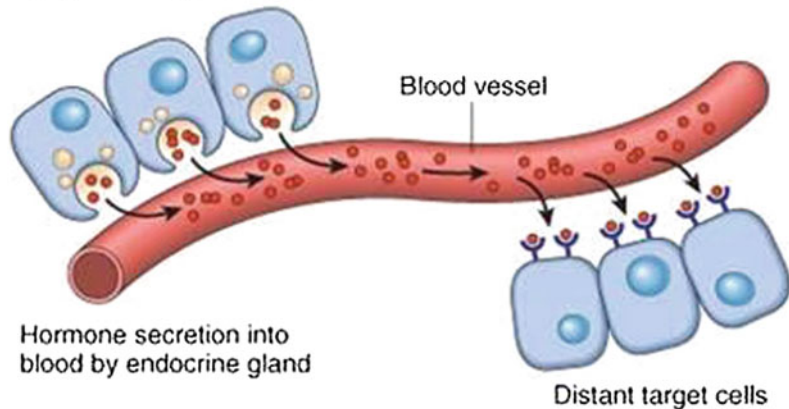
AUTOCRINE SIGNALING



PARACRINE SIGNALING



ENDOCRINE SIGNALING



domains. *The structure is discussed in Chap. 2 in detail.* The third intracellular loop plays role of mediator between receptor and G-protein. The receptor proteins have intrinsic property of exchanging GDP to GTP and vice versa on α subunit that's why they are called as G-protein-coupled receptors. There are around

16 isoforms of α five β , and 12 γ subunits have been identified till now in animals and constitute 20 families. The activated GPCR with bound ligand exchange GDP with GTP, which induces phosphorylation of receptor and conformation change in its structure resulting in disassociation of α subunit from β and γ for transducing signals.

The α subunit may regulate activate or inactivate metabolic pathways through various effector molecules like K^+ and Ca^{2+} channel, adenylate cyclase, phospholipase C and D and various kinases, tyrosine kinases (Src), while β and γ activate muscarinic K^+ channel, phospholipase A2, phospholipase C, inositol triphosphate kinase, β adrenergic receptors, and arachidonic acid. The intrinsic GTPase activity of α subunit hydrolyzes GTP to GDP which inactivates signal transduction in G-protein-dependent classical pathway. The dissociated GDP α subunit may join again β and γ complex in inactive form for next signaling event (Fig. 9.2).

The activators of G-protein signaling (AGS) and regulators of G-protein signaling (RGS) proteins may control signal transduction because of having **GTPase activating protein (GAP)**, guanine nucleotide exchange factor (GEF), or **guanine nucleotide dissociation inhibitor (GDI)** activities. The guanine exchange factors (GEFs) may promote GTP association with $G\alpha$ subunits at faster rate to enhance $G\alpha$ protein-mediated effects faster, while GDI proteins inhibit dissociation of GDP from $G\alpha$ subunits. RGS proteins with GAP activity enhance GTPase activity of $G\alpha$ subunits to reduce the magnitude and duration of $G\alpha$ protein mediated signaling. Recently, some GPCR ligands are identified to inhibit hypertrophic signal transduction in heart muscle and increase contraction of cardiac muscle in G-protein-independent manner. In heart, there are four prominent isoforms of α known as $G\alpha_s$, $G\alpha_{i/o}$, $G\alpha_{q/11}$, $G\alpha_{12/13}$. There are G-dependent and G-independent signaling.

9.3 G-Protein-Dependent Signaling Through cAMP

In heart muscle β adrenergic receptor stimulation generates cAMP by inner membrane-associated adenylyl cyclase. The cAMP phosphorylates protein kinase A, which phosphorylates ryanodine receptor (RyR), phospholamban (PLB), the L-type calcium channel (LTCC), cardiac troponin I (cTnI), and cardiomyosin-binding protein

for increasing contractibility. The RyR and LTCC enhance sarcoplasmic reticulum calcium release. The phospholamban (PLB) is SR calcium (SERCA) ATPase inhibitor, so it enhances calcium uptake by ER. The myofilament affinity to calcium is decreased by phosphorylated troponin I and cardiomyosin-binding protein because these proteins change dynamics of stimulation. In an another event, cAMP generation activates exchange protein activated by Camp (EPAC). The RYR and troponin I are phosphorylated through phosphorylated $PKC\epsilon$ and phospholipase $C\epsilon$ by EPAC. The EPAC also stimulate calmodulin kinase (CAMKII)-dependent calcium release from SR in short duration. β arrestin 1 and 2 is scaffold for calmodulin-dependent kinase CAMKII. The protein kinase A induces hyperpolarization through ATP-sensitive potassium channel phosphorylation, and EPAC is suggested to induce dephosphorylation of ATP-sensitive channel. While $G\alpha_s$ induces cAMP production, $G\alpha_i$ inhibits this. The β adrenergic receptors association with $G\alpha_i$ activate phosphodiesterase through inositol 3 kinase (PI3K) activity and regulate cAMP concentration. The G-protein β and γ subunit may inhibit L-type calcium channel, which increases hyperpolarization and decreases action potential duration (Fig. 9.3).

9.4 G-Protein-Coupled Receptor Kinases

G-protein-coupled receptors kinases (GPCRK/GRKs), a family of seven types serine/threonine kinase recognize and phosphorylate ligand-induced GPCR, desensitize it by recruiting β arrestin. This is the base of G-independent signaling. The β arrestin association with phosphorylated receptors is internalized by clathrin-coated vesicles for sending receptors back to membrane. The isoforms of GRKs are different in their function in tissue-specific manner (Fig. 9.4).

Recently, these kinases are found to phosphorylate many other proteins like platelet-derived growth factor (PDGF), synuclein,

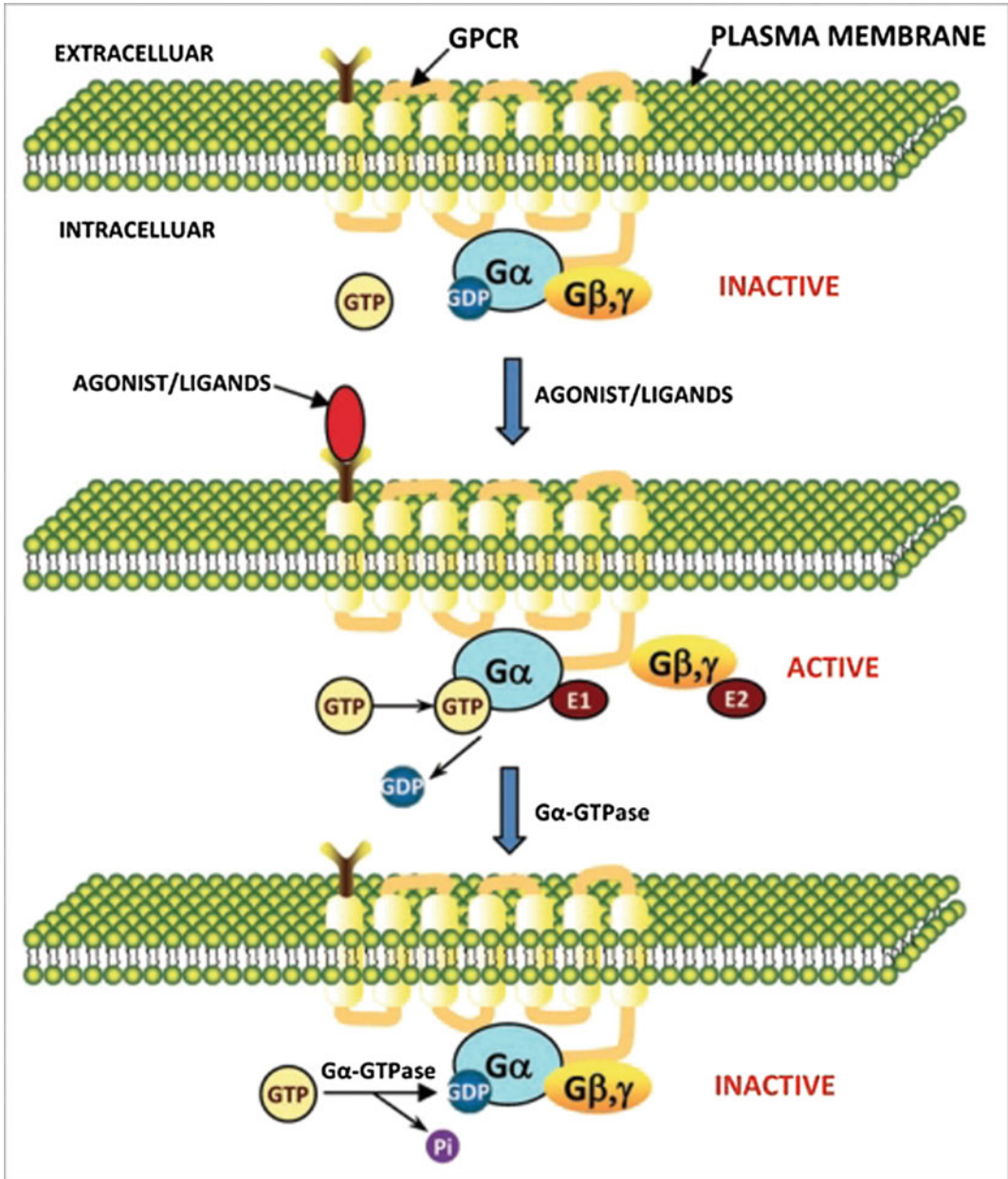
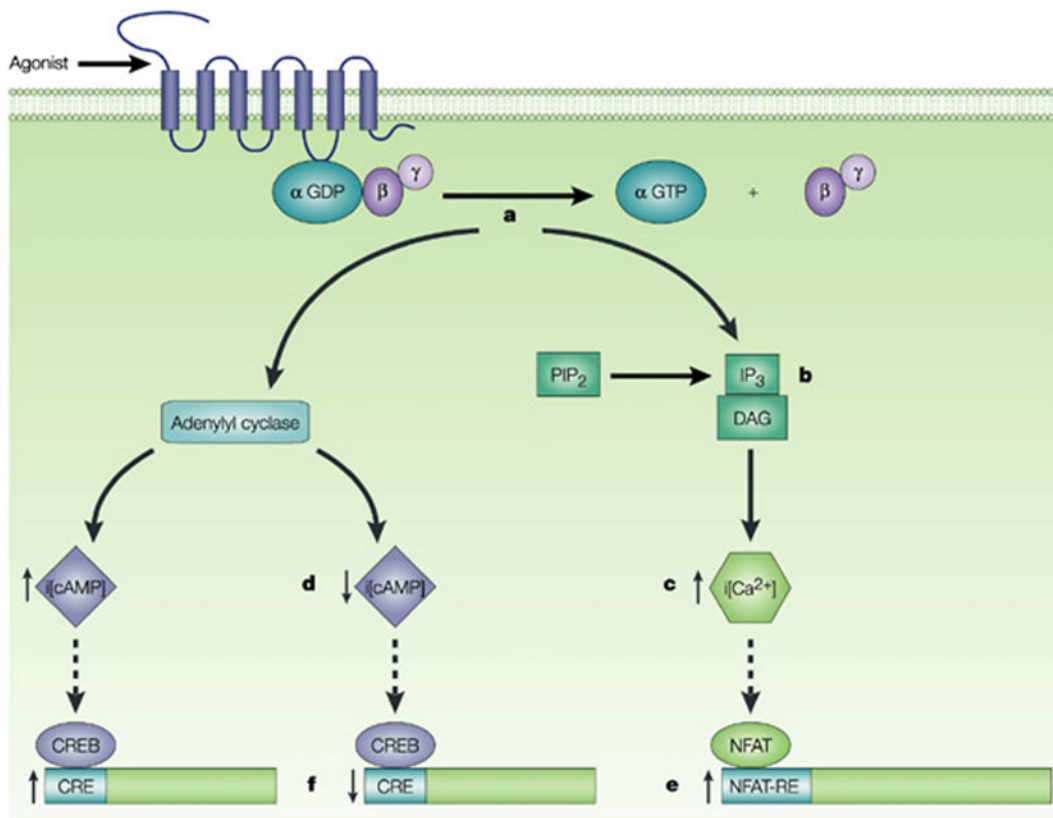


Fig. 9.2 Ligand-activated GPCR-mediated signal transduction by activation/inactivation of heterotrimeric G-proteins. The subunits of heterotrimeric G-proteins ($G\alpha$ GDP and $G\beta\gamma$) in their inactivated state are associated with each other. When ligand binds to GPCR, the change in conformation occurs in GPCR. The $G\alpha$ exchange GDP with GTP and gets disassociated from

$G\beta\gamma$. The separated $G\alpha$ and $G\beta\gamma$ have their own effectors (E1 and E2, respectively) for downstream signaling and initiate unique responses. After the signal transduction, the $G\alpha$ -GTPase activity hydrolyzes the bound GTP ($G\alpha$ -GTP) to GDP and P_i and inactivated $G\alpha$ reassociates with $G\beta\gamma$ and activation and inactivation cycle is completed



Nature Reviews | Drug Discovery

Fig. 9.3 G-protein activation by binding of an agonist and its downstream cascade. Nature Reviews Drug Discovery 3, 125–135 (February 2004). <https://doi.org/10.1038/nrd1306>

ribosomal protein P2, and inhibiting γ subunit of cGMP phosphodiesterases and β subunit of epithelial sodium channel. These kinases also modulate various cellular responses by interacting G α_q and G $\beta\gamma$ subunit of GPCR, PI3K, caveolin, and clathrin. These kinases along with β arrestin play important role in G-independent signaling. The GRK2 and GRK3 are actively involved in endocytosis. GRK3, GRK5, and GRK6 are universally present in mammal cells while 1, 4, and 6 isoforms are tissue-specific.

Structure of GRKs: G-receptor kinases, on the basis of sequence homology, have three subclasses known as rhodopsin kinase, which has GRK1 and GRK7, the GRK2 and GRK3 sub-families like β -adrenergic receptor kinases and

the GRK4 subfamily with GRK4, GRK5, and GRK6 as members. The GRKs proteins have conserved common structure with central catalytic domain of ~ 270 residues, N-terminal of ~ 185 amino acids (defining feature of all GRKs) and variable C-terminal of 105–203 amino acids. The N-terminal is involved in receptor recognition and intracellular membrane anchoring along with regulating G-protein signaling RH domain (120 amino acids). The phosphatidylinositol (4,5) biphosphate (PIP₂) binding to GRK4–GRK6 induces catalytic kinase activity. The C-terminal domain is responsible for subcellular localization and ligand-dependent translocation. The cytosolic domain of GRK2 and GRK3 has pleckstrin domain (PH) to bind with

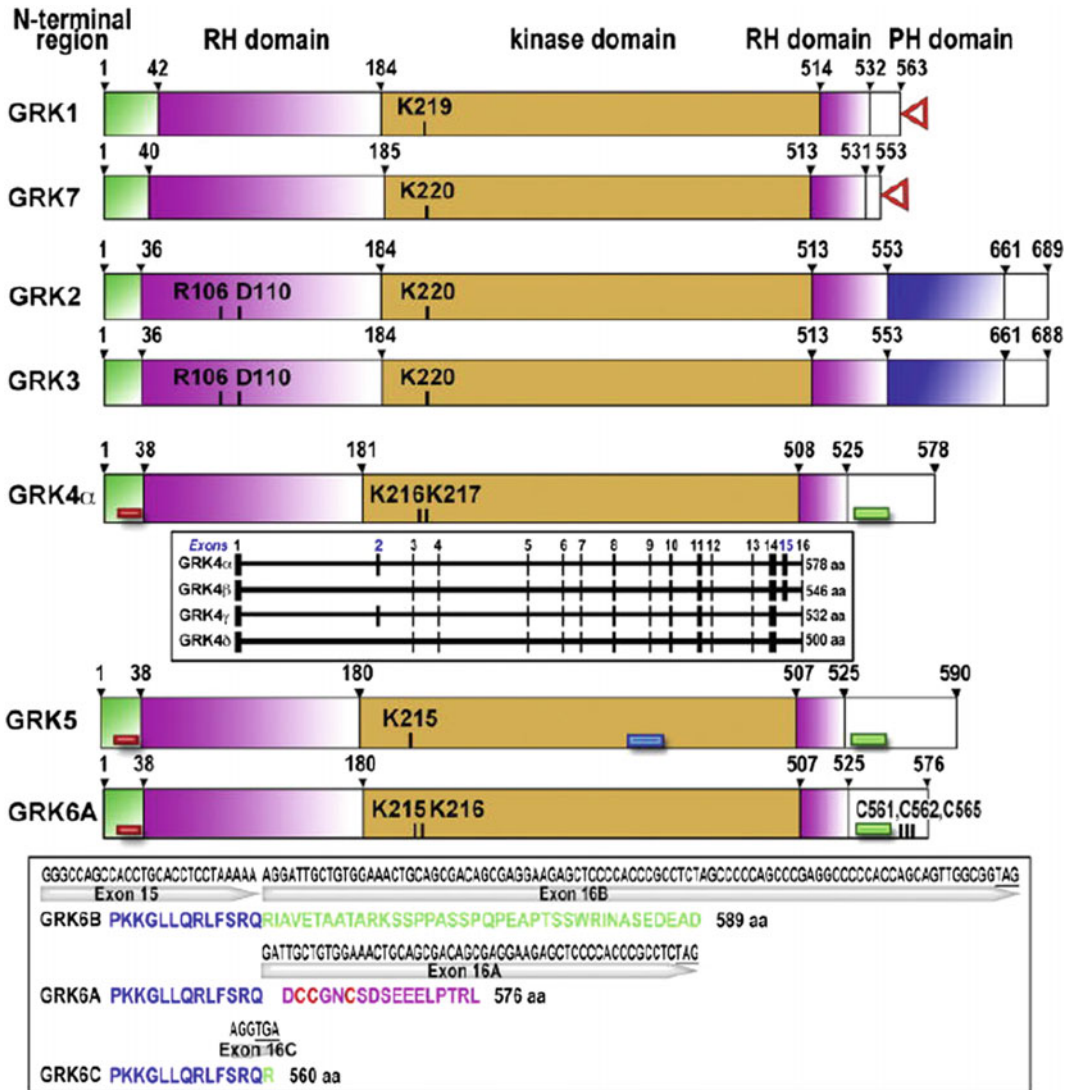
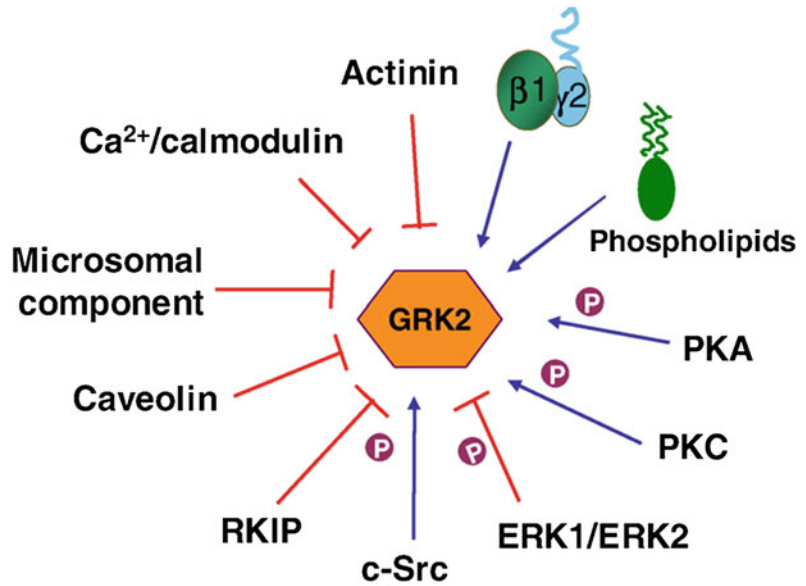


Fig. 9.4 The G-protein coupled receptor kinases (GRKs) with various domains of different sub families. The alphabet numbers indicate amino acids residues. Pharmacol Ther. Author manuscript; available in PMC 2013 Jan 1

phospholipids and free β and γ subunits. The subfamily of GRK1 has a prenylation site at C-terminal. The RH domain of GRK2 has nine α helices and two extra helices between kinase domain and PH domain. The RH domain regulates kinase activity by interacting with kinase and the PH domain. The α -10-helix of the RH domain interacts with β -2- β -3 and α -C- β -4 loops of the kinase domain and α -4- α -5 loop of the RH bundle with α -J-helix of the kinase

domain for regulation. The PH domain (phospholipid interaction and membrane targeting site) has seven β -strands and one C-terminal α -helix. At the interface RH has α -1 and α -9 helices and PH β -1 strand and α -CT helix interacts for allosteric regulation. The GRK2 kinase activity is inhibited by phosphorylation by MAPK at serine 670 at C-terminal (*G $\beta\gamma$ disturbed binding*) and increased in PKA-dependent manner phosphorylation at serine 685 (by increasing $G\beta\gamma$

Fig. 9.5 G-protein receptor kinases (GRK2) activity regulation by various effector molecules and kinases



affinity). The GRK2 and GRK3 RH domains interact with $G\alpha_q$ and $G\alpha_{11}$ but do not associate with $G\alpha_s$, $G\alpha_i$, $G\alpha_o$, or $G\alpha_{12/13}$, the isoforms predominantly found in heart muscles. The phosphorylation of GRK2 by c-Src in the RH region amino acid 86 and 92 near calmodulin-binding domain can increase its affinity toward soluble and membrane-bound substrates. GRK4/5/6 subfamily target membrane through palmitoylation (Fig. 9.5).

The RH domain GRK2 interacts with $G\alpha_q$ family and $G\alpha_{11}$ and stabilize inactive conformation of kinases. This is found to inhibit $G\alpha_q$ -modulated phospholipase C activity in “in vivo” and in “in vitro” by sequestering $G\alpha_q$ through protein–protein interaction. The GRKs desensitize various receptors like endothelin A and B, thromboxane A₂, muscarine cholinergic parathyroid hormone in phosphorylation-independent manner. The GRKs have caveolin-binding motif in PH domain (567–584) and in the N-terminal (63–71). The GRKs/caveolin interaction is important for kinases to interact with other signaling and regulatory molecule. The GRK2 and MEK1 interactions regulate chemokine induction of MAPK activation.

9.5 Tyrosine Kinase-Mediated Receptor Signaling

The-receptor tyrosine kinases (RTKs) are well established regulator for cell cycle, survival, differentiation, division, and other metabolic processes. In human, these RTKs are divided into 20 subfamilies with 58 identified members. Receptor tyrosine kinases (RTKs) functional domain is protein kinase domain in intracellular region of each RTK monomer. Ligand binding to the extracellular region of receptor increases tyrosine kinase activity and selective transautophosphorylation of tyrosine residues. Many of these sites maintain the active conformation of the kinase itself, and other acts as docking sites for different adaptor or effector scaffold proteins and enzymes (Fig. 9.6).

These receptors are made up of single trans-membrane with extracellular ligand-binding domain except insulin receptor (IR) subfamily, cytoplasmic domain for tyrosine phosphorylation and intracellular juxtamembrane regulatory region near C-terminal. The insulin receptor family includes insulin-like growth factor I

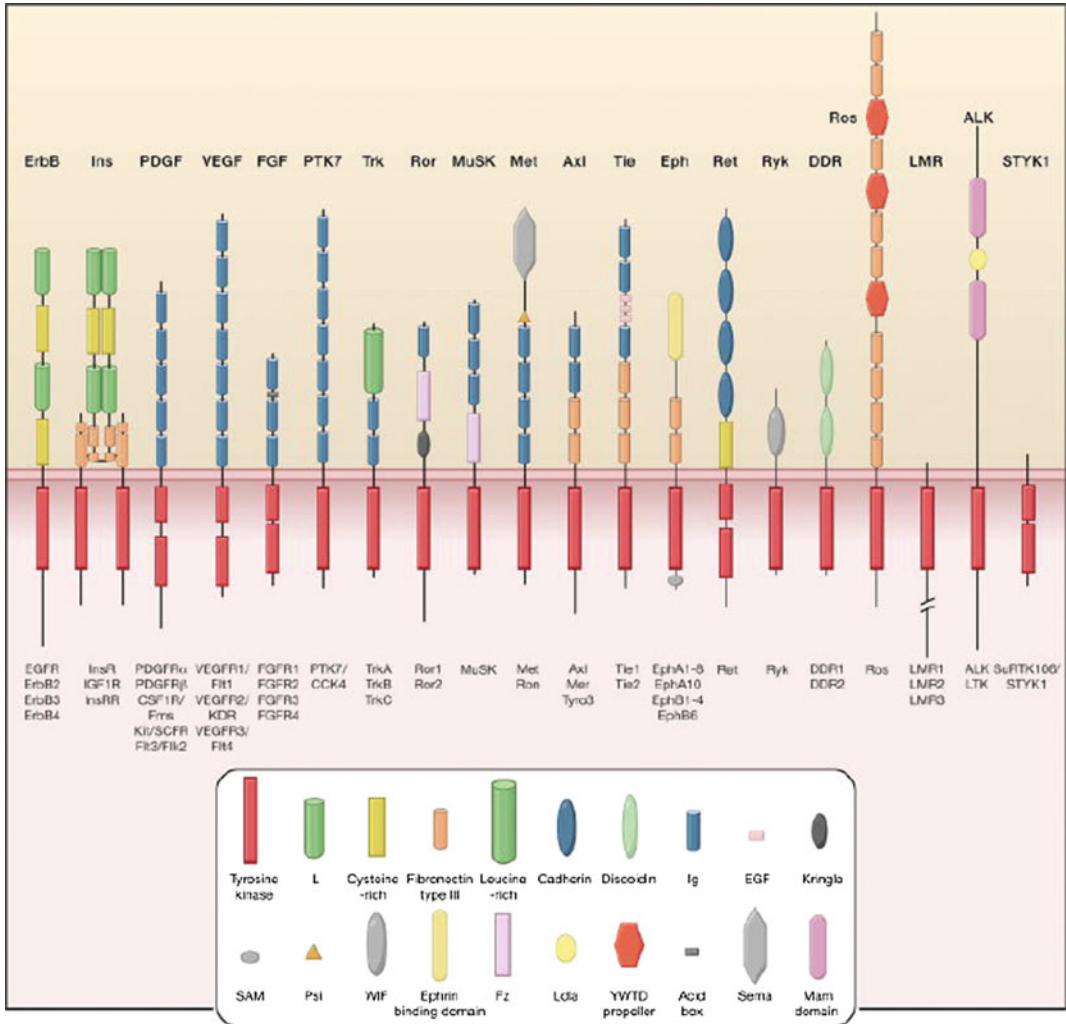


Fig. 9.6 Human receptor kinase families with various domain and their ligands. Cell. 2010 Jun 25; 141(7): 1117–1134. <https://doi.org/10.1016/j.cell.2010.06.011>

receptor (IGFIR), and the insulin receptor-related receptor (IRR) monomer generates α - and β -polypeptide and form heterotetramer, or an ($\alpha\beta$) homodimer through disulfide bonds, and transphosphorylation happens within the dimer. The one insulin ligand molecule binds to one ($\alpha\beta$) dimer. There are two separate ligand-binding regions in monomer known as site 1 and site 2. The ligand molecule binds to site 1 of one monomer and site 2 to other for cross-linking of monomers.

The structure, mechanism, and various components of signaling pathway are conserved in animals. The defect in receptors tyrosine kinases may lead to diseases like diabetes, cancer, bone disorders, arteriosclerosis and angiogenesis. The preactive form of receptors may be monomer or dimer (insulin or insulin growth factors 1-receptors) but binding of ligand-like growth factors induces active and stable dimerized or oligomerized (**Tie2—an angiopoietin receptor**) and stimulates the structural changes within these

dimeric or oligomeric receptors to enhance phosphorylation cell signaling. The receptor dimerization may be through receptor molecule or through ligand molecule direct interaction. The neurotropic tropomyocin receptor kinases (Trk) have leucine rich repeats (LRR) at extracellular side, which is followed by Ig-like domain C1 and C2. The C2 domain of KIT, a type III receptor tyrosine kinase in hematopoietic cells occurs through first three (D1–D3) Ig-like domains of extracellular region, which connect receptors without any conformational change. In fibroblast growth factor receptor (EGFR), the ligand binding and dimerization require three Ig-like extra cellular domain (D1–D3) and hair-pin intervening linker combination. The receptor interacts with each other by D2 domain, the receptor interaction with ligand and receptor heparin interactions stabilize the FGFR dimer.

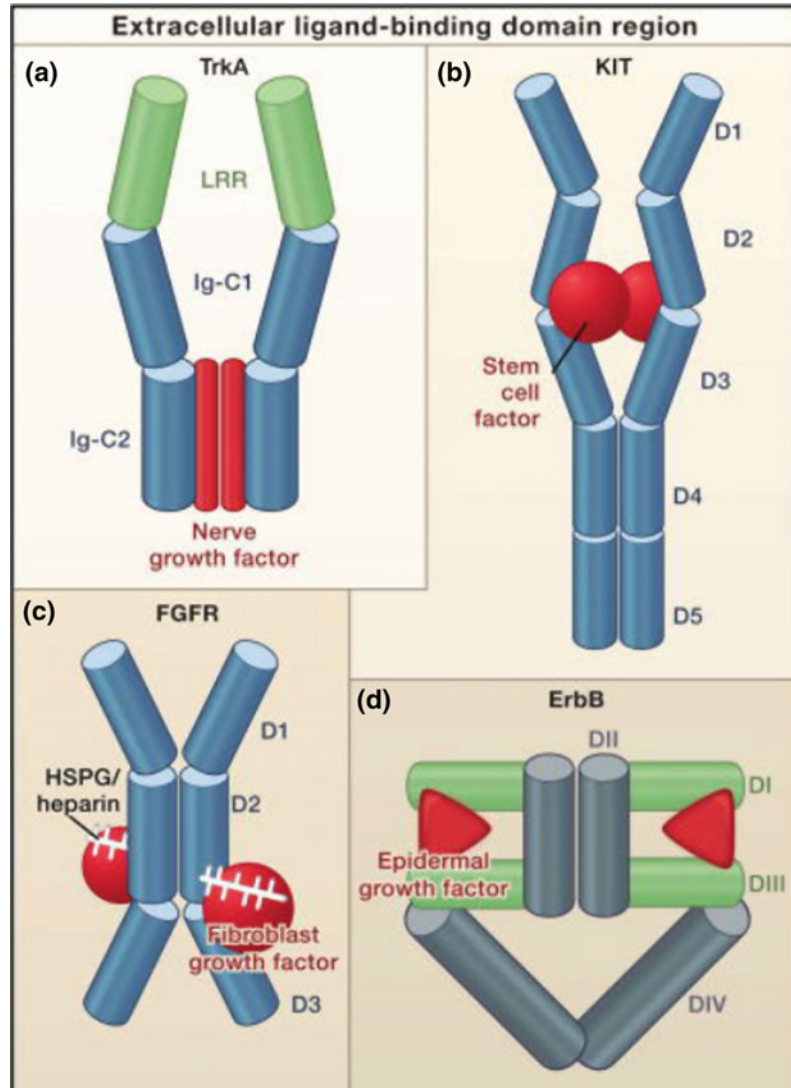
The ErbB family receptors may be divided into three subclasses. The ErbB class I binds to EGF, transforming growth factor (TGF) α , amphiregulin (AR), and epigen (EPG). The class II ErbB betacellulin (BTC), heparin-binding EGF (HB-EGF) have dual specificity for EGFR and ErbB4. The ErbB III neuregulins (NRGs) may bind to either ErbB3 or ErbB4 (NRG1 and NRG2) divided in two subcategories. The EGFR or ErbB receptors have extracellular ligand-binding domain of around 620 amino acids, single 25 amino acids transmembrane, intracellular juxtamembrane region of 40 AA residues, cytoplasmic kinase domain of approximately 270 AA residues and C-terminal region of 220–350 amino acids (tyrosine phosphorylation site). There are four domains (I–IV) in mammalian ErbB receptors extracellular region. The domains I or L1 and III/L2, the β -helix are leucine-rich repeats (LLR) domain, which is involved in ligand binding. The domains II/CR1 and IV/CR2 are cysteine-rich (CR) domain. These domains are also found in IR and IGFIR. The dimerization totally depends on receptor as shown in Fig. 9.7. The crystal structure of extracellular domain of EGFR with bound ligand and without ligand has revealed large conformational change during dimerization as the cysteine-rich dimerization site II/CR1 is hidden in

autoinhibited conformation with C-terminal domain IV-/CR2-rich region. The bivalent ligand contacts two separate sites within a single receptor molecule (domains I and III) unlike NGF (cross-linking occurs between two receptors). The ligand binding induced major conformational changes in the extracellular region of EGFR which reveals dimerization arm in domain II. The I-II/L1-CR1 moves away from IV/CR2 domain by bound ligand-induced rotation and is stabilized as an extended configuration with exposed II/CR1 and IV/CR2 loop of the EGFR to interact with other receptor. The total number of tyrosine residues found in each intracellular region and the number to be phosphorylated are different in various classes TRKs. The inactive tyrosine kinases difference in structure among various tyrosine kinase receptors family is correlated to diverse regulatory mechanism. The tyrosine kinase domain is in cis-autoinhibited conformation before ligand binding.

The intracellular JM region, needed for allosteric regulation, may be divided into two segments JMA and JMB. The JMA antiparallel helical dimer of dimerized receptor Glu663 and Glu666 is thought to participate in inter helical salt bridges to stabilize the helical dimer. The phorbol 12-myristate 13-acetate (PMA) stimulates Thr654 phosphorylation resulting in loss of cooperativity, which confirms JMA segment role in negative cooperativity in EGFR (Fig. 9.8).

Tyrosine kinase activation domain of the EGFR is found to be symmetric dimer in an inactive form and asymmetric dimer in active form. The helix α -C of the N-terminal lobe of the kinase domain in inactive conformation is moved to outside, and activation loop is buried inside the active site in such a way that no substrates is able to bind. In active state, the α -C helix moves toward the active site and activation loop is exposed to bind with substrates. At this point the C-terminal lobe of the activator or donor kinase contacts the N-terminal lobe of the adjacent receiver or acceptor kinase to stimulate conformational changes for receiver or acceptor kinase activation. The tyrosine kinase domain has activation loop α -C helix in N-lobe in special configuration for transfer of phosphoryl group. As

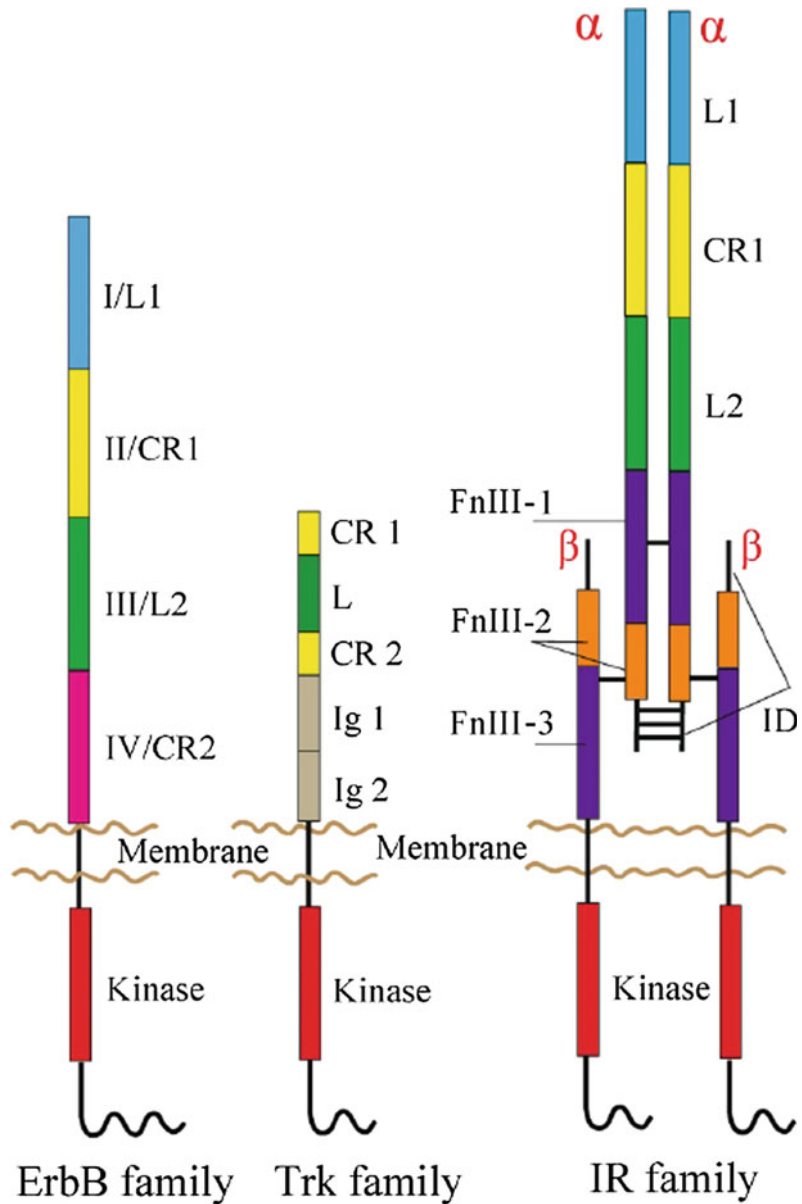
Fig. 9.7 Activation by dimerization of receptor molecules. **a** The nerve growth factor (TrkA) ligand and **b** stem cell factor interact across the dimer interface to stimulate dimerization of KIT (type III receptor tyrosine kinase) along with two Ig-like domains (D4 and D5) reorientation after stimulation so both ligand-mediated and receptor mediated dimerization modes occurs. **c** Two molecules of fibroblast growth factor receptor (FGFR) interact with one another through D2 (Ig-like) domain along with the accessory heparin molecule or with heparin sulfate proteoglycans (white sticks) for dimerization. **d** Ligand induced change in conformation as in epidermal growth factor receptor (EGFR) of Erb family expose a hidden dimerization site in Domain II (Color figure online)



seen with insulin receptor tyrosine kinase domain, tyrosine Y1162 of activation loop is protruded in active site and is autophosphorylated by its own kinase domain (cis-autophosphorylation). In ligand insulin bound receptor Y1162 of one monomer TKD domain is phosphorylated by another TKD domain of other monomer (transauto phosphorylation), which disturbs cis-autoinhibitory conformation and activation loop in phosphorylated forms adopt active conformation. *The transauto*

phosphorylation is discussed below. The N-lobe α helix rearrangement stabilizes ATP binding site and receptor in active form. Activation of tyrosine kinase may activate cellular signaling molecule with Src-homology 2(SH2) and phosphotyrosine-binding (PTB) domain, which may directly or indirectly interact with receptors through docking proteins. For insulin receptors, the docking proteins are known as FRS-2, IRS-1 (insulin substrates-1) and Gab 1 (Grb2-associated protein). The docking protein has N-terminal

Fig. 9.8 The various domains in three major family of tyrosine kinases. The abbreviations used as L leucine-rich; CR cysteine-rich; Ig immunoglobulin-like; FnIII fibronectin type III; ID insert domain. The L1, CR1, L2, and CR2 domains of the ErbB family are also known as domains I–IV. Cells. 2014 Jun; 3(2): 304–330. Published online 2014 Apr 22. <https://doi.org/10.3390/cells3020304>



target site with multiple tyrosine phosphorylation sites, where other cellular protein may come and bind.

The EGFR agonist like tumor growth factor α , β cellulin are synthesized as precursor, which are active after proteolysis. On binding of these ligands, the EFGR is phosphorylated to induce Ras/Mitogen-activated protein kinase pathway.

9.6 Transactivation of Epidermal Growth Factor Receptor by G-Protein Couple Receptors

The epidermal growth factor receptors tyrosine kinase has four members like ErbB1/Her1, ErbB2/Her2, ErbB3/Her3, and ErbB4/Her4,

where ErbB2 is an orphan receptor and ErbB2 with impaired kinase activity. These receptors are found to be activated by various stimuli without interacting them directly such as G-protein-coupled receptors, cytokines, chemokines, and other adhesion molecules. The signal for EGFR may be membrane polarization, heavy metals, UV, and γ radiations. The activated EGFR may form complex with various signaling proteins like Shc, Grb2, Src, PLC γ 1, Cbl, and the p85 α -subunit of phosphoinositide 3-kinase (PI3K) are shown in Fig. 9.9. The MEK-activated extracellular signal-regulated kinases (ERKs) stimulate ERK1 transcription factor directly and *c fos*, SRF TF through RSK. The EGFR-induced PLC γ 1 activation controls cell mitogenesis, and migration and activated PI3K/AKT pathway inhibits apoptosis. The agonist like lysophosphatidic acid, thrombin, and angiotensin II, or endothelin1 (in vascular smooth muscle cells, VSMC) binding to GPCR phosphorylates EGFR and ErbB2. The transactivation process of GPCR by Receptor tyrosine kinases was first given by Ullrich's group. The two major pathways for transactivation mechanism are widely accepted known as **triple membrane-passing signal (TMPS) pathway** and **ligand-independent intracellular pathway**. In TMPS pathway, the EGFR transactivation by GPCR depends on membrane bound matrix metalloproteases (MMPs) such as ADAM (a disintegrin and metalloprotease) family. MMPs hydrolyze EGFR ligands for binding to EGFR and activate receptors. The activated EGFR may activate various signaling pathways such as the Ras–Erk pathway and the PI3K–AKT pathway and regulates various cell functions. The various ligands like bombesin, 5-hydroxytryptamine, carbachol, angiotensin II, bradykinin, lysophosphatidic acid, endothelin 1, gonadotropin releasing hormone, phenylephrine, leptin, thrombin, deoxycholic acid, and prostaglandin E2 induce EGFR transactivation by MMPs pathway to regulate growth, development, and progression of many diseases such as cancers, kidney disease, and cardiovascular disease (Fig. 9.10).

In all ligand-independent pathways, intracellular protein tyrosine kinases RTKs like Src are activated, which phosphorylates the tyrosine residues in the cytosolic domain of EGFR, which may interact with downstream signaling proteins and activate various signaling pathways. The Src may also be activated by GPCR by different mechanisms. The third mechanism involves phosphorylation of p47phox by active GPCRs and NADPH oxidase activation to generate reactive oxygen species (ROS). The ROS might disturb the intracellular phosphorylation and enhance the activity of intracellular PTKs by two different pathways, either by inactivating protein tyrosine phosphatases (PTPs) by oxidizing its catalytic cysteine residue or by increasing negative regulatory proteins proteolysis and increase EGFR transactivation. The EGFR signaling may be important for targeting site in cancer and other diseases, if potential therapeutic agents are identified in EGFR transactivation by GPCR (Fig. 9.11).

9.7 G-Protein-Independent Signaling

The G-protein-coupled receptors (GPCRs) of seven transmembrane receptors are divided into three distinct classes as **ligand bias**, **receptor bias** and **tissue or cell bias** depending on the functional selectivity. The ligand bias is explained by various ligands interaction with same receptor. The receptor bias is the interaction of same ligand with various receptors and tissue bias includes same ligand and receptors signaling in different tissues. The biased signaling again may be either **G-protein-dependent** or **β arrestin-dependent signaling**.

9.7.1 β Arrestin-Dependent Signaling

The β arrestin, multifunctional protein participate in desensitization, G-independent signaling, internalization, structure reorganization and other signaling pathway. The role of β arrestin is well

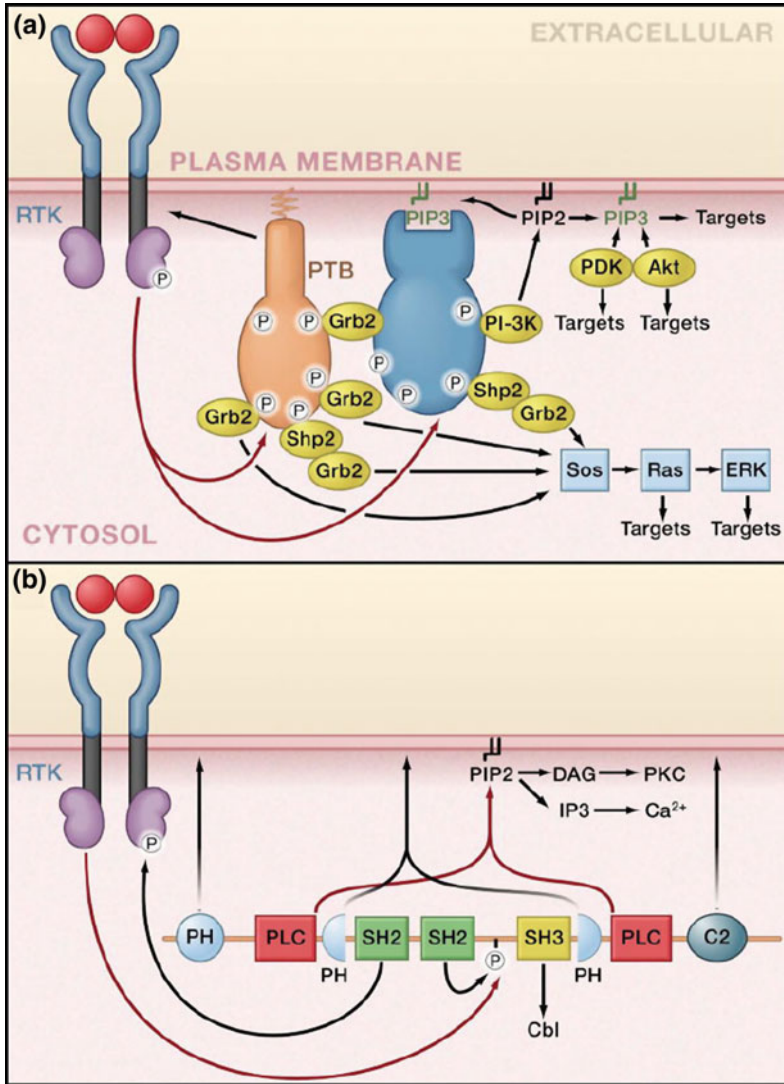


Fig. 9.9 The receptor tyrosine kinase signaling. **a** Coordinated assembly of multiprotein complexes in receptor tyrosine kinase (RTK) signaling and their branching points. The docking protein fibroblast growth factor (FGF) receptor substrate-2 (FRS2 α), which forms a complex with activated fibroblast growth factor (FGF) or nerve growth factor (NGF) receptors via its phosphor tyrosine-binding domain (PTB). The activated RTK phosphorylates FRS 2 α on multiple tyrosine, and the resulting phosphor tyrosine recruit multiple Grb2 and Shp2 molecules to bring a second docking protein, Gab1, into the complex. Gab1 is tyrosine phosphorylated and recruits additional signaling proteins, including phosphoinositide 3-kinase (PI3K). PI3K initiates a positive feedback loop in which PtdIns(3,4,5)P3 (PIP3), generated

by PI3K, recruits more Gab1, leading to further PI3K activation. **b** The multiple domains of phospholipase C- γ (PLC γ) cooperate to integrate multiple signals at the plasma membrane. The N-terminal SH2 domain is responsible for complex formation with activated receptor tyrosine kinases (RTKs). The C2 and PH domains cooperate with the SH2 domain to target PLC γ to the plasma membrane. One or both of the PH domains may also specifically recognize products of RTK-activated PI3K. RTK mediated tyrosine phosphorylation of PLC γ leads to intramolecular binding of the C-terminal SH2 domain to phosphotyrosine 783. This stimulates enzymatic activity of PLC γ , leading to hydrolysis of PtdIns(4,5)P2 (PIP2) and consequently leads to the formation of Ins(1,4,5)P3 (IP3) and diacylglycerol (DG)

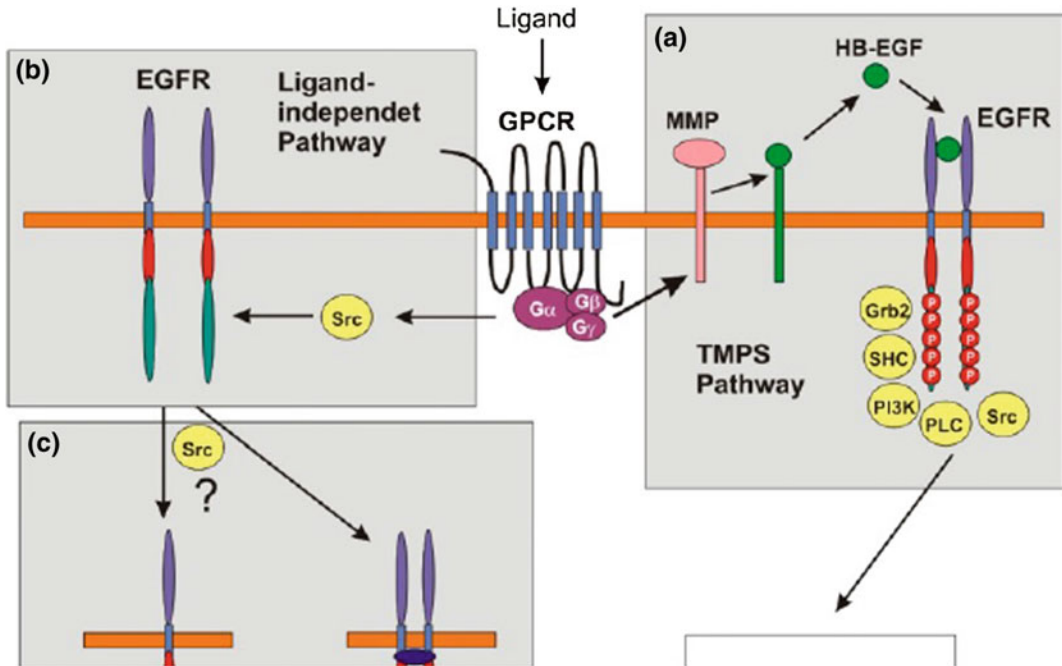


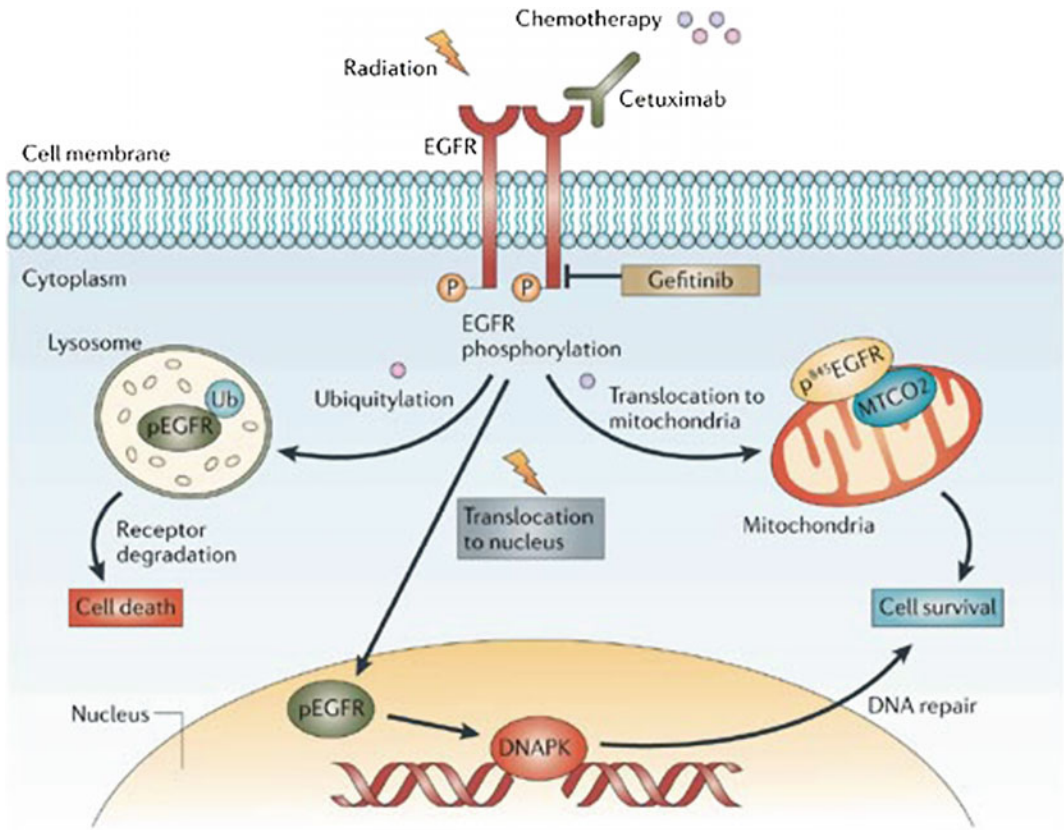
Fig. 9.10 Schematic representation of EGFR transactivation by GPCR. **a** Triple membrane-passing signal (TMPS) pathway (TMPS), where EGFR transactivation depends on the matrix metalloproteases (MMPs). The MMPs proteolyze EGFR ligands like HB-EGF to release in extracellular space for binding to EGFR. The binding may induce dimerization for activation of receptors, which activate signaling cascades. **b** Ligand-independent pathway, where intracellular protein tyrosine kinases (PTKs) such as Src-family proteins are activated. The Src phosphorylates the tyrosine residues in the cytosolic domain of EGFR, which may interact with downstream

signaling proteins and activate various signaling pathways. The Src may also be activated by GPCR by different mechanisms. **c** Future target for research should be on the EGFR transactivation by ligand-independent Src pathway. It is important to determine how Src activates EGFR, the activation status of Src-activated EGFR, and the effects of Src-activated EGFR on the downstream signaling cascades and cell functions. Does Src induce receptor dimerization or phosphorylate all the major phosphotyrosine (Y) residues of EGFR along with downstream signaling pathways and physiological consequence of this activation?

studied in human heart, where it activates MAPK and EFGR. The two isoforms β arrestin 1 and 2, universally present scaffold proteins, participates in G-independent signaling. β arrestin is known to inhibit G-protein signaling by uncoupling the interaction between a GPCR and its associated G-proteins. The β arrestin increases degradation of second messenger through phosphodiesterase and diacylglycerol kinase, respectively (Fig. 9.12).

The ligand-induced G-protein-coupled receptor phosphorylation at C-terminal by GRKs recruit β arrestin as discussed above. In HEK 293 cancer cells, β arrestin signalosomes proteins are found to be associated with AT1 R before and after Ang II stimulation. The AT1 R β

arrestin-dependent signaling enhances cardiomyocyte and cardiac contractility as shown in mouse cardiomyocytes, which is independent of G α q/11 protein activation. The AT 1R β arrestin 1-mediated signaling is found to enhance RhoA activation, which results in fiber reorganization. The β arrestin 2 has not affected this process. The RhoA activity may control PKC and PKD, which regulate cardiac contractility. The proteins like ROCK, actin, cofilin, myosin, and the myosin-binding subunit of myosin phosphatase (MYPT1) have shown changed phosphorylation status on interaction with β arrestin 1. The β arrestin-mediated ERKs scaffolding restricts ERK1/2 signaling to the cytosol



Copyright © 2006 Nature Publishing Group
 Nature Reviews | Cancer

Fig. 9.11 EGF signaling as a potential target for cancer therapy. *Nature Reviews Cancer* 6, 876–885 (November 2006). <https://doi.org/10.1038/nrc1953>

and this signaling may phosphorylate and activate ribosomal S6 kinase (p90RSK) in neonatal cardiomyocytes to increase DNA synthesis and proliferation. The Mnk1 and Mnk2 protein kinases are directly phosphorylated and activated by extracellular signal-regulated kinase (ERK) or p38 mitogen-activated protein (MAP) kinases to regulate protein synthesis. The Mnk1 is activated by β arrestin 2 interaction in an AT1R β arrestin ERK 1/2-dependent manner in vascular smooth muscle cell (VSMC) to phosphorylate eukaryotic translation initiation factor 4E (eIF4E) of protein synthesis (Fig. 9.13).

Recently bioluminescent resonance energy transfer (BRET)-based G-protein activation biosensors have identified G-protein activation by GRK β arrestin ligands. The angiotensin II type 1A receptor (AT1AR) is phosphorylated by GRK2 and GRK3 to cause desensitization and internalization. The GRK5-induced phosphorylation results in β arrestin-dependent ERK transactivation. The β 1 AR stimulated EFGR transactivation depends on β arrestin. The angiotensin II type 1A receptor (AT1AR), vasopressin receptor 2 (V2R), and β 2-adrenergic receptor (β 2-AR) activate extracellular kinase

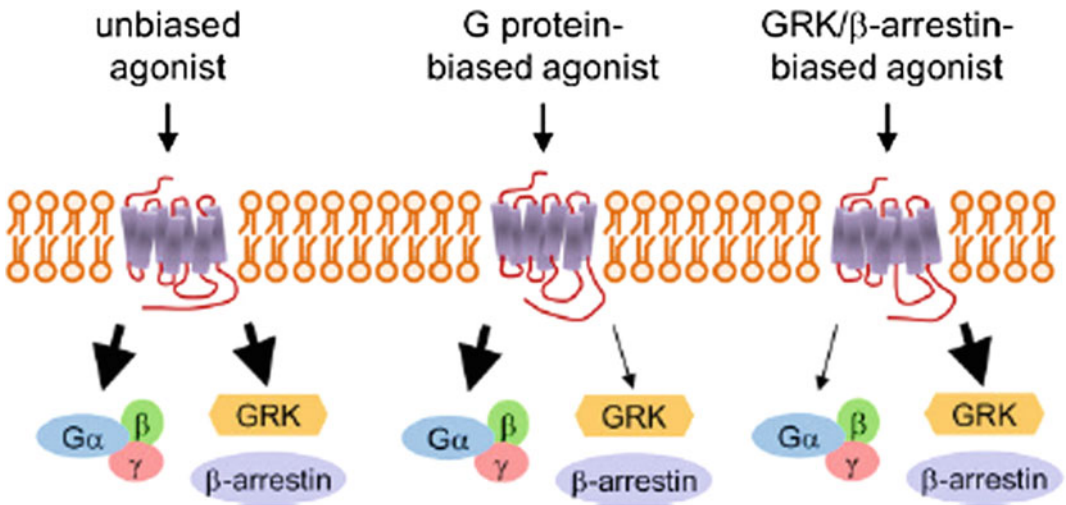


Fig. 9.12 G-receptor kinases in G-independent signaling in GRK/β arrestin-dependent manner. The ligand induces distinct conformational changes of GPCRs. The unbiased general ligand activate both G protein signaling and GRK/β arrestin-dependent signaling, whereas biased or

specific ligand activate either G protein- or GRK/β arrestin-dependent signaling (bold arrows) causing various Physiological responses mediated by GRK/β arrestin-dependent signaling different from G protein induced responses

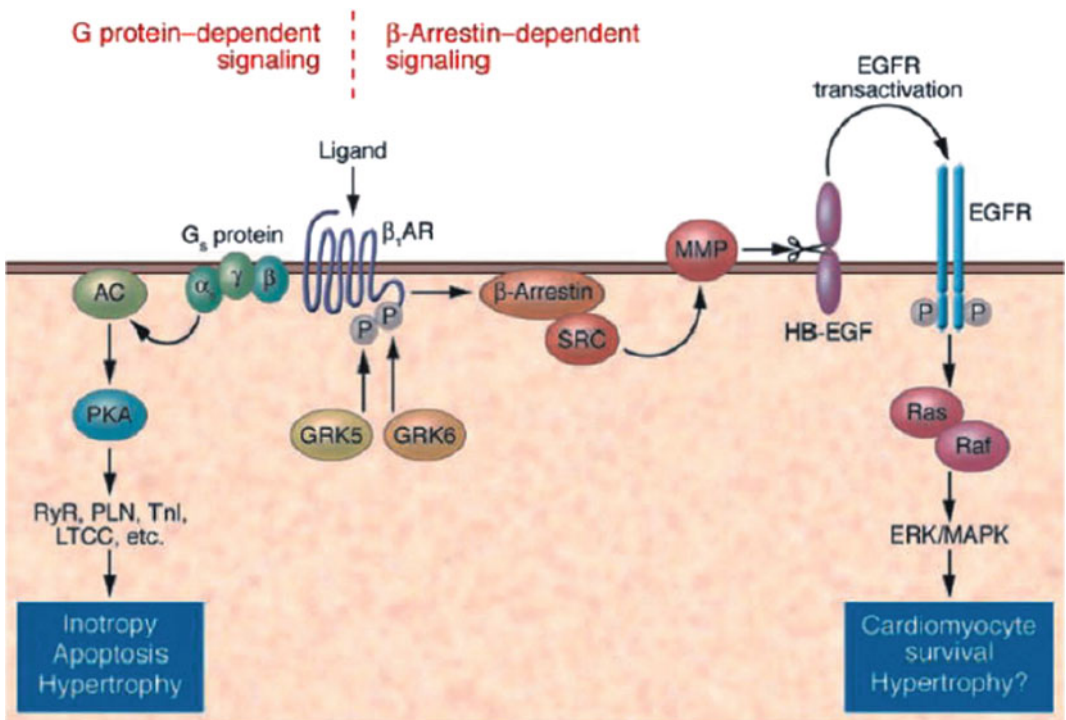


Fig. 9.13 The β-1-adrenergic receptor (β₁AR) induced transactivation of the epidermal growth factor receptor (EGFR). Stimulation of the β₁AR activates two independent signaling pathways, G_s-mediated and β arrestin-mediated pathways. The G_s stimulate adenylyl cyclase (AC) to produce cAMP for inducing downstream signaling. G_s-signaling activate short-term inotropy while

the catecholamine stimulation enhances harmful cardiac remodeling such as myocyte apoptosis, increased ventricular dilatation, and decreased fractional shortening. After β arrestin recruitment to GRK5/6-phosphorylated receptors, the β₁AR initiates cardioprotective β arrestin-mediated signaling through “transactivation” of the EGFR. *Circ J.* 2008 Nov; 72(11): 1725–1729

(ERK) in G-independent manner through GRK5 or GRK6.

The phosphorylation pattern in desensitization and signaling is also different as seen in GRK2 and GRK6 with different phosphorylation sites in β 2-adrenergic receptor. The G-receptor kinases phosphorylate β 1-AR at serine/threonine residues at C-terminal end. The GRKs may interact with various nonGPCR proteins like single transmembrane receptors, cytosolic proteins and nuclear proteins showing role in inflammation, cell motility, and cell cycle. The ERK1/2 activity downstream of some GPCRs is reciprocally regulated by β arrestins 1 and 2. The G-protein-independent ERK2 activation downstream of the AT1 R is mediated by β arrestin 2 but β arrestin 1 prevents β arrestin 2-mediated ERK2 scaffolding and subsequent activation.

The AT1AR and β 1AR classical G-protein signaling is detrimental in heart failure while β arrestin G-protein independent signaling protects cardiac cells. The biased ligands for β arrestin signaling activation and inhibitors for harmful G-protein signaling may be used as drug to prevent or reverse the harmful cardiac reorganization induced by catecholamine and angiotensin II in heart failure.

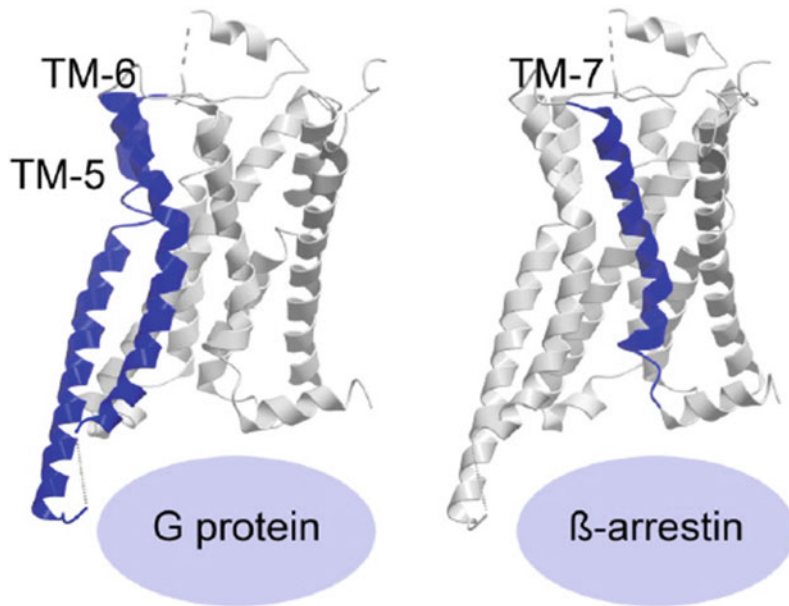
9.7.2 Chemokine Receptors Signaling

The seven transmembrane receptors have approximately 350 amino acids and their chemokines ligands of (8–12 kDa) peptides. The ligands, on the basis of two conserved cysteine residues position relative to each other, may be divided into two major and two minor groups. In the major group of CCL, the two cysteines are present together and in other major CXCL the two cysteines are separated by one amino acid. The minor chemokine CXCL1 subclass of single ligand has three amino acids in between the cysteines, while XCLs subclass of two ligands has only second cysteine. According to type of ligands, the chemokine receptors are grouped into 18 chemokine receptors in human like CCR110, CXCR16, CXCR1, and XCR1. The other receptors like ACKR14 and CCRL2 act as

decoy receptors to attenuate the chemokine-induced responses because these receptors may bind chemokine without stimulating intracellular signaling. The chemokine receptors are mostly $G\alpha_{i/o}$ coupled, which inhibit adenylate cyclase to decrease intracellular cAMP and activate of PKA. The chemokines are soluble proteins except two CXCL16 and CXCL1 integral membrane proteins, which are attached to negatively charged glucosamine glycans (GAGs) to be immobilized. The chemokines bind to their cognate receptors in two step such as N-loop chemokine core domain followed by the conserved cysteine motif recognize correct ligand for binding and the ligand N-terminal after first cysteine interacts with domains of receptors. The interaction between CCL14 and ACKR2 differs by involving the second proline of CCL14 (9–74) with the transmembrane bundle of ACKR2 during interaction for β arrestin recruitment and CCL14 degradation. The chemokines may be modified by glycosylation, sulfation, and citrullination, which may be reason for biased signaling through alternative pathway by same ligand. The dimerization state of receptors also influences the signaling as seen in CXCL12 monomer and dimer-activated G-protein-dependent signaling to control Ca flux and inhibition of forskolin-induced cAMP production with same efficiency but monomeric CXCL12 stimulated major response in β arrestin recruitment and chemotaxis. The monomeric CXCL12 interaction with CXCR4 causes slow phosphorylate ERK1/2, and dimeric CXCL12 have rapid and transient phosphorylation. The β -adrenergic receptor interaction with agonist and G-protein induces changes in the $G\alpha$ subunit for displacement and stabilization of the β adrenergic helices TM5 and TM6, curving TM6 extensively outward. The β -adrenergic receptor/agonist/G-protein complex involves ICL2 in addition to TM5 and TM6 at interface. No interaction is found between receptor and the $G\beta\gamma$ subunit and no interaction between the G-protein and receptor TM7 and helix 8 (Fig. 9.14).

The 7TM receptors being dynamic structure may exist in several functionally distinct

Fig. 9.14 Activation of seven transmembrane receptors. The blue color-active β_2 -adrenergic receptor with TM-5 and -6 or -7 interact with G protein or β arrestin, respectively. The structures are visualized with Molsoft Browser Pro©. *Front Immunol.* 2014; 5: 277 (Color figure online)



conformations, but these have similar helical movement in signaling and all have specific domain to regulate these helical movements. The endogenous CCR7 ligands CCL19 and CCL21 induce movement of various T-cell subpopulations and antigen presenting dendritic cells (DCs) to the lymph nodes. Recently, the β -adrenergic receptor and the serotonin 5HT receptor with agonists are found to initiate β arrestin signaling. The ergotamine (ERG) with 5-hydroxy tryptamine 2B 5HT 2B acts as β arrestin-biased agonist and unbiased in G-protein- β arrestin signaling with 5HT 1B, which can be correlated to change in overall helical rearrangements and microswitches-conserved amino acid sequences of seven transmembrane receptor family (Pro-Ile-Phe) in TM3, TM5, and TM6, Asp/Glu-Arg-Tyr in TM3, and Asn-Pro-x-x-Tyr in TM7. While the TM6 is highly significant for G-protein binding, the TM7 is majorly required for β arrestin coupling. The site-specific ^{19}F -NMR label study β -adrenergic receptor has confirmed two conformational states of cytoplasmic ends of TM6 and TM7 depending on whether the receptor-ligand interaction is β arrestin biased or non-biased. The unbiased ligands stimulate a basic shift

toward the active state of TM6, and β arrestin-biased ligands majorly affect the conformational states of TM7.

9.8 The Janus Kinases and Signal Transducers and Activators of Transcription

The Janus kinases (JAKs) and their downstream signal transducers and activators of transcriptions (STATs) mediate hematopoietic cytokine receptor signaling and growth factors signaling. The genetic mutation and translocations of the JAK2 gene are found to be involved in leukemia and other myeloproliferative disorders. The Janus kinases are divided into four families known as JAK1, JAK2, JAK3, and TYK2. The unique feature of the JAK kinases contains two motifs at half of amino-terminal, a Src homology-2 (SH2) domain and a band four point one, ezrin, radixin, moesin (FERM) domain. The SH2 domain was initially known as JH3 and partly JH4 domains. The JAKs have four functional domains, which are known as the FERM domain, the SH2 domain, the pseudo-tyrosine kinase domain, and a catalytically active tyrosine kinase domain (Fig. 9.15).

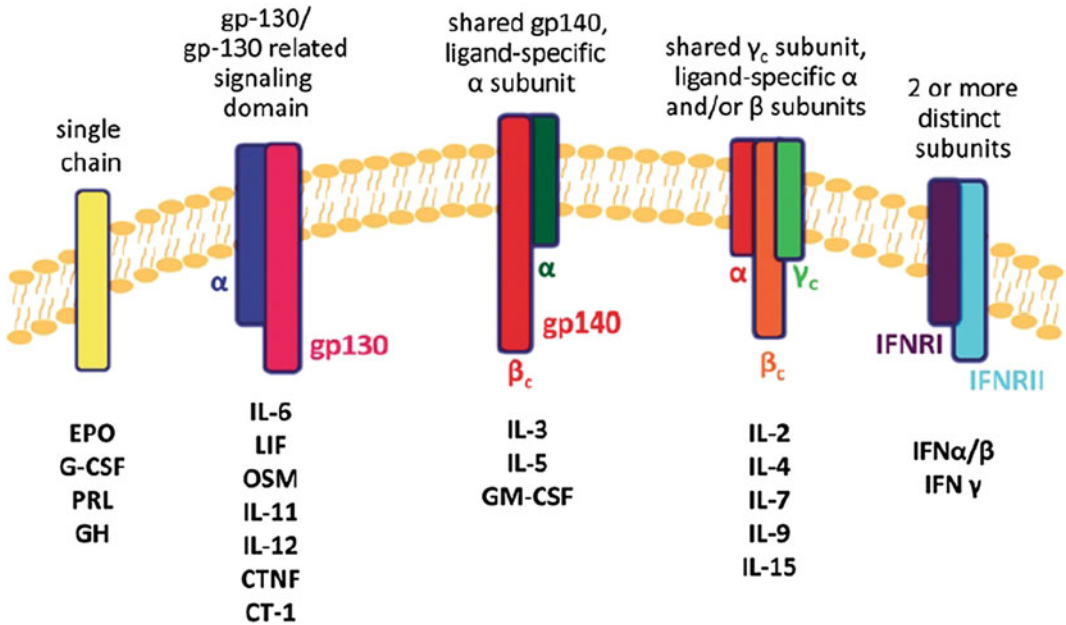


Fig. 9.15 The structure of five super families of cytokine receptor families. *Genes Cancer*. 2010 Oct; 1(10): 979–993

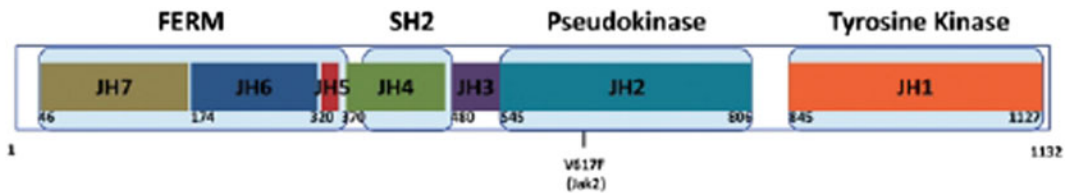


Fig. 9.16 Janus kinase four different domains like the FERM domain, the SH2 domain, the pseudo-tyrosine kinase domain and a catalytically active tyrosine kinase domain

The JH2 domain is negative regulator of JAK proteins. Initially known as JH5 to JH7 and part of the JH4 domains are part of FERM domain to regulate catalytic activity and stimulate association with receptors and other proteins. The FERM and SH2 domains act as receptor and phosphor tyrosine-binding domains, respectively, and the JAK2. The JH1 and JH2 have an extensive homology to tyrosine kinase domains (Fig. 9.16).

The JH1 domain, a functional tyrosine kinase domain has YY motif in the activation loop. Though the JH2 domain have most of the conserved amino acids (characteristic of functional kinases), but it does not have tyrosine kinase activity due to the amino acid binding and

catalytic amino acids. These kinase-like domain may play a significant role in the activity of JAK family proteins and cytokine-induced signaling regulation. The JAK2 and JAK3 JH2 domains negatively regulate the protein kinase activities.

9.8.1 Cytokine Receptor Signaling via JAKs

The agonist-induced homodimeric or heterodimeric interaction of receptor for dimerization or oligomerization causes juxtapositioning of JAKs, which are autophosphorylated or transphosphorylated by other JAKs or tyrosine kinases for increasing JAKs kinase activity. The activated

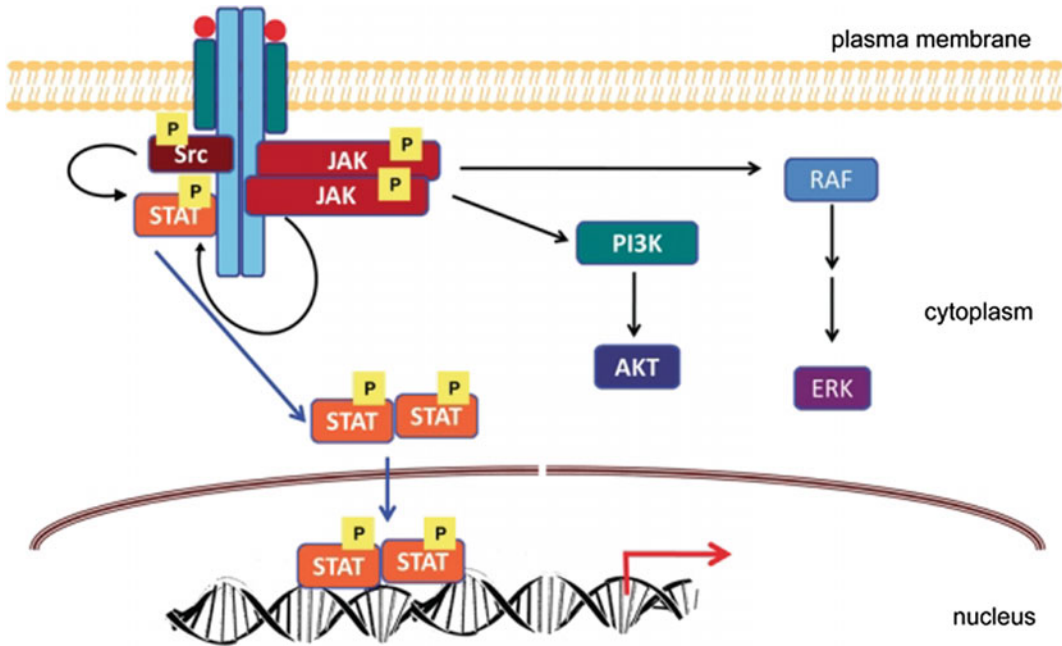


Fig. 9.17 Simple signaling pathways mediated by JAKs. Ligand binding to cytokine receptors induces their dimerization. JAKs, which bind to the receptor via their SH2 domains, undergo transphosphorylation and subsequently phosphorylate STATs. The activated STATs dimerize and translocate to the nucleus, whereby they activate or repress target gene promoters. STATs can also

be directly activated by Src kinases. In this model, JAKs phosphorylate the receptor and create binding sites for STATs. In addition to JAKs and STATs, cytokine receptors also activate additional signaling pathways involving proteins such as Akt and ERK. *Source* Baker et al. (2007)

JAKs may phosphorylate receptors tyrosine on docking site for binding of other SH2 domain-containing signaling molecules. These SH2 domain-containing molecules are STATs, Src kinases, protein phosphatases, and other signaling proteins like Shc, Grb2, and PI3 kinases. For example, the cytokine receptors dimerization is induced by ligand binding and receptor SH2 domain bound JAKs undergo transphosphorylation to phosphorylate STATs. The activated STATs after phosphorylation and dimerization are translocated to the nucleus to activate or repress target gene promoters. The STATs can also be directly activated by Src kinases. In this concept, the JAKs phosphorylate the receptor to create binding sites for STATs. As discussed above, the cytokine receptors in addition to JAKs and STATs may also activate additional signaling pathways through Akt and ERK proteins (Fig. 9.17).

9.8.2 Signal Transducers and Activators of Transcriptions (STATs)

The seven mammalian STAT encoding genes are isolated but alternative splicing, and posttranslational proteolytic cleavage may produce additional forms of STATs1 and STATs3. The STATs basically are transcriptional activators. The STAT4 and STAT5 have two isoforms known as STAT4 α , STAT4 β , and STAT5a, and STAT5b, respectively. The STATs have six well-defined domains known as conserved N-terminal conserved domain, a coiled-coil domain, a conserved DNA-binding domain, a linker region, an SH2 domain and a C-terminal transactivation domain. The STATs can also exist as stable, nonphosphorylated dimers in the absence of cytokine stimulation (Fig. 9.18).

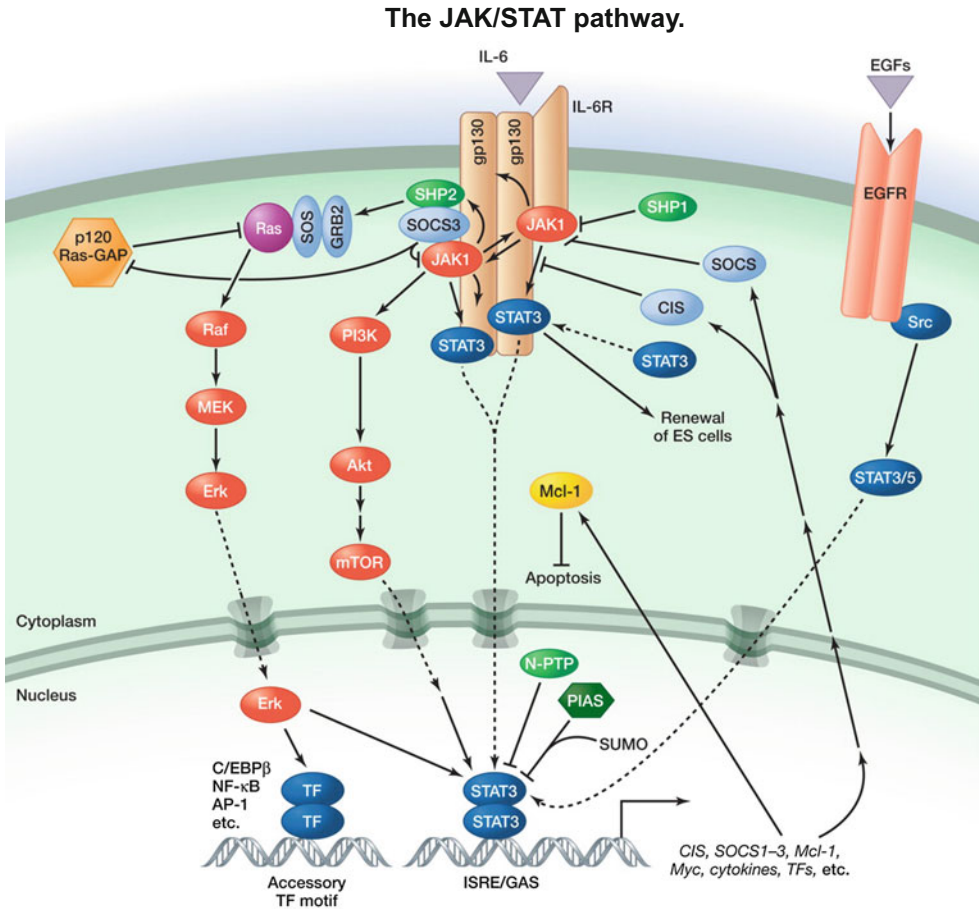


Fig. 9.18 Schematic representation of Janus kinases (JNKs) and signal transducers and activators of transcription (STAT) in detail. Harrison (2012). ©2012 by Cold Spring Harbor Laboratory Press

The STATs N-terminal domain participates in nuclear import, export, receptor binding, and in DNA-binding domain. The dimerization of STAT in inactive state is also regulated by the STATs N-terminal domain. The α -helical conformation of the coiled coil may associate with other regulatory proteins and participate in receptor binding. The activated STAT dimers in the nucleus may bind to consensus DNA-recognition motifs, known as gamma-activated sites (GAS).

Ten γ -activated sequence (GAS) elements with TTNCNNNA are bound by all the STATs except STAT2. The STAT1, STAT2 complex, and IFN regulatory factor (IRF) 9 binds to the IFN α - β -stimulated response element (ISRE),

which has AGTTN TTTC conserved sequence. The role of linker domain is to keep proper conformation between the dimerization and DNA-binding domains. The highly conserved SH2 domain is responsible for STATs recruitment to activated receptor complexes and for the interaction with JAK and Src kinases. The SH2 domain is also involved in STAT homodimerization and heterodimerization for nuclear localization and DNA-binding activities. The C-terminal transactivation domain varies among STATs family members (Fig. 9.19).

The STATs proteins are inactive, unphosphorylated cytosolic proteins without cytokine stimulation. In response to cytokine stimulation, the STATs are phosphorylated at conserved

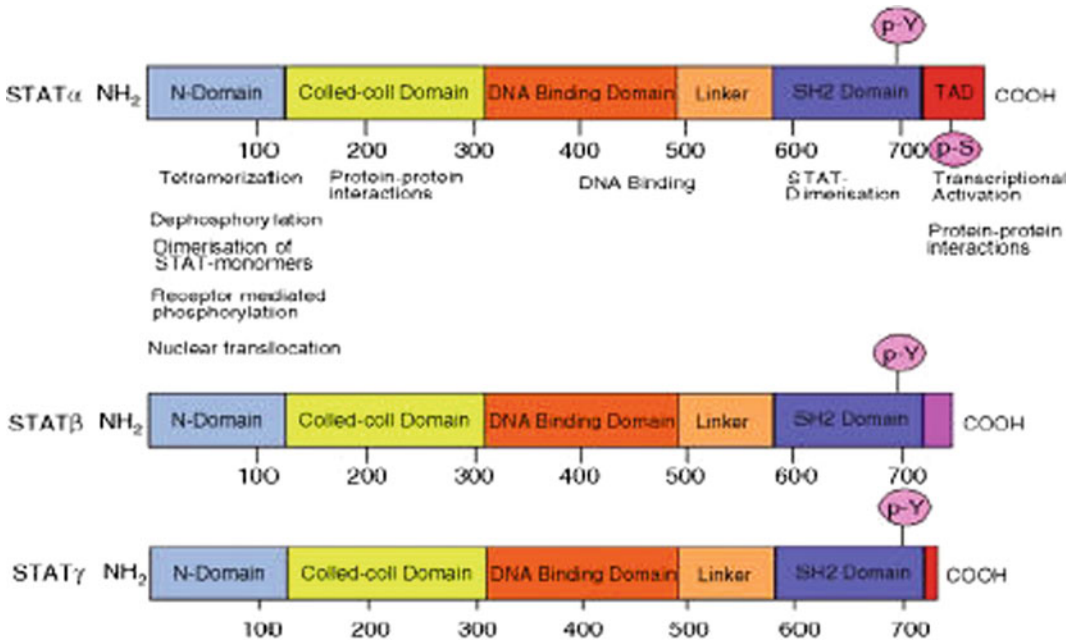


Fig. 9.19 The signal transducers and activator transcription factors (STATs) six domains are shown. The domains are known as N-terminal, coiled-coil, DNA binding, linker, SH2, and transactivation domains. Regulatory phosphotyrosine (pY) and phosphoserine residues (pS) are also shown. The STAT proteins can also be present as C-terminally truncated forms generated by

alternative splicing (STAT β) or by proteolytic processing (STAT γ). The C-termini of STAT β proteins differs from the corresponding STAT α protein not only by being truncated but also by having additional amino acids inserted as a result of the splicing event. *Immunology*. 2005 Mar; 114(3): 301–312

carboxyl-terminal tyrosine residue (Y694 in STAT 5). Apart from JNKs, the STAT is also activated by other tyrosine kinase. The number of inhibitors for Janus kinases has been identified for cancer chemotherapy, which may range from substrate competitive inhibitors like tyrphostin AG490 (canonical JAK2 inhibitor) to ATP competitive pyridones and pyrimidine analogs (Fig. 9.20).

9.9 Receptor Serine/Threonine Kinases

The serine–threonine kinases regulate the metabolism of the cell because protein phosphorylation on Ser, Thr, and Tyr residues is a key mechanism to regulate protein activity and cell function. The eukaryotic Ser/Thr and Tyr kinases are grouped on the basis of sequence homology

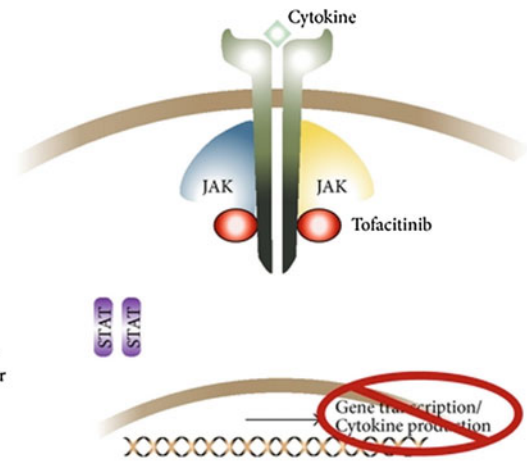
between kinase domains. The eukaryotic Ser/Thr kinase 12 subdomains are folded into a characteristic two-lobed catalytic core structure, where the conserved catalytic active site is formed at cleft. The small N-terminal lobe primarily binds and orients the phosphate donor ATP molecule and the bigger C-terminal lobe is involved in protein substrate binding and initiating phosphate group transfer. The catalytic domain-specific conserved motifs with 12 nearly invariant residues participate in positioning of the ATP molecule and the protein substrate for catalysis.

The Ser/Thr kinases may exist into inactive and active conformation and transition between them is regulated by binding of allosteric effectors and the subcellular localization of these kinases. The N-terminal lobe α -C helix and the C-terminal activation loop are subjected to major conformational change during inactive and active state transition (Fig. 9.21c, d). During transition,

Fig. 9.20 Inhibition of JAK-STAT pathway by Tofacitinib in rheumatoid arthritis. Site for drug targeting

- 1 Cytokine binding to its cell surface receptor leads to receptor polymerization [1]
- 2 Tofacitinib inhibits the phosphorylation and activation of JAKs [2,3]
- 3 JAKs cannot phosphorylate the cytokine receptors. Therefore, the receptors cannot dock STATs [2,3]
- 4 Since the STATs cannot dock, they are not phosphorylated or activated. Gene transcription and cytokine production are thereby inhibited [2,3]

Tofacitinib is a JAK inhibitor



the α -C-helix is shifted toward the active site and results in multiple interactions required for kinase activity between two lobes. The activation segment from conserved DFG to APE motifs has magnesium-binding loop, the activation loop, and the $P + 1$ loop. The variable regions of activation segment known as activation loop decide substrate specificity. The Ser/Thr residue of the activation loop can be either auto phosphorylated or transphosphorylated by other kinases for the various stabilizing interactions in the loop for substrate binding and catalysis. These interactions occur between the phosphorylated Serine/Threonine and the conserved arginine and aspartic acid of the catalytic loop. The phosphorylated Ser/Thr residue interaction with α -C-helix brings the two lobes together for active conformation, the $P + 1$ loop with conserved Ser/Thr decides substrate specificity. The consensus glycine-rich P loop is found to cover both β - and γ -phosphates and participates in phosphoryl transfer. These all interactions lead to major conformational changes for bringing ATP γ -phosphate, catalytic Asp residue and the substrate together for γ -phosphate group transfer from ATP to Ser or Thr residue of the substrates (Fig. 9.22c, d).

9.9.1 Serine/Threonine Kinase Signaling in T-Cell Proliferation

The T-cell antigen receptor (TCR) initiates signaling for T-lymphocyte proliferation and differentiation through cytosolic tyrosine kinases and adaptors. These kinases and adaptors connect TCR to serine–threonine kinases for sending signal from cell membrane to nucleus for gene transcription, which is required for T-cell proliferation and differentiation.

The inositol-(1,4,5)-trisphosphate (Ins(1,4,5) P3) and polyunsaturated diacylglycerols (DAGs) second messengers are generated by phosphatidylinositol-(4,5)-bisphosphate (PtdIns(4,5) P2) at the cell membrane by phospholipase C- γ (PLC- γ)-mediated TCR signaling cascade. The multiple DAG-binding serine–threonine kinases of protein kinase C (PKC) family are expressed on T-lymphocytes. The T-cell interaction with antigen-loaded antigen presenting cells along with MHC induces DAG concentration in the vicinity to activate PKCs and PKDs. The PKC has conserved T -loop motif within the catalytic domain of the enzyme, which has to be phosphorylated by phosphoinositide-dependent

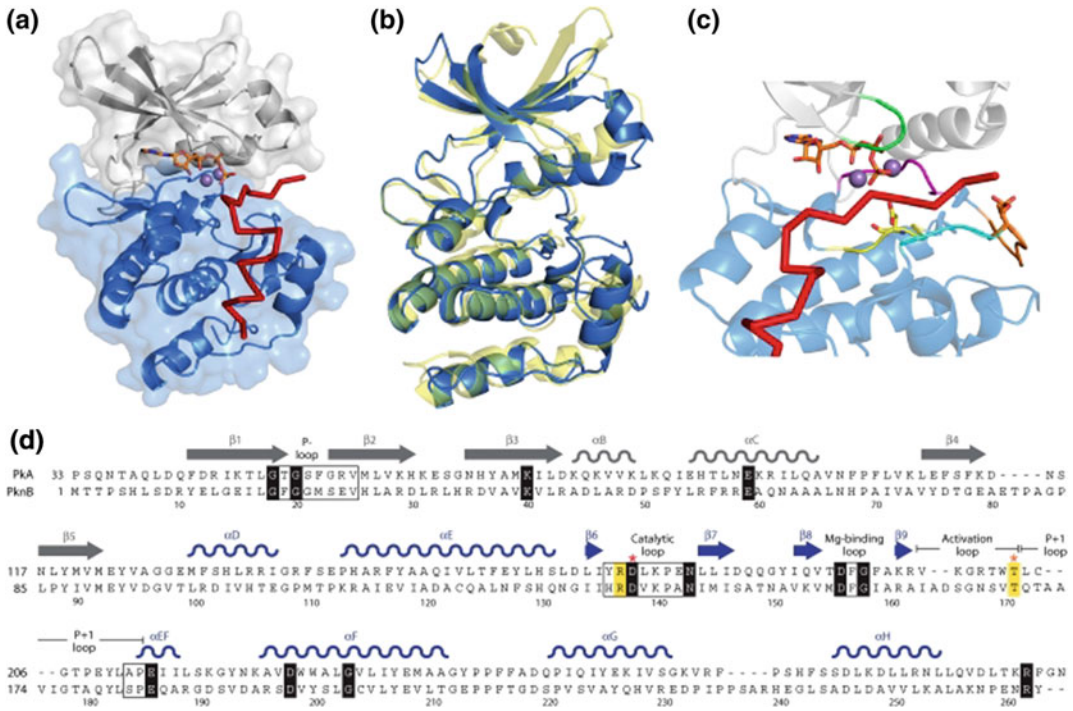


Fig. 9.21 The catalytic domain structure of Ser/Thr kinase in eukaryotes and bacteria. **a** The mouse protein kinase A (PKA) catalytic domain crystal structure complex with an ATP molecule and an inhibitor peptide [Protein Data Bank (PDB) accession number 1ATP]. The PKA N-terminal lobe is gray and the C-terminal lobe blue. The ATP as sticks, two manganese ions as spheres and the inhibitor peptide as a red line are depicted. **b** The PKA (blue) and the *M. tuberculosis* eSTK PknB (yellow) tertiary structure are superimposed PDB accession number 1MRU. **c** The regulatory elements forming catalytic domain between the N- and C-terminal lobes of the Ser/Thr kinase in PKA shown as P loop (green), catalytic loop (yellow) with the catalytic Asp residue,

magnesium-binding loop (magenta), activation loop with the phosphorylated threonine residue (orange) and P + 1 loop (cyan). ATP as sticks with two manganese ions as spheres and the inhibitor peptide as red line are represented. **d** The primary sequence alignment comparison between the PKA (residues 33–283) and PknB (residues 1–266) catalytic domains is shown. The N- and C-terminal lobes of PKA is shown in gray and blue respectively. The conserved motifs are shown in boxes, and the invariant residues are depicted in black. Other important residues are highlighted and/or shown in bold. <https://www.ncbi.nlm.nih.gov/pmc/articles/PMC3063355/> (Color figure online)

protein kinase 1 (PDK1) for PKC activity, so PKC localization and its activation by DAG generation may be limiting step for signal transduction in T-lymphocytes. The polarized exocytosis of the cytolytic granules and antigen receptor-induced reorientation of the centrosome by cytotoxic T-lymphocytes (CTLs) are executed by PKC enzyme. The T-cell adhesion and cell motility by TCR are also regulated by PKC. The guanine nucleotide exchange protein RapGEF2 phosphorylation by PKC- θ stimulated the

guanine nucleotide-binding protein Rap, which induces the integrin LFA-1 activation.

The β -chain of LFA-1 phosphorylation by PKC controls the interaction of LFA-1 with cytoskeletal proteins and regulates LFA-1-mediated cell adhesion. The DAG-PKC signaling cascades may regulate T-cell positioning within lymphoid tissues, T-cell transmigration across endothelial membranes and T-cell contacts with APCs.

The TCR signal generated DAG binds to an N-terminal regulatory domain in PKD2. The

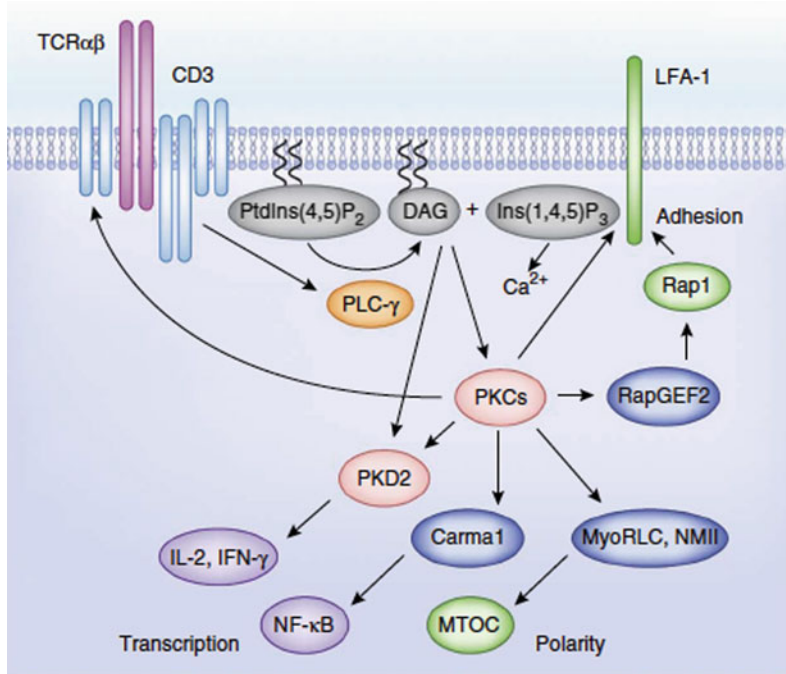


Fig. 9.22 T-cell antigen receptor (TCR) signaling through DAG-regulated serine–threonine kinases in T-cells by PLC- γ hydrolysis of PtdIns(4,5)P₂ to produce two second messenger molecules known as DAG and Ins(1,4,5)P₃. The DAG accumulation in the plasma membrane induces PKC and PKD kinases. The PKC substrates

control the T-cell various activation process like adhesion, building of polarity and transcription. The microtubule organizing center (MTOC), MyoRLC, myosin regulatory light chain (MyoRLC) and nonmuscle myosin (NMII)

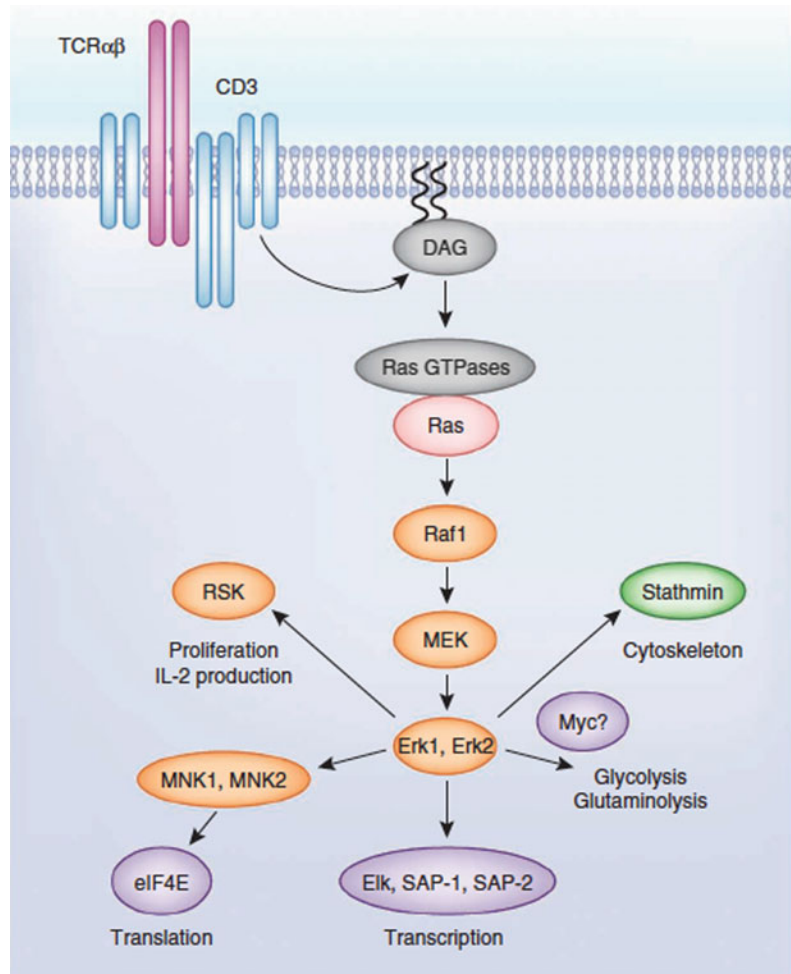
PKD2 is allosterically regulated by phosphorylation by PKC at Ser707 and Ser711 within PKD2 activation loop. The PKD2 activation may transduce TCR-mediated DAG increase from the cell membrane to the cytosol.

9.9.2 Serine–Threonine Kinase Pathways Regulation by Ras

The intracellular localization and PKC-mediated phosphorylation of Ras GRPs by TCR-mediated DAG production regulate Ras (Small GTPases) activity. The Ras GTPases may cycles rapidly between GDP-bound (inactive) and GTP-bound (active) states. In an active form, the Ras can bind to the serine-threonine kinase Raf-1 and activate mitogen-activated protein kinase

(MAPK) cascade to phosphorylate and activate the serine–threonine kinases Erk1 and Erk2. The Ras–Raf–Erk1–Erk2 pathway is involved in signaling for positive selection in thymus and peripheral T-cells. The Erk1 and Erk2 in T-cells phosphorylate transcription factors like ETS-domain transcription factors (Elk1, SAP1, and SAP2) to control expression of immediate early genes (c-Fos, Egr1 and Egr3) in T-cells. The activator protein-1 (AP-1) transcription complex formed by transcription factors c-Fos, Jun, Erk regulated c-Fos regulates transcription of dual-specificity (threonine/tyrosine) MAPK phosphatases to induce negative regulatory feedback pathway for regulating Erk activity time limit of duration and magnitude. Erk1 and Erk2 also control microtubule remodeling by phosphorylation and stathmin regulation. The Erk1 and Erk2 phosphorylate its substrate

Fig. 9.23 Ras GTPases-mediated serine–threonine kinase pathways. TCR-mediated DAG production induces Ras activation for the MAPK signaling cascades. The MAPK signaling induces Erk1 and Erk2 kinase activity for T-cell activation through different substrates, which are required for cytoskeleton remodeling, cell metabolism, transcription, translation, and proliferation



ribosomal protein S6 kinase (RSK), which is involved in cell cycle progression and cytokine production in T-cells (Fig. 9.23).

The signal is initiated by Erk1- and Erk2-mediated phosphorylation of RSK at Ser369, Thr365, and Thr577 in RSK C-terminal catalytic domain, which after activation autophosphorylates its Ser386 and forms PDK1 docking site. The final phosphorylation on Ser227 in the N-terminal RSK kinase domain changes into active conformation. Additionally, the Erk1 and Erk2 phosphorylate the MAPK signal-integrating kinases 1 and 2 (MNK1 and MNK2 and regulatory sites (outside the T-activation loop) in MNK and MNK2 for efficient activation. The MNK1 and MNK2 control

protein translation by phosphorylating eukaryotic translation initiation factor eIF4E in active form.

9.9.3 The Serine–Threonine Kinase Akt

The serine–threonine kinase Akt is regulated by the PtdIns-(3,4,5) P₃. In presence of costimulatory molecules like CD28 and continual activation of class 1 phosphatidylinositol-3-OH kinase (PI(3)K) p110 δ , the T-cells may produce and maintain large amounts of PtdIns(3,4,5)P₃ molecules. The PtdIns(3,4,5)P₃ regulates the serine–threonine **protein kinase B-activity** known as Akt. The phosphorylation of Thr308

in the Akt catalytic domain by PDK1 is found to be rate limiting. The binding of PtdIns(3,4,5)P₃ to Akt pleckstrin homology (PH) domain stimulates conformational change for phosphorylating Thr308 of Akt catalytic domain by PDK1 for activation. The two different mechanisms like co localization of PDK1 and Akt determine Akt activation efficiency. The first mechanism includes PtdIns(3,4,5)P₃ strong binding to the PDK1 PH domain, which is not required for PDK1 catalytic activity but needed for inducing translocation of PDK1 to the plasma membrane for colocalization with Akt. The second mechanism involves Akt phosphorylation on its C-terminal Ser-473 by the kinase complex mTORC2. The phosphorylated Akt dock to a substrate-docking motif on PDK1(PIF pocket). The mTORC2 includes mTOR serine–threonine kinase in complex with RICTOR, MLST8, and mSIN1.

The mTORC2 is understood to regulate hydrophobic motif phosphorylation of AGC family protein kinases like protein kinase A, protein kinase G, and PKC for colocalization and phosphorylation by PDK1 during signaling. The mTORC2 plays important role in differentiation of type 2 helper T(TH2) and TH17 cells by coupling TCR to serum- and glucocorticoid-induced protein kinase 1 (SGK1). There are two independent mechanisms are present for co localization of PDK1 and Akt, while the first one depends on mTORC2 and the PDK1-PIF pocket, the second mechanism relies on PtdIns(3,4,5)P₃ (Fig. 9.24a).

The Akt in TCR signaling regulates phosphorylation and localization of the Fox transcription factors (Fox-o1, Fox-o3a, and Fox-o4). The Fox transcription factors are active and present in nucleus but the phosphorylated by Akt forms complex with 14-3-3 proteins in the cytosol by exiting from nucleus to stop transcriptional activity (Fig. 9.24b).

The T-cells cytokines, cytokine receptors and transcription factors are targeted by Fox-os. The α -chain of the receptor for IL-7 is also induced by Fox-os. The T-cell regulator adhesion molecules transcription is regulated by transcription factor KLF2, which is under fox-os regulation.

As explained above, the TCR signaling can induce phosphorylation and inactivation of Foxes through Akt. The KLF2 enhances in L-selectin (CD62L) adhesion molecule gene transcription and it participates in the transmigration of T-cells across high endothelial cells. KLF2 acts as promoter for the chemokine receptor CCR7 and sphingosine 1-phosphate receptor S1P1 gene transcription also. The CD62L and CCR7 regulate lymphocyte entry and retention into secondary lymphoid tissues, and S1P1 control T-cell egress from lymph nodes.

9.10 Tumor Growth Factor (TGF- β) Signaling

The transforming growth factor β has TGF- β 1, TGF- β 2, and TGF- β 3, which are multifunctional pro-inflammatory cytokines. TGF- β is involved in various functions of the cell-like regulation of cell adhesion and migration, stimulation of extracellular matrix production, and regulation of immune and endocrine functions and produced as type II transmembrane protein arranged in stable homotrimers in variety of cells and secreted as latent precursor (latent TGF β 1) in complex with latent TGF β binding proteins (LTBP). The TGF β 1 is active only after proteolytic cleavage from LTBP by plasmin or reactive oxygen species or thrombospondin 1 or acid. The active soluble or membrane TGF may bind to TGF receptors family members, which are of two types of receptors known as type I and type II. The extracellular domain of TGF receptors-I (TGFR I) have three well-ordered cysteine-rich domains (CRD-1, CRD-2, and CRD-3) and fourth membrane-proximal cysteine-rich division. These cysteines may differentiate among TGF receptor superfamily. The number of cysteines may range from one to six. The N-terminal preligand-binding assembly domain supports preassembly of TNFR1 into trimeric complexes to stop spontaneous receptor auto activation (Fig. 9.25).

No enzyme activity is found in receptors intracellular domain, but TNF type I receptor has intracellular protein–protein interaction death

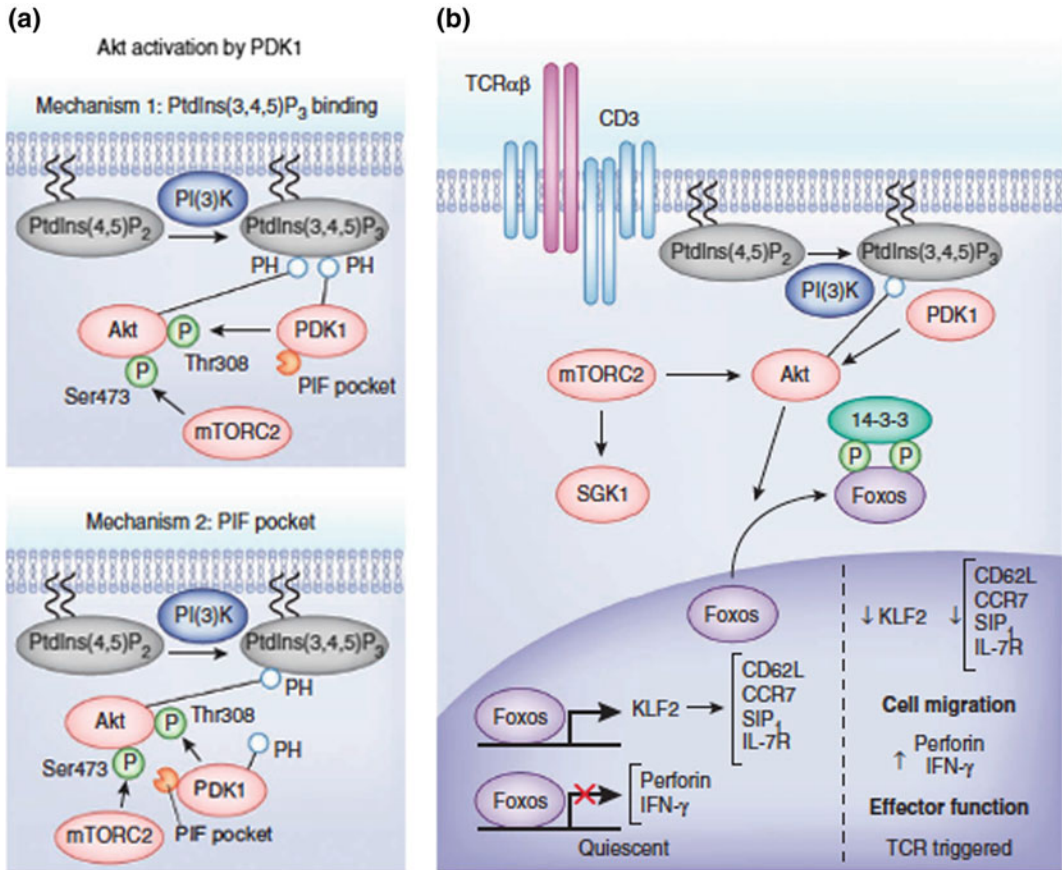


Fig. 9.24 The serine–threonine kinase Akt signaling induced by PtdIns(3,4,5)P₃. **a** Akt activation mechanism induced by PDK1. One of the two known mechanisms for co localization of Akt and PDK1 depends on PDK1 binding to PtdIns(3,4,5)P₃, and other depends on PDK1 recruitment to Akt via mTORC2-mediated Ser473

phosphorylation. **b** Role of the serine–threonine kinase Akt in TCR signal transduction. Akt activation by PDK1 regulates subcellular localization and Fox-o family of transcription factors in T-cell signaling. Fox-os regulate the expression of intermediate signaling molecules to control T-cell trafficking and effector molecules functions

domain (DD) to recruit other DD-containing proteins for apoptosis through caspase activation. The ligand binding to receptor induces dissociation of silencer of death domain and recruits the adapter protein TNF receptor-associated death domain (TRADD) on the exposed death domain. The TRADD association with TGF receptor may recruit other downstream signaling proteins such as TNF receptor associate factor-2 (TRAF2). The 55 kDa TNF receptor1 (TNFR1) present in all cells can activate nuclear factor kappa B (NF- κ B) and apoptosis according to cell environment. The bigger 75 kDa TNF receptor II (TNFR2) is expressed at low levels in immune cells in

normal physiological conditions. The TNF R II are expressed in neuronal subtypes, oligodendrocytes, microglia and astrocytes of the brain, endothelial cells, and certain T-cell subtypes such as lymphocytes (CD4⁺ and CD8⁺ T-cells), thymocytes and myocytes. While TNF receptor I indirectly recruit TNF receptor-associated factor (TRAF) for gene expression, the TNF receptor II directly involves in recruitment and cross talk with TNF receptor I also. The macrophages, lymphoid cells, mast cells, endothelial cells, fibroblasts, and neuronal tissue all may produce TNF. The tumor necrosis factor may exert its biological effect in paracrine or autocrine manner

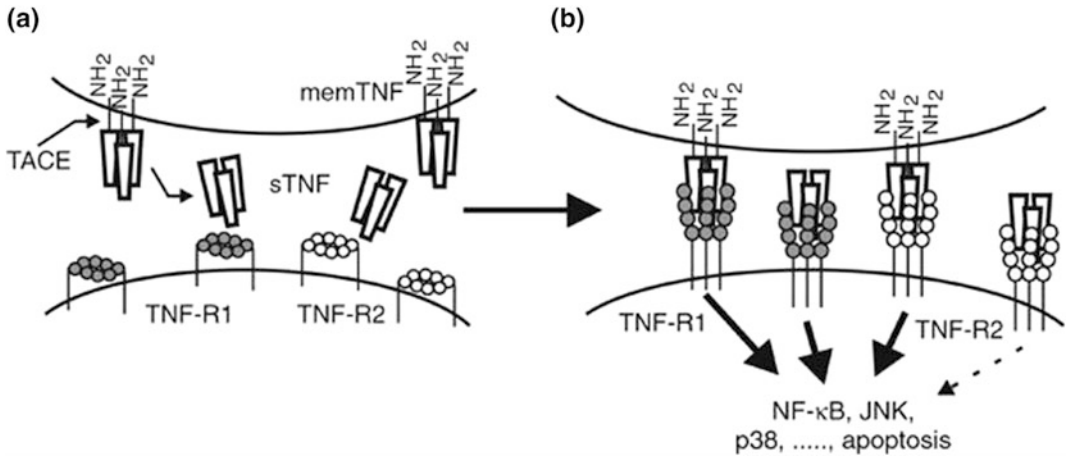


Fig. 9.25 The structure of tumor necrosis factor. **a** Membrane-bound TNF (memTNF). **b** Soluble TNF (sTNF). The TNF binds to both two types of the TNF receptor

superfamily, TNF receptor-I and TNF receptor-II. The membrane TNF may activates both types of TNF receptors. The soluble TNF majorly induces TNF receptor 1

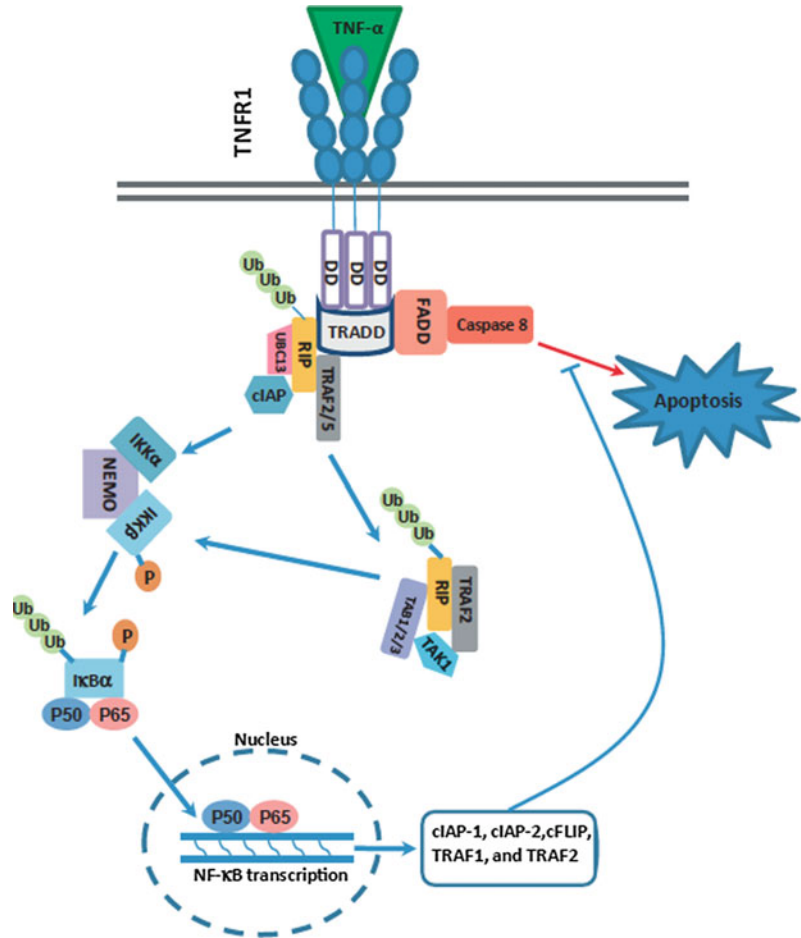
through Smad-dependent or Smad-independent signal pathway. Any defect in TGF- β factor may cause fibrosis, immunosuppression, cancer, and many other human diseases. The Smad-dependent signaling pathway induced by TNF β play a major role in many pathophysiological processes of kidney disease. The TGF β receptor type I (T β RI) kinase activation by binding of TGF β 1 to its receptor II (T β RII) can phosphorylate Smad2 and Smad3 and two receptor-associated Smads (R Smads). The phosphorylated Smad2 and Smad3 form the Smad complex by binding to Smad4 for translocation of the complex to nucleus for target gene transcription with the inhibitory Smad7. The Smad7 is negative regulator of Smad2 and Smad3, which cause degradation of the T β RI and Smads through ubiquitin proteasome (Fig. 9.26).

The highly upregulated TGF β 1 in renal fibrosis upregulates extracellular matrix (ECM) production and inhibits its degradation. The TGF β 1 stimulates tubular epithelial cells (TECs) transformation to myo fibroblasts by epithelial mesenchymal transition (EMT). TGF β 1 has well-defined anti-inflammatory function as

found in NF κ B-mediated renal inflammation through induced Smad7-dependent I κ B α -expression. The Smads like Smad2 and Smad3, which integrate signal by interacting with mitogen-activated protein kinase (MAPK) signaling pathway, can be activated by other molecules than TGF β 1 and participate in pathophysiological processes of kidney diseases. The advanced glycation end products (AGEs) in diabetes are found to stimulate Smad2 and Smad3 independent of TGF β 1 through ERK/p38 MAP kinase pathway. The angiotensin II may induce ECM generation through AT1 receptor-mediated ERK/p38 MAP kinase in hypertensive condition via Smad signaling as shown in Fig. 9.27. The TGF β 1 stimulation through Smad3 in renal fibrosis is very clear, but Smad2 role still is unknown in the kidney disease. The TGF β 1 also regulates angiogenesis and defective angiogenesis may cause progressive renal fibrosis.

The common Smad, Smad4 participate in various function for causing Smad3-mediated renal fibrosis and down regulating NF κ B-driven renal inflammation through Smad7-induced expression at transcription level (Fig. 9.28).

Fig. 9.26 The TGF or TNF-induced signaling via TNFR1. DD is death domain, cIAP is cellular inhibitor of apoptosis, FADD is called as Fas-associated death domain protein, cFLIP is caspase-8 homolog FLICE-inhibitory protein, IKK is I κ B kinase, I κ B α is known as inhibitor of kappa B, NF- κ B is nuclear factor kappa B, RIP is receptor interacting protein, TRADD is TNF receptor-associated death domain, TRAF is TNF receptor associate factor and TNF is tumor necrosis factor, and TNFR1 is tumor necrosis factor receptor-1



9.11 Atrial Natriuretic Peptide Signaling

The three types of natriuretic peptides (NPs) with their three cognate receptors are identified on the basis of their specific agonist and production of intracellular cGMP by guanylyl cyclase activity. The atrial and brain natriuretic peptides (ANP and BNP) bind natriuretic peptide receptor A (NPR A) for guanylyl cyclase activation. The other C-type natriuretic peptide (CNP) prefers to bind natriuretic peptide receptor B (NPR B) to activate guanylyl cyclase. The natriuretic peptide receptor-C (NPR C) is known as silent receptor and all three natriuretic peptides may bind to this receptor. The physiological function of atrial natriuretic factor/peptide (ANF/ANP) is to

regulate extracellular fluid volume, electrolyte balance, cardio vascular homeostasis, and arterial pressure in humans. These natriuretic peptides are also found to be ant hypertrophic, and anti-inflammatory. These NPs downregulate release of renin, aldosterone, and vasopressin and up regulate synthesis and release of testosterone progesterone and luteinizing hormone. The all three types of natriuretic peptides (NPs) enhance cGMP level during signaling but CAMP, calcium, and inositol triphosphate (IP) changes may vary in different cells. The atrial natriuretic peptides decrease cAMP, calcium, and IP concentration, and NPRC is found to increase these metabolic signaling molecules concentrations. The de Bold and his group in 1980 first isolated these natriuretic peptides from atrial extracts, but now it is known that ANP is primarily

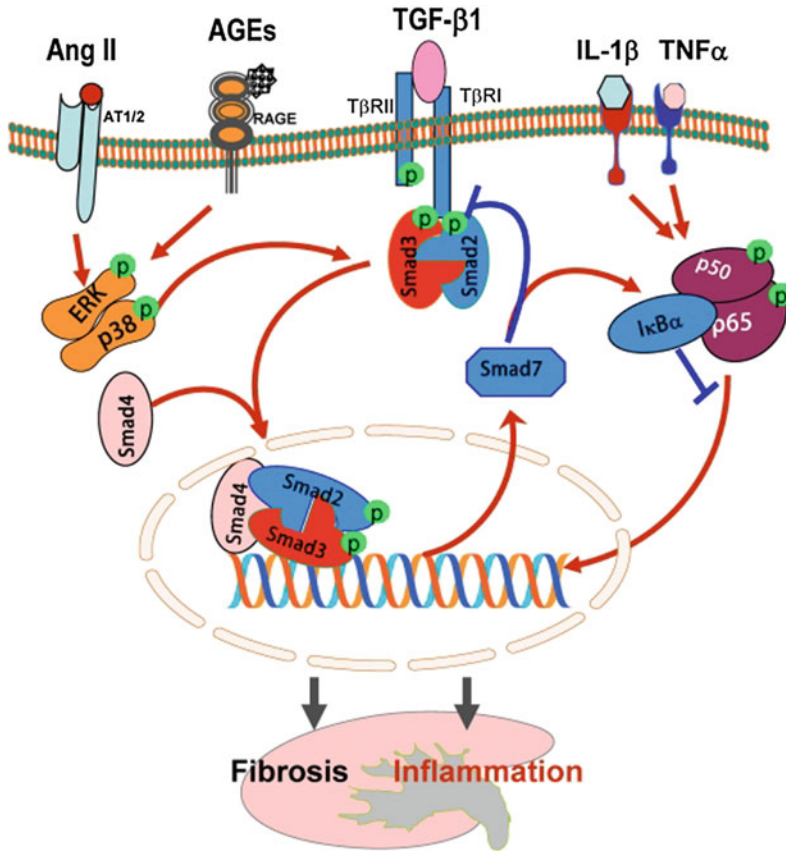


Fig. 9.27 TGF- β /Smads and crosstalk pathways in renal fibrosis and inflammation. After binding to T β RII, TGF- β 1 activates the T β RI-kinase which phosphorylates Smad2 and Smad3. The phosphorylated Smad2 and Smad3 forms Smad complex with Smad4. This complex is translocated in to nucleus for target gene transcription regulation along with inhibitory Smad7. The Smad7 block Smad2/3 activation through T β RI and Smad destruction

for inhibiting NF- κ B-driven inflammatory response by inducing I κ B α , which is an inhibitor of NF- κ B. The Ang II and AGEs can activate Smads independent of TGF- β 1 via the ERK/p38/MAPK crosstalk pathway. The Blue lines (symbols) depicts negative regulation pathways and red arrows (symbols) shows pathogenic or positive regulation pathways (Color figure online)

synthesized and secreted from heart atrium granules and BNP is majorly produced in the heart ventricle. The BNP has most variable amino acids sequence. The most conserved human NPC is mostly found in endothelial cells.

The ANP is produced as pre-pro-ANP of 152 amino acid residues with active peptide toward C-terminal, which is converted into active fragment of 28 amino acid residues (99–126). The disulfide bonded between cysteine 105 and 121 in active conformation of ANP is essential for biological activity. Infact, all three NPs share highly conserved 17 residues disulfide bonded

ring of amino acids but are variable in N-terminal and C-terminal domains.

The C-terminal sequence Asn-Phe-Arg-Tyr projecting from conserved cysteine ring structure is also necessary for the biological activity of ANP loop.

The NPs receptors molecular weight may range from 60–180 kDa. The active form of NPRA is found to be homodimer. The ANP and BNP has four defined domains such as extracellular ligand-binding domain, single transmembrane GC catalytic domain, intracellular protein kinase-like homology domain (protein-KHD) (Fig. 9.29).

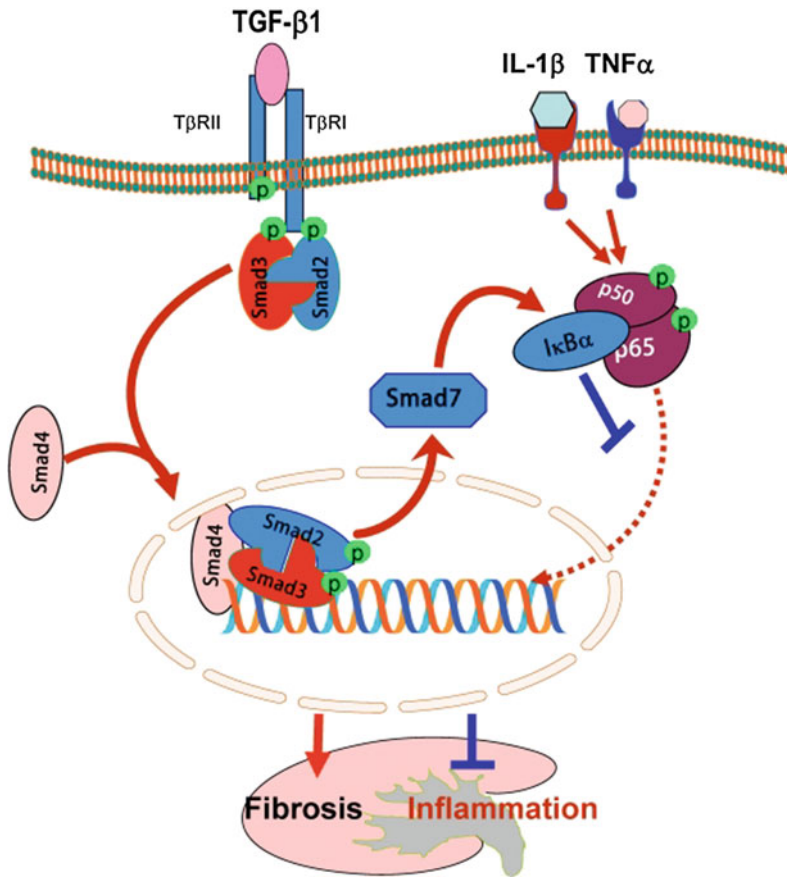


Fig. 9.28 Smad-4 diversified role in renal fibrosis and inflammation. The Smad4 may form the Smad complex by binding to phosphorylated Smad2/Smad3. The complex is translocated into nucleus for target genes

regulation involved in fibro genesis including Smad7. The over expression of Smad7 inhibits NF-κB/p50/p65 from being phosphorylated and nuclear translocation by inducing IκBα expression

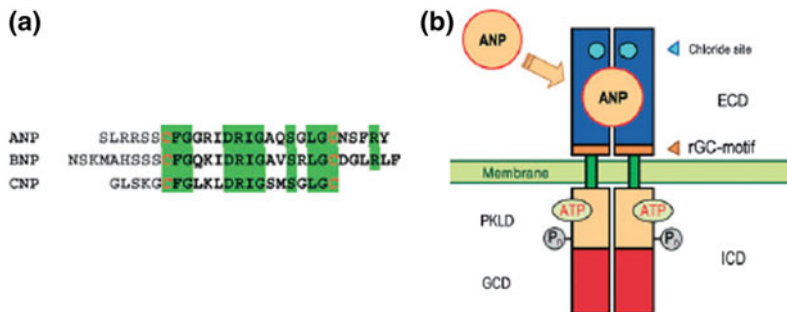


Fig. 9.29 **a** Amino acid sequences of ANP, BNP, and CNP from rat. Two cysteines in each peptide form an intramolecular disulfide bond, which is essential for the activity. The conserved residues are shaded. **b** The molecular topology of NPRA. NPRA occurs as a preformed homodimer. The diagrams depict each monomer with four different domains. The extracellular ligand binds ECD, transmembrane domain, and an intracellular

domain (consisting of a PKLD and a GCD). The ECD contains a highly conserved residues. The ligand in the picture is chloride and a juxtamembrane GC-signature motif is shown. The juxtamembrane GC-signature motif is important in transmembrane signal transduction. The PKLD binds the positive allosteric effector ATP and is phosphorylated at multiple sites

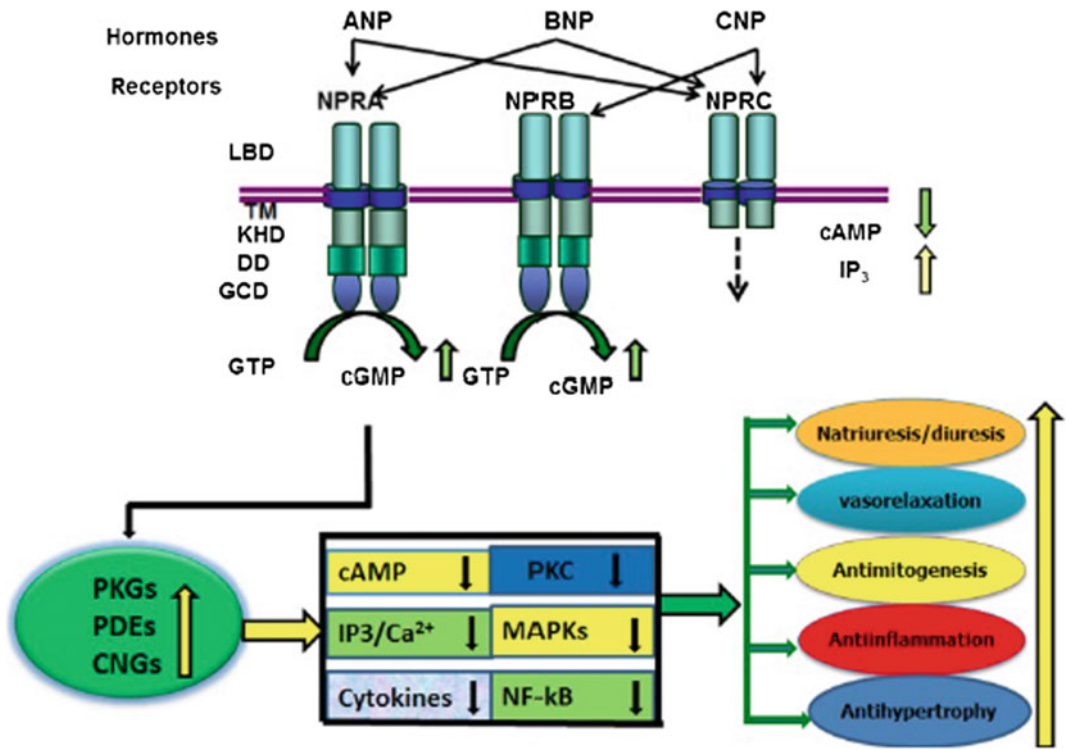


Fig. 9.30 GC-A/natriuretic peptides A receptor diagrammatic representation of the ligand specificity and functions. The intracellular cGMP production is stimulated by ANP binding to ligand to activate three cGMP effector molecules, which are known as cGMP-dependent protein kinases (PKGs), cGMP-dependent phosphodiesterase (PDEs), and cGMP-dependent ion-gated channels (CNGs). The ANP/NPRA/cGMP signaling might alienate the various pathways like the intracellular formation of

cAMP, calcium, inositol triphosphate, cytokine expression and the activation of protein kinase C (PKC), and mitogen-activated protein kinases (MAPKs). The resulting signaling cascade may copy or extend the physiological responses of ANP/NPRA. The abbreviations used are LBD-ligand-binding domain, TM transmembrane domain, protein-KHD-protein kinase-like homology domain, and GCD-guanylyl cyclase catalytic domain. <https://www.ncbi.nlm.nih.gov/pmc/articles/PMC4141235/figure/F1>

The dimerization region of these receptors is found between the KHD and GC catalytic domain, which may form an amphipathic alpha helix structure. The NPRC has large extracellular domain (496 amino acids residues), single transmembrane domain, and short cytoplasmic tail (37 amino acid residues) with no sequence homology with other known NPs receptors, that's why it is called as silent receptor. The two pairs of cysteine residues along with one isolated cysteine near transmembrane are present in extracellular domain, and three potential signals for N-glycosylation with many serine/threonine for O-linked glycosylation sites are found in the extracellular domain of NPRC. The NPRC plays

role in biological activity but not in clearance in other NPs. The ligand-induced internalization of receptors downregulate signaling. The transforming growth factor β , angiotensin II, and endothelium ET-1 downregulates NPRA at transcription level in various cultured cells. The receptors are suggested to exist into phosphorylated and unphosphorylated forms. The binding of ANP to its receptor enhances dephosphorylation, which caused reduced activity of GC catalytic domain (Fig. 9.30).

NPRC bound with ligand NPC is internalized through receptor mediated endocytosis for receptor down regulation. The cGMP generated may allosterically regulate receptor activity.

ATP is also regulating allosterically of GC catalytic activity because, the ATP interacts with KHD of receptor to enhance cGMP production with changing substrate affinity. The molecular cloning experiments have shown the ligand-induced activation of GC catalytic domain also requires ATP binding to KHD region of the receptor. The NPRA and NPRB have conserved and consensus ATP binding glycine-rich motif in KHD domain and hinge region of NPR. A near membrane on ligand binding undergoes conformation change, which might participate in transmembrane signaling. The conserved region in GC-A/NPRA is found to have numbers of proline with pair of cysteine and mutation in any proline may result in loss of GC catalytic activity without affecting ligand binding.

ANP is reported to inhibit auto phosphorylation and PKC enzyme activity in different types of cell. The potassium channels activation in ATP and PKG-dependent manner is induced by ANP. The positive effect of ANP on GC activity is well known, which might decrease cAMP, calcium and sodium influx or increase depending upon types of cell and act as antagonist for PKC and mitogen-activated kinases. This heterogeneity might involve different mechanism of signaling. The cytoplasmic decrease of calcium in vascular smooth muscle cells occurs through sarcoplasmic ATPase, which is activated by ANP-induced production of cGMP.

The ANP-dependent inhibitory effects on the phosphoinositide metabolism and PKC autophosphorylation, and enzyme activity might be exerted in complex or individual manner to negatively regulate the phosphoinositide, Ca, and PKC involving ANP/NPRA/cGMP/PKG cascade needs further detail study.

9.12 Cell Adhesion Receptors

The extracellular matrix (ECM) surrounds all cells in solid tissues to provide mechanical support, biochemical barrier, and a medium for extracellular communication. The extracellular matrix is made up mainly of proteins and carbohydrates. The extracellular matrix in plant cell

may be defined as cell wall and fibril or basement membrane in animal cells. The stability of cell shape and position is also provided by extracellular matrix, but the most important function of ECM is communication between cells. The cell adhesion molecules participate in signaling for carrying out cell–matrix interactions, cellular differentiation, morphogenesis, proliferation, and migration, embryogenesis, wound healing, inflammation, and cancer. The various cell adhesion receptors molecules are identified such as integrin, cadherins, selectins, syndecans, and the immunoglobulin superfamily of cell adhesion molecules (Ig-CAMs), which participate in signal transduction. The cooperation between cell adhesion receptors and conventional signaling receptors.

A. Signaling by Cadherins

The cadherins cell adhesion receptors participate in homotypic cell–cell adhesion in calcium-dependent manner. On the basis of their associated partners and cytoskeletal molecules, the cadherins are divided into two subfamilies. The first subfamily members are known as N, P, R, B, and E and have 10 other members also and these are resided in adherence-type junction to form linkage with actin protein of cytoskeleton. The second subfamily desmosome associated cadherins have desmogleins and desmocollins. The other protocadherins are found important in development of nervous system. On the cell surface, the cadherins receptor is serially dimerized in such a way that lateral movement of these receptors with the opposite dimers receptors at junction may zip up into stable adhesion between cells.

Cadherin receptors can be divided into three function domain, the extracellular N-terminal domain with five tandem repeats, a single transmembrane and approximately 150 amino acids residues containing C-terminal domain. The N-terminal repeat is site for ligand binding, and other tandem repeats are site for calcium binding. The C-terminal is interaction site for intracellular proteins, which are known as catenins. While the β catenins bind C-terminal end of cadherins

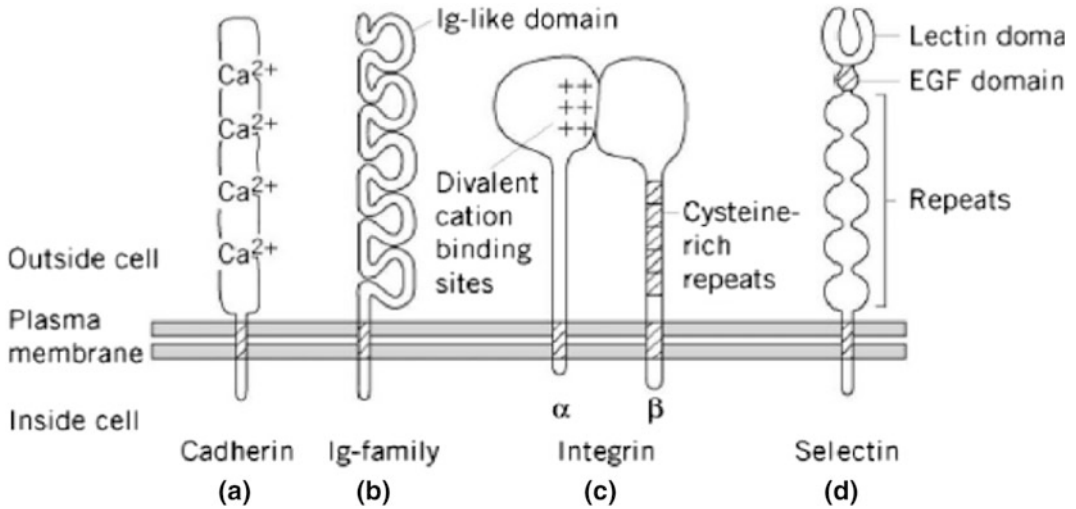


Fig. 9.31 The various types of cell adhesion receptor family

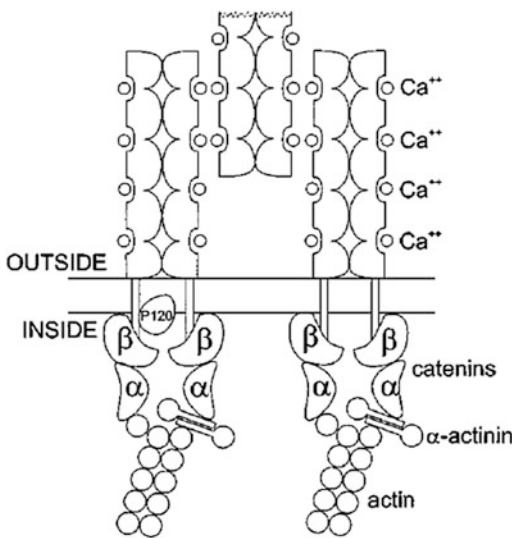


Fig. 9.32 Cell adhesion receptors cadherins with their associated cytoskeletal components and extracellular ligands and bound proteins that joins them to the actin cytoskeleton. *Annu. Rev. Pharmacol. Toxicol.* 2002. 42:283–323

directly, the α catenins bind through β catenins. The other p120 catenins bound to cadherins participates in Rho GTPases signaling (Fig. 9.31).

The cadherins are important for tissue organization and morphogenesis during development, any defect in expression may cause invasive and malignant tumor of epithelial cells (Fig. 9.32).

The cadherins and β catenin are involved in Wnt/wingless signaling for regulating the differentiation, development, and malignancy. The β catenin is found in three pools in the cell physically such as bound to cadherins at membrane, in the nucleus bound to LEF/TCF family of transcription factors and in cytoplasm bound either to adenomatous polyposis coli (tumor suppressor gene product) or with axin/conductin. The nuclear pool of β catenin with LEF controls cell cycle and epithelial regulator genes transcription such as cyclin D1 gene. The active glycogen synthetase 3 β kinase (GSK 3 β) induces phosphorylation of β catenin in APC/axin complex for its ubiquitination and proteasome-mediated degradation. The Wnt signaling protects β catenin from degradation and induces its transport to nucleus for its accumulation so it may regulate transcription. The homotypic interaction of N-cadherins induces cell cycle arrest by increasing the concentration of cyclin-dependent kinase inhibitor p27 and participates in muscle cell differentiation signaling. The E-cadherins are also involved in p27 upregulation. The β catenin linked axin protein acts as scaffold protein for c-Jun Kinase pathways proteins. The E cadherin homotypic interaction causes PI-3-kinase and protein kinase B activation through signaling. VE-cadherin in

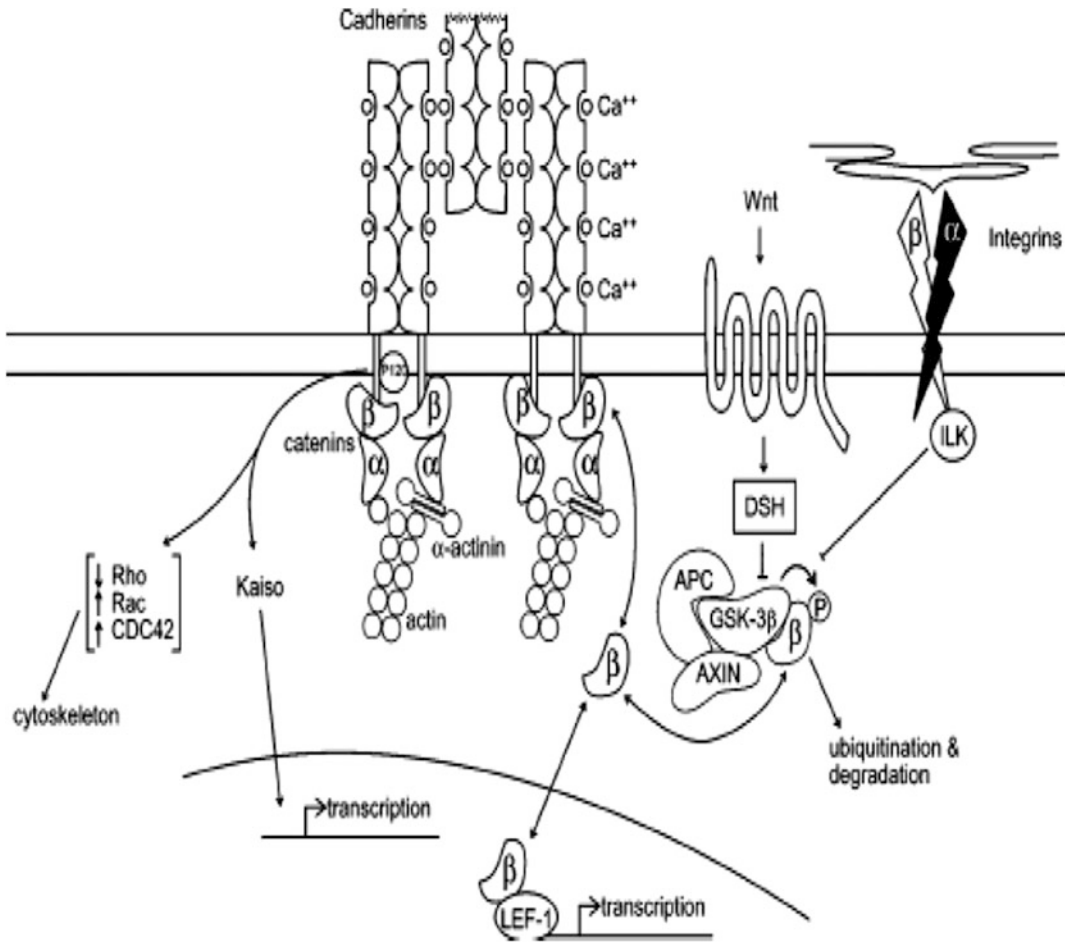


Fig. 9.33 Cadherins regulate signaling in the Wnt pathway. The ability of beta catenin for transport to nucleus and its participation in transactivation of genes is regulated by the concentration of its cytoplasmic pool, which in turn is controlled by binding of beta catenin to

cadherins at cell–cell adhesion sites and by the Wnt pathway. Cadherins also participates in other signal pathways like p120-catenin signals to Rho GTPases and to the transcription factor Kaiso

endothelial cells by forming with VEGFR-2, β catenin, and PI-3-kinase induce endothelial cell survival. The integrin-linked kinase (ILK), an ankyrin-repeat containing serine/threonine kinase upregulation is responsible for cell cycle progression and transformation, but in epithelial cells, the ILK disrupts cell–cell through β catenin signal pathway regulation (Fig. 9.33).

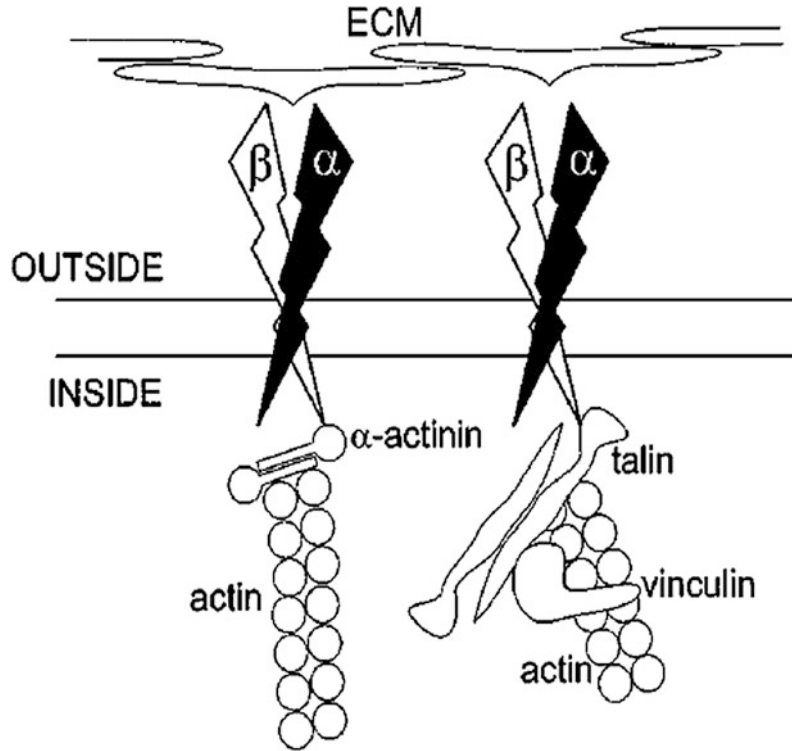
B. Signaling by the Integrins

The integrins like fibronectin, laminin, or collagen forms specialized complex, called as focal

adhesions sites at cell-ECM. The integrins belong to heterodimeric cell surface receptors having two dissimilar subunits α and β subunits joined noncovalently. There are till now 20 receptors of various 18 α , and 8 β subunits are identified in vertebrates as shown in Fig. 9.32.

Mostly, integrins are extracellular proteins but some like $\beta 2$ and $\alpha 4\beta 1$ integrins can participate in heterotypic cell–cell adhesion. The ligand specificities are decided by the α and β subunits number and associations on extracellular side. The integrins may bind to many ligands at one time, but the fibronectin $\alpha 5\beta 1$ exceptionally has

Fig. 9.34 Cell adhesion receptors integrin with their associated cytoskeletal components and extracellular ligands and bound proteins that join them to the actin cytoskeleton. *Annu. Rev. Pharmacol. Toxicol.* 2002. 42: 283–323



one ligand only. The many number of integrin receptors can also bind to same protein as seen with fibronectin, where many fibronectins bind to single protein. The integrins may bind to same region or different region of ligand (Fig. 9.34).

The ligand binding to integrins stimulate major conformational changes along with relative movements of subunits. The various affinity stage of ligand and integrins may be controlled by extracellular divalent ion and signaling pathways including R-Ras and Rap1 small GTPases. The cytoplasmic domain of both the subunits of integrin by interacting with various intracellular proteins of signal pathway plays an important role in cytoskeletal organization, cell motility, signal transduction and regulation. The integrins may directly activate signal pathway like integrin-mediated adhesion increase tyrosine phosphorylation through nonreceptor tyrosine kinase or focal adhesion kinase (FAK) (Fig. 9.35).

The FAK protein has central kinase domain between N-terminal and focal adhesion target site C-terminal. The C-terminal is involved in

recruitment of FAK, which in turn may bind to many other proteins like c-Src, PI-3-kinase, GRAF (a RhoGAP), paxillin, talin, and p130 Cas. The one model of activation explains the integrin interaction with ECM recruit FAK and auto phosphorylate it at Y397 to create binding site for c-Src SH2 domain and Src is recruited to phosphorylate FAK at additional sites. The one phosphorylated residue Y925 binds to SH2 domain of the adaptor protein Grb-2. The recruitment of Grb-2 and its partner Sos exchange factor induce Ras activation for downstream kinase cascade of Raf-1, Mek, and Erk activation.

The other model explains integrin mechanism through Erk cascade activation including the transmembrane protein caveolin-1, the Src-family kinase Fyn, and the adaptor protein Shc without FAK. The integrin α subunit induces phosphorylation of Shc by Fyn for the recruitment of Grb-2/Sos complex. These changes lead to Ras and downstream kinases leading finally Erk activation. The majority of integrins bind

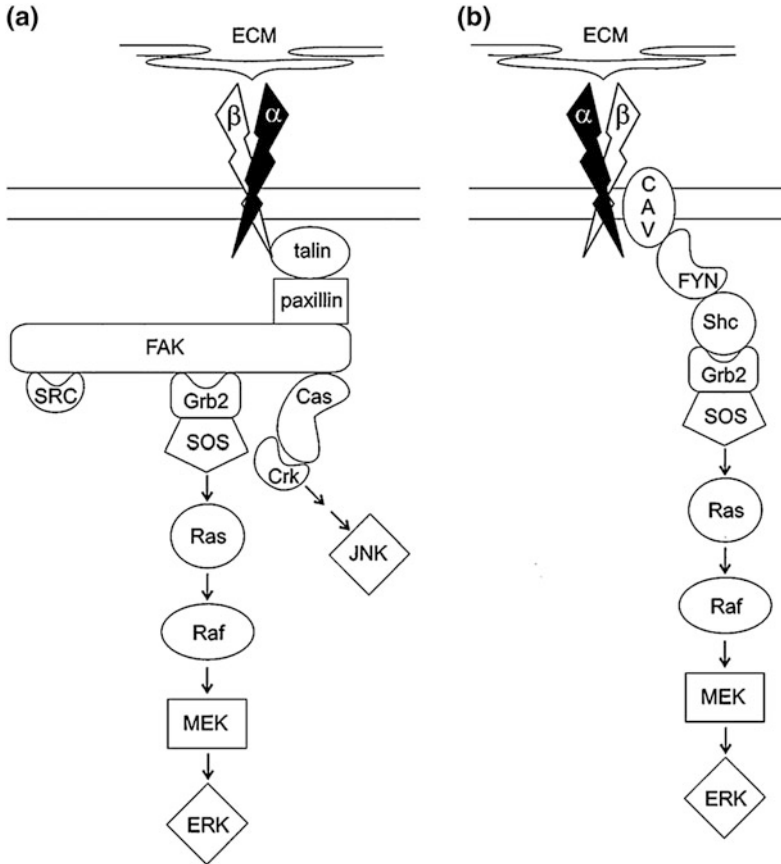


Fig. 9.35 Integrins signal pathway. There are two models explaining direct activation by integrin. One **a** is through Erk/MAPK cascade, where the integrin causes recruitment and activation of FAK along with its autophosphorylation to create a binding site for the Src tyrosine kinase for further phosphorylation of FAK. These changes induce the Grb2-SOS complex binding and

triggering Ras activation which in turn may activate Raf, Mek, and Erk signal pathways. A second pathway starts from p130 Cas and lead to Crk and c-Jun kinase activation. In the other model **(b)** some of the integrin molecules may interact with Fyn and Shc through caveolin. The phosphorylation of Shc by the Fyn tyrosine kinase recruits Grb2-SOS for activation of the cascade

caveolin, but few integrin heterodimers molecules can activate Fyn. The reason for the difference is not clear now but caveolin removal is found to disrupt integrin-mediated adhesion and signaling. The Ras is found to participate in both the model in integrin signaling.

The Rho-family of small GTPases along with many other cellular processes also regulates the actin cytoskeleton. The Rho regulates stress fibers, and Rac and CDC 42 control actin fibers like lamellipodia and filopodia. The Rho and Rac induced ROCK kinase and p21 activated kinase (PAK), respectively, activate by phosphorylation

to LIM kinase. The LIM kinase phosphorylates and inactivates actin depolymerizing protein cofilin for promoting actin filament assembly.

The Neu RTK and actin have been observed in mammary carcinoma cells integrin-mediated cell anchorage, and formation of cytoskeletal complexes is found to regulate the RTK/Ras/MAPK pathway in three different levels. First is at RTK activation, the second Ras to Raf coupling in the pathway, and third level is to control signal transmission between the cytoplasm and nucleus. The active integrin ligand complex may induce tyrosine phosphorylation of

epidermal growth factor (EGF), platelet-derived growth factor (PDGF), and fibroblast growth factor (FGF) receptors. The interaction between actin and Meu RTK is observed in mammary carcinoma cells supporting that interaction between integrins and RTKs through FAK increases probability of RTK dimerization and cross-phosphorylation.

The agonist like bombesin, gastrin, endothelin, and various muscarinic agents belonging to G-protein-coupled receptor (GPCR) are found to induce auto phosphorylation of FAK in Rho GTPase, which requires actin cytoskeleton and functional Rho GTPase. The muscarine acetylcholine receptor inhibits FAK activation in absence of Integrin and ECM interaction. The integrin is also found to regulate synthesis of some cytokines and cytokine receptors.

9.12.1 Selectins

The three members and calcium-dependent selectin family are a type I transmembrane glycoproteins. The three members are known as E-selectin, P-selectin, and L-selectin with similar topology. The selectins structurally can be divided into five domains such as an N-terminal lectin-like domain, an epidermal growth factor (EGF)-like domain, a changeable number of consensus repeats (CRs), a single transmembrane domain and small cytoplasmic tail. The consensus repeats (CRs) length, unique features of N-terminal lectin-like domain of selectin and posttranslational modification of ligand together decide the specific function and specificity of selectins. The epidermal growth factor (EGF)-like domain amino acid residues also contributes to some extent in selectin specificity and binding to ligand. The CRs number and length participate in selectin recognition by ligand (Fig. 9.32).

The selectins are majorly involved in leukocyte adherence to endothelial cells and platelets during inflammatory processes and carry out heterotypic cell-cell interactions through sialylated glycans recognition. The E-selectin (E-LAM1), glycosylated transmembrane, has molecular weight in the range of 107–115 kDa depending upon type of

glycosylation. The E-selectin may bind many diverse glycoconjugates in different hematopoietic and cancerous cells. The ligands are known as cutaneous lymphocyte-associated antigen (CLA), L-selectin, E-selectin ligand1, CD43, hematopoietic cell E, and L-selectin ligand (HCELL), β -2 integrins, glycolipids and death receptor3 (DR3) of colon carcinoma cells (Fig. 9.36).

The most studied 240 kDa sialomucin disulfide-linked homo dimer, P-selectin glycoprotein ligand-1 (PSGL1) is capable to bind all three E-, L- and P-selectins. The E-selectin transduce signals in response to ligands on endothelial cells.

P-selectin expression is found on platelets and endothelial cells on endothelial increase expression in inflammatory conditions. The L-selectin expression is found on leukocytes.

The serine and tyrosine phosphorylations in the cytoplasmic tail of endothelial E-selectin are controlled by E-selectin interaction with counter-receptors of leukocytes. The Phosphorylation of

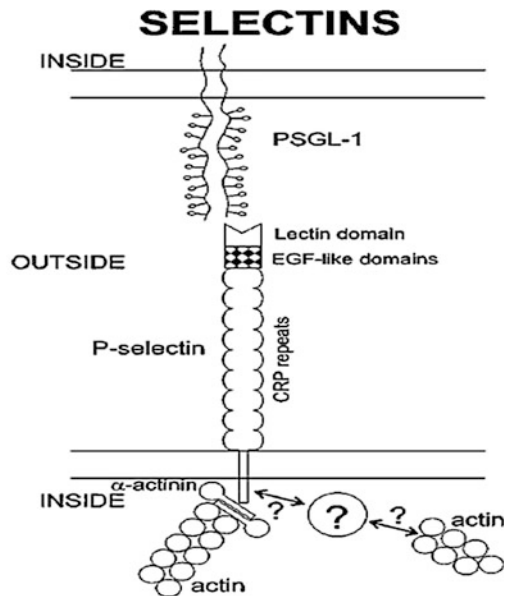


Fig. 9.36 Cell adhesion receptors selectins with their associated cytoskeletal components and extracellular ligands and bound proteins that join them to the actin cytoskeleton. *Annu. Rev. Pharmacol. Toxicol.* 2002. 42:283–323

serine/tyrosine may link E-selectin to cytoskeletal proteins or may change endothelial cell shape and these such rearrangements may increase permeability of the endothelial barrier by collecting stress fibers and supporting cellular diapedesis. The interaction of E-selectin, L-selectin, PSGL1, and/or CD44 expressed on leukocytes cell can enhance activation, expression, and clustering of α M β 2 (CD11b/CD18, Mac1) on the leukocyte membrane. Further, the interaction between E-selectin and integrins through phosphorylation of p38 and p42/44 MAPKs target neutrophils and other leukocytes movement through the endothelium to inflammatory foci. Recently, the E-selectin along with its glycoprotein co-receptor is reported to activate integrin in neutrophil cells through MAPK signal pathway.

The neutrophils circulate in blood in resting condition at average speed of approximately 40 μ m/s (characteristic rolling phenomenon), but in any inflammatory condition or microbial invasion the rolling velocity of neutrophils becomes approximately 5 μ m/s (slow rolling). These inflammatory conditions stimulate neutrophil extravasation to the inflamed interstitium through transmigration across the vessels. The steady state characteristic rolling results from the endothelial P-selectins interaction with their neutrophil glycoprotein counter receptors; primarily, PSGL-1 and slow rolling in inflammation are caused by E-selectins expression on the inflamed endothelium. These interactions induce change in conformation β 2-integrin LFA-1 on neutrophils with intermediate affinity, which further may enhance neutrophil–endothelial cell interactions because of LFA-1 binding to its endothelial counter receptor ICAM-1 during the slow rolling phase.

The slow rolling unlike steady state rolling is effectuated by both selectins and integrins. The other membrane-bound chemokines and cytokines expressed on inflamed endothelium also participate in neutrophil activation for forming high-affinity conformation of the neutrophil integrin LFA-1 to bind endothelial integrin ligands like the LFA-1 ligand ICAM-1 for arresting neutrophils at the endothelial surface, which results in firm adhesion. Now, the

neutrophil moves to interstitium through transmigration for chemotaxis. The leukocyte adhesion deficiency (LAD) type 1 is caused by β 2-integrin chain CD18 deficiency and LAD type 2 defect results from cellular fucose metabolism because the defect in fucose metabolism cause defective selectin-mediated cell–cell interactions. LAD type 3 is caused by defective inside-out signaling of various integrins including leukocyte β 2-integrins.

The tumor cells may release cytokines for inducing E-selectin expression on vascular walls because high level of E-selectin is found in patient blood, suffering from malignancies. The soluble E-selectin can be chemotactic during migration of tumor cells. The tumor cell or leukocytes diapedesis via endothelial cells is enhanced by E-selectin signaling.

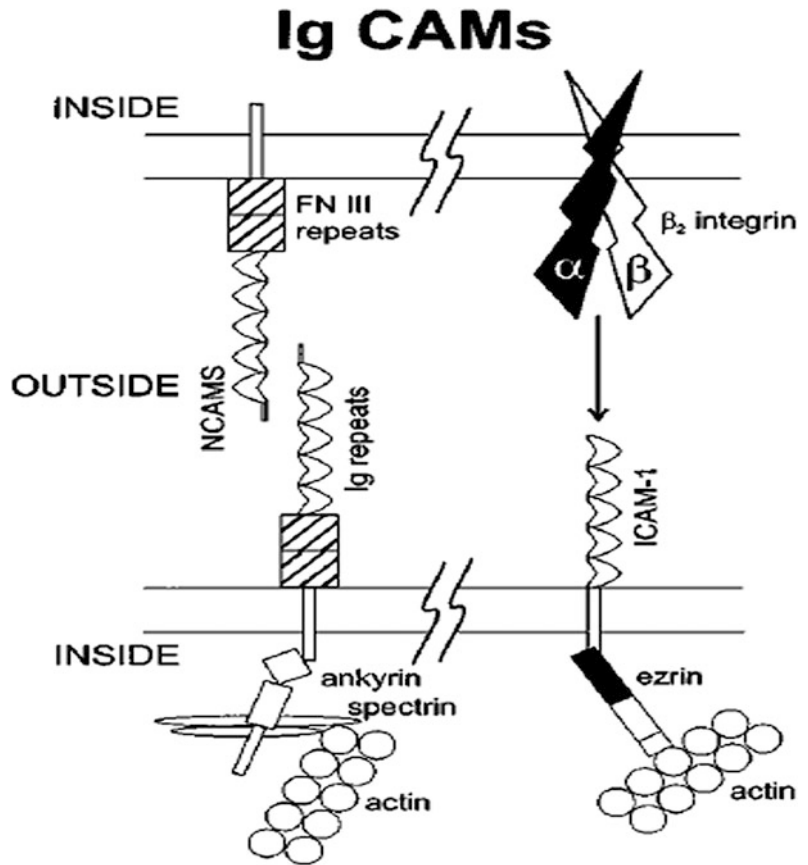
The E-selectin adhesion in cancer cells induces pseudo-podia formation, changes in cell morphology, and secretion of matrix degrading enzymes.

9.13 Immunoglobulin Superfamily Receptors

A. L1 CAM (L1) and Neural Cell Adhesion Molecule NCAM

The L1 cell adhesion molecule (CAM) identified in nerve cells are found to be involved in development, migration, synaptic plasticity, cell adhesion, axon outgrowth, cell migration, and myelination of nerve cells. The L1CAM either interacts with other L1CAM molecules (cis) as homophilic molecules or with other molecules like integrins, extracellular matrix proteins (ECM), neural cell adhesion molecules, CD24, neurocan, and neuropilin in trans heterophilic manner for cellular activities. The L1CAM is expressed in various types of cancers like colon, ovarian, malignant gliomas, renal, gallbladder, and extrahepatic cholangiocarcinoma (ECC) and the intensity of expression is directly proportional to tumor progression. The L1CAM, close homolog of L1 (CHL1), NrCAM, and Neurofascin are the L1CAM family members present in

Fig. 9.37 Cell adhesion receptors Ig CAM with their associated partners of cytoskeleton and extracellular ligands with bound proteins to link them to the actin. *Annu. Rev. Pharmacol. Toxicol.* 2002. 42:283–323



vertebrates. L1CAM is transmembrane glycoprotein belonging to immunoglobulin (Ig) superfamily. The molecular weight of L1CAM is in the range of 200–220 kDa, and it has six Ig-like domains and five fibronectins type III repeats with following transmembrane region and a highly conserved C-terminal domain. The cytoplasmic domain of L1CAM interacts with cytoskeletal proteins like ankyrin, actin, spectrin and ERM protein. The gene for L1CAM is present in X chromosome at q28 locus. The X linked mental retardation, recessive cerebral disorders, and schizophrenia are caused by L1CAM gene mutation. The other L1 syndrome may include mental retardation, aphasia, spastic paraplegia, and hydrocephalus, which are caused by defects in L1CAM intracellular transport, expression, or binding to ligands (Fig. 9.37).

The L1CAM cis-hemophilic binding occurs because of Ig domain 1–4 paired zipping along the intercellular boundaries supporting static cell adhesion. The two important factors contributing to function of L1 CAM are the cleavage of L1CAM via metalloproteinases and the binding of L1CAM to integrins or other receptor molecules through its RGD motif in the sixth Ig domain. These two steps may activate signaling pathways, which are different from homophilic activation. The serine proteinases plasmin or trypsin or the pro-protein convertase PC5A cleaving site (consensus cleaving sequence 840RKHSKR845) is in the third FN repeat of the ectodomain of L1CAM. This proteolysis may not necessarily release N-terminal fragment, but proteolysis by metalloproteases (ADAMs) and disintegrin definitely cleave to the release of the

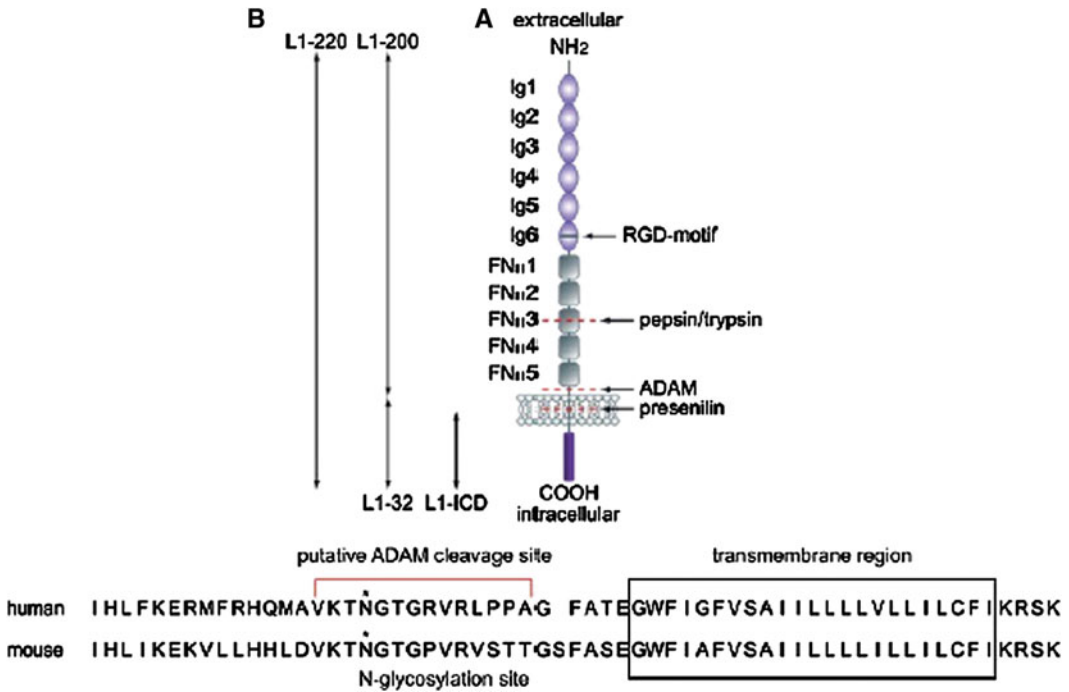


Fig. 9.38 The structure of type I transmembrane L1CAM and its proteolysis. **A** L1CAM has sixth immunoglobulin domains, five fibronectin-type III repeats and a conserved cytoplasmic tail. L1CAM can bind to L1CAM other molecule in cis-homophilic manner and in transheterophilic manner to other integrins, extracellular matrix proteins (ECM), neural cell adhesion molecules, CD24, neurocan and neuropilin ligands. The RGD-site in the sixth Ig domain is the binding site for integrins like $\alpha 5\beta 1$, $\alpha v\beta 3$, or $\alpha v\beta 5$. The metalloproteinases like

ADAM10 and ADAM17 may cleave L1CAM at plasma membrane to release soluble ectodomain of 200 and 32 kDa transmembrane domains remain intact. The RGD motif and proteolytic cleavage sites are specified. **B** The membrane-proximal cleavage site. The amino acid sequence of mouse and human L1CAM is depicted with ADAM-mediated cleavage. L1-32 cleavage is resistance to endoglycosidase because of N-linked glycans absence. <https://www.ncbi.nlm.nih.gov/pmc/articles/PMC3478260/figure/F1/>

water-soluble ecto domain (termed L1-200). The ectodomain shedding, the key mechanism for regulating the function of cell surface proteins has been observed in type I and type II transmembrane proteins receptor molecules like Ig-CAMs, selectins, epidermal growth factor receptor and cadherins. The proteolytic cleavage downregulates the cell surface expression and cell adhesion but activates intracellular signaling (Fig. 9.38).

After shedding of L1CAM ectodomain, the C-terminal fragment (L1-32) of 32 kDa remains in plasma membrane. The cleavage-dependent L1CAM nuclear signaling is found to be involved in induction of pro-tumorigenic and antiapoptotic genes expression and enhances cell

migration. The L1CAM-RGD-site in the sixth Ig domain appears to be essential because the RGD-site in the sixth Ig domain of L1CAM acts as substrates for RGD-binding integrins $\alpha v\beta 5$, $\alpha 5\beta 1$, $\alpha v\beta 1$, $\alpha v\beta 3$, and $\alpha IIb\beta 3$ for cell adhesion and motility enhancement. The L1CAM was observed to stimulate constitutive NF κ B activation in tumor cells. The increased L1CAM expression induces the phosphorylation of FAK at Y397 and Y925 and Src at Y416. This phosphorylation event may be correlated to a change in PI3K phosphorylation and Akt activation. As discussed above the PI3K and Akt activates NF κ B through I κ B κ , I κ B kinase β , and MAPKp38. The L1CAM-dependent NF κ B activation is mediated through integrin signaling.

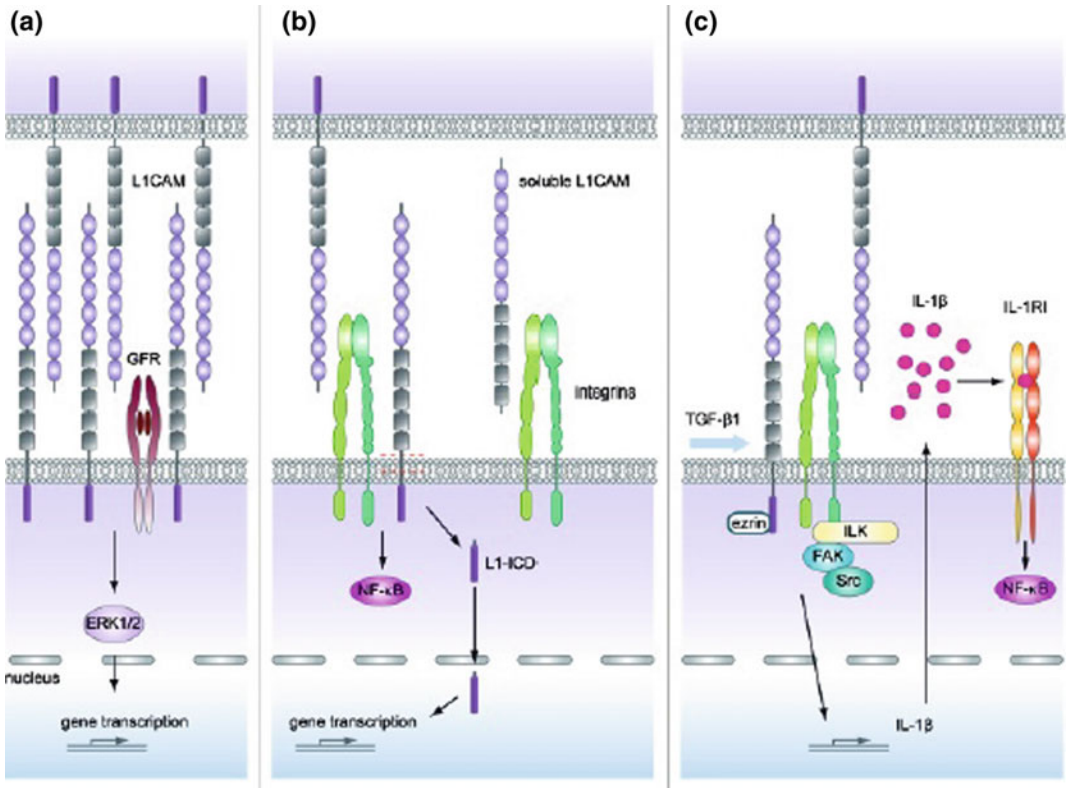


Fig. 9.39 The various signaling pathways of L1CAM. **a** L1CAM homophilic interactions may activate MAPK pathway through growth factor receptors (GFR) and induce static cell–cell binding. **b** The L1CAM binding to integrins stimulates NFκB activation for cell migration invasive property. The cleavage of L1CAM from the membrane releases soluble L1CAM, wand. The

intracellular fragment L1-ICD is translocated to the nucleus for gene transcription stimulation. **c** TGF-β upregulate L1CAM for L1CAM-integrin downstream signaling via FAK-Src, which has been discussed above for production and release of IL-1β. The IL-1β then activates NFκB via binding to the IL-1 receptor (IL-1RI)

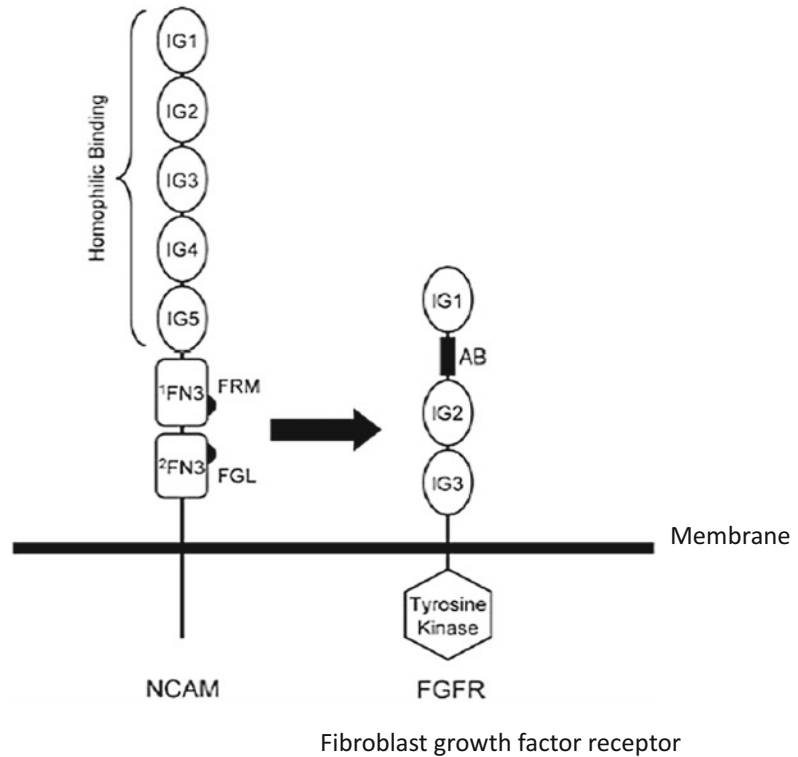
The downstream signaling of integrins is explained above. The depletion of α5- and β1-integrin, ILK, FAK, and p110β is observed to NFκB activation and IL-1β expression in breast cancer cell line (Fig. 9.39).

B. Neural Cell Adhesion Molecule

The neural cell adhesion molecule (NCAM), CD56, an immunoglobulin-like neuronal surface glycoprotein is found on the cell surface of neurons, astrocytes and oligodendrocytes, where it participates in homophilic and heterophilic interactions and cause adhesion, guidance, and differentiation during neuronal growth by binding to different adhesion molecules. The NCAM

gene by alternate splicing produces three different size classes, which are known (on molecular weight basis) as NCAM-180, NCAM-140 and NCAM-120, and these have same extracellular domain with different membrane attachment and cytosolic regions. The NCAM function is also regulated by an unusual posttranslational modification by adding polysialic acid to Ig5. While the NCAM-120 has a glycol phosphatidyl (GPI) anchor for membrane attachment, the NCAM-180 and NCAM-140 has transmembrane domain. The extracellular domain of NCAM has five immunoglobulin-like (Ig) domains, which are followed by two fibronectins type III (FNIII) domains. While the Ig domain participates in homophilic binding to NCAM, the FNIII

Fig. 9.40 Schematic presentation of neural cell adhesion molecule (NCAM) and FGFR at the cell surface. Ig domain is oval and FNIII is rectangle. The hexagonal is cytosolic tyrosine kinase domain of FGFR, and the acid box (AB) is shown as filled black rectangle. The arrow directs the interaction of two NCAM regions (FRM and FGL) with FGFR. *J Mol Biol.* 2008 Mar 21; 377(2): 524–534. <https://doi.org/10.1016/j.jmb.2008.01.030>



domains activate signaling for neurite outgrowth. The NCAM may activate neurite outgrowth through homophilic (NCAM–NCAM) and heterophilic (NCAM–fibroblast growth factor receptor) interactions by activating various intracellular signaling pathways. The NCAM-induced intracellular signaling depends on cytoplasmic calcium concentration. The NCAM signaling controls cell migration, neurite extension, fasciculation, and synapses formation in the brain (Fig. 9.40).

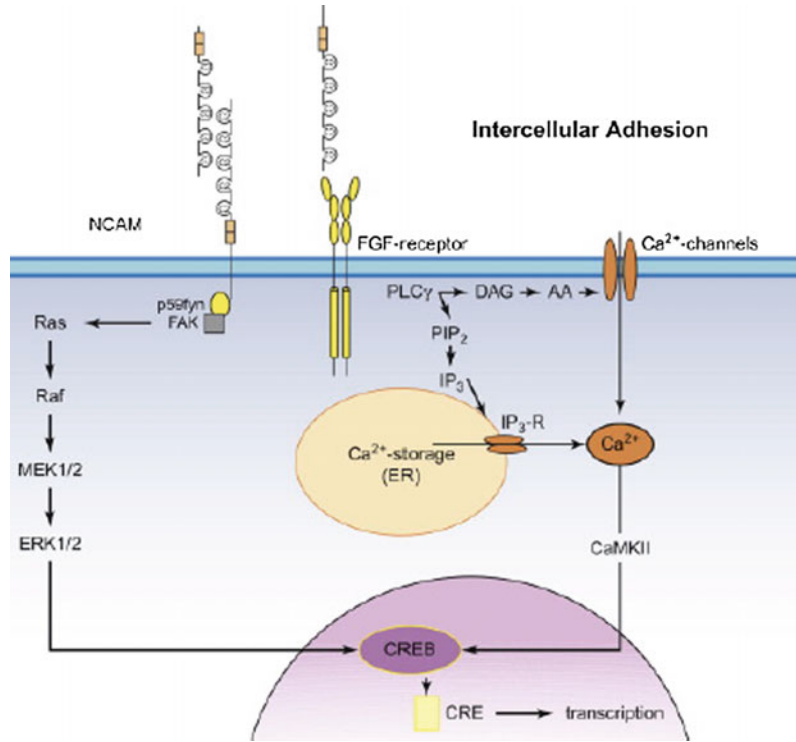
The glycan like α -2,8-linked polysialic acid on NCAM has high negative charge and big hydration volume so their presence in NCAM reduces homophilic NCAM interactions. 1 The NCAM carries out its function by activating fibroblast growth factor receptor-1 (FGFR1) through cis-interaction of NCAM and FGFR. The FGFR-4 receptors with 48 isoforms and 23 growth factor ligands are known to perform various functions. The longest ecto domain of FGFR-1 has three Ig domains (D1–D3) along with acidic amino acids (acid box) in between the

D1–D2 linker. The shorter ecto domain does not have D1 and the acid box. The NCAM–FGFR1 interaction occurs through direct binding of the FN3 domains of NCAM to FGFRs. The NCAM derived peptide like FRM peptide derived from the first FN3 domain of NCAM, and FGL peptide derived from the second FN3 domain induces FGFR 1 signaling for neurite outgrowth. The FN3–FN3 domain is flexible and may adopt a bending conformation for stabilized interactions. The FGFR belong to receptor tyrosine kinases. The lavendustin A, the inhibitor of RTKs and the Src (protein tyrosine kinases) downregulates NCAM signaling and neurite outgrowth (Fig. 9.41).

A. T-Cell Receptors (TCRs)

The T-cell receptor (TCR) signaling play a central role in adaptive immune response by recognizing antigen, and T-cell receptor (TCR)–CD3 complex explains in general the principles of receptor assembly, ligand recognition, and

Fig. 9.41 NCAM-induced signaling pathway. <http://ars.els-cdn.com/content/image/3-s2.0-B9780123749475000092-f09-04-9780123749475.jpg?httpAccept=%2A%2F%2A>



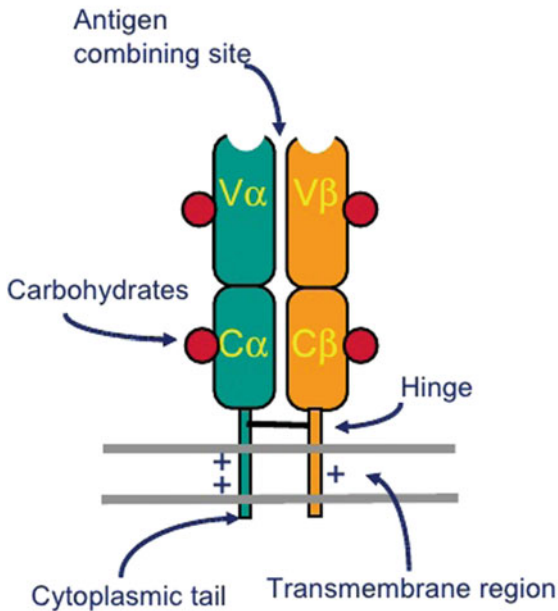
signaling in the immune system which depends on basic and acidic amino acids residues of transmembrane for assembly cell receptors have no signaling domains by themselves, so they are associated with a conserved multi subunit signaling CD3 complex of CD3εγ, CD3εδ, and CD3ζζ dimers. The majority of T-cells receptors (TCR) are made up of two glycoproteins known as α and β but some might have γ and δ glycoproteins. The TCR binds antigens exhibited by major histocompatibility complexes (MHCs) and MHC-like molecules (Fig. 9.42).

The TCR-CD3 complex contains four dimeric modules like TCRαβ (or γδ), CD3δε, CD3γε, and ζζ which are linked through transmembrane residues. Each unit of signaling dimers is associated with particular basic amino acids residues in TCR, resulting in octomaeric complex. The aspartic acid pair D6-D6 at the helix dimer interface mediates assembly with TCR, which is stabilized by inter helical H-bonds between side-chain oxygens and backbone amide protons (dotted lines). The methyl and aromatic packing like L9-L9 and two tyrosine-threonine

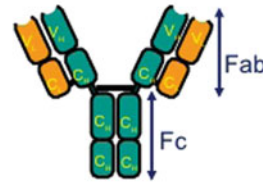
H-bonds between Y12 and T17 at interface are also important for dimer formation.

The TCR recognition of antigen peptide displayed by major histocompatibility complex (MHC) can stimulate conformational changes in the associated CD3 chains, which cause their phosphorylation and interaction with downstream proteins. The CD3 δ-, γ-, ε-, and ζ-chains all have immune receptor tyrosine-based activation motifs (ITAMs), and these ITAMs motifs are phosphorylated by the Src kinase leukocyte-specific tyrosine kinase (Lck) after TCR recognition of antigen. Constitutively, the Src kinase leukocyte-specific tyrosine kinase (Lck) is also associated with T-helper cells CD4 coreceptor. The CD3ε cytoplasmic domains intrinsic binding to ζ chains in the inner leaflet of the plasma membrane has shown new mechanism of activation, where CD3ε-specific tyrosine insertion into the hydrophobic membrane may stop their phosphorylation before receptor engagement. The antigen recognition mechanism is found different in three classes of TCR ligands. The CD4 interaction with MHC molecule recruit

The T cell antigen receptor



Resembles an Ig Fab fragment



Domain structure: Ig gene superfamily
Monovalent

No alternative constant regions

Never secreted

Heterodimeric, chains are disulfide-bonded

Very short intracytoplasmic tail

Positively charged amino acids in the TM region

Antigen combining site made of juxtaposed V α and V β regions

30,000 identical specificity TcR per cell

Fig. 9.42 The T-cell antigen receptor

LcK to TCR complexes and phosphorylated CD3 immune receptor tyrosine-based activation motifs (ITAMs) engage the Syk family kinase Zeta activated protein 70 kDa (Zap70) through Src-homology-2 (SH2)-domain interactions. The Zap70 after being recruited on TCR, phosphorylates multiple tyrosine residues in linker for the activation of T-cells scaffolding protein (LAT). The LAT after phosphorylation recruits the SIp76 (SH2 domain-containing leukocyte protein) via Grb-related protein 2, which is also called Gads. The Zap70 phosphorylate SIp76 to form LAT-SIp76 complex for signaling effectors interactions. The C- γ (PLC γ) lipase interacts with LAT-SIp76 complex and hydrolyzes phosphatidylinositol bisphosphate (PIP₂) to generate diacylglycerol (DAG), and inositol trisphosphate (IP₃) for signal transduction.

The released DAG may activate MAPK pathway as shown in Fig. 9.43 through various intermediate signal molecules like protein kinase C- θ

(PKC θ), Ras GRP (RAS guanylyl nucleotide-releasing protein GEF) etc. (Fig. 9.44).

The phosphorylated SIp76 may also bind directly to the Tec family kinase interleukin-2-inducible T-cell kinase (ITK). The LAT-SIp76 complex components can interact with many other signaling molecules in cooperative manner, which is the base for TCR signaling via joining various signal pathway branches.

9.13.1 Major Histocompatibility Complex (MHC)

T-cytotoxic and T-helper cells lymphocytes express CD8 and CD4 membrane proteins on their surface to increase T-cells response and sensitivity toward antigenic peptide along with major histocompatibility complex (pMHC) ligands. The T-cell receptor sensitivity and response increase either might be because of stabilization of CD4

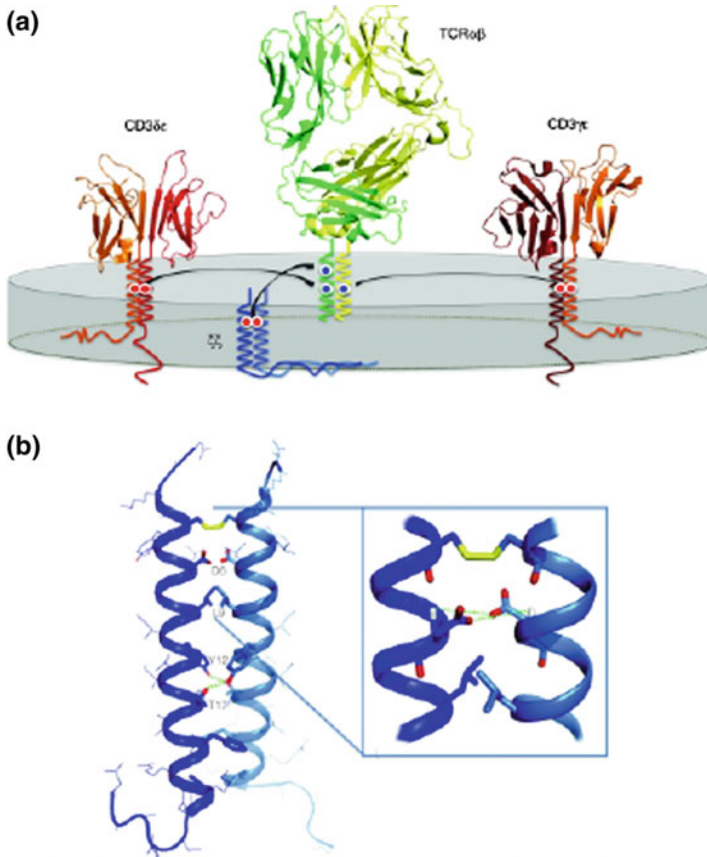


Fig. 9.43 TCR–CD3 complex structure contains four dimeric modules like TCRαβ (or γδ), CD3δϵ, CD3γϵ, and ζζ which are linked through transmembrane residues. Each unit of signaling dimers is associated by particular basic amino acids residues in TCR, resulting in octomeric complex. **a** The ribbon structures from PDB entries 1MI5 (LC13 αβTCR), 1XMW (CD3δϵ), and 1SY6 (CD3γϵ) are shown. **b** NMR structure of the ζζ TM

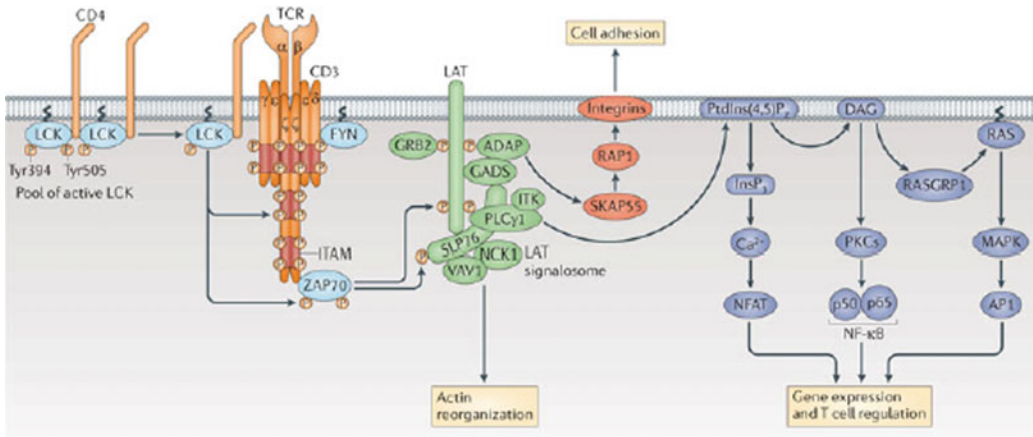
homodimer (PDB entry 2HAC). The aspartic acid pair D6–D6 at the helix dimer interface mediates assembly with TCR, which is stabilized by interhelical H-bonds between side-chain oxygens and backbone amide protons (dotted lines). The methyl and aromatic packing like L9–L9 and two tyrosine–threonine H-bonds between Y12 and T17 at interface are also important for dimer formation. Cold Spring Harb Perspect Biol. 2010 Apr; 2(4):a0051

and CD8 to MHC class I and class II interaction or may be because of the Src kinase (Lck) recruitment to the TCR complex as discussed above. The MHCII initiates antigen specific immune response and also activates intracellular signaling for apoptosis. The professional antigen-presenting cells (APC) like dendritic cells, B-lymphocytes, monocytes, macrophages, and epithelial cells have constitutive.

MHC class II expression and nonprofessional APC like fibroblasts, keratinocytes display

inducible MHC class II in presence of inflammatory cytokines. The class II MHC molecules isoforms, found in human are known as HLA-DR, HLA-DQ, and HLA-DP. The MHC class II expression is seen after 3–5 days after T-cell activation contrary to generation of cytokines like interferon γ and interleukin (IL)-4 within a few hours after TCR-triggering and co-stimulation (Fig. 9.45).

The MHC class II expression is regulated by class II transactivator (CIITA). The class II



Nature Reviews | Immunology

Fig. 9.44 Overview of TCR signaling. The following abbreviations are used as AP-activator protein 1, DAG-diacylglycerol, InsP₃-inositol-1,4,5-trisphosphate, NFAT-nuclear factor of activated T-cells, PKC-protein kinase C,

PtdIns(4,5)P₂-phosphatidylinositol-4,5-bisphosphate, RASGRP1-RAS guanylyl-releasing protein 1, and SKAP55 SRC kinase-associated phosphoprotein of 55 kDa

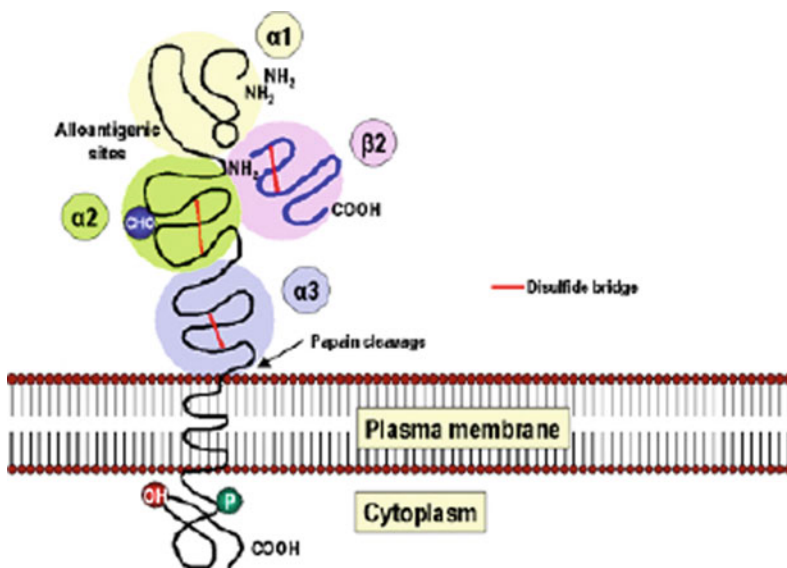


Fig. 9.45 The MHC class 1 structure with three globular domains alpha 1 (yellow), alpha 2 (green) and alpha 3 (blue). The alpha 3 domains are in close association with the non-MHC beta 2 microglobulin (pink), which is

stabilized by a disulfide bridge (red) and has similarity to immunoglobulin domain. The alloantigenic sites which carry determinants specific to each individual are found in the alpha 1 and 2 domains (Color figure online)

transactivator (CIITA) is constitutively expressed in antigen-presenting cells but expressed by induction in other cell types. The CIITA gene is controlled by at least three independent promoter

units (CIITA-PI, CIITA-PIII, and CIITA-PIV), each transcribing a unique first exon. We and others have recently established that normal human in vivo activated T cells exclusively use

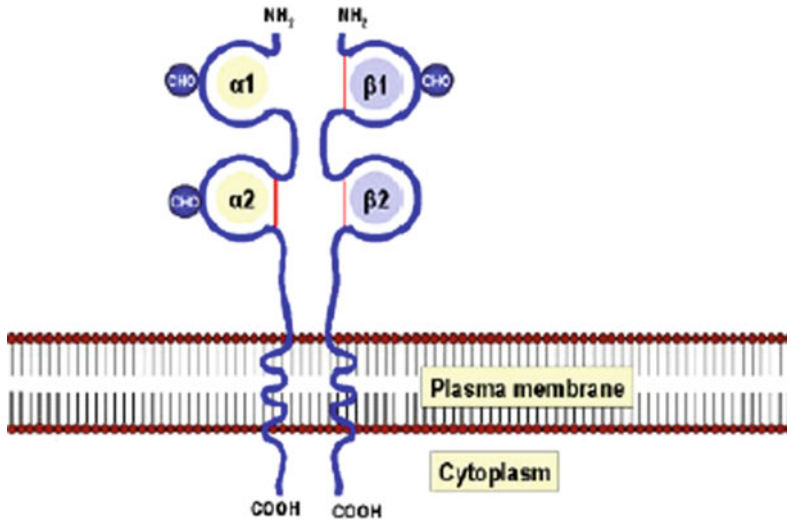


Fig. 9.46 MHC class II molecules structure with two nonidentical peptides (alpha and beta) in noncovalently association, which traverses the plasma membrane with extra cellular N terminus. All domains except alpha 1

domain are stabilized by disulfide bridges (red). The alpha and beta chains are glycosylated. The beta chain is smaller than alpha chain (beta mol. wt. = 28,000) and contains the alloantigenic sites (Color figure online)

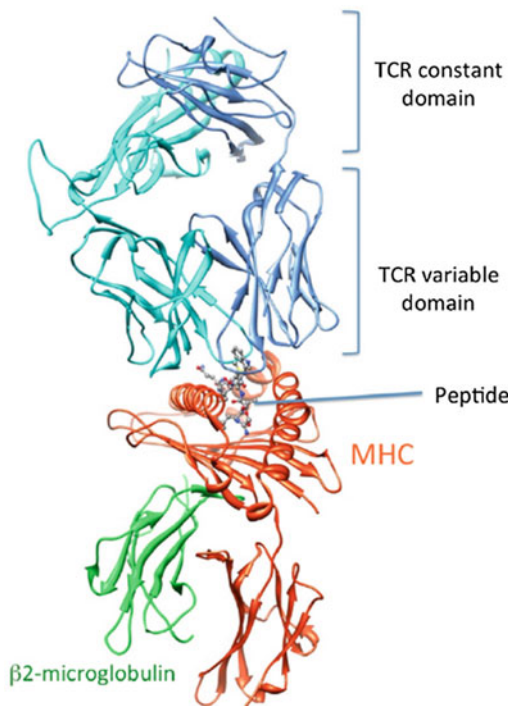


Fig. 9.47 The TCR–peptide MHC complex 3D structure. The TCR α , TCR β , MHC, and b2-microglobulin are colored in blue, cyan, orange, and green, respectively. The NY-ESO-1 peptide is displayed in ball and stick (Color figure online)

CIITA promoter III (CIITA-PIII), whereas unstimulated T-cells lacked CIITA expression. In malignancies of T-cell origin, we have recently shown that the lack of MHC class II expression in a panel of T-cell acute lymphoblastic leukemia (T-ALL) cell lines coincides with lack of CIITA expression, and stimulation of these T-ALL cells with well-known T-cell activation agents did not result in the induction of CIITA and congruent MHC class II expression (Fig. 9.46).

In humans these genes are called **Human Leukocyte Antigen** or HLA genes, as they were first discovered through antigenic differences between white blood cells from different individuals; in the mouse, they are known as the **H-2** genes. There are three class I α -chain genes in humans, called *human-leukocyte-associated* antigens HLA-A, HLA-B, and HLA-C. There are also three pairs of MHC class II α - and β -chain genes, called HLA-DR, HLA-DP, and HLA-DQ. However, in many cases the HLA-DR cluster contains an extra β -chain gene whose product can pair with the DR α -chain. This means that the three sets of genes can give rise to four types of MHC class II molecule (Fig. 9.47).

9.13.2 Surface Immunoglobulins

The B-lymphocytes produce soluble antibodies or immunoglobulins for humoral immunity, which is a part of the adaptive immune system in mammals. The immunoglobulins heterodimeric proteins belonging to IgsF superfamily, structurally are made up of two heavy (H) and two light (L) peptide chains, which can functionally be separated into variable (V) domains antigens binding and constant (C) domains to interact with various effector molecules like complement or Fc receptors for immune response. The variable domains are resulted because of gene rearrangement and somatic hypermutation after antigen interaction. On the basis of sequence, the variable region V again may be divided into three such as complementarity determining regions (CDRs) and four framework regions (FRs) with relatively constant sequences. The antigenic site is defined by three CDRs of the H-chain pairing with the three CDRs of the L chain. The immunoglobulins are classified into five classes, known as IgM, IgG, IgA, IgD, and IgE isotypes. IgG has four subclasses like IgG1, IgG2, IgG3, and IgG4, and IgA is with two IgA1 and IgA2 subclasses.

The constant domains of the H-chain can be switched to allow altered effector function while maintaining antigen specificity. The light chain may have κ or λ -peptide (Fig. 9.48).

The heavy chain with three constant C-domains includes one spacer *hinge* region between the first (C_{H1}) and second (C_{H2}) domains. While the digestion of IgG by papain release two Fab fragments and both can bind antigen, the IgG digestion by pepsin forms an Fc fragment and one dimeric $F(ab)_2$ with the property of cross-linking and antigen binding. The Fab includes one entire L chain along with portion of heavy chain, V and C_{H1} H (Fig. 9.46). The Fab is again divided into a variable fragment (Fv), which is made up of the V_H and V_L domains along with constant fragment (Fb) of the C_L and C_{H1} domains. The presence of immunoglobins without chain is found in nurse shark and in some other minor species.

Fc receptors, a family of membrane-associated and soluble glycoproteins is expressed in various immune cells like B-lymphocytes, follicular dendritic cells, natural killer cells, macrophages, neutrophils, eosinophils, basophils, human platelets, and mast cells

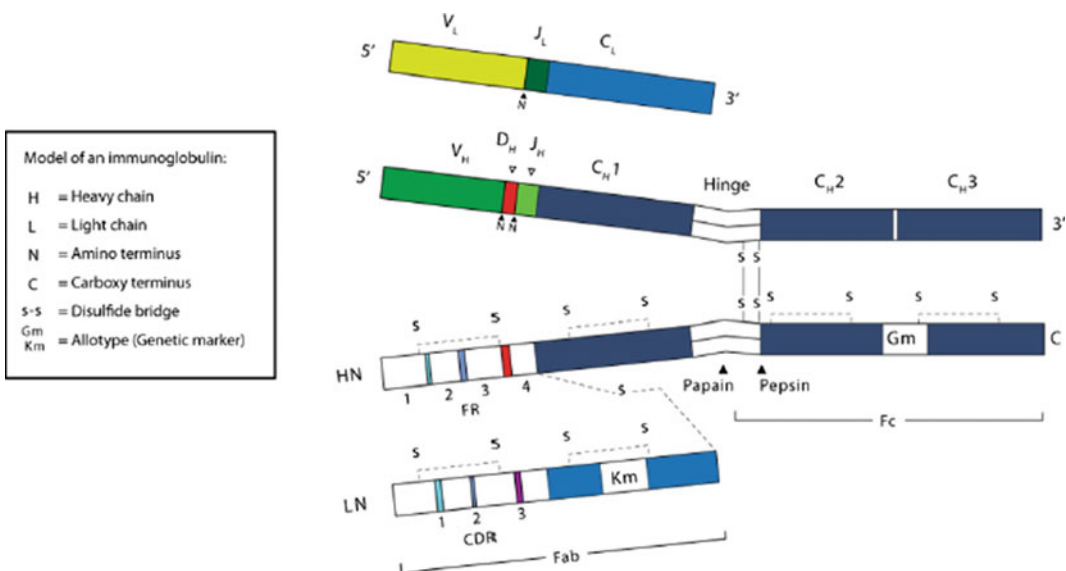


Fig. 9.48 Two-dimensional structure of surface immunoglobulin, showing light and heavy chain with hinge region of sulfide linkage

for signaling of different functions induced by immune complexes. The various isoforms of Fc receptors enhance the B-lymphocytes activation and differentiation via an increased antigen presentation associated with IgG such as Fc gamma RIIb2, Fc gamma RIII, Fc epsilon RII, or by inducing cytokine synthesis from mast cells through Fc epsilon RI, Fc gamma RIII, and natural killer cells through Fc gamma RIII receptors. The B-cell activation is reduced by interaction of Fc gamma RIIb1 to membrane Ig. The immunoglobins production is also enhanced by soluble forms of Fc Receptor Fc-ε RII through interleukin4 and decreased by Fc γ Receptor. The various structural motifs of Fc receptors are responsible for different immune responses. The various Fc low-affinity Fc receptors of neutrophils primarily recognize Ig-opsonized pathogens but also involved in immune complex-mediated inflammatory processes. The human neutrophil expresses two types of Fc receptor, known as Fc-γ RIIA single-chain transmembrane receptor with c-terminal tyrosine-based activation motif (ITAM) and extracellular GPI anchored to plasma membrane FcγRIII B receptor. Both the receptors FcγRIIA and FcγRIIB are required in neutrophils activation by immune complexes. The FcγRIIB leads initial contact and holding immune complexes following synergistic interaction with of followed FcγRIIA induce neutrophil cells.

The cross-linking of FcγRIIB and FcγRIIA induces dual tyrosine phosphorylation of the ITAM sequence motifs (short consensus sequences of YxxL/Ix(6–12) YxxL/I where x may be any amino acid) as discussed above for Syk tyrosine kinase recruitment to the receptor complex via two tandem SH2-domains of Syk to the two phosphorylated ITAM tyrosines. These interactions may result in Syk activation and phosphorylate various tyrosine kinase substrates for further downstream signaling. The mechanism is similar to ITAM-mediated signal transduction by antigen receptors of B- and T-cell receptors (Fig. 9.49).

As discussed above in T-cells, the Src-family kinases are important in ITAM phosphorylation and activation via Syk-related ZAP-70 kinase.

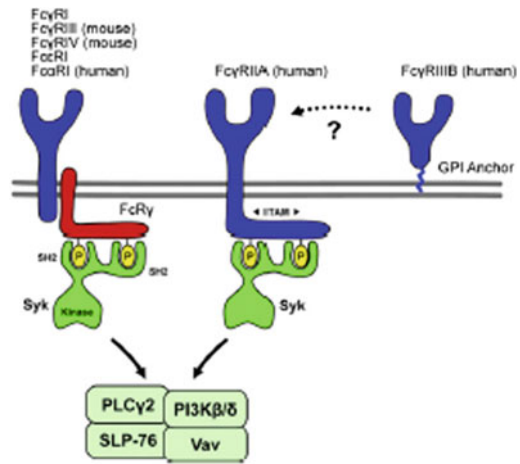


Fig. 9.49 Neutrophil Fc receptors signaling in neutrophils. The low-affinity Fcγ-receptors signal through cytoplasmic ITAM motifs in activated form and recruit and activate the Syk tyrosine kinase for further downstream signaling

Unlike ZAP-70, which may not phosphorylate the TCR-associated ITAM sequences, the Syk is found to induce phosphorylation of ITAM sequences. The Syk-mediated signal transduction initiation is observed even in the absence of Src-family kinase also. The B-cell receptor-mediated ITAM phosphorylation is found to be insensitive to combined deficiency of Blk, Fyn, and Lyn. The Syk deficiency in macrophage results in complete failure of phagocytosis while inactive Src-family kinases Hck, Fgr, and Lyn only delay and decrease phagocytosis of IgG-coated red blood cells.

The FcγR-mediated Ca²⁺-flux and superoxide production and neutrophil activation require SLP-76, PLCγ2 phospholipases, guanine exchange factor, Rac small GTPase, PI3-kinase isoforms PI3Kβ, and PI3Kδ with a predominant role for PI3Kβ also.

References

- Aplin E, Howe A, Alahari SK, Juliano RL (1998) Signal transduction and signal modulation by cell adhesion receptors: the role of integrins, cadherins, immunoglobulin-cell adhesion molecules, and selectins. *Pharmacol Rev* 50(2):197–264

- Barnes NM et al (2009) The 5-HT₃ receptor—the relationship between structure and function. *Neuropharmacology* 56:273–284
- Baker SJ, Rane SG, Reddy EP (2007) Hematopoietic cytokine receptor signaling. *Oncogene* 26(47):6724–37
- Cambell ID, Humphries MJ (2011) Integrin structure, activation, and interactions. *Cold Spring Harbor Perspect Biol* 3(3). <https://doi.org/10.1101/cshperspect.a004994>. Source: PubMed
- Chen H, Levine YC, Golan DE et al (2007) Atrial natriuretic peptide-initiated cGMP pathways regulate vasodilator-stimulated phosphoprotein phosphorylation and angiogenesis in vascular endothelium. *J Biol Chem* 283:4439–4447
- Deem TL, Cook-Mills JM (2004) Vascular cell adhesion molecule 1 (VCAM-1) activation of endothelial cell matrix metalloproteinases: role of reactive oxygen species, and associated components. *Braz J Med Biol Res* 40:1025–1035
- Derynck R, Zhang YE (2003) Smad-dependent and Smad-independent pathways in TGF- β family signaling. *Nature* 425:577–584
- Ghanemi A (2015) Targeting G protein coupled receptor related pathways as emerging molecular therapies. *Saudi Pharm J* 23(2):115–129
- Gurevich EV, Tesmer JJJ, Mushegian A, Gurevich VV (2011) G protein-coupled receptor kinases: more than just kinases and not only for GPCRs. *Pharmacol Ther* 133(1):40–69
- Harrison DA (2012) *Cold Spring Harb Perspect Biol* 4:a011205
- Huse M (2009) The T-cell-receptor signaling network. *J Cell Sci* 122:1269–1273 (Published by The Company of Biologists)
- Huttenlocher A, Horwitz AR (2011) Integrins in cell migration. *Cold Spring Harbor Perspect Biol*
- Juliano RL (2002) Signal transduction by cell adhesion receptors and the cytoskeleton: functions of integrins, cadherins, selectins and immunoglobulin-superfamily members. *Annu Rev Pharmacol Toxicol* 42:283–323
- Kobilka BK (2007) G protein coupled receptor structure and activation. *Biochim Biophys Acta (BBA) Biomembranes* 1768(4):794–807
- Lemmon MA, Schlessinger J (2010) Cell signaling by receptor tyrosine kinases. *Cell* 14(7):1117–1134
- Ley K (2003) The role of selectins in inflammation and disease. *Trends Mol Med* 9(6):263–268
- Ma L, Xiang X (2011) Atrial natriuretic peptide/natriuretic peptide receptor A (ANP/NPRA) signaling pathway: a potential therapeutic target for allergic asthma. *Med Hypothesis* 77(5):832–833. <http://dx.doi.org/10.1016/j.mehy.2011.07.048>
- Südhof TC (2013) A molecular machine for neurotransmitter release: synaptotagmin and beyond. *Nat Med* 19:1227–1231
- Wuchterpfennig KW, Gagnon E, Call MJ et al (2010) Structural biology of the T-cell receptor: insights into receptor assembly, ligand recognition, and initiation of signaling. *Cold Spring Harb Perspect Bio* 2(4):a0005140. <https://doi.org/10.1101/cshperspect.a0005140>

10.1 Introduction

The membrane-enclosed small cell organelle containing biomolecules for transport, either from one organelle to other or from one cell to other cell, is known as **vesicles**. All living organism plasma membrane needs these **vesicles** for synthesis, maintenance, and various physiological functions of the cell. The larger molecules like lipids and proteins, which cannot cross membrane themselves, are transported through these vesicles by **exocytosis** or **endocytosis**. The transport vesicles are dynamic structures and are constantly formed at the specific region of **endoplasmic reticulum** and **Golgi complex membrane**. The membrane bulges out and is pinched off for the formation and release of vesicle, respectively, at specific region of membrane. The vesicle travels to its destination, merges with target membrane to release its freight of molecules without interaction of freight molecules to membrane components. The various type vesicles are known as **lysosomes**, **vacuoles**, **transport vesicle**, and **secretary vesicles** on the basis of their structure and physiological functions. The vesicles may be **uncoated** or **coated vesicles** depending on their outer components. The coated vesicles have **COPI**, **COPII**, or **clathrin** coat proteins on the outer side of vesicles. The mechanism of transport may be secretary, called **exocytosis** or the freight is internalized by **endocytosis**. These vesicles are recycled after their cargo delivery. **Clathrin-dependent** and **clathrin-independent**

endocytosis (CIE) are different from each other in respect to vesicle formation and mode of transport. Clathrin-independent endocytosis may occur by **caveola**, **Phagocytosis** to internalize large molecules, while **micropinocytosis** is involved in fluid uptake by cell. The vesicle synthesis, functions, its interaction with various components, and regulation are discussed in this chapter. Transport by **areolae** may be dynamin dependent and dynamin independent. **Caveolae**, a vesicle with four isoforms of **caving coat** protein complex, a flask-like invaginations of the plasma membrane functions in **endocytosis**, **transcytosis**, and **pinocytosis**. The endocytosis may be **clathrin dependent** and **clathrin independent**. The **Glycosylic phosphatidic inositol**-anchored proteins are also involved in clathrin- and areolae-independent endocytosis.

10.2 Type of Vesicle Transport

The vesicles originate from cell membrane only. The formation starts at particular region of membrane. The vesicles found in the cell may be **coated** or **uncoated vesicles**. The **coated vesicles** are of three different types depending on their coat proteins. They may have customer protein **COPI**, **COPII**, or **clathrin**. These coat proteins have two important functions in transport. One is the selection of right kind of freight for transport, and other one is to form curvature in the specific region of plasma membrane by clustering required proteins for vesicle formation. Vesicle

formation is very regulated process and that is why the same type of vesicles has similar size. **COPI vesicles** are involved in **retrograde** transport for recycling proteins between *cis*-golgi complex to endoplasmic reticulum and intra golgi complex transport. COPI also regulates functioning of Golgi complex. COPII vesicles transport newly formed proteins from rough endoplasmic reticulum to Golgi complex and this transport is called **anterograde** transport. **Clathrin-coated vesicles** internalize their freight of molecules from plasma membrane by endocytosis and also transport proteins from *trans*-Golgi complex. Clathrin-coated vesicle plays an important role in mitosis and in **endosomal sorting complex required for transport (ESCRT)**-dependent proteins segregation at endosomes. After endocytosis, the clathrin coat protein is removed from vesicle to form **uncoated vesicle**. The **uncoated vesicle**, known as **primary endosome**, may fuse with early or **sorting endosome** with the help of MYO6 (myosin), which helps in escaping of this uncoated vesicle from the

actin mesh of epithelial cells. The distribution of transported molecules by endosome depends on geometry of organelle and not on protein–protein interaction like clathrin-coated vesicles endocytosis. The **caveolae**, a vesicle with four isoforms of **caving coat** protein complex, a flask-like invaginations of the plasma membrane functions in **endocytosis, transcytosis** and **pinocytosis**. The endocytosis may be **clathrin dependent** and **clathrin independent**. **Glycosylc phosphatidyl inositol**-anchored protein is also involved in clathrin- and areolae-independent endocytosis by tubular structure, which is sensitive to small GTP binding protein (CDC42) inhibition but not to dynamin or clathrin inhibitions. Clathrin independent (CI) pathways again may be divided into two types, one having **dynammin-dependent** scission and other **dynammin-independent**. The dynammin-dependent endocytosis may further be divided into **alveolar** and **Rho A** regulated endocytosis, while **dynammin independent** includes **CDC42** and **ARF6** regulated endocytosis (Fig. 10.1).

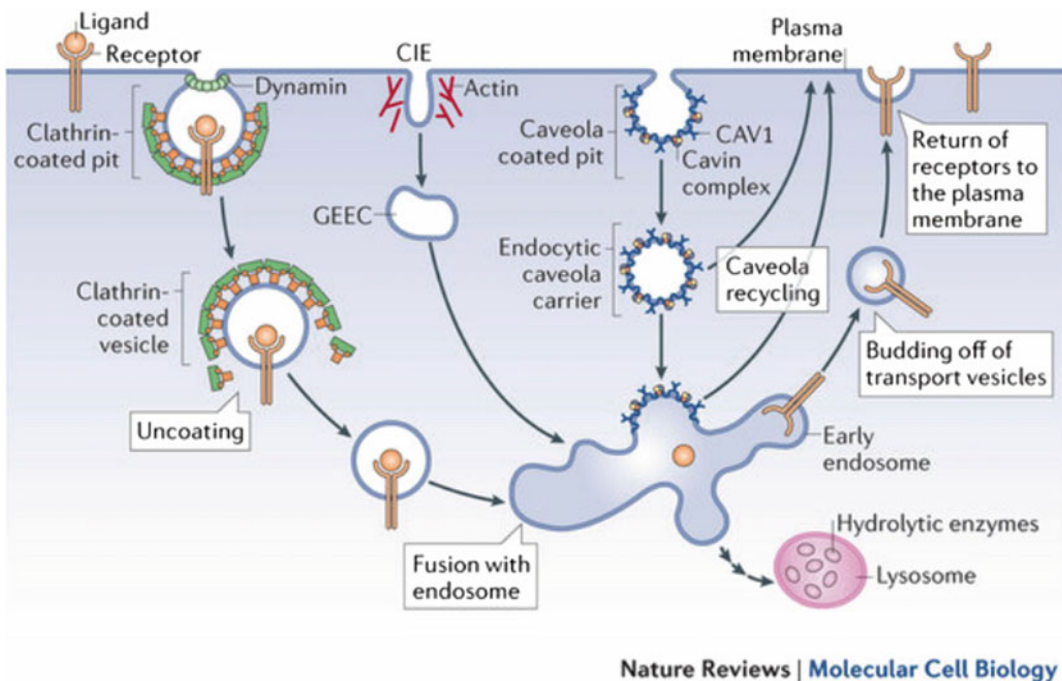


Fig. 10.1 Endocytosis by clathrin-dependent, clathrin-independent (CIE), and caveola-dependent proteins

10.3 Clathrin-Coated Vesicles Mediated Endocytosis and Recycling of Membrane

The **Clathrin-coated vesicles** are universally present in all eukaryotic polar (yeast and nerve cells) and nonpolar (fibroblast) cells. These vesicles cause endocytosis of freight of molecules. Clathrin-coated vesicles (CCV) carry out various function like recycling of proteins and lipids, internalization of nutrients like low-density lipoprotein, transferrin loaded with iron, activation of signaling receptor after internalization, sending various molecules to lysosomes for degradation. The pathogenic viruses like **influenza virus** and bacterial toxins like **shiga toxins** also depend on CCV for their internalization into host cell. **The human placental cell** receives maternal immunoglobulins through clathrin-coated vesicles for fetus development. The clathrin-mediated membrane bulging at the membranes of the *trans*-Golgi network (TGN) forms vesicles for freight transport to endosomes. The mannose-6-phosphate receptors interaction with mannose-6-phosphate labeled lysosomal hydrolases in the *trans*-Golgi lumen induce packaging of these enzymes into CCVs for transport to endosomes/lysosomes. Any defect in this pathways leads to release of these hydrolases causing abnormal function of lysosomal and development of lysosomal storage disease.

The active clathrin protein is made up of three heavy (**clathrin heavy chain, CHC**) and three light chains (**clathrin light chain, CLC**), all projecting outwardly. The three light chains interacts with three heavy chains to form **a triskelion** and many triskelia polymerize themselves around the vesicle to form lettuce like structure. The heavy chain N-terminal is β -propeller domain with seven WD40 repeats, which is followed in the polypeptide chain by 42 α -helical zig-zags of roughly 30 amino acid residues each, a longer α -helix at the threefold contact, and a 45-residue carboxy-terminal segment. Heat shock protein (HSc70) interacts with C-terminal to facilitate uncoating of CCV. The 42 zig-zags form an extended, slightly curved “leg” for the clathrin *triskelion*. The amino- and

carboxy-terminal of light chain are disordered. Clathrin triskelions may form sharply curved small or large coat (Fig. 10.2).

The clathrin-coated vesicle has to cross five stages of completion for endocytosis, which can be divided as 1. **initiation or nucleation**, 2. **freight loading**, 3. **clathrin polymerization**, 4. **scission** from membrane, and 5. **uncoating**. After passing the stage of initiation or nucleation and freight loading, the **clathrin triskelia** may form hexagonal net-like structure. The clathrin protein does not interact with membrane, ligand, or receptors directly but interacts with adapter protein and other associated factors for its recruitment to membrane. Some of the receptors like **low-density lipoprotein** have to interact with ligand for internalization while others like **transferrin receptor** are internalized directly without ligand interaction.

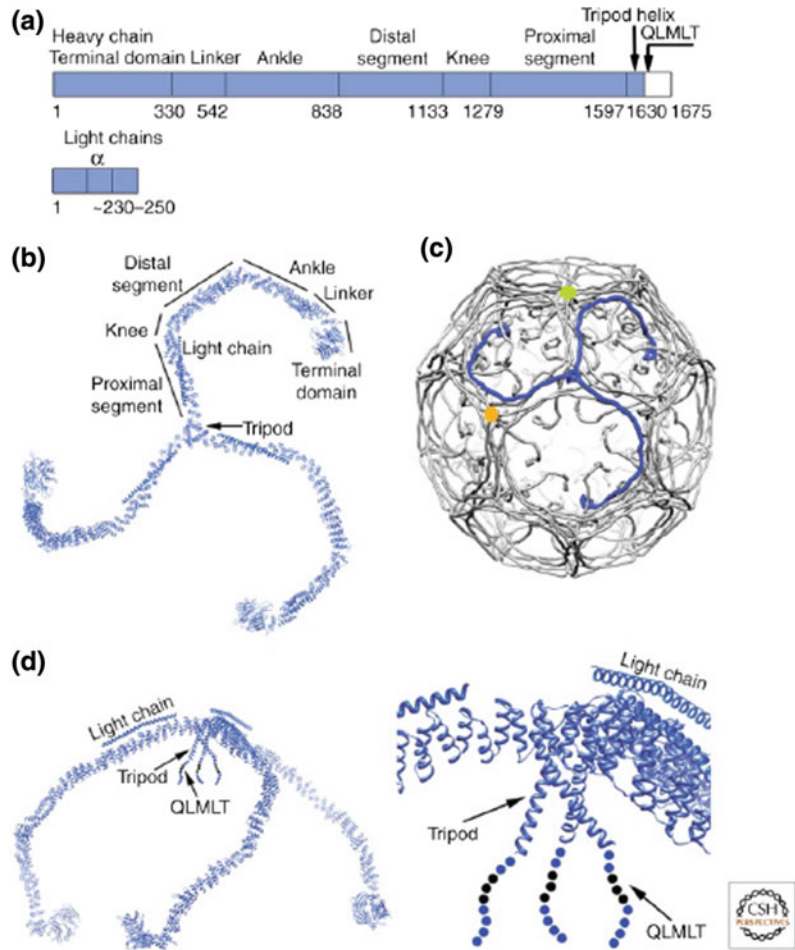
Once the transported molecules are internalized, clathrin coat is removed and these vesicles will convert to primary and **late** or **sorting endosomes** to separate different freight components, which may be sent back to either membrane surface or targeted to **mature endosomes** and then to **lysosomes**. (*Endosomes are discussed ahead*) (Fig. 10.3).

10.3.1 The Clathrin-Coated Vesicle (CCV) Cycling

The formation of clathrin-coated vesicle starts with putative nucleation module by highlighting the area on membrane for vesicle budding and clathrin recruitment because of phosphatidyl inositides (PtdIns). This requires **FCHO protein**, **EPS15** (AP2 clustering and scaffolding proteins), and **intersectin** (scaffolding protein). The FCHO is **F-BAR containing** protein; its signal decides the site for CCV formation before **AP2** or clathrin proteins appear. FCHO protein is responsible for **adapter protein (AP2)** and clathrin localization in membrane from cytosol. FCHO also participates in freight selection of transported molecules.

The putative nucleation module proteins define the site for membrane vesicle formation

Fig. 10.2 Clathrin protein. **a** Assembly of the heavy- and light-peptides. **b** α -carbon ($C\alpha$) display of a clathrin triskelion with various segments labeled of the heavy chain, central α -helical region of the light chain on each leg. **c** Triskelions formation in a clathrin coat. **d** Side view of the triskelion. <https://www.ncbi.nlm.nih.gov/pmc/articles/PMC3996469/figure/A016725F1>



and recruit the most abundant adapter protein (AP2) of **clathrin-coated vesicle (CCV)** along with other accessory proteins. These proteins may interact directly with adapter protein but not with clathrin. The **adapter proteins** are conserved, hetero-tetrameric complex of $\alpha\beta 2$ and $\mu 2$ and $\sigma 2$ subunits. The adapter proteins along with freight molecules bind to inner leaflet phosphatidylinositol (4,5) bisphosphate [PtdIns(4,5)P₂] through their α - and $\mu 2$ -adaptin subunits. The conversion of phosphatidylinositol (4,5) bisphosphate from phosphatidyl inositides (PtdIns) is regulated by kinases. At the *trans*-Golgi network, the members of the **Arf family** of **small GTPases** recruit and activate phospholipid kinases that mediate PtdIns (4,5)P₂ synthesis. The transitory increases in PtdIns(4,5)P₂ concentration at specific region of

inner leaflet creates temporary low-affinity nucleation site, where AP-2 interacts strongly with the membrane.

The AP2 interact with phosphatidylinositol 4,5 bis phosphate directly by binding to receptor cytosolic tail through its μ and σ subunit and indirectly to freight or cargo molecules with its extended domain. The other accessory adapter proteins interact with AP2, the core protein only. The accessory proteins **AP180** and **epsin** bind **with** amino-terminal domains to membrane for bending modules and also interact with freight of molecules. The next step in clathrin-coated vesicle formation is the recruitment of **clathrin** protein from cytosol to nucleation site by AP2 and accessory protein. The clathrin polymerization stabilizes curvature. At this point, the

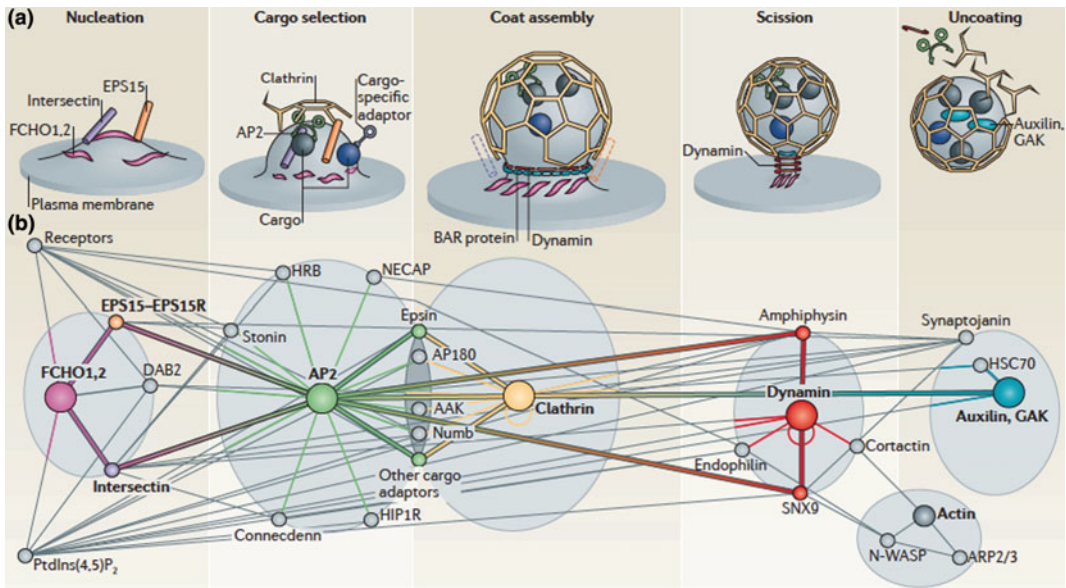


Fig. 10.3 a Various stages of clathrin coated vesicle formation. b Interaction of various proteins

accessory proteins like **EPS 15** and **epsin** move toward periphery of vesicles. The budding of **CCV** requires **dynamin**, which is recruited by **amphiphysin**, **endophilin**, and sorting **nexin 9** proteins. These **BAR domain** containing proteins prefer to bind at the curvature of the vesicle neck and form the neck more sharply by binding to proline-rich region of dynamin. The **BAR (Bin/Amphiphysin/Rvs; pfam03114 and SMART00721)** domain is the most highly conserved feature of amphiphysin from yeast to humans. The two BAR domains form a crescent-shaped homodimer with positive charge residues distributed along the membrane interacting concave face. Proteins of the **BAR superfamily** function in remodeling of membrane by interacting with acidic phospholipids. They can stabilize or induce membrane curvature in response to the molecular geometry of membrane-binding surface. Proteins with **F-BAR domains**, like **FCH domain only protein 1 (FCHO1)** and **FCHO2**, are involved at early stages of the process, whereas proteins with **N-BAR domains** (with an *N*-terminal amphipathic helix preceding the BAR domain), such as

endophilin and **amphiphysin**, are active with deeply invaginated pits at late stages of dynamin recruitment. On the one hand, the dynamin protein disrupts continuity of newly formed CCV on membrane and reseals the scission vesicles. The process requires GTP hydrolysis to cause both scaffolding of curvature and membrane insertions. The polymerization around the neck of newly formed vesicle causes membrane fission by induced GTP hydrolysis. The GTP hydrolysis induced conformational change in proteins that cause **scission or separation** of vesicle. When the heat shock protein **HSC70 ATPase** and **auxilin** or **cyclin G-associated kinase (GAK)** starts promoting triskelia formation from lettuce conformation, slowly clathrin starts dissociating from CCV and finally vesicle is without clathrin and starts moving. **Synaptojanin lipid phosphatase**-induced changes in phosphoinositides composition cause final uncoating of vesicle from clathrin (Fig. 10.4).

The phenylarsine oxide (PAO), monodansylcadaverine (MDC), Potassium depletion, acidic cytosolic pH, and chlorpromazine are found to inhibit clathrin-dependent endocytosis.

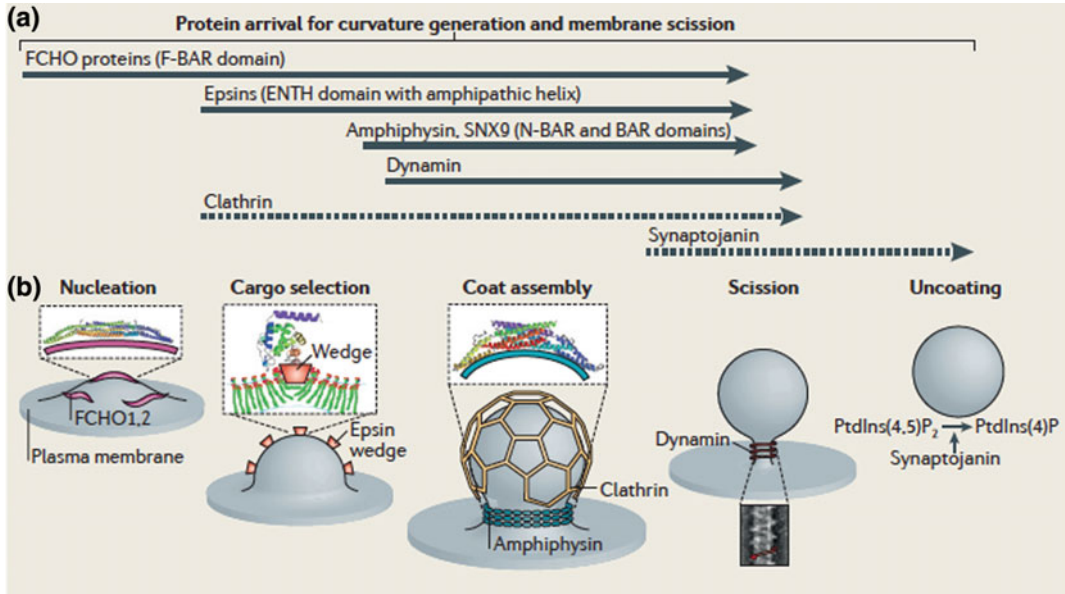


Fig. 10.4 **a** Many different curvature effector proteins work in clathrin-mediated endocytosis to form curved cargo-loaded vesicle. **b** Bending occurs because of various interactions with the membrane

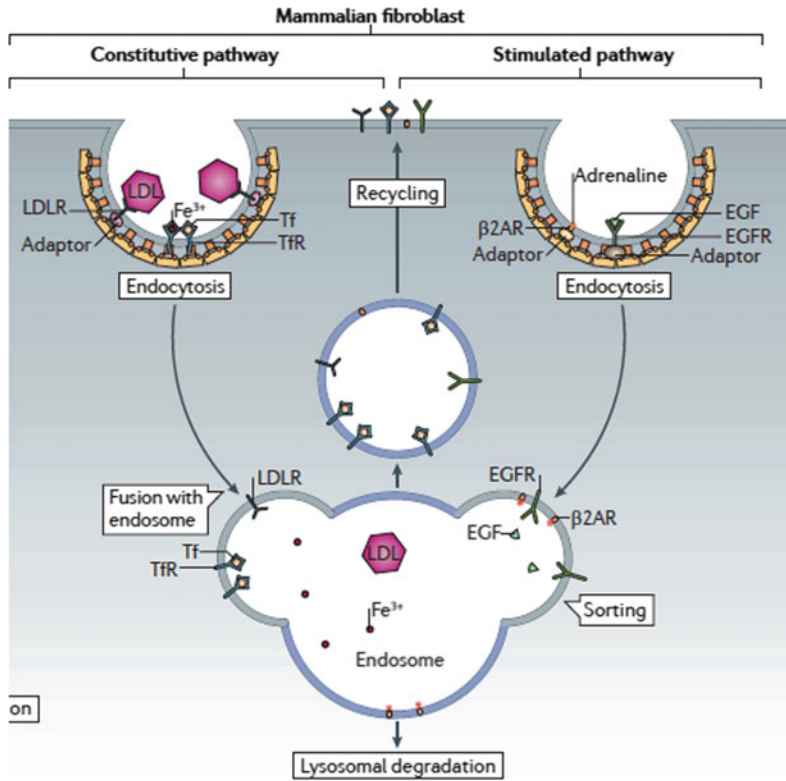
10.3.2 Constitutive and Inducible Endocytosis by Clathrin Coating Vesicle

Clathrin-mediated endocytosis may play role in signal proliferation, signal termination, and signal delay response. Some of the receptors like **Transferrin bound with iron (tfr)** and **low-density lipoprotein receptors (LDLR)** are internalized constitutively, while some other receptors as **tyrosine kinases (RTKs)**, **epidermal growth factors (EGFR)**, and **G protein coupled (GPCR)** need induction for endocytosis. In the inducible receptors, binding of ligand induces dimerization (RTKs) or change in conformation (GPCR) of receptors for loading to clathrin-coated vesicle by AP2 protein. As discussed above, AP2 and other accessory proteins recognize motif of cytoplasmic tails of constitutive. The low-density lipoprotein receptor (LDLR) contains an internalization sequence **FDNPVY**, resembling to consensus internalization motif **FXNPXY** for interaction with AP-2. After internalization, receptors are separated from their ligand and sent back to cell membrane or to lysosomes causing termination of signal or

delay in signal (if ligand is in small quantity). Sometimes endosome becomes the site for **signal amplification**. **Amphiphysin** and **dynamin** mutation may cause **centronuclear myopathy** and **neuropathy**. Single nucleotide polymorphism and altered gene expression of clathrin-dependent endocytic components are correlated to **bipolar disorder**, **schizophrenia**, and **neurodegenerative diseases** (Fig. 10.5).

10.4 Noncoated Vesicles in Endocytosis

As discussed above, the early and late endosomes are without any coat proteins. When **clathrin coat** is removed from vesicles after endocytosis, the vesicle is said to be newly formed known as **early endosomes**, whose function is to sort out all the receptors, proteins and other freight molecules. The term early endosomes include two different endosomes—the **sorting endosome** and **endocytic recycling compartment (ERC)**. The newly formed sorting endosomes fuse with other newly formed or preformed endosomes only for few minutes. These endosomes, having pH



NATURE REVIEWS | MOLECULAR CELL BIOLOGY, vol 12, 2012

Fig. 10.5 Transferrin receptor (TfR) and low-density lipoprotein receptor (LDLR), do not bound to their freight for internalization during clathrin-dependent endocytosis (the constitutive pathway), but epidermal growth factor receptor (EGFR) and β 2 adrenergic receptor (β 2AR) are endocytosed upon ligand binding. Endocytic motifs

present in the cytoplasmic tails of constitutively endocytosed receptors are recognized by adaptor protein 2 (AP2). During stimulated endocytosis, ligand-induced receptor dimerization (EGFR) or deprotection (β 2AR) (dimerization and deprotection not shown) allow receptors to bind AP2 for recruitment

around 6, are tubular vesicular structure. When the sorting endosomes translocate and stop fusing, their pH becomes more acidic (pH 5–5.5) and these endosomes are matured into **late endosomes**. The late endosomes are heterogeneous endocytic endosomes without any connection to clathrin vesicle. Because of low pH, the ligands and receptors with other molecules are uncoupled in the late endosomes and are sent back to their destination either to their specific destination or to endocytic recycling compartment. The fusion of early endosome is controlled by **endosome antigen (EEA1)**, **Rab5**, and **SNAREs**. Microtubules are observed to enhance transport of freight from sorting to late endosome. **Bafilomycin A1**, an ATPase inhibitor, inhibits transport

from sorting endosome to late endosome and to lysosome. The details of Rab5 and SNAREs are discussed in the following topics.

10.5 Clathrin-Independent Endocytosis (CIE)

10.5.1 Endocytosis by Caveolae

Though clathrin is major coat proteins involved in endocytosis of cargo but the freight of molecules may also be internalized by clathrin-independent pathways as mentioned above. A special membrane domain **caveolae** is omega shaped and detergent resistant invagination on the plasma

membrane of various muscle tissues and adipocytes, which is involved in internalization of freight of molecules independently of clathrin. The major resident molecules of caveolae are **caveolin** protein, **cavin protein**, **cholesterol**, **sphingomyelin**, and **glycosphingolipids**. Caveolae carry out **endothelial transport** and various **receptors uptake** in the membrane. It also has role in **membrane repair**, **protection against lipotoxicity**, cell signaling, lipid regulation. The various viruses like **SV40**, **polyoma**, **HIV** and pathogens as **ganglioside-bound cholera toxin** are internalized by caveolae. Interaction of caveolar components with freight molecules ligands like **protein albumin**, **ligand folic acid**, alkaline phosphatase, and lactosyl ceramide promote internalization of caveolae.

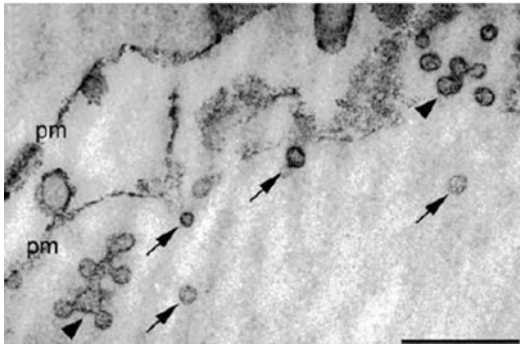
The caveolin protein has four isoforms like caveolin 1 α , caveolin 1 β , caveolin 2, and caveolin 3. The caveolin 1 protein plays a very important role in caveolae formation stabilization of caveolae in membranes. Recently, a new class of protein has been identified in mammals known as **Cavins** with four members as **Cavin1**, transcript release factor (**PTRF**), **Cavin2** (**SDPR**), **Cavin3** (**PRKCDBP**), and the muscle-specific isoform **Cavin4** (**MURC**). The other cytoskeletal and regulatory proteins are also involved in caveolae internalization. The transmembrane with conserved hydrophobic residue, **caveolin** protein has both N- and C-terminal toward cytosolic side and its 19–21 amino acids participate in signal regulation. Its 34 amino acids form hairpin structure in inner leaflet of the membrane without extrapasmic exposure. The N-terminal part of the proteins functions as scaffolding domain, which bind to cholesterol and sphingolipid-rich membrane domains. The C terminus is palmitoylated on many residues to align itself along the inner leaflet. Cholesterol is also required for caveolae formation and caveolin transcription because cholesterol inhibitor **filipin** or **nystatin** loses caveolin and caveola. Caveolar budding is regulated by kinases and phosphatases. As the simultaneous phosphorylation of caveolin 1 tyrosine 14 and tyrosine 19 of caveolin-2 induced **caveolae budding and internalization**. **Herbimycin A** and **genistein**,

the tyrosine kinase inhibitors have been found to prevent vesicle formation. The phosphatases also play an important role in regulation. The tyrosine phosphatase inhibitor **Vanadate** stimulates caveolar endocytosis by causing hyperphosphorylation of tyrosine residues of caveolin-1. The okadaic acid, polyether metabolite of the black marine sponge *Halichondria okadai*, serine/threonine phosphatase inhibitor also promote caveolar internalization. Caveolae formation depends on **dynamain protein**, which is also found to be important in clathrin-mediated endocytosis. The dynamain protein interacts with caveolae for a short period to cause fission of caveolae from the neck by **using GTPase enzyme**. **Intersectin-2** regulates GTPase activity of dynamain for caveolae internalization. The **endothelial NO synthase (eNOS)-trafficking inducer**, **NOSTRIN** is also found to recruit dynamain-2 molecules at caveolae in vascular tissue. The cytoskeletal proteins play a role in the formation and internalization of caveolae. The inward movement of caveolae happens because of cortical actin network local disassembly. The **Filamin** (an actin cross-linking protein) is a ligand for caveolin-1. The virus also uses caveolae for their entry.

SV40 virus present in caveolae generates endocytic signal, which results in tyrosine phosphorylation and depolymerization of cortical actin cytoskeleton. Actin monomers are recruited to the virus loaded caveolae for caveolae budding. Once caveolae are internalized, the cytoskeleton goes back to their original position. **Okadaic acid** helps in targeting actin cytoskeleton to go back to its original position, for caveolar internalization. As studied in SV40 virus endocytosis, the caveolae loaded with viruses, after internalization, interact with each other to form caveolar complexes, known as **caveosomes** of neutral pH. These complexes never fuse with lysosomes. This may be reason of **virus escapism** from lysosomal enzyme. These **caveosomes** are heterogenous multicaveolar structures (Fig. 10.6).

The viruses may be sorted from caveosomes into vesicular and tubular structures that travel along microtubules to the smooth endoplasmic

(a)



(b)

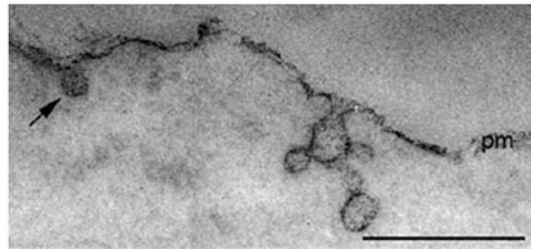


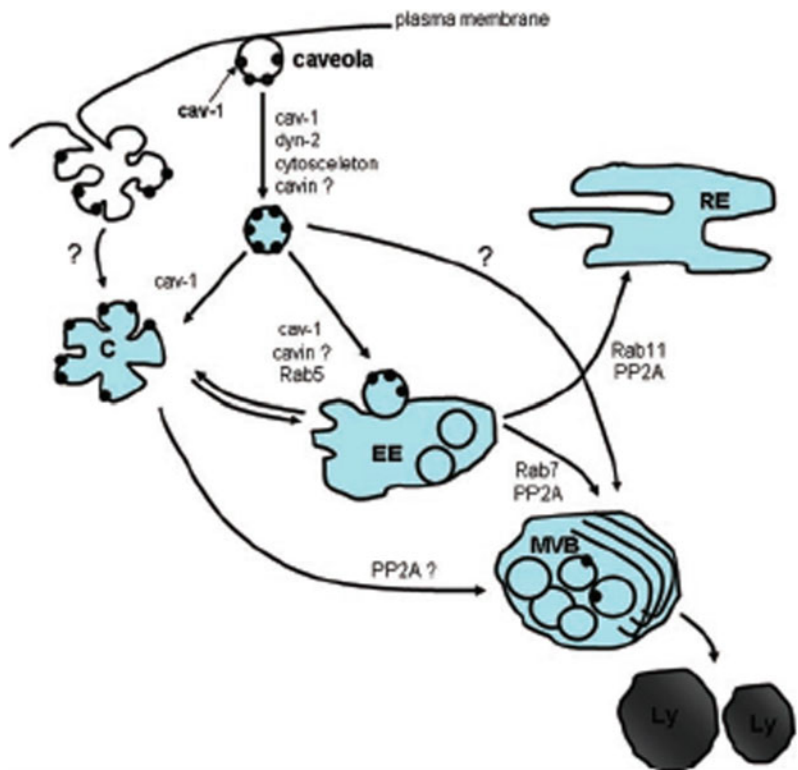
Fig. 10.6 Electron micrographs of caveolae mediated internalization. Ruthenium red (Ru red) is used to label the cell surface, single vesicles (arrows) as well as caveolar bundle (arrow heads) are Ruthenium positive. The

caveolar bundles (arrow heads) are known as caveosomes. pm: plasma membrane. Bars: 400 nm. Journal compilation © 2009 Foundation for Cellular and Molecular Medicine/Blackwell Publishing Ltd

reticulum. There are other examples of freight internalization by caveolae, which passes through early endosome like receptor-mediated endocytosis. The pathogen **cholera toxin** after internalization enters into early endosomes Golgi complex targeting (Fig. 10.7).

The caveolae either forms **caveosomes** or may move to early endosome. In this process Rab5-GTPase is needed. The caveolae may dock on endosomal membrane, and their membrane domains do not mix with each other. After some time, the caveolin-1 subdomains pinch off from

Fig. 10.7 Recycling of caveolae. Phosphorylation of dynamin, cytoskeleton reorganization causes budding of caveolae. Caveolae may form cluster in cytoplasm. Single endocytic caveolae may fuse with early endosomes (EE) or with pre-existing caveosomes (C) or can form caveosomes. This pathway is bi directional



early endosomes as membrane vesicles by picking some of the cargo. This kind of transport is understood as **bidirectional transport**. **Dephosphorylation** of caveolin is necessary for the recycling of caveolae to the cell surface.

10.5.2 The Clathrin-Independent Carrier (CLIC)—GPI-Anchored Protein-Enriched Early Endosomal Compartment (GEEC) Cycling

The internalization of freight of molecules may also be mediated by tubular and ring-shaped membrane endosomes, different than clathrin and caveolae-mediated endocytosis, which depend on small **GTP binding protein cyclin-dependent kinase (CDC42)**, **ADP-ribosylation factor 1 (ARF1)**, **GTPase regulator associated with focal adhesion kinase 1 (GTPase activating protein for Rho, GRAF1)**, cholesterol and actin. GRAF1, a **BAR domain**, is membrane curvature and CDC42 regulator protein. The other proteins involved in clathrin- and caveolin-independent pathway are **Glycosylphosphatidylinositol (GPI)-anchored proteins**, which is called as **clathrin-independent carrier (CLIC)—GPI-anchored protein-enriched early endosomal compartment (GEEC) pathway**. CLIC–GEEC carriers may fuse with early endosomes in phosphatidylinositol 3-kinase dependent manner. The **major histocompatibility class I (MHC I)** molecules are also internalized by this process, which is fused with endosomes after internalization. A member of the Ras superfamily of monomeric G protein **RAB22**, membrane-associated RING-CH (**MARCH**) ubiquitin ligases help in sorting of **GPI-anchored proteins, CD44**, and **MHC I** after internalization. The RING-CH MARCH proteins of ligases family have catalytic ring finger and are membrane bound. The formation of transporting spherical or tubular bud occurs by local mechanical deformation of the flat plasma membrane. The energy needed for this localized tubular structure formation per unit of

area (F_b) from the membrane is formulated by Helfrich Hamiltonian as:

$$F_b = \frac{\kappa}{2} C^2$$

where C is local curvature, κ **varies with composition of membrane**, known as membrane bending modulus.

This energy (F_b) is provided by **kinesins, dyneins, or myosins** (especially class I myosins) molecular motors, which can pull membrane by binding and moving along microtubule to form tubular membrane structures. This mechanism of tube formation has been confirmed by several in vitro experiments. The cytoskeletal protein **actin** involved actively in forming specific lipid domain in the membrane for vesicle budding and scission.

The other less energy-consuming and more spontaneous tube formation occurs by **asymmetric distribution of proteins and lipids** in two leaflets of the membrane, which causes natural bending of the membrane.

The energy requirement is reduced in this way for bending and formula becomes

$$F_b = \frac{k}{2} (C - C_0)^2$$

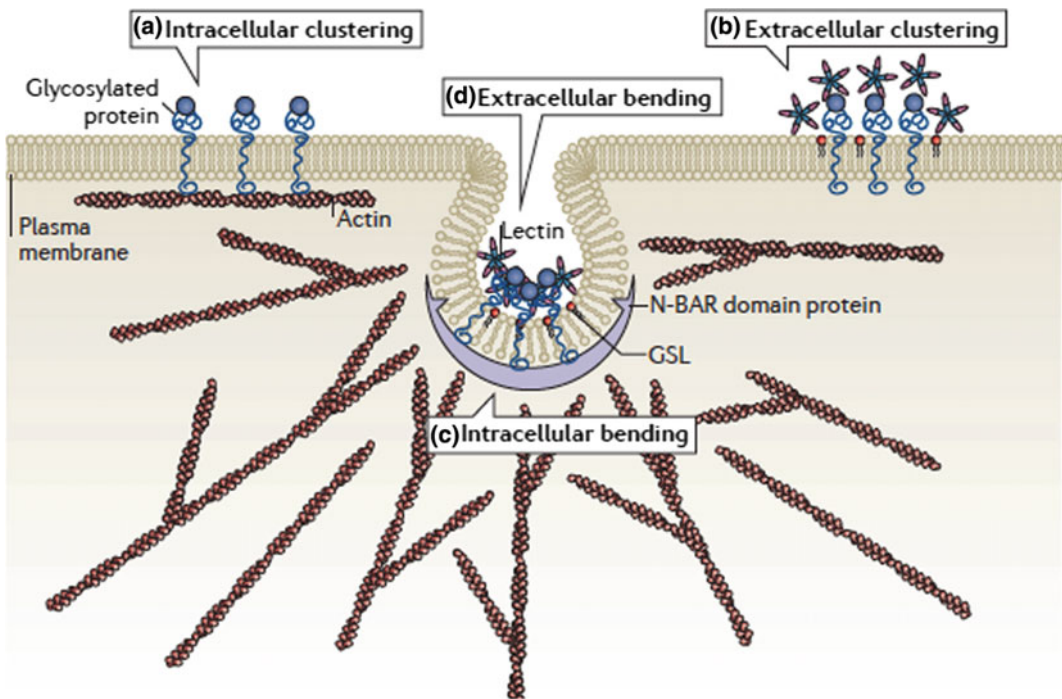
where C_0 indicates the spontaneous membrane curvature in absence of external support. The spontaneous bending is supported by inserting hydrophobic proteins in the membrane (as observed by **epsins**), or by modulating the membrane (as observed by crescent-shaped BAR domain proteins.), or by locally clustering of proteins.

In the **RHO-A GTPase-dependent pathway** of CIE, elaborate actin-recruiting machineries like **cortactin, p21-activated kinase 1 (PAK1)**, and **neural Wiskott–Aldrich syndrome protein (N-WASP)** are required for internalization. The N-WASP protein enhances actin polymerization. In clathrin-independent internalization, the transformation of CDC42 between GTP bound active conformation and GDP-bound inactive conformation regulates actin polymerization and internalization. **Macropinocytosis** is another

stimulated, clathrin-independent endocytosis, which is carried by large endocytic vesicles, called as **Macropinosomes** in actin-dependent manner. Macropinosomes size may range from 0.2 to 0.5 μm in diameter. These macropinosomes internalize MHC glycoproteins bound to foreign antigen on dendritic antigen presenting cells. **The GSL globotriaosylceramide (Gb3GSLs)** is found to be involved in the cellular entry of a large number of pathogens and pathogenic factors, including viruses such as **polyoma viruses, rotavirus, influenza virus, and HIV** and **toxins** such as **shiga, cholera, botulinum, and tetanus toxins** because their carbohydrate **lectins** bind to receptor. The **lectins are pentamers** and induce membrane invaginations on interacting with GSLs. The receptor C-terminal of SV40 and GSL monosialotetrahexosylganglioside (GM1)

were found to be important for internalization and infection. The cellular **lectin galectin 3** drives the biogenesis of CLICs and the cellular uptake of the CLIC freight. The CD44 and $\beta 1$ integrin proteins are involved in cell migration and adhesion. **Galectin 3** seems to function as an **endocytic adaptor** that recruits cargoes (glycosylated proteins) and curvature-inducing components (GSLs) into molecular environments.

Lectin also forms **tubule** for CIE. The cellular receptor of **shiga toxin** is the **GSL globotriaosylceramide (Gb3)**, and Gb3 is also important for the clathrin-independent formation of endocytic pit. The **dynamamin, actin,** and the BAR domain protein **endophilin A2** induce vesicle scission through actin polymerization on endocytic membrane (Figs. 10.8, 10.9 and 10.10).



Nature Reviews Molecular Cell Biology | AOP, published online 10 April 2015; doi:10.1038/nrm3968

Fig. 10.8 Clathrin independent vesicle formation. A membrane invagination is shown in the centre. Four different process are explained. **a** Intracellular collection. **b** Extracellular collection of glycosylated membrane proteins with lectins. **c** N-Bin–Amphiphysin–Rvs

(N-BAR) domain proteins or helix-inserting epsins recruitment by freight proteins for membrane curvature. **d** The curvature can be induced by glycosphingolipids (GSLs) organization by lectins

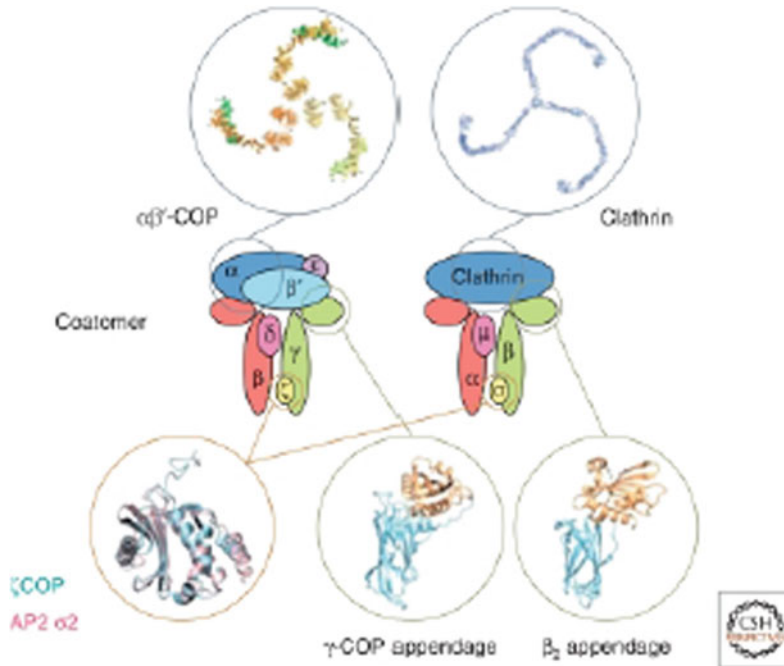


Fig. 10.9 Similarities between COPI heptameric complex and clathrin/adaptor complex AP2. The stable complex coatomer can be dissociated *in vitro* into subcomplexes: a trimer ($\alpha\beta'\epsilon$) and a tetramer ($\beta\gamma\delta\zeta$). Within the tetrameric subcomplex of coatomer structural similarities are reported

for ζ -COP and AP2 σ 2 and for the γ -COP and the β 2 appendage domains. Thus, the trimeric COPI-subcomplex is thought to resemble the clathrin part, and the tetrameric COPI subcomplex the adaptor part of a clathrin-coated vesicle. <https://www.ncbi.nlm.nih.gov/pmc/articles/PMC3220356/>

10.6 Coatomer Protein (COP) Vesicles

10.6.1 The Coatomer Protein I (COP) in Transport

COPI vesicles are involved in **retrograde** transport for recycling proteins between *cis*-Golgi complex to endoplasmic reticulum and intra Golgi complex transport. COPI also regulates functioning of Golgi complex. **COPII** vesicles transport newly formed proteins from rough endoplasmic reticulum to Golgi complex, and this transport is called **anterograde** transport as explained above.

The Golgi complex has a central place between endoplasmic reticulum secretory protein and other endocytic compartment. The anterograde transport through the Golgi is mediated by **cisternal maturation**. GTPase CDC42 is a

regulator to control freight movement in either direction in Golgi with the help of COPI in **freight selection and vesicle formation**. CDC42 also helps in bending of membrane for COPI tubule formation. The COPI tubular transport is associated with cisternal maturation. The Coatomer protein I is a protein complex of seven different types of subunits, $\alpha\beta'\epsilon/\beta\gamma\delta\zeta$ which is found on Golgi complex, endoplasmic reticulum intermediate compartment (IC) and on coated vesicles surrounding the Golgi (COPI vesicles).

The **vascular model** and **maturation and progressive model** were given for functioning of coatomer proteins, where **Vesicular model** deals with Golgi complex being stationary and COPI vesicles being mobile. COPI leaves their freight of proteins and lipids to cisternae in this model. In **maturation and progressive model**, the cisternae are moving along the Golgi from *cis*- to *trans*-Golgi complex and finally get disassembled there. COPI activates maturation of the

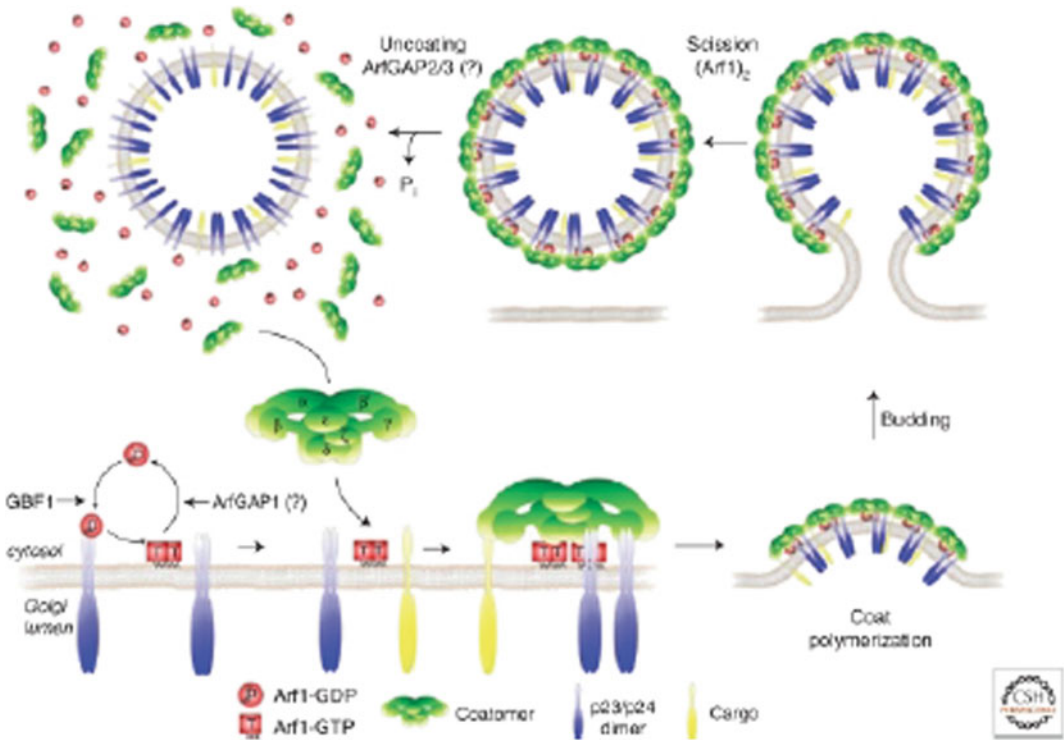


Fig. 10.10 Individual steps in the formation of a COPI vesicle. <https://www.ncbi.nlm.nih.gov/pmc/articles/PMC3220356/figure/A005231F2/>

cisternae along the cistrans axis of the Golgi in this model. The majorly accepted **percolating model** combines the feature of these two models to explain that COPI vesicles mediate bidirectional transport between two adjacent cisternae randomly. In **anterograde** transport, the newly formed proteins enters *cis*-Golgi and leaves from *trans*-Golgi.

10.6.2 Coatomer Protein (COP)II Vesicles in Transport

As mentioned above, the coatomer protein II is involved in transport from endoplasmic reticulum (ER) to Golgi complex (TGN), which is known as **anterograde** transport. The defective COPII transport for procollagen is found to secrete and deposit defective collagen protein. In the yeast live cells, the time lapse fluorescence microscopy has confirmed COPII vesicles as kinetically stable vesicles on the ER membrane

because the same site is used again and again for vesicle formation.

Sar1 family of GTPase and guanine exchange factor (GEF) play an important role in COPII recruitment on membrane of ER. The nascent formed protein is transported from ER to Golgi for modification and further destination. The COPII might be recruited at different sites of smooth endoplasmic reticulum or **ER exit sites (ERES)** or **transitional endoplasmic reticulum (tER)**. Yeast COPII components “in vitro” has identified two more heterodimeric complexes of Sec23/24p and Sec13/31 apart from Sar1 protein. The GEF-Sec12 promote the Sar1GTPase protein in cytoplasm in the similar way like Arf1. The arf initiate bulging out of membrane by inserting its N-terminal α helix into lipid bilayer. The sar1-GTP after binding to membrane catalyzes loading of Sec23-Sec24 by interacting with Sec23 subunit. The Sec23 acts as GTPase activating protein (GAP). The whole complex is known as **prebudding complex**. The activated

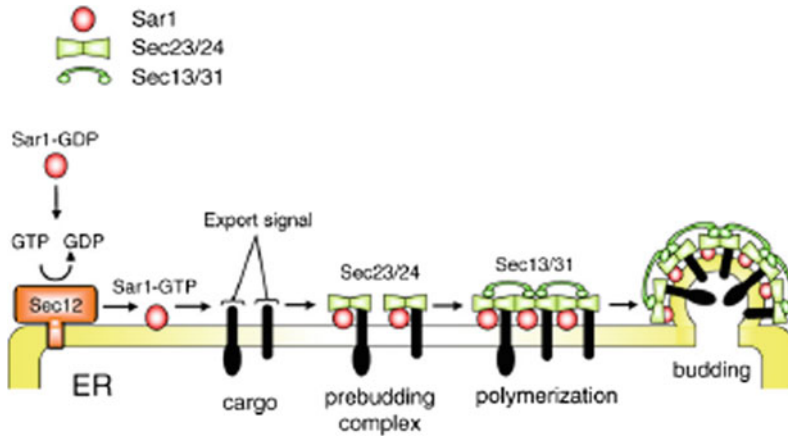


Fig. 10.11 Selective uptake of freight molecules by COPII vesicle by Sar1 through Sec12 GEF. Activated Sar1-GTP load Sec23/24 sub complex binds to the ER membrane and the freight C terminal signal interact with

Sec24 with proteins in pre budding stage. The whole pre budding protein complexes is concentrated by the Sec13/31 proteins to form COPII-coated vesicles

complex of **sar1-/Sec23-Sec24** carry out freight selection of molecules and recruit **Sec13-Sec31** for forming outer layer of COPII vesicle. Sec13-Sec31 induce polymerization for membrane bending for vesicle formation. Sec16 and Sec4 provide additional scaffold for COPII-coated vesicle assembly. Immediately after budding, these COPII vesicles lose their coat and get fused with each other to form intermediate compartments (IC). These multiple fused vesicles (IC) now travel along microtubule with secretory proteins for transport with freight molecules (Fig. 10.11).

Sec23-Sec24 complexes perform two different functions, the Sec23 acts as GTPase activating protein for sar1 and the Sec24 interacts with various ER exporting signals of freight protein via its different domain for specific selection and provides more flexibility to vesicles. As explained in COPI vesicles transport, the freight proteins are found to have export signal at their C-terminal, which interact with COPII vesicle proteins. For example, lectin-like receptor for glycoproteins has **diphenylamine motif** at their C-terminal and vesicular stomatitis virus glycoprotein has **di-acidic sorting signal** (Aspartic acid-X-glutamic acid or DXE) sequence for its transport from ER to Golgi. The soluble proteins are selected in two different ways, either by

default or through specific interaction of coat protein to membrane receptor of protein.

Rab protein in COPII vesicle transports mediate tethering and fusion of COPII vesicle to their target membrane. The activated Rab proteins act through its effector molecules like **golgin p115**. Golgins are supercoiled protein family, which also play role in Golgi shape formation. The **Rab1 protein** load p115 protein to COPII vesicle for tethering and organising transitional ER site (tER). The p115 is also present in intermediate compartment (IC) for IC to Golgi transport. Vesicle fusion is executed by another effector protein SNAREs. The role of SNARE is explained in membrane fusion (Figs. 10.12 and 10.13).

10.7 Internalization by the Exomer Complex

Recently identified exomer protein complex is a putative coat and freight adapter like AP2, which directly transport freight molecules from *trans*-Golgi network to plasma membrane in response to environment stress in cell cycle-dependent manner. The **chitin synthetase (Chs3)**, **pheromone response mediator Fus1**, and **Pin 3** are identified protein, which are internalized in response to stress. The Chs3 may be exported

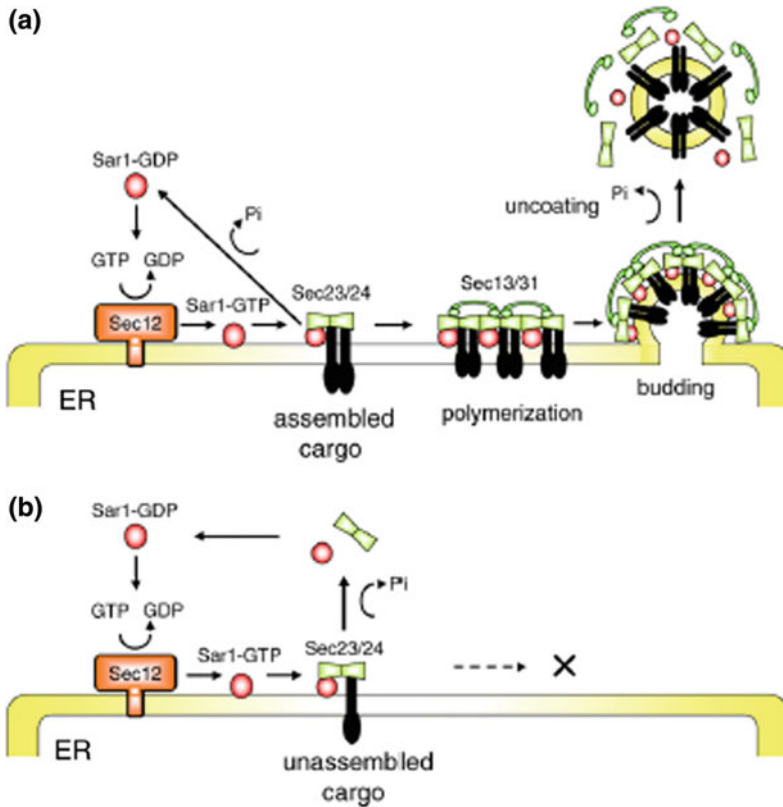


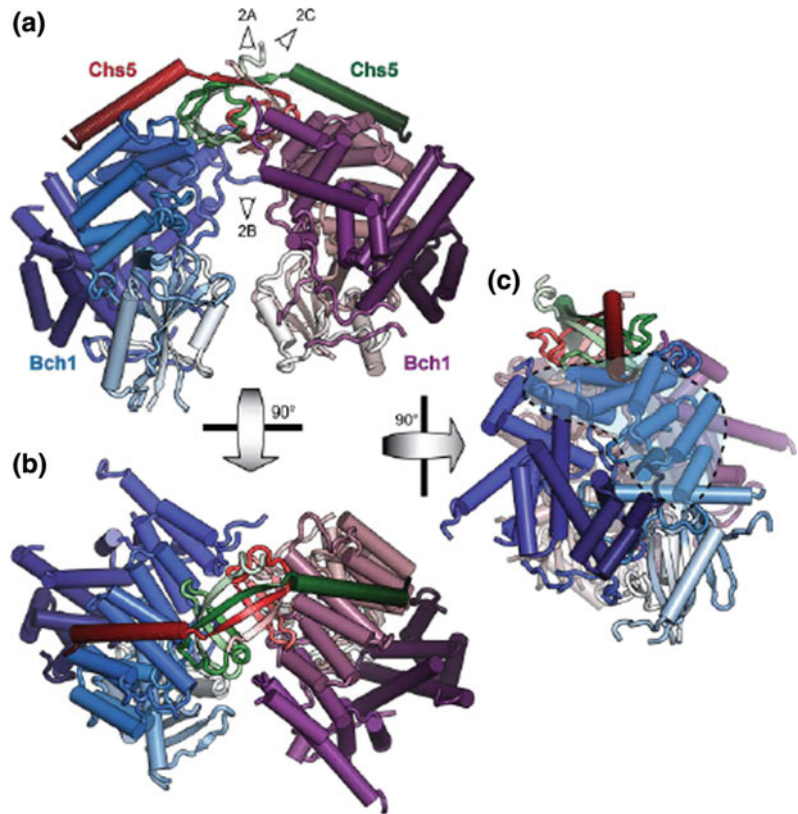
Fig. 10.12 A model for GTPase-driven proof-reading by Sar1. The assembled cargo has a high affinity for the Sec23/24 because of the combined export signals. This cargo-Sec23/24 association persists during the nucleotide exchange reaction of Sar1 catalyzed by Sec12 (a). In contrast, the Sar1 GTP hydrolysis dissociates the weak

association between the coat and unassembled cargo before polymerizing into COPII coats (b). Thus, the prebudding complex stabilities are biased towards the complex including assembled cargo, ensuring that the fully assembled cargo is preferentially incorporated into COPII vesicles

back to plasma membrane with time gap after internalization and provide strength to cell membrane. The Pin3 protein stays back in transGolgi complex till the stress is settled or removed. Once the cell is relaxed, Pin3 moves back to membrane. The exomer-dependent transport might be important to mark stress responsive protein at plasma membrane. The exomer protein complex **ChAPs** includes five peripheral *trans*-Golgi proteins, known as **Chs5**, **Chs6**, **Bud7**, **Bch1**, and **Bch2**. The soluble complex is found to have two copies of Chs5 and two copies of any other ChAP. The half of the protein from N-terminal of Chs5 has similarity to API and COPI. The exomer recruited is

dependent on ARF1. The whole protein is a scaffold for assembly. Chs5 recruit ChAPs to transGolgi complex in Arf1GTP manner. The structural analysis of Chs5 reveals the subunits flexibility at dimeric N-terminal domain. The flexible hinge domain of Chs5 is responsible for stable interaction with other proteins in dynamic environment of cell. The structural data suggest that the complex is very flexible around the dimeric N-terminal domain of the Chs5 subunits, which might adopt to a noncanonical trans β -sandwich fold. ChAPs protein interacts directly with freight molecules of proteins and lipids similar to adapter protein and binding at the exporting site needs Arf1/Sar1 GTPases.

Fig. 10.13 Crystal structure of exomer protein complex tetramer, showing subunits of the Chs5/Bch1



10.8 Recycling of Synaptic Vesicle

Membrane fusion is the first step for various physiological functions like endocytosis, exocytosis, signal transduction, and fertilization. The membrane fusion can be explained as merging of the components of two separate lipid bilayer of membrane where role of SNARE proteins is very important.

The chemical signals propagate by neurotransmitters through the synapses as discussed in Chap. 7 from presynaptic cell to postsynaptic cell. These neurotransmitters are packed in the vesicles for Ca^{2+} dependent exocytosis. The presynaptic cells have thousands of vesicles, which need to be cycled immediately after exocytosis for continuous signal propagation. **Clathrin-mediated endocytosis** plays an important role in recycling of synaptic vesicle and in regulation vesicle size in cell. The

significance of clathrin-mediated endocytosis (CME) is observed by mutation study of pathway components in *C. elegans* and in *D. melanogaster*. In the other study, the nerve cell extract was found to be rich in clathrin-coated vesicles and has brain-specific adapter and accessory proteins like **AP180**, **Epsin1**, **amphiphysin1**, **dynammin1**, and splice forms of **EPS15** and **amphiphysin2**. At synapse endocytosis and exocytosis is regulated by **phosphorylation** and **dephosphorylation** event. Endocytosis is initiated by calcium-dependent **calcineurin protein** mediated dephosphorylation of endocytic components and phosphorylation occurs after endocytosis by **cyclin-dependent Kinases (CDKs)**, because dephosphorylation generally enhances protein-protein interactions. At the synapse signal propagation and transport of neurotransmitter study gives combined result including clathrin-dependent and -independent pathways together because of populated cells. Endocytosis is much

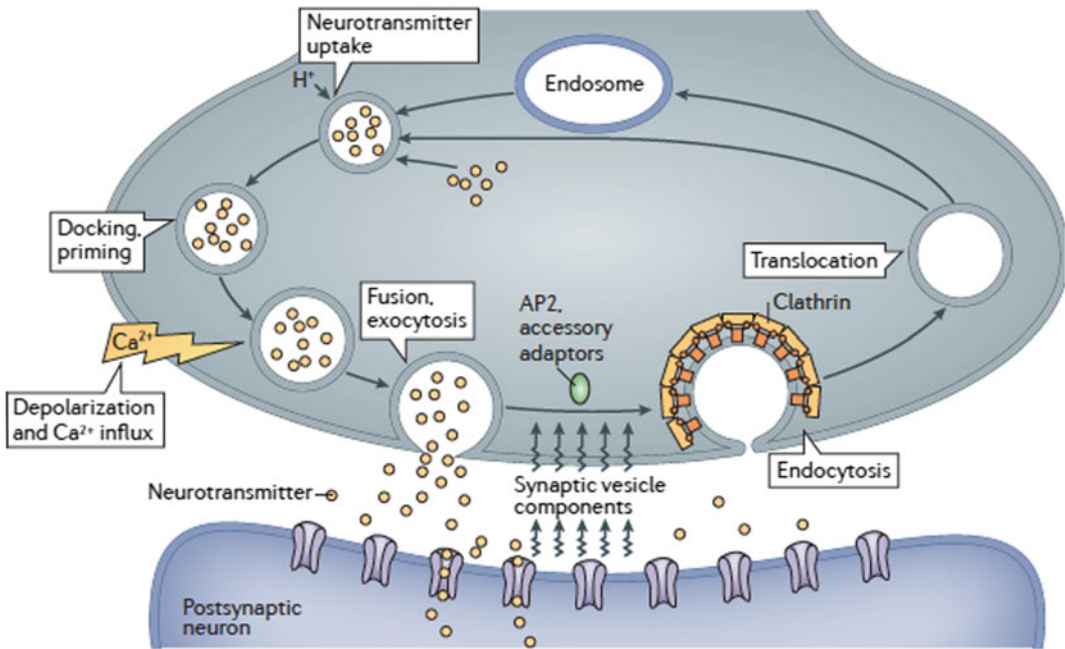


Fig. 10.14 Synaptic vesicle components, SNAREs, synaptotagmin and neurotransmitter transporters are separated into clathrin-coated vesicles by AP2 and freight specific adaptors. Synaptic vesicles are recycled to endosomes

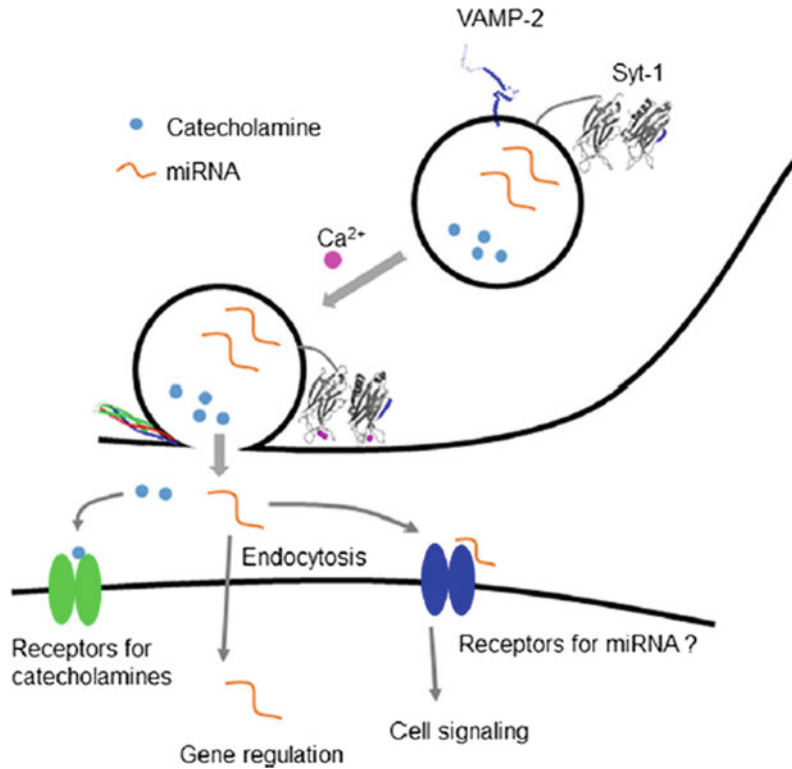
faster in nerve cells in comparison to other cells, so it is difficult to observe endocytosis in single cell. Clathrin-coated vesicles are smaller at synapse, and clathrin-dependent endocytosis is specifically coupled to exocytotic stimulus for recycling of synaptic vesicle components as SNAREs and neurotransmitter transporters rather than for up taking of ligands. The action potential and depolarization induced calcium influx triggers synaptic vesicle fusion and transmitter release (Refer to Chap. 7 in detail). The synaptic vesicle components like SNAREs, synaptotagmin, and neurotransmitter transporters are loaded into clathrin-coated pits by binding AP2 and cargo-specific adaptors. Recycled synaptic vesicles are translocated to endosomes, where they may bind with new neurotransmitters for another round of signaling. The synaptic vesicle (SV) interacts with five types of proteins majorly, the SNARE protein **synaptobrevin** for fusion, **synaptotagmin** for calcium binding, **neurotransmitter transporter**, **rab proteins** for docking and **synaptophysin** with poorly understood function. Synaptic vesicles proteins also

interact with coat protein. The mechanism of endocytosis is discussed above (Fig. 10.14).

10.9 Exocytosis

Exocytosis is the most important mechanism for neurotransmitters release for communication at synapse. The neurotransmitters, present in presynaptic vesicles, are stimulated to fuse with the presynaptic membrane to form pore for releasing of molecules. These vesicles may be divided into two types according to their size; **small synaptic vesicles (SSV)** involved in neurotransmitters release and the other one is **large dense core vesicles (LDCV)** with **densely packed protein matrix**. The LDCV may also be found cells, like exocrine, endocrine, and neuroendocrine cells. Both LDCV and synaptic vesicles are originated from the *trans*-Golgi network (TGN). The formation of LDCVs occurs because of aggregation of secretory proteins as seen in fibroblasts in **chromogranin A**, while in **PC12 cells**, low expression of chromogranin

Fig. 10.15 Exocytosis of miR-375 RNA along with neurotransmitter by LDCVs. The exocytosis is mediated by the SNARE complex in calcium dependent manner. Secreted miRNAs control gene expression and signal transduction



inhibits LDCV formation. **Cholesterol** and **dynamin II** facilitate the budding of these vesicles from the Golgi network. The neurotransmitter vesicle has pH of 5.4 because of H⁺-ATPase presence in the vesicle membrane. This pH gradient is important for loading of by **antiport transporter** protein of vesicular membrane, which transports the neurotransmitter molecules into the vesicle at acidic pH. The **vesicular monoamine transporter** or the **VMAT** (VMAT1 in endocrine cells and VMAT2 in neurons) are involved in **monoamine** and **dopamine** transport, against a steep concentration gradient. The synaptic vesicle and large dense-core vesicle (LDCV) use **soluble N-ethylmaleimide-sensitive factor activating protein receptor** (SNARE) proteins and calcium sensor Synaptotagmin 1 protein for releasing their freight. The LDCV or **chromaffin granules** participate in **mi RNA exocytosis** along with neurotransmitter like **dopamine**, **adrenaline**. Usually mi RNA of 20–24 nucleotides was supposed to be present only in cell, where it

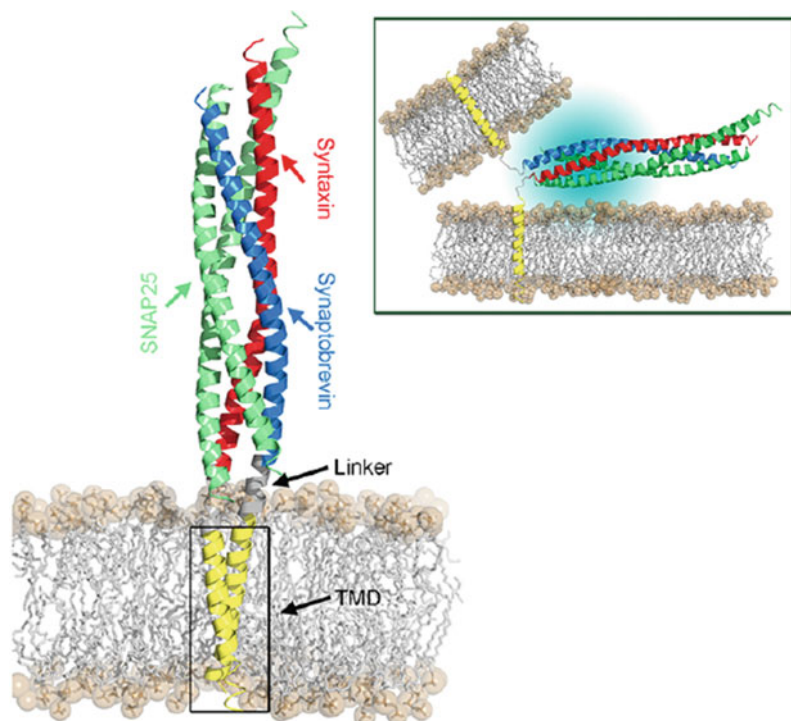
controls gene expression. Recently, mi RNA is detected in serum and at synapse and in extra-cellular compartment. The mi RNA is released by nerve cell at synapse to play possible role in pain signaling. The two different length mi RNA, mi R-229 and mi R-125, are detected at synapse with neurotransmitter, secreted in calcium-dependent manner. The next-generation sequencing in LDCV from bovine chromaffin cells has confirmed the presence of mi RNA in these vesicles. These results are also supported by in vitro artificial vesicle fusion and artificial neurotransmitter release. The mi RNA along with neurotransmitter secretion may regulate gene expression and signal transduction. To know the exact mechanism of mi RNA exocytosis, further investigations are required (Fig. 10.15).

The exocytosis can be divided into following steps; 1. **tethering**, 2. **priming or docking**, 3. **fusion initiation**, 4. **Hemifusion** between two membranes, 5. **Pore opening** by fusion of two membranes, and 6. **Release of freight** by complete disintegration of membrane.

The SNAREs protein superfamily with α helical configuration participate actively in membrane fusion by lowering energy requirement. The conserved motif of 60–70 amino acids in SNARE complex is called as **SNARE domain**, which brings together vesicle and target membrane together in close proximity. The SNARE complex of vesicles and target is called as **v SNARE** and **t SNARE**, respectively, for understanding. The v-SNAREs are enriched with arginine (R) in the SNARE domain center and may be called as R SNARE. **SNAP 25** and **syntaxin** are called as QSNARE because of glutamine (Q) presence. The other proteins such as calcium sensor protein, **Synaptotagmin**, **Rab**, **Rab5 effector protein EEA1** (early endosomal antigen 1) are also involved in membrane fusion for exocytosis. SNAREs can be monomer or polymer. For exocytotic membrane fusion, SNAREs are polymerized as homo- or hetero-polymer in helical form. The polymerization causes energy release to form compact bundle of SNAREs (Figs. 10.16 and 10.17).

The spontaneous folding of SNARE complex regulates priming of vesicle to target membrane. SNARE linker region of v SNARE proteins transmembrane catalyze fusion by transferring cytosolic core complex force to membrane aligned fusion site. The positive charge amino acids of linker are found to be supportive of fusion because interaction between positive charge amino acids with anionic membrane surface disrupts water ordering and bringing two membrane closures. The two tryptophan present in SNARE (W89 W90) at fusion site, change electrostatic potential at the site by acting as fusion clamp in Ca^{2+} dependent manner. The change in conformation of SNARE and its interaction with lipid bilayer of membrane promotes lipids disorder and mixing. Hemifusion, the intermediate nonlamellar structure, needed for fusion pore formation is also stabilized by transmembrane domain of SNAREs. The polymerization of SNAREs enhances interaction between the SNARE domain of SNAP25 and syntaxin via forming an ionic couple to link neighboring SNARE complex to form radial

Fig. 10.16 SNARE proteins complex consisting of synaptobrevin (in blue), syntaxin-1A (in red), and two SNAP-25 (sn1 and sn2, both in green) proteins (PDB:1SFC). http://www.frontiersin.org/files/Articles/244875/fphys-08-00005-HTML/image_m/fphys-08-00005-g003.jpg (Color figure online)



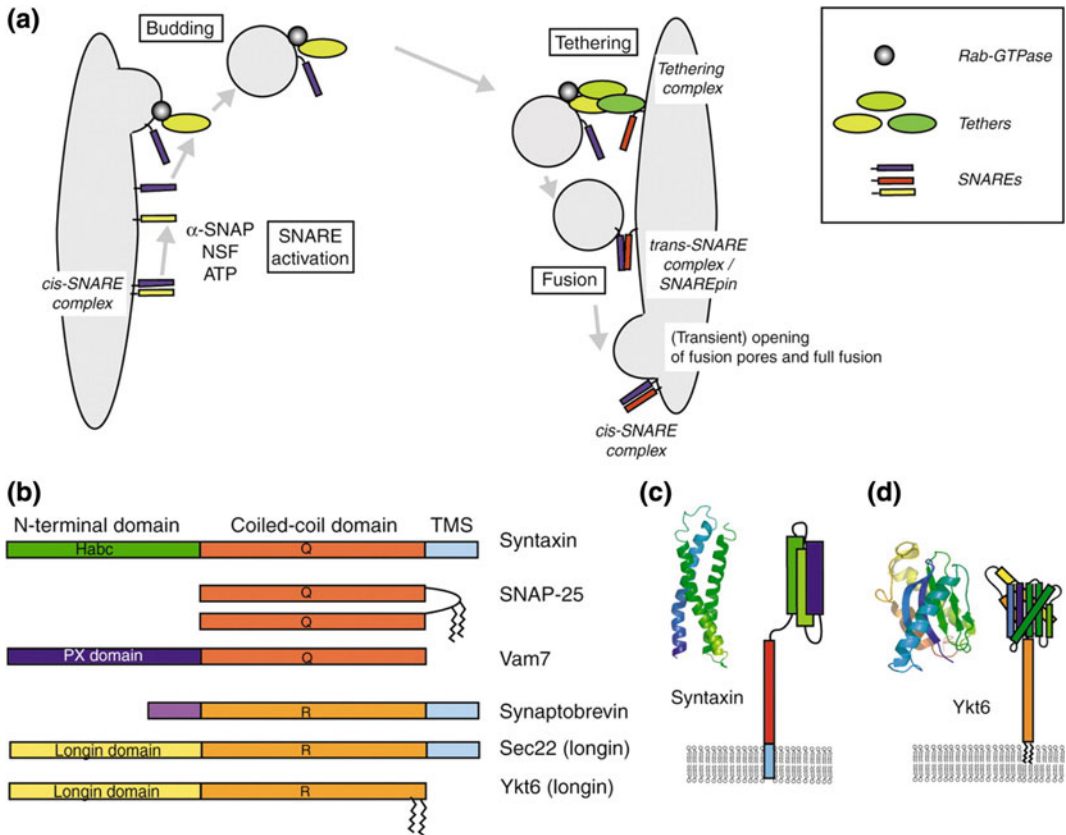


Fig. 10.17 SNARE function in trafficking and SNARE domain structure. *Source* Ungermann and Langosch (2005)

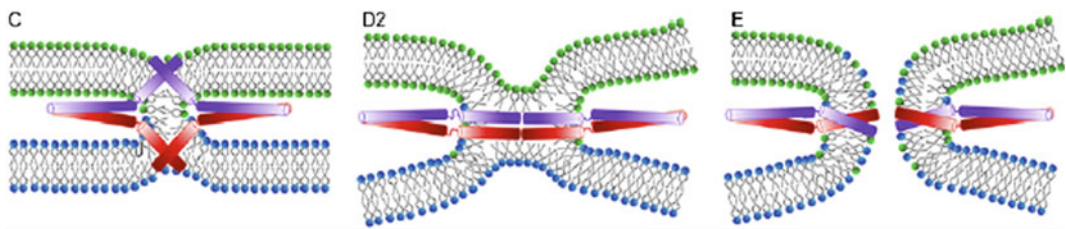


Fig. 10.18 Fusion pore formation by the insertion of the TMDs into the membrane interior as suggested by Fang and Lindau (2014), Fang et al. (2013)

organization (**Fusion**). SNARE transmembrane enhances pore formation after fusion because SNARE assembly and displacement of C-terminal generate mechanical pulling force (Fig. 10.18).

The generated pulling force and zippering action pulls the uncharged C-terminal of transmembrane movement into membrane interior to

initiate pore formation. In the synaptic vesicle and on the target membrane, the SNAREs are concentrated at specific region of membrane fusion for neurotransmitters release. The t SNARE syntaxin density increases because of dynamic clustering by weak protein–protein interaction. The concentration of SNARE protein at fusion site determines fusion kinetics.

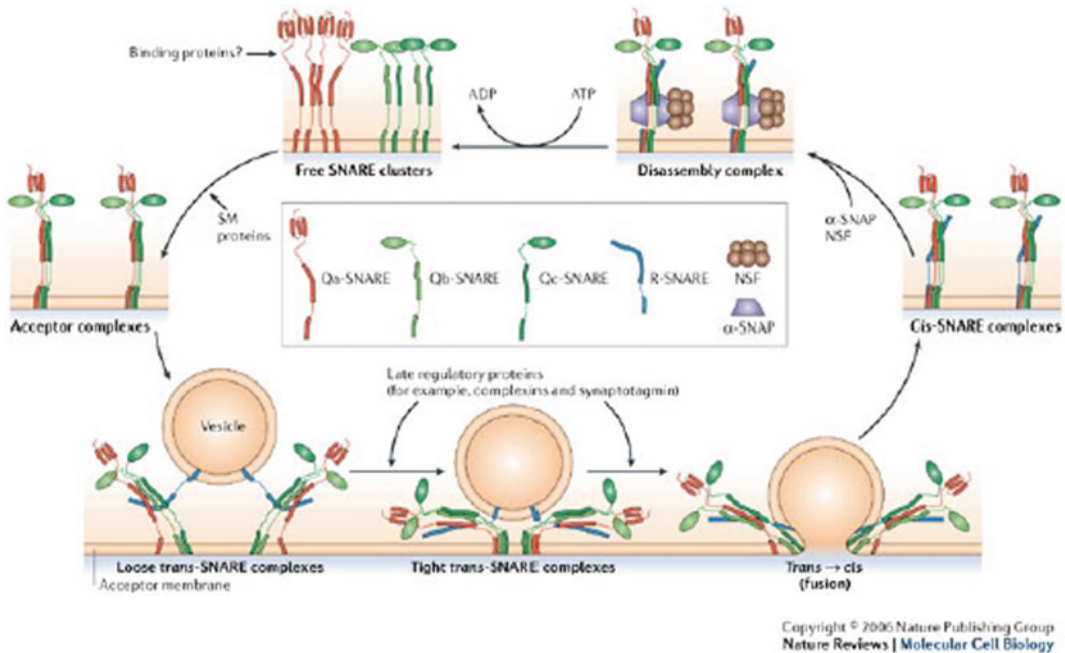


Fig. 10.19 Vesicle docking and membrane fusion By SNARE conformation change cycle. The vesicle 3 R SNAREs interact with R t SNARE on target membrane.

In cluster Q SNARE assembled on target membrane in SM dependent manner. Both t SNARE and v SNARE interact for membrane fusion and pore formation

Syntaxin interaction with SNAP 25 increases polymerization (Fig. 10.19).

Rab is 20–25 Kda monomeric Ras-like GTPases, which cycle between GDP and GTP bound state in guanine exchange factor (GEF) dependent manner. It plays role in both exocytosis and endocytosis. v SNARE of vesicle and t SNARE of target membrane form transSNARE complex. t SNARE complex forms fusion pore and finally fusion of membrane for transport. Rab recruits its effector proteins like early endosome antigen (EEA) to interact with t SNARE and syntaxin for membrane fusion. The Rab cycle is explained diagrammatically in Fig. 10.20 (Table 10.1).

The t SNARE complex contains four parallel helices with two copies of **SNAP 25** and each copy of **syntaxin** and **synaptobrevin** or **VAMP**. The many neurotoxins like **botulinium** cleave these proteins and stop neurotransmission.

During the fusion process, the SNAREs complex changes conformation from trans SNARE (parallel Peptides) to *cis*-SNARE (folding peptides) for fusion (Fig. 10.21).

The defective **α-Synuclein** protein causes **Parkinson's disease** in human patients as **α-synuclein** promotes **SNARE complex assembly**. The neurotransmitter release at synapse requires the following sequence of events (1) physical connection of synaptic vesicles, calcium channels, and other presynaptic components into a single complex, thereby ensuring efficient colocalization of the elements that enable rapid synaptic transmission; (2) organize presynaptic receptors to allow presynaptic modulation of neurotransmitter release, for example, by **endocannabinoids** or by **auto receptors**; and (3) mediate various forms of short- and long-term **presynaptic plasticity**.

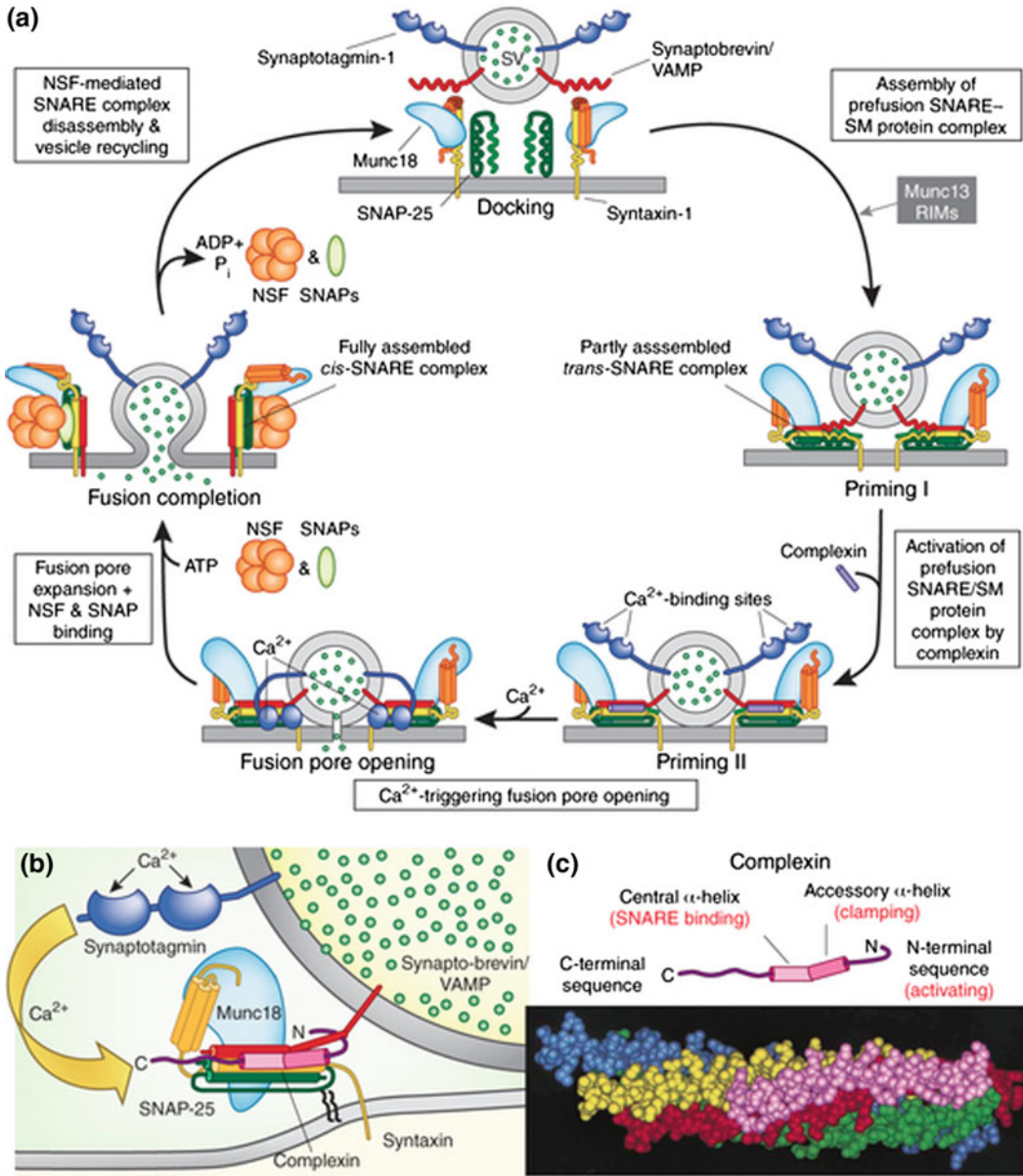


Fig. 10.20 **a** Overview of the SNARE-SM protein cycle and the points of action of complexin and synaptotagmin. Superimposed on the SNARE-SM protein cycle is the association of complexin with partially assembled *trans*-SNARE complexes, which enhances vesicle priming for fusion, and the step of calcium triggering of fusion pore opening by synaptotagmin. **b** Expanded view of the primed synaptic vesicle fusion complex (an assembly of

SNARE proteins, Munc18-1 and complexin) with synaptotagmin poised to trigger fusion pore opening upon calcium binding. **c** Modular domain structure of complexin with functional assignments of the complexin sequences, and a space-filling model of the atomic structure of the SNARE complex containing bound complexin

Table 10.1 The major proteins required for clathrin coated vesicle formations


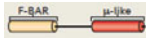
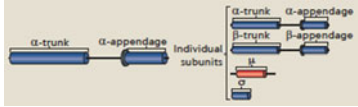

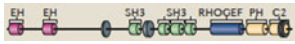


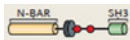
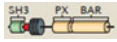



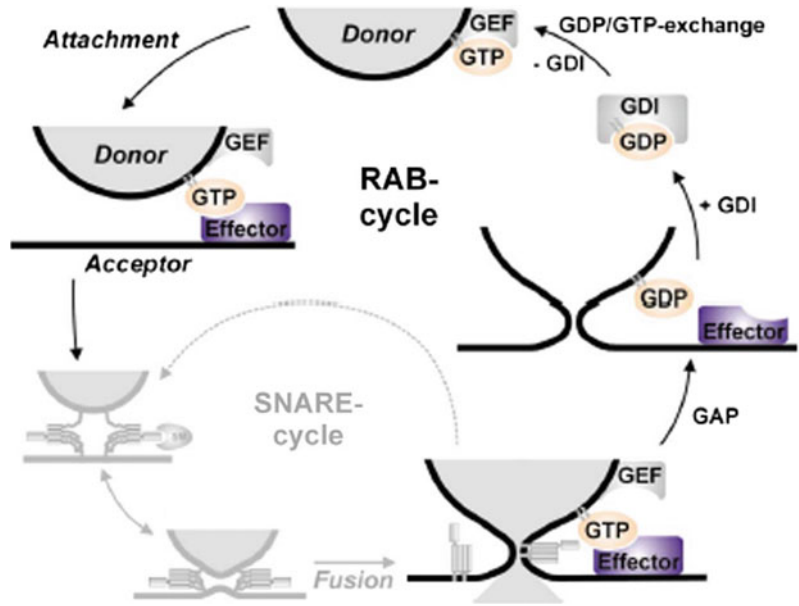
Protein	Human genes	Function	Domain architecture*
<i>Core components</i>			
Clathrin	<i>CLTA</i> , <i>CLTB</i> , <i>CLTC</i>	Self-polymerizing protein composed of three heavy and three light chains that form clathrin triskelion, which can polymerize into flat lattices or cages	
FCHO	<i>FCHO1</i> , <i>FCHO2</i>	F-BAR domain-containing proteins that nucleate clathrin-coated pits and generate the initial membrane curvature	
AP ₂	<i>AP2A1</i> , <i>AP2A2</i> , <i>AP2B1</i> , <i>AP2M1</i> , <i>AP2S1</i>	A heterotetrameric adaptor complex (α -, β 2, μ 2 and σ 2 subunits) that links membrane cargo to clathrin and accessory proteins	
EPS15– EPS15R	<i>EPS15</i> , <i>EPS15R</i>	AP2 clustering and scaffolding proteins	
Intersectin	<i>ITSN1</i> , <i>ITSN2</i>	Scaffolding protein linking various components of the clathrin machinery	
AP180, CALM [§]	<i>SNAP91</i> , <i>PICALM</i>	ANTH domain-containing PtdIns(4,5) P ₂ -binding protein that binds AP ₂ and clathrin and is thought to regulate vesicle size	
Epsin	<i>EPN1</i> , <i>EPN2</i>	ENTH domain-containing membrane-bending protein that is a cargo-specific adaptor for monoubiquitinated receptors	
Amphiphysin	<i>AMPH1</i> , <i>BIN1</i>	N-BAR domain-containing protein that bends the membrane and recruits dynamin to clathrin-coated pits	
SNX ₉	<i>SNX9</i>	BAR domain-containing protein that binds AP ₂ and dynamin	
Dynamin	<i>DNM1</i> , <i>DNM2</i> , <i>DNM3</i>	Self-polymerizing mechanoenzyme that triggers vesicle scission upon GTP hydrolysis	
Auxilin, GAK	<i>DNAJC6</i> , <i>GAK</i>	J domain-containing protein that recruits HSC70 to clathrin cages for uncoating	
HSC70	<i>HSPA8</i>	ATPase triggering uncoating of clathrin cages	

Fig. 10.21 The Rab protein interaction with SNARE for Membrane Fusion. GDI is a guanine dissociation inhibitor to remove all GDP-Rab proteins from the membrane. The guanine nucleotide exchange factor (GEF) initiates GDP-GTP conversion along with displacement of GDI and membrane binding



References

- Fang Q, Lindau M (2014) How could SNARE proteins open a fusion pore? *Physiology* 29(4):278–285
- Fang Q, Zhao Y, Lindau M (2013) Juxtamembrane tryptophans of synaptobrevin 2 control the process of

membrane fusion. *FEBS Lett* 587:67–72. <https://doi.org/10.1016/j.febslet.2012.11.002>

- Ungermann C, Langosch D (2005) Functions of SNAREs in intracellular membrane fusion and lipid bilayer mixing. *J Cell Sci* 118:3819–3828